Ferocenski analozi biomolekula: strukturna karakterizacija i biološka evaluacija (IP-2020-02-9162)_Plan upravljanja istraživačkim podacima

Barišić, Lidija

Data management plan / Plan upravljanja istraživačkim podacima

Plan upravljanja istraživačkim podacima

Opće informacije		
	Ime i prezime predlagatelja	Lidija Barišić
	Matična organizacija	Prehrambeno-biotehnološki fakultet
	Naziv projekta	Ferocenski analozi biomolekula: strukturna karakterizacija i biološka evaluacija (IP-2020-02-9162) FER-AN-BIOMOL
	Upravitelj podacima	Lidija Barišić (lidija.barisic@pbf.unizg.hr)
1.	Prikupljanje podataka i dokumentacija	
	Koje ćete podatke prikupljati, obrađivati, stvarati ili se ponovno njima koristiti? (navedite format, vrstu i opseg podataka)	Podaci prikupljeni istraživanjem mogu se svrstati u tri kategorije: • Reakcijski putevi za pripravu različitih tipova ferocenskih konjugata s biomolekulama • Spektroskopska karakterizacija i konformacijska analiza spojeva sintetiziranih tijekom projekta • Podaci o biološkoj aktivnosti spojeva sintetiziranih tijekom projekta. Podaci u prvoj kategoriji bit će dokumentirani u PDF formatu. IR spektroskopski podaci iz 2. kategorije bit će snimljeni u .prn ili .sp formatu i konvertirani u txt.format ili asci.format za daljnju uporabu. IR spektri obradit će se u programu Origin te pohraniti u .opj formatu, pri čemu se za potrebe publikacija ili izvješća mogu konvertirati u .pgn format. NMR spektroskopski podaci iz druge kategorije bit će snimljeni u fid file NMR formatu i konvertirani u spektralne podatke (spectrum file NMR format) za daljnje korištenje. Obrađeni podaci bit će pohranjeni u PDF formatu. CD spektroskopski podaci bit će snimljeni u .jws formatu i konvertirani u .asci format za daljnju uporabu. Obradom tako spremljenih podataka, spektri će se iscrtati u programu Origin, spremiti u .opj formatu te za za potrebe publikacija ili izvješća konvertirati u .pgn format. Podaci iz 3. kategorije vezani za antitumorsku aktivnost pohranit će se u digitalnom obliku u formatu koji se dobije izravno s instrumenta, a obrađeni podaci bit će pohranjeni u excel i PDF formatu. Podatci će bit snimljeni u različitim softverski specifičnim formatima poput: • VISIONlite files za spektrofluorimetrijske metode • Cary Eclipse files za spektrofotometrijske metode • Rezultati protočne citometrije prikupit će se u fcs. formatu te će se nakon obrade snimiti u excel i PDF formatu • Slike stanica sa svjetlosnog mikroskopa i slike gelova prikupit će se u tiff. ili jpeg.formatu • Rezultati qPCR-a i čitača mikrotitarskih pločica prikupit će se u xlsx. i txt. formatu te nakon obrade snimiti u excel formatu. Za mjerenje NOD2 aktivnosti koristit će se čitač mikrotitarskih pločica (BioTek Synergy). Mjerenja i kvantifikacija (osim slika sa svjetlosnog mikroskopa) sirovih podataka pohranit će u excel obliku.

		Podaci iz ove kategorije vezani za antimikrobnu aktivnost prikupit će se u jpg. formatu, dok će rezultati antioksidativne aktivnosti biti prikupljeni u obliku xls. datoteke te će biti konvertirani u pdf. format za daljnju uporabu. Zone inhibicije rasta test mikroorganizama dokumentirat će se slikanjem, a antioksidativna aktivnost zapisivanjem spektrofotometrijski izmjerenih apsorbancija. Svi prikupljeni podaci bit će u PDF formatu dostupni nakon objavljivanja publikacija i isteka ukupnih projektnih aktivnosti. Procjenjujemo da će opseg prikupljenih podataka iznositi do 50 GB prostora.
	Kako će se podaci prikupljati, obrađivati ili stvarati? (ukratko navedite metodologiju i procese osiguranja kvalitete te načine organiziranja podataka)	Svi prikupljeni podaci i dobiveni rezultati najprije će se zapisivati u laboratorijskim dnevnicima istraživača. Potom će se: 1. eksperimentalni protokoli i s njima povezana karakterizacija spojeva zapisivati u skladu s predloškom časopisa u koji će rezultati biti poslani na recenziju odnosno predlošcima završnih i diplomskih radova, u PDF dokumentu. 2. IR, NMR, CD i MS spektri pohraniti u PDF obliku, raspoređeni u skupine prema planu publiciranja. 3. Podaci o biološkoj aktivnosti pohranit će se u PDF obliku, raspoređeni u skupine prema planu publiciranja. Svi eksperimenti bit će podvrgnuti kontroli kako bi se osigurala valjanost dobivenih podataka. Kemijske sinteze najprije će se izvoditi na manjoj skali, a nakon optimizacije procesa ponovit će se na većoj skali pri čemu iskorištenja u višestruko ponovljenim istim postupcima moraju biti ujednačena. Kvaliteta prikupljenih podataka osiguravat će se te kontrolom i optimizacijom procesnih parametara (koristit će se reagensi i otapala visoke čistoće, sterilni uvjeti prilikom rada sa stanicama, testiranje stanica na kontaminaciju mikoplazmama, korištenje stanica niskog broja pasaža). Svi konačni produkti bit će pročišćavani tankoslojnom i kolonskom kromatografijom sve dok se NMR spektroskopijom ili HPLC-analizom ne dokaže čistoća viša od 95% (prema standardima ACS). Svi uzorci na kojima će se prikupljati podaci pripremit će se prema validiranim protokolima za ovo područje, slijedeći upute proizvođača reagenasa i kitova. U eksperimentima je uključena odgovarajuća kontrola čime se osigurava valjanost podataka (npr. pozitivna kontrola, slijepa proba, kontrola s dodatkom otapala i sl.). Pouzdanost podatka postići će se višekratnim ponavljanjem eksperimenata s istim ulaznim varijablama, umjeravanjem instrumenata, korištenjem standardiziranih protokola, usporedbom dobivenih podataka s relevantnim literaturnim podacima itd. Svi eksperimentalni podatci automatski će se pohraniti u računalni repozitorij mjernog uređaja, a dodatna kopija pohraniti na matičnom računalu istraživača. Također, vodit će osobni laboratorijski dnevnici istraživača u koje će se zapisivati protokoli, opažanja i zapisi eksperimenata te će se prevesti u digitalni oblik u skladu s predloškom časopisa za javnu objavu. Svi će mjerni instrumenti biti redovito kalibrirani. Analitički podatci prikupljeni s instrumenata koji ih generira procesirat će se koristeći njihove matične programe kao što je navedeno u prethodnom odgovoru. NMR spektri bit će snimljeni na instrumentu Avance III HD (Bruker) i obrađeni pomoću programa TopSpin (verzija 4.1.4), CMC-assist za AVANCE III HD (verzija 2.23), Spinworks i Mestre Nova. IR spektri bit će snimljeni na Perkin Elmer Spectrum Two spektrofotometru i obrađeni u programu Perkin Elmer Spectrum. CD spektri bit će snimljeni na Jasco-810 spektropolarimetru te obrađeni u programu J-810 Spectra Manager. Matični programi Microvisible i Alliance koristit

		će se za prikupljanje slika stanica i slika gelova sa svjetlosnog mikroskopa (Micros) i s UV kamere (Uvitec Cambridge). BD FACSuite software korisitit će se za prikupljanje podataka s protočnog citometra (BD FACSVerse) te FlowJo za njihovu obradu. MikroWin2000 i Agilent AriaMx programi koristit će se za prikupljanje rezultata apsorbancija s čitača mikrotitarskih pločica (Hidex Chameleon V) i fluorescencije s qPCR-a (Agilent AriaMx). Programi Microsoft Excel i GraphPad Prism će se korisititi za završnu obradu podataka i spremanje u tablični i grafički prikaz. Svi podaci prikupljeni na odgovarajućim mjernim instrumentima bit će označeni datumom kojeg su prikupljeni u formatu GGGG-MM-DD. Za testove antimikrobne i antioksidativne aktivnosti koristit će se spektrofotometar Specord Plus (Analytik Jena, Njemačka) s pripadajućim matičnim operativnim programom. Također, prikupljat će se i analizirati relevantni znanstveni članci i općenito literaturni podaci. Navedeno će se vršiti definiranjem ključnih riječi i upita, na znanstvenim platformama poput Web of Science i Scopus. Zahvaljujući institucionalnoj (Prehrambeno-biotehnološki Fakultet, Sveučilište u Zagrebu) pretplati na baze podataka, sadržaj odabrane literature preuzimat će se u doc, .pdf ili .xls obliku, te adekvatno skladištiti. Prikupljene podatke članovi istraživačke skupine međusobno će dijeliti korištenjem web-aplikacije FileSender.
	Koju ćete dokumentaciju i metapodatke ustupiti osim podataka? (navedite koje su informacije potrebne korisnicima kako bi mogli čitati i interpretirati podatke u budućnosti te koji će se standardi koristiti pri tumačenju podataka)	1. Svi sintetski podaci bit će popraćeni PDF dokumentom u kojem će biti detaljno opisani svi koraci u sintezi, prema metodološkim standardima propisanima od strane znanstvenih časopisa. 2. Rezultati spektroskopske karakterizacije bit će popraćeni PDF dokumentom sa skeniranim spektrima, prema metodološkim standardima propisanima od strane znanstvenih časopisa. 3. Rezultati biološke aktivnosti bit će popraćeni excel tablicama i PDF dokumentom s grafičkim prikazima i detaljnim opisom svih koraka u određivanju biološke aktivnosti kako bi se osigurala ponovljivost eksperimenata prema metodološkim standardima propisanima od strane znanstvenih časopisa. Dokumenti će se nazvati na sljedeći način: 1. HRZZ_FER-AN-BIOMOL_sinteza 2. HRZZ_FER-AN-BIOMOL_spektroskopska karakterizacija 3. HRZZ_FER-AN-BIOMOL_biološka evaluacija. Opisani dokumenti bit će javno dostupni nakon objavljivanja, ukoliko prikupljeni podaci neće biti korišteni za pripremu i objavu dodatnih publikacija.
2.	Pravna i sigurnosna pitanja	
	Jeste li ograničeni sporazumom o povjerljivosti? Imate li potrebna dopuštenja za prikupljanje, obradu, čuvanje i dijeljenje podataka? Jesu li osobe čiji se podaci pohranjuju informirani o tome i jesu li dali privolu? Kojim ćete se metodama	Pri izvedbi ovog projekta neće se kršiti etička načela. Napomena: u istraživanjima koristimo humane/animalne stanice, ali ne primarne stanične kulture, nego kontinuirane komercijalne stanične kulture koje ne podliježu zakonskim propisima RH.

	koristiti u svrhu zaštite osjetljivih podataka (GDPR - posebne kategorije osobnih podataka)?	
	Kako će se regulirati pristup podacima i njihova sigurnost? Koji su potencijalni rizici koje treba uzeti u obzir? Kako ćete osigurati sigurnost pohrane osjetljivih podataka?	Ovim projektom ne koriste se i ne obrađuju se osobni ili osjetljivi podaci. Dobiveni podaci dijelit će samo između članova istraživačke skupine putem aplikacije FileSender koja ima vremenski ograničen pristup podacima.
	Kako ćete upravljati zaštitom autorskih prava i intelektualnog vlasništva? Tko će biti vlasnik podataka? Koje će se licencije primjenjivati na podatke? Koja će se ograničenja primjenjivati na ponovnu uporabu osobnih podataka?	Prava na intelektualno vlasništvo regulirana su preporukama matične institucije. Podaci prikupljeni po završetku projektnih aktivnosti služit će za objavljivanje u znanstvenim časopisima i prezentaciju na znanstvenim konferencijama. Ne očekujemo da će naša istraživanja rezultirati patentom, a ako do toga ipak dođe autorska prava i intelektualno vlasništvo zaštitit će sukladno preporukama matične institucije.
3.	Pohrana i čuvanje podataka	
	Kako će podaci biti pohranjeni i kako će biti napravljena sigurnosna kopija podataka (*backup*) tijekom istraživanja? Koji su kapaciteti čuvanja podataka kojim raspolažete? Kojim se procedurama koristite za sigurnosnu kopiju (*backup*)?	Istraživači će laboratorijske dnevnike čuvati u svojim laboratorijima, dok će elektronički podaci biti čuvani na računalu glavnog istraživača i na računalima suradnika. Podaci će se nakon objavljivanja ili po isteku projektnih aktivnosti s računala glavnog istraživača kopirati u nacionalni sustav za pohranu i dijeljenje podataka Puh. Glavni istraživač će redovito raditi sigurnosnu kopiju s uredskog računala na osobno prijenosno računalo i vanjski disk.
	Koji je vaš plan čuvanja podataka? U kojim će se formatima čuvati?	Sve podatci prikupljeni tijekom provedbe projekta čuvat će se na računalima istraživača u txt., xslx., docx i pdf.formatu.
4.	Dijeljenje i ponovna uporaba podataka	
	Kako i gdje će se podaci dijeliti? Na kojem repozitoriju planirate dijeliti	Podaci prikupljeni tijekom provedbe projekta bit će diseminirani na znanstvenim konferencijama i u znanstvenim publikacijama, te će se trajno pohraniti u institucijskom repozitoriju Fakulteta uspostavljenom u nacionalnom sustavu Dabar. Osim toga, dio podataka će objavljivanjem u Open Access časopisima biti vidljiv potencijalnim korisnicima.

	podatke? Kako će potencijalni korisnici doznati za podatke?	
	Ako postoje podaci koji se ne smiju dijeliti (prijavitelji vezani zakonskim, etičkim, autorskim pravila, povjerljivošću i sl.), pojasnite razloge ograničenja.	Diseminirani podaci bit će dostupni u rukopisu i dodatnim, popratnim materijalima predmetnog časopisa, dok će neobjavljeni podaci biti pohranjeni na računalu glavnog istraživača.
	Potvrdite da ćete se koristiti digitalnim repozitorijem koji je u skladu s načelima *FAIR-a*.	Potvrđujemo da ćemo se koristiti digitalnim repozitorijem koji je u skladu s načelima FAIR-a.
	Potvrdite da ćete se koristiti digitalnim repozitorijem koji održava neprofitna organizacija (ako ne, objasnite zašto ne možete dijeliti podatke na digitalnom repozitoriju koji nije komercijalan).	Potvrđujemo da ćemo se koristiti digitalnim repozitorijem koji održava neprofitna organizacija.

Ref:
[1] Celjak, D., Dorotić Malič, I., Matijević, M., Poljak, Lj., Posavec K. i Turk, I.: „Istraživački podaci - što s njima?“ Istraživački podaci - što s njima? : priručnik o upravljanju istraživačkim podacima | Digitalni repozitorij Srca (unizg.hr)

HRZZ_FER-AN-BIOMOL_sinteza

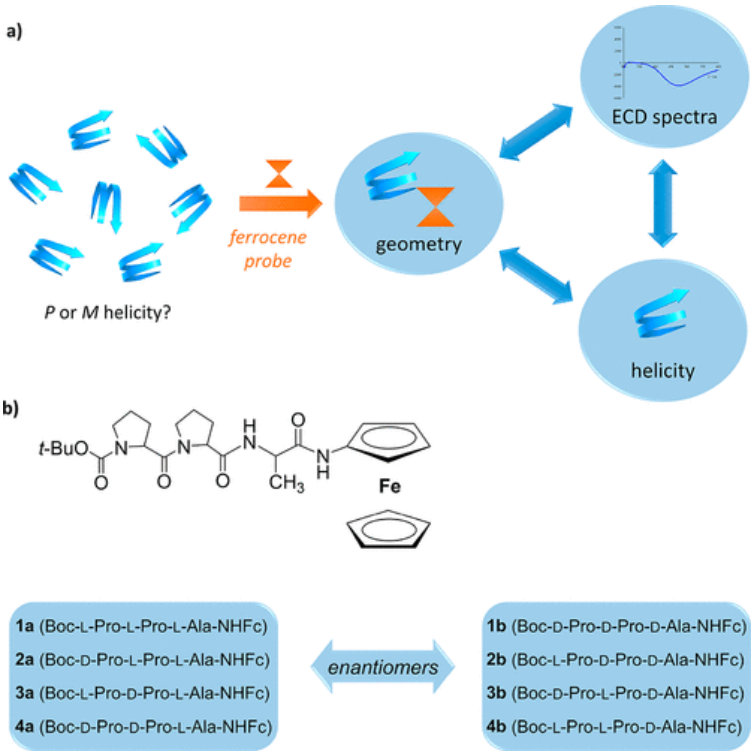

Derivatives **1**–**4** were synthesized using stepwise 1-hydroxybenzotriazole (HOBt)/1-ethyl-3-(3-dimethylaminopropyl)carbodiimide hydrochloride (EDC)-mediated coupling technique starting from Boc-protected aminoferrocene (more details in the Experimental Section). (27) We expected the same experimental observations for scalar properties of both enantiomers (**a** and **b** for each compound); thus experimental data are thoroughly described only for one series (**1a**–**4a**). Additionally, properties depending on the sign of torsion angles are reported for each enantiomer.

General Procedure

The precursors *t*BuCO–AA_2–AA_1–NHFc (AA_1 = L-Ala, D-Ala; AA_2 = L-Pro, D-Pro) were prepared using previously described stepwise solution-phase peptide synthesis. (20,21) A solution of *t*BuCO–AA_2–AA_1–NHFc (188 mg, 0.4 mmol) in dichloromethane (20 mL) was cooled to 0 °C and treated with gaseous HCl for 2 h. Thereafter, the mixture was evaporated to dryness, and the resulting hydrochloride was treated with Et_3N in CH_2Cl_2 to pH ∼8. The free amine was coupled with Boc–AA_3–OH (AA_3 = L-Pro, D-Pro) (172 mg, 0.8 mmol), previously activated using standard EDC/HOBt protocol [EDC (169 mg, 0.88 mmol); HOBt (119 mg, 0.88 mmol)]. The reaction mixture was stirred at room temperature until consumption of the starting material, as monitored by thin-layer chromatography (TLC). The mixture was washed three times with a saturated aqueous solution of $NaHCO_3$ (30 mL), 10% aqueous solution of citric acid (30 mL), and H_2O (30 mL), dried over Na_2SO_4, and evaporated. TLC purification of crude products on silica gel with CH_2Cl_2/EtOAc (10:1) gave a yellow powder of peptides **1**–**4**.

Boc-L-Pro-L-Pro-L-Ala-NHFc (1a):

Yield 216 mg (95%). Mp 181–183 °C. $[\alpha]_D$ +15.9° (*c* = 1.1 $CHCl_3$). FT-IR ($CHCl_3$, ν_{max}, cm^{-1}): 3410 vw (NH_{free}), 3317 m (NH_{assoc}), 1682 s (amide I), 1618 m (amide I), 1556 m (amide II), 1528 m (amide II). ^1H NMR ($CDCl_3$, δ, ppm): 8.26 (s, 1 H, NH_{Fc}), 7.66 (d, 1H, *J* = 8.0 Hz, NH_{Ala}), 4.86 (s, 1H, H-2, Fc), 4.79 (s, 1H, H-5, Fc), 4.6–

4.56 (m, 1H, CHα$_{Pro2}$), 4.51–4.44 (m, 2H, CHα$_{Pro1}$, CH$_{Ala}$), 4.15 (s, 5H, Fc), 3.93 (s, 1H, H-3, Fc), 3.92 (s, 1H, H-4, Fc), 3.64–3.60 (m, 2H, CHδ$_{Pro1}$), 3.40–3.37 (m, 2H, CHδ$_{Pro}$), 2.47–2.40 (m, 1H, CHβ$_{Pro1}$), 2.38–2.30 (m, 1H, CHβ$_{Pro2}$), 2.11–2.05 (m, 1H, CHγ$_{Pro}$), 2.05–1.91 (m, 1H CHβ$_{Pro2}$, 1H CHβ$_{Pro1}$, 1H CHγ$_{Pro2}$, 2H CHγ$_{Pro1}$), 1.49 (bs, 3H, CH$_{3Ala}$), 1.46 (s, 9H, CH$_{3Boc}$). ^{13}C NMR ($CDCl_3$, δ, ppm): 172.1 (CO$_{Pro1}$), 171.4 (CO$_{Pro2}$), 170.7 (CO$_{Ala}$), 154.9 (CO$_{Boc}$), 95 (C-1), 81.0 (Cq$_{Boc}$), 69.3 (Cp), 64.4 (C-3, Fc), 64.3 (C-4, Fc), 62.4 (CHα$_{Pro2}$), 62.3 (CHα$_{Pro1}$), 61.7 (C-2, Fc), 61.6 (C-5, Fc), 49.8 (CH$_{Ala}$), 47.0 (CHδ$_{Pro1}$), 46.8 (CHδ$_{Pro2}$), 29.1 (CHβ$_{Pro1}$), 28.6 (CHβ$_{Pro2}$), 28.5 (CH$_{3Boc}$), 24.8 (CHγ$_{Pro1}$), 26.1 (CHγ$_{Pro2}$), 17.5 (CH$_{3Ala}$). HRMS (ESI): calcd for $C_{28}H_{38}N_4O_5Fe$ 566.2191; found 566.2198.

Boc-D-Pro-L-Pro-L-Ala-NHFc (2a):

Yield 216 mg (95%). Mp 181–183 °C. $[\alpha]_D$ +30.1° (*c* = 1.1 $CHCl_3$). FT-IR ($CHCl_3$, ν_{max}, cm^{-1}): 3323 m (NH$_{assoc}$), 1667 s (amide I), 1651 s (amide I), 1558 m (amide II), 1540 m (amide II), 1515 m (amide II). ^{1}H NMR ($CDCl_3$, δ, ppm): 8.26 (s, 1 H, NH$_{Fc}$), 7.10 (d, 1H, *J* = 8.0 Hz, NH$_{Ala}$), 5.01 (m, 1H, H-2, Fc), 4.63–4.55 (m, 2H, CHα$_{Pro2}$, CH$_{Ala}$), 4.43–4.40 (m, 2H, H-5 Fc, CHα$_{Pro1}$), 4.16 (s, 5H, Fc), 4.09–4.04 (m, 1H, CHδ$_{Pro1}$), 3.95 (m, 1H, H-3, Fc), 3.89 (m, 1H, H-4, Fc), 3.63–3.56 (m, 1H, CHδ$_{Pro1}$), 3.40–3.37 (m, 2H, CHδ$_{Pro2}$), 2.36–2.27 (m, 1H, CHβ$_{Pro2}$), 2.25–2.13 (m, 2H CHβ$_{Pro1}$, 1H CHγ$_{Pro2}$), 2.10–2.02 (m, 1H CHβ$_{Pro2}$, 2 H CHγ$_{Pro1}$), 1.96–1.86 (m, 1H, CHγ$_{Pro2}$), 1.47 (d, 2H, *J* = 7.6 Hz, CH$_{3Ala}$), 1.26 (s, 9H, CH$_{3Boc}$). ^{13}C NMR ($CDCl_3$, δ, ppm): 173.7 (CO$_{Pro1}$), 171.0 (CO$_{Pro2}$), 170.0 (CO$_{Ala}$), 155.1 (CO$_{Boc}$), 94.6 (C-1), 80.7 (Cq$_{Boc}$), 69.4 (Cp), 64.8 (C-3, Fc), 63.7 (C-4, Fc), 62.7 (C-2, Fc), 61.7 (CHα$_{Pro2}$), 61.1 (C-5, Fc), 57.8 (CHα$_{Pro1}$), 49.7 (CH$_{Ala}$), 48.0 (CHδ$_{Pro1}$), 47.5 (CHδ$_{Pro2}$), 29.7 (CHβ$_{Pro2}$), 29.7 (CHβ$_{Pro1}$), 28.4 (CH$_{3Boc}$), 25.1 (CHγ$_{Pro2}$), 24.9 (CHγ$_{Pro1}$), 17.2 (CH$_{3Ala}$). HRMS (ESI): calcd for $C_{28}H_{38}N_4O_5Fe$ 566.2191; found 566.2192.

Boc-L-Pro-D-Pro-L-Ala-NHFc (3a):

Yield 220 mg (97%). Mp 181–183 °C. $[\alpha]_D$ −25.5° (*c* = 1.1 $CHCl_3$). FT-IR ($CHCl_3$, ν_{max}, cm^{-1}): 3424 w (NH$_{free}$), 3346 m (NH$_{assoc}$), 3324 m (NH$_{assoc}$), 1670 s (amide I), 1552 m (amide II), 1520 m (amide II). ^{1}H NMR ($CDCl_3$, δ, ppm): 8.04 (s, 1 H, NH$_{Fc}$), 7.52 (d, 1H, *J* = 6.4 Hz, NH$_{Ala}$), 4.70 (m, 1H, H-2, Fc), 4.67 (m, 1H, H-5, Fc), 4.64–4.62 (m, 1H, CHα$_{Pro1}$), 4.46–4.42 (m, 1H, CHα$_{Pro2}$), 4.15 (s, 5H, Fc), 4.13–4.10 (m, 1H, CH$_{Ala}$), 3.99–3.95 (m, 1H, CHδ$_{Pro1}$), 3.94–3.90 (m, 2H, H-3, H-4, Fc), 3.60–3.46 (m, 1H CHδ$_{Pro1}$, 2H CHδ$_{Pro2}$), 2.28–1.88 (m, 2H CHβ$_{Pro1}$, 2H CHβ$_{Pro2}$, 2 H CHγ$_{Pro1}$, 2H CHγ$_{Pro2}$), 1.49 (d, 2H, *J* = 7.2 Hz, CH$_{3Ala}$), 1.38 (s, 9H, CH$_{3Boc}$). ^{13}C NMR ($CDCl_3$, δ, ppm): 173.1 (CO$_{Pro1}$), 171.5 (CO$_{Pro2}$), 170.6 (CO$_{Ala}$), 155.0 (CO$_{Boc}$), 94.9 (C-1), 80.4 (Cq$_{Boc}$), 69.3 (Cp), 64.4 (C-3, Fc), 64.3 (C-4, Fc), 61.7 (C-2, Fc), 61.6 (C-5, Fc), 60.8 (CHα$_{Pro1}$), 58.0 (CHα$_{Pro2}$), 51.4 (CH$_{Ala}$), 47.5 (CHδ$_{Pro1}$), 47.4 (CHδ$_{Pro2}$), 29.4 (CHβ$_{Pro1}$), 28.6 (CH$_{3Boc}$), 28.4 (CHβ$_{Pro2}$), 25.0 (CHγ$_{Pro1}$), 24.8 (CHγ$_{Pro2}$), 16.6 (CH$_{3Ala}$). HRMS (ESI): calcd for $C_{28}H_{38}N_4O_5Fe$ 566.2191; found 566.2194.

Boc-D-Pro-D-Pro-L-Ala-NHFc (4a):

Yield 205 mg (90%). Mp 181–183 °C. $[\alpha]_D$ +40.6° (*c* = 1.1 $CHCl_3$). FT-IR ($CHCl_3$, ν_{max}, cm^{-1}): 3423 m (NH$_{free}$), 3315 m (NH$_{assoc}$), 1691 s (amide I), 1647 s (amide I), 1557 m (amide II), 1516 m (amide II). ^{1}H NMR ($CDCl_3$, δ, ppm): 8.58 (s, 1 H, NH$_{Fc}$), 6.61 (d, 1H, *J* = 8.6 Hz, NH$_{Ala}$), 4.87 (m, 1H, H-2 Fc), 4.78 (m, 1H, H-5 Fc), 4.60–4.46 (m, 2H, CHα$_{Pro1}$, CH$_{Ala}$), 4.42–4.30 (m, 1H, CHα$_{Pro2}$), 4.10 (s, 5H, Fc), 3.94–3.90 (m, 2H, H-3 Fc, H-4 Fc), 3.77–3.40 (m, 4H, CHδ$_{Pro1}$, CHδ$_{Pro2}$), 2.22–1.94 (m, 2H CHβ$_{Pro2}$, 2H CHβ$_{Pro1}$, 2H CHγ$_{Pro2}$, 2H CHγ$_{Pro1}$), 1.50 (s, 9H, CH$_{3Boc}$), 1.42 (s, 3H, CH$_{3Ala}$). ^{13}C NMR ($CDCl_3$, δ, ppm): 172.1 (CO$_{Pro1}$), 172.1 (CO$_{Pro2}$), 170.1 (CO$_{Ala}$), 154.7 (CO$_{Boc}$), 95.3 (C-1), 79.9 (Cq$_{Boc}$), 69.2 (Cp), 64.3 (C-3, Fc), 64.1 (C-4, Fc), 61.4 (C-2, Fc), 61.4 (C-5, Fc), 61.1 (CHα$_{Pro1}$), 58.3 (CHα$_{Pro2}$), 49.5 (CH$_{Ala}$), 47.3 (CHδ$_{Pro1}$), 47.2 (CHδ$_{Pro2}$), 29.3 (CHβ$_{Pro1}$), 28.7 (CH$_{3Boc}$), 28.6 (CHβ$_{Pro2}$), 25.8 (CHγ$_{Pro1}$), 24.7 (CHγ$_{Pro2}$), 17.7 (CH$_{3Ala}$). HRMS (ESI): calcd for $C_{28}H_{38}N_4O_5Fe$ 566.2191; found 566.2195.

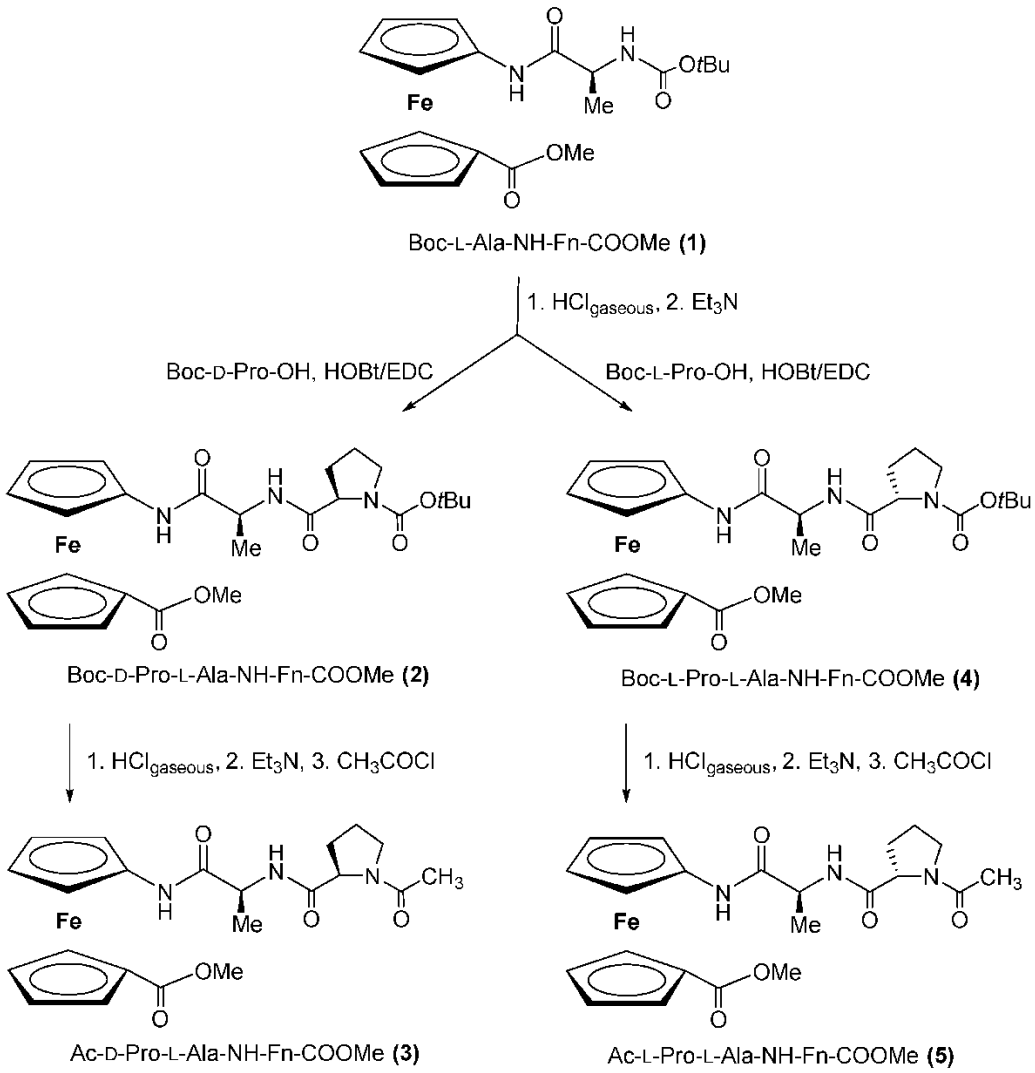

Synthesis of Boc-(**2**,**4**) and Ac-protected peptides (**3**,**5**) containing homo-and heterochiral Pro-Ala sequences

***Synthesis of Peptides* 2–5**

The previously established simple and efficient synthetic route to ferrocene-containing peptides [13,14,16,17] was applied here to obtain peptides **2**–**5** (Scheme 1). Boc-deprotection of Boc-L-Ala-NH-Fn-COOMe **1** [16] in the presence of gaseous HCl gave a hydrochloride salt, which was processed with an excess of NEt_3 to give the free amine required for the coupling step. Then, *C*-activated Boc-L-Pro-OH and Boc-D-Pro-OH were added to the unstable amine to obtain diastereomeric Boc-peptides **2** and **4**, respectively. Conversion of carbamates **2** and **4** to acetamides **3** and **5** was accomplished by (i) acidic Boc-deprotection and (ii) Ac-protection in the presence of acetyl chloride [14]. The characterization data with IR, NMR, and MS spectra of conjugates **2**–**5** can be found in the Supplementary Material, Figures S2–S51.

Materials and Methods

General Procedure and Methods

The synthesis of peptides **2**–**5** was carried out under argon atmosphere and the chemicals used for the reactions were analytically pure. CH_2Cl_2 used for synthesis, CD measurements and FTIR was dried

(P_2O_5), distilled over CaH_2, and stored over molecular sieves (4 Å). EDC (Acros Organics, Geel, Belgium), HOBt (Aldrich, Santa Clara, CA, USA) and acetyl chloride (Aldrich), were used as received. The synthesis of Boc-L-Ala-NH-Fn-COOMe (**1**) has been described previously [16]. Its *N*-terminus was deprotected by exposure to gaseous HCl. The *N*-termini of L- and D-proline were protected in the presence of sodium hydroxide, aqueous dioxane and di-*tert*-butyldicarbonate to give Boc-L-Pro-OH and Boc-D-Pro-OH, respectively. Boc-L-Pro-OH and Boc-D-Pro-OH were activated with the coupling reagent HOBt for 1 h in CH_2Cl_2. The products were purified by preparative thin layer chromatography on silica gel (Kieselgel 60 HF254, KGaA, Darmstadt, Germany) using EtOAc/CH_2Cl_2 mixture or pure EtOAc as eluent

Synthesis of Boc-D-Pro-L-Ala-NH-Fn-COOMe (2) and Boc-L-Pro-L-Ala-NH-Fn-COOMe (4)

The HCl_{gas} was purged through the suspension of Boc-L-Ala-NH-Fn-COOMe (**1**) (1000 mg, 2.32 mmol) in dry CH_2Cl_2 (5 mL) at 0 °C. After 30 min, the solvent was evaporated in vacuo, leaving a dark yellow hydrochloride salt, which was then suspended in CH_2Cl_2 and treated with NEt_3 (pH ~ 8) to afford an unstable free amine suitable for coupling to Boc-L-Pro-OH or Boc-D-Pro-OH (998 mg, 4.64 mmol) using the standard EDC/HOBt method; EDC (1007 mg, 5.57 mmol), HOBt (753 mg, 5.57 mmol). The reaction mixtures were then stirred at room temperature until the ferrocene amine was completely consumed, which was monitored by TLC (~1 h). Standard work-up (washing with a saturated aqueous solution of $NaHCO_3$, a 10% aqueous solution of citric acid and brine, drying over Na_2SO_4 and evaporation in vacuo) including TLC purification of the crude products (EtOAc: CH_2Cl_2 = 1: 5; R_f = 0.52 (**2**), R_f = 0.55 (**4**)) gave orange solids of **2** (1107 mg, 89%) and **4** (1213 mg, 92%).

Boc-D-Pro-L-Ala-NH-Fn-COOMe (**2**): m.p. = 119.2 °C. IR (CH_2Cl_2) $\breve{\nu}_{max}$/cm^{-1}: 3418 w (NH_{free}), 3325 m ($NH_{assoc.}$), 1705 s (C = O_{COOMe}), 1684 s, 1671 s (C = O_{CONH}), 1557 s, 1531 s (amide II). IR (KBr) $\breve{\nu}_{max}$/cm^{-1}: 3509 w(NH_{free}), 3308 m ($NH_{assoc.}$), 1714 s (C = O_{COOMe}), 1695 s, 1671 s (C = O_{CONH}). ^{1}H-NMR (600 MHz, $CDCl_3$) δ/ppm: 8.37 (s, 0.89H, $NH_{Fn\ trans}$), 7.70 (s, 0.11H, $NH_{Fn\ cis}$), 7.24 (d, *J* = 6.3 Hz, 0.89H, $NH_{Ala\ trans}$), 6.66 (d, 0.11H, $NH_{Ala\ cis}$), 5.09 (s, 1H, H-3), 4.81 (s, 2H, H-8), 4.72–4.69 (m, 2H, H-9, CH_{Ala}) 4.58 (s, 1H, H-4), 4.40 (s, 1H, H-7), 4.35 (s, 1H, H-10), 4.16 (s, 1H, CH-α (Pro)), 4.01 (s, 1H, H-2), 3.95 (s, 1H, H-5), 3.79 (s, 3H, COOMe), 3.53 (td, *J* = 10.3 Hz, 6,7 Hz, 1H, CH_2-δ (Pro)), 3.46 (s, 1H, CH_2-δ′ (Pro)), 2.22–2.07 (m, 2H, CH_2-β, CH_2-β′ (Pro)), 1.89–1.86 (m, 2H, CH_2-γ, CH_2-γ′ (Pro)), 1.50 (s, 9H, $(CH_3)_{3\ Boc}$), 1.48 (d, *J* = 7.30 Hz, 3H, $CH_{3\ Ala}$). ^{13}C-NMR (150 MHz, $CDCl_3$) δ/ppm: 172.47 (CO_{Fn}), 172.10 (CO_{COOMe}), 170.89 (CO_{Ala}), 155.26 (CO_{Boc}), 96.31 (C-1, Fn), 80.37 ($C_{q\ Boc}$), 72.79 (C-7), 72.45 (C-10), 71.88 (C-6), 71.75 (C-8), 71.43 (C-9), 66.59 (C-2), 65.40 (C-5), 63.94 (C-4), 62.54 (C-3), 61.10 (C-α, Pro), 51.87 ($CH_{3\ COOMe}$), 48.59 (CH_{Ala}), 47.53 (CH_2-δ, Pro), 29.87 (CH_2-β, Pro), 28.58 ($(CH_3)_{3\ Boc}$), 24.96 (CH_2-γ, Pro), 17.56 ($CH_{3\ Ala}$). ESI-MS (H_2O:MeOH = 50:50): *m*/*z* 526.1 ((M − H)$^-$). MALDI-HRMS *m*/*z* = 527.1708 (calculated for $C_{25}H_{33}N_3O_6Fe$ = 527.1718).

Boc-D-Pro-L-Ala-NH-Fn-COOMe (**4**): m.p. = 66.9 °C. IR (CH_2Cl_2) $\breve{\nu}_{max}$/cm^{-1}: 3418 w (NH_{free}), 3310 m ($NH_{assoc.}$), 1705 s (C = O_{COOMe}), 1674 s (C = O_{CONH}), 1555 s, 1503 s (amide II). IR (KBr) $\breve{\nu}_{max}$/cm^{-1}: 3505 w (NH_{free}), 3296 m ($NH_{assoc.}$), 1715 s (C = O_{COOMe}), 1669 s, 1660 s (C = O_{CONH}). ^{1}H-NMR (600 MHz, $CDCl_3$) δ/ppm: 8.15 (s, 0.9H, $NH_{Fn\ trans}$), 7.74 (s, 0.1H, $NH_{Fn\ cis}$), 6.85 (d, *J* = 6.3 Hz, 0.9H, $NH_{Ala\ trans}$), 6.67 (d, 0.1H, $NH_{Ala\ trans}$), 4.81 (s, 1H, H-3), 4.76 (s, 2H, H-8, H-9), 4.60 (s, 1H, H-4), 4.48 (m, 1H, CH_{Ala}), 4.38 (s, 1H, H-7), 4.37 (s, 1H, H-10), 4.34 (s, 1H, CH-α (Pro)), 4.00 (s, 2H, H-2, H-5), 3.78 (s, 3H, COOMe), 3.50–3.45 (m, 2H, CH_2-δ, CH_2-δ′ (Pro)), 2.22–2.16 (m, 2H, CH_2-β, CH_2-β′ (Pro)), 1.92–1.91 (m, 2H, CH_2-γ, CH_2-γ′ (Pro)), 1.49 (s, 9H, $(CH_3)_{3\ Boc}$), 1.42 (d, *J* = 6.98 Hz, 3H, $CH_{3\ Ala}$). ^{13}C-NMR (150 MHz, $CDCl_3$) δ/ppm: 172,35 (CO_{Fn}), 171.95 (CO_{COOMe}), 170.45 (CO_{Ala}), 156.34 (CO_{Boc}), 95.79 (C-1, Fn), 81.24 ($C_{q\ Boc}$), 73.08 (C-7), 72.97 (C-10), 71.90 (C-6), 71.41 (C-8), 71.08 (C-9), 66.56 (C-2), 66.39 (C-5), 63.15 (C-4), 62.71 (C-3), 60.97 (C-α, Pro), 51.70 ($CH_{3\ COOMe}$), 49.74 (CH_{Ala}), 47.57 (CH_2-δ, Pro), 29.14 (CH_2-β, Pro), 28.54 ($(CH_3)_{3\ Boc}$), 24.84 (CH_2-γ, Pro), 17.54 ($CH_{3\ Ala}$). ESI-MS (H_2O:MeOH = 50:50): *m*/*z* 526.1 ((M − H)$^-$). MALDI-HRMS *m*/*z* = 527.1729 (calculated for $C_{25}H_{33}N_3O_6Fe$ = 5.271.718).

Synthesis of Ac-D-Pro-L-Ala-NH-Fn-COOMe (3) and Ac-L-Pro-L-Ala-NH-Fn-COOMe (5)

The transformation of carbamates **2** and **4** (1000 mg, 1.89 mmol) to acetamides **3** and **5** began with the acidic Boc-deprotection described above. Their free amines, obtained by treating the hydrochloride salt with NEt_3 (2.07 mL, 23.7 mmol), were cooled to 0 °C and acetyl chloride (807 µL, 11.34 mmol) was added dropwise, stirring in an ice bath. After TLC monitoring showed complete conversion of the starting materials, the reaction mixtures were poured into water and extracted with CH_2Cl_2. The combined organic phases were washed with a brine, dried over Na_2SO_4 and evaporated to dryness in vacuo. The resulting crude products were purified by TLC on silica gel (EtOAc; R_f = 0.33 (**3**), R_f = 0.35 (**5**)) to give orange solids of **3** (1132 mg, 60%) and **5** (1213 mg, 64%).

Ac-D-Pro-L-Ala-NH-Fn-COOMe (**3**): m.p. = 132.3 °C. IR (CH_2Cl_2) $\breve{\upsilon}_{max}/cm^{-1}$: 3424 w ($NH_{free}$), 3303 m ($NH_{assoc.}$), 1706 s (C = O_{COOMe}), 1688 s, 1630 s (C = O_{CONH}), 1557 s, 1541 s, 1521 m (amide II). IR (KBr) $\breve{\upsilon}_{max}/cm^{-1}$: 3542 w ($NH_{free}$), 3308 s, 3259 s, 3222 m ($NH_{assoc.}$), 1714 s (C = O_{COOMe}), 1690 s, 1679 s, 1688 s (C = O_{CONH}). ^{1}H-NMR (600 MHz, $CDCl_3$) δ/ppm: 8.58 (s, 1H, NH_{Fn}), 7.08 (d, *J* = 9.1 Hz, 1H, NH_{Ala}), 5.05 (s, 1H, H-3), 4.78 (s, 1H, H-8), 4.76 (s, 1H, H-9), 4.70 (s, 1H, H-4), 4.62 (dq, *J* = 8.5 Hz, 7.1 Hz, 1H, CH_{Ala}), 4.40 (s, 1H, H-7), 4.35 (s, 1H, H-10), 4.26 (dd, *J* = 7.7 Hz, 5,6 Hz, 1H, CH-α (Pro)), 3.98 (s, 1H, H-2), 3.95 (s, 1H, H-5), 3.77 (s, 3H, COOMe), 3.68 (td, *J* = 9.8 Hz, 6,9 Hz, 1H, CH_2-δ (Pro)), 3.55 (td, *J* = 9.8 Hz, 6,5 Hz, 1H, CH_2-δ′ (Pro)), 2.28–2.23 (m, 1H, CH_2-γ Pro)), 2.21–2.18 (m, 1H, CH_2-β (Pro)), 2.16 (s, 3H, $CH_{3\ Ac}$), 2.15–2.11 (m, 1H, CH_2-β′ (Pro)), 2.00–1.95 (s, 1H, CH_2-γ′ (Pro)), 1.49 (d, *J* = 7.2 Hz, 3H, $CH_{3\ Ala}$). ^{13}C-NMR (150 MHz, $CDCl_3$) δ/ppm: 172.08 (CO_{Ac}), 172.03 (CO_{COOMe}), 170.63 (CO_{Ala}), 170.31 (CO_{Fn}), 96.56 (C-1, Fn), 72.80 (C-7), 72.64 (C-10), 71.91 (C-6), 71.46 (C-8), 71.20 (C-9), 66.45 (C-2), 65.74 (C-5), 63.25 (C-4), 62.69 (C-3), 61.19 (C-α, Pro), 51.78 ($CH_{3\ COOMe}$), 49.11 (CH_{Ala}), 48.66 (CH_2-δ, Pro), 29.23 (CH_2-β, Pro), 25.52 (CH_2-γ, Pro), 22.87 ($CH_{3\ Ac}$), 17.55 ($CH_{3\ Ala}$). ESI-MS (H_2O:MeOH = 50:50): *m*/*z* 468.1 ($(M - H)^-$). MALDI-HRMS *m*/*z* = 469.1280 (calculated for $C_{22}H_{27}N_3O_5Fe$ = 4.691.300).

Ac-L-Pro-L-Ala-NH-Fn-COOMe (**5**): m.p. = 125.1 °C. IR (CH_2Cl_2) $\breve{\upsilon}_{max}/cm^{-1}$: 3420 w ($NH_{free}$), 3309 m ($NH_{assoc.}$), 1705 s (C = O_{COOMe}), 1696 s, 1680 s, 1636 s (C = O_{CONH}), 1555 s, 1540 s, 1507 m (amide II). IR (KBr) $\breve{\upsilon}_{max}/cm^{-1}$: 3499 w ($NH_{free}$), 3288 m ($NH_{assoc.}$), 1714 s (C = O_{COOMe}), 1673 s, 1630 s (C = O_{CONH}). ^{1}H-NMR (600 MHz, $CDCl_3$) δ/ppm: 7.99 (s, 0.95H, $NH_{Fn\ \textit{trans}}$), 7.65 (s, 0.05H, $NH_{Fn\ \textit{cis}}$), 7.22 (d, *J* = 7.1 Hz, 0.94H, $NH_{Ala\ \textit{trans}}$), 6.86 (d, 0.06H, $NH_{Ala\ \textit{cis}}$), 4.78 (s, 1H, H-8), 4.76 (s, 1H, H-3), 4.74 (s, 1H, H-9), 4.67 (s, 1H, H-4), 4.57 (m, 1H, CH-α (Pro)), 4.48 (dq, *J* = 8.4 Hz, 7,1 Hz, 1H, CH_{Ala}), 4.39 (s, 1H, H-7), 4.37 (s, 1H, H-10), 4.02 (s, 1H, H-2), 3.96 (s, 1H, H-5), 3.77 (s, 3H, COOMe), 3.67–3.64 (m, 1H, CH_2-δ, (Pro)), 3.52–3.50 (m, 1H, CH_2-δ′ Pro)), 2.32 (s, 1H, CH_2-γ, Pro)), 2.18 (s, 3H, $CH_{3\ Ac}$), 2.08–2.06 (m, 2H, CH_2-β, CH_2-β′ (Pro)), 1.93 (s, 1H, CH_2-γ′ (Pro)), 1.42 (d, *J* = 7.0 Hz, 3H, $CH_{3.Ala}$). ^{13}C-NMR (150 MHz, $CDCl_3$) δ/ppm: 171.82 (CO_{Ac}), 171.81 (CO_{COOMe}), 171.66 (CO_{Ala}), 170.28 (CO_{Fn}), 95.76 (C-1, Fn), 72.67 (C-7), 72.65 (C-10), 72.21 (C-6), 71.43 (C-8), 71.08 (C-9), 66.62 (C-2), 66.01 (C-5), 63.04 (C-4), 62.87 (C-3), 60.65 (C-α, Pro), 51.76 ($CH_{3\ COOMe}$), 49.58 (CH_{Ala}), 48.67 (CH_2-δ, Pro), 28.68 (CH_2-β, Pro), 25.21 (CH_2-γ, Pro), 22.93 ($CH_{3\ Ac}$), 17.22 ($CH_{3\ Ala}$). ESI-MS (H_2O:MeOH = 50:50): *m*/*z* 468.1 ($(M - H)^-$). MALDI-HRMS *m*/*z* = 469.1280 (calculated for $C_{22}H_{27}N_3O_5Fe$ = 469.1300).

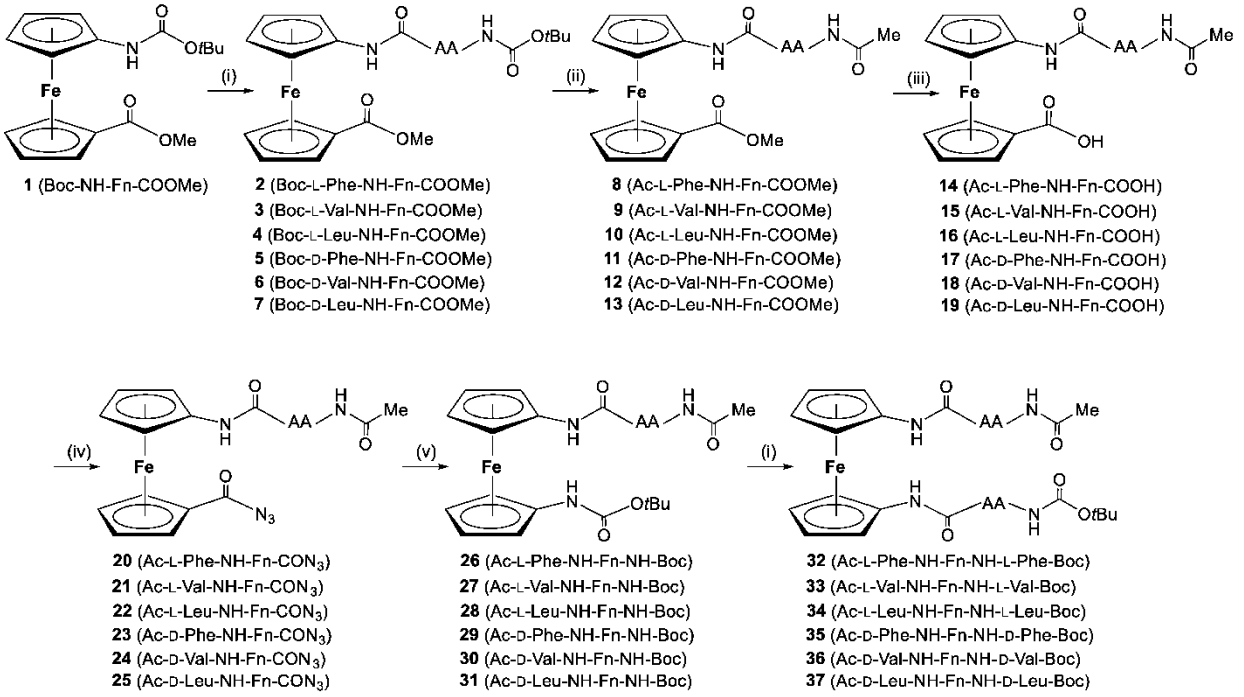

1 (Boc-NH-Fn-COOMe)

2 (Boc-L-Phe-NH-Fn-COOMe)
3 (Boc-L-Val-NH-Fn-COOMe)
4 (Boc-L-Leu-NH-Fn-COOMe)
5 (Boc-D-Phe-NH-Fn-COOMe)
6 (Boc-D-Val-NH-Fn-COOMe)
7 (Boc-D-Leu-NH-Fn-COOMe)

8 (Ac-L-Phe-NH-Fn-COOMe)
9 (Ac-L-Val-NH-Fn-COOMe)
10 (Ac-L-Leu-NH-Fn-COOMe)
11 (Ac-D-Phe-NH-Fn-COOMe)
12 (Ac-D-Val-NH-Fn-COOMe)
13 (Ac-D-Leu-NH-Fn-COOMe)

14 (Ac-L-Phe-NH-Fn-COOH)
15 (Ac-L-Val-NH-Fn-COOH)
16 (Ac-L-Leu-NH-Fn-COOH)
17 (Ac-D-Phe-NH-Fn-COOH)
18 (Ac-D-Val-NH-Fn-COOH)
19 (Ac-D-Leu-NH-Fn-COOH)

20 (Ac-L-Phe-NH-Fn-CON_3)
21 (Ac-L-Val-NH-Fn-CON_3)
22 (Ac-L-Leu-NH-Fn-CON_3)
23 (Ac-D-Phe-NH-Fn-CON_3)
24 (Ac-D-Val-NH-Fn-CON_3)
25 (Ac-D-Leu-NH-Fn-CON_3)

26 (Ac-L-Phe-NH-Fn-NH-Boc)
27 (Ac-L-Val-NH-Fn-NH-Boc)
28 (Ac-L-Leu-NH-Fn-NH-Boc)
29 (Ac-D-Phe-NH-Fn-NH-Boc)
30 (Ac-D-Val-NH-Fn-NH-Boc)
31 (Ac-D-Leu-NH-Fn-NH-Boc)

32 (Ac-L-Phe-NH-Fn-NH-L-Phe-Boc)
33 (Ac-L-Val-NH-Fn-NH-L-Val-Boc)
34 (Ac-L-Leu-NH-Fn-NH-L-Leu-Boc)
35 (Ac-D-Phe-NH-Fn-NH-D-Phe-Boc)
36 (Ac-D-Val-NH-Fn-NH-D-Val-Boc)
37 (Ac-D-Leu-NH-Fn-NH-D-Leu-Boc)

Synthesis of homochiral conjugates of ferrocene-1,1'-diamine with L- and D-Phe (**32**/**35**), L- and D-Val (**33**/**36**) and L- and D-Leu (**34**/**37**). (i) 1. HClgaseous, 2. Et_3N, 3. Boc–AA–OH, HOBT/EDC; (ii) 1. HClgaseous, 2. NEt_3, 3. AcCl; (iii) $NaOH/H_2O$, MeOH; (iv) 1. Et_3N, 2. ClCOOEt, 3. NaN_3; (v) *t*-BuOH/Δ.

Results and Discussion

Synthesis of Peptides **32**–**37**

The goal peptides **32**–**37** were synthesized according to the protocols established for the synthesis of ferrocene peptides **III** [19] and **VI** [26] (Scheme 1). The *N*-terminus of Boc–NH–Fn–COOMe [48] was deprotected in the presence of gaseous HCl to afford the hydrochloride salt, which was treated with an excess of NEt_3. The free amine obtained was then coupled with *C*-activated Boc–AA–OH (AA = L-Phe, L-Val, L-Leu, D-Phe, D-Val, D-Leu), respectively, to give carbamates **2**–**7** which were Boc-deprotected and converted to the acetamides **8**–**13**. The ester groups attached to the lower Cp rings of **8**–**13** were then carefully hydrolyzed to give the acids **14**–**19** (an equimolar amount of NaOH was used to prevent racemization, and the reactions were carried out at 80 °C for 1 h). The orthogonally protected goal precursors **26**–**31** were prepared by an in situ Curtius rearrangement of the unstable azides **20**–**25** obtained from acids **14**–**19**. To avoid the conversion of the intermediate isocyanate group to undesired *sym*-urea that could occur during the Curtius rearrangement, *t*-BuOH was freshly dried, and the reaction temperature was maintained at 65 °C. The conversion of azide (~2135 cm^{-1}) to carbamate via isocyanate (~2270 cm^{-1}) was monitored by IR spectroscopy and was complete when both IR bands disappeared. This was followed by acidic Boc-deprotection of the goal precursors **26**–**31** to give free *N*-termini, which were coupled with *C*-activated Boc–AA–OH to give the goal peptides **32**–**37**.

Materials and Methods

General Procedure and Methods

Peptides **2–37** were synthesized under argon atmosphere using chemicals of analytical purity. (The synthetic procedures and spectroscopic characterization of precursor **2**–**31** can be found in

the **Supplementary Material**.) CH_2Cl_2 used for synthesis, CD measurements, and FTIR was dried (P_2O_5), distilled over CaH_2, and stored over molecular sieves (4 Å). EDC (Acros Organics), HOBt (Aldrich), and acetyl chloride (Aldrich) were used as received. The synthesis of Boc–NH–Fn–COOMe **(1)** has been reported previously by us [41]. Its *N*-terminus was deprotected by action of gaseous HCl. The *N*-termini of L- and D-AA (AA = Phe, Val and Leu) were protected in the presence of sodium hydroxide, aqueous dioxane, and di-*tert*-butyldicarbonate to give Boc-L-AA-OH and Boc-D-AA-OH, respectively. Boc-L-AA-OH and Boc-D-AA-OH were activated with the coupling reagent HOBt for 1h in CH_2Cl_2. The products were purified by preparative thin layer chromatography on silica gel (Merck, Kieselgel 60 HF_{254}) using EtOAc/CH_2Cl_2 mixture or pure EtOAc as eluent.

Synthesis of Ac–L-AA–NH–Fn–NH–AA–Boc (32–37)

The HCl_{gas} was purged through the suspension of Ac–L-AA–NH–Fn–NH–Boc (**26**–**28**) and Ac–D-AA–NH–Fn–NH–Boc (**29**–**31**) (1 mmol) in dry CH_2Cl_2 (5 mL) at 0 °C, respectively. After approx. 30–120 min, the solvent was evaporated in vacuo, and the obtained hydrochloride salt was then suspended in CH_2Cl_2 and treated with NEt_3 (pH~8) to give an unstable free amine suitable for coupling to Boc-L-AA-OH or Boc-D-AA-OH (2 mmol) using the standard EDC/HOBt method (EDC (3 mmol); HOBt (3 mmol)). The reaction mixtures were then stirred at room temperature until the ferrocene amine was completely consumed, which was monitored by TLC (~2 h). Standard work-up (washing with a saturated aqueous solution of $NaHCO_3$, a 10% aqueous solution of citric acid and brine, drying over Na_2SO_4 and evaporation in vacuo) including TLC purification of the crude products (EtOAc: CH_2Cl_2 = 1: 5; R_f = 0.83 (**32**), R_f = 0.58 (**33**), R_f = 0.44 (**34**), R_f = 0.80 (**35**), R_f = 0.57 (**36**), R_f = 0.45 (**37**)) gave orange solids of **32** (160 mg, 25%), **33** (223 mg, 40%), **34** (187 mg, 32%), **35** (140 mg, 22%), **36** (190 mg, 35%), and **37** (150 mg, 25%).

Ac–L-Phe–NH–Fn–NH–L-Phe–Boc **(32):** Mp = 145.2 °C. IR (CH_2Cl_2) $\breve{\upsilon}_{max}/cm^{-1}$: 3430 m ($NH_{free}$), 3302, 3266, 3217 s ($NH_{assoc.}$), 1731 s, 1706 s, 1683 s, 1668 s ($C{=}O_{CONH}$), 1648 s 1575 s, 1541 s, 1498 s, 1467 s, 1457 s (amide II). IR (KBr) $\breve{\upsilon}_{max}/cm^{-1}$: 3294 m ($NH_{assoc.}$), 1658 s, 1651 s ($C{=}O_{CONH}$), 1568 s, 1533 s, 1499 (amide II). ^{1}H-NMR (600 MHz, $CDCl_3$) δ: 9.21 (1H, s, NH^b_{Fn}), 9.15 (1H, s, NH^a_{Fn}), 7.30–7.17 (11H, m, $CH^{a\ and\ b}_{phenyl}$ and NH_{Ac}), 5.47–5.26 (3H, m, CH-7_{Fn}, CH-10_{Fn} and NH_{Boc}), 4.84–4.76 (1H, s, $CH^a_{\alpha\text{-Phe}}$), 4.67–4.59 (1H, s, $CH^b_{\alpha\text{-Phe}}$), 4.09–3.88 (6H, m, CH-2_{Fn}, CH-3_{Fn}, CH-4_{Fn}, CH-5_{Fn}, CH-8_{Fn} and CH-9_{Fn}), 3.19 (1H, dd, J = 14.14; 4.46 Hz, $CH^a_{\beta1\text{-Phe}}$), 3.14 (1H, dd, J = 14.89; 5.21 Hz, $CH^b_{\beta1\text{-Phe}}$), 2.98 (1H, dd, J = 13.80; 10.42 Hz, $CH^a_{\beta2\text{-Phe}}$), 2.89 (1H, dd, J = 14.14; 10.05 Hz, $CH^b_{\beta2\text{-Phe}}$), 2.06 (s, 3H, $CH_{3\text{-Ac}}$), 1.43 (9H, s, $(CH_3)_{3\text{-Boc}}$) ppm. ^{13}C-NMR (150 MHz, $CDCl_3$) δ: 171.8 (1C, CO_{Ac}), 170.9 (1C, CO^b_{Fn}), 170.7 (1C, CO^a_{Fn}), 157.3 (1C, CO_{Boc}), 136.9 (1C, $C_q{}^{a\ or\ b}_{\gamma\text{-Phe}}$), 136.7 (1C, $C_q{}^{a\ or\ b}_{\gamma\text{-Phe}}$), 129.3 (2C, $CH^{aor\ b}_{\delta\text{-Phe}}$), 129.2 (2C, $CH^{aor\ b}_{\delta\text{-Phe}}$), 128.9 (2C, $CH^{aor\ b}_{\varepsilon\text{-Phe}}$), 128.8 (2C, $CH^{aor\ b}_{\varepsilon\text{-Phe}}$), 127.1 (1C, $CH^{aor\ b}_{\zeta\text{-Phe}}$), 127.0 (1C, $CH^{aor\ b}_{\zeta\text{-Phe}}$), 95.9 (1C, C_q-6_{Fn}), 95.6 (1C, C_q-1_{Fn}), 81.0 (1C, C_{qBoc}), 65.9 (2C, CH-8_{Fn} and CH-9_{Fn}), 65.0 (1C, CH-5_{Fn}), 64.9 (1C, CH-4_{Fn}), 63.1 (1C, CH-7_{Fn}), 62.9 (1C, CH-10_{Fn}), 61.8 (1C, CH-3_{Fn}), 61.5 (1C, CH-2_{Fn}), 56.6 (1C, $CH^b_{\alpha\text{-Phe}}$), 56.3 (1C, $CH^a_{\alpha\text{-Phe}}$), 38.1 (1C, $CH_2{}^b_{\beta\text{-Phe}}$), 37.7 (1C, $CH_2{}^a_{\beta\text{-Phe}}$), 28.7 (3C, $(CH_3)_{3\text{-Boc}}$), 23.1 (1C, $CH_{3\text{-Ac}}$) ppm. ESI-MS (H_2O:MeOH= 50:50): *m/z* 653.3 ($(M+H)^+$). MALDI-HRMS *m/z* = 652.2337 (calculated for $C_{35}H_{40}N_4O_5Fe$ = 652.2348).

Ac–L-Val–NH–Fn–NH–L-Val–Boc **(33):** Mp = 182.4 °C. IR (CH_2Cl_2) $\breve{\upsilon}_{max}/cm^{-1}$: 3434 m ($NH_{free}$), 3305 s, 3249 m ($NH_{assoc.}$), 1733 s, 1716 s, 1683 s, 166 s ($C{=}O_{CONH}$), 1637 s, 1571 s, 1540 s, 1505 s, 1458 s (amide II). IR (KBr) $\breve{\upsilon}_{max}/cm^{-1}$: 3293 s ($NH_{assoc.}$), 1672 s, 1652 s, 1578 s ($C{=}O_{CONH}$), 1563 s, 1508 s, 1480 s, 1467 s (amide II). ^{1}H-NMR (600 MHz, $CDCl_3$) δ: 9.20 (1H, s, NH^b_{Fn}), 9.02 (1H, s, NH^a_{Fn}), 6.74 (1H, d, J = 7.26 Hz, NH_{Ac}), 5.34 (2H, s, CH-7_{Fn} and CH-10_{Fn}), 5.20 (1H, d, J = 8.38 Hz, NH_{Boc}), 4.14 (1H, t, J = 7.95 Hz, $CH^a_{\alpha\text{-Val}}$), 4.03 (1H, s, CH-2_{Fn}), 3.98–3.94 (3H, m, CH-3_{Fn}, CH-4_{Fn} and $CH^b_{\alpha\text{-Val}}$), 3.92 (1H, s, CH-5_{Fn}), 3.88 (2H, s, CH-8_{Fn} and CH-9_{Fn}), 2.10 (3H, s, $CH_{3\text{-Ac}}$), 2.05–1.98 (1H, m, $CH^a_{\beta\text{-Val}}$), 1.98–1.91 (1H, m, $CH^b_{\beta\text{-Val}}$), 1.45 (9H, s, $(CH_3)_{3\text{-Boc}}$), 1.04 (3H, d, J = 6.60 Hz, $CH_3{}^a_{\gamma\text{-Val}}$), 1.02 (3H, d, J = 6.80 Hz, $CH_3{}^b_{\gamma\text{-Val}}$), 0.98 (6H, d, J = 6.60 Hz, $CH_3{}^a_{\gamma\text{-Val}}$ and $CH_3{}^b_{\gamma\text{-Val}}$) ppm. ^{13}C-NMR (150 MHz, $CDCl_3$) δ: 171.6 (1C, CO_{Ac}), 171.0 (1C, CO^b_{Fn}), 170.7 (1C, CO^a_{Fn}), 157.3 (1C, CO_{Boc}), 95.9 (1C, C_q-6_{Fn}), 95.6 (1C, C_q-1_{Fn}), 80.6 (1C, C_{qBoc}), 65.7 (2C, CH-8_{Fn} and CH-9_{Fn}), 65.1 (1C, CH-5_{Fn}), 64.9 (1C, CH-4_{Fn}), 62.9 (1C, CH-7_{Fn}), 62.8 (1C, CH-10_{Fn}), 61.9 (1C, CH-3_{Fn}), 61.4 (1C, CH-2_{Fn}), 61.3 (1C, $CH^b_{\alpha\text{-Val}}$), 61.1

(1C, $CH^{a}_{\alpha\text{-Val}}$), 30.5 (1C, $CH^{b}_{\beta\text{-Val}}$), 30.3 (1C, $CH^{a}_{\beta\text{-Val}}$), 28.7 (3C, $(CH_3)_{3\text{-Boc}}$), 23.4 (1C, $CH_{3\text{-Ac}}$), 19.7 (1C, $CH_3{}^{a\text{ or }b}_{\gamma\text{-Val}}$), 19.44 (2C, $CH_3{}^{a\text{ and }b}_{\gamma\text{-Val}}$), 19.36 (1C, $CH_3{}^{a\text{ or }b}_{\gamma\text{-Val}}$) ppm. ESI-MS ($H_2O$:MeOH= 50:50): *m/z* 579.3 ($(M+Na)^+$). MALDI-HRMS *m/z* = 556.2339 (calculated for $C_{27}H_{40}N_4O_5Fe$ = 556.2348).

Ac–L-Leu–NH–Fn–NH–L-Leu–Boc **(34):** Mp = 206.6 °C. IR (CH_2Cl_2) $\breve{\upsilon}_{max}/cm^{-1}$: 3434 m ($NH_{free}$), 3301 s, 3253 s ($NH_{assoc.}$), 1733 s, 1684 s, 1668 s ($C{=}O_{CONH}$), 1653 s, 1573 s, 1540 s, 1506 s, 1457 s (amide II). IR (KBr) $\breve{\upsilon}_{max}/cm^{-1}$: 3281 s ($NH_{assoc.}$), 1667 s, 1650 s ($C{=}O_{CONH}$), 1568 s, 1530 s, 1484 s (amide II). ^{1}H-NMR (600 MHz, $CDCl_3$) *δ*: 9.36 (1H, s, NH^{b}_{Fn}), 9.13 (1H, s, NH^{a}_{Fn}), 7.28 (1H, d, *J* = 6.20 Hz, NH_{Ac}), 5.35 (1H, s, CH-7_{Fn}), 5.34 (1H, s, CH-10_{Fn}), 5.14 (1H, d, *J* = 8.02 Hz, NH_{Boc}), 4.49–4.43 (1H, m, $CH^{a}_{\alpha\text{-Leu}}$), 4.31–4.25 (1H, m, $CH^{b}_{\alpha\text{-Leu}}$), 4.05 (1H, s, CH-$3_{Fn}$), 3.98 (1H, s, CH-$4_{Fn}$), 3.95 (1H, s, CH-$2_{Fn}$), 3.90 (1H, s, CH-$5_{Fn}$), 3.87 (2H, s, CH-$8_{Fn}$ and CH-9_{Fn}), 2.09 (3H, s, $CH_{3\text{-Ac}}$), 1.79–1.65 (3H, m, $CH^{a}_{\beta1\text{-Leu}}$, $CH^{a}_{\gamma\text{-Leu}}$ and $CH^{b}_{\gamma\text{-Leu}}$), 1.59–1.50 (3H, m, $CH^{a}_{\beta2\text{-Leu}}$, $CH^{b}_{\beta1\text{-Leu}}$ and $CH^{b}_{\beta2\text{-Leu}}$), 1.45 (9H, s, $(CH_3)_{3\text{-Boc}}$), 0.92 (6H, t, *J* = 6.80 Hz, $CH_3{}^{b}_{\delta1\text{-Leu}}$ and $CH_3{}^{b}_{\delta2\text{-Leu}}$), 0.86 (6H, d, *J* = 6.58 Hz, $CH_3{}^{a}_{\delta1\text{-Leu}}$ and $CH_3{}^{a}_{\delta2\text{-Leu}}$) ppm. ^{13}C-NMR (150 MHz, $CDCl_3$) *δ*: 172.0 (1C, CO_{Ac}), 171.75 (1C, CO^{b}_{Fn}), 171.67 (1C, CO^{a}_{Fn}), 157.3 (1C, CO_{Boc}), 96.2 (1C, C_q-6_{Fn}), 95.9 (1C, C_q-1_{Fn}), 80.7 (1C, C_{qBoc}), 65.7 (2C, CH-8_{Fn} and CH-9_{Fn}), 64.9 (1C, CH-5_{Fn}), 64.7 (1C, CH-4_{Fn}), 62.9 (1C, CH-7_{Fn}), 62.7 (1C, CH-10_{Fn}), 61.6 (1C, CH-3_{Fn}), 61.3 (1C, CH-2_{Fn}), 54.1 (1C, $CH^{b}_{\alpha\text{-Leu}}$), 53.9 (1C, $CH^{a}_{\alpha\text{-Leu}}$), 41.1 (1C, $CH_2{}^{b}_{\beta\text{-Leu}}$), 40.6 (1C, $CH_2{}^{a}_{\beta\text{-Leu}}$), 28.7 (3C, $(CH_3)_{3\text{-Boc}}$), 25.0 (1C, $CH^{b}_{\gamma\text{-Leu}}$), 24.9 (1C, $CH^{a}_{\gamma\text{-Leu}}$), 23.5 (1C, $CH_{3\text{-Ac}}$), 23.1, 23.0, 21.8 and 21.7 (4C, $CH_3{}^{a}_{\delta1\text{- and }\delta2\text{-Leu}}$ and $CH_3{}^{b}$ $_{\delta1\text{- and }\delta2\text{-Leu}}$) ppm. ESI-MS ($H_2O$:MeOH= 50:50): *m/z* 607.3 ($(M+Na)^+$). MALDI-HRMS *m/z* = 584.2641 (calculated for $C_{29}H_{44}N_4O_5Fe$ = 584.2661).

Ac–D-Phe–NH–Fn–NH–D-Phe–Boc (**35):** Mp = 140.1 °C. IR (CH_2Cl_2) $\breve{\upsilon}_{max}/cm^{-1}$: 3432 m ($NH_{free}$), 3301 s ($NH_{assoc.}$), 1731 s, 1682 s, 1668 s ($C{=}O_{CONH}$), 1571 s, 1498 s, 1455 s, 1442 s (amide II). IR (KBr) $\breve{\upsilon}_{max}/cm^{-1}$: 3293 s ($NH_{assoc.}$), 1657 s, 1651 s ($C{=}O_{CONH}$), 1570 s, 1547 m, 1531 m, 1498 m, 1491 m, 1454 s (amide II). ^{1}H-NMR (600 MHz, $CDCl_3$) *δ*: 9.18 (1H, s, NH^{b}_{Fn}), 9.12 (1H, s, NH^{a}_{Fn}), 7.30–7.17 (10H, m, $CH^{a\text{ and }b}_{phenyl}$), 7.07 (1H, s, NH_{Ac}), 5.36 (1H, s, CH-7_{Fn}), 5.34 (1H, s, CH-10_{Fn}), 5.30 (1H, s, *J* = 5.88 Hz, NH_{Boc}), 4.79 (1H, s, $CH^{a}_{\alpha\text{-Phe}}$), 4.62 (1H, s, $CH^{b}_{\alpha\text{-Phe}}$), 4.08–3.89 (6H, m, CH-$2_{Fn}$, CH-$3_{Fn}$, CH-$4_{Fn}$, CH-$5_{Fn}$, CH-$8_{Fn}$ and CH-9_{Fn}), 3.21–3.10 (2H, m, $CH^{a}_{\beta1\text{-Phe}}$ and $CH^{b}_{\beta1\text{-Phe}}$), 2.97 (1H, t, *J* = 10.91 Hz, $CH^{a}_{\beta2\text{-Phe}}$), 2.88 (1H, t, *J* = 10.91 Hz, $CH^{a}_{\beta2\text{-Phe}}$), 2.05 (3H, s, $CH_{3\text{-Ac}}$), 1.42 (9H, s, $(CH_3)_{3\text{-Boc}}$) ppm. ^{13}C-NMR (150 MHz, $CDCl_3$) *δ*: 171.8 (1C, CO_{Ac}), 170.9 (1C, CO^{b}_{Fn}), 170.6 (1C, CO^{a}_{Fn}), 157.3 (1C, CO_{Boc}), 136.9 (1C, $C_q{}^{a\text{ or }b}_{\gamma\text{-Phe}}$), 136.7 (1C, $C_q{}^{a\text{ or }b}_{\gamma\text{-Phe}}$), 129.3 (2C, $CH^{a\text{ or }b}_{\delta\text{-Phe}}$), 129.2 (2C, $CH^{a\text{ or }b}_{\delta\text{-Phe}}$), 128.9 (2C, $CH^{a\text{ or }b}_{\varepsilon\text{-Phe}}$), 128.8 (2C, $CH^{a\text{ or }b}_{\varepsilon\text{-Phe}}$), 127.2 (1C, $CH^{a\text{ or }b}_{\zeta\text{-Phe}}$), 127.1 (1C, $CH^{a\text{ or }b}_{\zeta\text{-Phe),}}$ 95.9 (1C, C_q-6_{Fn}), 95.5 (1C, C_q-1_{Fn}), 81.0 (1C, C_{qBoc}), 65.9 (2C, CH-8_{Fn} and CH-9_{Fn}), 65.0 (1C, CH-5_{Fn}), 64.8 (1C, CH-4_{Fn}), 63.1 (1C, CH-7_{Fn}), 62.9 (1C, CH-10_{Fn}), 61.9 (1C, CH-3_{Fn}), 61.5 (1C, CH-2_{Fn}), 56.6 (1C, $CH^{b}_{\alpha\text{-Phe}}$), 56.3 (1C, $CH^{a}_{\alpha\text{-Phe}}$), 38.1 (1C, $CH_2{}^{b}_{\beta\text{-Phe}}$), 37.7 (1C, $CH_2{}^{a}_{\beta\text{-Phe}}$), 28.7 (3C, $(CH_3)_{3\text{-Boc}}$), 23.1 (1C, $CH_{3\text{-Ac}}$) ppm. ESI-MS (H_2O:MeOH= 50:50): *m/z* 653.1 ($(M+H)^+$), calculated for $C_{35}H_{40}N_4O_5Fe$ = 652.2348.

Ac–D-Val–NH–Fn–NH–D-Val–Boc **(36):** Mp = 201.4 °C. IR (CH_2Cl_2) $\breve{\upsilon}_{max}/cm^{-1}$: 3435 m ($NH_{free}$), 3306 s ($NH_{assoc.}$), 1731 s, 1681 s, 1667 s ($C{=}O_{CONH}$), 1571 s, 1503 s (amide II). IR (KBr) $\breve{\upsilon}_{max}/cm^{-1}$: 3287 s ($NH_{assoc.}$), 1671 s, 1652 s ($C{=}O_{CONH}$), 1577 s, 1564 s, 1508 s (amide II). ^{1}H-NMR (600 MHz, $CDCl_3$) *δ*: 9.21 (1H, s, NH^{b}_{Fn}), 9.05 (1H, s, NH^{a}_{Fn}), 6.78 (1H, d, *J* = 6.91 Hz, NH_{Ac}), 5.36 (2H, s, CH-7_{Fn} and CH-10_{Fn}), 5.21 (1H, d, *J* = 8.41 Hz, NH_{Boc}), 4.16 (1H, t, *J* = 8.04 Hz, $CH^{a}_{\alpha\text{-Val}}$), 4.04 (1H, s, CH-$2_{Fn}$), 4.01–3.96 (3H, m, CH-$3_{Fn}$, CH-$4_{Fn}$ and $CH^{b}_{\alpha\text{-Val}}$), 3.94 (1H, s, CH-$5_{Fn}$), 3.90 (2H, s, CH-$8_{Fn}$ and CH-9_{Fn}), 2.11 (3H, s, $CH_{3\text{-Ac}}$), 2.04 (1H, q, *J* = 6.96 Hz, $CH^{a}_{\beta\text{-Val}}$), 1.97 (1H, q, *J* = 6.96 Hz, $CH^{b}_{\beta\text{-Val}}$), 1.47 (9H, s, $(CH_3)_{3\text{-Boc}}$), 1.07 (3H, d, *J* = 6.69 Hz, $CH_3{}^{a}_{\gamma\text{-Val}}$), 1.04 (3H, d, *J* = 6.69 Hz, $CH_3{}^{b}_{\gamma\text{-Val}}$), 1.00 (6H, d, *J* = 6.69 Hz, $CH_3{}^{a}_{\gamma\text{-Val}}$ and $CH_3{}^{b}_{\gamma\text{-Val}}$) ppm. ^{13}C-NMR (150 MHz, $CDCl_3$) *δ*: 171.5 (1C, CO_{Ac}), 171.0 (1C, CO^{b}_{Fn}), 170.7 (1C, CO^{a}_{Fn}), 157.3 (1C, CO_{Boc}), 95.9 (1C, C_q-6_{Fn}), 95.6 (1C, C_q-1_{Fn}), 80.6 (1C, C_{qBoc}), 65.7 (2C, CH-8_{Fn} and CH-9_{Fn}), 65.1 (1C, CH-5_{Fn}), 64.9 (1C, CH-4_{Fn}), 62.9 (1C, CH-7_{Fn}), 62.8 (1C, CH-10_{Fn}), 61.8 (1C, CH-3_{Fn}), 61.4 (1C, CH-2_{Fn}), 61.2 (1C, $CH^{b}_{\alpha\text{-Val}}$), 61.1 (1C, $CH^{a}_{\alpha\text{-Val}}$), 30.4 (1C, $CH^{b}_{\beta\text{-Val}}$), 30.2 (1C, $CH^{a}_{\beta\text{-Val}}$), 28.7 (3C, $(CH_3)_{3\text{-Boc}}$), 23.4 (1C, $CH_{3\text{-Ac}}$), 19.7 (1C, $CH_3{}^{a\text{ or }b}_{\gamma\text{-Val}}$), 19.44 (2C, $CH_3{}^{a\text{ and }b}_{\gamma\text{-Val}}$), 19.38 (1C, $CH_3{}^{a\text{ or }b}_{\gamma\text{-Val}}$) ppm. ESI-MS ($H_2O$:MeOH= 50:50): *m/z* 579.1 ($(M+Na)^+$), calculated for $C_{27}H_{40}N_4O_5Fe$ = 556.2348.

Ac–D-Leu–NH–Fn–NH–D-Leu–Boc **(37):** Mp = 207.8 °C. IR (CH_2Cl_2) $\breve{\upsilon}_{max}/cm^{-1}$: 3434 m ($NH_{free}$), 3292 s ($NH_{assoc.}$), 1733 w, 1663 s ($C{=}O_{CONH}$), 1492 s (amide II). IR (KBr) $\breve{\upsilon}_{max}/cm^{-1}$: 3287 s ($NH_{assoc.}$), 1683 s, 1667 s, 1651 s ($C{=}O_{CONH}$), 1565 m, 1526 m, 1483 m (amide II). ^{1}H-NMR (600 MHz, $CDCl_3$) δ: 9.36 (1H, s, $NH^b{}_{Fn}$), 9.14 (1H, s, $NH^a{}_{Fn}$), 7.25 (1H, s, NH_{Ac}), 5.38 (2H, s, CH-7_{Fn} and CH-10_{Fn}), 5.15 (1H, d, J = 7.77 Hz, NH_{Boc}), 4.51–4.41 (1H, m, $CH^a{}_{\alpha\text{-Leu}}$), 4.32–4.24 (1H, m, $CH^b{}_{\alpha\text{-Leu}}$), 4.13–3.83 (6H, m, CH-$2_{Fn}$, CH-$3_{Fn}$, CH-$4_{Fn}$, CH-$5_{Fn}$, CH-$8_{Fn}$ and CH-9_{Fn}), 2.09 (3H, s, $CH_{3\text{-Ac}}$), 1.79–1.64 (3H, m, $CH^a{}_{\beta1\text{-Leu}}$, $CH^a{}_{\gamma\text{-Leu}}$ and $CH^b{}_{\gamma\text{-Leu}}$), 1.60–1.49 (3H, m, $CH^a{}_{\beta2\text{-Leu}}$, $CH^b{}_{\beta1\text{-Leu}}$ and $CH^b{}_{\beta2\text{-Leu}}$), 1.45 (9H, s, $(CH_3)_{3\text{-Boc}}$), 0.92 (6H, t, J = 6.62 Hz, $CH_3{}^b{}_{\delta1\text{-Leu}}$ and $CH_3{}^b{}_{\delta2\text{-Leu}}$), 0.86 (6H, d, J = 6.49 Hz, $CH_3{}^a{}_{\delta1\text{-Leu}}$ $CH_3{}^a{}_{\delta2\text{-Leu}}$) ppm. ^{13}C-NMR (150 MHz, $CDCl_3$) δ: 171.9 (1C, CO_{Ac}), 171.6 (2C, $CO^a{}_{Fn}$ and $CO^b{}_{Fn}$), 157.2 (1C, CO_{Boc}), 96.2 (1C, C_q-6_{Fn}), 95.9 (1C, C_q-1_{Fn}), 80.7 (1C, C_{qBoc}), 65.7 (2C, CH-8_{Fn} and CH-9_{Fn}), 65.0 (1C, CH-5_{Fn}), 64.8 (1C, CH-4_{Fn}), 62.9 (1C, CH-7_{Fn}), 62.7 (1C, CH-10_{Fn}), 61.5 (1C, CH-2_{Fn}), 61.3 (1C, CH-3_{Fn}), 54.0 (1C, $CH^b{}_{\alpha\text{-Leu}}$), 53.9 (1C, $CH^a{}_{\alpha\text{-Leu}}$), 41.0 (1C, $CH_2{}^b{}_{\beta\text{-Leu}}$), 40.5 (1C, $CH_2{}^a{}_{\beta\text{-Leu}}$), 28.7 (3C, $(CH_3)_{3\text{-Boc}}$), 25.0 (1C, $CH^b{}_{\gamma\text{-Leu}}$), 24.8 (1C, $CH^a{}_{\gamma\text{-Leu}}$), 23.4 (1C, $CH_{3\text{-Ac}}$), 23.1, 23.0, 21.7 and 21.6 (4C, $CH_3{}^a{}_{\delta1\text{- and }\delta2\text{-Leu}}$ and $CH_3{}^b{}_{\delta1\text{- and }\delta2\text{-Leu}}$) ppm. ESI-MS ($H_2O$:MeOH = 50:50): *m/z* 607.2 ($(M+Na)^+$), calculated for $C_{29}H_{44}N_4O_5Fe$ = 584.2661.

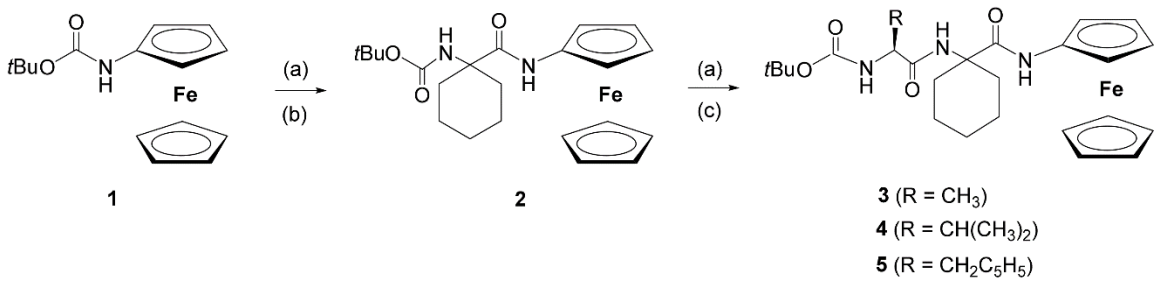

Syntheses of derivatives **2**–**5**: (**a**) HCl(*g*)/EtOAc; (**b**) 1. HOBt/EDC, CH_2Cl_2; 2. Boc−Ac6c−OH, CH_2Cl_2; (**c**) 1. HOBt/EDC, MeCN; 2. Boc−AA−OH

Results and Discussion

The targeted compound Boc−Ac6c−NH−Fc (**2**) was synthesized in a 91% yield by HOBt/EDC-mediated coupling of aminoferrocene, obtained by deprotection of Boc−NHFc (**1**) [33] with Boc−Ac6c−OH (Scheme 1). Target dipeptides **3–5** were synthesized using the procedure described in [34]. Coupling of *N*-deprotected **2** with HOBt/EDC-activated Boc−AA−OH in acetonitrile at an elevated temperature (65 °C) gave **3** (79%), **4** (68%), and **5** (72%), respectively.

*Synthesis of Boc−Ac6c−NH−Fc (**2**) and Boc−AA−Ac6c−NH−Fc (**3**–**5**)*

Boc−NH−Fc (**1**) or Boc−Ac6c−NH−Fc (**2**) (1 mmol) was deprotected by the action of gaseous HCl in dry CH_2Cl_2 (10 mL) at 0 °C for two hours. After evaporation of the solvent, the resulting hydrochloride was suspended in MeCN, treated with Et_3N (pH~8) and coupled with HOBt/EDC (2.2 mmol) activated Boc−AA−OH (2 mmol). The reaction mixture was stirred for two hours at RT (**2**) or for 24 h at 65 °C (**3**–**5**) and evaporated to dryness. The residue was diluted with CH_2Cl_2, washed three times with saturated $NaHCO_3$ solution, 10% aqueous citric acid solution, brine, and dried over Na_2SO_4. After removing the solvent, the crude products were purified by preparative TLC on silica gel using mixtures of dichloromethane and ethyl acetate as eluents.

3.2.1. Boc–Ac6c–NH–Fc (**2**)

Yield 388 mg (91%), mp 130–131 °C. ^{1}H-NMR ($CDCl_3$, c = 0.1 mol dm^{-3}) δ/ppm: 8.27 (s, 1H, NH_{Fc}), 4.71 (s, 1H, NH_{Ac6c}), 4.64 (s, 2H, H-2, H-5), 4.17 (s, 5H, Fc), 4.0 (bs, 2H, H-3, H-4), 2.07–2.01 (m, 2H, $CH_2\beta_{Ac6c}$), 1.94–1.88 (m, 2H, $CH_2\beta_{Ac6c}$), 1.70–1.61 (m, 4H, $CH_2\gamma_{Ac6c}$), 1.49 (s, 9H, $C(CH_3)_3$), 1.45–1.31 (m, 2H, CH_2d_{Ac6c}). ^{13}C-NMR ($CDCl_3$, c = 0.1 mol dm^{-3}) δ/ ppm: 172.7 (CO_{Ac6c}), 155.3 (CO_{Boc}), 95.1 (C-1), 80.5 (Cq_{Boc}), 69.3 (Cp), 64.5 (C-3, C-4), 61.2 (C-2, C-5), 59.7 ($C\alpha_{Ac6c}$), 32.1 ($CH_2\beta_{Ac6c}$), 29.7 ($CH_2\beta_{Ac6c}$), 28.3 (CH_{3Boc}), 25.2 (CH_2d_{Ac6c}), 21.3 ($CH_2\gamma_{Ac6c}$). Elemental analysis calcd for $C_{22}H_{30}N_2O_3Fe$: C 61.98, H 7.09, N 6.57, found: C 57.86, H 7.01, N 6.48. IR (CH_2Cl_2): ν_{max}/cm^{-1}: 3426 m (NHfree), 2976 sh, 2932 m, 2859 m (CH_2), 1722 s, 1694 s (amide I).

3.2.2. Boc–L–Ala–Ac6c–NH–Fc (**3**)

Yield 348 (79%), mp 98 °C. ^{1}H-NMR ($CDCl_3$, c = 0.1 mol dm^{-3}) δ/ppm: 8.43 (s, 1H, NH_{Fc}), 6.34 (s, 1H, NH_{Ac6c}), 5.00 (s, 1H, NH_{Ala}), 4.79 (s, 1H, H-2), 4.67 (s, 1H, H-5), 4.17 (s, 5H, Fc), 4.06 (m, 1H, $CH\alpha_{Ala}$), 3.99 (bs, 2H, H-3, H-4), 2.28–2.23 (s, 1H, $CH_2\beta_{Ac6c}$), 2.04–1.95 (m, 2H, $CH_2\beta_{Ac6c}$), 1.91–1.85 (m, 1H, $CH_2\beta_{Ac6c}$), 1.71–1.60 (m, 4H, $CH_2\gamma_{Ac6c}$), 1.49 (s, 9H, $C(CH_3)_3$), 1.40 (d, J = 6.6 Hz, 3H, CH_{3Ala}), 1.33–1.28 (m, 2H, CH_2d_{Ac6c}).^{13}C-NMR ($CDCl_3$, c = 0.1 mol dm^{-3}) δ/ppm: 172.3 (CO_{Ac6c}), 172.2 (CO_{Ala}), 156.2 (CO_{Boc}), 92.6 (C-1), 81.1 (Cq_{Boc}), 69.4 (Cp), 64.5 (C-3), 64.3 (C-4), 61.4 (C-2), 61.0 (C-5), 60.5 ($C\alpha_{Ac6c}$), 51.7 ($CH\alpha_{Ala}$), 33.0 ($CH_2\beta_{Ac6c}$), 30.9 ($CH_2\beta_{Ac6c}$), 28.3 (CH_{3Boc}), 25.1 (CH_2d_{Ac6c}), 21.4 ($CH_2\gamma_{Ac6c}$), 21.3 ($CH_2\gamma_{Ac6c}$), 17.4 (CH_{3Ala}). Elemental analysis calcd for $C_{25}H_{35}N_3O_4Fe$: C 60.37, H 7.09, N 8.45, found: C 60.29, H 7.05, N 8.51. IR (CH_2Cl_2): ν_{max}/cm^{-1}: 3425 m (NHfree), 3342 m (NHassoc.), 2935 m, 2860 m (CH_2), 1699 s (amide I).

3.2.3. Boc–L–Val–Ac6c–NH–Fc (**4**)

Yield 357 mg (68%), mp 102–103 °C. ^{1}H-NMR ($CDCl_3$, c = 0.1 mol dm^{-3}) δ/ppm: 8.48 (s, 1H, NH_{Fc}), 6.18 (s, 1H, NH_{Ac6c}), 4.98 (d, J = 5.4 Hz, 1H, NH_{Val}), 4.74 (s, 1H, H-2), 4.60 (s, 1H, H-5), 4.16 (s, 5H, Fc), 3.96 (bs, 2H, H-3, H-4), 3.82 (t, J = 6.0 Hz, 1H, $CH\alpha_{Val}$), 2.32–2.22 (m, 2H, $CH\beta_{Val}$, $CH_2\beta_{Ac6c}$), 2.04–1.96 (m, 2H, $CH_2\beta_{Ac6c}$), 1.93–1.86 (m, 1H, $CH_2\beta_{Ac6c}$), 1.73–1.60 (m, 4H, $CH_2\gamma_{Ac6c}$), 1.48 (s, 9H, $C(CH_3)_3$), 1.35–1.28 (m, 2H, CH_2d_{Ac6c}), 1.06 (d, J = 6.6 Hz, 3H, CH_{3Val}), 1.01 (d, J = 6.6 Hz, 3H, CH_{3Val}). ^{13}C-NMR ($CDCl_3$, c = 0.1 mol dm^{-3}) δ/ppm: 172.1 (CO_{Ac6c}), 171.6 (CO_{Val}), 156.5 (CO_{Boc}), 92.5 (C-1), 80.9 (Cq_{Boc}), 69.4 (Cp), 64.6 (C-3), 64.3 (C-4), 61.6 (C-2), 61.4 (C-5), 61.0 ($CH\alpha_{Val}$), 60.9 ($C\alpha_{Ac6c}$), 52.1 ($CH\alpha_{Val}$), 33.3 ($CH_2\beta_{Ac6c}$), 30.9 ($CH_2\beta_{Ac6c}$), 29.7 ($CH\beta_{Val}$), 28.6 (CH_{3Boc}), 25.1 (CH_2d_{Ac6c}), 21.4 ($CH_2\gamma_{Ac6c}$), 21.3 ($CH_2\gamma_{Ac6c}$), 19.6 (CH_{3Val}), 18.0 (CH_{3Val}). Elemental analysis calcd for $C_{27}H_{39}N_3O_4Fe$: C 61.72, H 7.48, N 8.0, found: C 61.80, H 7.45, N 8.05. IR (CH_2Cl_2): ν_{max}/cm^{-1}: 3429 m (NHfree), 3340 m (NHassoc.), 2976 sh, 2932 m, 2858 m (CH_2), 1702 m (amide I).

3.2.4. Boc–L–Phe–Ac6c–NH–Fc (**5**)

Yield 413 mg (72%), mp 113 °C. ^{1}H-NMR ($CDCl_3$, c = 0.1 mol dm^{-3}) δ/ppm: 8.38 (s, 1H, NH_{Fc}), 7.35–7.32 (m, 2H, $CH\gamma_{Phe}$), 7.29–7.27 (m, 1H, CHd_{Phe}), 7.25–7.23 (m, 2H, $CH\beta_{Phe}$), 6.09 (s, 1H, NH_{Ac6c}), 4.99 (bs, 1H, NH_{Phe}), 4.72 (s, 1H, H-2), 4.69 (s, 1H, H-5), 4.25–4.20 (m, 1H, $CH\alpha_{Phe}$), 4.19 (s, 5H, Fc), 4.00 (bs, 2H, H-3, H-4), 3.24–3.19 (m, 1H, $CH_2\beta_{Phe}$), 3.06–3.01 (m, 1H, $CH_2\beta_{Phe}$), 2.15–2.10 (m, 1H, $CH_2\beta_{Ac6c}$), 2.00–1.94 (m, 2H, $CH_2\beta_{Ac6c}$), 1.91–1.85 (m, 1H, $CH_2\beta_{Ac6c}$), 1.68–1.53 (m, 4H, $CH_2\gamma_{Ac6c}$), 1.45 (s, 9H, $C(CH_3)_3$), 1.30–1.19 (m, 2H, CH_2d_{Ac6c}). ^{13}C-NMR ($CDCl_3$, c = 0.1 mol dm^{-3}) δ/ ppm: 171.9 (CO_{Ac6c}), 171.0 (CO_{Phe}), 156.1 (CO_{Boc}), 136.3 (CαPhe), 129.1 (CβPhe), 129.0 (CγPhe), 127.3 (CdPhe), 94.7 (C-1), 81.2 (Cq_{Boc}), 69.4 (Cp), 64.5 (C-3), 64.3 (C-4), 61.3 (C-2), 61.1 (C-5), 60.8 ($C\alpha_{Ac6c}$), 57.2 ($CH\alpha_{Phe}$), 37.2 ($CH_2\beta_{Phe}$), 32.1 ($CH_2\beta_{Ac6c}$), 29.7 ($CH_2\beta_{Ac6c}$), 28.2 (CH_{3Boc}), 25.2 (CH_2d_{Ac6c}), 21.3 ($CH_2\gamma_{Ac6C}$). Elemental analysis calcd for $C_{31}H_{39}N_3O_4Fe$: C 64.92, H 6.85, N 7.33 found: C 64.98, H 6.79, N 7.29. IR (CH_2Cl_2): ν_{max}/cm^{-1}: 3422 m (NHfree), 3342 m (NHassoc.), 2930 m, 2858 m (CH_2), 1710 m (amide I).

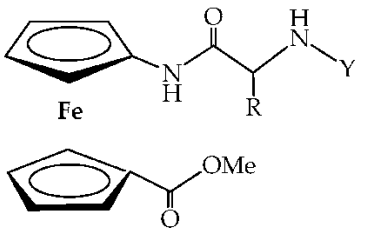

L- and D-**1a** (R = $CH(CH_3)_2$, Y = $COCH_3$) L- and D-**1b** (R = $CH(CH_3)_2$, Y = $COOC(CH_3)_3$)

L- and D-**2a** (R = $CH_2CH(CH_3)_2$, Y = $COCH_3$) L- and D-**2b** (R = $CH_2CH(CH_3)_2$, Y = $COOC(CH_3)_3$)

L- and D-**3a** (R = $CH_2C_6H_5$, Y = $COCH_3$) L- and D-**3b** (R = $CH_2C_6H_5$, Y = $COOC(CH_3)_3$)

Ferrocene dipeptides with hydrophobic amino acids

Synthesis of Boc–AA–NH–Fn–COOMe (**1b-3b**): Boc–NH–Fn–COOMe (1) (1000 mg, 2.78 mmol) was Boc-deprotected in the presence of HClgas in dry CH_2Cl_2 (5 ml) at 0 °C. After 2 hours, the solvent was evaporated in vacuo to afford the hydrochloride salt which was then suspended in CH_2Cl_2 and treated with NEt_3 (pH ~ 8) to give free amine suitable for coupling to Boc–L-AA–OH or Boc–D-AA–OH (5.57 mmol) (AA = Phe, Val and Leu) using the standard EDC/ HOBt method [EDC (2135 mg, 11.1 mmol); HOBt (1505 mg, 11.1 mmol)]. The reaction mixtures were then stirred at room temperature until total consumption of ferrocene amine, which was monitored by TLC (~ 1-3 hour). Standard work-up (washing with a saturated aqueous solution of $NaHCO_3$, a 10% aqueous solution of citric acid and brine, drying over Na2SO4 and evaporation in vacuo) including TLC purification of the crude products [EtOAc : CH_2Cl_2 = 1 : 5; Rf = 0.75, Rf = 0.63, Rf = 0.83, Rf = 0.72, Rf = 0.66, Rf = 0.80] gave orange solids of **1b-3b** (1053 mg, 75%), (815 mg, 64%), (850 mg, 65%), (982 mg, 70%), (764 mg, 60%) and (771 mg, 59%).

Boc–L–Phe–NH–Fn–COOMe: IR (CH_2Cl_2) νmax/cm^{-1}: 3416 m (NHfree), 3324 w (NHassoc.), 1709 s (C=OCOOMe), 1685 s (C=OBoc), 1640 m (C=OCONH), 1535 m, 1496 m, 1466 m (amide II). ^{1}H-NMR (600 MHz, $CDCl_3$) δ: 7.34-7.24 (m, 5H, CHPhe), 7.32 (s, 1H, NHFn), 5.15 (s, 1H, NHBoc), 4.72 (s, 1H, CHFn), 4.68 (s, 1H, CHFn), 4.61 (s, 1H, CHFn), 4.44 (s, 1H, CHFn), 4.39 (d, J = 6.6 Hz, 1H, CHα-Phe), 4.32 (s, 2H, CHFn), 4.02 (s, 1H, CHFn), 4.00 (s, 1H, HFn), 3.78 (s, 3H, CH_3-COOMe), 3.17 (dd, J= 6.1, 13.1 Hz, 1H, CHβ1-Phe), 3.09 (dd, J = 7.1, 13.5 Hz, 1H, CHβ2-Phe), 1.42 [s, 9H, $(CH_3)_3$-Boc] ppm. ^{13}C-NMR (150 MHz, $CDCl_3$) δ: 171.84 (1C, COa Fn), 169.93 (1C, COb Fn), 155.66 (1C, COBoc), 136.92 (1C, Cq-γPhe), 129.53 (2C, CHPhe), 128.87 (2C, CHPhe), 127.14 (1C, CHPhe), 94.51 (1C, Cq-1Fn), 80.62 (1C, CqBoc), 72.76 (1C, CHFn), 72.05 (1C, Cq-6Fn), 71.36, 71.32, 66.79, 66.57, 63.74, 63.25 (7C, CHFn), 56.38 (1C, CHα-Phe), 51.81 (1C, CH_3-COOMe), 38.37 (1C, CH_2β-Phe), 28.43 [3C, $(CH_3)_3$-Boc] ppm.

Boc–L–Val–NH–Fn–COOMe: IR (CH_2Cl_2) νmax/cm^{-1}: 3422 m (NHfree), 3324 w (NHassoc.), 1710 s (C=OCOOMe), 1683 s (C=OBoc), 1636 m (C=OCONH), 1534 m, 1498 m, 1466 m (amide II). 1H-NMR (600 MHz, $CDCl_3$) δ: 7.35 (s, 1H, NHFn), 5.14 (s, 1H, NHBoc), 4.75 (s, 2H, CHFn), 4.65 (s, 1H, CHFn), 4.54 (s, 1H, CHFn), 4.39 (s, 2H, CHFn), 4.04 (s, 2H, CHFn), 3.94 (t, J = 6.8 Hz, 1H, CHα–Val), 3.81 (s, 3H, CH_3- COOMe), 2.22 (s, 1H, CHβ-Val), 1.47 [s, 9H, $(CH_3)_3$-Boc], 1.02 [d, J = 6.7 Hz, 3H, (CH_3)γ-aVal], 0.98 [d, J = 6.7 Hz, 3H, (CH3) γ-bVal] ppm. ^{13}C-NMR (150 MHz, $CDCl_3$) δ: 172.04 (1C, COa Fn), 170.39 (1C, COb Fn), 156.25 (1C, COBoc), 94.75 (1C, Cq-1Fn), 80.26 (1C, CqBoc), 72.77 (1C, CHFn), 72.00 (1C, Cq-6Fn), 71.42, 71.34, 66.80, 66.60, 63.70 (7C, CHFn), 63.36 (1C, CHα-Val), 51.85 (1C, CH_3-COOMe), 30.65 (1C, CHβ-Val), 28.51 [3C, $(CH_3)_3$-Boc], 19.59 [1C, (CH3)γ-aVal], 17.94 [1C, (CH_3)γ-bVal] ppm.

Boc–L–Leu–NH–Fn–COOMe: IR (CH_2Cl_2) νmax/cm^{-1}: 3425 m (NHfree), 3320 w (NHassoc.), 1708 s (C=OCOOMe), 1685 s (C=OBoc), 1654 m (C=OCONH), 1534 m, 1499 m, 1467 m (amide II). ^{1}H-NMR (600 MHz, $CDCl_3$) δ: 7.57 (s, 1H, NHFn), 5.01 (d, J = 8.1 Hz, 1H, NHBoc), 4.76 (pt, 2H, CHFn), 4.68 (s, 1H, CHFn), 4.55 (s, 1H, CHFn), 4.39 (pt, 2H, CHFn), 4.16-4.11 (m, 1H, CHα-Leu), 4.04 (s, 1H, CHFn), 4.01 (s, 1H, CHFn), 3.81 (s, 3H, CH_3-COOMe), 1.79-1.71 (m, 2H, CH2-β1-Leu, CHγ-Leu), 1.56-1.51 (m, 1H, CH_2-β2- Leu), 1.48 [s, 9H, $(CH_3)_3$-Boc], 0.97 [t, J= 6.7 Hz, 6H, (CH_3) 2-δ-Leu] ppm. ^{13}C-NMR (150 MHz, $CDCl_3$) δ: 171.92 (1C, COa Fn), 171.11 (1C, COb Fn), 156.22 (1C, COBoc), 95.17 (1C, Cq-1Fn), 80.63 (1C, CqBoc), 3 72.81, 72.78 (2C, CHFn), 72.29 (1C, Cq-6Fn), 72.03, 71.39, 71.27, 66.76, 66.46 (5C, CHFn), 63.43 (CHαLeu), 63.06 (1C, CHFn), 51.82 (1C, CH_3-COOMe), 40.91 [1C, (CH_2)β-Leu], 28.52 [3C, $(CH_3)_3$-Boc], 24.95 (1C, CHγ-Leu), 23.14, 22.15 [2C, (CH_3)2-δ-Leu] ppm.

Boc–D–Phe–NH–Fn–COOMe: IR (CH_2Cl_2) νmax/cm^{-1}: 3412 m (NHfree), 3323 w (NHassoc.), 1709 s (C=OCOOMe), 1687 s (C=OBoc), 1605 m (C=OCONH), 1557 m, 1536 m, 1508 m, 1496 m (amide II). ^{1}HNMR (600 MHz, $CDCl_3$) δ: 7.34-7.31 (m, 5H, CHPhe), 7.27 (s, 1H, NHFn), 5.15 (s, 1H, NHBoc), 4.71 (s, 1H, CHFn), 4.68 (m, 1H, CHFn), 4.62 (pt, 1H, CHFn), 4.43 (s, 1H, CHFn), 4.40-4.39 (m, 1H, CHα-Phe), 4.32 (pt, 2H, CHFn), 4.03-4.01 (m, 2H, CHFn), 3.78 (s, 3H, CH_3-COOMe), 3.17 (m, 1H, CHβ1-Phe), 3.10-3.06 (m, 1H, $CH\beta_2$-Phe), 1.42 [s, 9H, $(CH_3)_3$-Boc] ppm. ^{13}C-NMR (150 MHz, $CDCl_3$) δ: 171.90 (1C, COa Fn), 169.93 (1C, COb Fn), 155.76 (1C, COBoc), 136.89 (1C, Cq-αPhe), 129.53 (2C, CHPhe), 128.88 (2C, CHPhe), 127.14 (1C, CHPhe), 94.46 (1C, Cq-1Fn), 80.59 (1C, CqBoc), 72.76 (1C, CHFn), 72.02 (1C, Cq-6Fn), 71.35, 71.31, 66.80, 66.57, 63.73, 63.25 (7C, CHFn), 56.36 (1C, CHα-Phe), 51.84 (1C, CH_3-COOMe), 38.34 (1C, CH2β- Phe), 28.42 [3C, $(CH_3)_3$-Boc] ppm.

Boc–D–Val–NH–Fn–COOMe: IR (CH_2Cl_2) νmax/cm^{-1}: 3425 s (NHfree), 3323 m (NHassoc.), 1709 s (C=OCOOMe), 1688 s (C=OCONH), 1534 s, 1498 s (amide II). ^{1}H-NMR (600 MHz, $CDCl_3$) δ: 7.48 (s, 1H, NHFn), 5.20 (d, J = 8.55 Hz, 1H, NHBoc), 4.74 (pt, 2H, CHFn), 4.65 (s, 1H, CHFn), 4.55 (s, 1H, CHFn), 4.38 (pt, 2H, CHFn), 4.03 (pt, 2H, CHFn), 3.96-3.93 (m, 1H, CHα-Val), 3.80 (s, 3H, CH_3-COOMe), 2.19 (s, 1H, CHβ-Val), 1.46 (s, 9H, $(CH_3)_3$-Boc), 1.02 (d, J = 6.8 Hz, 3H, (CH_3)γ-aVal), 0.98 (d, J = 6.9 Hz, 3H, (CH_3)γ-bVal) ppm. ^{13}C-NMR (150 MHz, $CDCl_3$) δ: 172.06 (1C, COa Fn), 170.44 (1C, COb Fn), 156.21 (1C, COBoc), 94.83 (1C, Cq-1Fn), 80.28 (1C, CqBoc), 72.77 (1C, CHFn), 71.91 (1C, Cq-6Fn), 71.34, 71.27, 66.75, 66.56, 63.54, 63.27 (7C, CHFn), 60.62 (1C, CHα-Val), 51.85 (1C, CH_3-COOMe), 30.71 (1C, CHβ-Val), 28.49 [3C, $(CH_3)_3$-Boc], 19.57 [1C, (CH_3)γ-aVal], 17.98 [1C, (CH_3)γ-bVal] ppm.

Boc–D–Leu–NH–Fn–COOMe: IR (CH_2Cl_2) νmax/cm^{-1}: 3416 s (NHfree), 3322 m (NHassoc.), 1709 s (C=OCOOMe), 1685 s (C=OBoc), 1603 m (C=OCONH), 1584 s, 1534 m, 1506 m, 1499 m (amide II). ^{1}HNMR (600 MHz, $CDCl_3$) δ: 7.62 (s, 1H, NHFn), 5.03 (d, J = 8.03 Hz, 1H, NHBoc), 4.74 (pt, 2H, CHFn), 4.67 (s, 1H, CHFn), 4.55 (s, 1H, CHFn), 4.37 (pt, 2H, CHFn), 4.15-4.12 (m, 1H, CHα-Leu), 4.03 (s, 1H, CHFn), 4.01 (s, 1H, CHFn), 3.80 (s, 3H, CH_3-COOMe), 1.78-1.70 (m, 2H, CH_2-β1-Leu, CHγ-Leu), 1.55-1.51 (m, 1H, CH_2-β2-Leu), 1.47 [s, 9H, $(CH_3)_3$-Boc], 0.97 [t, J= 6.3 Hz, 6H, (CH3)2-δ-Leu] ppm. ^{13}C-NMR (150 MHz, $CDCl_3$) δ: 171.96 (1C, COa Fn), 171.12 (1C, COb Fn), 154.34 (1C, COBoc), 100.13 (1C, CqBoc), 95.17 (1C, Cq-1Fn), 72.81 (1C, CHFn), 72.79 (1C, Cq-6Fn), 71.95, 71.35, 71.24, 66.73, 66.44 (6C, CHFn), 63.37 (1C, CHα-Leu), 63.01 (1C, CHFn), 51.83 (1C, CH_3-COOMe), 40.90 [1C, (CH_2)β-Leu], 28.49 [3C, $(CH_3)_3$-Boc], 24.91 (1C, CHγ-Leu), 23.13, 22.15 [2C, $(CH_3)_2$-δ-Leu] ppm.

Synthesis of Ac–AA–NH–Fn–COOMe (**1a-3a**): The transformation of carbamates **1b-3b** (2 mmol) to acetamides **1a-3a** began with the acidic Boc-deprotection described above. Their free amines, obtained by treating the hydrochloride salt with NEt_3 (25.1 mmol), were cooled to 0°C and acetyl chloride (12 mmol) was added dropwise, stirring in an ice bath. After TLC monitoring showed complete conversion of the

starting materials, the reaction mixtures were poured into water and extracted with CH_2Cl_2. The combined organic phases were washed with a brine, dried over Na_2SO_4 and evaporated to dryness in vacuo. The resulting crude products were purified by TLC on silica gel [EtOAc : CH_2Cl_2 = 1 : 5; Rf = 0.25, Rf = 0.16, Rf = 0.33, Rf = 0.21, Rf = 0.13, Rf = 0.32] to give orange solids of acetamides of **1a-3a** (394 mg, 76%), (538 mg, 78%), (498 mg, 60%), (357 mg, 69%), (496 mg, 72%) and (540 mg, 65%).

Ac–L–Phe–NH–Fn–COOMe: IR (CH_2Cl_2) νmax/cm^{-1}: 3418 m (NHfree), 3290 m, 3248 w (NHassoc.), 1709 s (C=OCOOMe), 1696 s, 1668 s (C=OCONH), 1574, 1558, 1540, 1535, 1516, 1507, 1498, 1466 (amide II). ^{1}H-NMR (600 MHz, $CDCl_3$) δ: 7.68 (s, 1H, NHFn), 7.33-7.24 (m, 5H, CHPhe), 6.43 (d, J = 7.6 Hz, 1H, NHAc), 4.77 (q, J = 7.3 Hz, 1H, CHα-Phe), 4.69 (s, 1H, CHFn), 4.65 (s, 1H, CHFn), 4.57 (s, 1H, CHFn), 4.45 (s, 1H, CHFn), 4.29 (s, 2H, CHFn), 4.03 (s, 1H, CHFn), 4.00 (s, 1H, CHFn), 3.78 (s, 3H, CH_3-COOMe), 3.1 (dd, J= 7.4 Hz, 13.8 Hz, 1H, CHβ1-Phe), 3.09 (dd, J= 6.8 Hz, 13.9 Hz, 1H, CHβ_2-Phe), 2.02 [s, 3H, CH_3- Ac] ppm. ^{13}C-NMR (150 MHz, $CDCl_3$) δ: 171.92 (1C, COb Fn), 170.62 (1C, COa Fn), 169.71 (1C, COAc), 136.78 (1C, Cq-γPhe), 129.49, 129.46, 128.85, 127.21 (5C, CHPhe), 94.40 (1C, Cq-1Fn), 72.72 (1C, CHFn), 72.05 (1C, Cq-6Fn), 71.40, 71.28, 66.84, 66.58, 63.89, 63.44 (7C, CHFn), 55.01 (1C, CHα-Phe), 51.82 (1C, CH_3-COOMe), 38.23 (1C, CH2β-Phe), 23.35 (CH_3-Ac) ppm.

Ac–L–Val–NH–Fn–COOMe: IR (CH_2Cl_2) νmax/cm^{-1}: 3421 m (NHfree), 3287 m, 3245 m (NHassoc.), 1711 s (C=OCOOMe), 1684 s, 1670 s, 1661 s (C=OCONH), 1569, 1559, 1540, 1517, 1508, 1490, 1466 (amide II). ^{1}H-NMR (600 MHz, $CDCl_3$) δ: 8.21 (s, 1H, NHFn), 6.49 (d, J = 8.7 Hz, 1H, NHAc), 4.74 (s, 1H, CHFn), 4.73 (s, 1H, CHFn), 4.61 (s, 1H, CHFn), 4.60 (s, 1H, CHFn), 4.41 (t, J = 7.7 Hz, 1H, CHα-Val), 4.37 (s, 2H, CHFn), 4.03 (s, 2H, CHFn), 3.78 (s, 3H, CH_3-COOMe), 2.18-2.13 (m, 1H, CHααVal), 2.10 (s, 3H, CH_3- Ac), 1.04 [d, J = 6.7 Hz, 3H, (CH_3)γ-aVal], 1.01 [d, J = 6.7 Hz, 3H, (CH_3) γ-bVal] ppm. ^{13}C-NMR (150 MHz, $CDCl_3$) δ: 172.04 (1C, COb Fn), 170.70 (1C, COa Fn), 170.25 (1C, COAc), 95.00 (1C, Cq-1Fn), 72.73, 72.68 (2C, CHFn), 72.01 (1C, Cq-6Fn), 71.39, 71.22, 66.72, 66.60, 63.42, 63.38 (6C, CHFn), 59.13 (1C, CHα-Val), 51.80 (1C, CH_3-COOMe), 31.16 (1C, CHβ-Val), 23.51 (1C, CH_3-Ac), 19.50 [(CH_3)γ-aVal], 18.49 [(CH_3)γ-bVal] ppm.

Ac–L–Leu–NH–Fn–COOMe: IR (CH_2Cl_2) νmax/cm^{-1}: 3425 m (NHfree), 3289 m, 3241 w (NHassoc.), 1709 s (C=OCOOMe), 1693 s, 1673 s, 1669 s (C=OCONH), 1562, 1557, 1538, 1520, 1515, 1467 (amide II). ^{1}H-NMR (600 MHz, $CDCl_3$= δ: 8.07 (s, 1H, NHFn), 6.33 (d, J = 8.3 Hz, 1H, NHAc), 4.74 (s, 1H, CHFn), 4.71 (s, 1H, CHFn), 4.62 (s, 1H, CHFn), 4.59 (s, 1H, CHFn), 4.53 (q, J = 8.3 Hz, 1H, CHα-Leu), 4.36 (pt, 2H, CHFn), 4.03 (s, 1H, CHFn), 4.00 (s, 1H, CHFn), 3.80 (s, 3H, CH_3-COOMe), 2.07 (s, 3H, CH_3-Ac), 1.81-1.76 (m, 1H, CH_2-β1-Leu), 1.73-1.68 (m, 1H, CHγ-Leu), 1.60-1.55 (m, 1H, CH_2-β2-Leu), 0.98 [d, J = 6.6 Hz, 3H, (CH_3)δ-aLeu], 0.96 [d, J = 6.6 Hz, 3H, (CH_3)δ-b-Leu] ppm. ^{13}C-NMR (150 MHz, $CDCl_3$) δ: 171.95 (1C, COb Fn), 170.90 (1C, COa Fn), 170.78 (1C, COAc), 95.17 (1C, Cq-1Fn), 72.70, 72.66 (2C, CHFn), 72.08 (1C, Cq-6Fn), 71.43, 71.22, 66.72, 66.39, 63.48, 63.21 (6C, CHFn), 52.29 (1C, CHα-Leu), 51.83 (1C, CH_3-COOMe), 40.83 [1C, (CH_2)β-Leu], 24.99 (1C, CHγ-Leu), 23.38 (1C, CH_3-Ac), 23.04, 22.41 [2C, (CH_3)$_2$-δ-Leu] ppm.

Ac–D–Phe–NH–Fn–COOMe: IR (CH_2Cl_2) νmax/cm^{-1}: 3419 m (NHfree), 3310 w, 3292 m, 3243 w (NHassoc.), 1707 s (C=OCOOMe), 1690 s, 1666 s, 1654 s (C=OCONH), 1605, 1575, 1558, 1539, 1506, 1497 (amide II). ^{1}H-NMR (600 MHz, $CDCl_3$) δ: 7.77 (d, 1H, NHFn), 7.32-7.24 (m, 5H, CHPhe), 6.46 (pt, 1H, NHAc), 4.79-4.75 (m, 1H, CHα-Phe), 4.68 (m, 1H, CHFn), 4.64 (m, 1H, CHFn), 4.58-4.55 (m, 1H, CHFn), 4.46 (m, 1H, CHFn), 4.29 (m, 2H, CHFn), 4.03 (s, 1H, CHFn), 4.00 (s, 1H, CHFn), 3.76 (s, 3H, CH_3-COOMe), 3.17-3.13 (m, 1H, CHβ1-Phe), 3.10-3.05 (m, 1H, CHβ_2-Phe), 2.02 [s, 3H, CH_3Ac] ppm. ^{13}C-NMR (150 MHz, 5 $CDCl_3$) δ: 171.99 (1C, COb Fn), 170.60 (1C, COa Fn), 169.70 (1C, COAc), 136.74 (1C, Cq-γPhe), 129.47, 129.45, 128.83, 127.19 (5C, CHfenil), 94.38 (1C, Cq-1Fn), 72.72 (1C, CHFn), 71.98 (1C, Cq-6Fn), 71.40, 71.26, 66.62, 66.57, 66.42, 63.89, 63.44 (7C, CHFn), 54.96 (1C, CHα-Phe), 51.85 (CH_3-COOMe), 38.22 (1C, CH_2β-Phe), 23.35 (1C, CH_3-Ac) ppm.

Ac–D–Val–NH–Fn–COOMe: IR (CH_2Cl_2) νmax/cm^{-1}: 3420 m (NHfree), 3286 m, 3235 m (NHassoc.), 1707 s (C=OCOOMe), 1686 s, 1672 s, 1660 s (C=OCONH), 1605, 1569, 1539, 1514, 1508, 1489 (amide II). ^{1}H-NMR (600 MHz, $CDCl_3$) δ: 8.19 (s, 1H, NHFn), 6.45 (d, J = 8.91 Hz, 1H, NHAc), 4.74 (s, 1H, CHFn), 4.72 (s, 1H, CHFn), 4.61 (s, 1H, CHFn), 4.59 (s, 1H, CHFn), 4.40 (t, J = 8.3 Hz, 1H, CHα-Val), 4.37 (pt, 2H, CHFn), 4.03 (pt, 2H, CHFn), 3.78 (s, 3H, CH_3-COOMe), 2.19-2.13 (m, 1H, CHβ-Val), 2.10 (s, 3H, CH_3-Ac), 1.04 [d, J = 6.8 Hz, 3H, (CH_3)γ-aVal], 1.01 [d, J = 6.6 Hz, 3H, (CH_3) γ-bVal] ppm. ^{13}C-NMR (150 MHz, $CDCl_3$) δ: 172.06 (1C, COb Fn), 170.66 (1C, COa Fn), 170.19 (1C, COAc), 94.96 (1C, Cq-1Fn), 72.72, 72.68 (2C, CHFn), 71.95 (1C, Cq-6Fn), 71.37, 71.20, 66.71, 66.59, 63.39, 63.36 (6C, CHFn), 59.07 (1C, CHα-Val), 51.82 (1C, CH_3-COOMe), 31.16 (1C, CHβ-Val), 23.53 (1C, CH_3-Ac), 19.50 [1C, (CH_3)γ-aVal], 18.47 [1C, (CH_3)γ-bVal] ppm.

Ac–D–Leu–NH–Fn–COOMe: IR (CH_2Cl_2) νmax/cm^{-1}: 3421 m (NHfree), 3290 m, 3241 w (NHassoc.), 1708 s (C=OCOOMe), 1699 s, 1652 s, 1636 s (C=OCONH), 1574, 1556, 1541, 1516, 1508, 1488 (amide II). ^{1}H-NMR (600 MHz, $CDCl_3$) δ: 8.23 (s, 1H, NHFn), 6.47 (d, J = 8.22 Hz, 1H, NHAc), 4.73 (pt, 1H, CHFn), 4.71 (pt, 1H, CHFn), 4.61 (pt, 2H, CHFn), 4.54 (q, J = 8.3 Hz, 1H, CHα-Leu), 4.02 (pt, 2H, CHFn), 4.00 (pt, 2H, CHFn), 3.79 (s, 3H, CH_3-COOMe), 2.05 (s, 3H, CH_3-Ac), 1.78-1.74 (m, 1H, CH_2-β1-Leu), 1.71-1.69 (m, 1H, CHγ-Leu), 1.60-1.55 (m, 1H, CH_2-β2-Leu), 0.98 [d, J = 6.6 Hz, 3H, (CH_3)δ-a-Leu], 0.96 [d, J = 6.6 Hz, 3H, (CH_3)δ-b-Leu] ppm. ^{13}C-NMR (150 MHz, $CDCl_3$) δ: 171.97 (1C, COb Fn), 170.90 (1C, COa Fn), 169.92 (1C, COAc), 95.22 (1C, Cq-1Fn), 72.71, 72.67 (2C, CHFn), 71.99 (1C, Cq-6Fn), 71.38, 71.19, 66.67, 66.40, 63.34, 63.16 (6C, CHFn), 52.28 (1C, CHα-Leu), 51.82 (1C, CH_3-COOMe), 40.86 [1C, (CH_2)β-Leu], 24.97 (1C, CHγ-Leu), 23.34 (1C, CH_3-Ac), 23.03, 22.39 [2C, $(CH_3)_2$-δ-Leu] ppm.

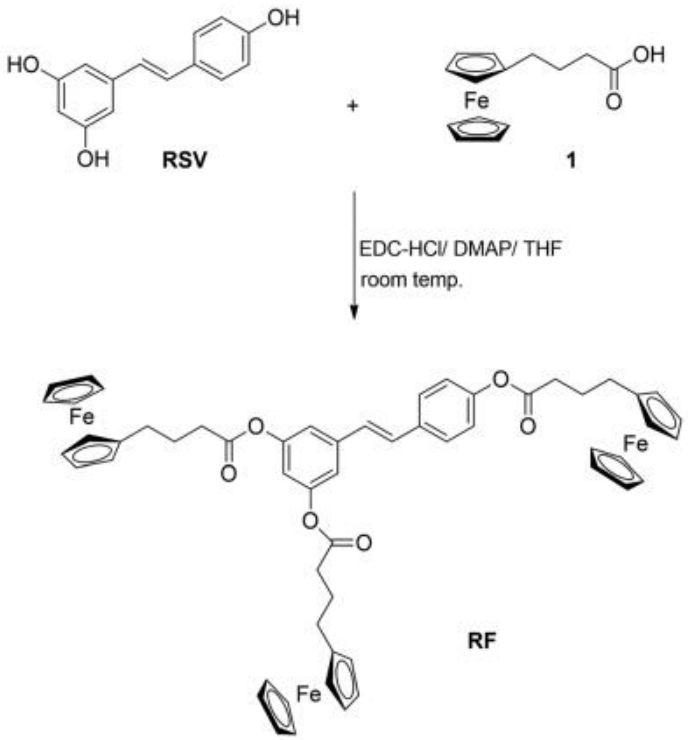

SCHEME 1 The synthesis of ferrocene-containing resveratrol derivative, RF

3.1 | Synthetic procedure of resveratrol derivative preparation

The synthetic route of RF preparation is shown in Scheme 1. In the modified Steglich esterification (Neises & Steglich, 1978) of ferrocenebutyric acid with RSV in a molar ratio of 3:1 in the presence of *N*-(3-dimethylaminopropyl)-*N*-ethylcarbodiimide hydrochloride (EDC-HCl) and a catalytic amount of 4-dimethylaminopyridine (DMAP), only one product was displayed on the TLC plate. Due to the poor solubility of RSV in dichloromethane (DCM), tetrahydrofuran (THF) was used as solvent. After isolation and TLC purification of the

crude material, the compound was obtained in a yield of 53%, and its structure was confirmed by IR and NMR spectra (spectroscopy data of a new compound are given in the supporting information). The involvement of all three RSV hydroxyl groups in the ester bond was confirmed by the disappearance of the broad absorption band at about 3,300 cm^{-1} attributed to the OH-stretching vibrations and the appearance of the strong absorption band at about 1,758 cm^{-1} corresponding to the $C{=}O_{ester}$ stretching vibration in IR spectra. Moreover, new signals of ester carbonyl groups were observed at 172.09 and 171.55 ppm in the ^{13}C NMR spectra, while the signal of the hydroxyl group could not be detected in the ^{1}H NMR spectra. *Trans*-orientation of the two phenyl rings of RSV was confirmed by the value of the coupling constant J(H,H) = 16.3 Hz between the two alkene hydrogen atoms Hα and Hα′ in the ^{1}H NMR spectra. Signals of ferrocene protons were detected at 4.13 ppm (15 hydrogen atoms of the unsubstituted ferrocene rings) and at 4.11 and 4.08 ppm (12 hydrogen atoms of the substituted ferrocene rings). Methylene groups of alkyl chains were detected at 2.59 and 2.48 ppm as two triplets (6 CH_2 groups in total) and at 1.99–1.94 ppm as one multiplet (3 CH_2 groups in total). The IR and the NMR data have proved beyond doubt the presence of three ferrocene units formed by esterification of all three RSV hydroxyl groups.

2.1.2 | Synthesis of *trans*-3,5,4′-tri (4-ferrocenylbutanoyloxy)-stilbene (RF)

To solution of RSV (0.438 mmol) in dry THF (3 ml) ferrocenebutyric acid **1** (1.314 mmol), EDC-HCl (1.314 mmol) and a catalytic amount of DMAP (0.060 mmol) were added (Scheme 1). The reaction mixture was stirred at room temperature for 6 days, until TLC monitoring showed consumption of the starting material. After the reaction mixture was filtered and the solvent evaporated in vacuo, the residue was purified by TLC on silica gel (DCM/hexane = 1/1) to give yellow crystals of RF (229 mg, 53%). M.p. 83–85°C; $R_f = 0.59$ in DCM/hexane = 2/1; IR (CH_2Cl_2) $_{max}/cm^{-1}$: 1,758 s $(C{=}O)_{ester}$, 1,126 s (C-O); ^{1}H NMR (600 MHz, $CDCl_3$, TMS) δ/ppm: 7.49 (d, $J = 8.5$ Hz, 2H, H2′ H6′), 7.11 (d, $J = 8.5$ Hz, 2H, H3′ H5′), 7.10 (bs, 1H, H2), 7.08 (bs, 1H, H6), 7.07 (d, $J = 16.3$ Hz, 1H, Hα′), 6.98 (d, $J = 16.3$ Hz, 1H, Hα), 6.82 (pt, 1H, H4), 4.13 (s, 15H, H_{Fc}), 4.11 (s, 6H, H_{Fc}), 4.08 (s, 6H, H_{Fc}), 2.59 (t, $J = 2.6$ Hz, 6H, $CH_{2\beta}$), 2.48 (t, $J = 2.5$ Hz, 6H, $CH_{2\delta}$), 1.99–1.94 (m, 6H, $CH_{2\gamma}$).^{13}C NMR APT (150 MHz, $CDCl_3$, TMS) δ/ppm: 172.09, 171.55 (C=O), 151.50 (C3, C5), 150.46 (C4′), 139.65 (C1), 134.68 (C1′), 129.79 (Cα′), 127.78 (C2′, C6′), 127.35 (Cα), 122.03 (C3′, C5′), 117.03 (C2, C6), 114.47 (C4), 87.98 (C_{qFc}), 68.73, 68.33, 67.49 (C_{Fc}), 34.03 ($CH_{2\beta}$), 29.00 ($CH_{2\delta}$), 26.19 ($CH_{2\gamma}$).

IR spectra

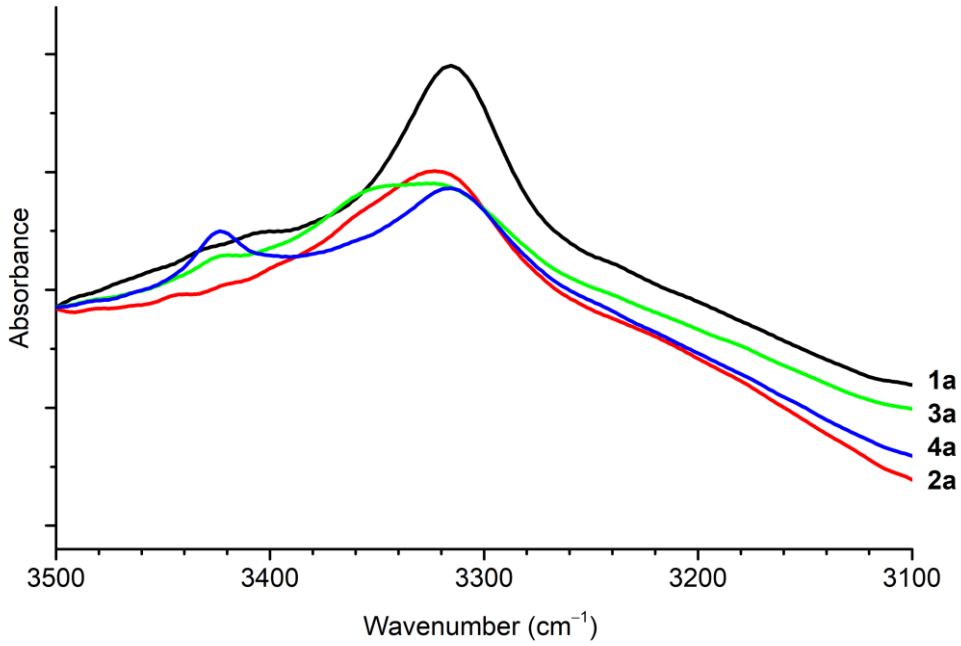

Figure S1. The NH stretching vibrations of **1a**–**4a** in CH_2Cl_2 ($c = 1 \cdot 10^{-3}$ mol·dm^{-3})

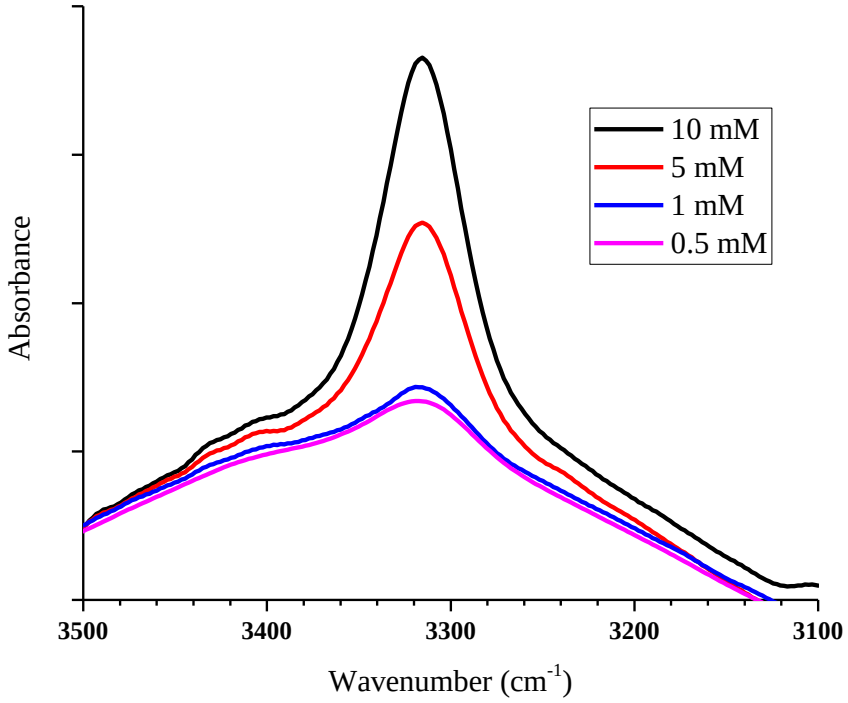

Figure S2. The NH stretching vibrations of compound **1a** during dilution

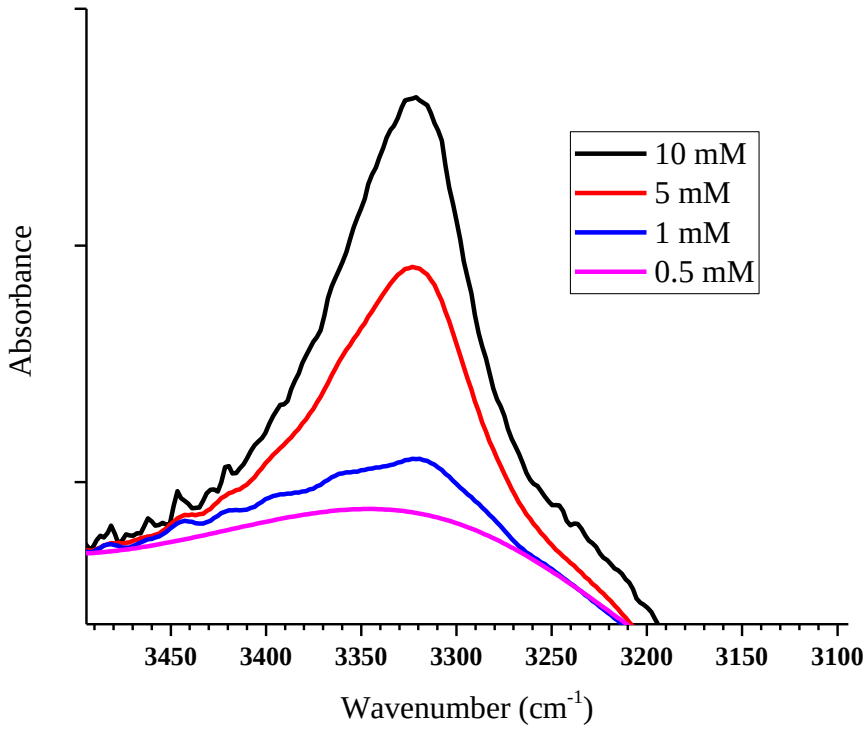

Figure S3. The NH stretching vibrations of compound **2a** during dilution

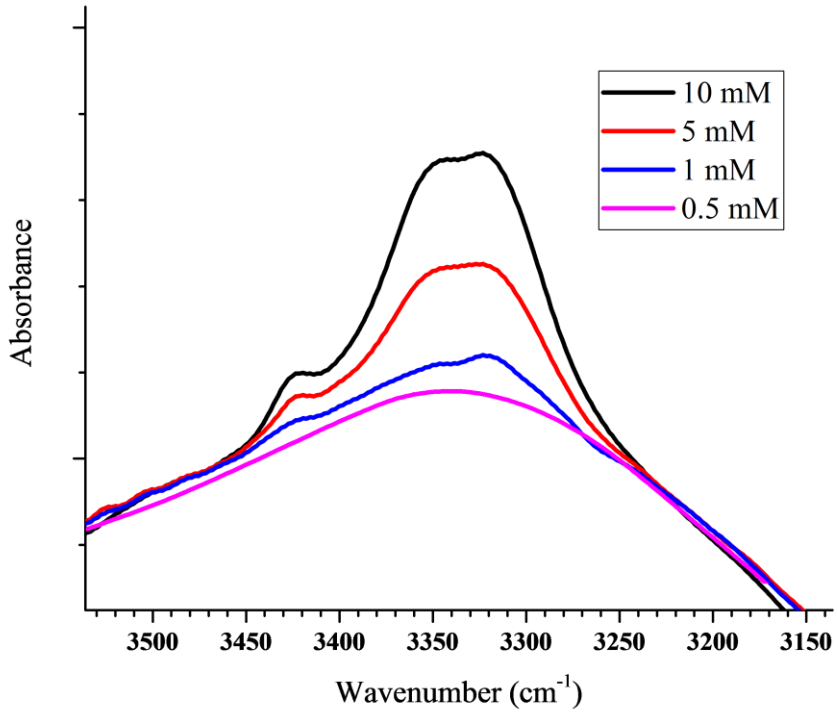

Figure S4. The NH stretching vibrations of compound **3a** during dilution

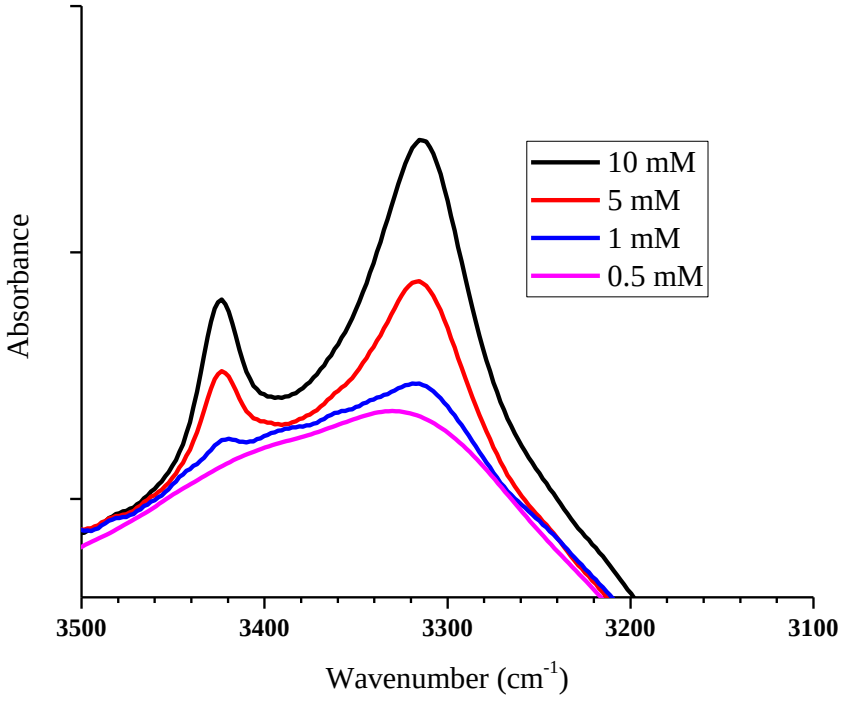

Figure S5. The NH stretching vibrations of compound **4a** during dilution

Table S1. NH and CO absorption frequencies of compounds **1a**-**4a** in DCM (c = 1 mM)

Compound	ν NH (free)	ν NH (assoc.)	amide I	amide II
1a CH_2Cl_2	-	3315	1666, 1629	1558, 1525
2a CH_2Cl_2	-	3323	1666	1556, 1541, 1515
3a CH_2Cl_2	3420	3326	1672	1541, 1520
4a CH_2Cl_2	3423	3315	1691, 1645	1556, 1541, 1514

NMR spectra

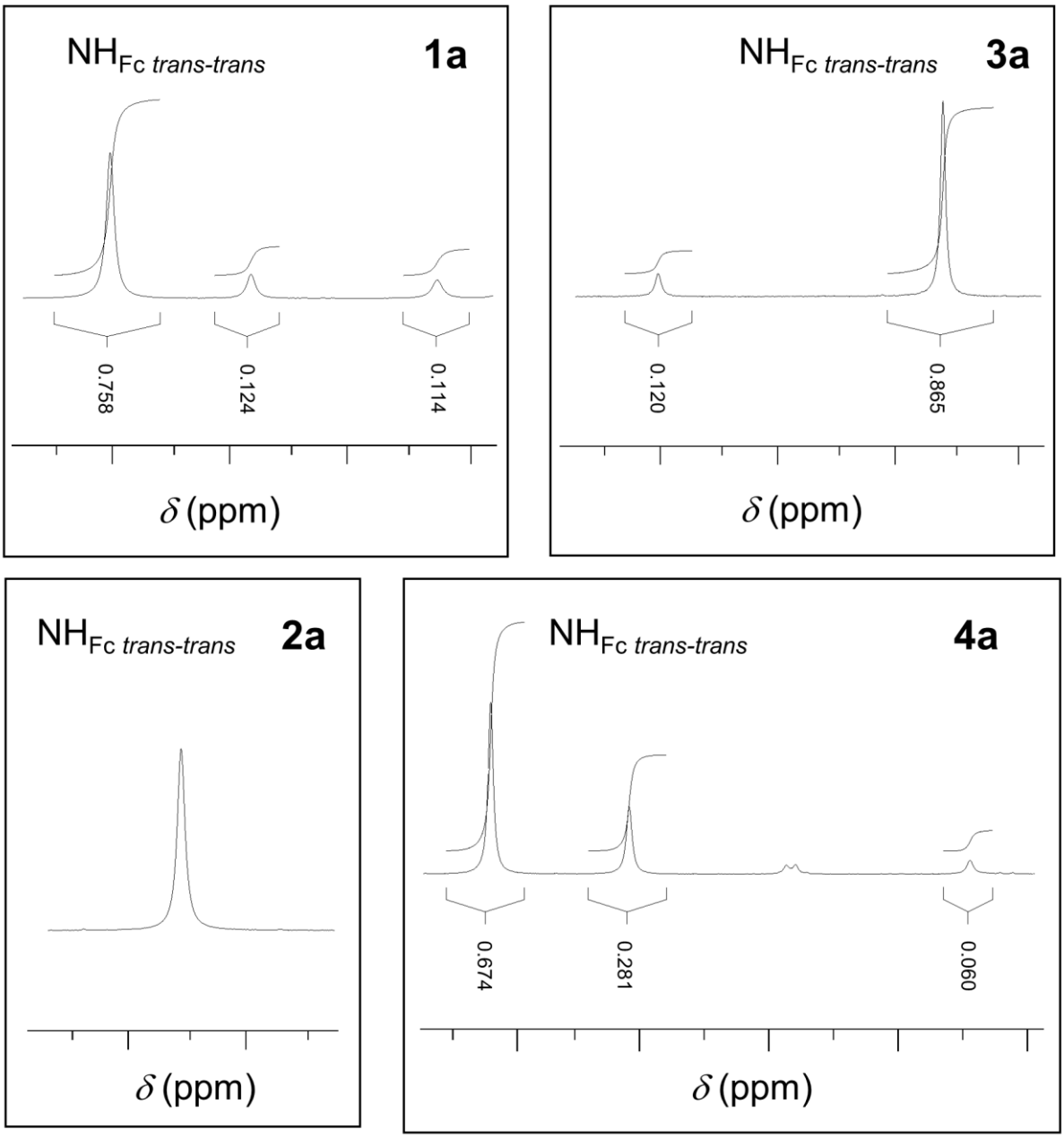

Figure S6. NH region of the ^{1}H NMR spectrum of **1a**–**4a** (c = 2·10^{-3} mol·dm^{-3} at 25°C) showing signals corresponding to the major and minor isomers.

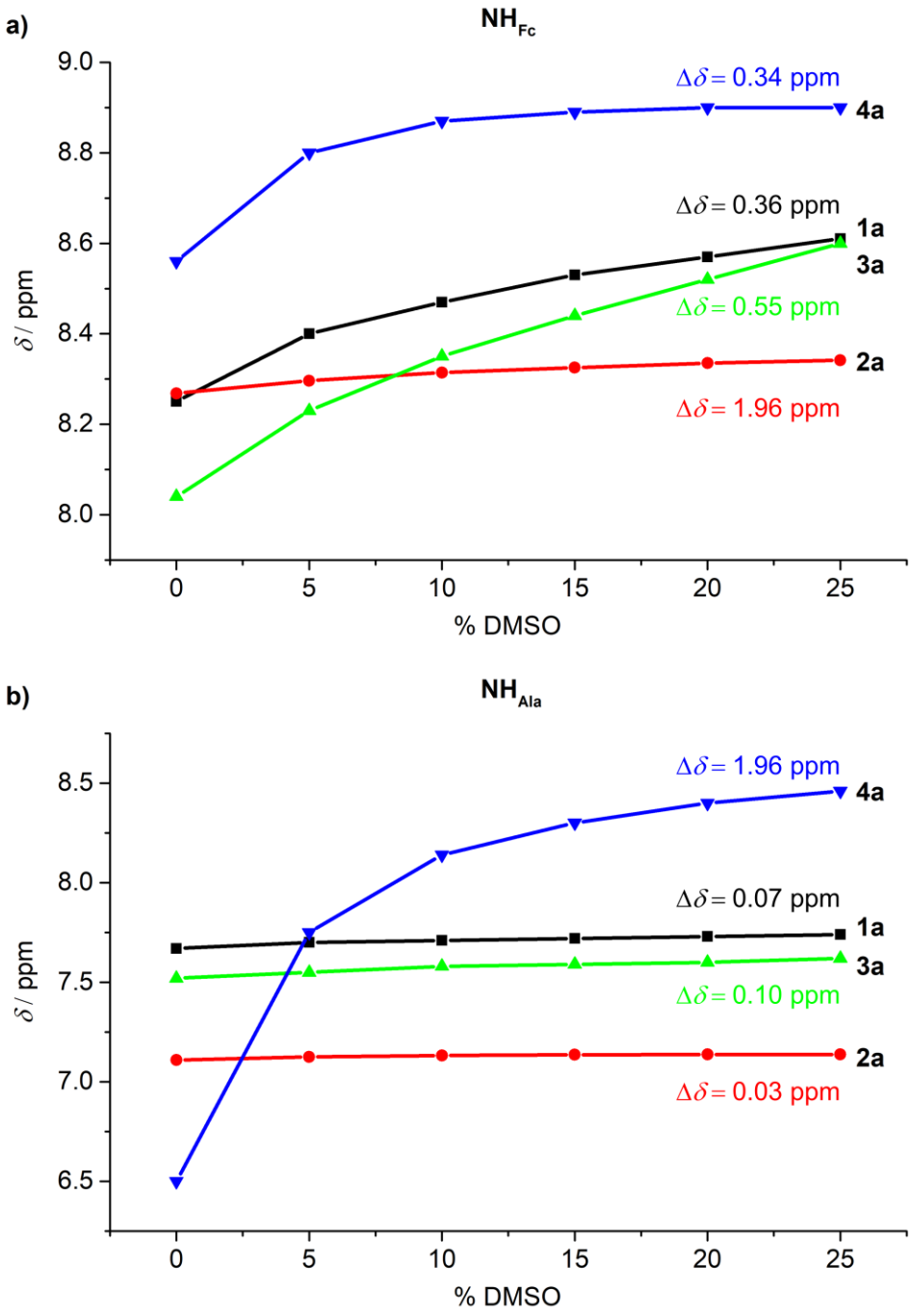

Figure S7. Solvent dependence of the amide proton chemical shifts of **1a**–**4a** while increasing concentration of *d*6-DMSO in $CDCl_3$ ($c = 1 \cdot 10^{-3}$ mol·dm^{-3}).

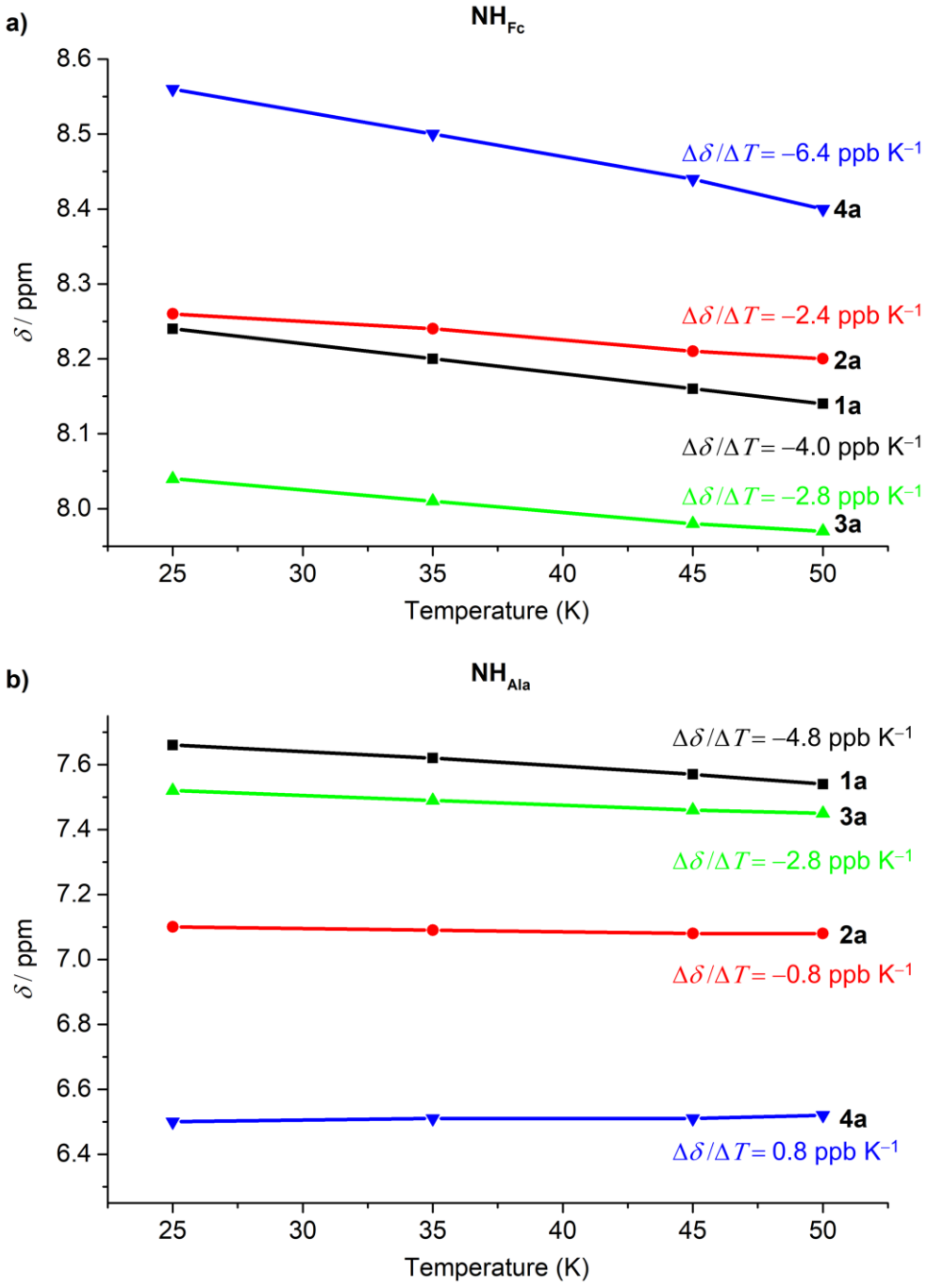

Figure S8. Temperature dependence of the amide proton chemical shifts for **1a**–**4a** in $CDCl_3$ ($c = 2 \cdot 10^{-3}$ mol·dm^{-3}).

Compound 1a

^{1}H NMR spectra

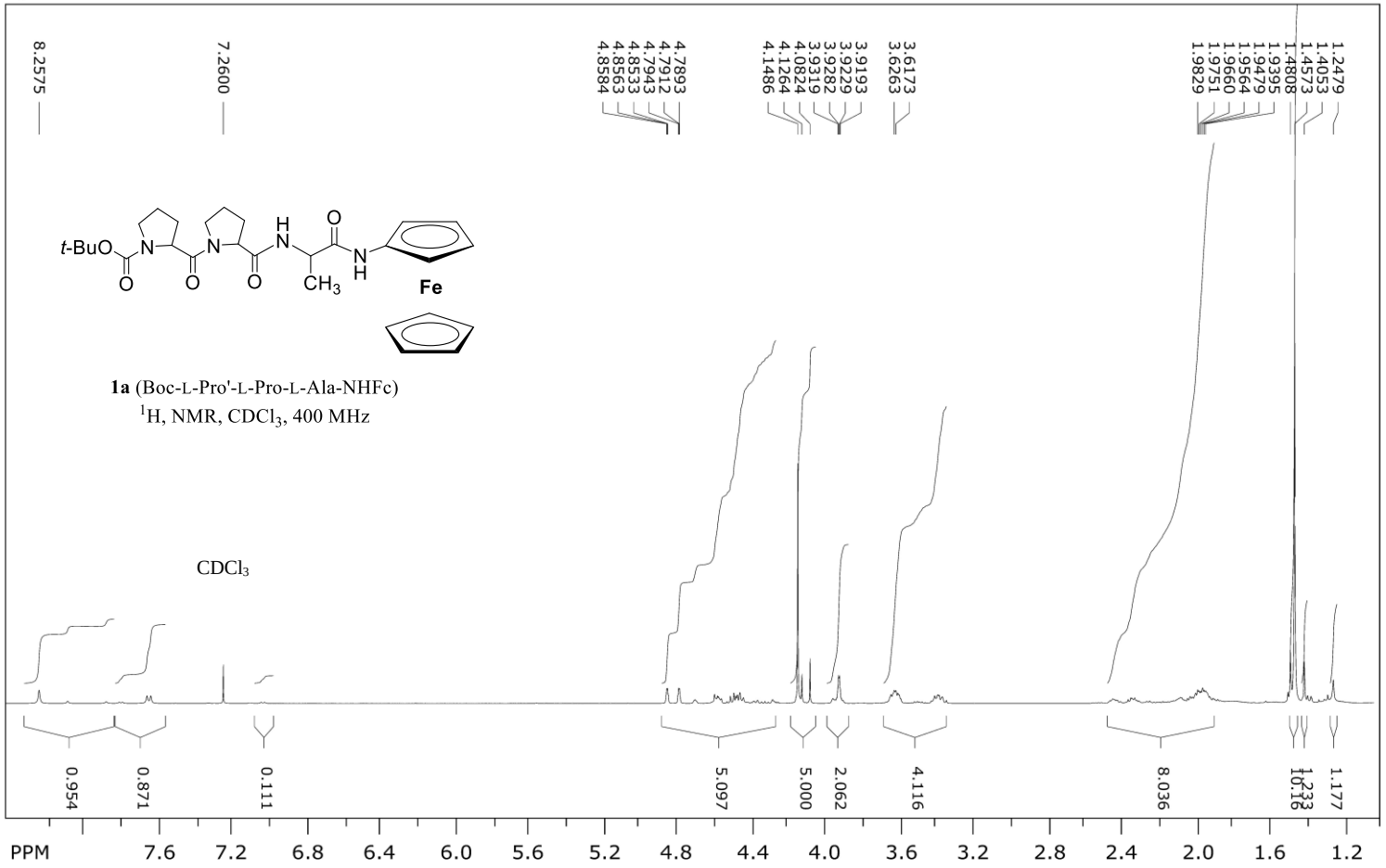

Figure S9. ^{1}H NMR spectrum, full range

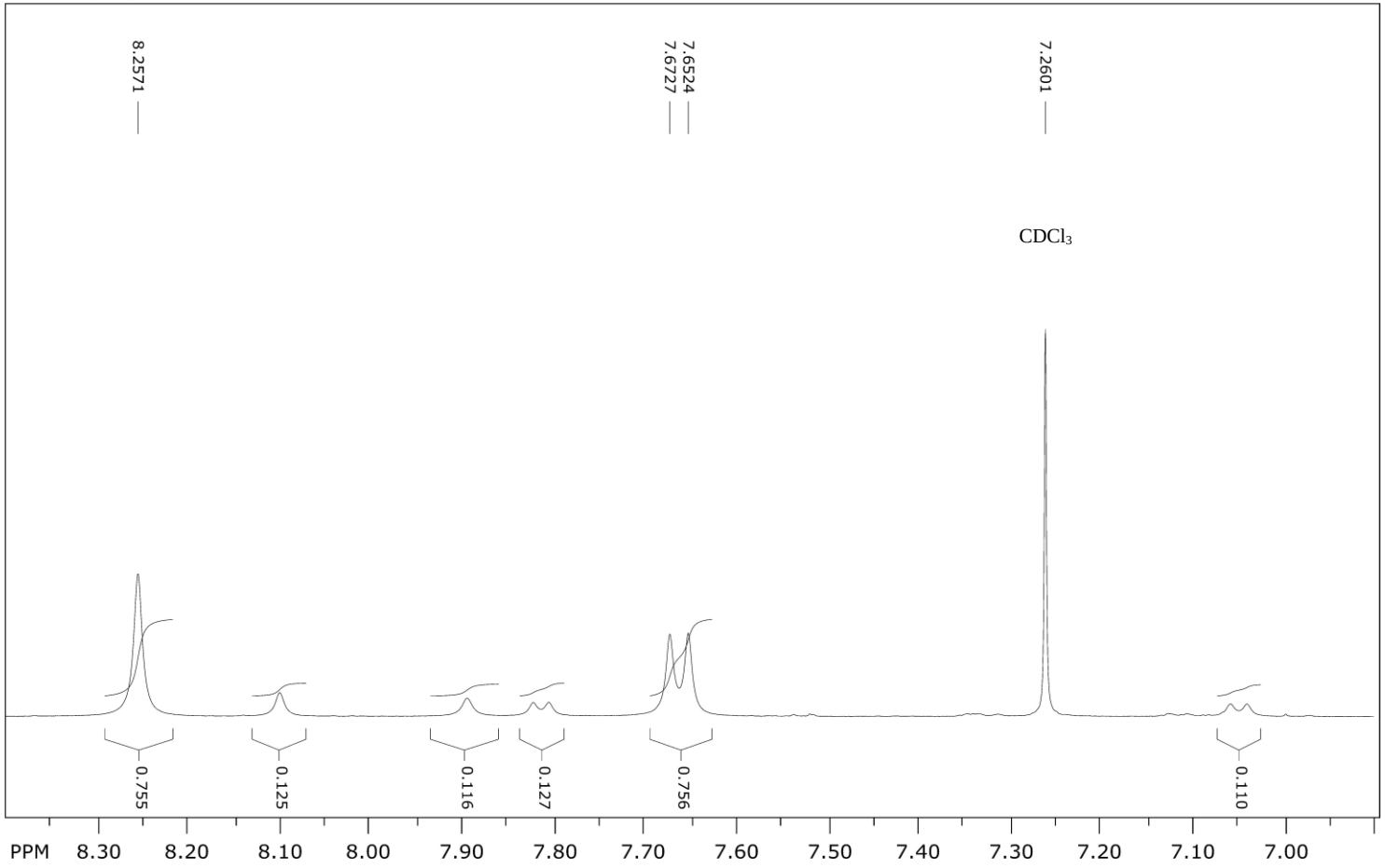

Figure S10. ^{1}H NMR spectrum, downfield range

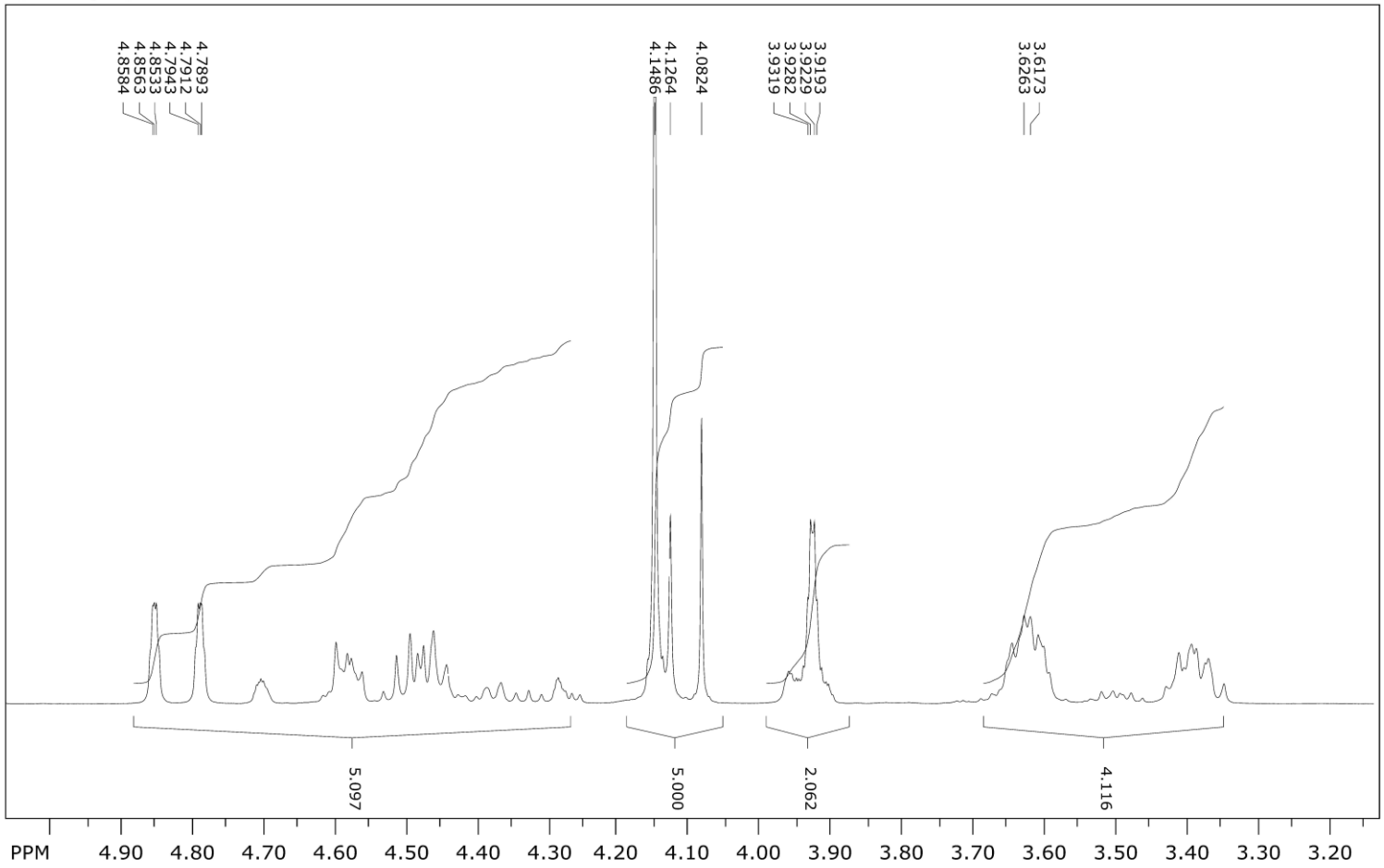

Figure S11. ^{1}H NMR spectrum, upfield range

^{13}C NMR spectra

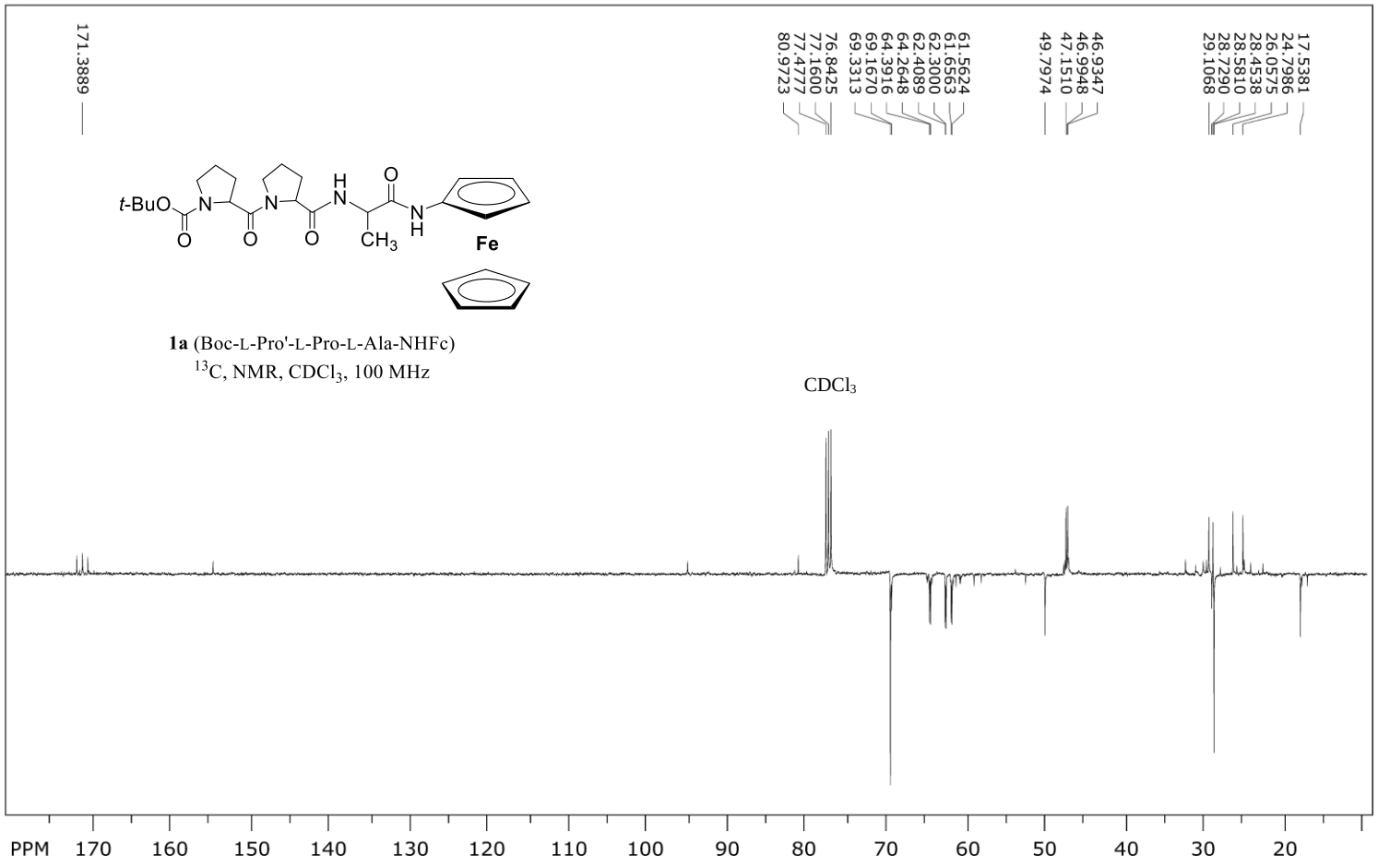

Figure S12. ^{13}C NMR spectrum, full range

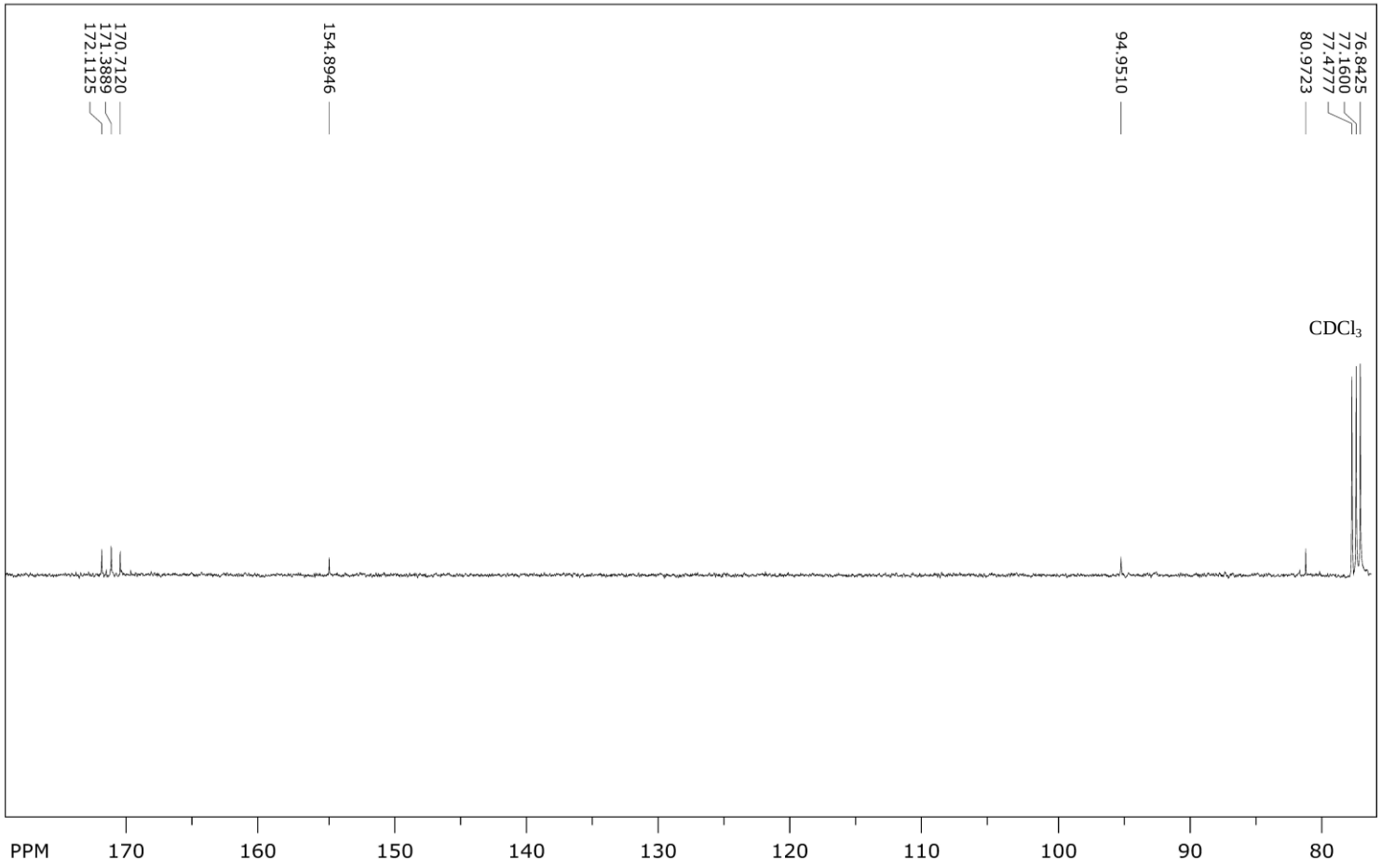

Figure S13. ^{13}C NMR spectrum, downfield range

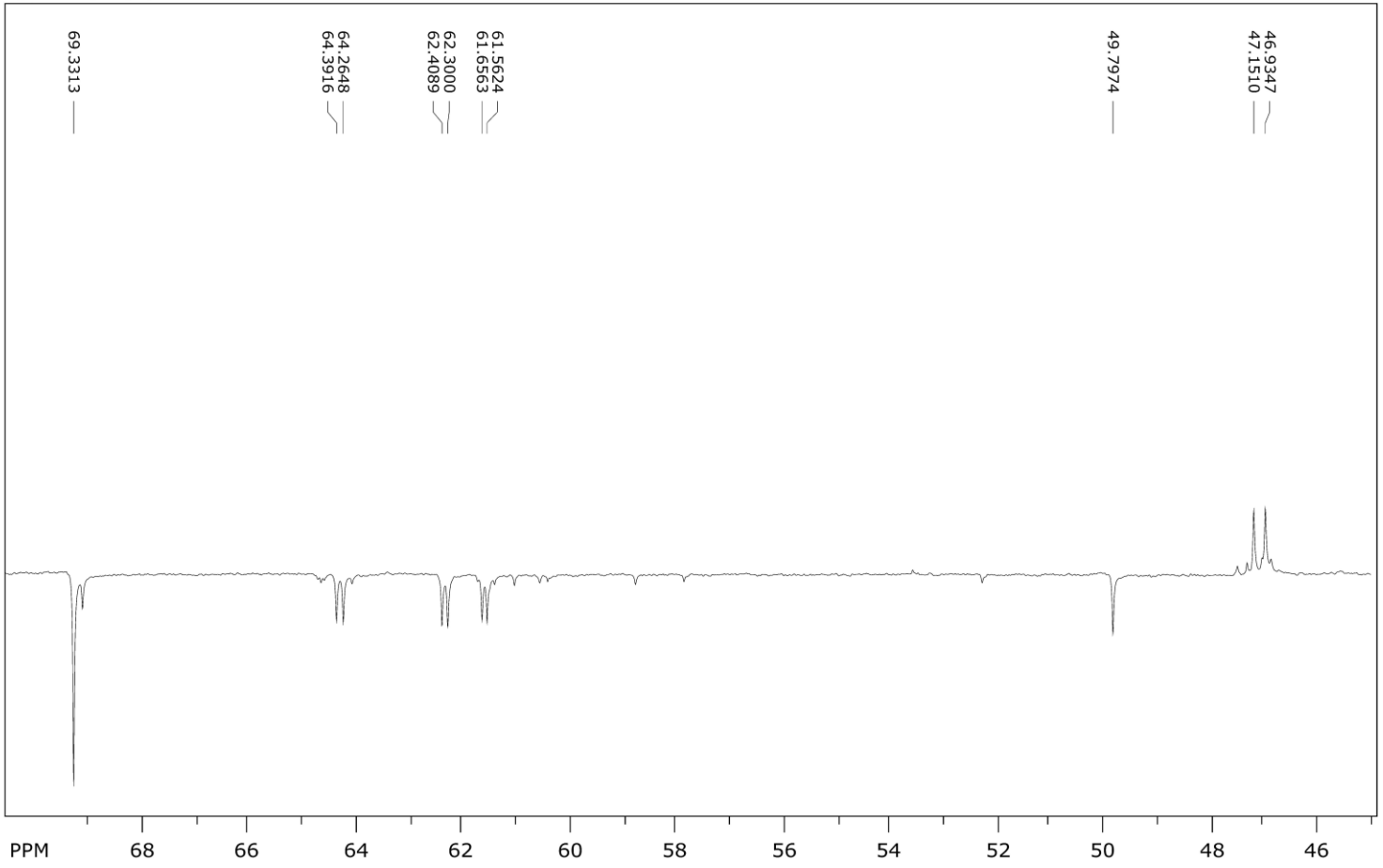

Figure S14. ^{13}C NMR spectrum, upfield range

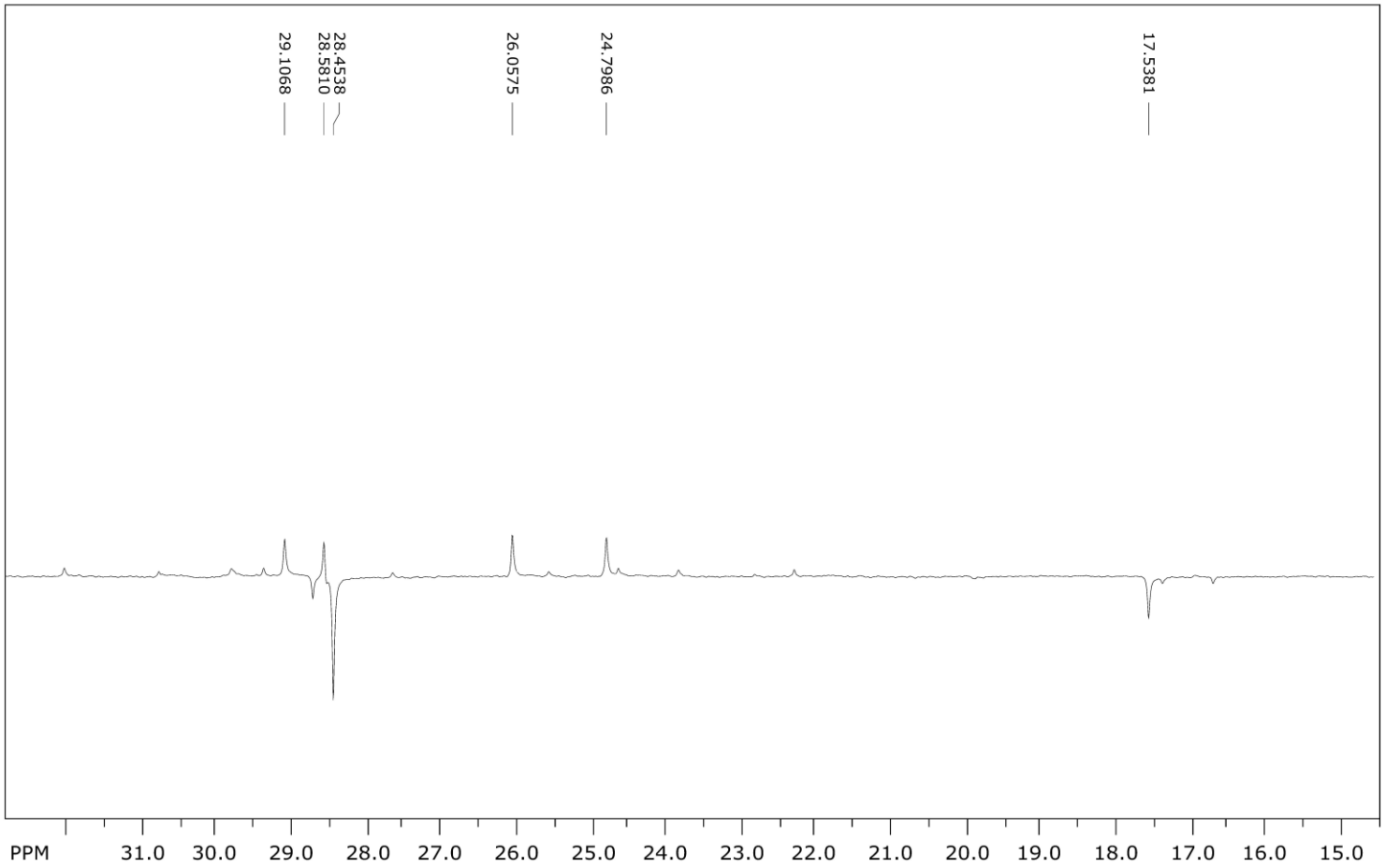

Figure S15. ^{13}C NMR spectrum, upfield range

Compound 2a

^{1}H NMR spectra

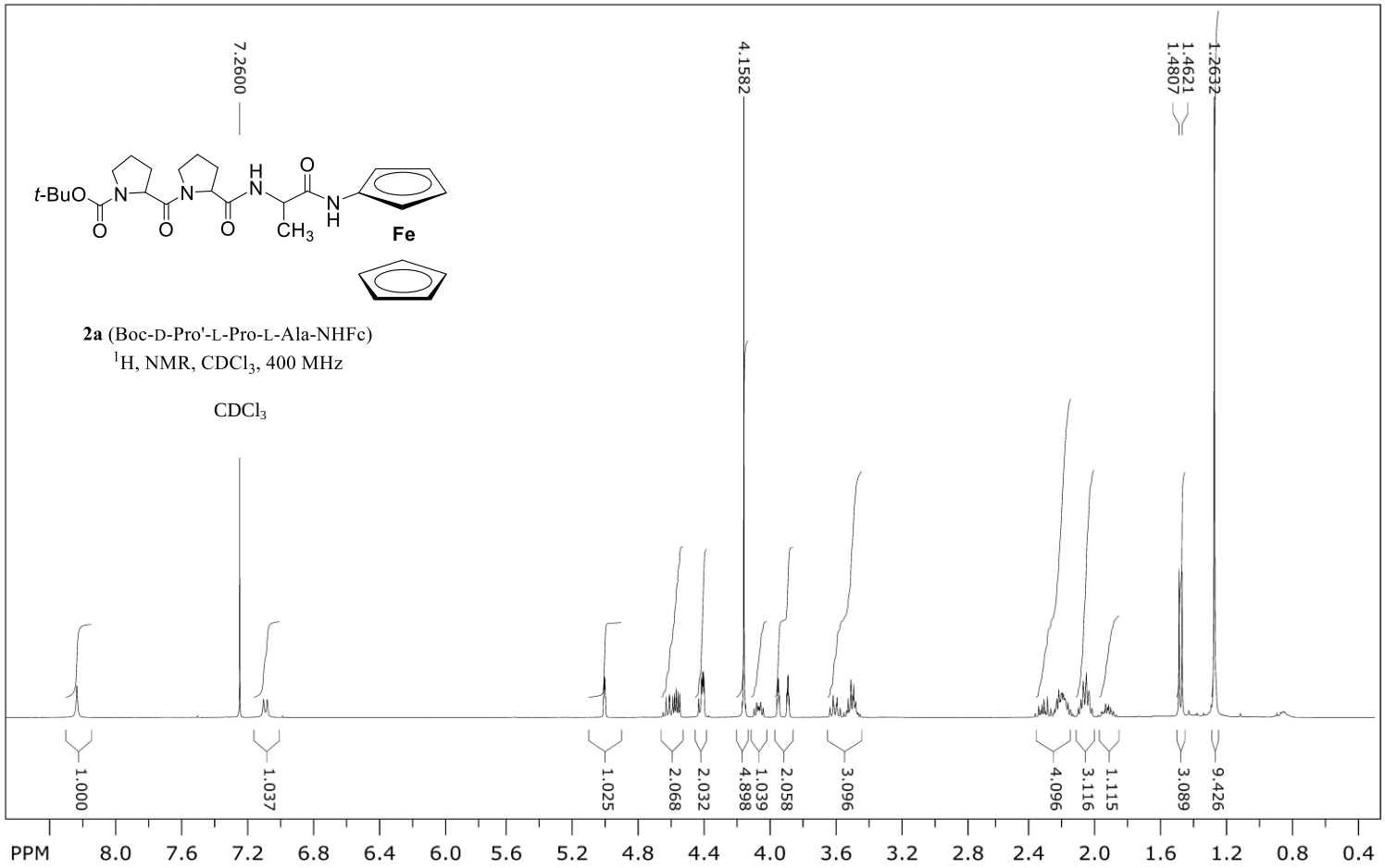

Figure S16. ^{1}H NMR spectrum, full range

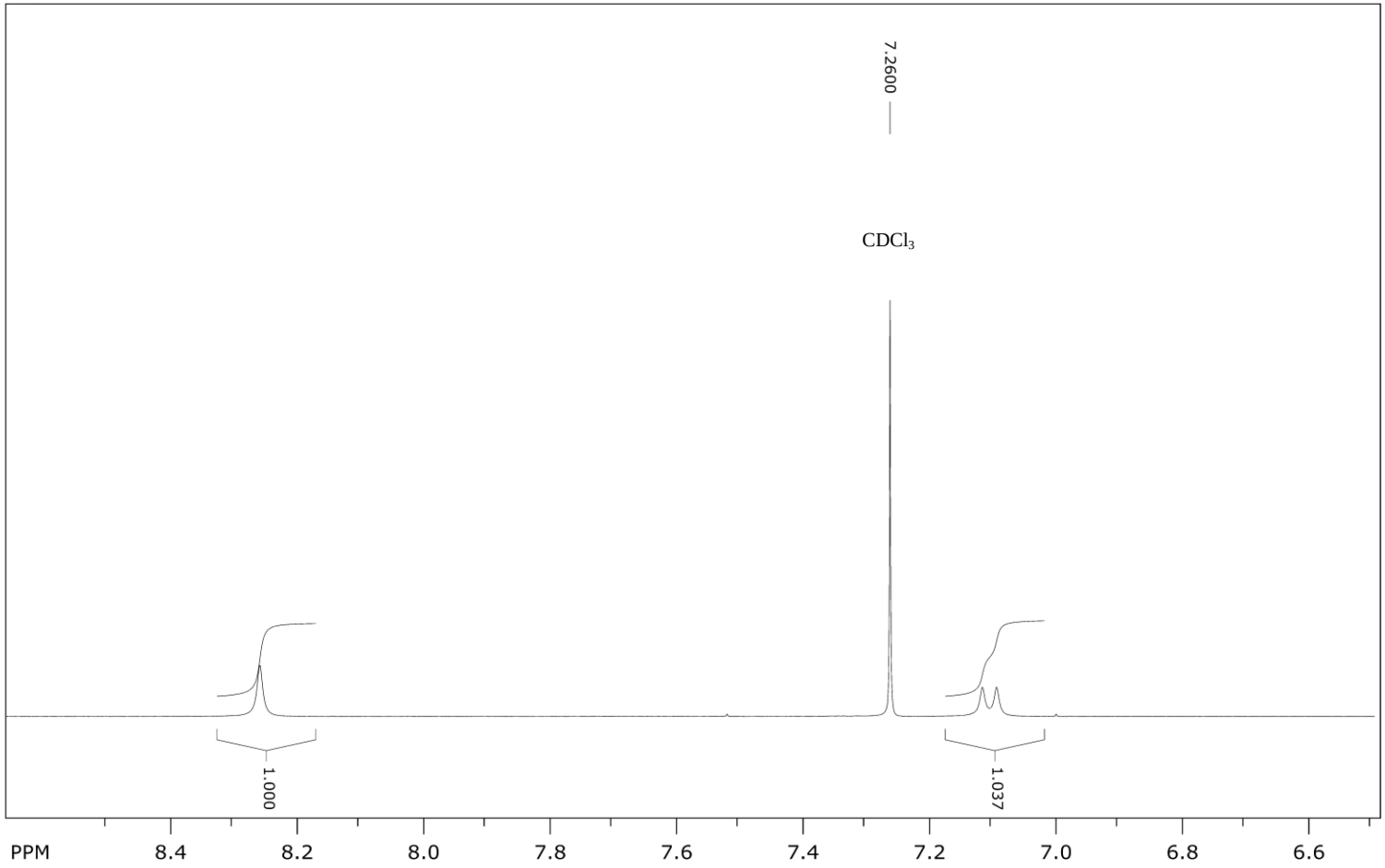

Figure S17. ^{1}H NMR spectrum, downfield range

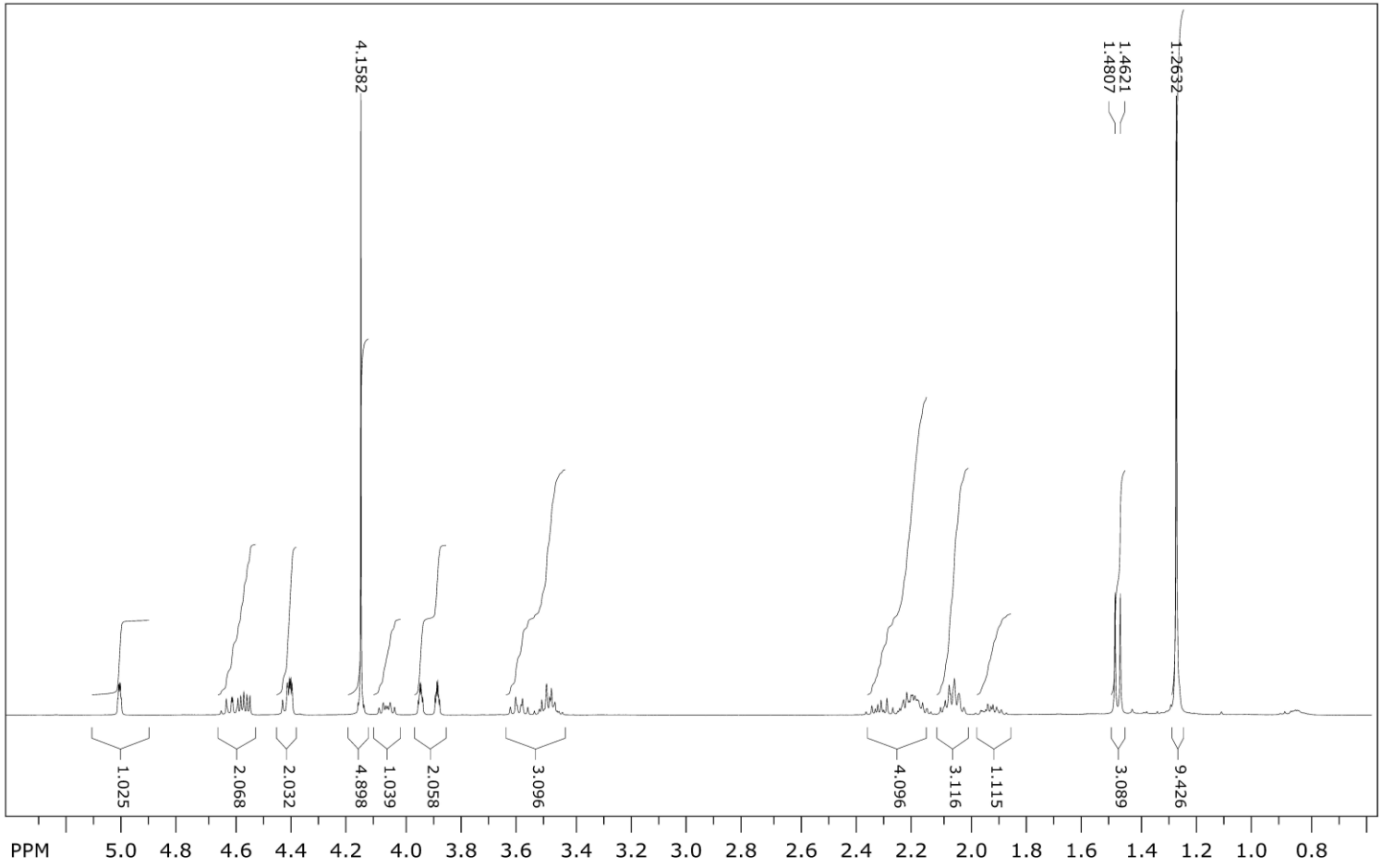

Figure S18. ^{1}H NMR spectrum, upfield range

^{13}C NMR spectra

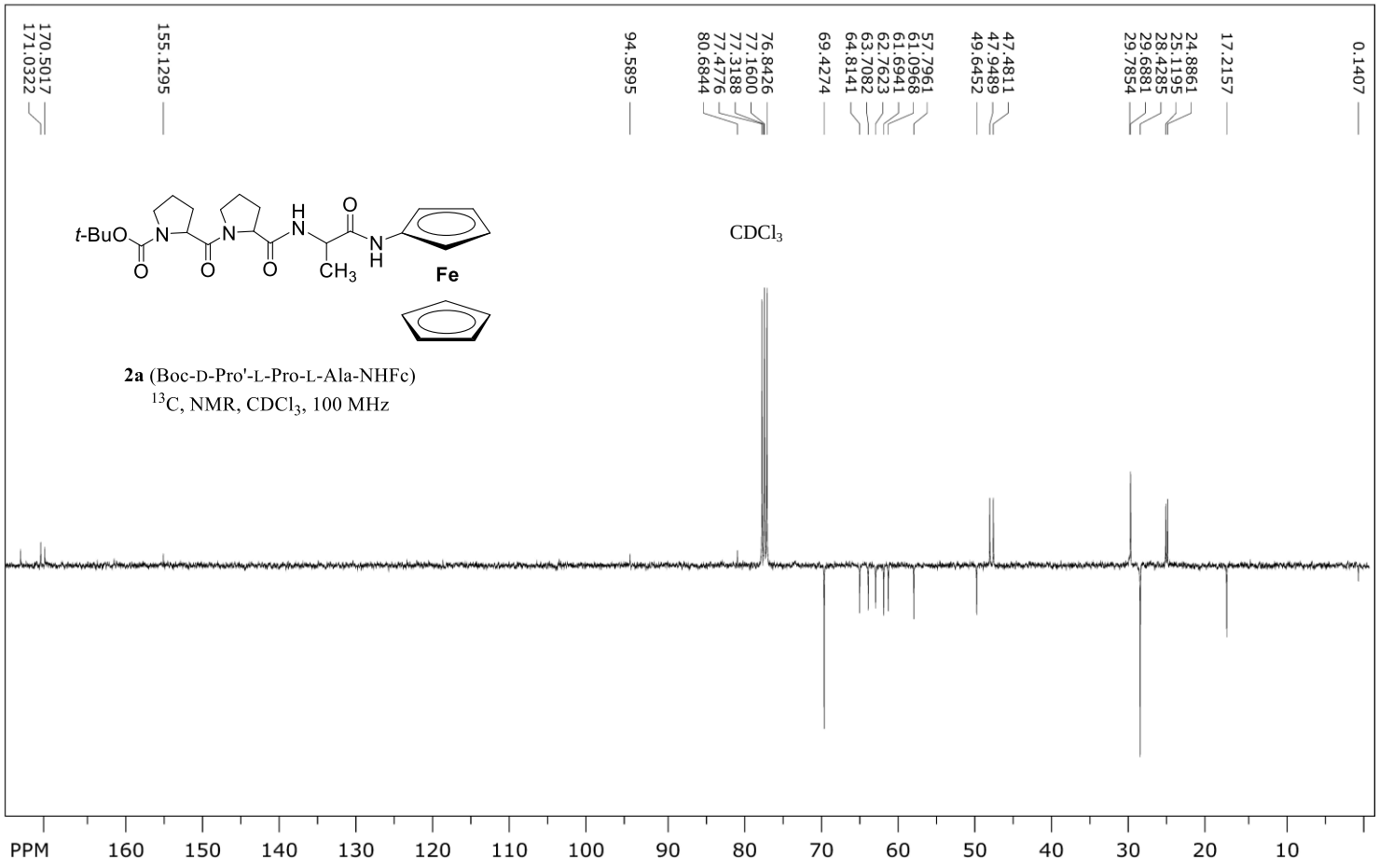

Figure S19. ^{13}C NMR spectrum, full range

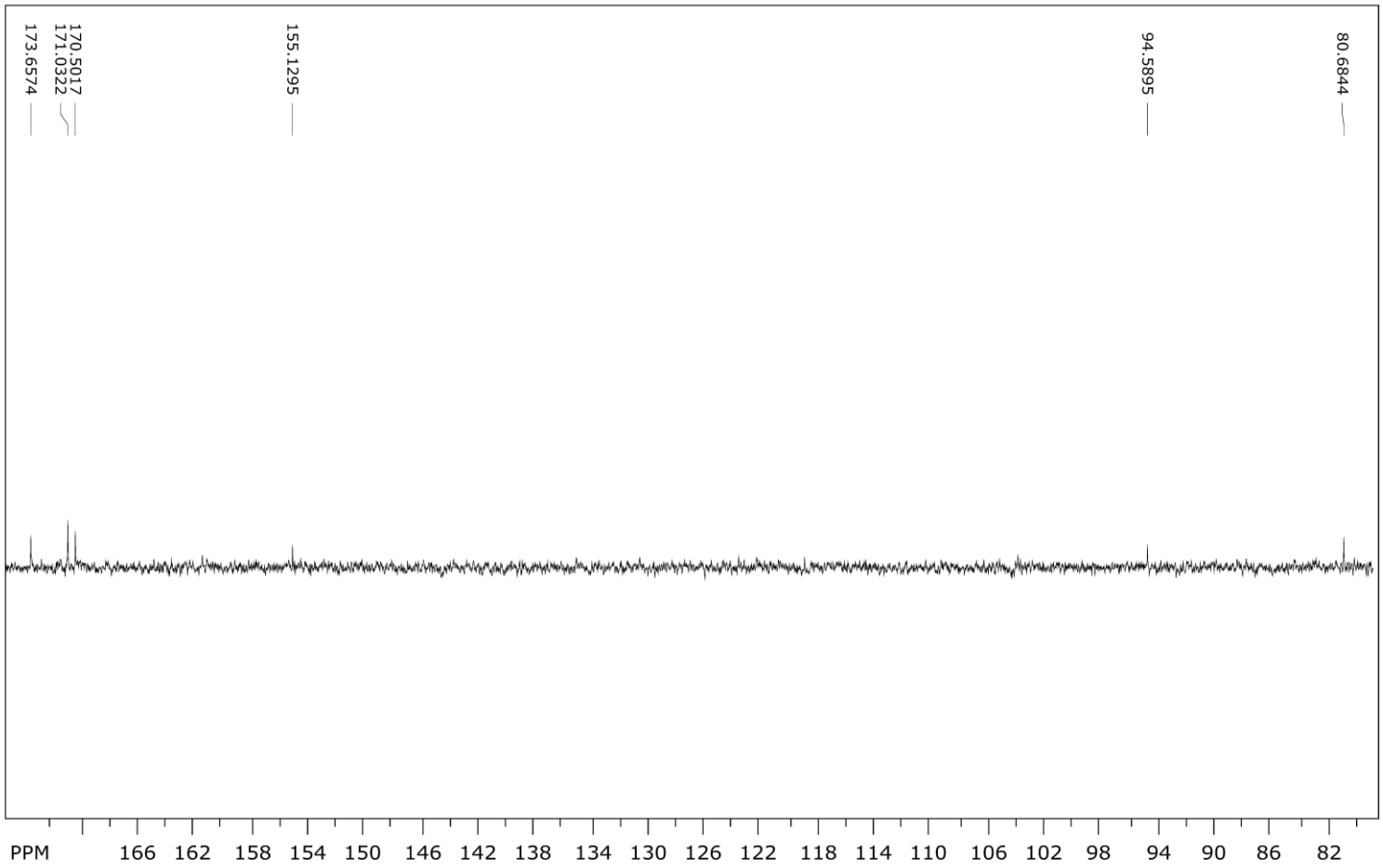

Figure S20. ^{13}C NMR spectrum, downfield range

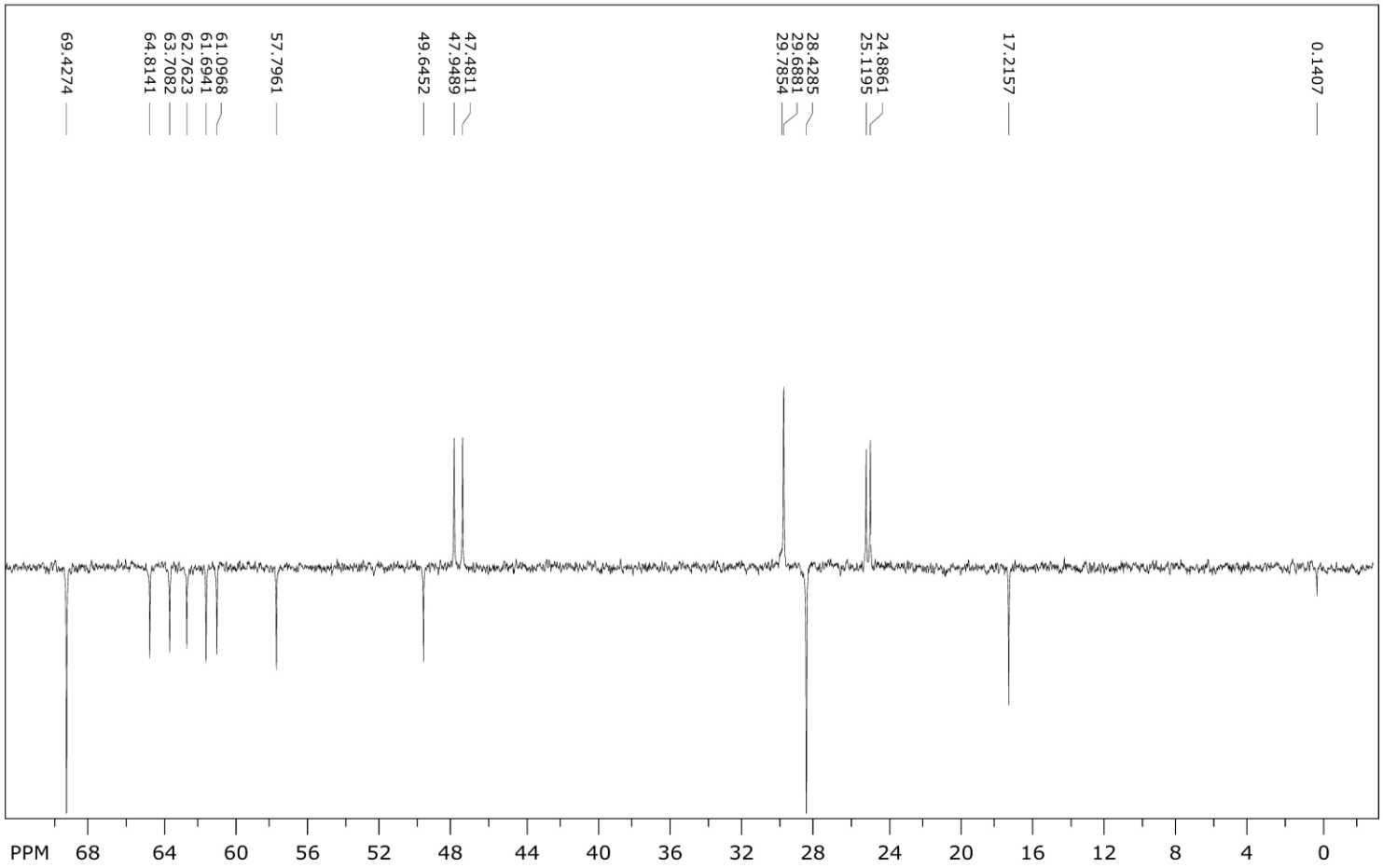

Figure S21. ^{13}C NMR spectrum, upfield range

Compound 3a

^{1}H NMR spectra

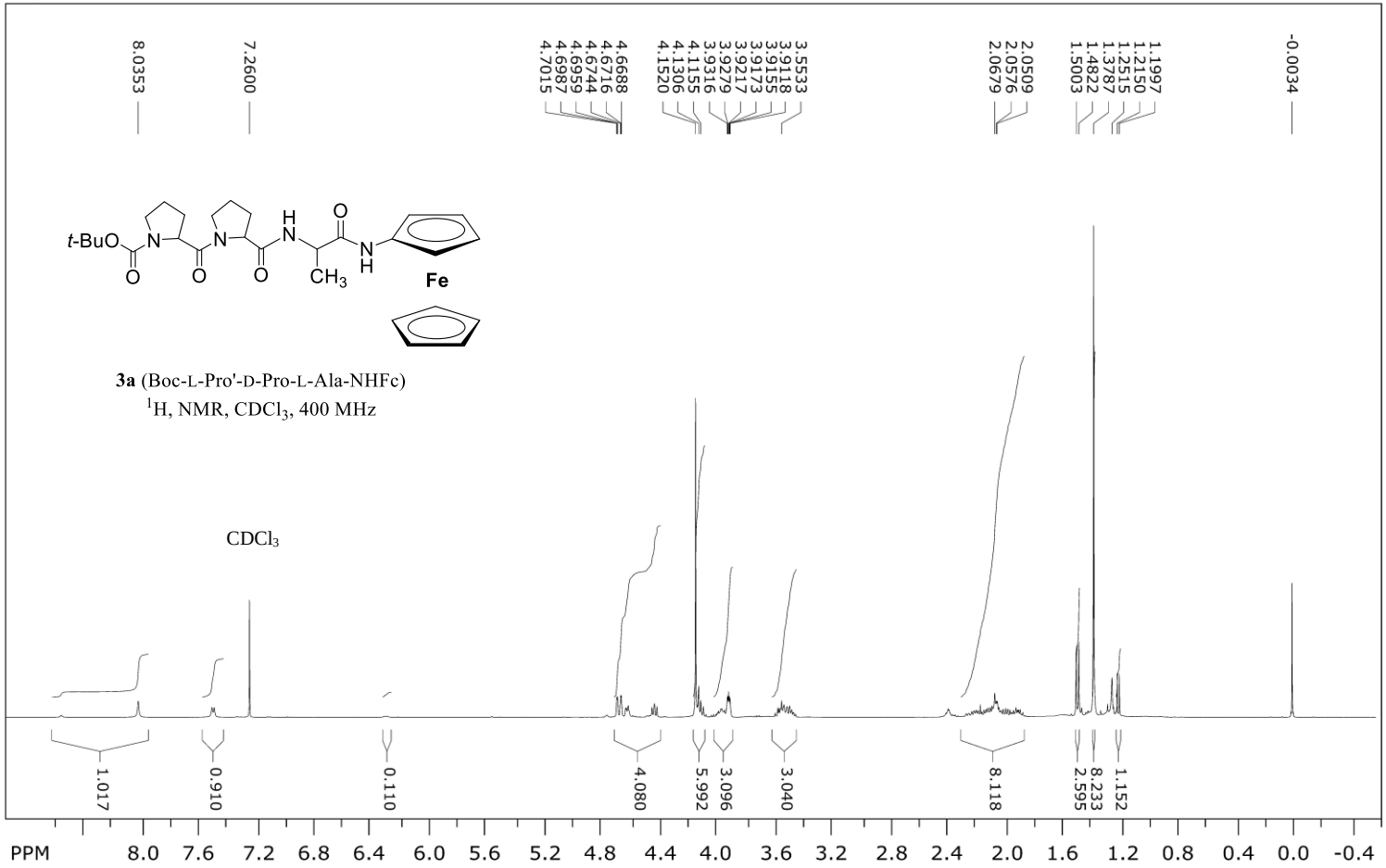

Figure S22. ^{1}H NMR spectrum, full range

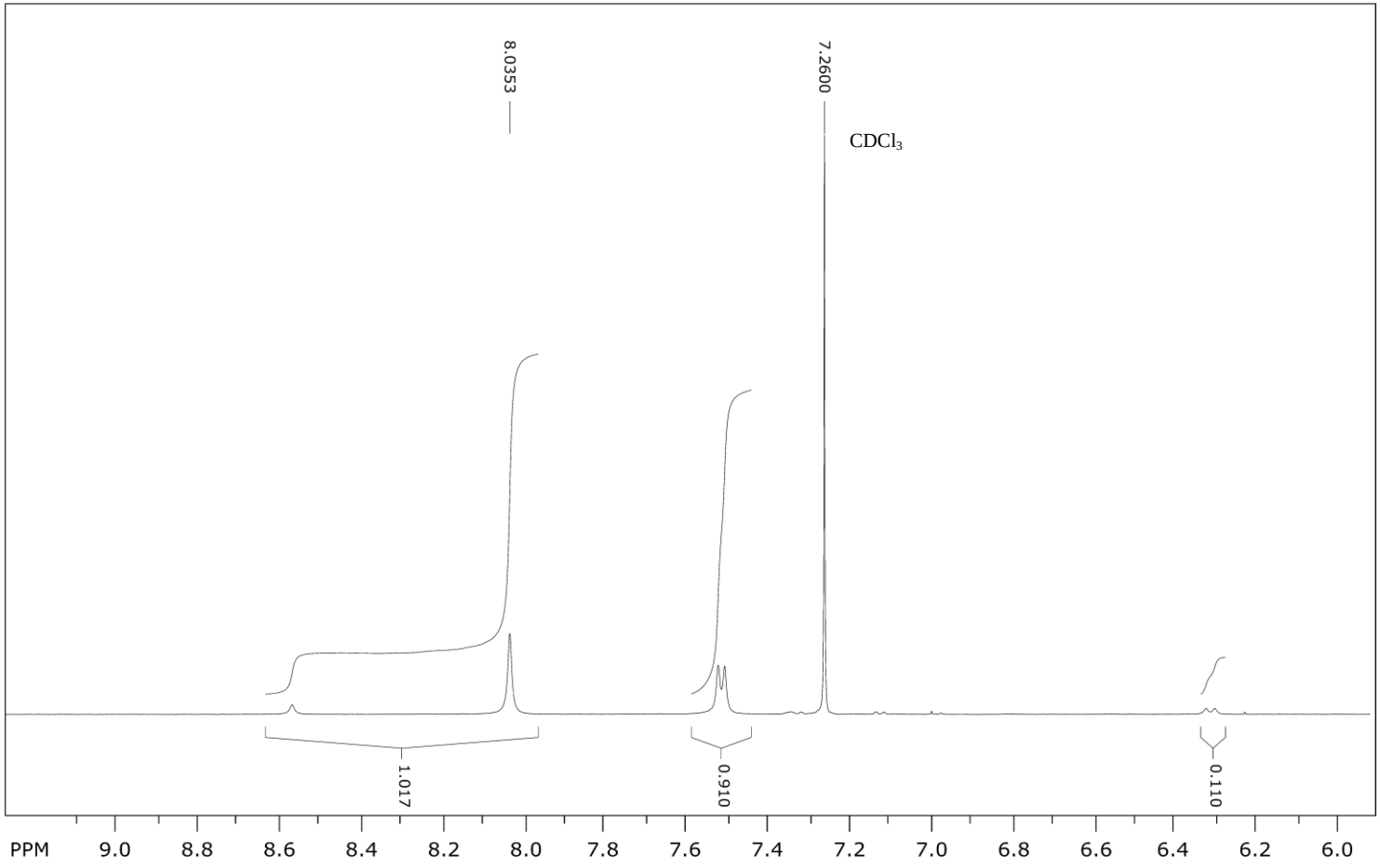

Figure S23. ^{1}H NMR spectrum, downfield range

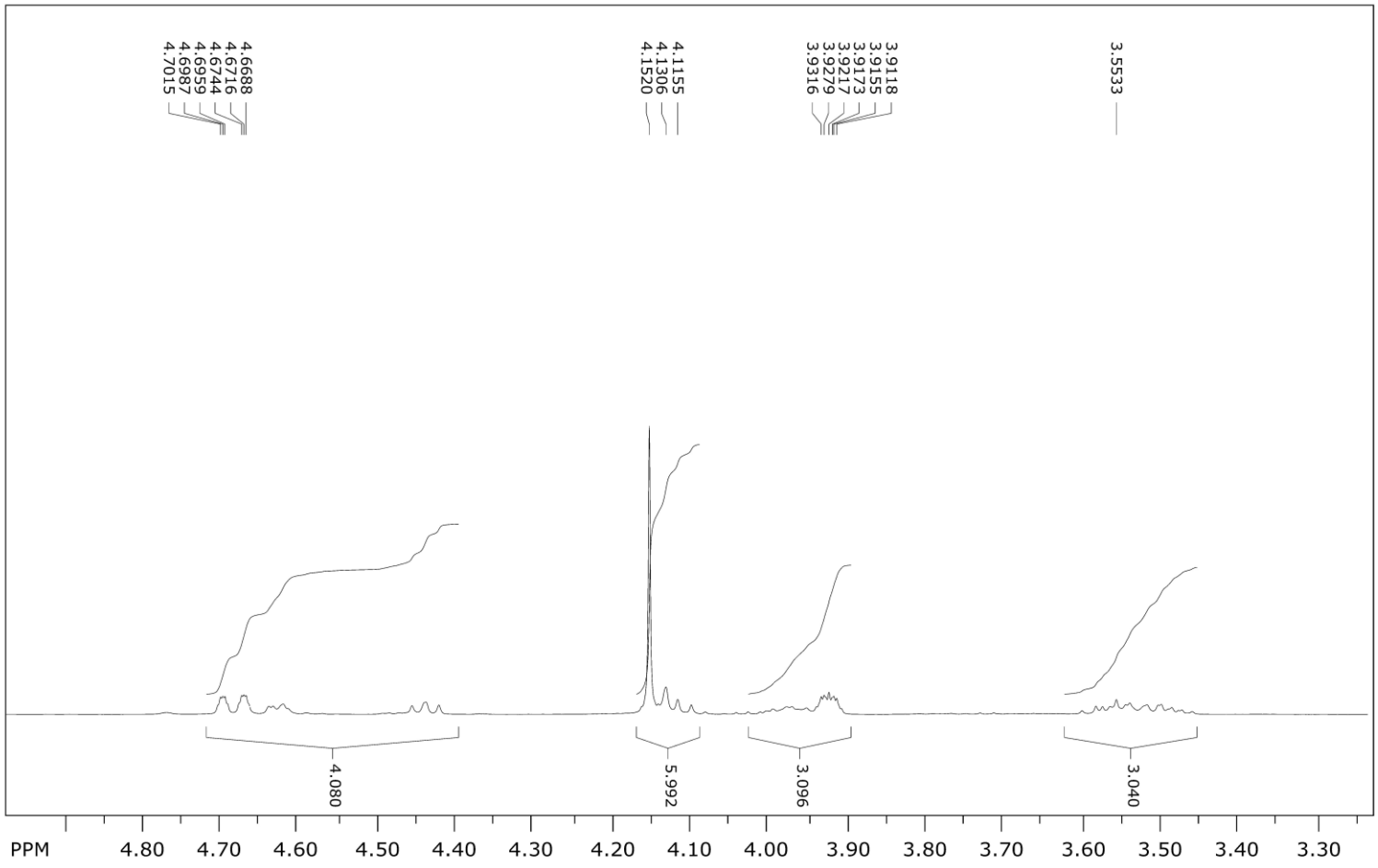

Figure S24. ^{1}H NMR spectrum, upfield range

^{13}C NMR spectra

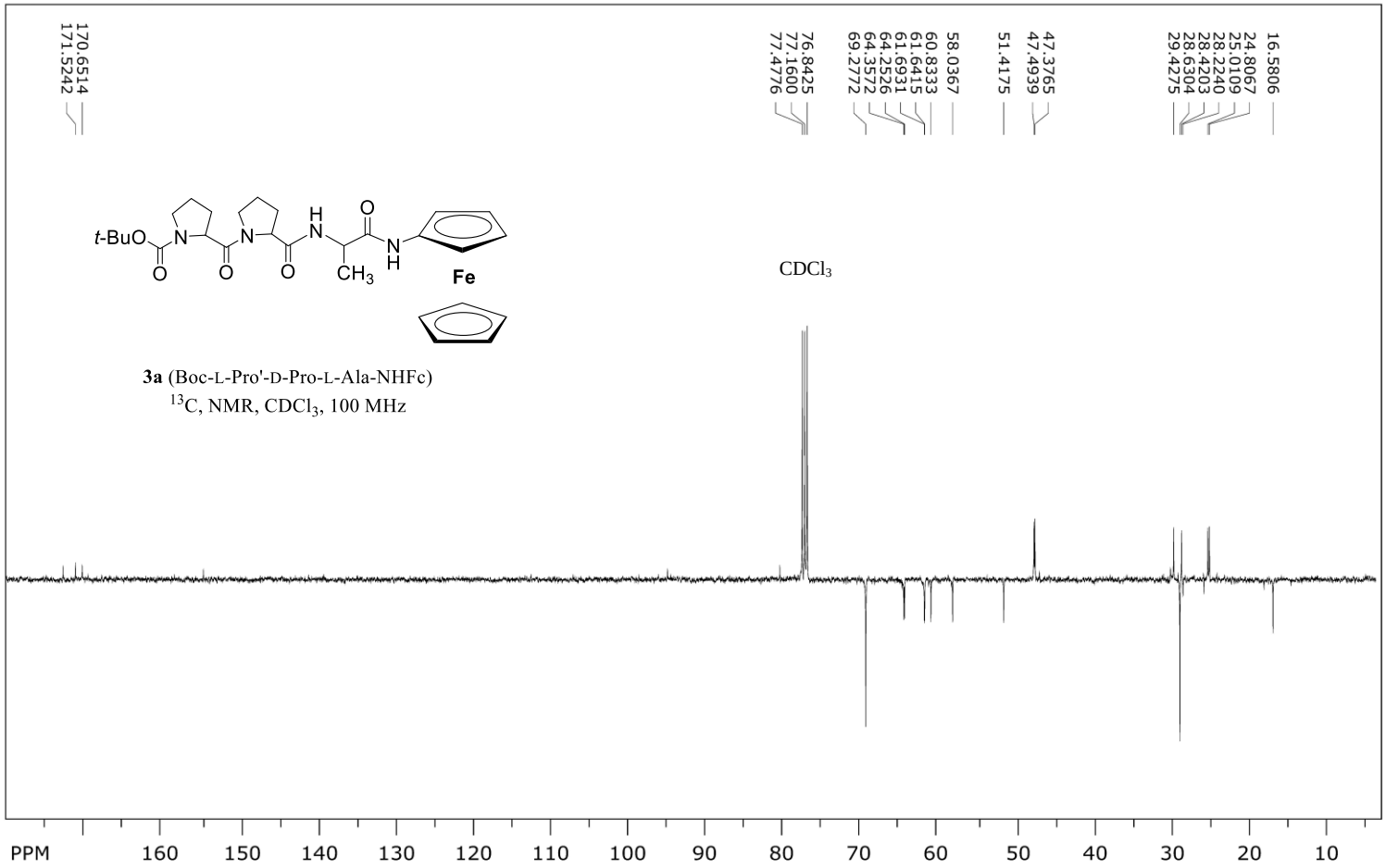

Figure S25. ^{13}C NMR spectrum, full range

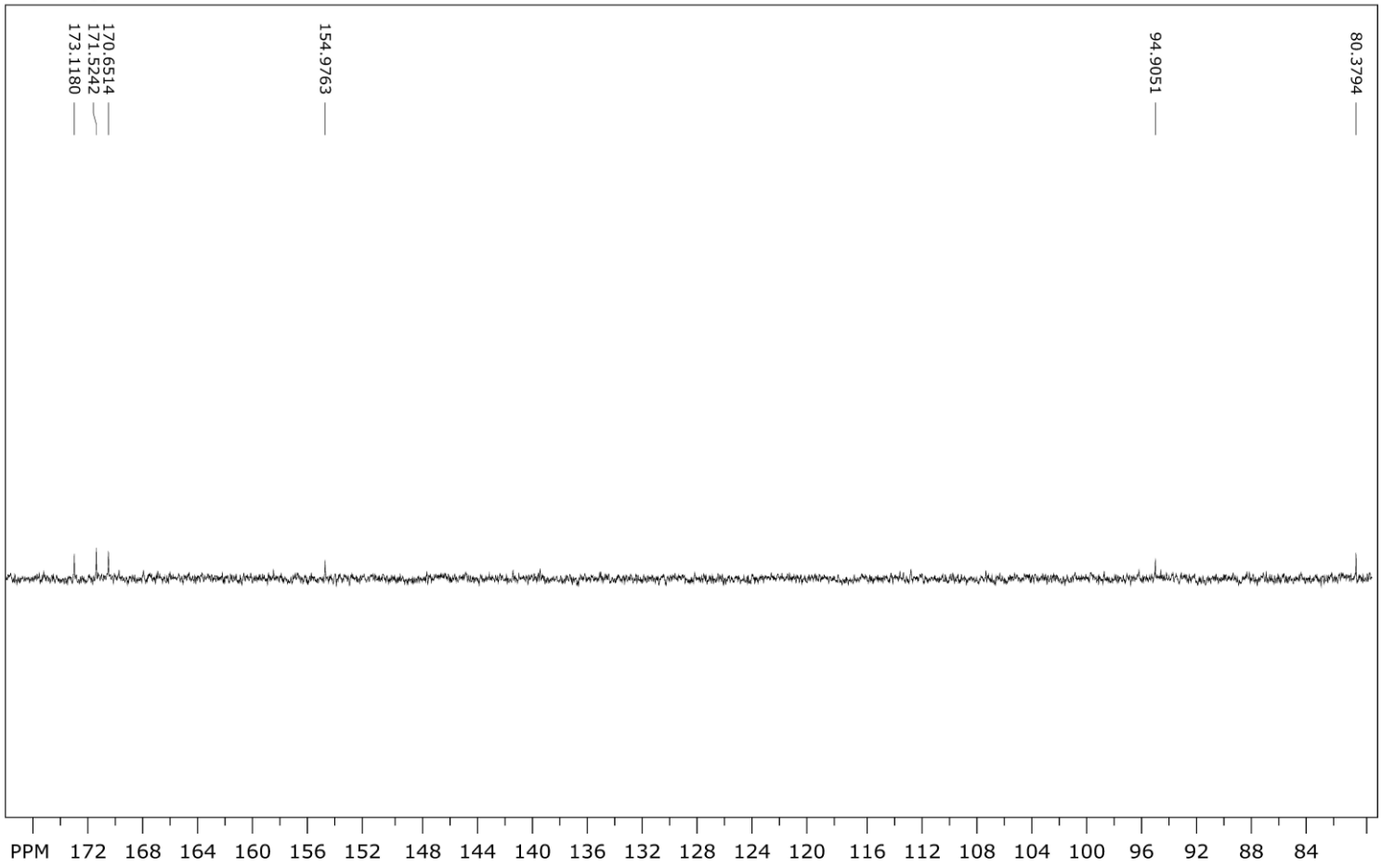

Figure S26. ^{13}C NMR spectrum, downfield range

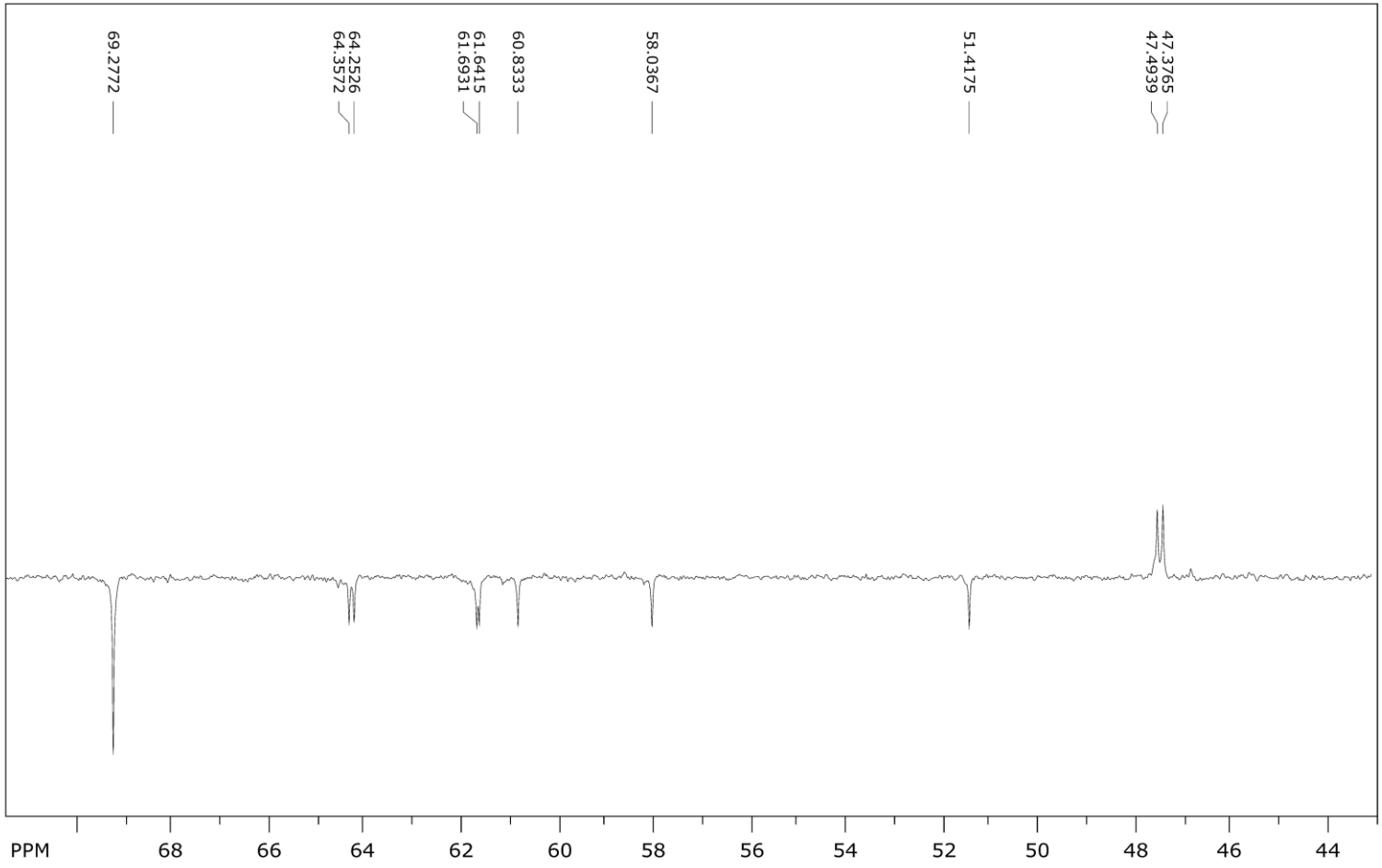

Figure S27. ^{13}C NMR spectrum, upfield range

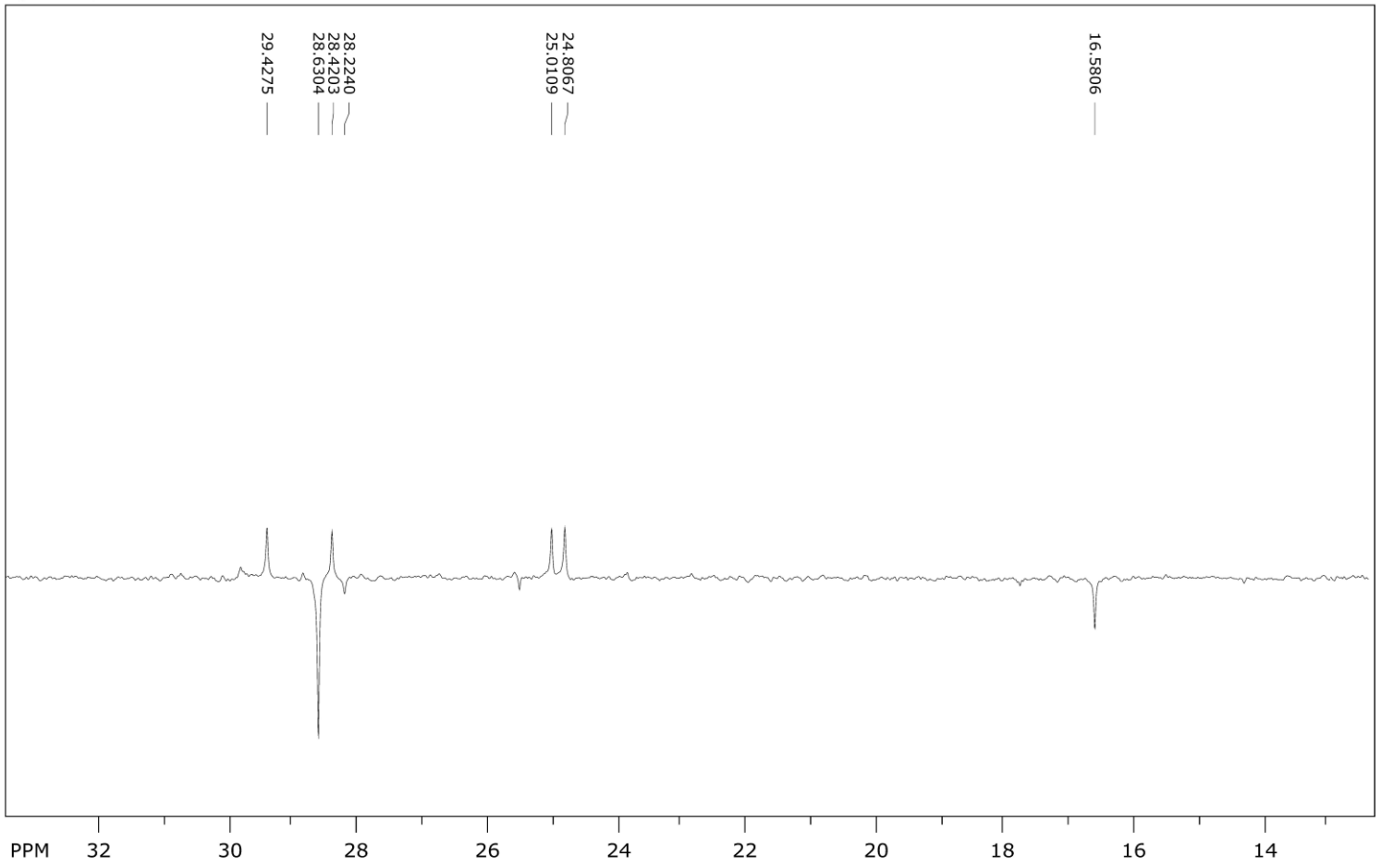

Figure S28. ^{13}C NMR spectrum, upfield range

Compound 4a

^{1}H NMR spectra

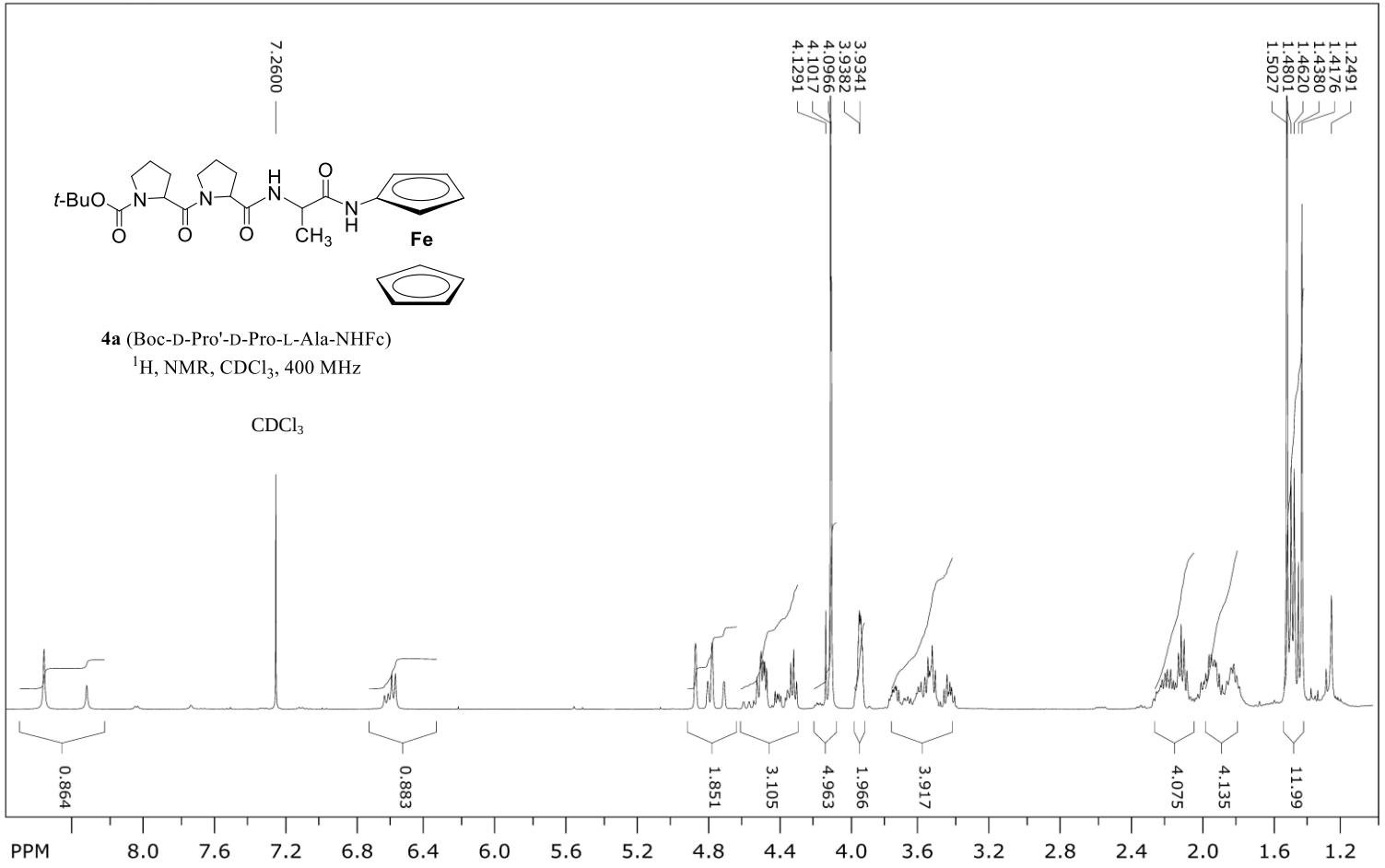

Figure S29. ^{1}H NMR spectrum, full range

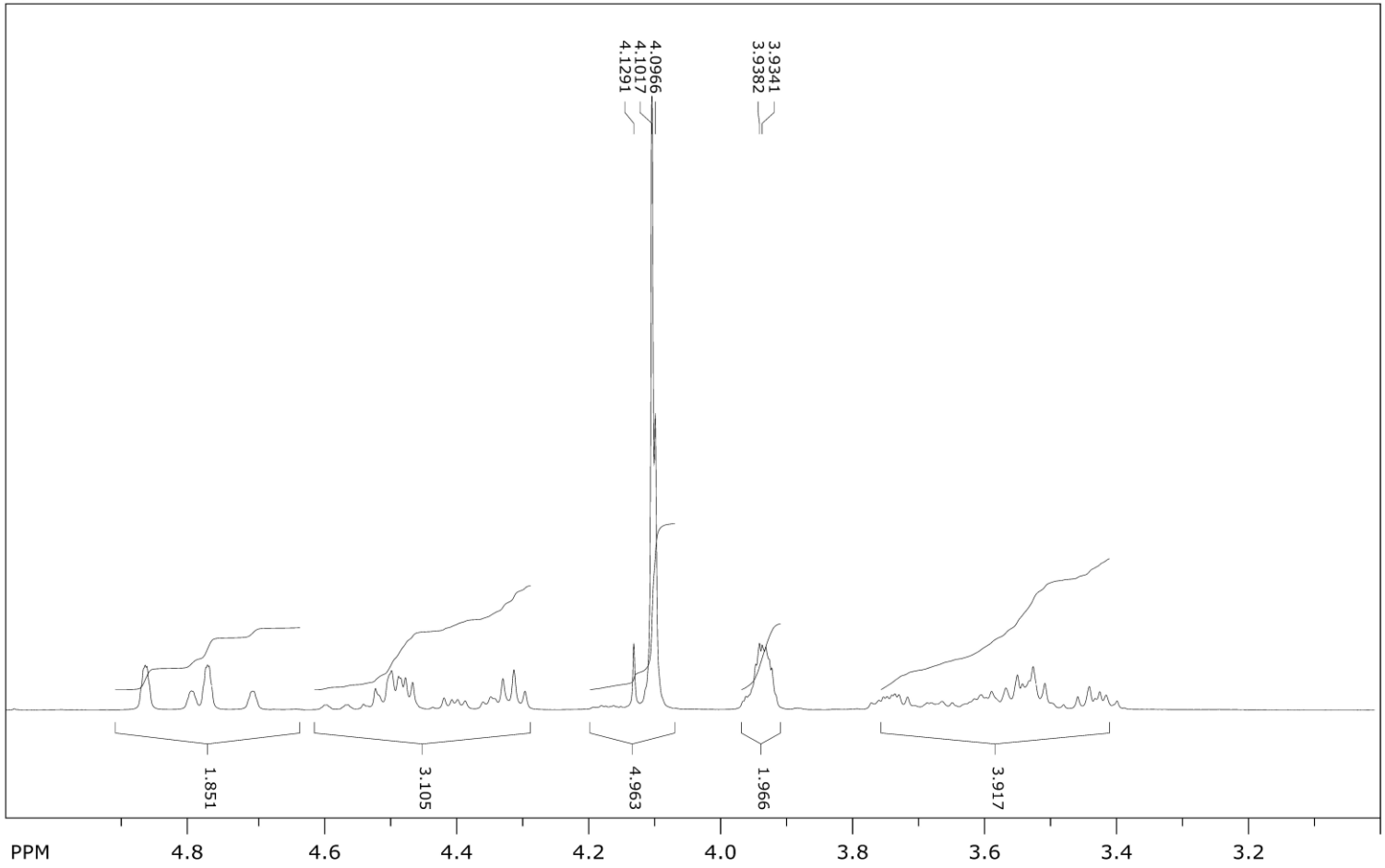

Figure S30. ^{1}H NMR spectrum, upfield range

^{13}C NMR spectra

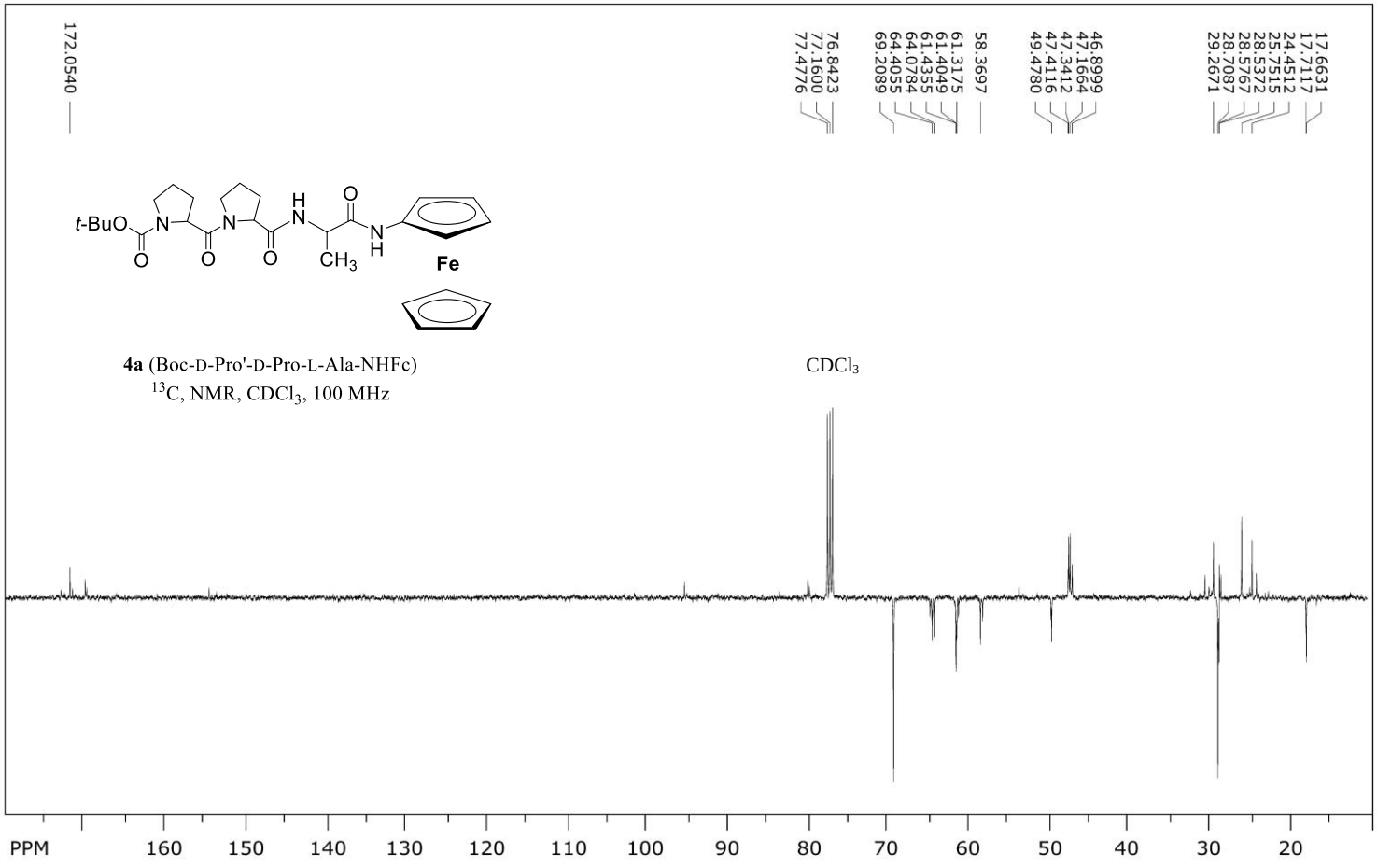

Figure S31. ^{13}C NMR spectrum, full range

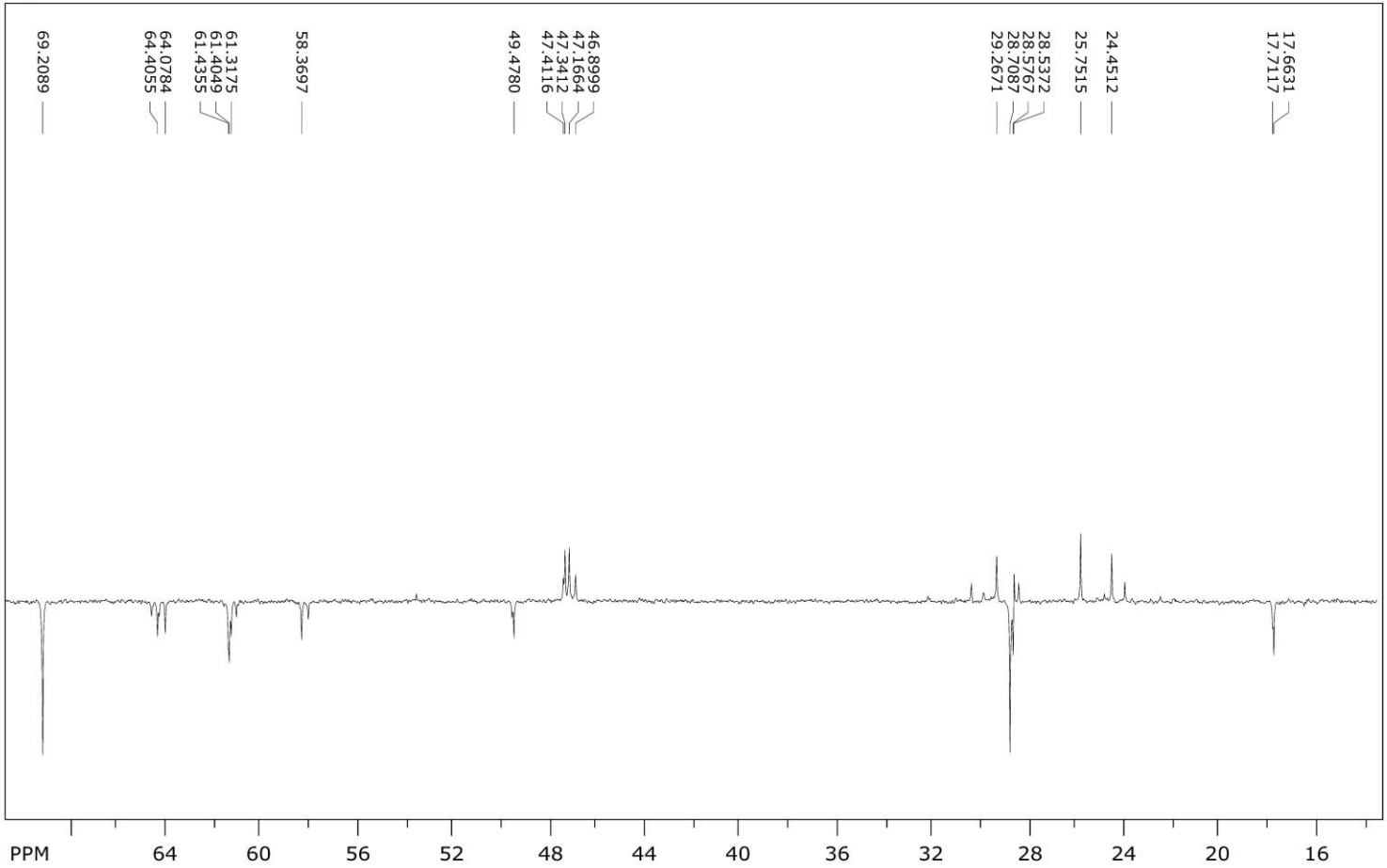

Figure S32. ^{13}C NMR spectrum, upfield range

Cis-trans isomerization of proline imide bonds of compounds 1a-4a.

Table S2. Influence of temperature and volume fraction of DMSO on *cis-trans* isomerization of proline imide bonds of compounds **1a-4a**.

	Temperature							
	298.15 K		**308.15 K**		**318.15 K**		**323.15 K**	
	trans-trans isomer (%)	other isomers (%)	*trans-trans* isomer (%)	other isomers (%)	*trans-trans* isomer (%)	other isomers (%)	*trans-trans* isomer (%)	other isomers (%)
1a	76	13, 11	71	16, 12	66	18, 16	66	18, 16
2a	100	-	100	-	100	-	100	-
3a	87	13	85	15	82	18	83	17
4a	67	27, 6	52	26, 22	48	27, 25	45	30, 25

Table S3. Influence of temperature and volume fraction of DMSO on *cis-trans* isomerization of proline imide bonds of compounds **1a-4a**.

	φ (DMSO)									
	0.5		**0.9**		**0.13**		**0.17**		**0.2**	
	trans-trans isomer (%)	other isomers (%)	*trans-trans* isomer (%)	other isomers (%)	*trans-trans* isomer (%)	other isomers (%)	*trans-trans* isomer (%)	other isomers (%)	*trans-trans* isomer (%)	other isomers (%)
1a	83	17	63	25, 12	60	31, 9	60	31, 9	52	35, 13
2a	100	-	100	-	100	-	100	-	100	
3a	75	25	62	34, 4	46	28, 14, 12	41	35, 14, 10	40	39, 12, 9
4a	67	33	63	37	64	36	58	42	58	42

NOESY spectra

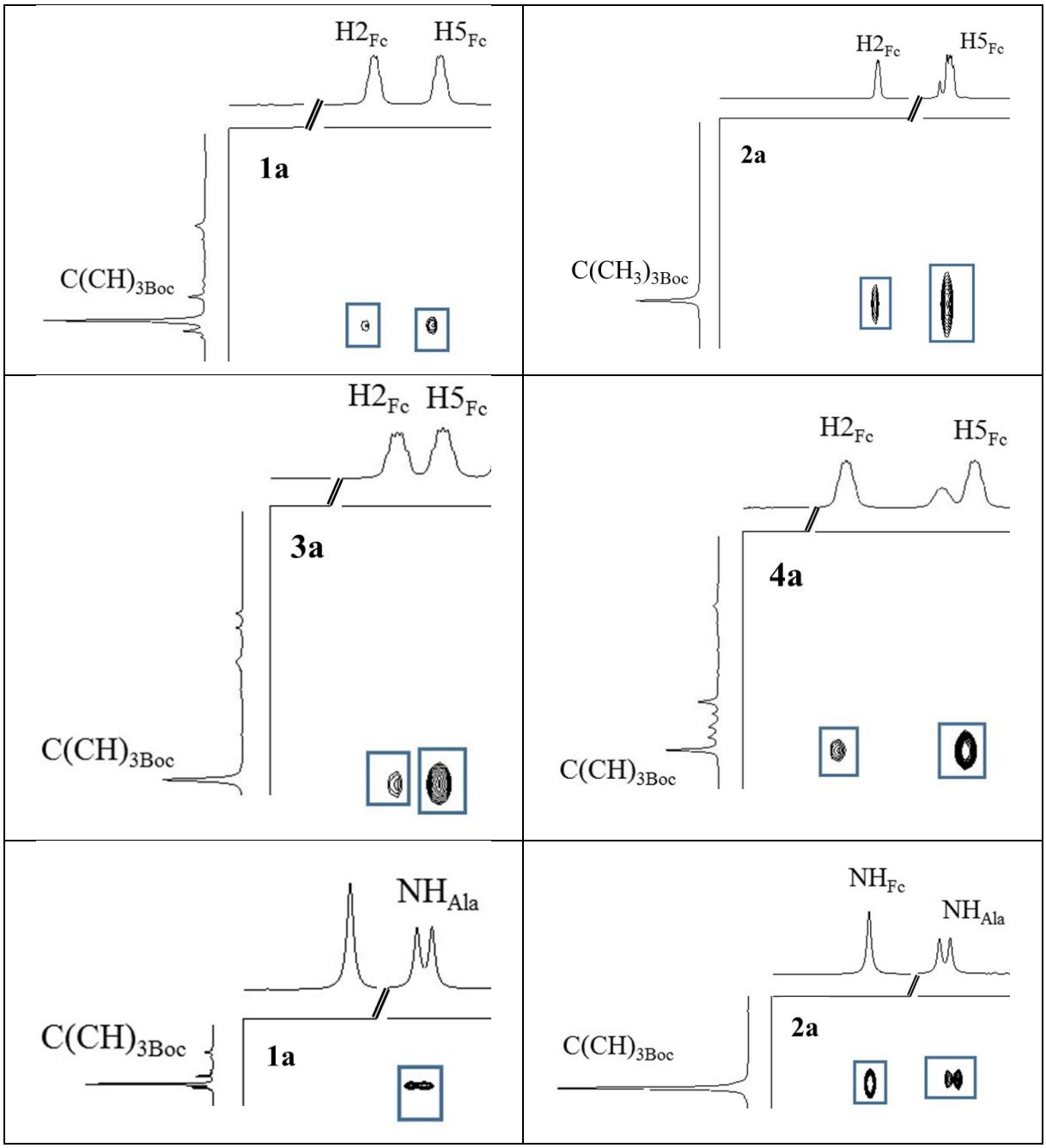

Figure S33. Long [$C(CH_3)_3$-$H2_{Fc}$/$H5_{Fc}$ i $C(CH_3)_3$-NH_{Fc}] and medium range [$C(CH_3)_3$-NH_{Ala}] NOE contacts in spectra of **1a**-**4a**.

Boc-D-Pro-L-Ala-NH-Fn-COOMe (2)

Ion type	Calc. mass	Measured mass	Mass error / ppm	Mol. Formula	Int. CAL
M+	527.1719	527.1708	2.1	$C_{25}H_{33}N_3O_6Fe$	azitromicin

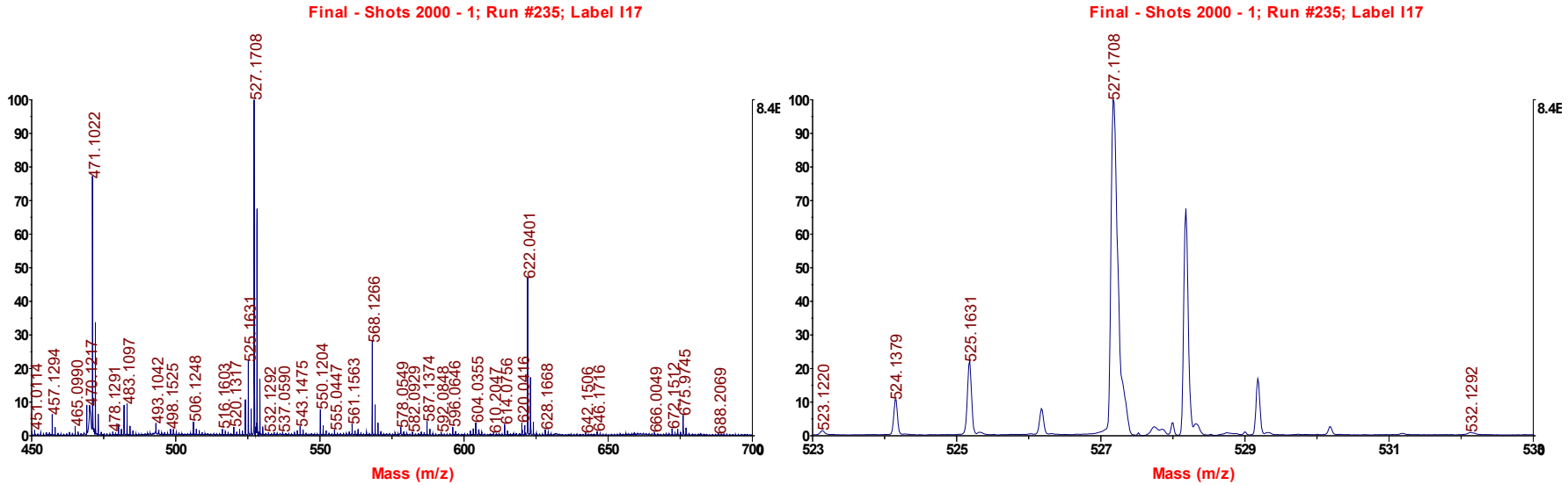

Figure S2. HRMS spectrum of compound **2.**

Qualitative Analysis Report

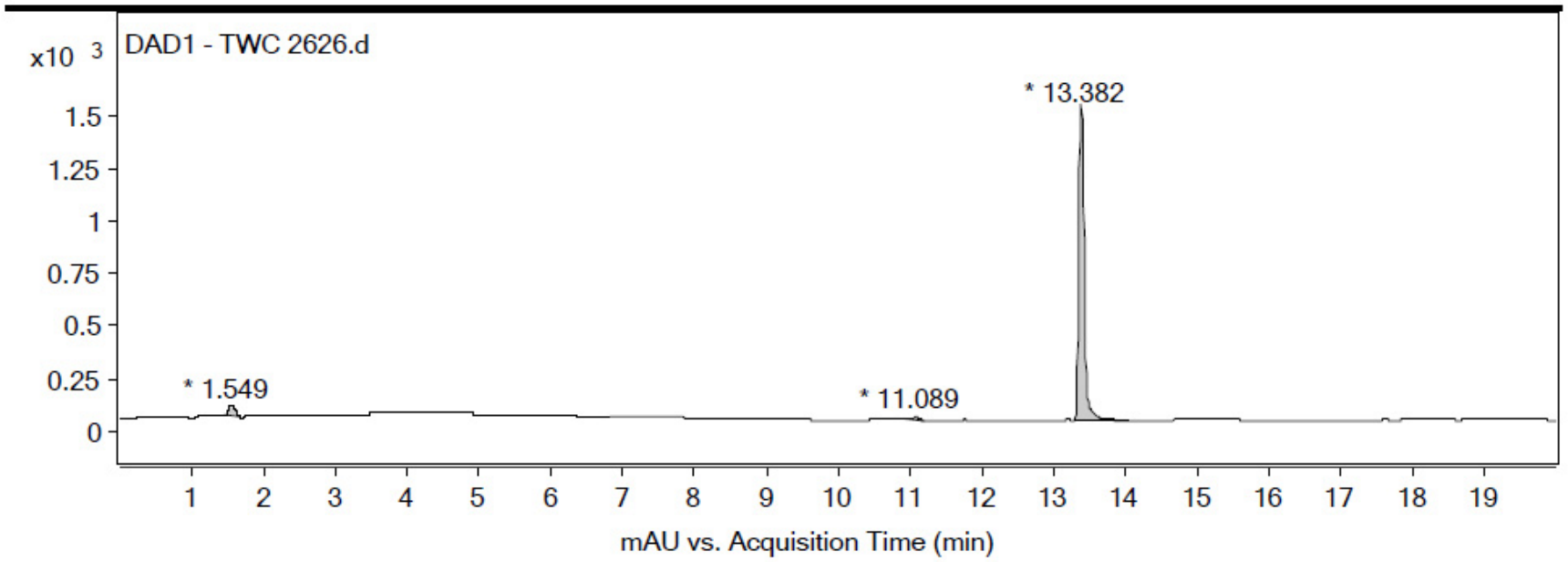

Integration Peak List

Peak	Start	RT	End	Height	Area	Area %
1	1.462	1.549	1.656	45.16	305.73	3.78
2	10.916	11.089	11.189	16.1	81.62	1.01
3	13.296	13.382	14.062	1513.94	8085.83	100

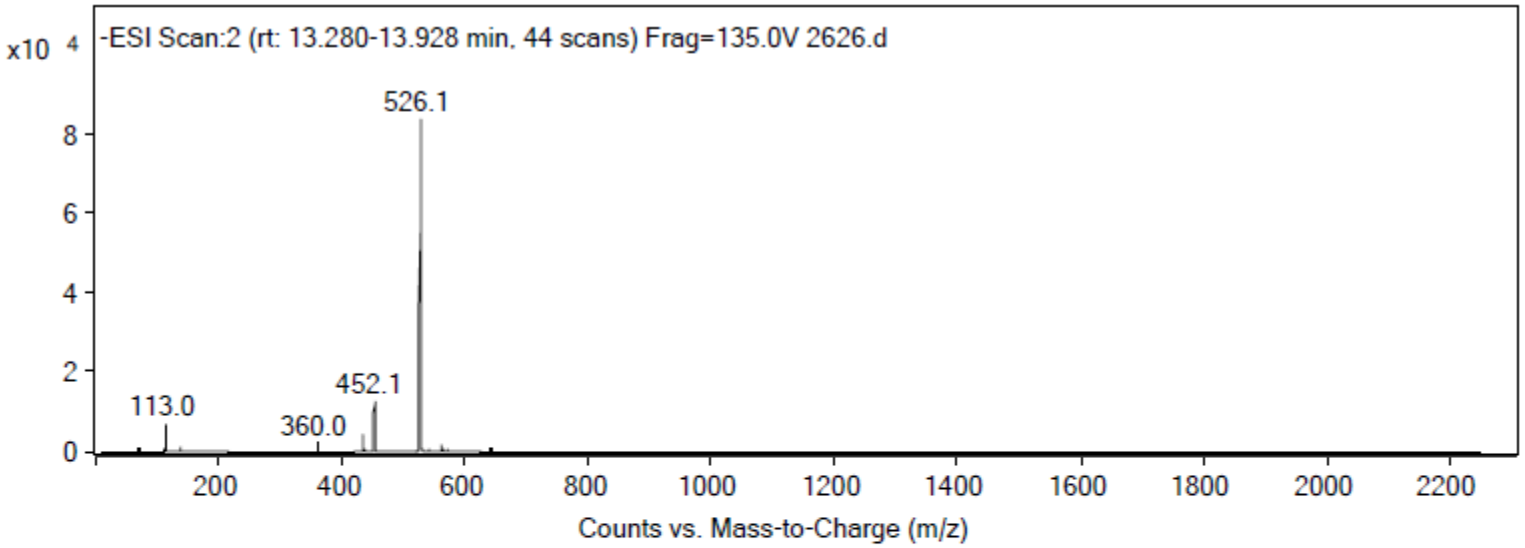

Peak List

m/z	z	Abund
113		6729.59
360		1854.58
434.1		3931.85
452.1	1	12571.55
453.1	1	3524.29
524.1		4976.46
526.1	1	83682.7
527.2	1	25827.74
528.1	1	5049.3
562.1		1647.65

Figure S3. HPLC-ESI spectra of compound **2.**

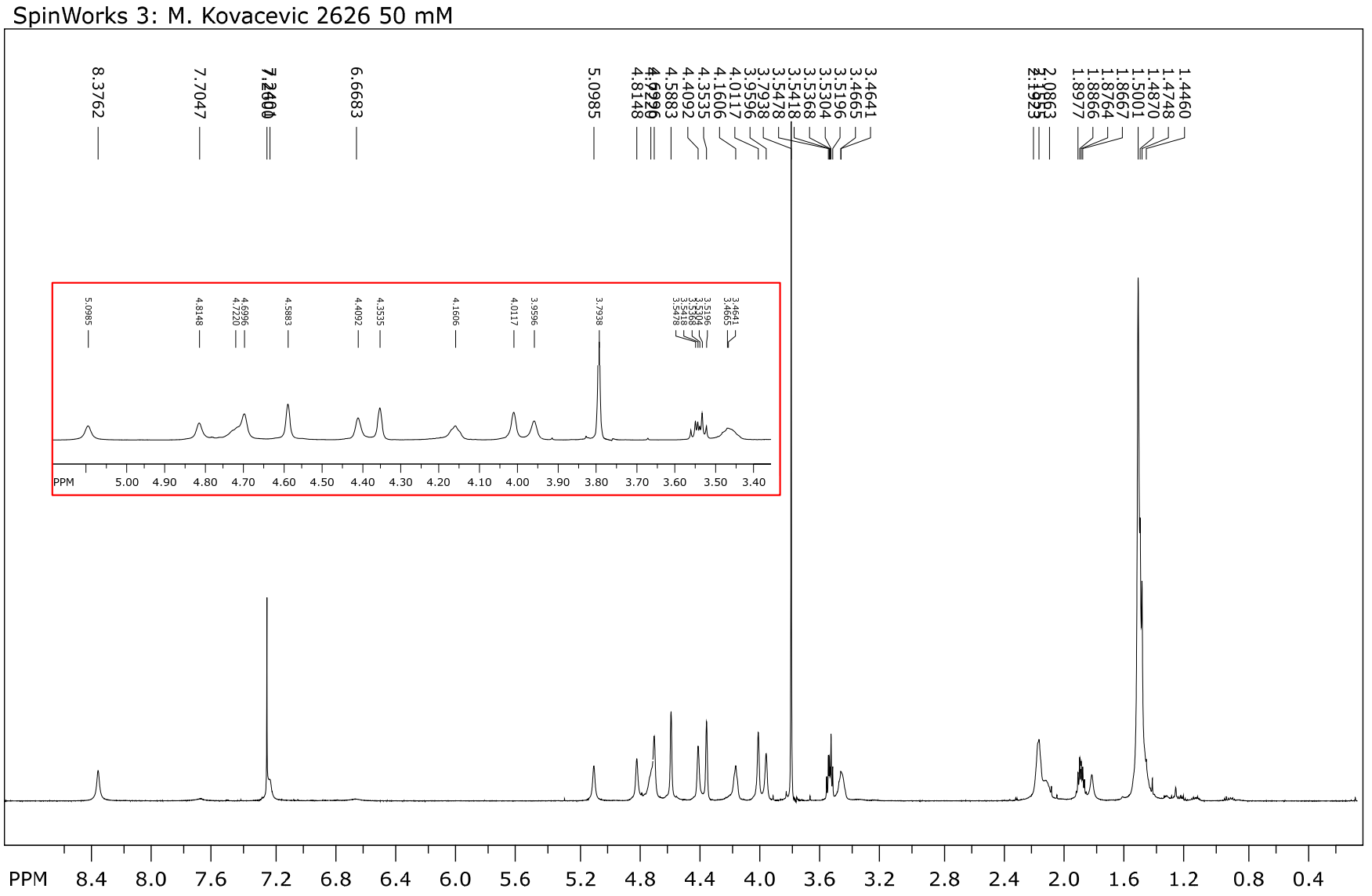

Figure S4. ^{1}H NMR spectrum of compound **2** ($c = 5 \times 10^{-2}$ M).

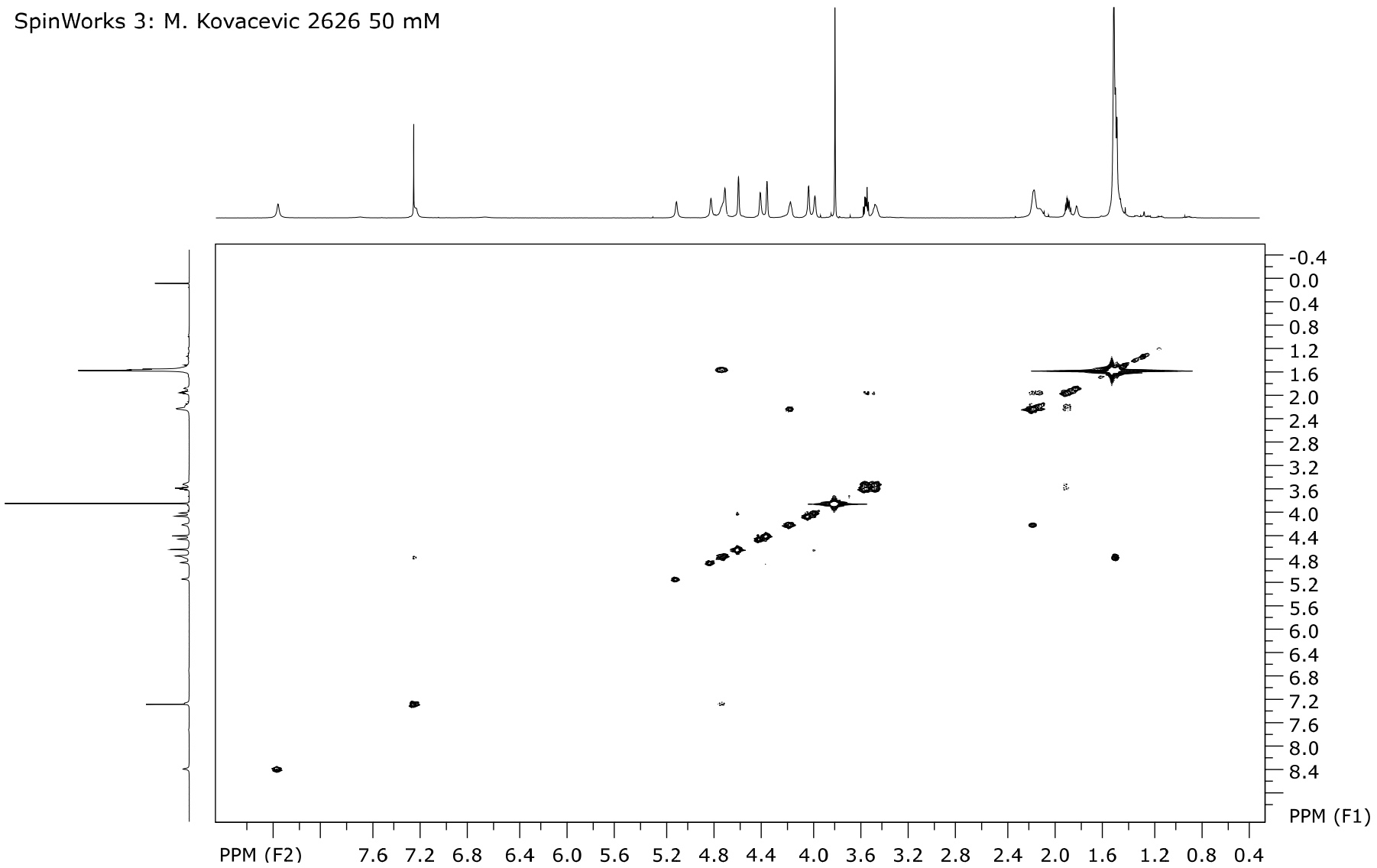

Figure S5. ^{1}H-^{1}H COSY NMR spectrum of compound **2** ($c = 5 \times 10^{-2}$ M).

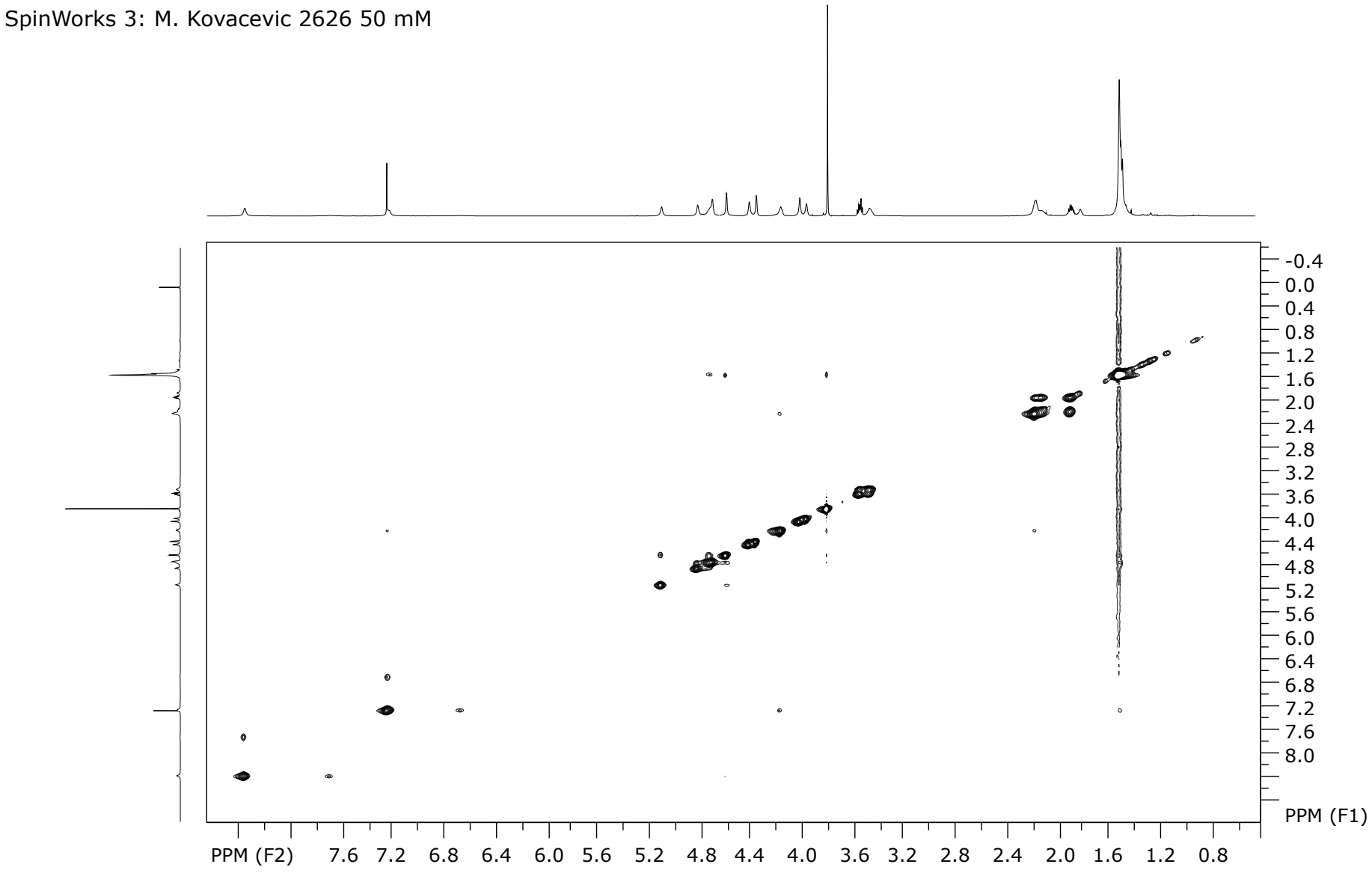

Figure S6. ^{1}H-^{1}H NOESY NMR spectrum of compound **2** ($c = 5 \times 10^{-2}$ M).

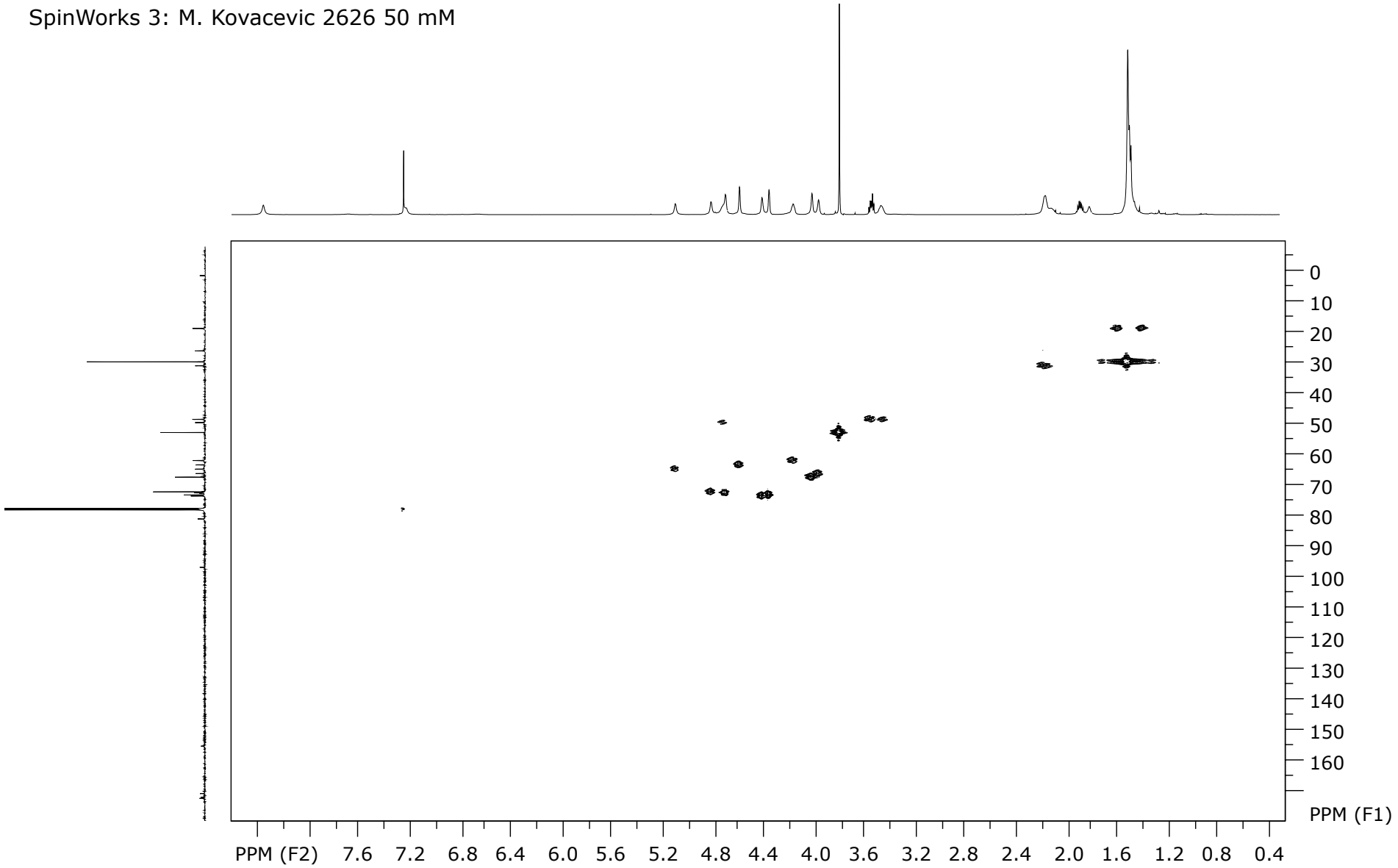

Figure S7. ^{1}H-^{13}C HMQC spectrum of compound **2** ($c = 5 \times 10^{-2}$ M).

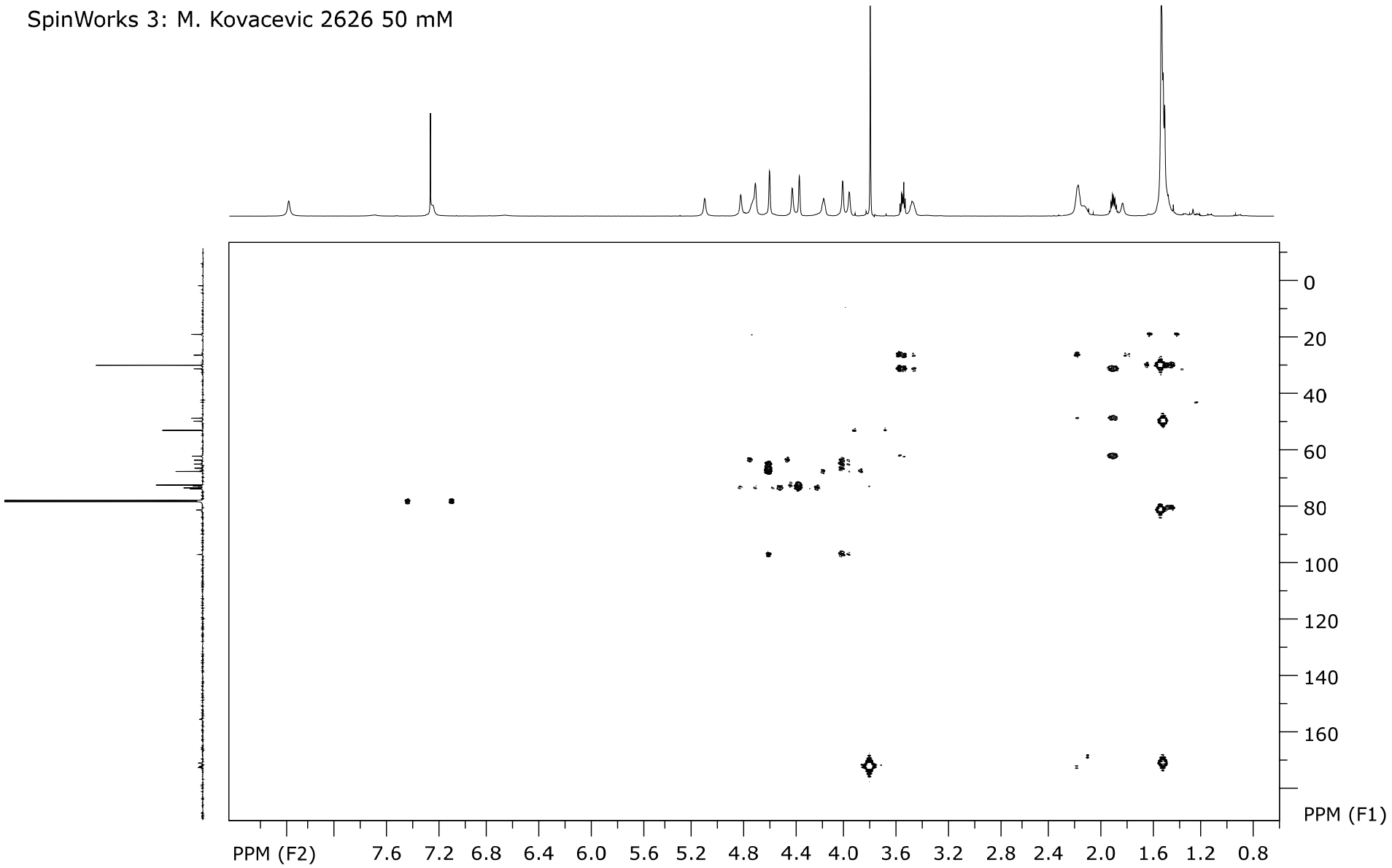

Figure S8. ^{1}H-^{13}C HMBC spectrum of compound **2** ($c = 5 \times 10^{-2}$ M).

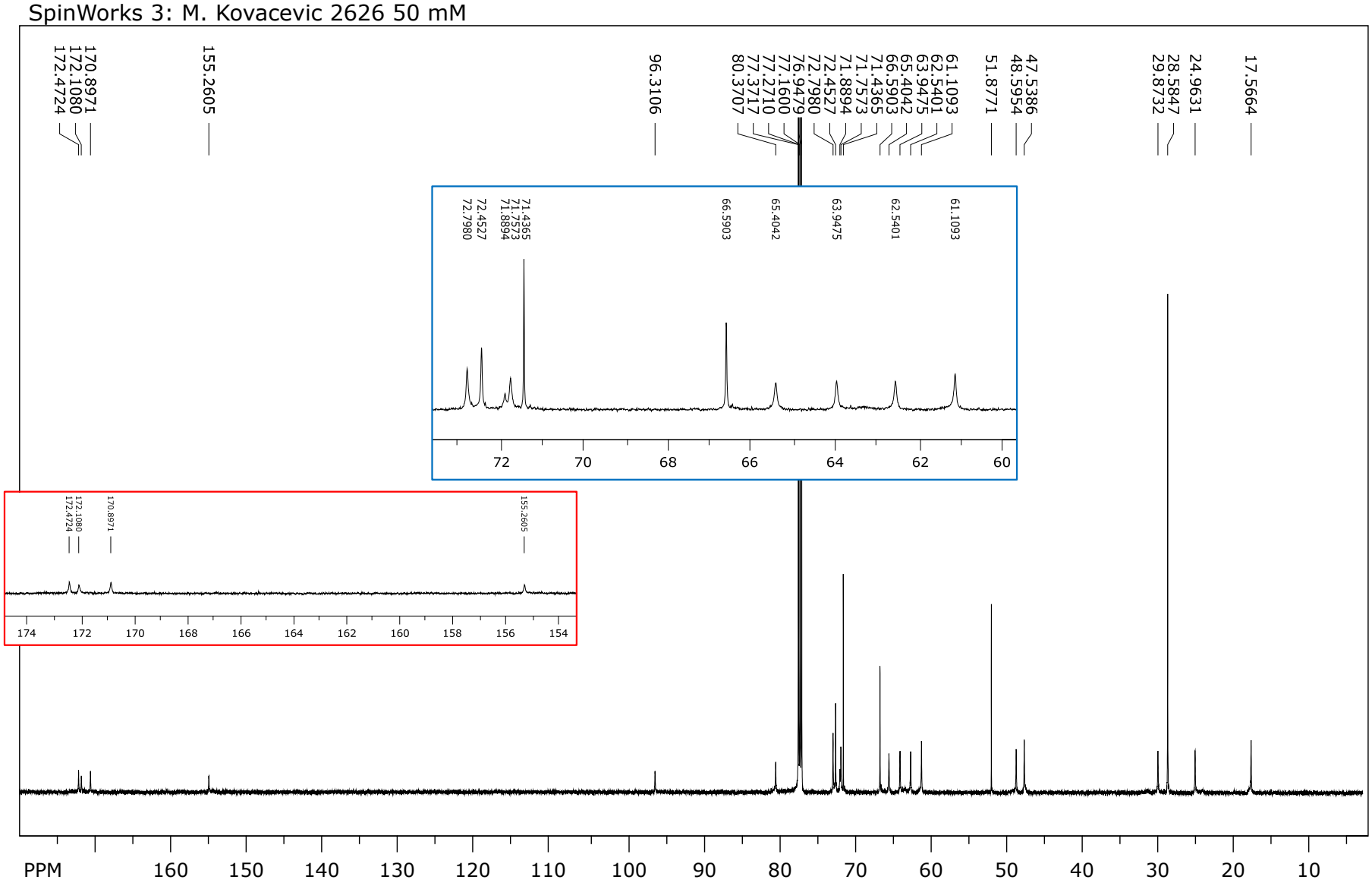

Figure S9. $^{13}C\{^{1}H\}$ NMR spectrum of compound **2** ($c = 5 \times 10^{-2}$ M).

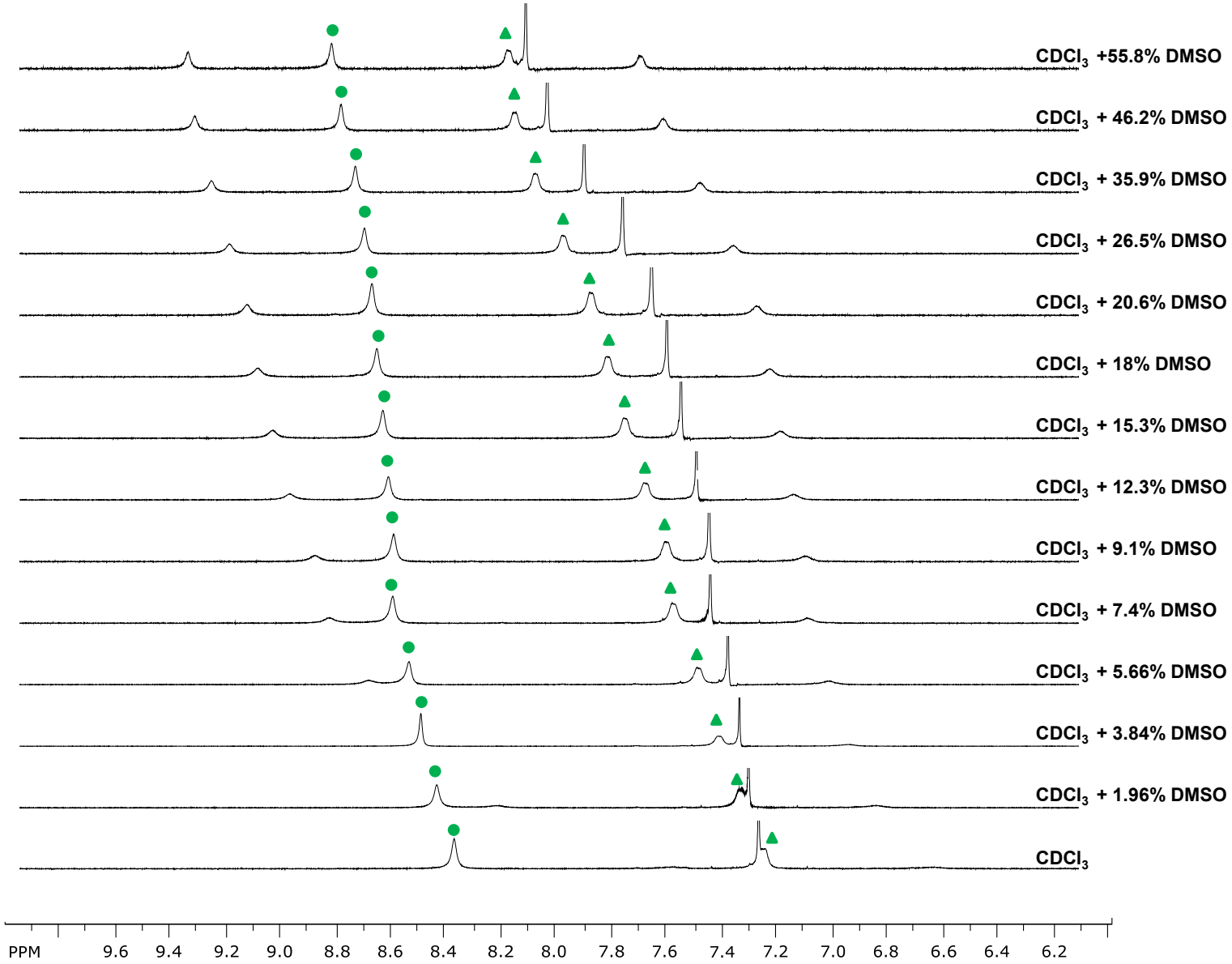

Figure S10. Solvent dependence of NH chemical shifts of compound **2** at varying concentrations of DMSO in $CDCl_3$ (c = 2.5 × 10-2 M).

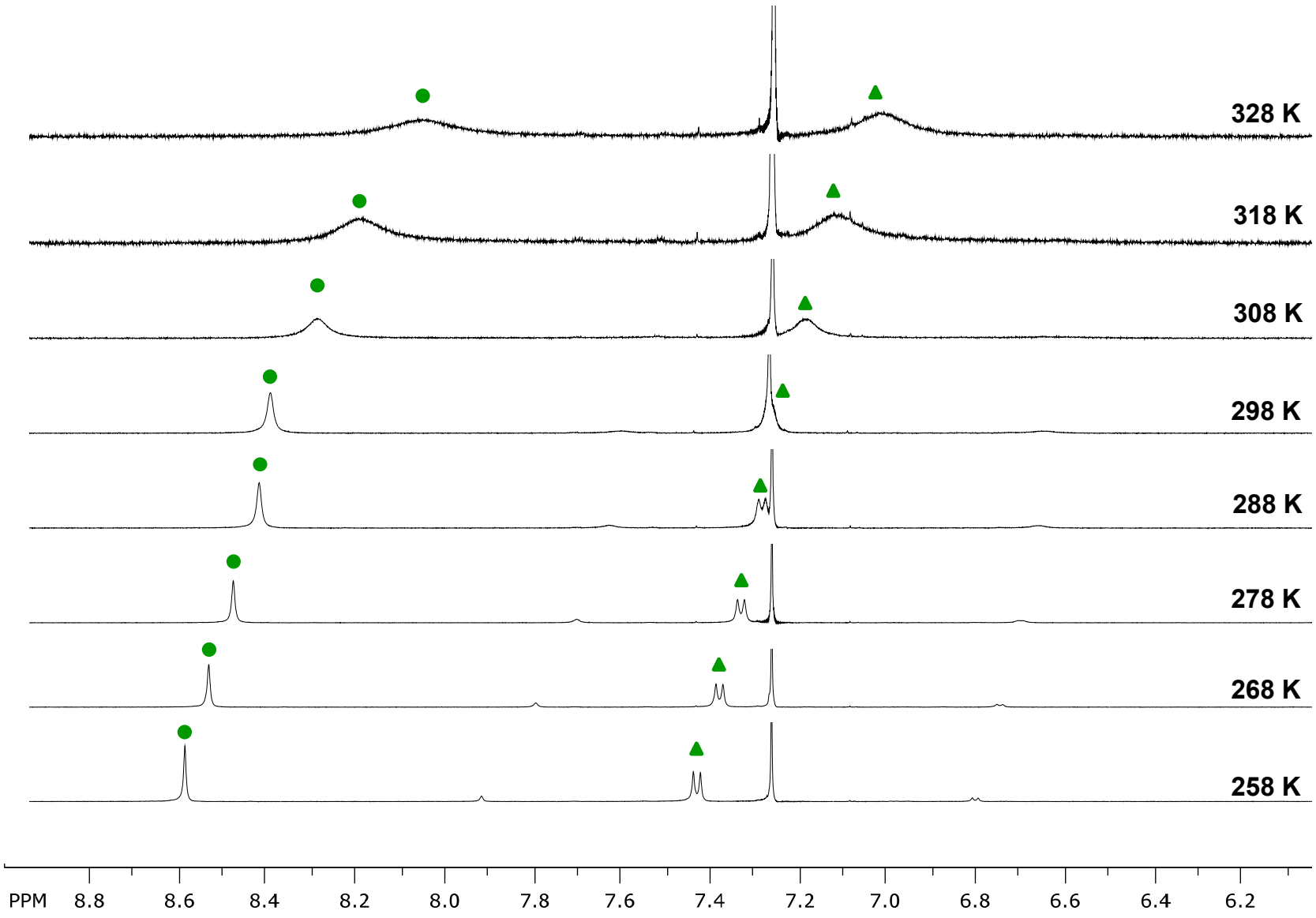

Figure S11. Temperature-dependent NH chemical shifts of compound **2** ($c = 1 \times 10^{-2}$ M).

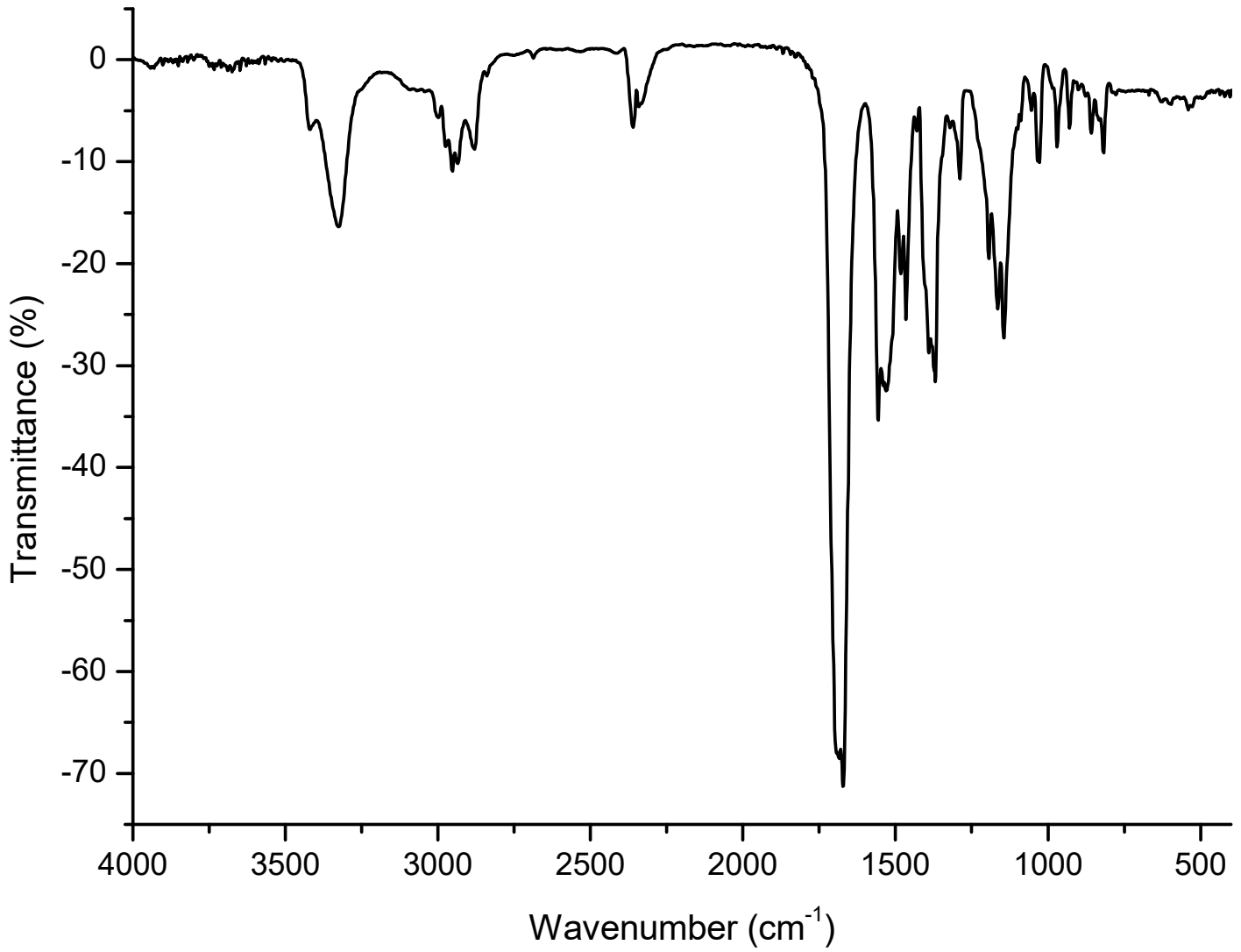

Figure S12. IR spectrum of compound **2** ($c = 5 \times 10^{-2}$ M) in DCM.

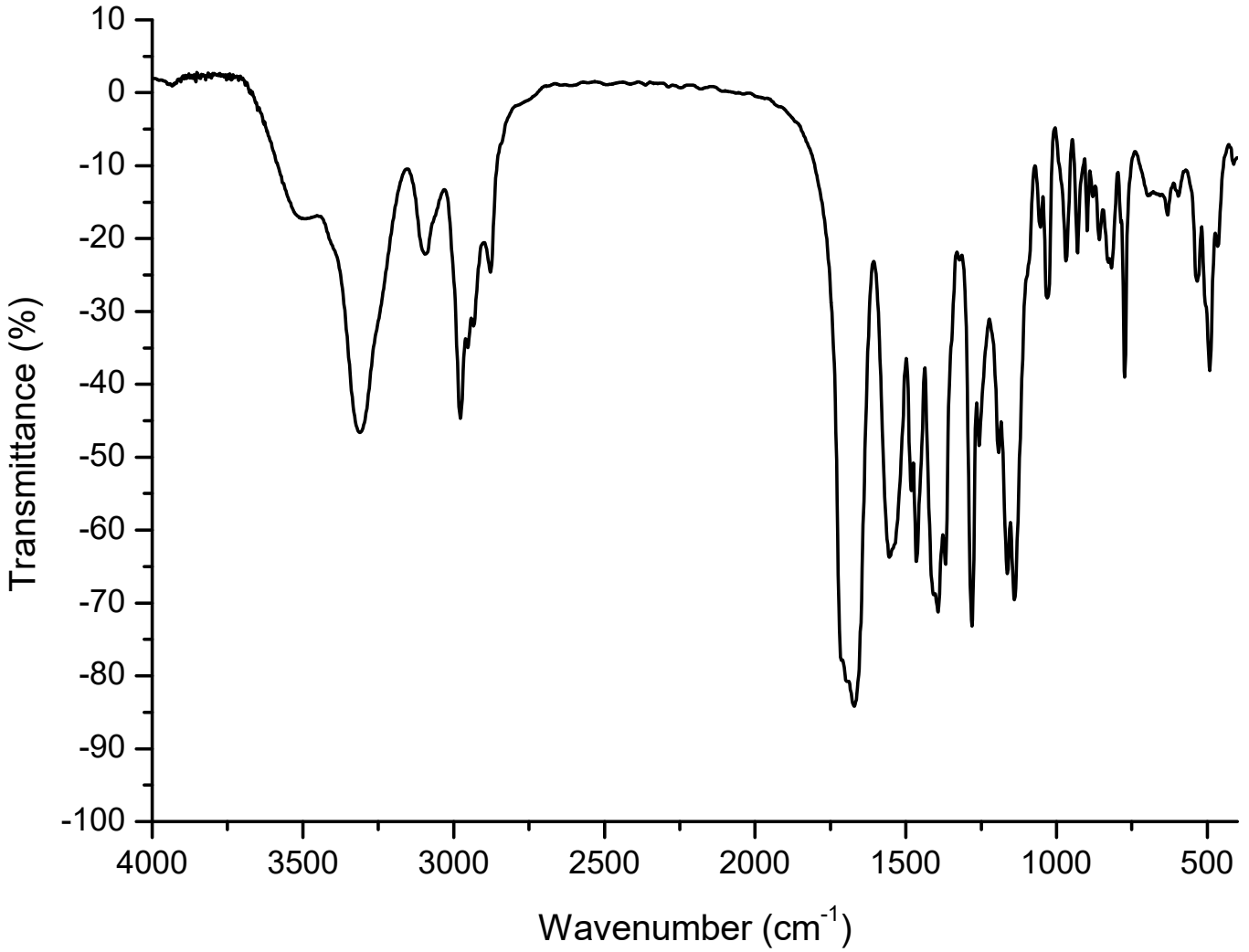

Figure S13. IR spectrum of compound **2** (2 mg) in KBr (200 mg).

Ac-D-Pro-L-Ala-NH-Fn-COOMe (3)

Ion type	Calc. mass	Measured mass	Mass error / ppm	Mol. Formula	Int. CAL
M+	469.1300	469.1280	4.5	$C_{22}H_{27}N_3O5Fe$	azitromicin

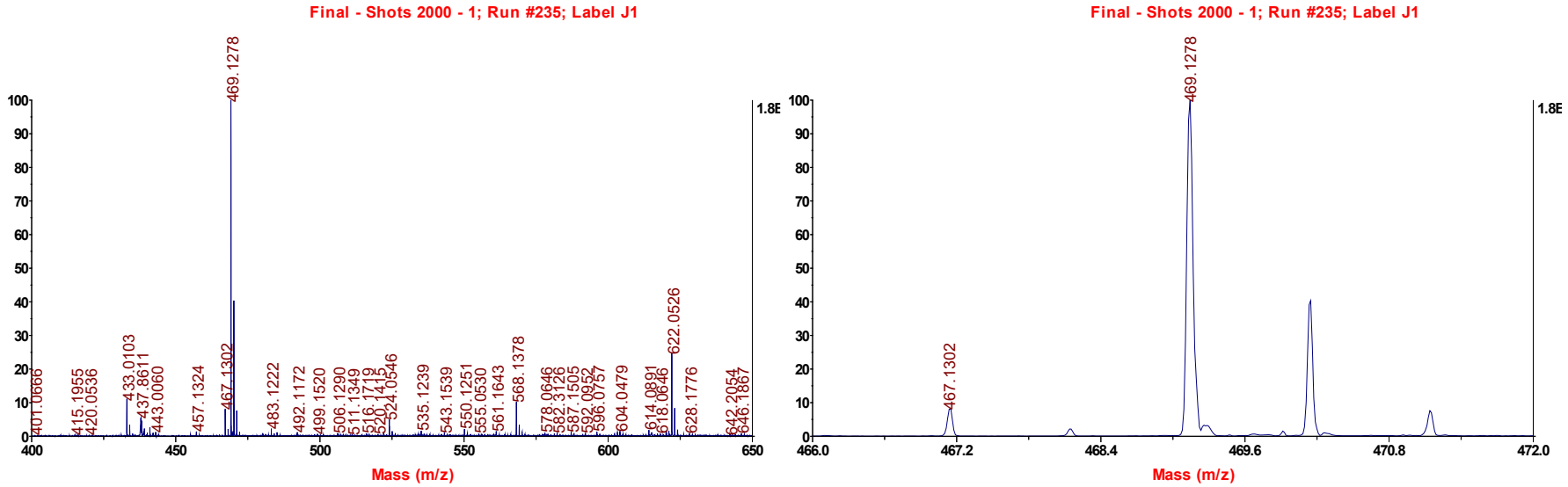

Figure S14. HRMS spectrum of compound **3.**

Qualitative Analysis Report

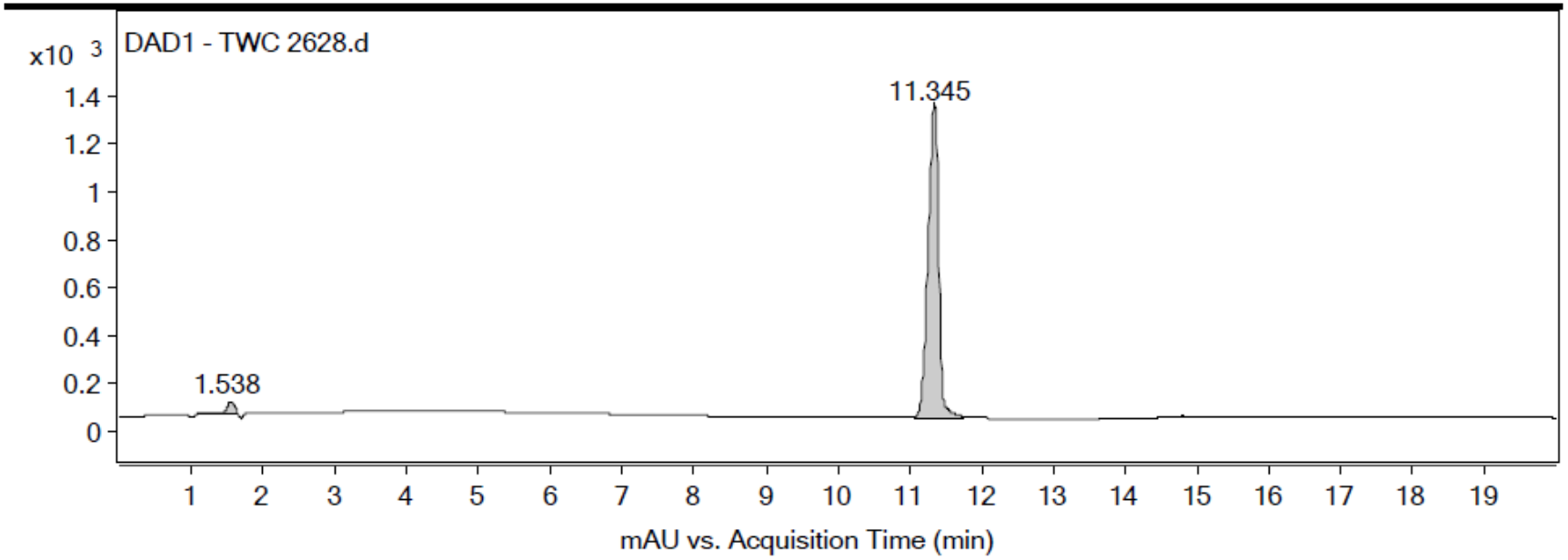

Integration Peak List

Peak	Start	RT	End	Height	Area	Area %
1	1.091	1.538	1.649	49.75	497.3	3.62
2	11.065	11.345	11.751	1322.47	13733.02	100

Spectrum Source	Fragmentor Voltage	Collision Energy	Ionization Mode
Peak (1) in "+/- TIC Scan"		0	ESI

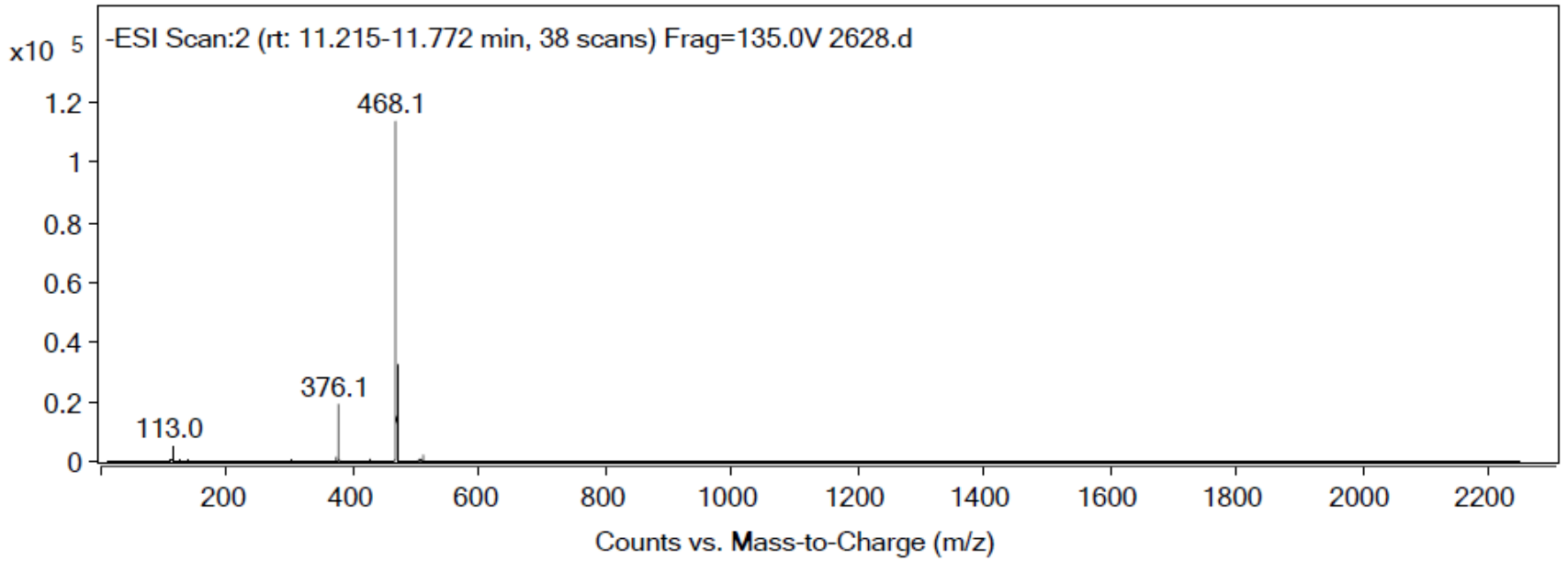

Peak List

m/z	z	Abund
113		5043.04
374		1191.55
376.1	1	19153.22
377	1	3753.97
466.1		7309.16
468.1	1	113881.13
469.1	1	32806.95
470.1	1	5590.01

Figure S15. HPLC-ESI spectra of compound **3.**

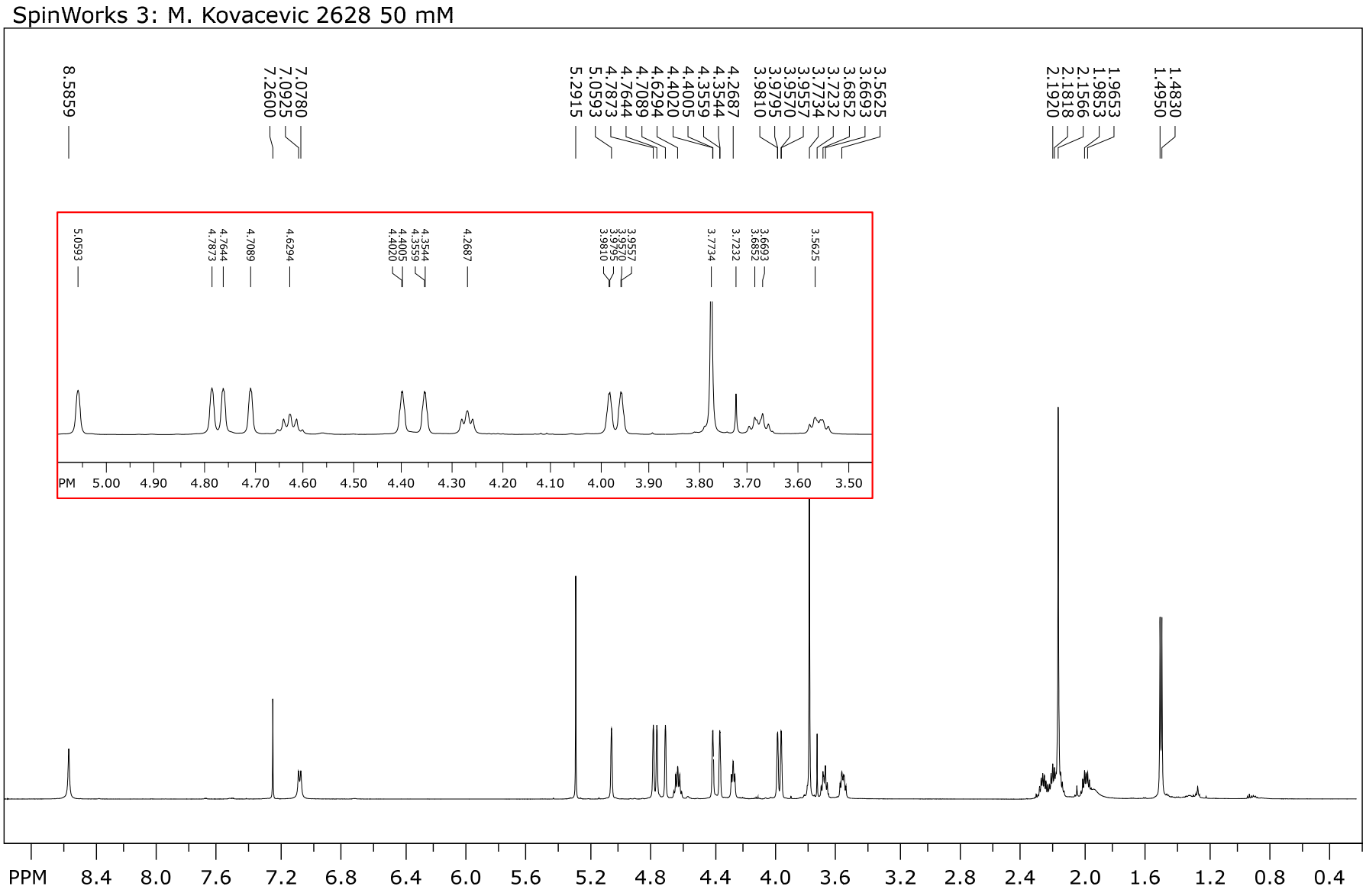

Figure S16. ^{1}H NMR spectrum of compound **3** ($c = 5 \times 10^{-2}$ M).

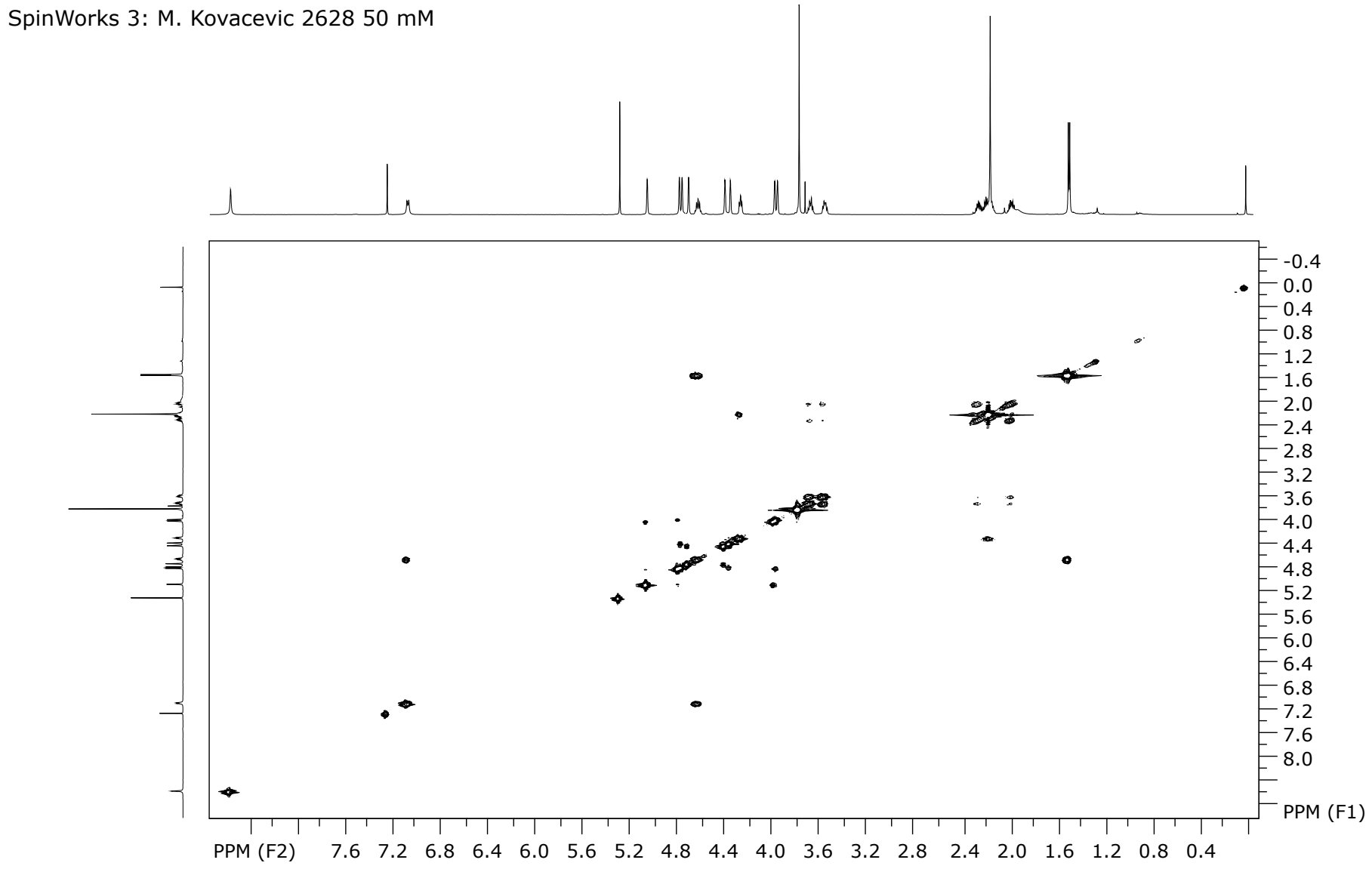

Figure S17. ^{1}H-^{1}H COSY NMR spectrum of compound **3** ($c = 5 \times 10^{-2}$ M).

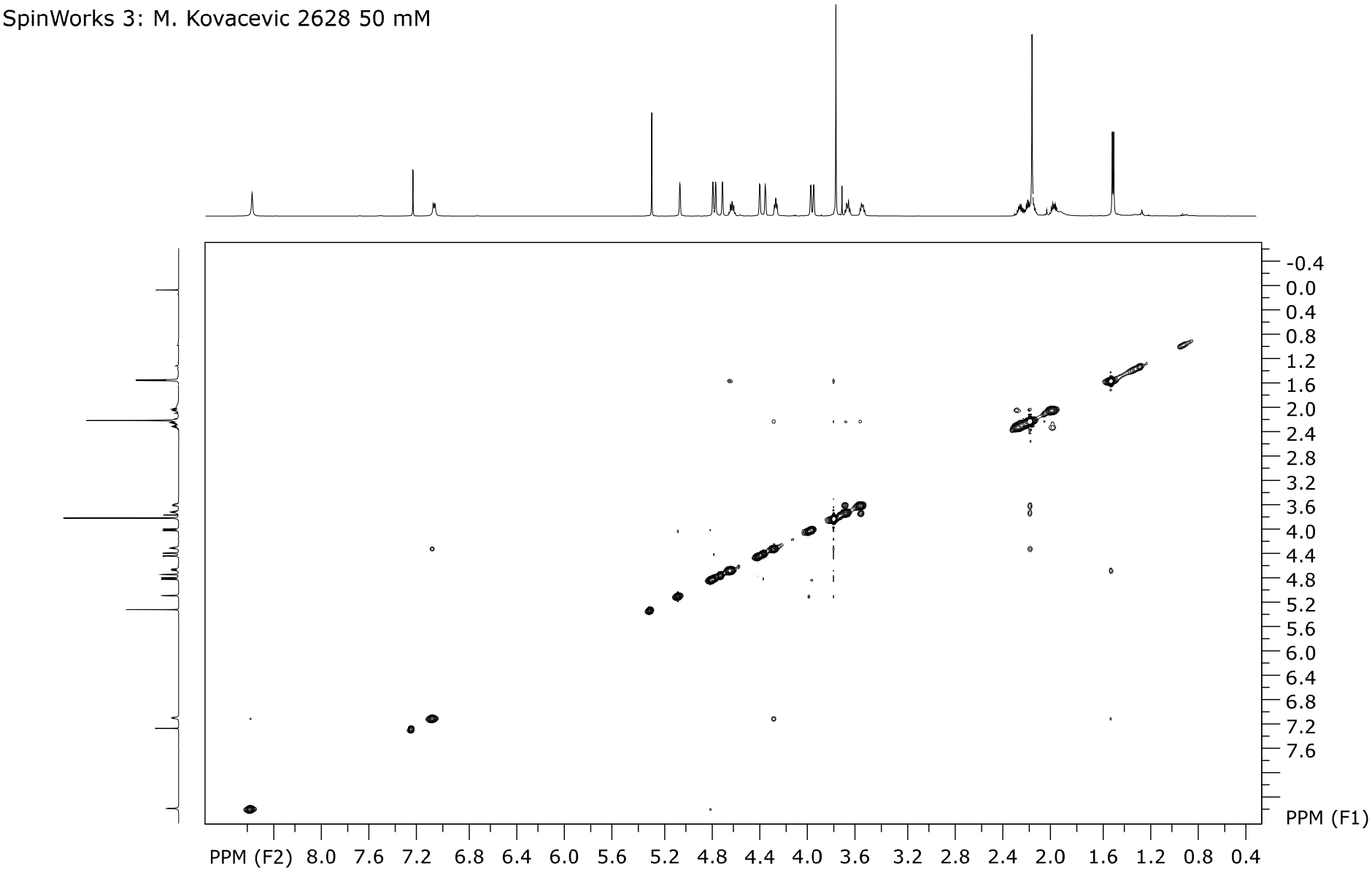

Figure S18. ^{1}H-^{1}H NOESY NMR spectrum of compound **3** ($c = 5 \times 10^{-2}$ M).

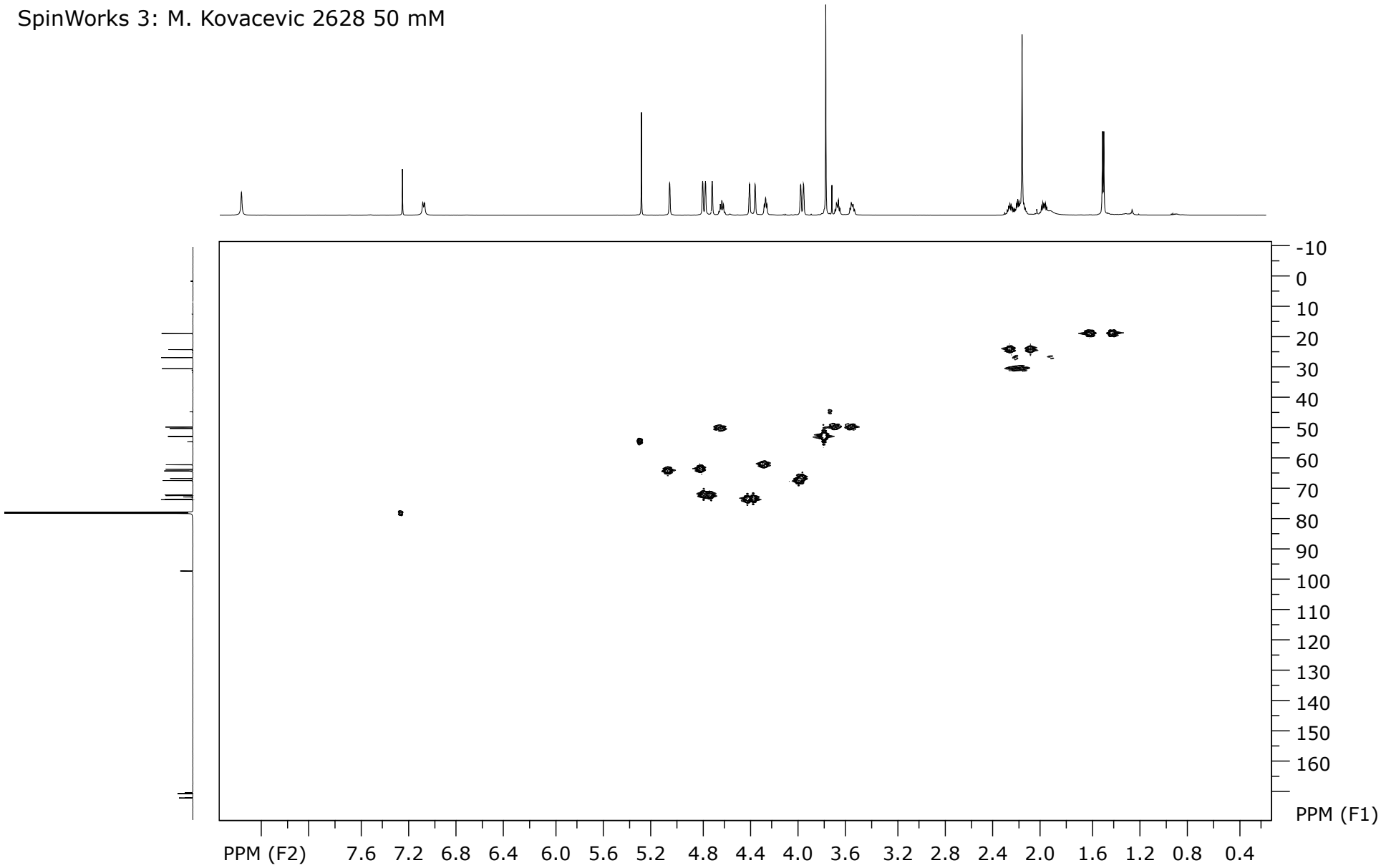

Figure S19. ^{1}H-^{13}C HMQC spectrum of compound **3** ($c = 5 \times 10^{-2}$ M).

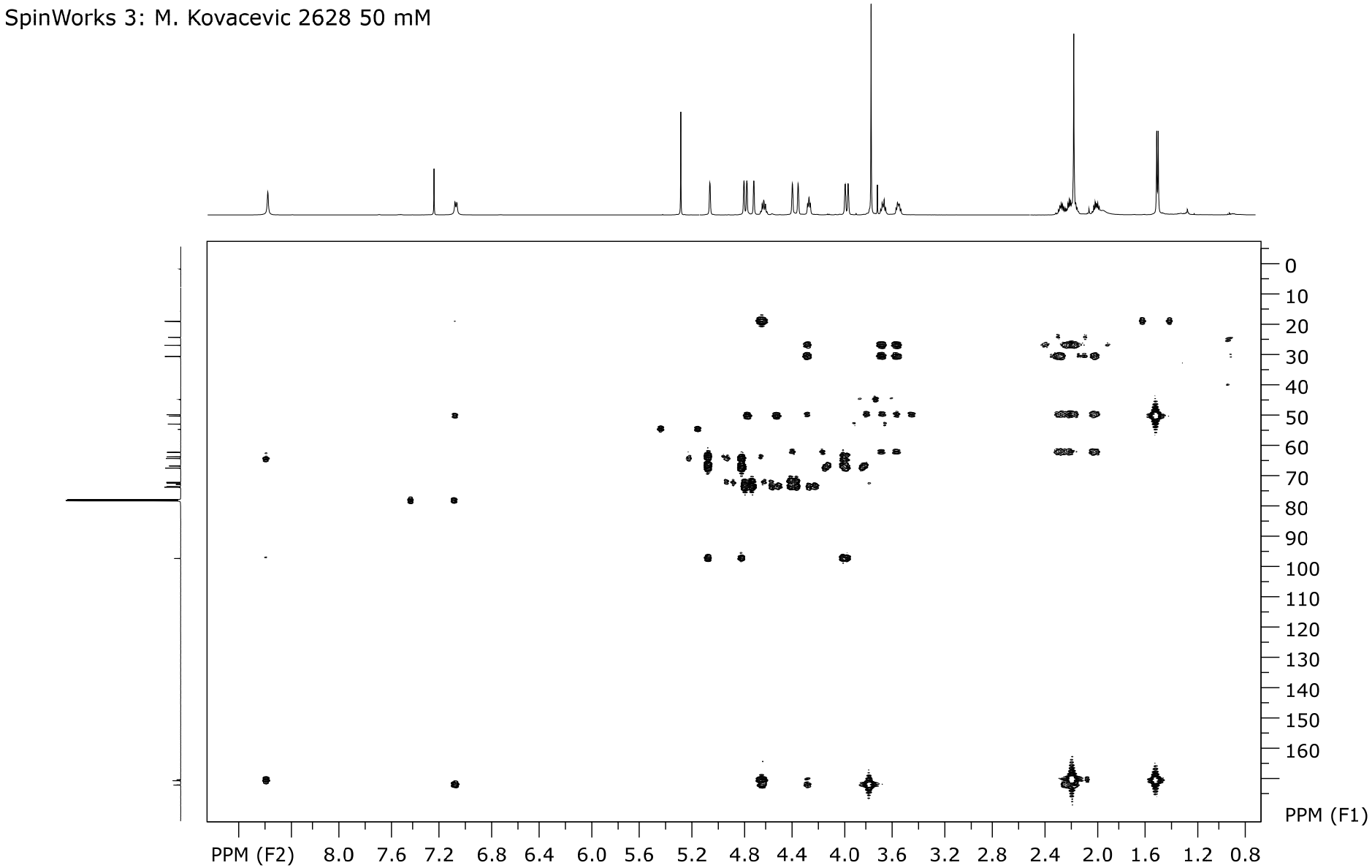

Figure S20. ^{1}H-^{13}C HMBC spectrum of compound **3** ($c = 5 \times 10^{-2}$ M).

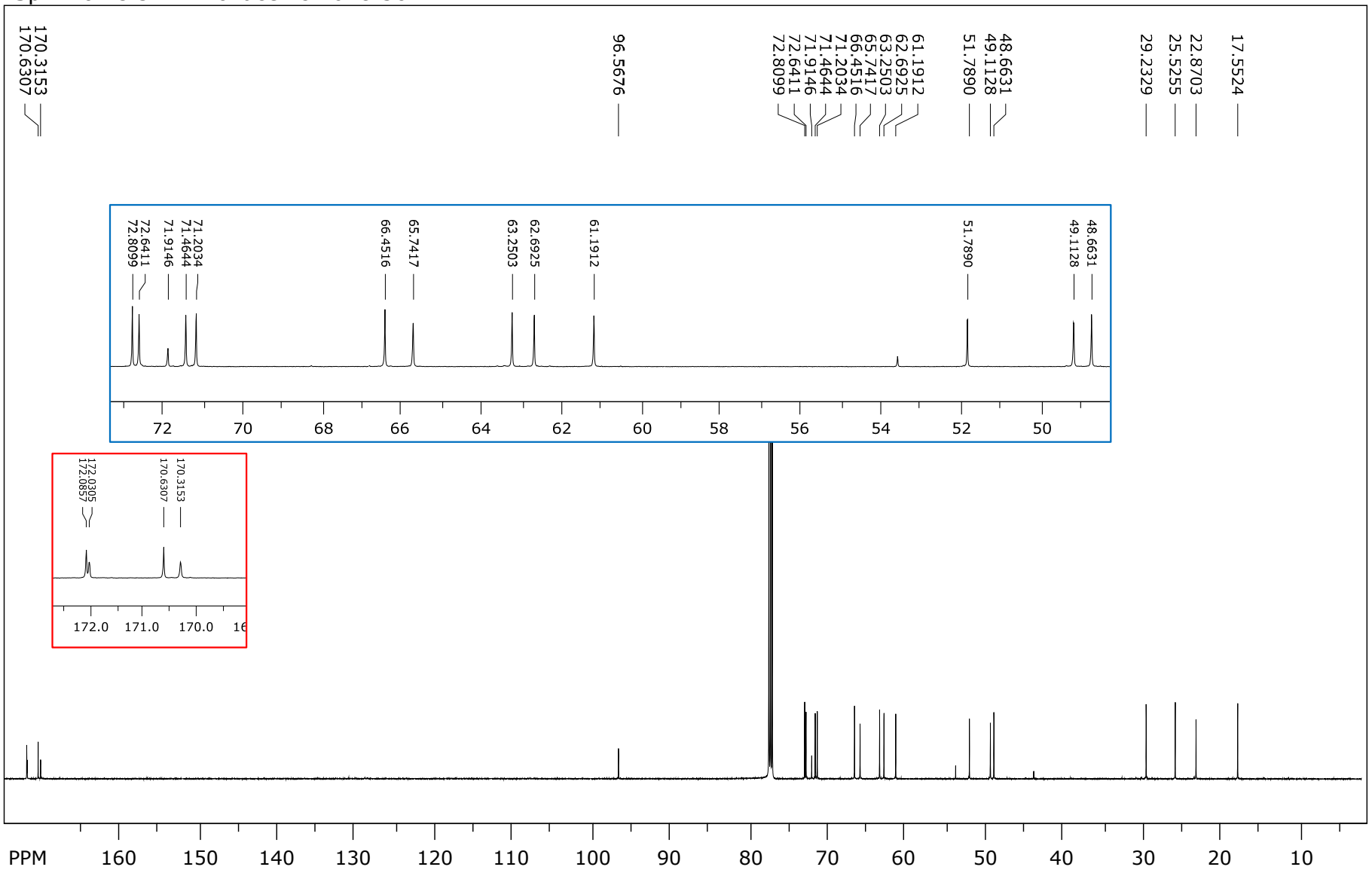

Figure S21. $^{13}C\{^{1}H\}$ NMR spectrum of compound **3** ($c = 5 \times 10^{-2}$ M).

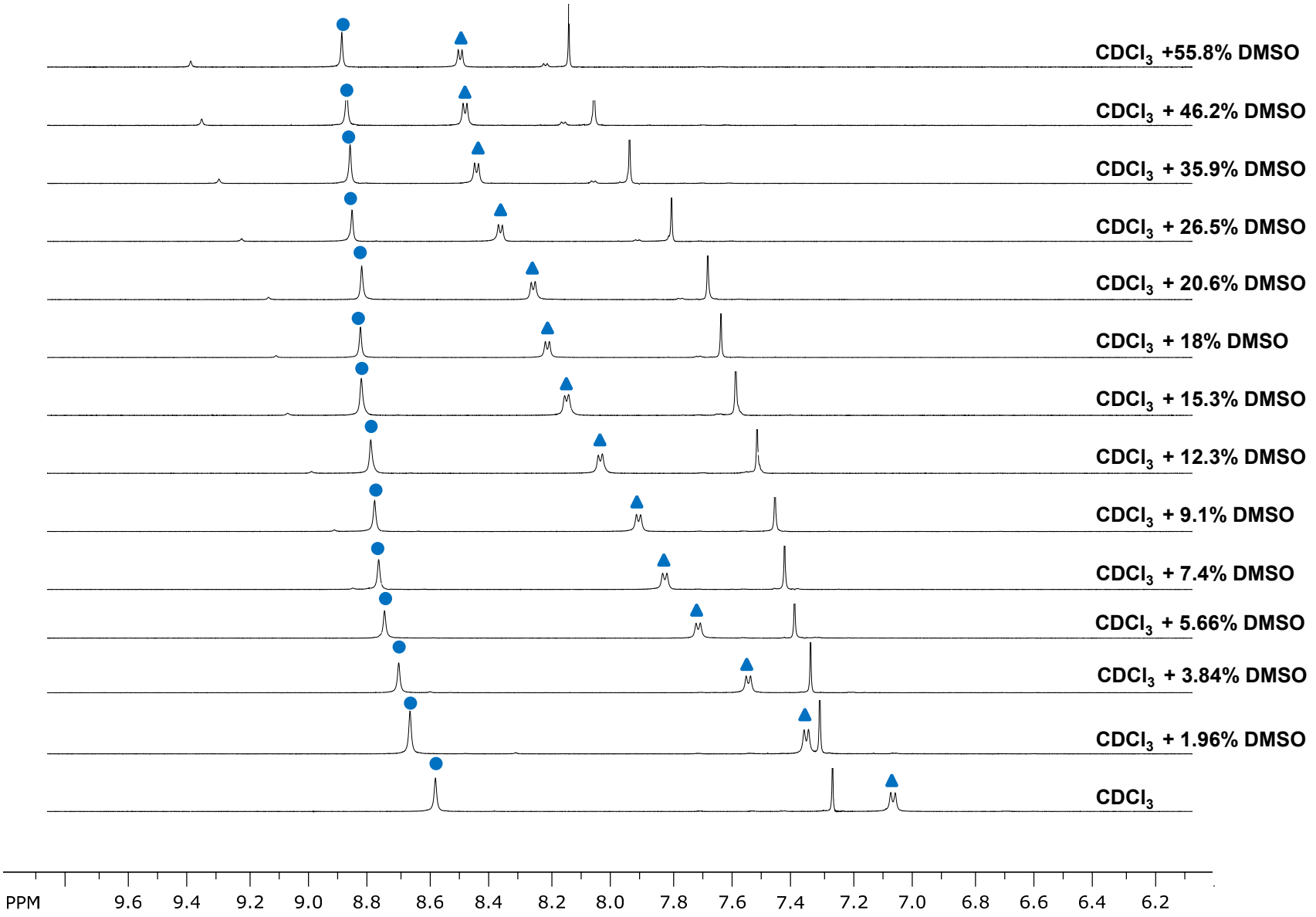

Figure S22. Solvent dependence of NH chemical shifts of compound **3** at varying concentrations of DMSO in $CDCl_3$ ($c = 2.5 \times 10^{-2}$ M).

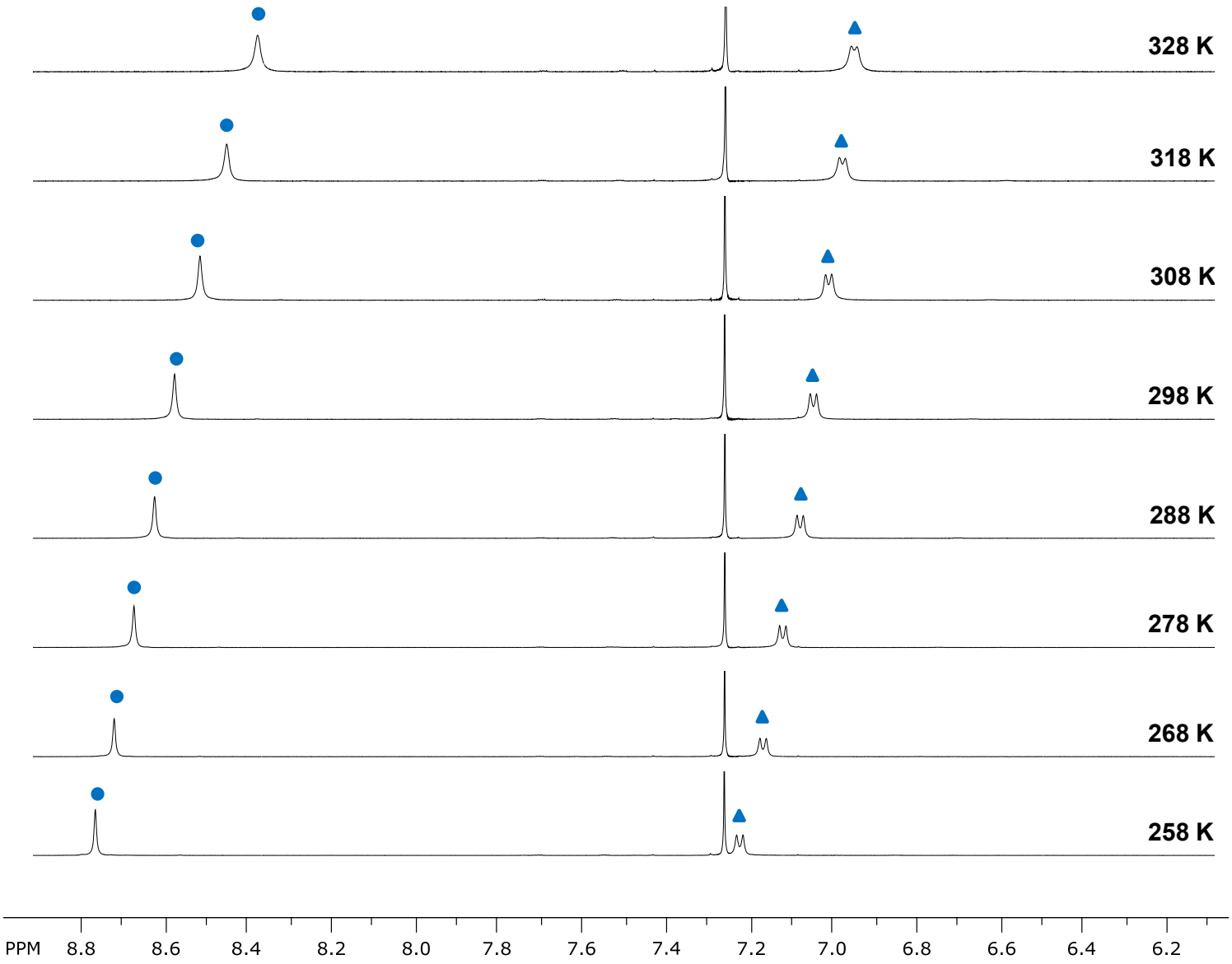

Figure S23. Temperature-dependent NH chemical shifts of compound **3** ($c = 1 \times 10^{-2}$ M).

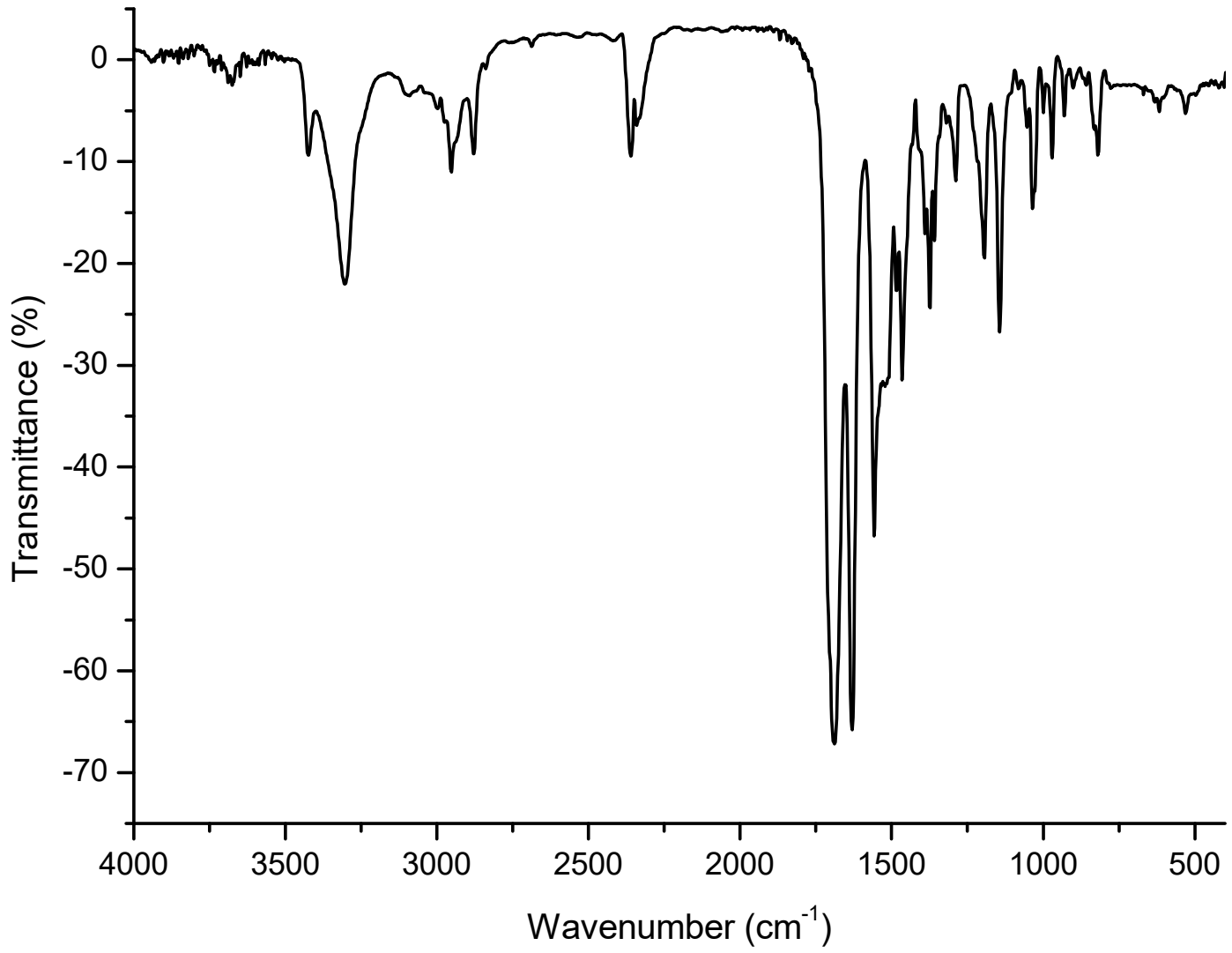

Figure S24. IR spectrum of compound **3** ($c = 5 \times 10^{-2}$ M) in DCM.

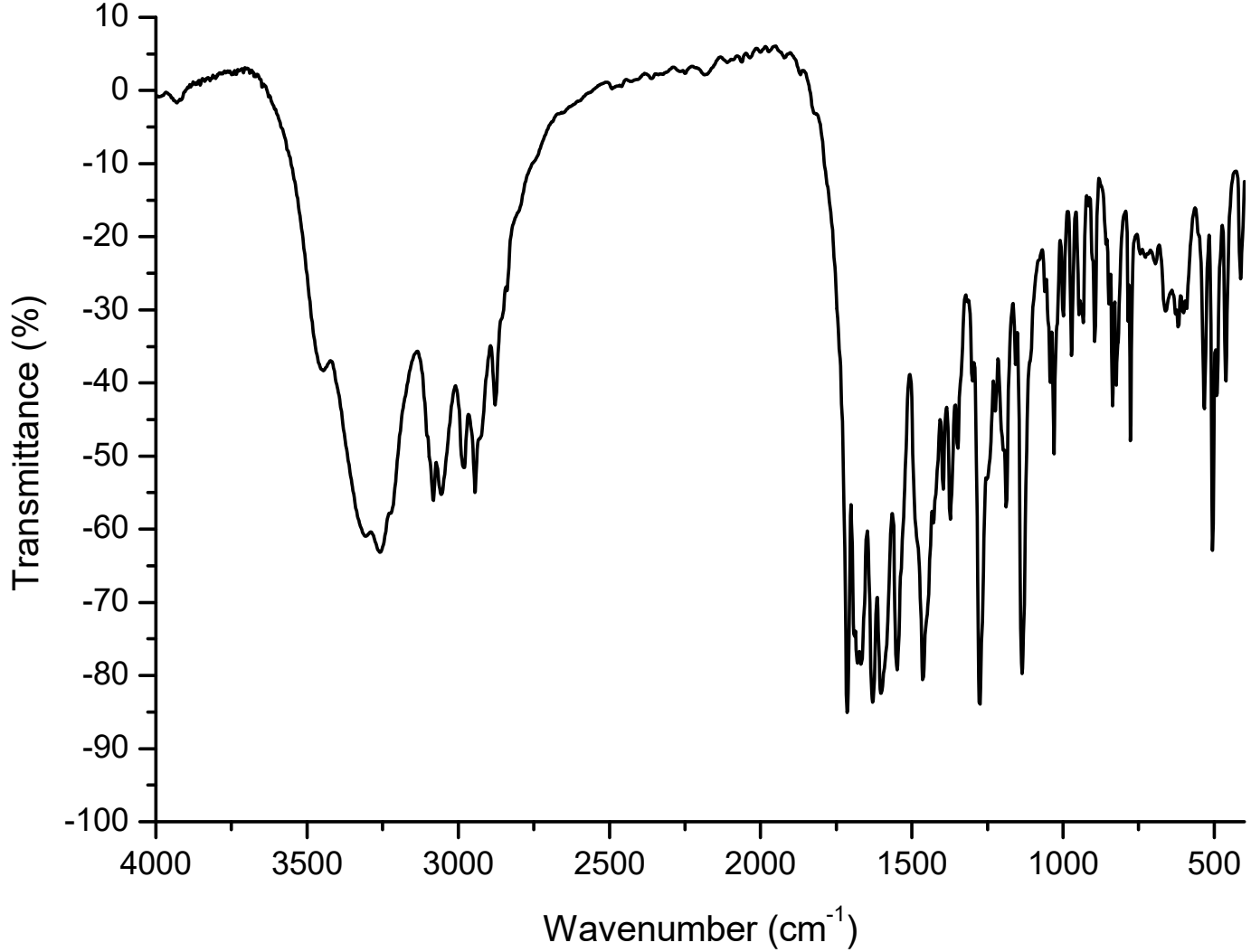

Figure S25. IR spectrum of compound **3** (2 mg) in KBr (200 mg).

Boc-L-Pro-L-Ala-NH-Fn-COOMe (4)

Ion type	Calc. mass	Measured mass	Mass error / ppm	Mol. Formula	Int. CAL
M+	527.1719	527.1729	1.9	$C_{25}H_{33}N_3O_6Fe$	azitromicin

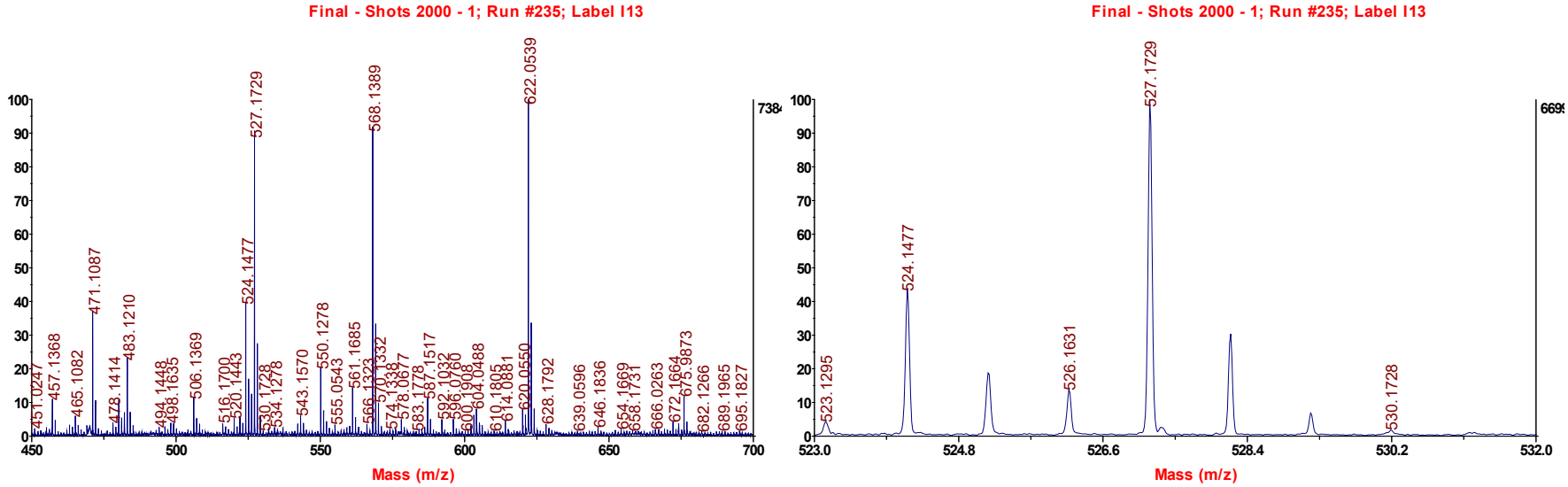

Figure S26. HRMS spectrum of compound **4.**

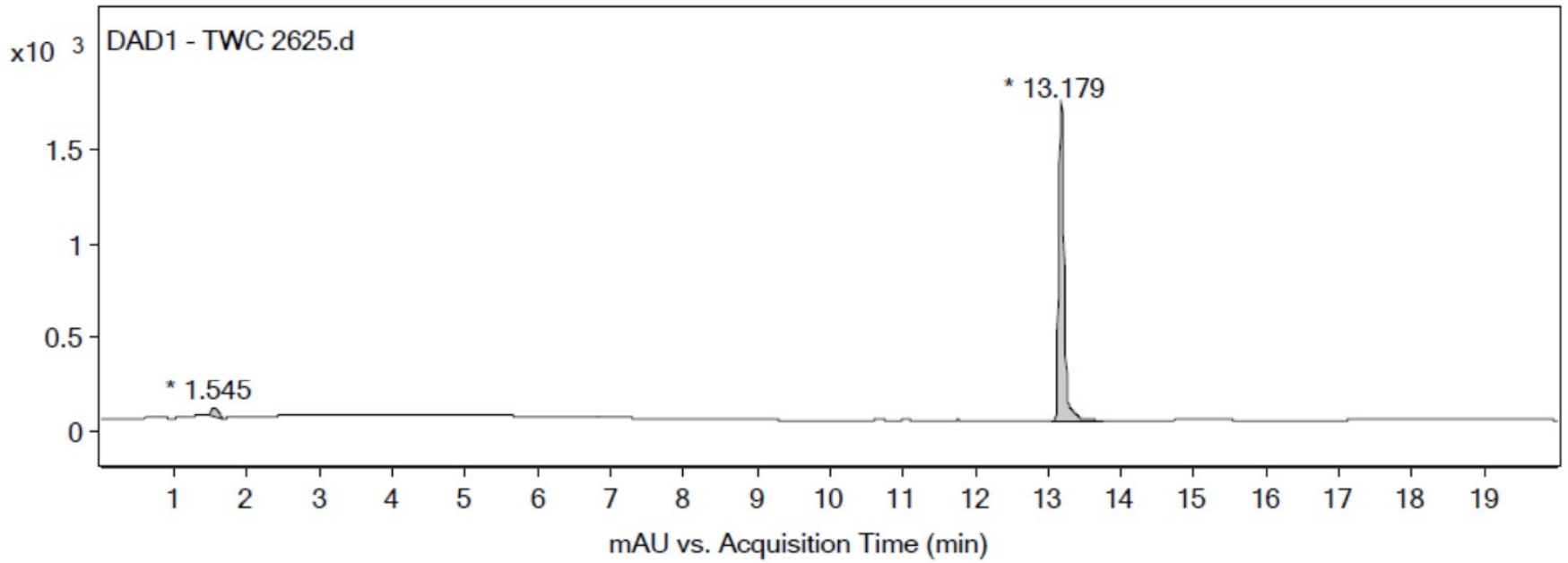

Integration Peak List

Peak	Start	RT	End	Height	Area	Area %
1	1.452	1.545	1.679	49.37	370.02	4.04
2	13.065	13.179	13.765	1702.41	9150.92	100

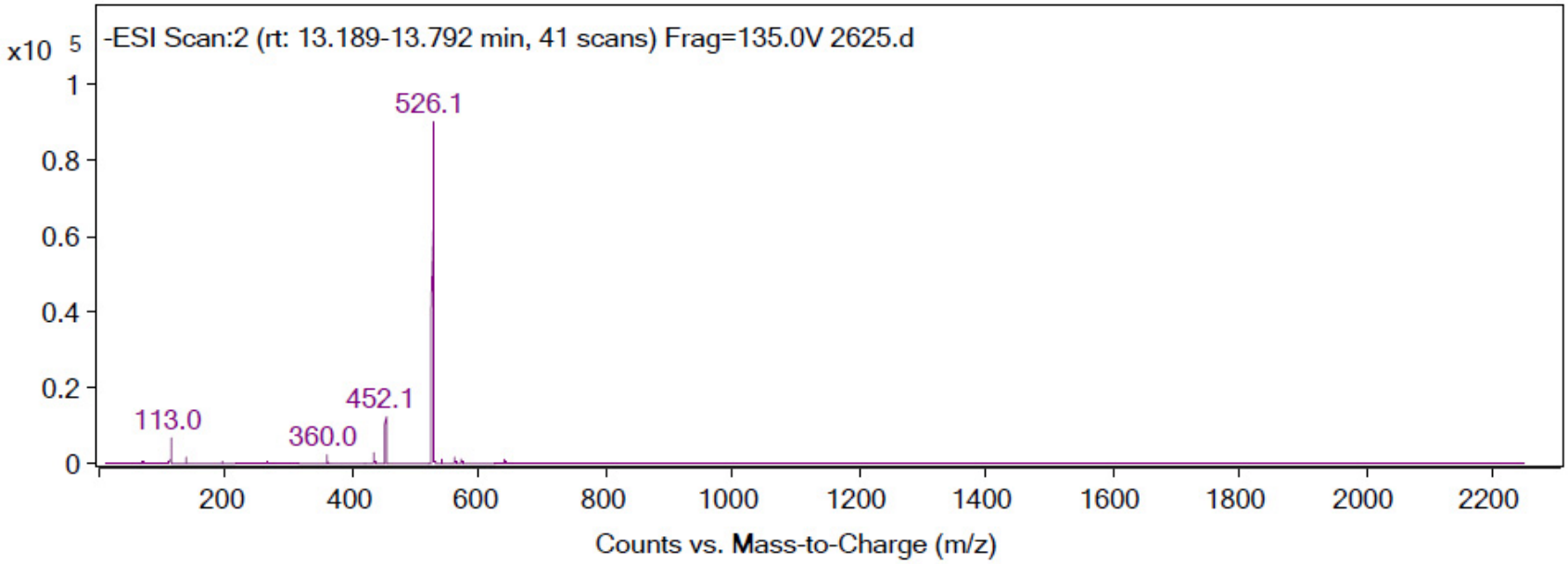

Peak List

m/z	z	Abund
113		6847.82
360		1990.32
434.1		2932.19
452.1	1	12574.58
453	1	3605.96
524.1		6158.28
526.1	1	90050.9
527.2	1	30406.55
528.1	1	6029.68
562		1833.22

Figure S27. HPLC-ESI spectra of compound **4.**

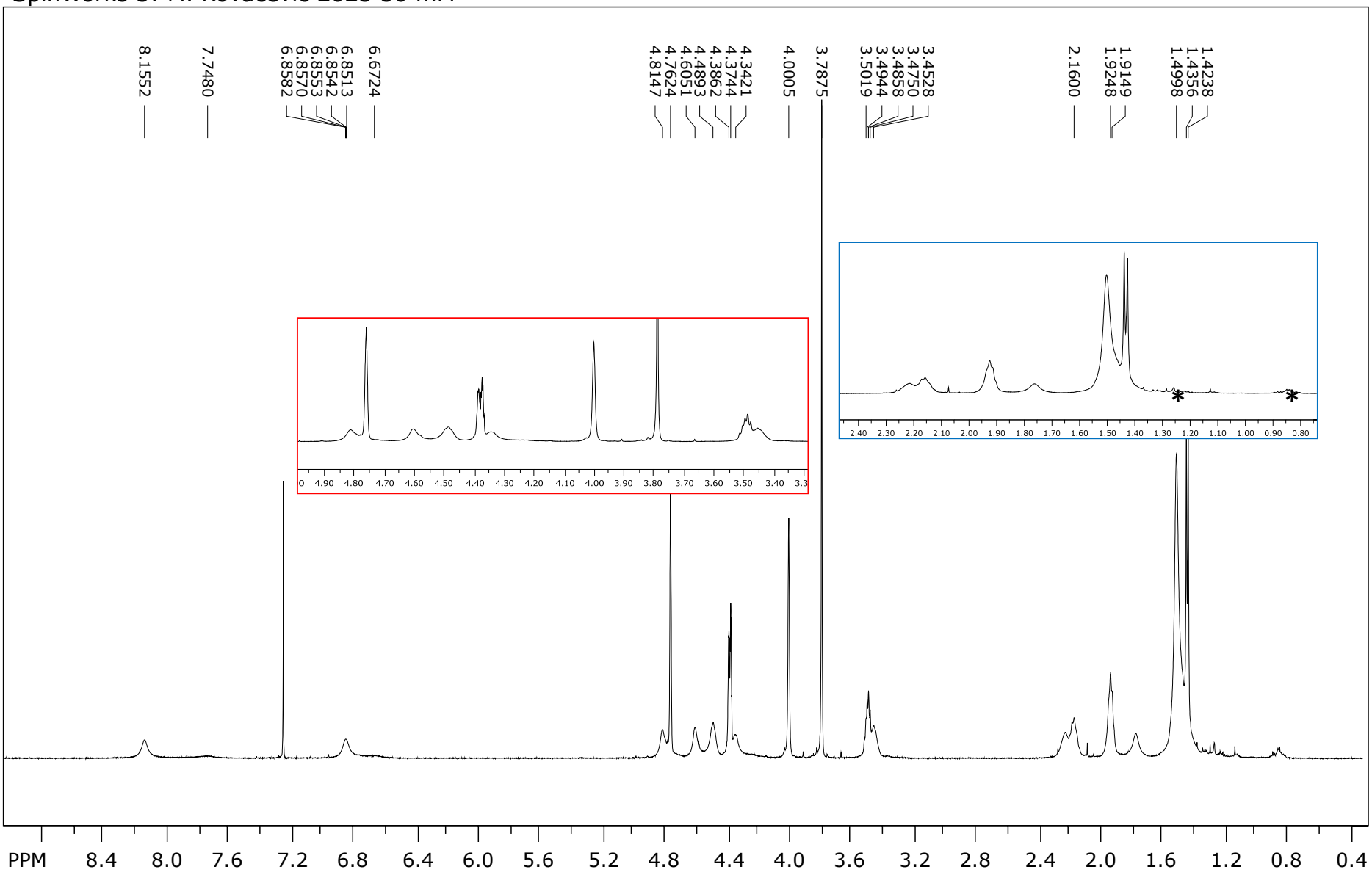

Figure S28. ^{1}H NMR spectrum of compound **4** ($c = 5 \times 10^{-2}$ M).

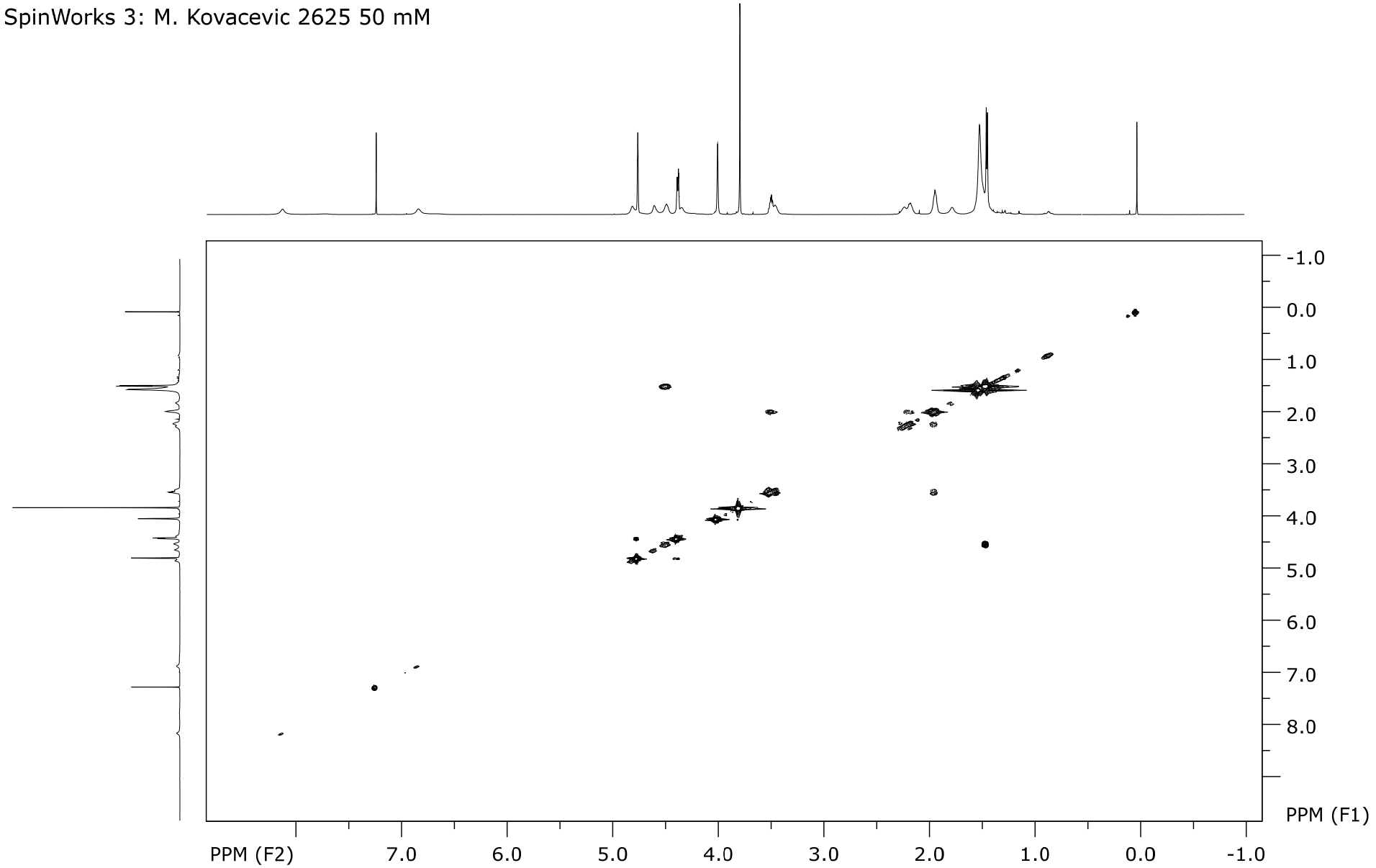

Figure S29. ^{1}H-^{1}H COSY NMR spectrum of compound **4** ($c = 5 \times 10^{-2}$ M).

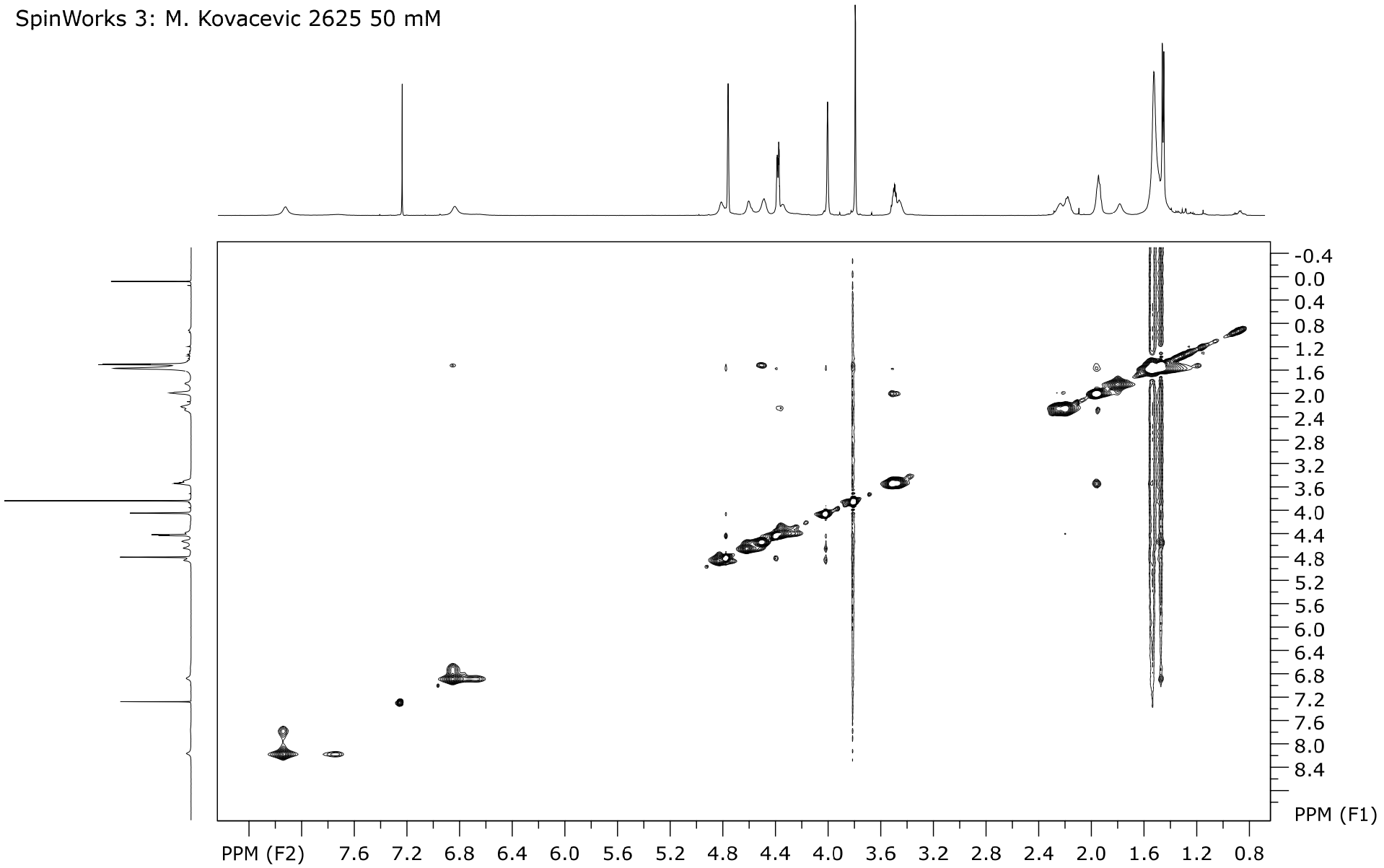

Figure S30. ^{1}H-^{1}H NOESY NMR spectrum of compound **4** ($c = 5 \times 10^{-2}$ M).

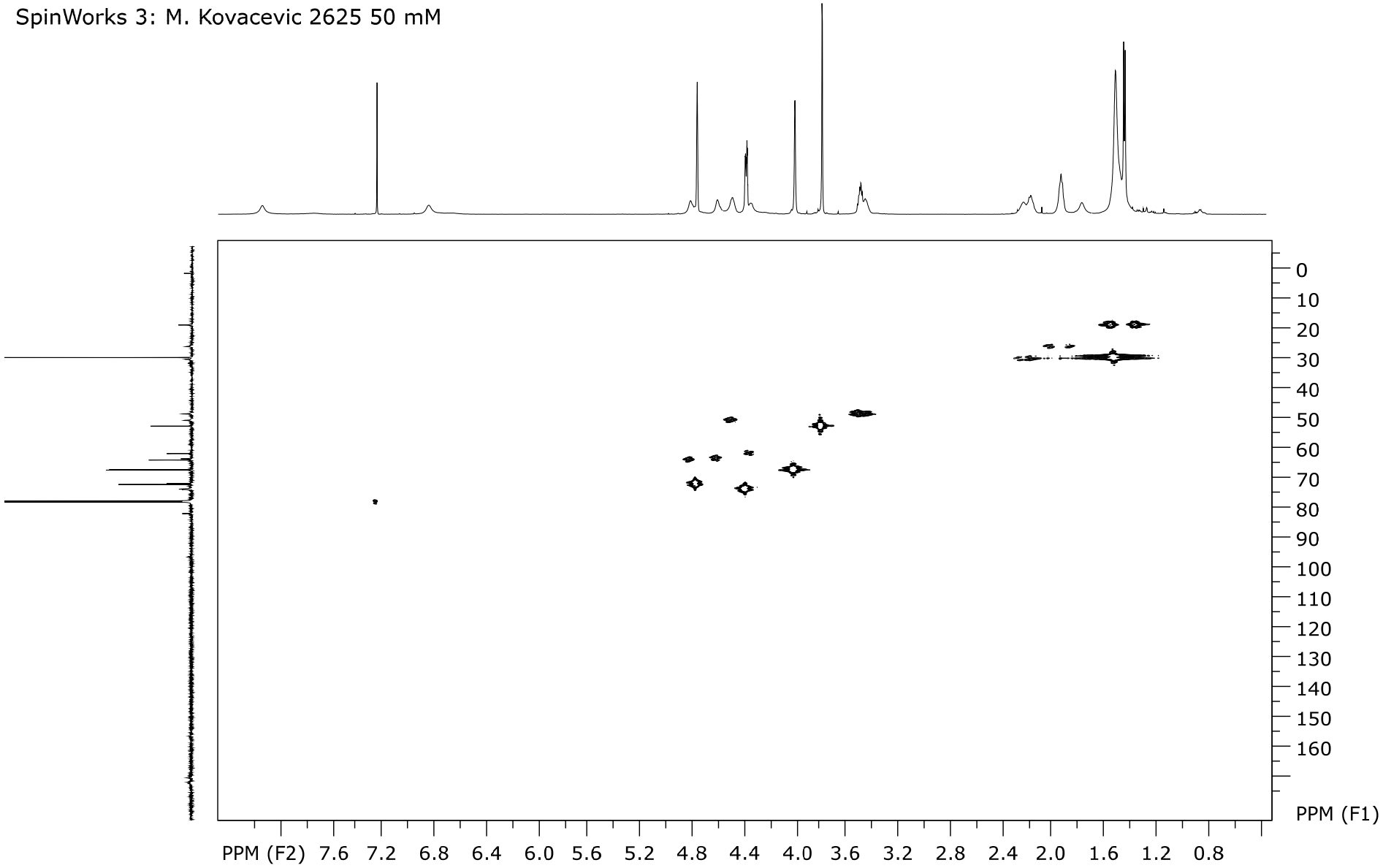

Figure S31. ^{1}H-^{13}C HMQC spectrum of compound **4** ($c = 5 \times 10^{-2}$ M).

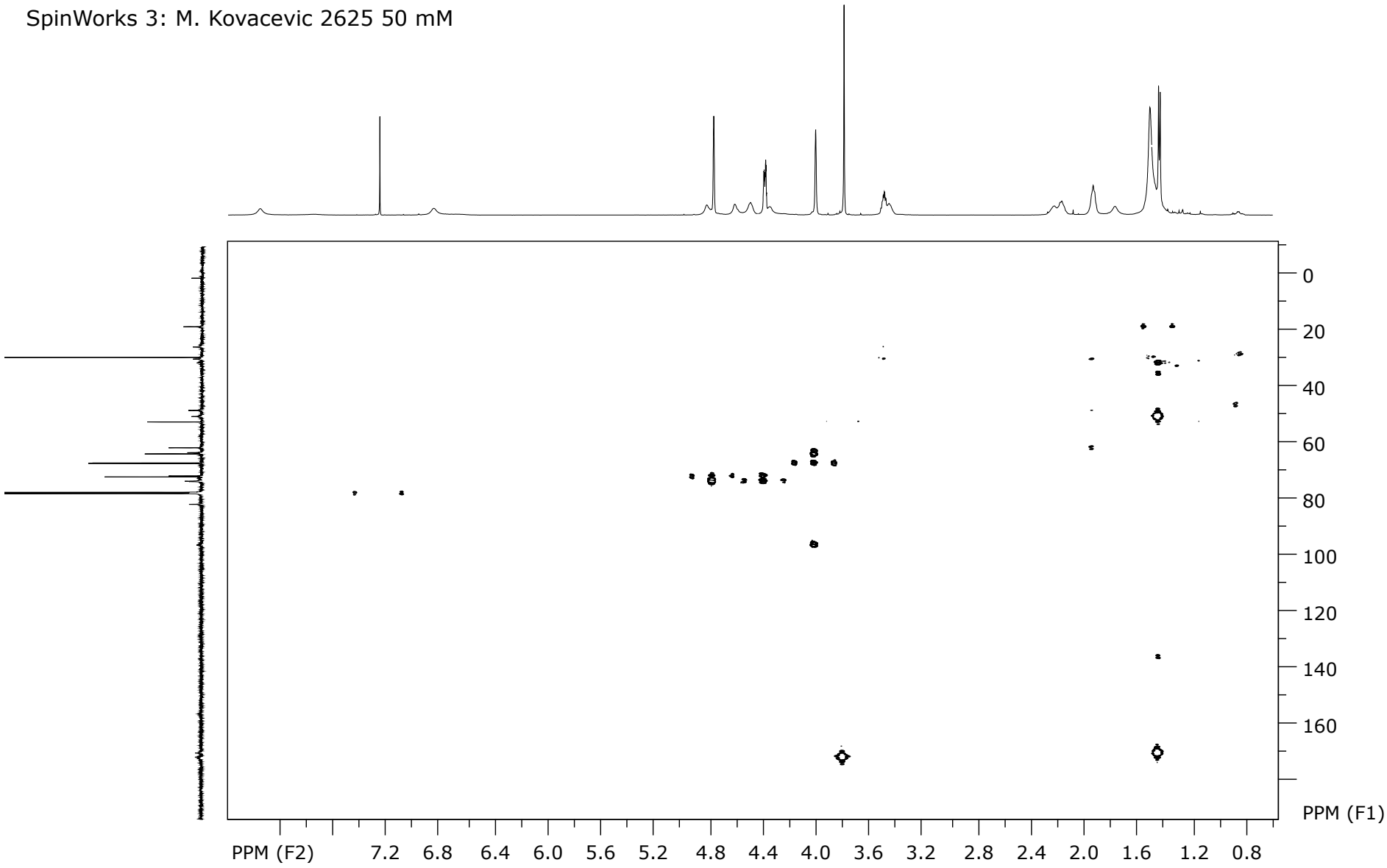

Figure S32. ^{1}H-^{13}C HMBC spectrum of compound **4** ($c = 5 \times 10^{-2}$ M).

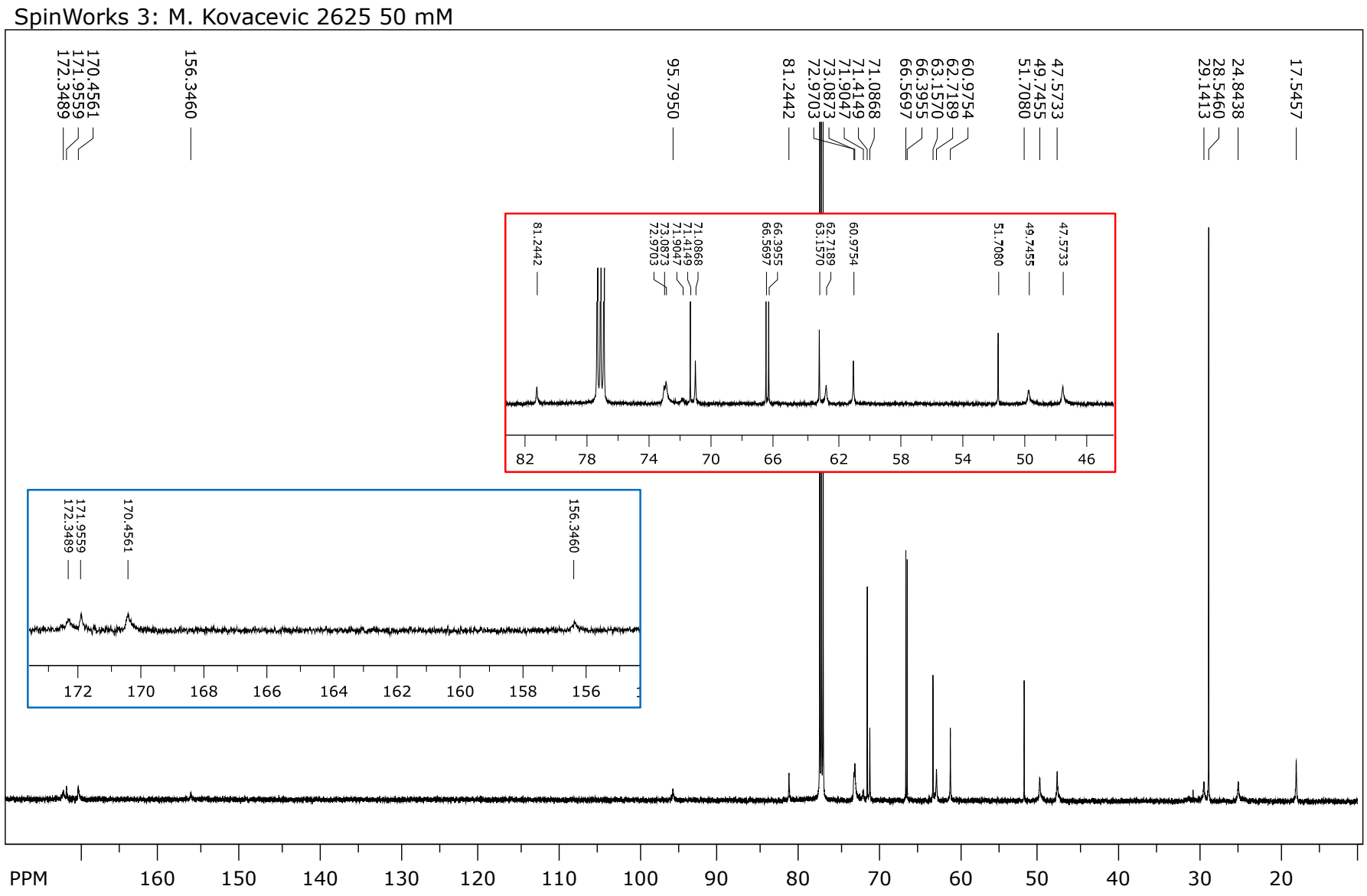

Figure S33. $^{13}C\{^{1}H\}$ NMR spectrum of compound **4** ($c = 5 \times 10^{-2}$ M).

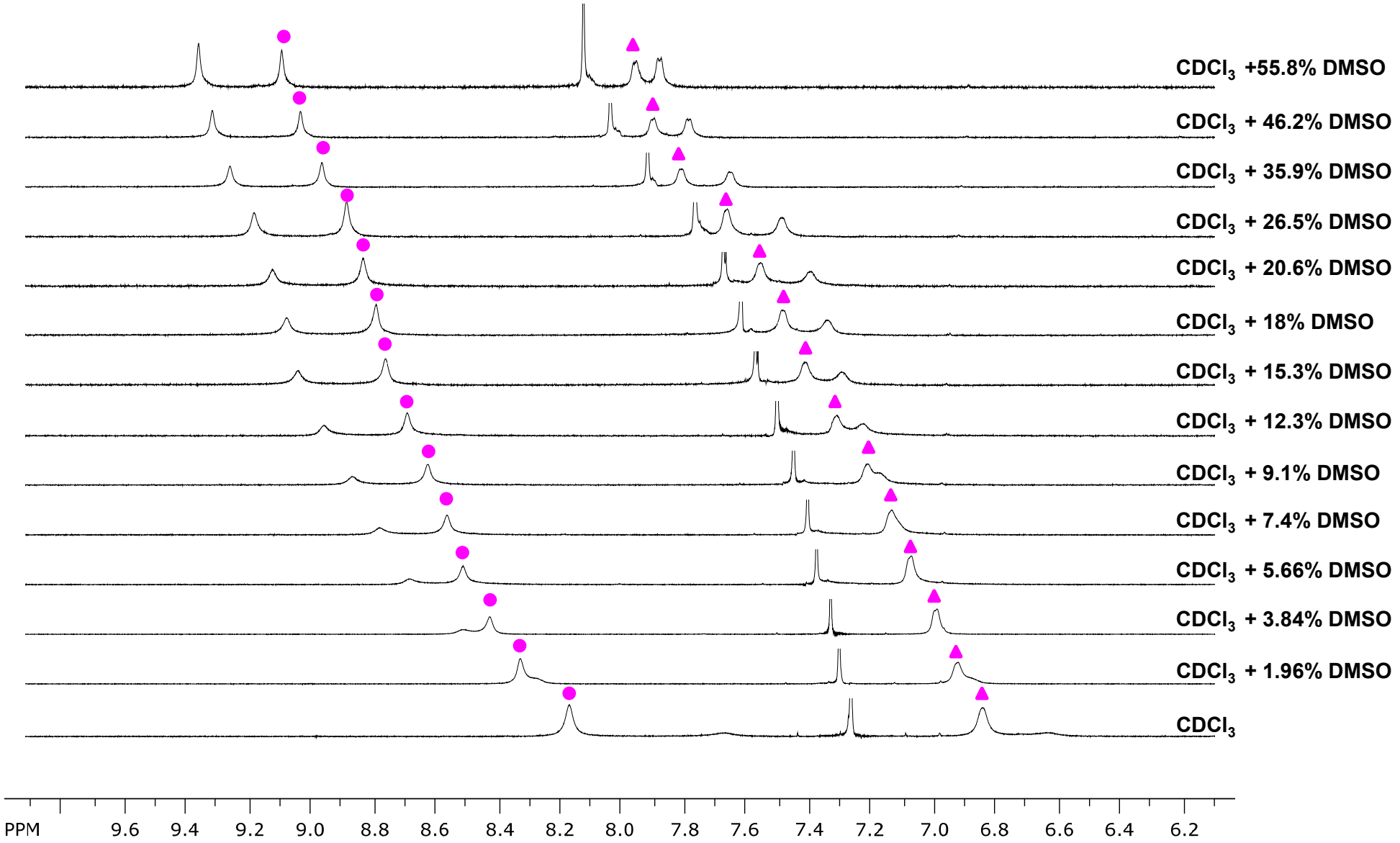

Figure S34. Solvent dependence of NH chemical shifts of compound **4** at varying concentrations of DMSO in $CDCl_3$ ($c = 2.5 \times 10^{-2}$ M).

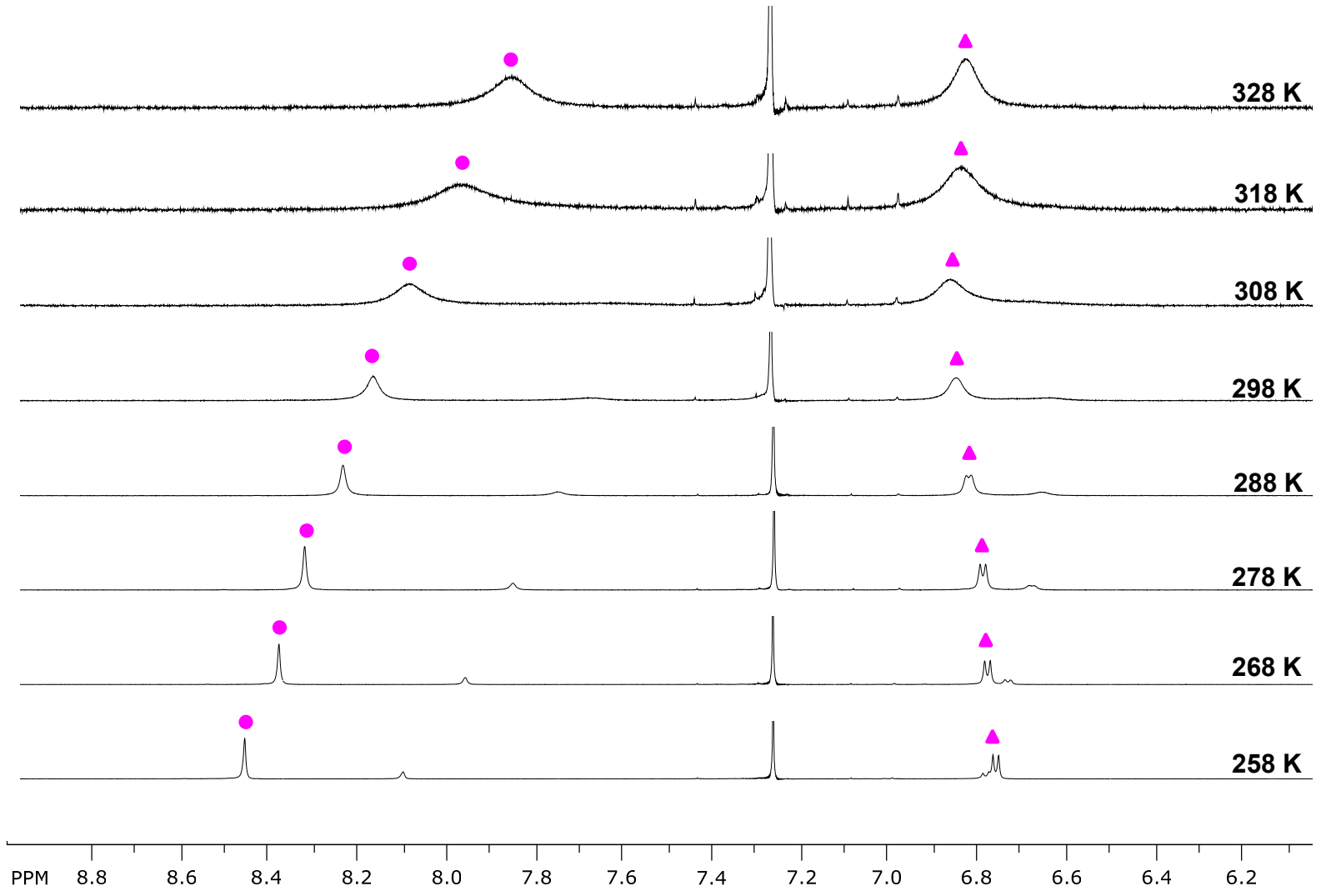

Figure S35. Temperature-dependent NH chemical shifts of compound **4** ($c = 1 \times 10^{-2}$ M).

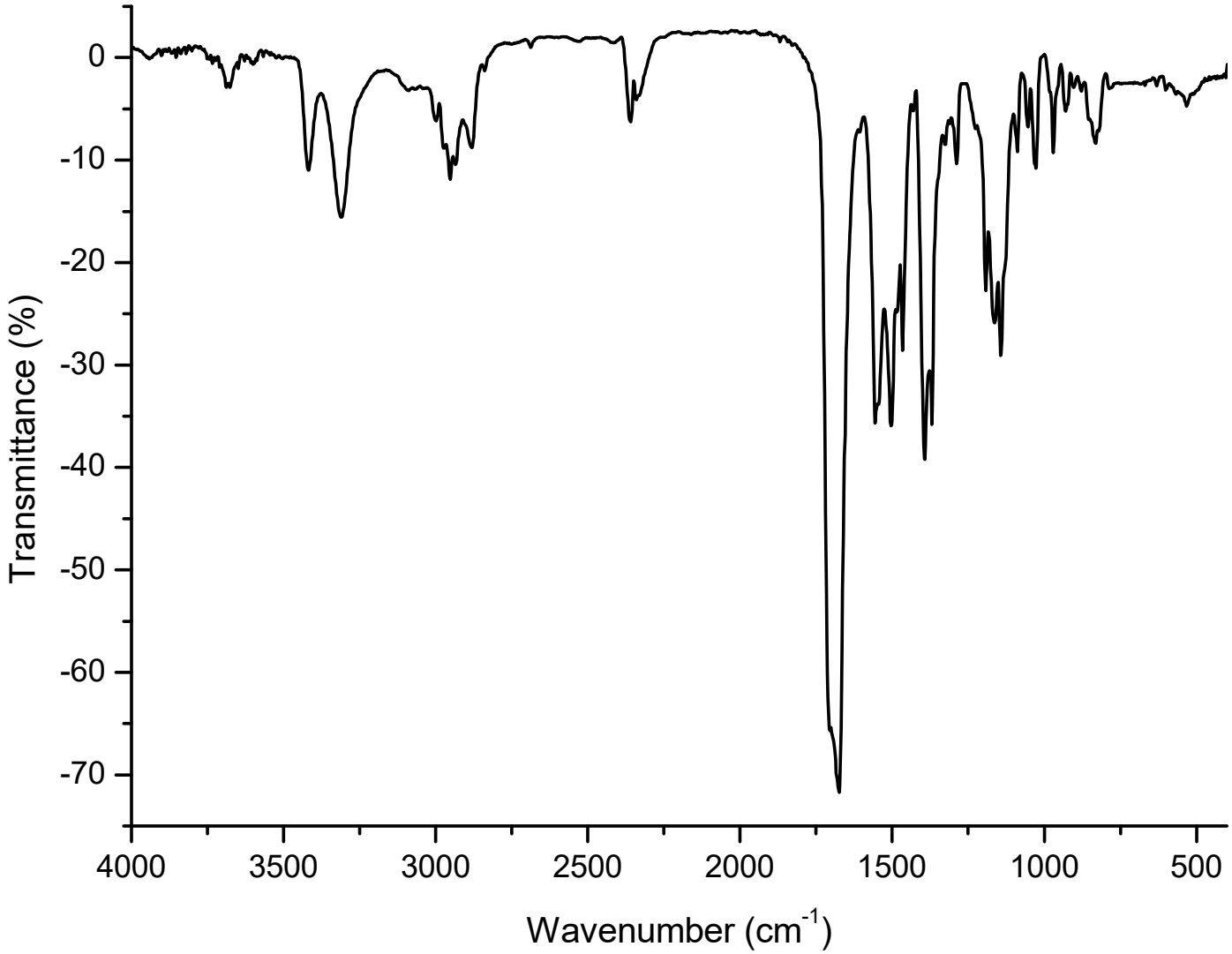

Figure S36. IR spectrum of compound **4** ($c = 5 \times 10^{-2}$ M) in DCM.

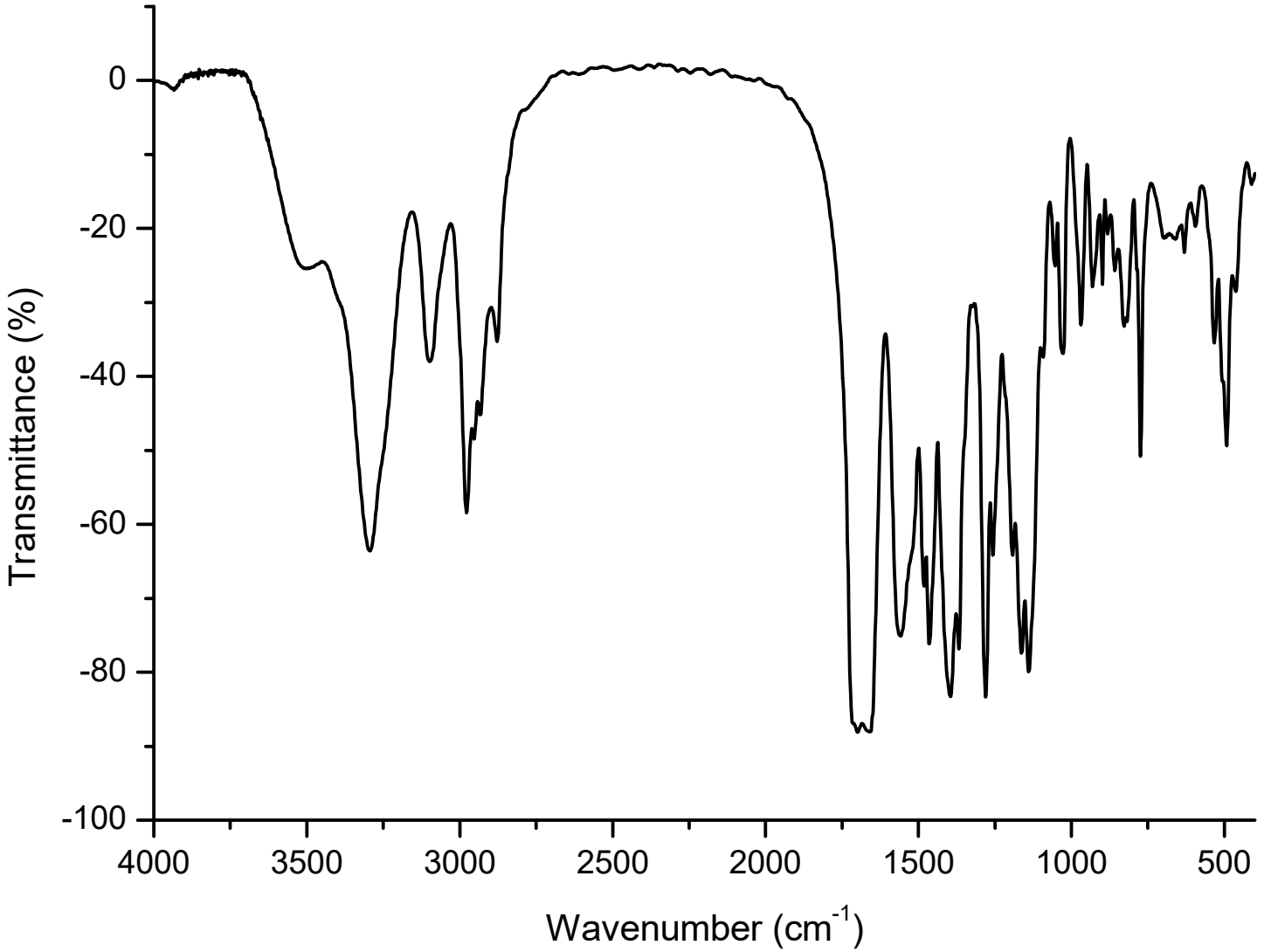

Figure S37. IR spectra of compound **4** (2 mg) in KBr (200 mg).

Ac-L-Pro-L-Ala-NH-Fn-COOMe (5)

Ion type	Calc. mass	Measured mass	Mass error / ppm	Mol. Formula	Int. CAL
M+	469.1300	469.1280	4.3	$C_{22}H_{27}N_3O5Fe$	azitromicin

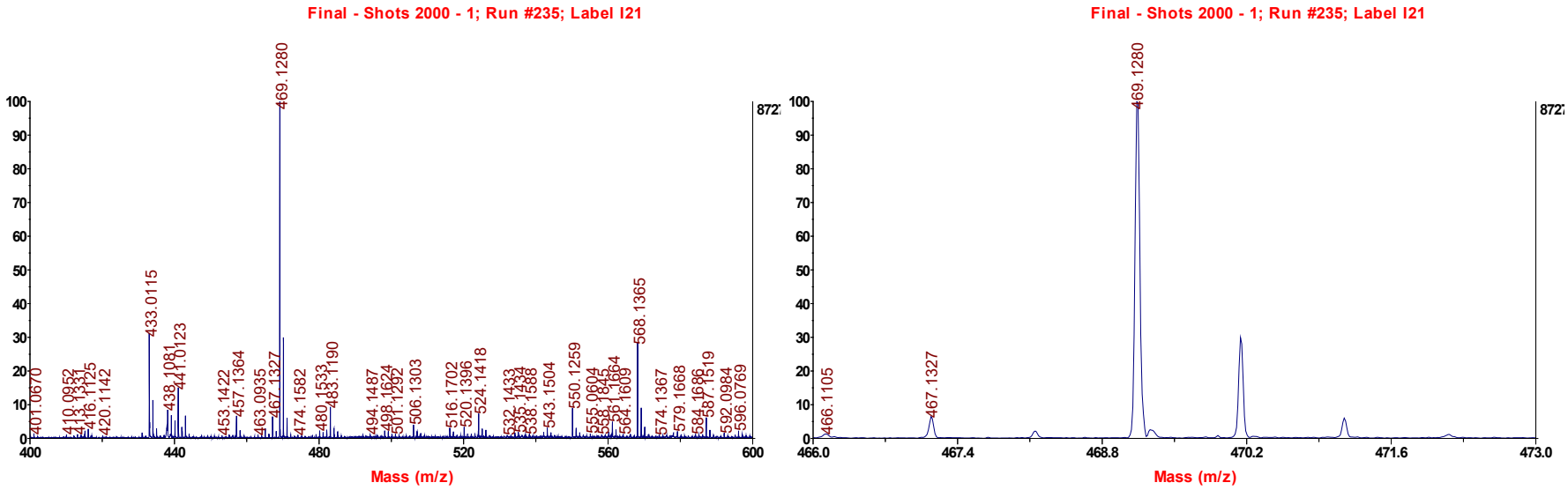

Figure S38. HRMS spectrum of compound **5.**

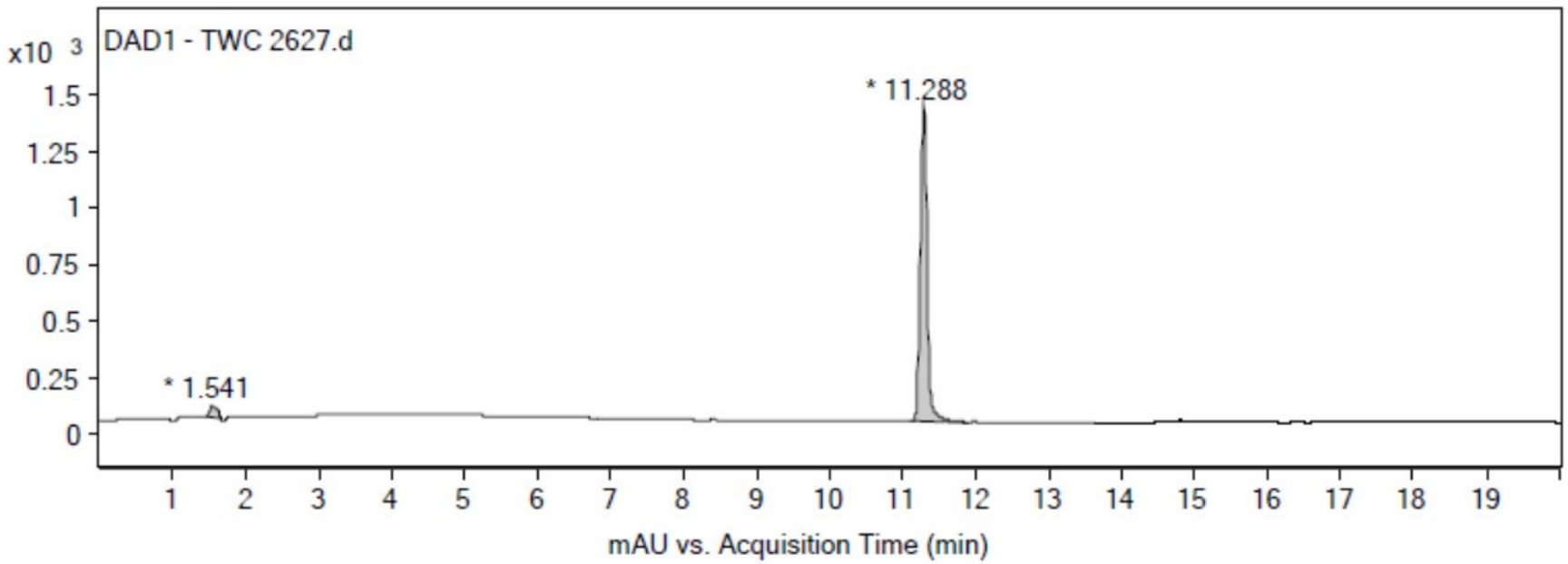

Integration Peak List

Peak	Start	RT	End	Height	Area	Area %
1	1.461	1.541	1.648	46.76	329.46	3.47
2	11.101	11.288	11.881	1411.81	9488.61	100

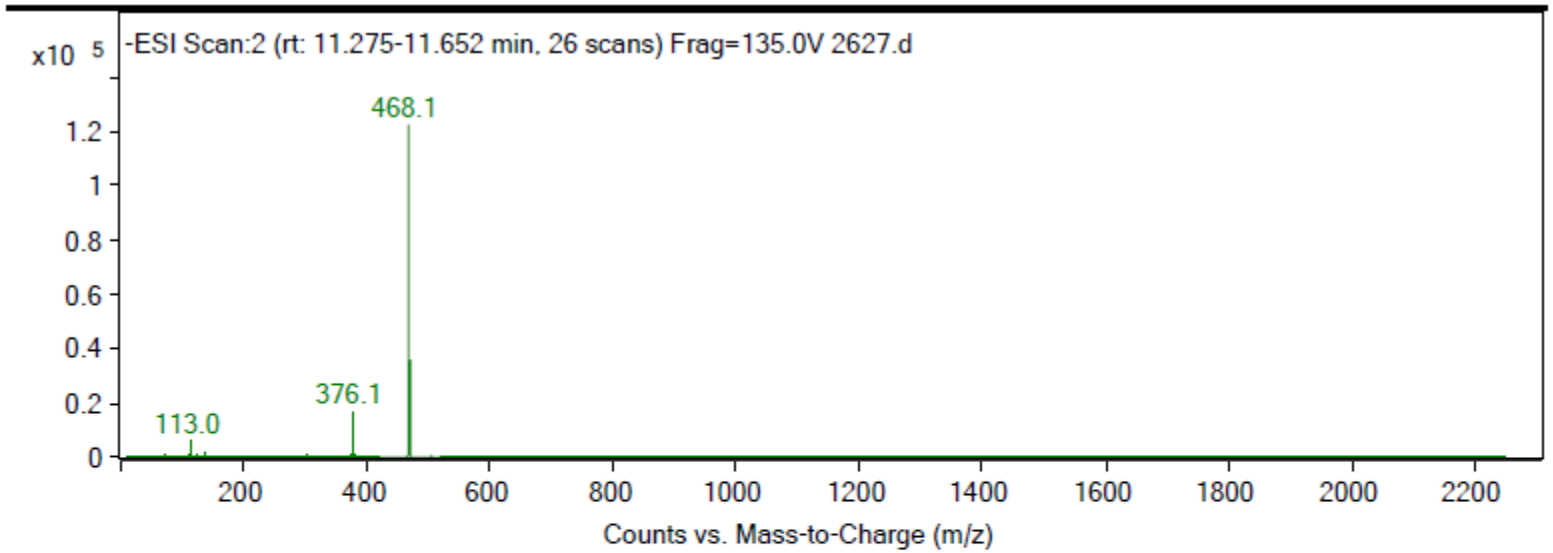

Peak List

m/z	z	Abund
113		6106.96
137		1766.12
376.1	1	16761.93
377	1	2996.78
466.1		8795.53
468.1	1	122427.03
469.1	1	35895.96
470.1	1	6283.23

Figure S39. HPLC-ESI spectra of compound **5.**

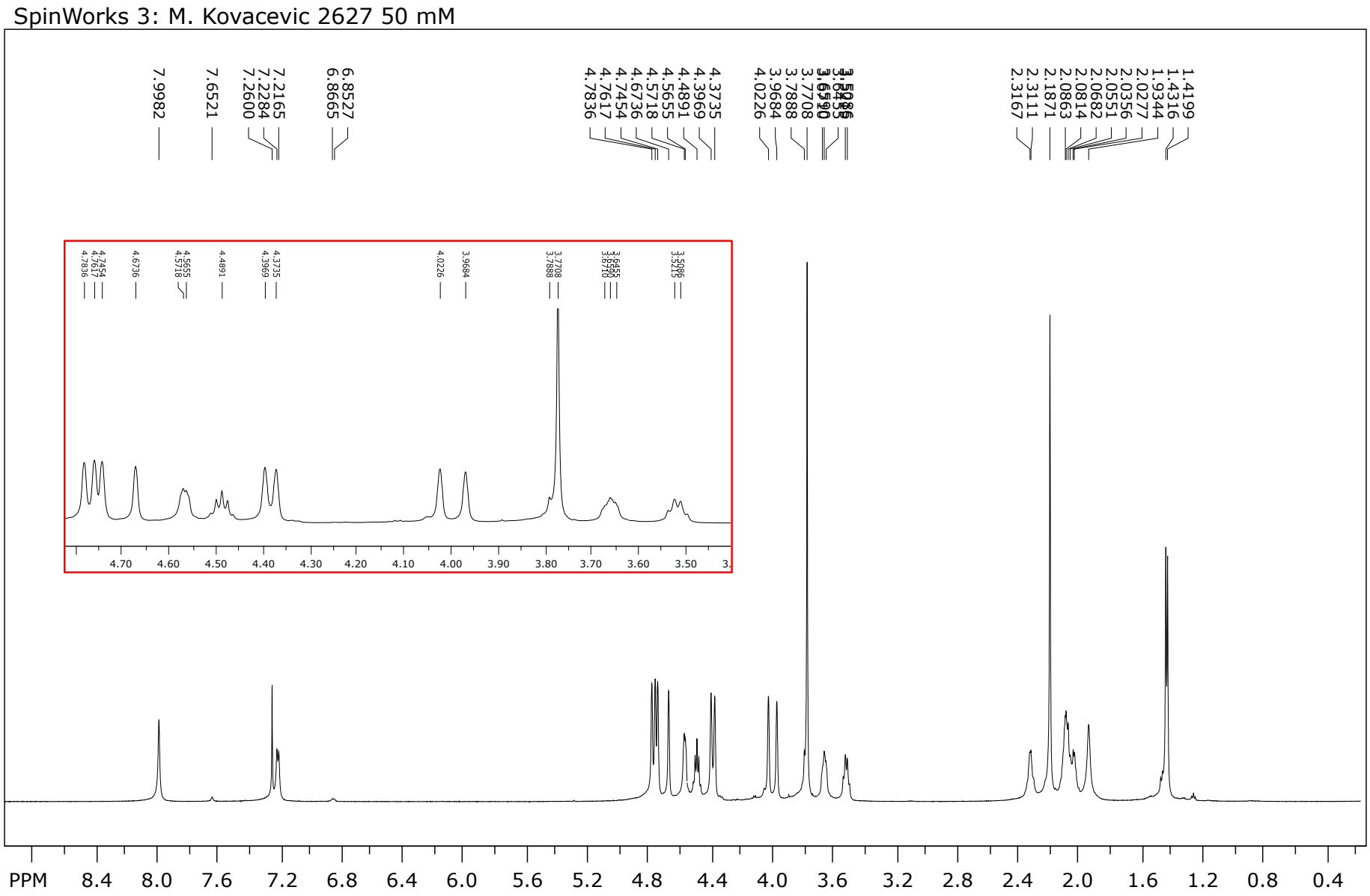

Figure S40. ^{1}H NMR spectrum of compound **5** ($c = 5 \times 10^{-2}$ M).

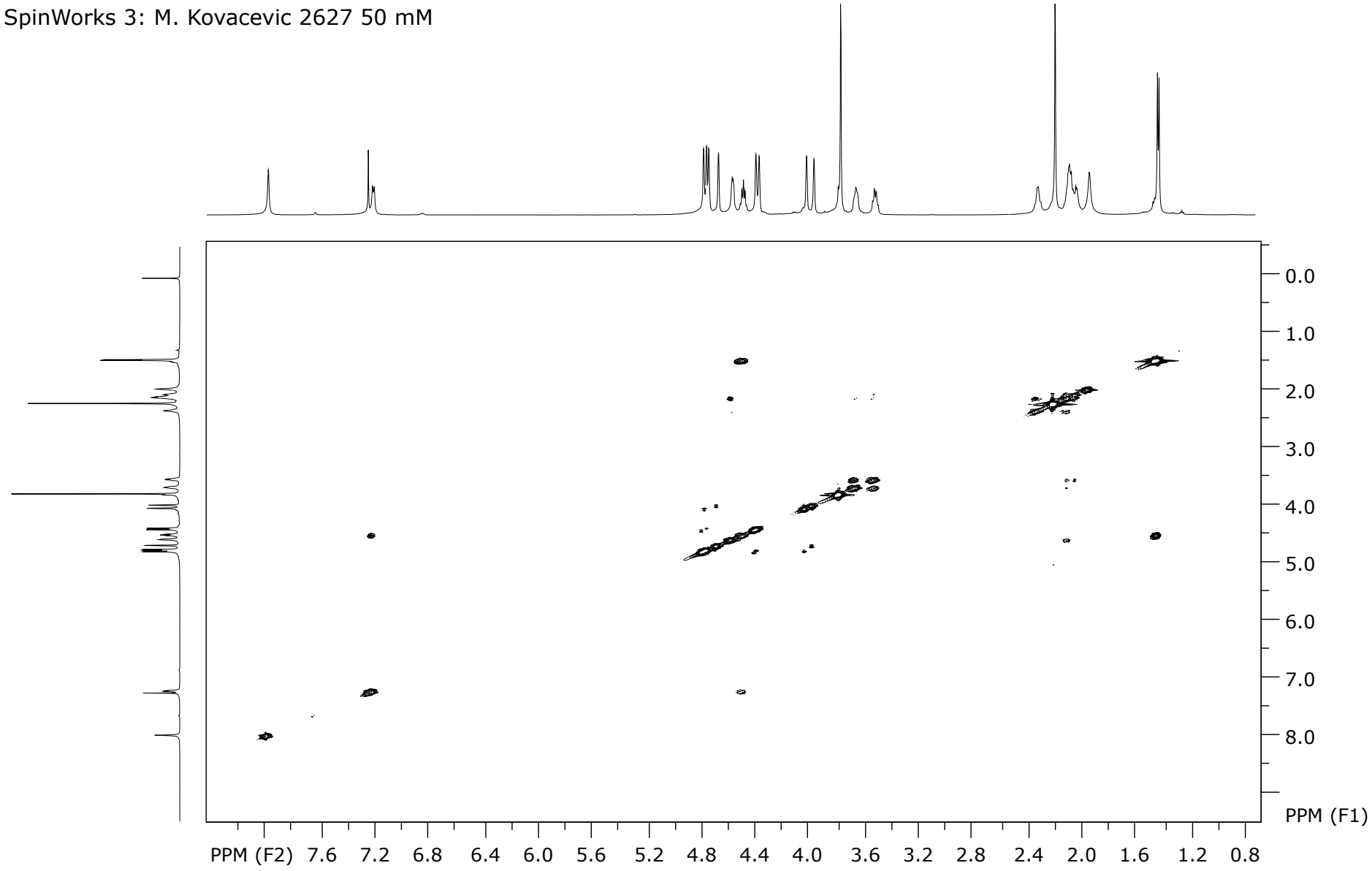

Figure S41. ^{1}H-^{1}H COSY NMR spectrum of compound **5** ($c = 5 \times 10^{-2}$ M).

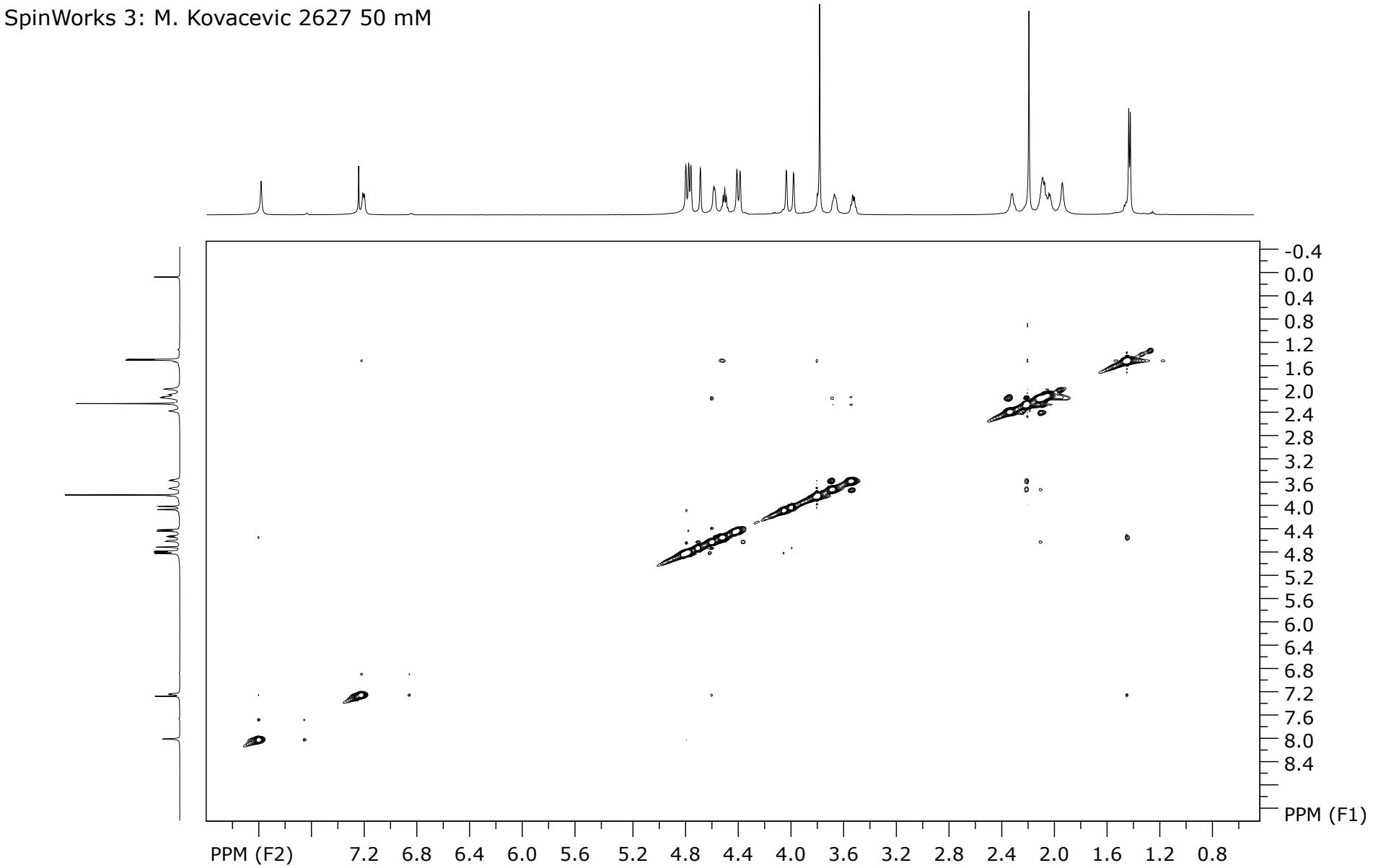

Figure S42. ^{1}H-^{1}H NOESY NMR spectrum of compound **5** ($c = 5 \times 10^{-2}$ M).

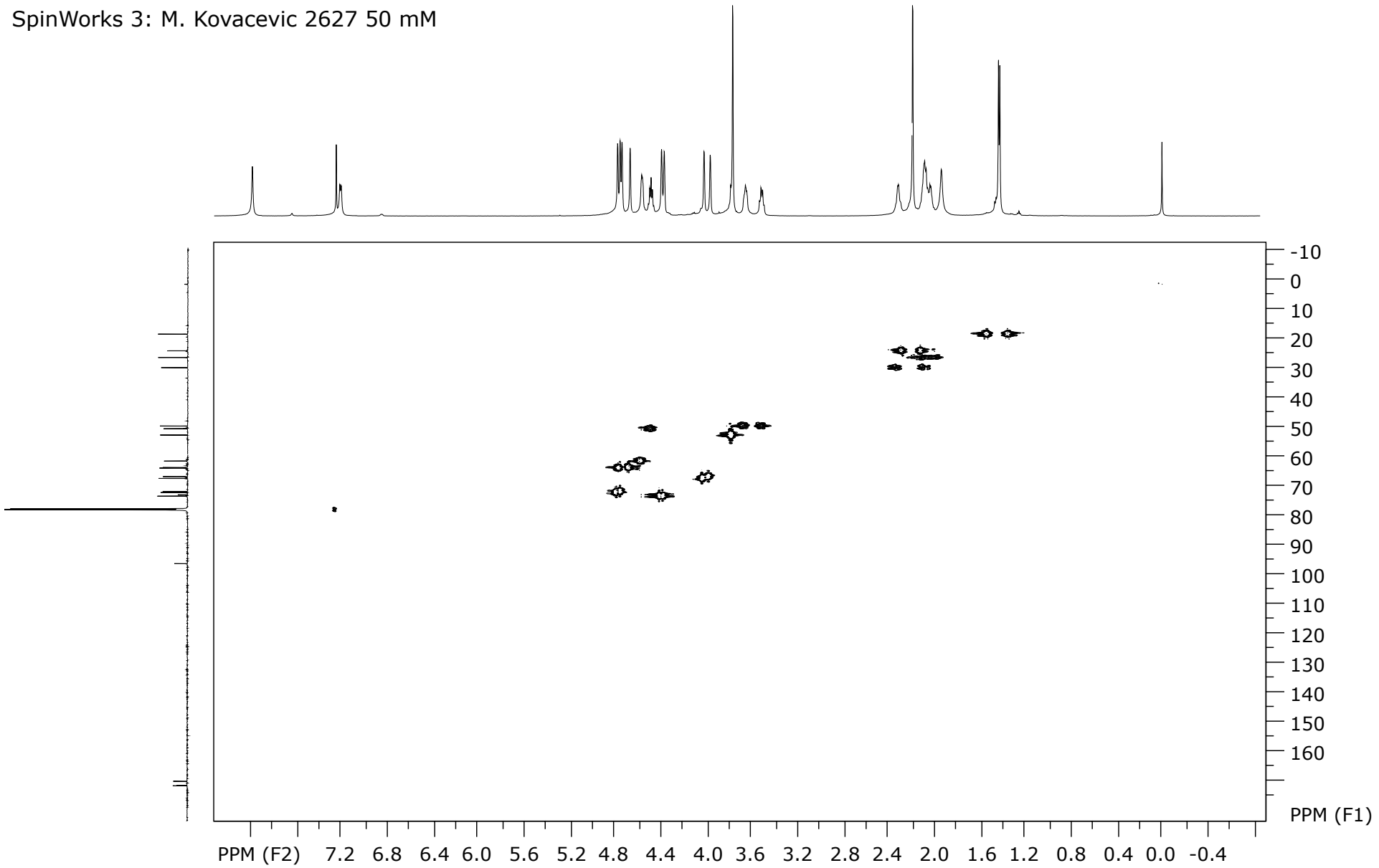

Figure S43. ^{1}H-^{13}C HMQC spectrum of compound **5** ($c = 5 \times 10^{-2}$ M).

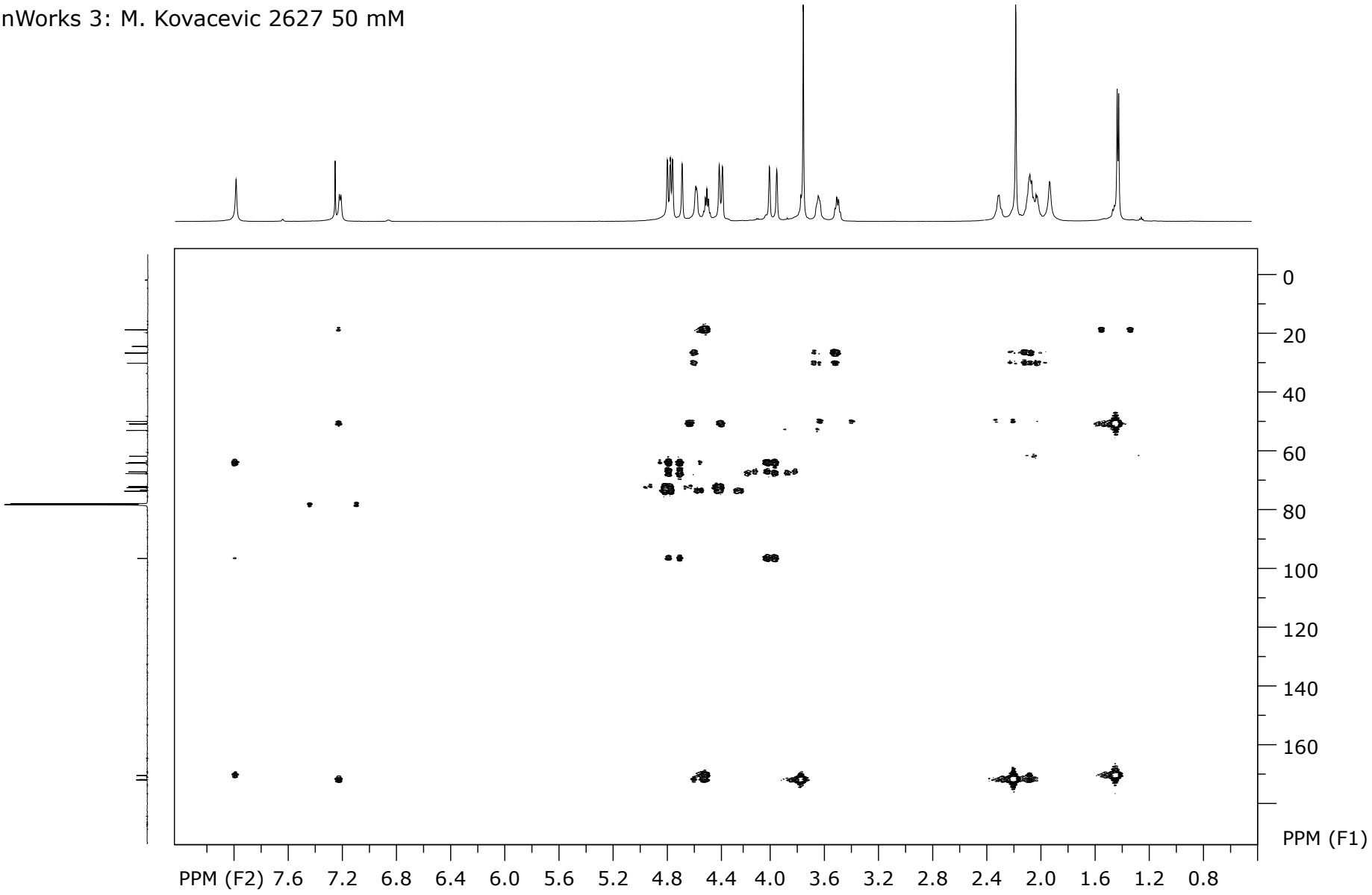

Figure S44. ^{1}H-^{13}C HMBC spectrum of compound **5** ($c = 5 \times 10^{-2}$ M).

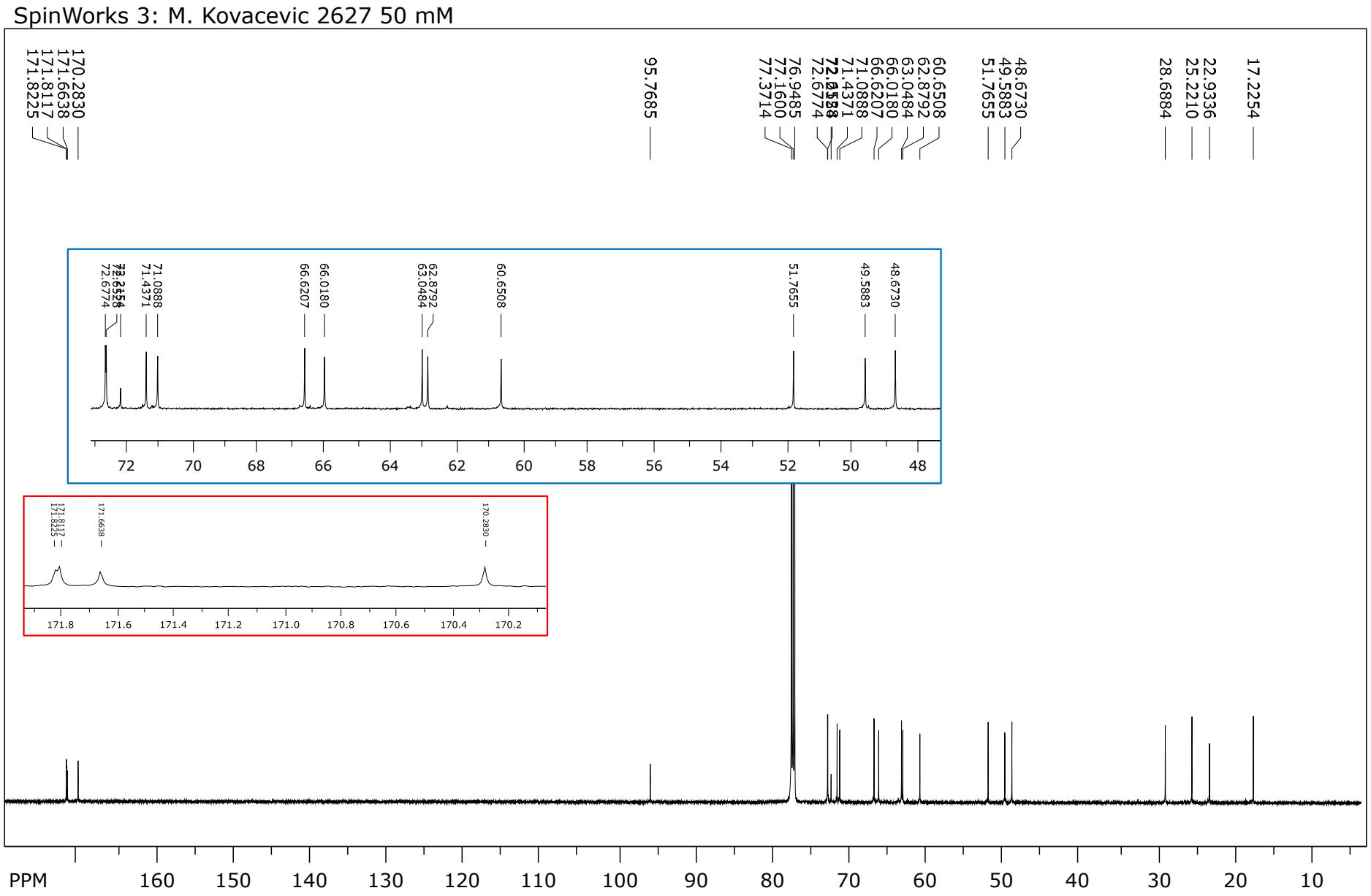

Figure S45. $^{13}C\{^{1}H\}$ NMR spectrum of compound **5** ($c = 5 \times 10^{-2}$ M).

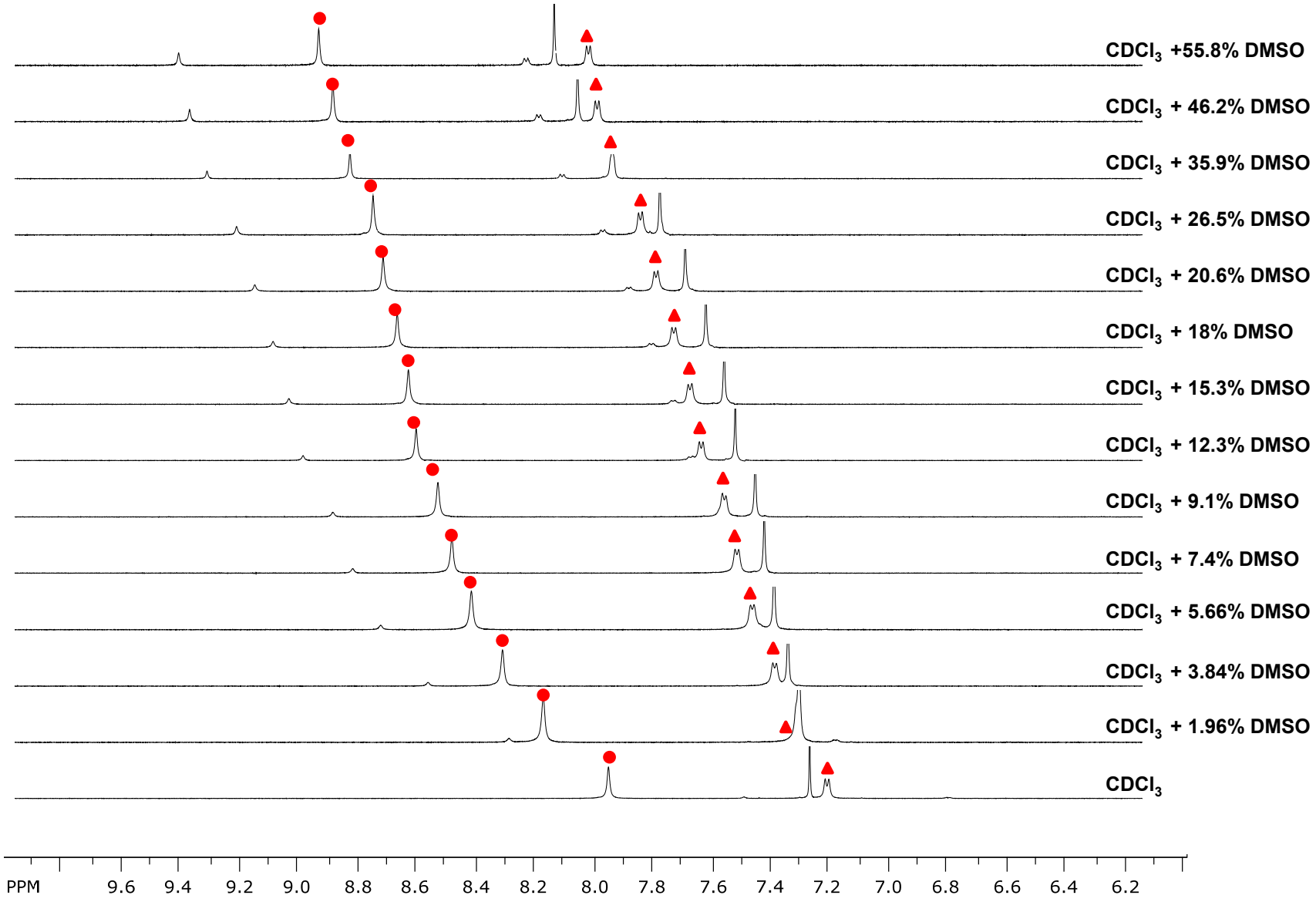

Figure S46. Solvent dependence of NH chemical shifts of compound **5** at varying concentrations of DMSO in $CDCl_3$ ($c = 2.5 \times 10^{-2}$ M).

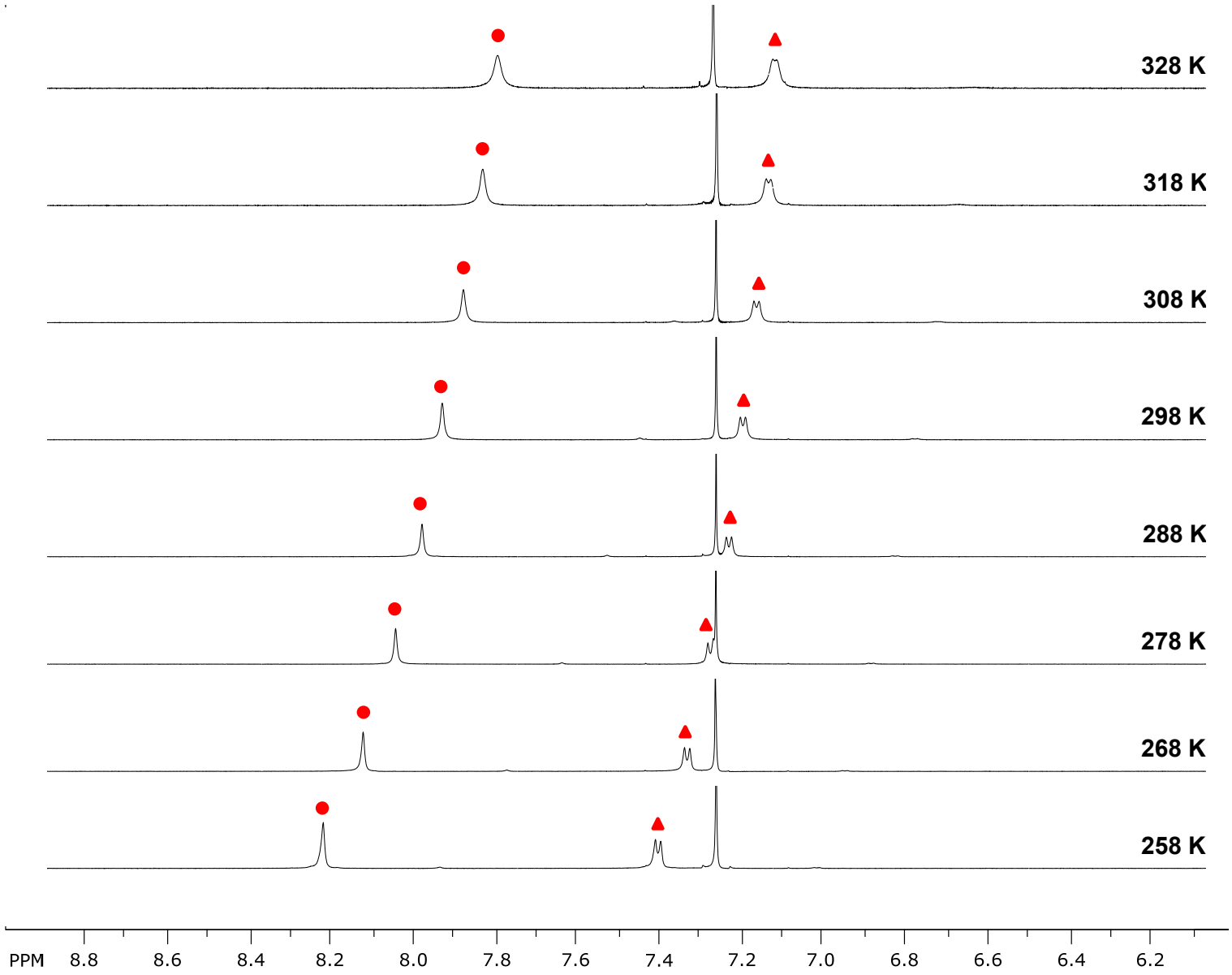

Figure S47. Temperature-dependent NH chemical shifts of compound **5** ($c = 1 \times 10^{-2}$ M).

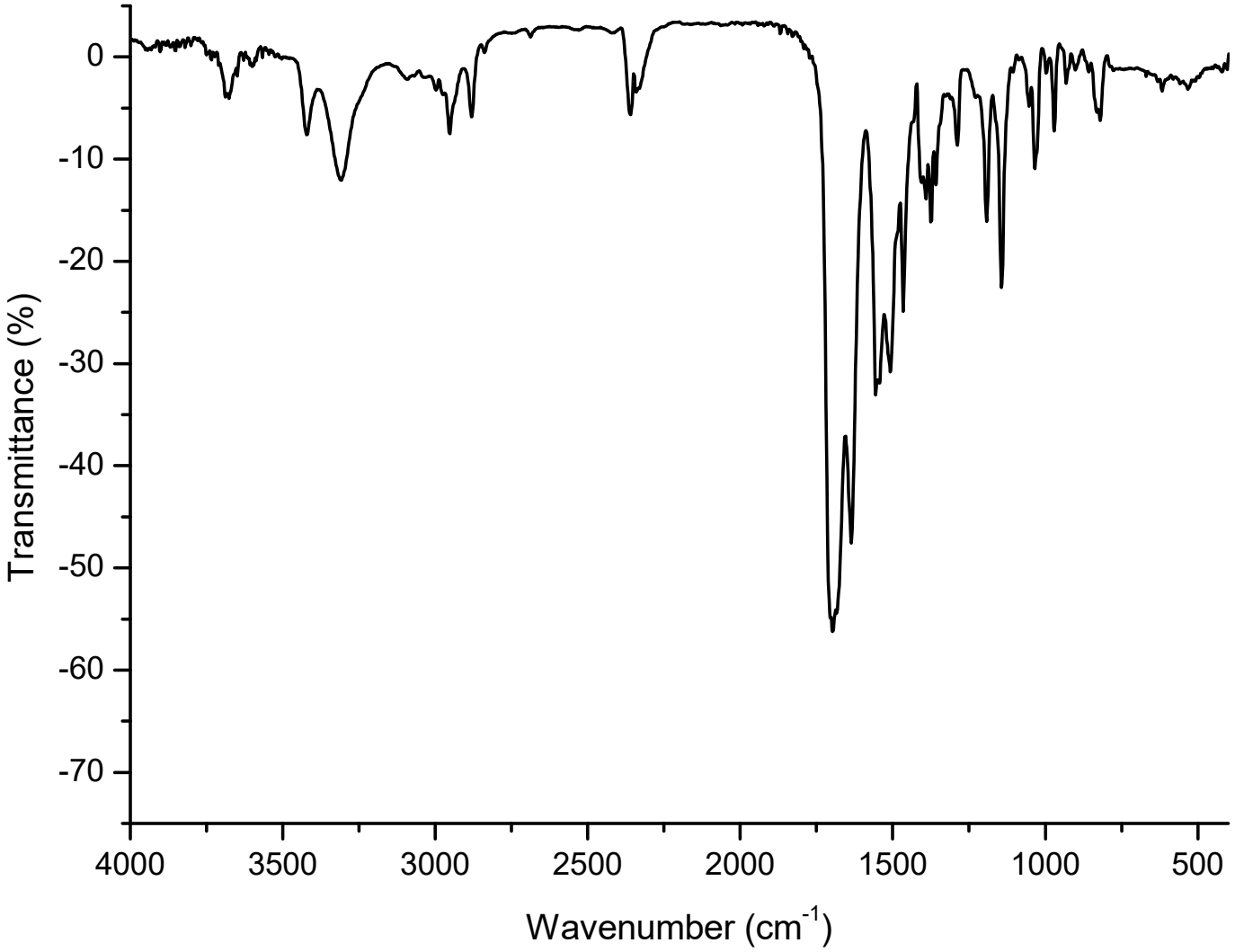

Figure S48. IR spectrum of compound **5** ($c = 5 \times 10^{-2}$ M) in DCM.

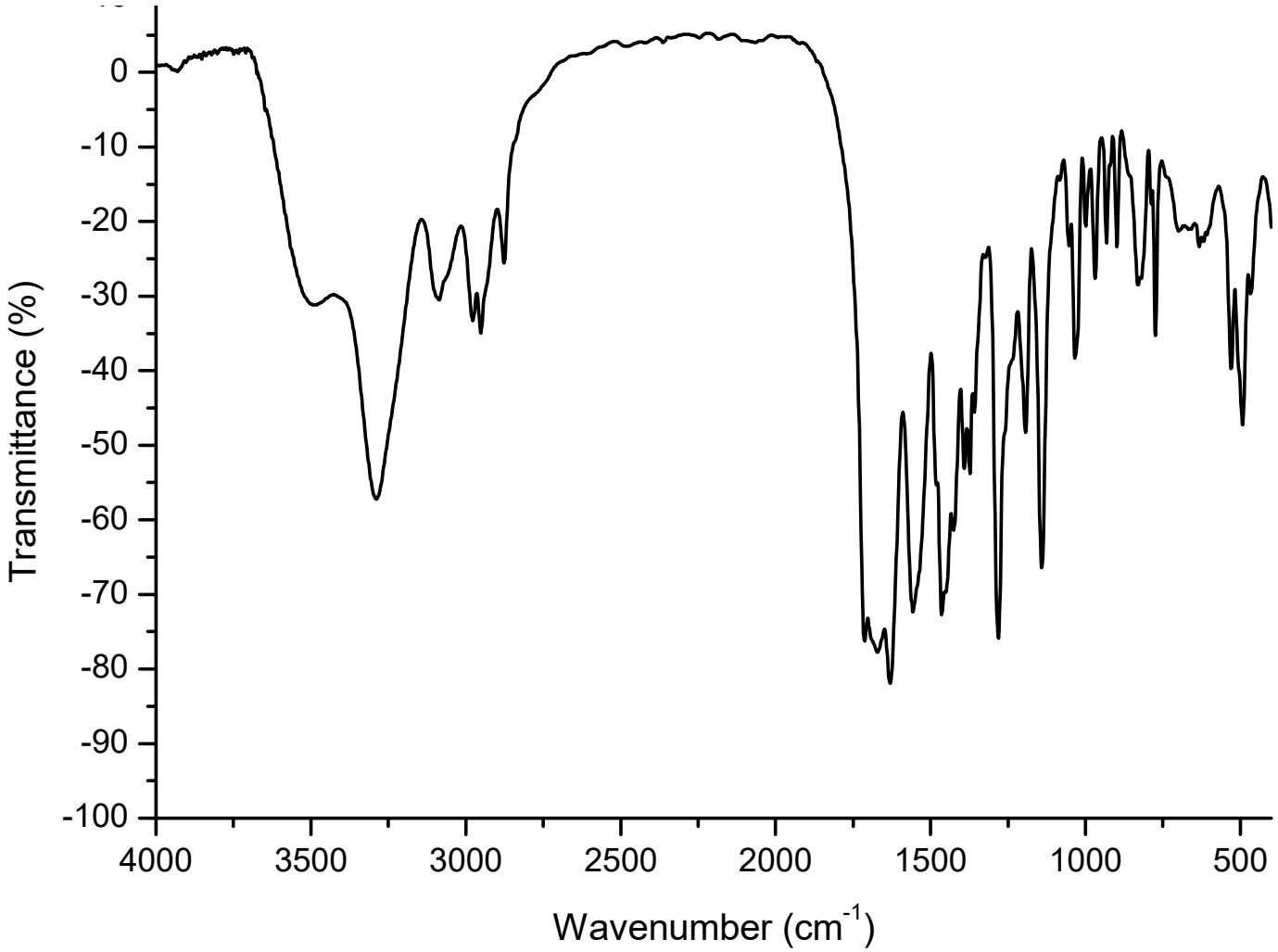

Figure S49. IR spectrum of compound **5** (2 mg) in KBr (200 mg).

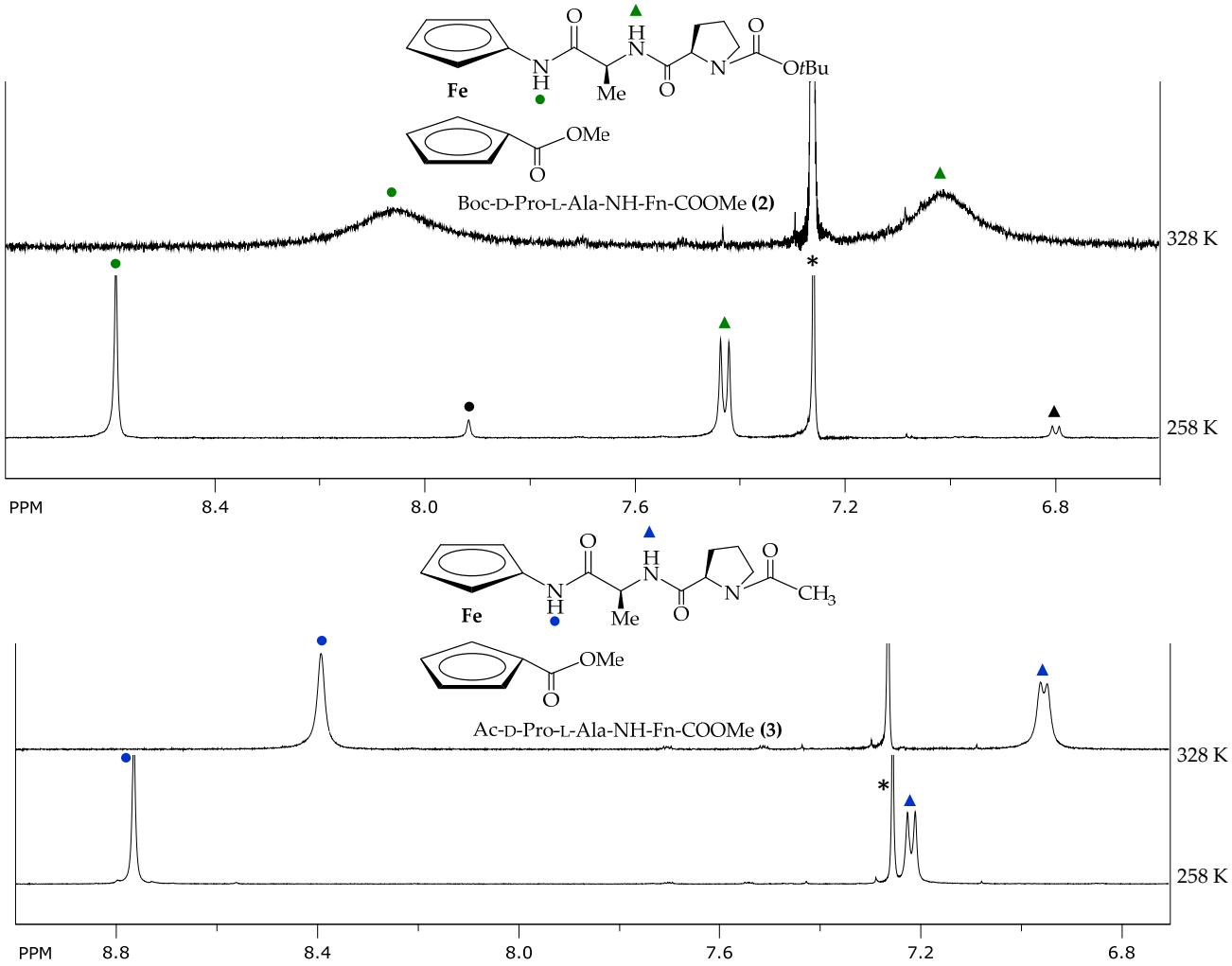
Fe
Me
OtBu
OMe
Boc-D-Pro-L-Ala-NH-Fn-COOMe (2)
328 K
258 K
PPM
8.4
8.0
7.6
7.2
6.8
Fe
Me
CH3
OMe
Ac-D-Pro-L-Ala-NH-Fn-COOMe (3)
328 K
258 K
PPM
8.8
8.4
8.0
7.6
7.2
6.8

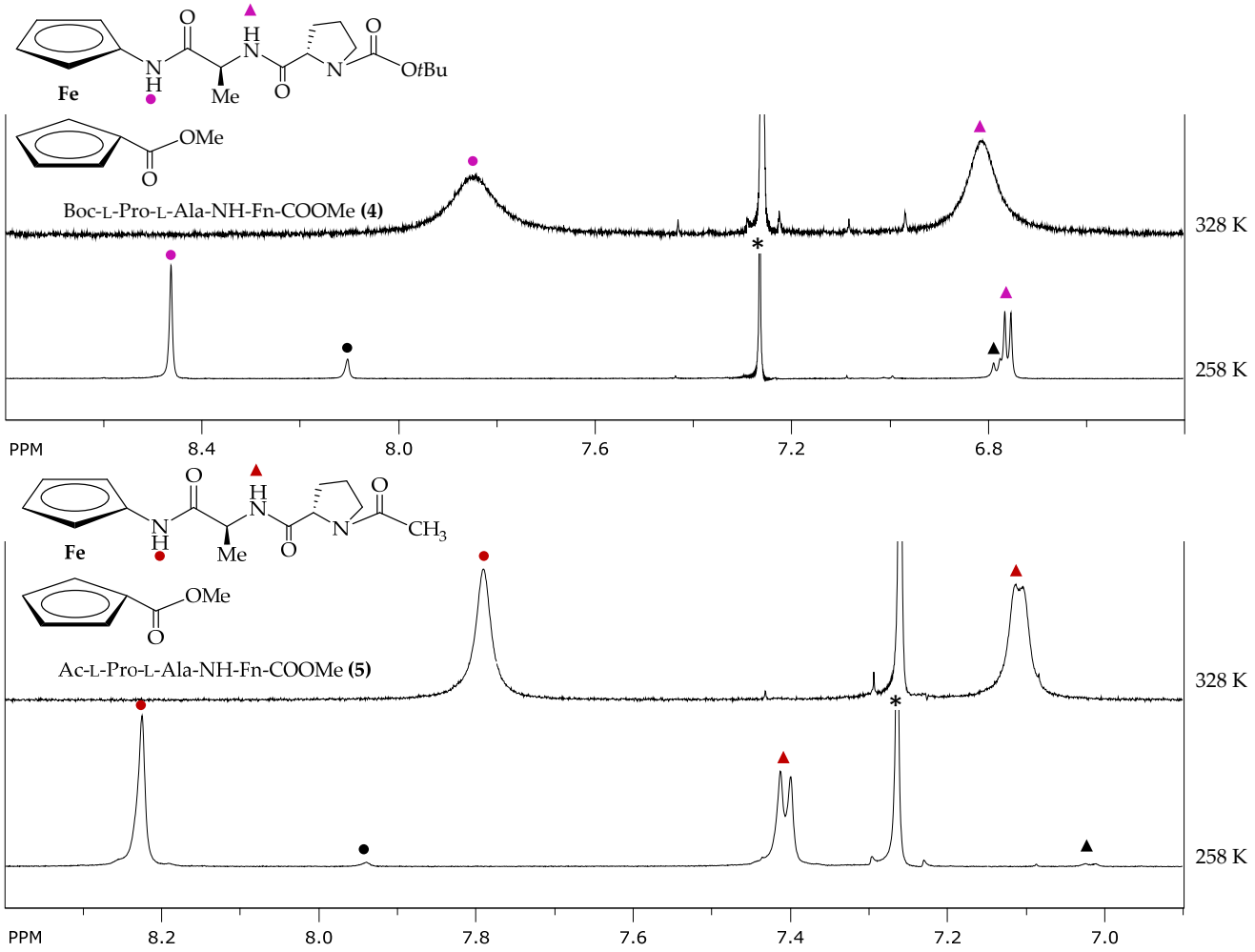

Figure S50. The influence of increased temperature on the *cis*/*trans* signals coalescence in peptides **2-5.**

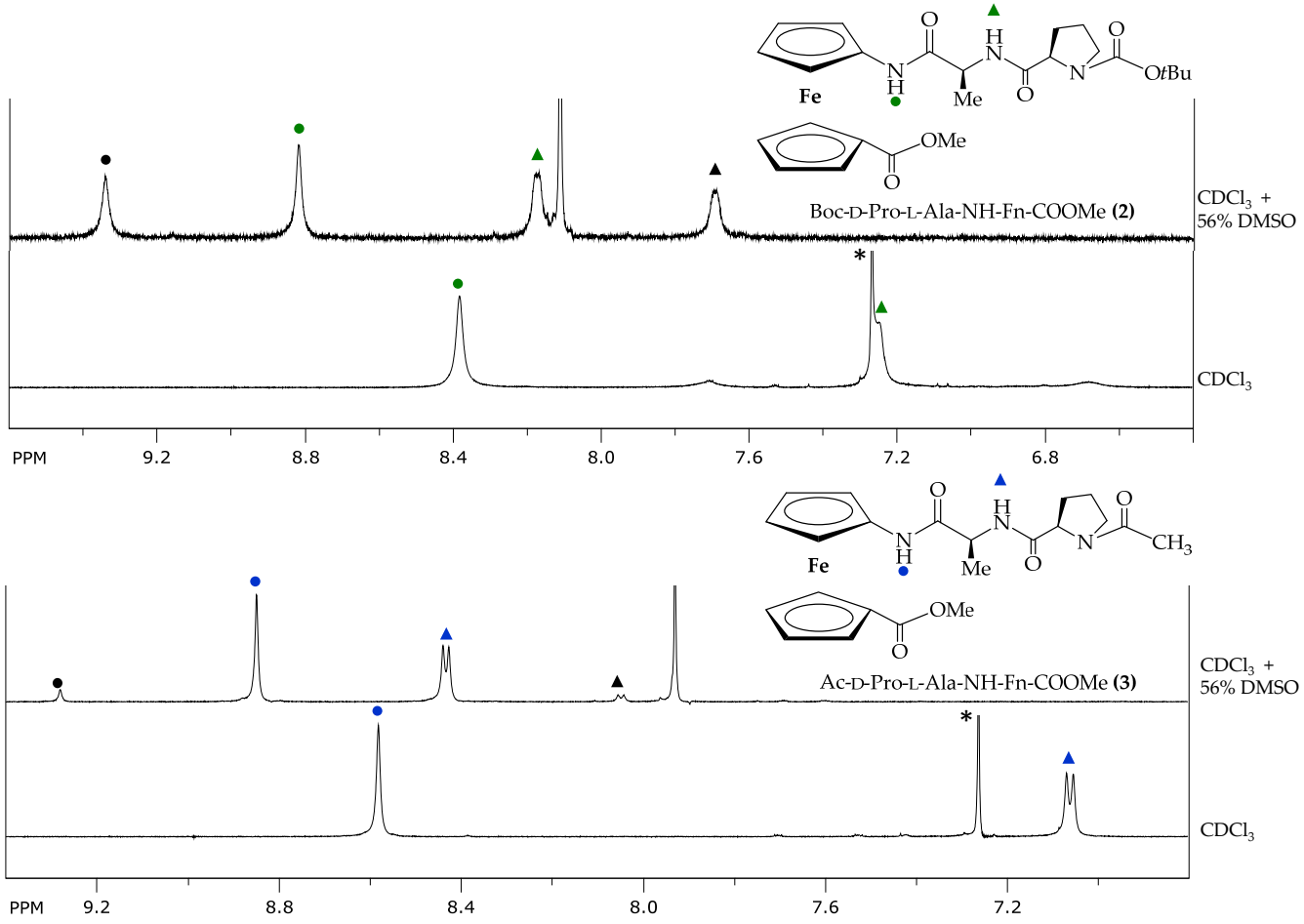
Fe
Me
OtBu
OMe
Boc-D-Pro-L-Ala-NH-Fn-COOMe (2)
CDCl3 + 56% DMSO
CDCl3
PPM
9.2
8.8
8.4
8.0
7.6
7.2
6.8
Fe
Me
CH3
OMe
Ac-D-Pro-L-Ala-NH-Fn-COOMe (3)
CDCl3 + 56% DMSO
CDCl3
PPM
9.2
8.8
8.4
8.0
7.6
7.2

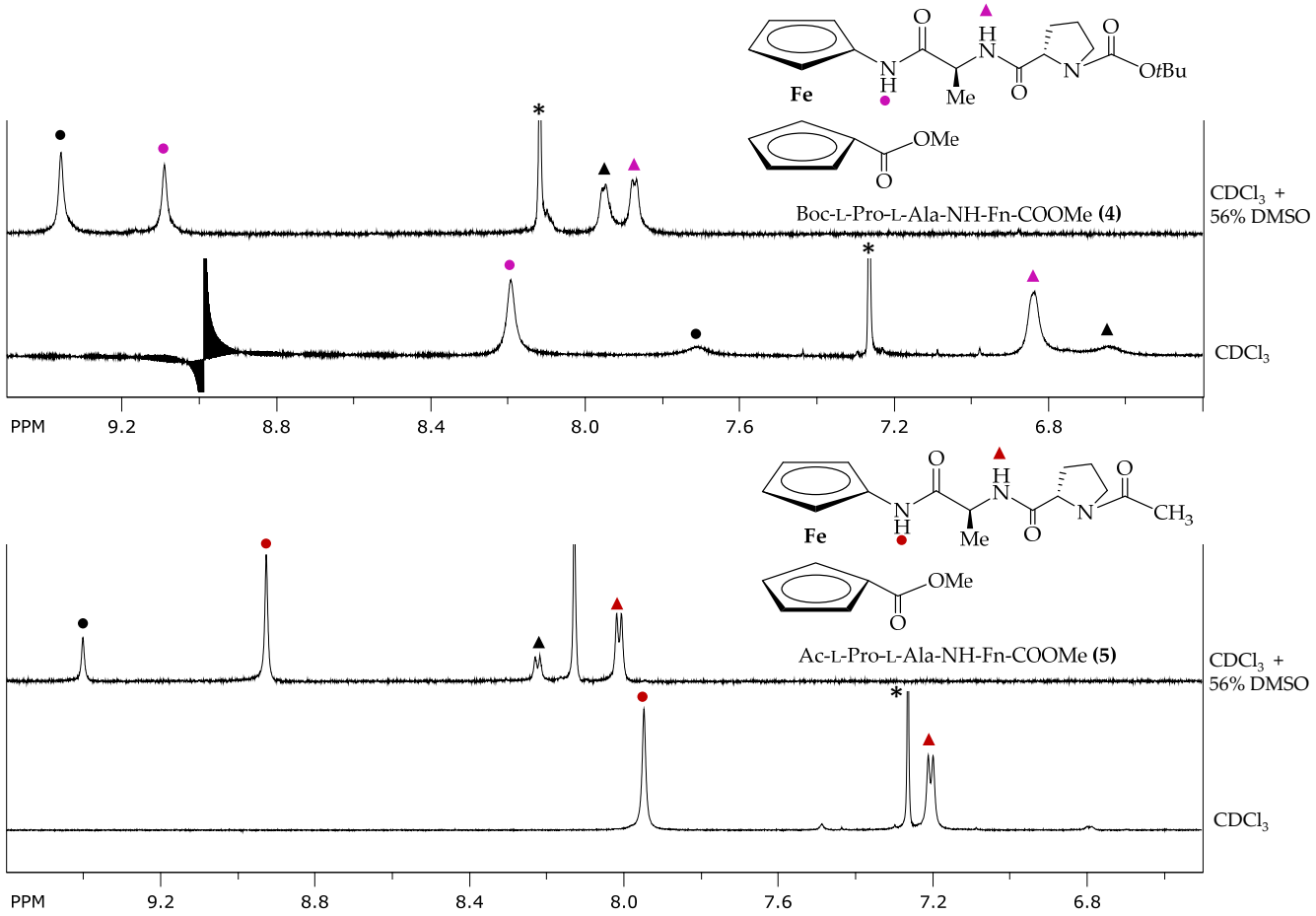

Figure S51. The influence of DMSO on *cis-trans* isomerization of a proline imide bond in peptides **2-5.**

X-ray crystal structure analysis

Table S52. Crystallographic, data collection and refinement data.

Compound	**2**	**5**
Empirical formula	$C_{25}H_{33}FeN_3O_6$	$C_{22}H_{26}FeN_3O_6$
Formula wt. / g mol^{-1}	527.39	484.31
Colour	yellow	yellow
Crystal dimensions / mm	0.20 x 0.09 x 0.05	0.15 x 0.09 x 0.04
Space group	$P\,2_12_12_1$	$C\,2$
a / Å	5.88390(10)	22.3927(8)
b / Å	17.6280(2)	6.2677(3)
c / Å	24.6876(4)	16.5434(7)
α / °	90	90
β / °	90	104.007(4)
γ / °	90	90
Z	4	4
V / Å^3	2560.63(7)	2252.84(17)
D_{calc} / g cm^{-3}	1.368	1.475
λ / Å	1.54179 (Cu$K\alpha$)	1.54179 (Cu$K\alpha$)
μ / mm^{-1}	5.094	5.742

Compound	**2**	**5**
Θ range / °	3.58 – 79.66	2.75 – 76.27
T / K	293(2)	293(1)
Diffractometer type	Synergy S	Xcalibur Nova
Range of h, k, l	$-4 < h < 7$; $-20 < k < 22$; $-31 < l < 26$	$-28 < h < 25$; $-5 < k < 7$; $-20 < l < 15$
Reflections collected	18409	5290
Independent reflections	5486	3415
Observed reflections ($I \geq 2\sigma$)	5251	2765
Absorption correction	Multi-scan	Multi-scan
T_{min}, T_{max}	0.1844; 1.0000	0.2363; 1.0000
R_{int}	0.0314	0.0862
R (F)	0.0293	0.0702
R_w (F^2)	0.0791	0.1998
Goodness of fit	1.071	1.019
H atom treatment	Constrained	Constrained
No. of parameters	316	280
No. of restraints	0	41
$\Delta\rho_{max}$, $\Delta\rho_{min}$ (eÅ^{-3})	0.367; -0.371	0.535; -0.623

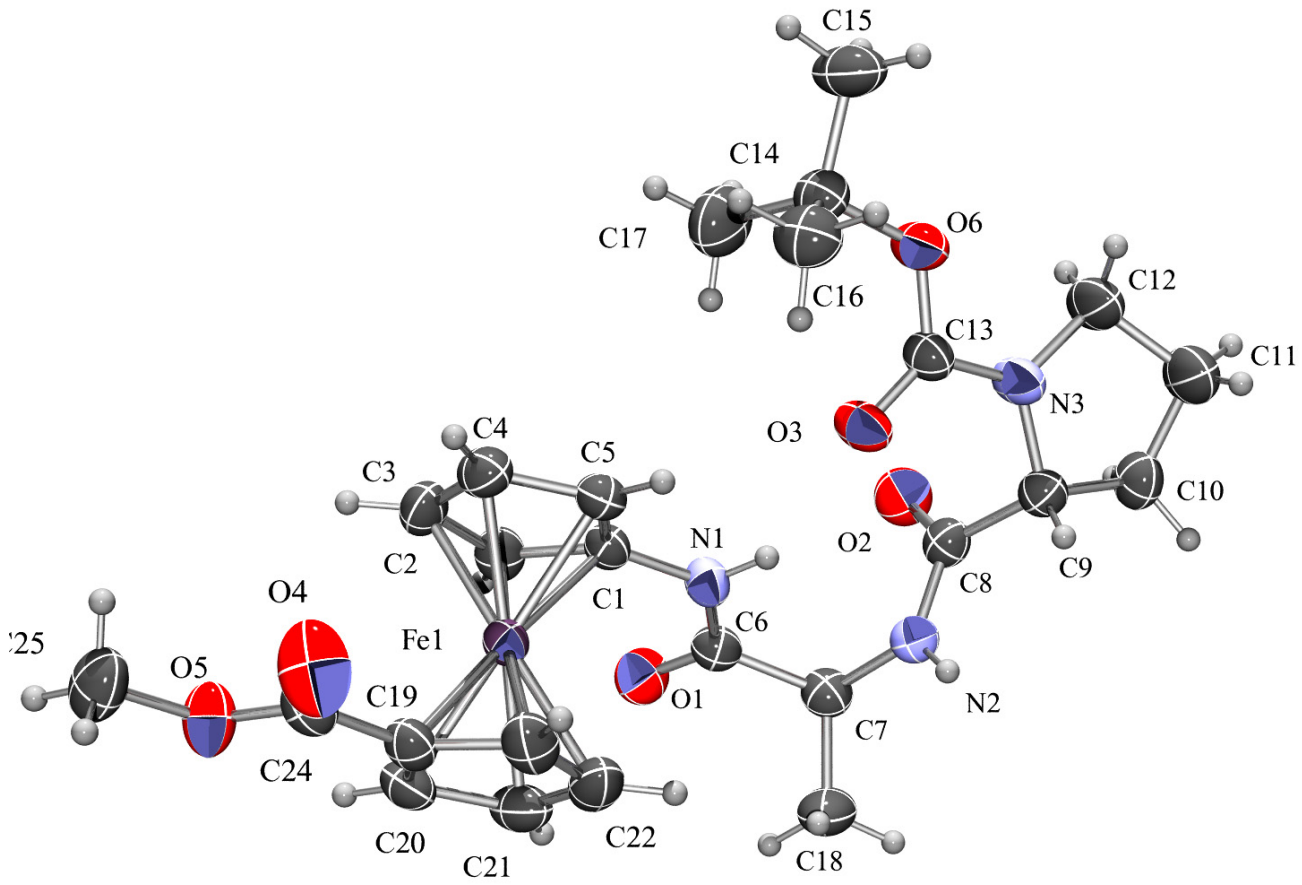

Figure S53. ORTEP-3 drawing of a molecule of **2**. Displacement ellipsoids are drawn for the probability of 50 % and hydrogen atoms are shown as spheres of arbitrary radii.

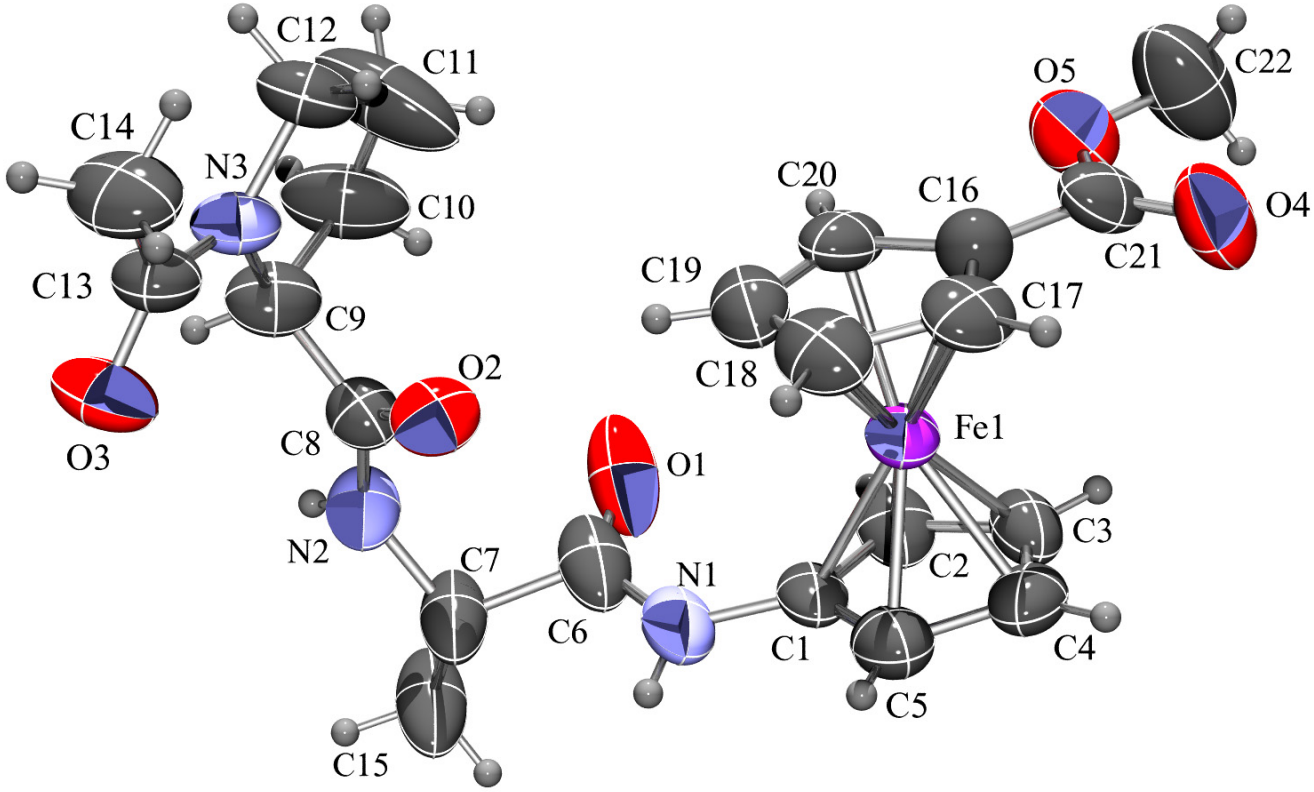

Figure S54. ORTEP-3 drawing of a molecule of **5**. Displacement ellipsoids are drawn for the probability of 50 % and hydrogen atoms are shown as spheres of arbitrary radii.

Table S55. Geometric parameters of hydrogen bonding (Å, °).

	D–H / Å	H···*A* / Å	*D*···*A* / Å	*D*–H···*A* / º	Symm. op. on *A*
		2			
N1–H1···O3	0.86	2.11	2.898(3)	151	*x*, *y*, *z*
N1–H1···N2	0.86	2.32	2.749(3)	111	*x*, *y*, *z*
N2–H2···O1	0.86	2.11	2.954(3)	168	–1+*x*, *y*, *z*
C2–H2A···O1	0.93	2.51	2.940(3)	108	*x*, *y*, *z*
C5–H5···O3	0.93	2.80	3.326(4)	117	*x*, *y*, *z*
C10–H10A···O2	0.97	2.55	3.226(3)	127	–1+*x*, *y*, *z*
C16–H16B···O3	0.96	2.34	2.961(3)	122	*x*, *y*, *z*
C17–H17C···O3	0.96	2.45	3.048(4)	120	*x*, *y*, *z*
C4–H4···O2	0.93	2.80	3.598(4)	144	*x*, –1/2+*y*, 3/2–*z*
C23–H23··O5	0.93	2.71	3.442(4)	136	–1+*x*, *y*, *z*
C15–H15C···O5	0.96	2.79	3.723(4)	165	1/2–*x*, –*y*, –1/2+*z*
		5			
N1–H1···O6	0.86	1.95	2.754(16)	156	*x*, *y*, *z*
N2–H2···O3	0.86	2.01	2.847(12)	163	1/2–*x*, –1/2+*y*, –*z*
C2–H2A···O1	0.93	2.59	2.980(11)	106	*x*, *y*, *z*
C10–H10B···O2	0.97	2.53	3.158(13)	122	*x*, –1+*y*, *z*
C15–H15C···O6	0.96	2.53	3.37(2)	145	*x*, –1+*y*, *z*
C19–H19···O2	0.93	2.42	3.325(10)	164	*x*, *y*, *z*
C12–H12A···O4	0.96	2.68	3.174(12)	112	1/2–*x*, –1/2+*y*, 1–*z*
C5–H5···O1	0.93	2.71	3.519(11)	147	*x*, 1+*y*, *z*

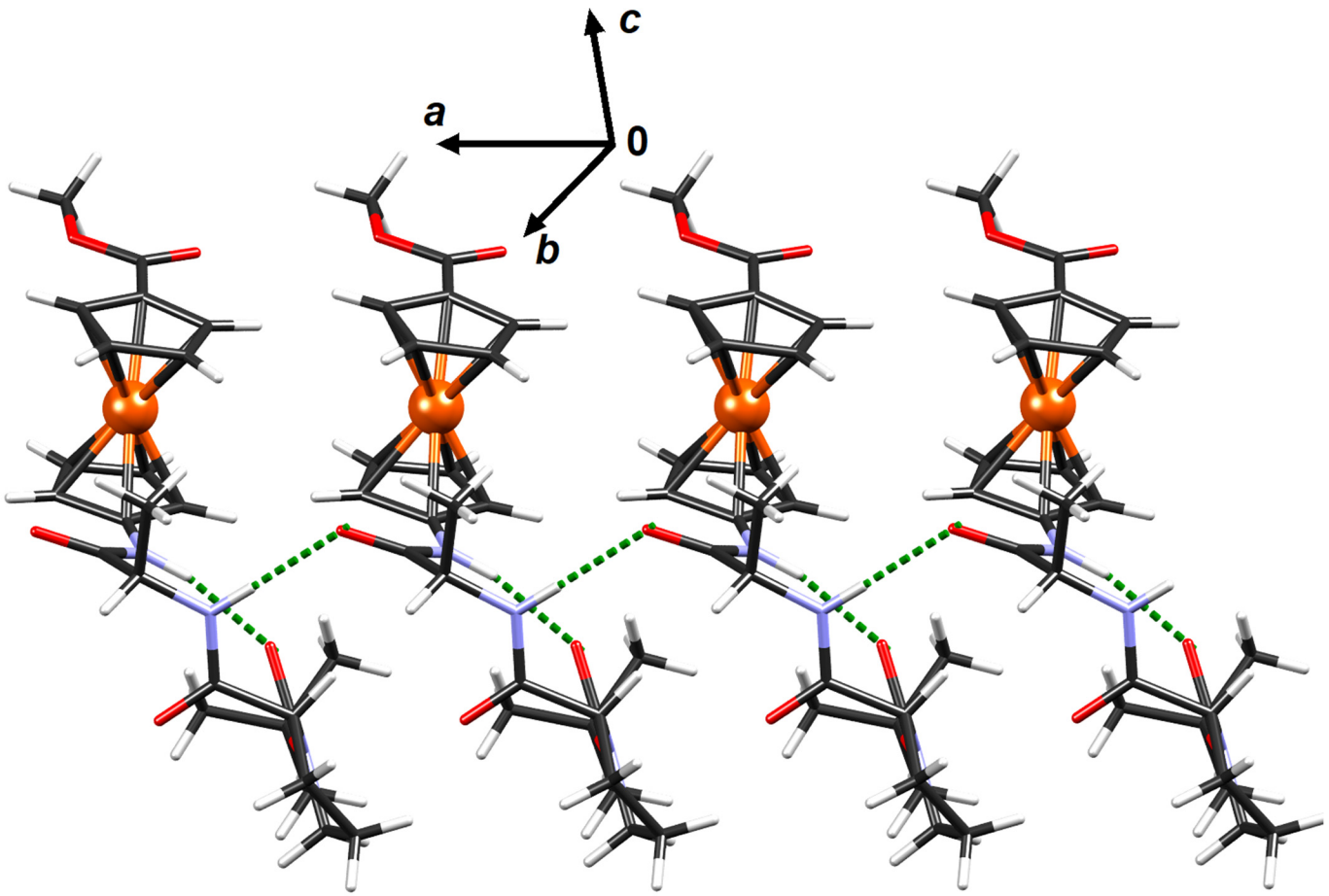

Figure S56. Hydrogen bonded chains in crystal packing of compound **2**. Hydrogen bonds are shown as dashed lines.

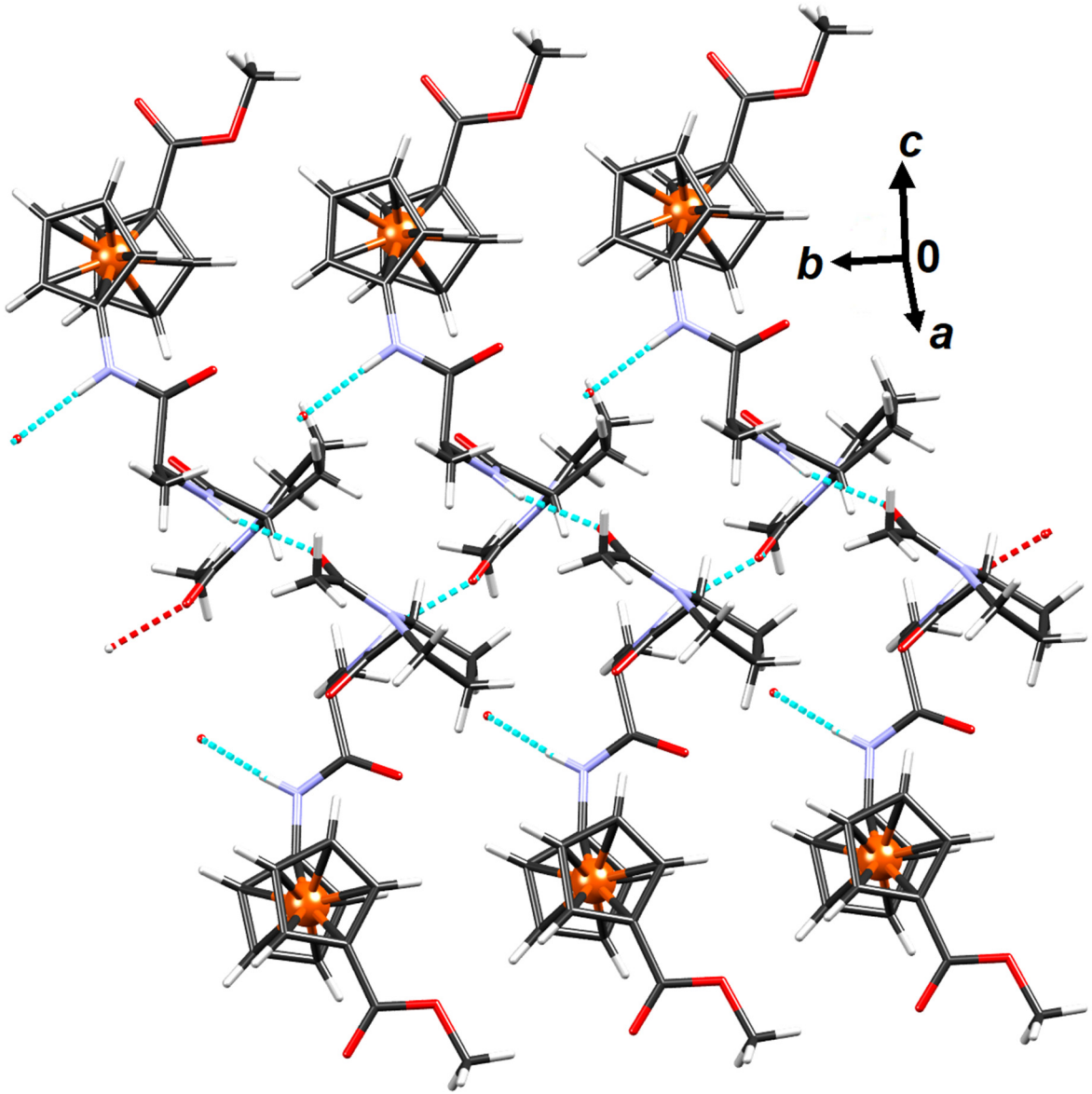

Figure S57. Hydrogen bonded chains in crystal packing of compound **5**. Hydrogen bonds are shown as dashed lines.

Synthesis of precursors 2–31

Synthesis of Boc–L–AA–NH–Fn–COOMe (2–7): Boc–NH–Fn–COOMe (**1**) (1000 mg, 2.78 mmol) was Boc-deprotected in the presence of HCl_{gas} in dry CH_2Cl_2 (5 ml) at 0 °C. After 2 hours, the solvent was evaporated *in vacuo* to afford the hydrochloride salt which was then suspended in CH_2Cl_2 and treated with NEt_3 (pH ~ 8) to give free amine suitable for coupling to Boc–L-AA–OH or Boc–D-AA–OH (5.57 mmol) (AA = Phe, Val and Leu) using the standard EDC/ HOBt method [EDC (2135 mg, 11.1 mmol); HOBt (1505 mg, 11.1 mmol)]. The reaction mixtures were then stirred at room temperature until total consumption of ferrocene amine, which was monitored by TLC (~ 1-3 hour). Standard work-up (washing with a saturated aqueous solution of $NaHCO_3$, a 10% aqueous solution of citric acid and brine, drying over Na_2SO_4 and evaporation in vacuo) including TLC purification of the crude products [EtOAc : CH_2Cl_2 = 1 : 5; R_f = 0.75 **(2)**, R_f = 0.63 **(3)**, R_f = 0.83 **(4)**, R_f = 0.72 **(5)**, R_f = 0.66 **(6)**, R_f = 0.80 **(7)**] gave orange solids of **2** (1053 mg, 75%), **3** (815 mg, 64%), **4** (850 mg, 65%), **5** (982 mg, 70%), **6** (764 mg, 60%) and **7** (771 mg, 59%).

Boc–L–Phe–NH–Fn–COOMe (2): **IR** (CH_2Cl_2) ν_{max}/cm^{-1}: 3416 m (NH_{free}), 3324 w ($NH_{assoc.}$), 1709 s ($C{=}O_{COOMe}$), 1685 s ($C{=}O_{Boc}$), 1640 m ($C{=}O_{CONH}$), 1535 m, 1496 m, 1466 m (amide II). **^{1}H-NMR** (600 MHz, $CDCl_3$) *δ*: 7.34-7.24 (m, 5H, CH_{Phe}), 7.32 (s, 1H, NH_{Fn}), 5.15 (s, 1H, NH_{Boc}), 4.72 (s, 1H, CH_{Fn}), 4.68 (s, 1H, CH_{Fn}), 4.61 (s, 1H, CH_{Fn}), 4.44 (s, 1H, CH_{Fn}), 4.39 (d, *J* = 6.6 Hz, 1H, $CH_{\alpha\text{-Phe}}$), 4.32 (s, 2H, CH_{Fn}), 4.02 (s, 1H, CH_{Fn}), 4.00 (s, 1H, H_{Fn}), 3.78 (s, 3H, $CH_{3\text{-COOMe}}$), 3.17 (dd, *J*= 6.1, 13.1 Hz, 1H, $CH_{\beta1\text{-Phe}}$), 3.09 (dd, *J* = 7.1, 13.5 Hz, 1H, $CH_{\beta2\text{-Phe}}$), 1.42 [s, 9H, $(CH_3)_{3\text{-Boc}}$] ppm. **^{13}C-NMR** (150 MHz, $CDCl_3$) *δ*: 171.84 (1C, CO^a_{Fn}), 169.93 (1C, CO^b_{Fn}), 155.66 (1C, CO_{Boc}), 136.92 (1C, $C_{q\text{-}\gamma Phe}$), 129.53 (2C, CH_{Phe}), 128.87 (2C, CH_{Phe}), 127.14 (1C, CH_{Phe}), 94.51 (1C, C_q-1_{Fn}), 80.62 (1C, C_{qBoc}), 72.76 (1C, CH_{Fn}), 72.05 (1C, C_q-6_{Fn}), 71.36, 71.32, 66.79, 66.57, 63.74, 63.25 (7C, CH_{Fn}), 56.38 (1C, $CH_{\square\text{-Phe}}$), 51.81 (1C, CH_{3}-$_{COOMe}$), 38.37 (1C, $CH_{2\beta\text{-Phe}}$), 28.43 [3C, $(CH_3)_{3\text{-Boc}}$] ppm.

Boc–L–Val–NH–Fn–COOMe (3): **IR** (CH_2Cl_2) ν_{max}/cm^{-1}: 3422 m (NH_{free}), 3324 w ($NH_{assoc.}$), 1710 s ($C{=}O_{COOMe}$), 1683 s ($C{=}O_{Boc}$), 1636 m ($C{=}O_{CONH}$), 1534 m, 1498 m, 1466 m (amide II). **^{1}H-NMR** (600 MHz, $CDCl_3$) *δ*: 7.35 (s, 1H, NH_{Fn}), 5.14 (s, 1H, NH_{Boc}), 4.75 (s, 2H, CH_{Fn}), 4.65 (s, 1H, CH_{Fn}), 4.54 (s, 1H, CH_{Fn}), 4.39 (s, 2H, CH_{Fn}), 4.04 (s, 2H, CH_{Fn}), 3.94 (t, *J* = 6.8 Hz, 1H, $CH_{\alpha\text{–Val}}$), 3.81 (s, 3H, $CH_{3\text{-}COOMe}$), 2.22 (s, 1H, $CH_{\beta\text{-Val}}$), 1.47 [s, 9H, $(CH_3)_{3\text{-Boc}}$], 1.02 [d, *J* = 6.7 Hz, 3H, $(CH_3)_{\gamma\text{-aVal}}$], 0.98 [d, *J* = 6.7 Hz, 3H, $(CH_3)_{\gamma\text{-bVal}}$] ppm. **^{13}C-NMR** (150 MHz, $CDCl_3$) *δ*: 172.04 (1C, CO^a_{Fn}), 170.39 (1C, CO^b_{Fn}), 156.25 (1C, CO_{Boc}), 94.75 (1C, C_q-1_{Fn}), 80.26 (1C, C_{qBoc}), 72.77 (1C, CH_{Fn}), 72.00 (1C, C_q-6_{Fn}), 71.42, 71.34, 66.80, 66.60, 63.70 (7C, CH_{Fn}), 63.36 (1C, $CH_{\alpha\text{-Val}}$), 51.85 (1C, $CH_{3\text{-COOMe}}$), 30.65 (1C, $CH_{\beta\text{-Val}}$), 28.51 [3C, $(CH_3)_{3\text{-Boc}}$], 19.59 [1C, $(CH_3)_{\gamma\text{-aVal}}$], 17.94 [1C, $(CH_3)_{\gamma\text{-bVal}}$] ppm.

Boc–L–Leu–NH–Fn–COOMe (4): **IR** (CH_2Cl_2) ν_{max}/cm^{-1}: 3425 m (NH_{free}), 3320 w ($NH_{assoc.}$), 1708 s ($C{=}O_{COOMe}$), 1685 s ($C{=}O_{Boc}$), 1654 m ($C{=}O_{CONH}$), 1534 m, 1499 m, 1467 m (amide II). **^{1}H-NMR** (600 MHz, $CDCl_3$) *δ*: 7.57 (s, 1H, NH_{Fn}), 5.01 (d, *J* = 8.1 Hz, 1H, NH_{Boc}), 4.76 (pt, 2H, CH_{Fn}), 4.68 (s, 1H, CH_{Fn}), 4.55 (s, 1H, CH_{Fn}), 4.39 (pt, 2H, CH_{Fn}), 4.16-4.11 (m, 1H, $CH_{\alpha\text{-Leu}}$), 4.04 (s, 1H, CH_{Fn}), 4.01 (s, 1H, CH_{Fn}), 3.81 (s, 3H, $CH_{3\text{-COOMe}}$), 1.79-1.71 (m, 2H, $CH_{2\text{-}\beta1\text{-Leu}}$, $CH_{\gamma\text{-Leu}}$), 1.56-1.51 (m, 1H, $CH_{2\text{-}\beta2\text{-Leu}}$), 1.48 [s, 9H, $(CH_3)_{3\text{-Boc}}$], 0.97 [t, *J*= 6.7 Hz, 6H, $(CH_3)_{2\text{-}\delta\text{-Leu}}$] ppm. **^{13}C-NMR** (150 MHz, $CDCl_3$) *δ*: 171.92 (1C, CO^a_{Fn}), 171.11 (1C, CO^b_{Fn}), 156.22 (1C, CO_{Boc}), 95.17 (1C, C_q-1_{Fn}), 80.63 (1C, C_{qBoc}),

72.81, 72.78 (2C, CH_{Fn}), 72.29 (1C, C_q-6_{Fn}), 72.03, 71.39, 71.27, 66.76, 66.46 (5C, CH_{Fn}), 63.43 ($CH_{\alpha\text{-Leu}}$), 63.06 (1C, CH_{Fn}), 51.82 (1C, CH_3-$_{COOMe}$), 40.91 [1C, $(CH_2)_{\beta\text{-Leu}}$], 28.52 [3C, $(CH_3)_{3\text{-Boc}}$], 24.95 (1C, $CH_{\gamma\text{-Leu}}$), 23.14, 22.15 [2C, $(CH_3)_2$-$_{\delta\text{-Leu}}$] ppm.

Boc–D–Phe–NH–Fn–COOMe (5): **IR** (CH_2Cl_2) ν_{max}/cm^{-1}: 3412 m (NH_{free}), 3323 w ($NH_{assoc.}$), 1709 s ($C{=}O_{COOMe}$), 1687 s ($C{=}O_{Boc}$), 1605 m ($C{=}O_{CONH}$), 1557 m, 1536 m, 1508 m, 1496 m (amide II). **^{1}H-NMR** (600 MHz, $CDCl_3$) δ: 7.34-7.31 (m, 5H, CH_{Phe}), 7.27 (s, 1H, NH_{Fn}), 5.15 (s, 1H, NH_{Boc}), 4.71 (s, 1H, CH_{Fn}), 4.68 (m, 1H, CH_{Fn}), 4.62 (pt, 1H, CH_{Fn}), 4.43 (s, 1H, CH_{Fn}), 4.40-4.39 (m, 1H, $CH_{\alpha\text{-Phe}}$), 4.32 (pt, 2H, CH_{Fn}), 4.03-4.01 (m, 2H, CH_{Fn}), 3.78 (s, 3H, CH_3-$_{COOMe}$), 3.17 (m, 1H, $CH_{\beta1\text{-Phe}}$), 3.10-3.06 (m, 1H, $CH_{\beta2\text{-Phe}}$), 1.42 [s, 9H, $(CH_3)_{3\text{-Boc}}$] ppm. **^{13}C-NMR** (150 MHz, $CDCl_3$) δ: 171.90 (1C, CO^a_{Fn}), 169.93 (1C, CO^b_{Fn}), 155.76 (1C, CO_{Boc}), 136.89 (1C, $C_{q\text{-}}$□$_{Phe}$), 129.53 (2C, CH_{Phe}), 128.88 (2C, CH_{Phe}), 127.14 (1C, CH_{Phe}), 94.46 (1C, C_q-1_{Fn}), 80.59 (1C, C_{qBoc}), 72.76 (1C, CH_{Fn}), 72.02 (1C, C_q-6_{Fn}), 71.35, 71.31, 66.80, 66.57, 63.73, 63.25 (7C, CH_{Fn}), 56.36 (1C, $CH_{\alpha\text{-Phe}}$), 51.84 (1C, CH_3-$_{COOMe}$), 38.34 (1C, $CH_{2\beta\text{-Phe}}$), 28.42 [3C, $(CH_3)_{3\text{-Boc}}$] ppm.

Boc–D–Val–NH–Fn–COOMe (6): IR (CH_2Cl_2) ν_{max}/cm^{-1}: 3425 s (NH_{free}), 3323 m ($NH_{assoc.}$), 1709 s ($C{=}O_{COOMe}$), 1688 s ($C{=}O_{CONH}$), 1534 s, 1498 s (amide II). **^{1}H-NMR** (600 MHz, $CDCl_3$) δ: 7.48 (s, 1H, NH_{Fn}), 5.20 (d, J = 8.55 Hz, 1H, NH_{Boc}), 4.74 (pt, 2H, CH_{Fn}), 4.65 (s, 1H, CH_{Fn}), 4.55 (s, 1H, CH_{Fn}), 4.38 (pt, 2H, CH_{Fn}), 4.03 (pt, 2H, CH_{Fn}), 3.96-3.93 (m, 1H, $CH_{\alpha\text{-Val}}$), 3.80 (s, 3H, CH_3-$_{COOMe}$), 2.19 (s, 1H, $CH_{\beta\text{-Val}}$), 1.46 (s, 9H, $(CH_3)_{3\text{-Boc}}$), 1.02 (d, J = 6.8 Hz, 3H, $(CH_3)_{\gamma\text{-aVal}}$), 0.98 (d, J = 6.9 Hz, 3H, $(CH_3)_{\gamma\text{-bVal}}$) ppm. **^{13}C-NMR** (150 MHz, $CDCl_3$) δ: 172.06 (1C, CO^a_{Fn}), 170.44 (1C, CO^b_{Fn}), 156.21 (1C, CO_{Boc}), 94.83 (1C, C_q-1_{Fn}), 80.28 (1C, C_{qBoc}), 72.77 (1C, CH_{Fn}), 71.91 (1C, C_q-6_{Fn}), 71.34, 71.27, 66.75, 66.56, 63.54, 63.27 (7C, CH_{Fn}), 60.62 (1C, $CH_{\alpha\text{-Val}}$), 51.85 (1C, CH_3-$_{COOMe}$), 30.71 (1C, $CH_{\beta\text{-Val}}$), 28.49 [3C, $(CH_3)_{3\text{-Boc}}$], 19.57 [1C, $(CH_3)_{\gamma\text{-aVal}}$], 17.98 [1C, $(CH_3)_{\gamma\text{-bVal}}$] ppm.

Boc–D–Leu–NH–Fn–COOMe (7): **IR** (CH_2Cl_2) ν_{max}/cm^{-1}: 3416 s (NH_{free}), 3322 m ($NH_{assoc.}$), 1709 s ($C{=}O_{COOMe}$), 1685 s ($C{=}O_{Boc}$), 1603 m ($C{=}O_{CONH}$), 1584 s, 1534 m, 1506 m, 1499 m (amide II). **^{1}H-NMR** (600 MHz, $CDCl_3$) δ: 7.62 (s, 1H, NH_{Fn}), 5.03 (d, J = 8.03 Hz, 1H, NH_{Boc}), 4.74 (pt, 2H, CH_{Fn}), 4.67 (s, 1H, CH_{Fn}), 4.55 (s, 1H, CH_{Fn}), 4.37 (pt, 2H, CH_{Fn}), 4.15-4.12 (m, 1H, $CH_{\alpha\text{-Leu}}$), 4.03 (s, 1H, CH_{Fn}), 4.01 (s, 1H, CH_{Fn}), 3.80 (s, 3H, CH_3-$_{COOMe}$), 1.78-1.70 (m, 2H, $CH_{2\text{-}\beta1\text{-Leu}}$, $CH_{\gamma\text{-Leu}}$), 1.55-1.51 (m, 1H, $CH_{2\text{-}\beta2\text{-Leu}}$), 1.47 [s, 9H, $(CH_3)_{3\text{-Boc}}$], 0.97 [t, J= 6.3 Hz, 6H, $(CH_3)_2$-$_{\delta\text{-Leu}}$] ppm. **^{13}C-NMR** (150 MHz, $CDCl_3$) δ: 171.96 (1C, CO^a_{Fn}), 171.12 (1C, CO^b_{Fn}), 154.34 (1C, CO_{Boc}), 100.13 (1C, C_{qBoc}), 95.17 (1C, C_q-1_{Fn}), 72.81 (1C, CH_{Fn}), 72.79 (1C, C_q-6_{Fn}), 71.95, 71.35, 71.24, 66.73, 66.44 (6C, CH_{Fn}), 63.37 (1C, $CH_{\alpha\text{-Leu}}$), 63.01 (1C, CH_{Fn}), 51.83 (1C, CH_3-$_{COOMe}$), 40.90 [1C, $(CH_2)_{\beta\text{-Leu}}$], 28.49 [3C, $(CH_3)_{3\text{-Boc}}$], 24.91 (1C, $CH_{\gamma\text{-Leu}}$), 23.13, 22.15 [2C, $(CH_3)_2$-$_{\delta\text{-Leu}}$] ppm.

Synthesis of Ac–L–AA–NH–Fn–COOMe (**8**–**13**): The transformation of carbamates **2–7** (2 mmol) to acetamides **8–13** began with the acidic Boc-deprotection described above. Their free amines, obtained by treating the hydrochloride salt with NEt_3 (25.1 mmol), were cooled to 0°C and acetyl chloride (12 mmol) was added dropwise, stirring in an ice bath. After TLC monitoring showed complete conversion of the starting materials, the reaction mixtures were poured into water and extracted with CH_2Cl_2. The combined organic phases were washed with a brine, dried over Na_2SO_4 and evaporated to dryness in vacuo. The resulting crude products were purified by TLC on silica gel [EtOAc : CH_2Cl_2 = 1 : 5; R_f =

0.25 (**8**), R_f = 0.16 (**9**), R_f = 0.33 (**10**), R_f = 0.21 (**11**), R_f = 0.13 (**12**), R_f = 0.32 (**13**)] to give orange solids of acetamides of **8** (394 mg, 76%), **9** (538 mg, 78%), **10** (498 mg, 60%), **11** (357 mg, 69%), **12** (496 mg, 72%) and **13** (540 mg, 65%).

Ac–L–Phe–NH–Fn–COOMe (8): **IR** (CH_2Cl_2) ν_{max}/cm^{-1}: 3418 m (NH_{free}), 3290 m, 3248 w ($NH_{assoc.}$), 1709 s ($C{=}O_{COOMe}$), 1696 s, 1668 s ($C{=}O_{CONH}$), 1574, 1558, 1540, 1535, 1516, 1507, 1498, 1466 (amide II). **^{1}H-NMR** (600 MHz, $CDCl_3$) δ: 7.68 (s, 1H, NH_{Fn}), 7.33-7.24 (m, 5H, CH_{Phe}), 6.43 (d, J = 7.6 Hz, 1H, NH_{Ac}), 4.77 (q, J = 7.3 Hz, 1H, $CH_{\alpha\text{-Phe}}$), 4.69 (s, 1H, CH_{Fn}), 4.65 (s, 1H, CH_{Fn}), 4.57 (s, 1H, CH_{Fn}), 4.45 (s, 1H, CH_{Fn}), 4.29 (s, 2H, CH_{Fn}), 4.03 (s, 1H, CH_{Fn}), 4.00 (s, 1H, CH_{Fn}), 3.78 (s, 3H, $CH_{3\text{-COOMe}}$), 3.1 (dd, J= 7.4 Hz, 13.8 Hz, 1H, $CH_{\beta1\text{-Phe}}$), 3.09 (dd, J= 6.8 Hz, 13.9 Hz, 1H, $CH_{\beta2\text{-Phe}}$), 2.02 [s, 3H, $CH_{3\text{-Ac}}$] ppm. **^{13}C-NMR** (150 MHz, $CDCl_3$) δ: 171.92 (1C, $CO^b{}_{Fn}$), 170.62 (1C, $CO^a{}_{Fn}$), 169.71 (1C, CO_{Ac}), 136.78 (1C, $C_{q\text{-}\gamma Phe}$), 129.49, 129.46, 128.85, 127.21 (5C, CH_{Phe}), 94.40 (1C, C_q-1_{Fn}), 72.72 (1C, CH_{Fn}), 72.05 (1C, C_q-6_{Fn}), 71.40, 71.28, 66.84, 66.58, 63.89, 63.44 (7C, CH_{Fn}), 55.01 (1C, $CH_{\alpha\text{-Phe}}$), 51.82 (1C, $CH_{3\text{-COOMe}}$), 38.23 (1C, $CH_{2\beta\text{-Phe}}$), 23.35 ($CH_{3\text{-Ac}}$) ppm.

Ac–L–Val–NH–Fn–COOMe (9): **IR** (CH_2Cl_2) ν_{max}/cm^{-1}: 3421 m (NH_{free}), 3287 m, 3245 m ($NH_{assoc.}$), 1711 s ($C{=}O_{COOMe}$), 1684 s, 1670 s, 1661 s ($C{=}O_{CONH}$), 1569, 1559, 1540, 1517, 1508, 1490, 1466 (amide II). **^{1}H-NMR** (600 MHz, $CDCl_3$) δ: 8.21 (s, 1H, NH_{Fn}), 6.49 (d, J = 8.7 Hz, 1H, NH_{Ac}), 4.74 (s, 1H, CH_{Fn}), 4.73 (s, 1H, CH_{Fn}), 4.61 (s, 1H, CH_{Fn}), 4.60 (s, 1H, CH_{Fn}), 4.41 (t, J = 7.7 Hz, 1H, $CH_{\square\text{-Val}}$), 4.37 (s, 2H, CH_{Fn}), 4.03 (s, 2H, CH_{Fn}), 3.78 (s, 3H, $CH_{3\text{-COOMe}}$), 2.18-2.13 (m, 1H, $CH_{\square\square Val}$), 2.10 (s, 3H, $CH_{3\text{-Ac}}$), 1.04 [d, J = 6.7 Hz, 3H, $(CH_3)_{\gamma\text{-aVal}}$], 1.01 [d, J = 6.7 Hz, 3H, $(CH_3)_{\gamma\text{-bVal}}$] ppm. **^{13}C-NMR** (150 MHz, $CDCl_3$) δ: 172.04 (1C, $CO^b{}_{Fn}$), 170.70 (1C, $CO^a{}_{Fn}$), 170.25 (1C, CO_{Ac}), 95.00 (1C, C_q-1_{Fn}), 72.73, 72.68 (2C, CH_{Fn}), 72.01 (1C, C_q-6_{Fn}), 71.39, 71.22, 66.72, 66.60, 63.42, 63.38 (6C, CH_{Fn}), 59.13 (1C, $CH_{\alpha\text{-Val}}$), 51.80 (1C, $CH_{3\text{-COOMe}}$), 31.16 (1C, $CH_{\beta\text{-Val}}$), 23.51 (1C, $CH_{3\text{-Ac}}$), 19.50 [$(CH_3)_{\gamma\text{-aVal}}$], 18.49 [$(CH_3)_{\gamma\text{-bVal}}$] ppm.

Ac–L–Leu–NH–Fn–COOMe (10): **IR** (CH_2Cl_2) ν_{max}/cm^{-1}: 3425 m (NH_{free}), 3289 m, 3241 w ($NH_{assoc.}$), 1709 s ($C{=}O_{COOMe}$), 1693 s, 1673 s, 1669 s ($C{=}O_{CONH}$), 1562, 1557, 1538, 1520, 1515, 1467 (amide II). **^{1}H-NMR** (600 MHz, $CDCl_3$) δ: 8.07 (s, 1H, NH_{Fn}), 6.33 (d, J = 8.3 Hz, 1H, NH_{Ac}), 4.74 (s, 1H, CH_{Fn}), 4.71 (s, 1H, CH_{Fn}), 4.62 (s, 1H, CH_{Fn}), 4.59 (s, 1H, CH_{Fn}), 4.53 (q, J = 8.3 Hz, 1H, $CH_{\alpha\text{-Leu}}$), 4.36 (pt, 2H, CH_{Fn}), 4.03 (s, 1H, CH_{Fn}), 4.00 (s, 1H, CH_{Fn}), 3.80 (s, 3H, $CH_{3\text{-COOMe}}$), 2.07 (s, 3H, $CH_{3\text{-Ac}}$), 1.81-1.76 (m, 1H, $CH_{2\text{-}\beta1\text{-Leu}}$), 1.73-1.68 (m, 1H, $CH_{\gamma\text{-Leu}}$), 1.60-1.55 (m, 1H, $CH_{2\text{-}\beta2\text{-Leu}}$), 0.98 [d, J = 6.6 Hz, 3H, $(CH_3)_{\delta\text{-a-Leu}}$], 0.96 [d, J = 6.6 Hz, 3H, $(CH_3)_{\delta\text{-b-Leu}}$] ppm. **^{13}C-NMR** (150 MHz, $CDCl_3$) δ: 171.95 (1C, $CO^b{}_{Fn}$), 170.90 (1C, $CO^a{}_{Fn}$), 170.78 (1C, CO_{Ac}), 95.17 (1C, C_q-1_{Fn}), 72.70, 72.66 (2C, CH_{Fn}), 72.08 (1C, C_q-6_{Fn}), 71.43, 71.22, 66.72, 66.39, 63.48, 63.21 (6C, CH_{Fn}), 52.29 (1C, $CH_{\alpha\text{-Leu}}$), 51.83 (1C, $CH_{3\text{-COOMe}}$), 40.83 [1C, $(CH_2)_{\beta\text{-Leu}}$], 24.99 (1C, $CH_{\gamma\text{-Leu}}$), 23.38 (1C, $CH_{3\text{-Ac}}$), 23.04, 22.41 [2C, $(CH_3)_{2\text{-}\delta\text{-Leu}}$] ppm.

Ac–D–Phe–NH–Fn–COOMe (11): **IR** (CH_2Cl_2) ν_{max}/cm^{-1}: 3419 m (NH_{free}), 3310 w, 3292 m, 3243 w ($NH_{assoc.}$), 1707 s ($C{=}O_{COOMe}$), 1690 s, 1666 s, 1654 s ($C{=}O_{CONH}$), 1605, 1575, 1558, 1539, 1506, 1497 (amide II). **^{1}H-NMR** (600 MHz, $CDCl_3$) δ: 7.77 (d, 1H, NH_{Fn}), 7.32-7.24 (m, 5H, CH_{Phe}), 6.46 (pt, 1H, NH_{Ac}), 4.79-4.75 (m, 1H, $CH_{\alpha\text{-Phe}}$), 4.68 (m, 1H, CH_{Fn}), 4.64 (m, 1H, CH_{Fn}), 4.58-4.55 (m, 1H, CH_{Fn}), 4.46 (m, 1H, CH_{Fn}), 4.29 (m, 2H, CH_{Fn}), 4.03 (s, 1H, CH_{Fn}), 4.00 (s, 1H, CH_{Fn}), 3.76 (s, 3H, $CH_{3\text{-COOMe}}$), 3.17-3.13 (m, 1H, $CH_{\beta1\text{-Phe}}$), 3.10-3.05 (m, 1H, $CH_{\beta2\text{-Phe}}$), 2.02 [s, 3H, CH_{3Ac}] ppm. **^{13}C-NMR** (150 MHz,

$CDCl_3$) δ: 171.99 (1C, CO^b_{Fn}), 170.60 (1C, CO^a_{Fn}), 169.70 (1C, CO_{Ac}), 136.74 (1C, $C_{q\text{-}\gamma Phe}$), 129.47, 129.45, 128.83, 127.19 (5C, CH_{fenil}), 94.38 (1C, $C_q\text{-}1_{Fn}$), 72.72 (1C, CH_{Fn}), 71.98 (1C, $C_q\text{-}6_{Fn}$), 71.40, 71.26, 66.62, 66.57, 66.42, 63.89, 63.44 (7C, CH_{Fn}), 54.96 (1C, $CH_{\alpha\text{-}Phe}$), 51.85 ($CH_3\text{-}COOMe$), 38.22 (1C, $CH_{2\beta\text{-}Phe}$), 23.35 (1C, $CH_{3\text{-}Ac}$) ppm.

Ac–D–Val–NH–Fn–COOMe (12): IR (CH_2Cl_2) ν_{max}/cm^{-1}: 3420 m (NH_{free}), 3286 m, 3235 m ($NH_{assoc.}$), 1707 s ($C{=}O_{COOMe}$), 1686 s, 1672 s, 1660 s ($C{=}O_{CONH}$), 1605, 1569, 1539, 1514, 1508, 1489 (amide II). **^{1}H-NMR** (600 MHz, $CDCl_3$) δ: 8.19 (s, 1H, NH_{Fn}), 6.45 (d, J = 8.91 Hz, 1H, NH_{Ac}), 4.74 (s, 1H, CH_{Fn}), 4.72 (s, 1H, CH_{Fn}), 4.61 (s, 1H, CH_{Fn}), 4.59 (s, 1H, CH_{Fn}), 4.40 (t, J = 8.3 Hz, 1H, $CH_{\alpha\text{-}Val}$), 4.37 (pt, 2H, CH_{Fn}), 4.03 (pt, 2H, CH_{Fn}), 3.78 (s, 3H, $CH_{3\text{-}COOMe}$), 2.19-2.13 (m, 1H, $CH_{\beta\text{-}Val}$), 2.10 (s, 3H, $CH_{3\text{-}Ac}$), 1.04 [d, J = 6.8 Hz, 3H, $(CH_3)_{\gamma\text{-}aVal}$], 1.01 [d, J = 6.6 Hz, 3H, $(CH_3)_{\gamma\text{-}bVal}$] ppm. **^{13}C-NMR** (150 MHz, $CDCl_3$) δ: 172.06 (1C, CO^b_{Fn}), 170.66 (1C, CO^a_{Fn}), 170.19 (1C, CO_{Ac}), 94.96 (1C, $C_q\text{-}1_{Fn}$), 72.72, 72.68 (2C, CH_{Fn}), 71.95 (1C, $C_q\text{-}6_{Fn}$), 71.37, 71.20, 66.71, 66.59, 63.39, 63.36 (6C, CH_{Fn}), 59.07 (1C, $CH_{\alpha\text{-}Val}$), 51.82 (1C, $CH_{3\text{-}COOMe}$), 31.16 (1C, $CH_{\beta\text{-}Val}$), 23.53 (1C, $CH_{3\text{-}Ac}$), 19.50 [1C, $(CH_3)_{\gamma\text{-}aVal}$], 18.47 [1C, $(CH_3)_{\gamma\text{-}bVal}$] ppm.

Ac–D–Leu–NH–Fn–COOMe (13): IR (CH_2Cl_2) ν_{max}/cm^{-1}: 3421 m (NH_{free}), 3290 m, 3241 w ($NH_{assoc.}$), 1708 s ($C{=}O_{COOMe}$), 1699 s, 1652 s, 1636 s ($C{=}O_{CONH}$), 1574, 1556, 1541, 1516, 1508, 1488 (amide II). **^{1}H-NMR** (600 MHz, $CDCl_3$) δ: 8.23 (s, 1H, NH_{Fn}), 6.47 (d, J = 8.22 Hz, 1H, NH_{Ac}), 4.73 (pt, 1H, CH_{Fn}), 4.71 (pt, 1H, CH_{Fn}), 4.61 (pt, 2H, CH_{Fn}), 4.54 (q, J = 8.3 Hz, 1H, $CH_{\alpha\text{-}Leu}$), 4.02 (pt, 2H, CH_{Fn}), 4.00 (pt, 2H, CH_{Fn}), 3.79 (s, 3H, $CH_{3\text{-}COOMe}$), 2.05 (s, 3H, $CH_{3\text{-}Ac}$), 1.78-1.74 (m, 1H, $CH_{2\text{-}\beta1\text{-}Leu}$), 1.71-1.69 (m, 1H, $CH_{\gamma\text{-}Leu}$), 1.60-1.55 (m, 1H, $CH_{2\text{-}\beta2\text{-}Leu}$), 0.98 [d, J = 6.6 Hz, 3H, $(CH_3)_{\delta\text{-}a\text{-}Leu}$], 0.96 [d, J = 6.6 Hz, 3H, $(CH_3)_{\delta\text{-}b\text{-}Leu}$] ppm. **^{13}C-NMR** (150 MHz, $CDCl_3$) δ: 171.97 (1C, CO^b_{Fn}), 170.90 (1C, CO^a_{Fn}), 169.92 (1C, CO_{Ac}), 95.22 (1C, $C_q\text{-}1_{Fn}$), 72.71, 72.67 (2C, CH_{Fn}), 71.99 (1C, $C_q\text{-}6_{Fn}$), 71.38, 71.19, 66.67, 66.40, 63.34, 63.16 (6C, CH_{Fn}), 52.28 (1C, $CH_{\alpha\text{-}Leu}$), 51.82 (1C, $CH_{3\text{-}COOMe}$), 40.86 [1C, $(CH_2)_{\beta\text{-}Leu}$], 24.97 (1C, $CH_{\gamma\text{-}Leu}$), 23.34 (1C, $CH_{3\text{-}Ac}$), 23.03, 22.39 [2C, $(CH_3)_2\text{-}\delta\text{-}Leu$] ppm.

Synthesis of Ac–L–AA–NH–Fn–COOH (14–19): Esters **8–13** (1 mmol) were dissolved in MeOH (3 mL) and hydrolyzed by heating at reflux in the presence of NaOH (1 mmol) and H_2O (0.1 mL) for 1 h. The reaction mixtures were concentrated *in vacuo* to leave the salts, which were dissolved in 5% $NaHCO_3$ and washed with CH_2Cl_2 to remove the residual esters. The water phases were acidified with 10% HCl and extracted with EtOAc. The organic phases were washed with brine, dried with Na_2SO_4, and concentrated in vacuo to get the crude products of the desired acids **14** (348 mg, 81%), **15** (322 mg, 84%), **16** (342 mg, 86%), **17** (344 mg, 80%), **18** (307 mg, 80%) and **19** (314 mg, 79%) as orange resins.

Ac–L–Phe–NH–Fn–COOH (14): IR (CH_2Cl) ν_{max}/cm^{-1}: 3411 m (NH_{free}), 3285 m, 3256 m ($NH_{assoc.}$), 3143-3073 br (OH, COOH), 1716 s, 1696 s, 1683 s, 1654 s ($C{=}O_{COOH,\ CONH}$), 1575, 1569, 1558, 1540, 1533, 1522, 1508, 1498, 1485, 1474 (amide II).

Ac–L–Val–NH–Fn–COOH (15): IR (CH_2Cl) ν_{max}/cm^{-1}: 3417 m (NH_{free}), 3280 m, 3237 m ($NH_{assoc.}$), 3152-3056 br (OH, COOH), 1712 s, 1684 s, 1656 s ($C{=}O_{COOH,\ CONH}$), 1574, 1540, 1521, 1478 (amide II).

Ac–L–Leu–NH–Fn–COOH (16): IR (CH_2Cl) ν_{max}/cm^{-1}: 3419 m (NH_{free}), 3287 m, 3277 m ($NH_{assoc.}$), 3161-3070 br (OH, COOH), 1714 s, 1696 s, 1686 s, 1653 s ($C{=}O_{COOH,\ CONH}$), 1569, 1558, 1539, 1533, 1528, 1522, 1509, 1472 (amide II).

Ac–D–Phe–NH–Fn–COOH (17): IR (CH_2Cl) ν_{max}/cm^{-1}: 3419 m (NH_{free}), 3292 m, 3243 m ($NH_{assoc.}$), 3150-3070 br (OH, COOH), 1716 s, 1690 s, 1666 s, 1654 s ($C{=}O_{COOH,\ CONH}$), 1605, 1575, 1558, 1539, 1506, 1497 (amide II).
Ac–D–Val–NH–Fn–COOH (18): IR (CH_2Cl) ν_{max}/cm^{-1}: 3420 m (NH_{free}), 3286 m, 3235 m ($NH_{assoc.}$), 3150-3055 br (OH, COOH), 1715 s, 1686 s, 1672 s, 1660 s ($C{=}O_{COOH,\ CONH}$), 1605, 1569, 1539, 1514, 1508, 1489 (amide II).
Ac–D–Leu–NH–Fn–COOH (19): IR (CH_2Cl) ν_{max}/cm^{-1}: 3421 m (NH_{free}), 3290 m, 3241 m ($NH_{assoc.}$), 3161-3071 br (OH, COOH), 1715 s, 1699 s, 1652 s, 1636 s ($C{=}O_{COOH,\ CONH}$), 1574, 1556, 1541, 1516, 1508, 1488 (amide II).

Synthesis of Ac–L–AA–NH–Fn–NH–Boc (26–31): The carboxylic acid groups of **14–19** were converted to carbamates **26–31** *via* unstable azides **20–25**. The acid precursors **14–19** (1 mmol) were suspended in water (0.5 mL), and sufficient acetone was added to complete the solutions. Triethylamine (1.14 mmol) in acetone (3 mL) was added at 0 °C, and the intermediate amines were transferred to mixed anhydrides by action of ethyl chloroformate (0.75 mmol) in acetone (0.8 mL). After stirring for 30 min at 0 °C, a solution of sodium azide (1.5 mmol) in water (1 mL) was added. The mixtures were stirred for 1 h at 0 °C and concentrated *in vacuo* to afford an unstable azides **20–25** which were then converted *in situ* to the corresponding carbamates by heating with *t*-BuOH (5 mL) at 65 °C for 5 h. The reaction mixtures were concentrated *in vacuo* and purified by preparative chromatography [EtOAc; R_f = 0.78 **(26)**, R_f = 0.59 **(27)**, R_f = 0.80 **(28)**, R_f = 0.75 **(29)**, R_f = 0.52 **(30)**, R_f = 0.82 **(31)**] to give orange solids of acetamides of **26** (147 mg, 29 %), **27** (138 mg, 30%), **28** (166 mg, 35%), **29** (126 mg, 25 %), **30** (133 mg, 29%) and **31** (142 mg, 30%).
Ac–L–Phe–NH–Fn–NH–Boc (26): IR (CH_2Cl_2) ν_{max}/cm^{-1}: 3427 m (NH_{free}), 3318 w ($NH_{assoc.}$), 1704 s, 1683 s, 1673 s ($C{=}O_{CONH}$), 1531, 1507, 1498, 1456 (amide II). **^{1}H-NMR** (600 MHz, $CDCl_3$) δ: 7.77 (s, 1H, $NH^a{}_{Fn}$), 7.32-7.20 (m, 5H, CH_{Phe}), 6.30 (d, J = 7.6 Hz, 1H, NH_{Ac}), 5.90 (d, J = 7.6 Hz, 1H, $NH^b{}_{Fn}$), 4.70 (q, J = 7.2 Hz, 1H, CH_{Phe}), 4.51 (pt, 2H, CH_{Fn}), 4.32 (pt, 2H, CH_{Fn}), 4.16-4.08 (m, 4H, CH_{Fn}), 3.16-3.08 (m, 2H, $CH_{\beta\text{-}1\text{-}Phe}$, $CH_{\beta\text{-}2\text{-}Phe}$), 1.99 [s, 3H, $CH_{3\text{-}Ac}$], 1.49 [s, 9H, $(CH_3)_{3\text{-}Boc}$] ppm. **^{13}C-NMR** (150 MHz, $CDCl_3$) δ: 170.98 (1C, $CO^a{}_{Fn}$), 169.46 (1C, CO_{Ac}), 153.87 (1C, $CO^b{}_{Fn}$), 136.75 (1C, $C_{q\text{-}\gamma Phe}$), 129.58, 128.82, 127.20 (5C, CH_{Phe}), 80.62 (1C, C_{qBoc}), 62.63, 62.54, 62.53, 62.51 (8C, CH_{Fn}), 55.06 (1C, $CH_{\alpha\text{-}Phe}$), 38.37 (1C, $CH_{2\beta\text{-}Phe}$), 28.58 [3C, $(CH_3)_{3Boc}$], 23.37 (1C, $CH_{3\text{-}Ac}$) ppm.
Ac–L–Val–NH–Fn–NH–Boc (27): IR (CH_2Cl_2) ν_{max}/cm^{-1}: 3427 m (NH_{free}), 3322 w, 3311 w, 3290 w ($NH_{assoc.}$), 1704 s, 1684 s, 1671 s ($C{=}O_{CONH}$), 1630, 1507, 1457 (amide II). **^{1}H-NMR** (600 MHz, $CDCl_3$) δ: 8.00 (s, 1H, $NH^a{}_{Fn}$), 6.25 (s, 1H, NH_{Ac}), 6.02 (s, 1H, $NH^b{}_{Fn}$), 4.66 (pt, 2H, CH_{Fn}), 4.55 (pt, 2H, CH_{Fn}), 4.39-4.30 (m, 1H, $CH_{\alpha\text{-}Val}$), 4.12 (s, 2H, CH_{Fn}), 4.05 (s, 2H, CH_{Fn}), 2.19-2.14 (m, 1H, $CH_{\beta\text{–}Val}$), 2.05 (s, 3H, $CH_{3\text{-}Ac}$), 1.50 [s, 9H, $(CH_3)_{3\text{-}Boc}$], 1.01 [d, J = 6.3 Hz, 3H, $(CH_3)_{\gamma\text{-}aVal}$], 0.98 [d, J = 6.2 Hz,3H, $(CH_3)_{\gamma\text{-}bVal}$] ppm. **^{13}C-NMR** (150 MHz, $CDCl_3$) δ: 169.79 (1C, $CO^a{}_{Fn}$), 169.15 (1C, CO_{Ac}), 153.12 (1C, $CO^b{}_{Fn}$), 79.95 (1C, C_{qBoc}), 74.45 (1C, C_q-1_{Fn}), 72.93, 71.87, 70.81, 70.69, 67.45, 66.27, 63.54, 62.14 (8C, CH_{Fn}), 58.45 (1C, $CH_{\alpha\text{-}Val}$), 30.47 (1C, $CH_{\beta\text{-}Val}$), 27.87 [3C, $(CH_3)_{3Boc}$], 22.81 (1C, $CH_{3\text{-}Ac}$), 18.81 [1C, $(CH_3)_{\gamma\text{-}aVal}$], 17.71 [1C, $(CH_3)_{\gamma\text{-}bVal}$] ppm.

Ac–L–Leu–NH–Fn–NH–Boc (28): IR (CH_2Cl_2) ν_{max}/cm^{-1}: 3428 m ($NH_{slobodni}$), 3306 w ($NH_{assoc.}$), 1704 s, 1682 s, 1673 s ($C{=}O_{CONH}$), 1531, 1507, 1480, 1458, 1438, 1420 (amide II). **^{1}H-NMR** (600 MHz, $CDCl_3$) δ: 8.02 (s, 1H, NH_{Fn}), 6.20 (s, 1H, NH_{Ac}), 6.02 (s, 1H, $NH^b{}_{Fn}$), 4.69-4.54 (m, 2H, CH_{Fn}), 4.32 (s, 2H, CH_{Fn}), 4.49-4.46 (m, 1H, $CH_{\alpha\text{-Leu}}$), 4.23-4.13 (m, 4H, CH_{Fn}), 2.02 (s, 3H, $CH_{3\text{-Ac}}$), 1.75-1.51 [m, 3H, $(CH_2)_{\beta\text{-Leu}}$, $CH_{\gamma\text{-Leu}}$], 1.49 [s, 9H, $(CH_3)_{3\text{-Boc}}$], 0.98-0.96 [m, 6H, $(CH_3)_{\delta\text{-a-Leu}}$, $(CH_3)_{\delta\text{-b-Leu}}$] ppm. **^{13}C-NMR** (150 MHz, $CDCl_3$) δ: 170.62 (1C, $CO^a{}_{Fn}$), 170.52 (1C, CO_{Ac}), 150.30 (1C, $CO^b{}_{Fn}$), 80.56 (1C, C_{qBoc}), 70.76 (1C, $C_q\text{-}1_{Fn}$), 67.73, 63.05, 63.02, 62.82, 62.80 (8C, CH_{Fn}), 52.36 (1C, $CH_{\alpha\text{-Leu}}$), 41.29 [1C, $(CH_2)_{\beta\text{-Leu}}$], 28.57 [3C, $(CH_3)_{3Boc}$], 24.99 (1C, $CH_{\gamma\text{-Leu}}$), 23.38 (1C, $CH_{3\text{-Ac}}$), 23.09, 22.41 [2C, $(CH_3)_{2\text{-}\delta\text{-Leu}}$] ppm.

Ac–D–Phe–NH–Fn–NH–Boc (29): IR (CH_2Cl_2) ν_{max}/cm^{-1}: 3427 m (NH_{free}), 3316 w ($NH_{assoc.}$), 1701 s, 1680 s, 1670 s ($C{=}O_{CONH}$), 1530, 1505, 1499, 1455 (amide II). **^{1}H-NMR** (600 MHz, $CDCl_3$) δ: 7.90 (s, 1H, $NH^a{}_{Fn}$), 7.32-7.23 (m, 5H, CH_{Phe}), 6.42 (s, 1H, NH_{Ac}), 5.93 (s 1H, $NH^b{}_{Fn}$), 4.72-4.71 (m, 1H, CH_{Phe}), 4.49 (s, 2H, CH_{Fn}), 4.30 (s, 2H, CH_{Fn}), 4.14-4.01 (m, 4H, CH_{Fn}), 3.16-3.07 (m, 2H, $CH_{\beta\text{-1-Phe}}$, $CH_{\beta\text{-2-Phe}}$), 1.98 [s, 3H, $CH_{3\text{-Ac}}$], 1.48 [s, 9H, $(CH_3)_{3\text{-Boc}}$] ppm. **^{13}C-NMR** (150 MHz, $CDCl_3$) δ: 170.37 (1C, $CO^a{}_{Fn}$), 169.61 (1C, CO_{Ac}), 153.90 (1C, $CO^b{}_{Fn}$), 136.69 (1C, $C_{q\text{-}\gamma Phe}$), 129.55, 128.78, 127.17 (5C, CH_{Phe}), 80.59 (1C, C_{qBoc}), 74.97 (1C, $C_q\text{-}1_{Fn}$), 69.67, 66.37, 65.71, 64.70, 64.49, 92.90, 62.60, 60.54 (8C, CH_{Fn}), 55.04 (1C, $CH_{\alpha\text{-Phe}}$), 38.42 (1C, $CH_{2\beta\text{-Phe}}$), 28.54 [3C, $(CH_3)_{3Boc}$], 23.36 (1C, $CH_{3\text{-Ac}}$) ppm.

Ac–D–Val–NH–Fn–NH–Boc (30): IR (CH_2Cl_2) ν_{max}/cm^{-1}: 3425 m (NH_{free}), 3320 w, 3309 w, 3288 w ($NH_{assoc.}$), 1703 s, 1680 s, 1671 s ($C{=}O_{CONH}$), 1629, 1506, 1456 (amide II). **^{1}H-NMR** (600 MHz, $CDCl_3$) δ: 8.04 (s, 1H, $NH^a{}_{Fn}$), 6.31 (s, 1H, NH_{Ac}), 6.00 (s,1H, $NH^b{}_{Fn}$), 4.74 (pt, 2H, CH_{Fn}), 4.60 (pt, 2H, CH_{Fn}), 4.29-4.20 (s, 4H, CH_{Fn}), 4.11 (q, J =7.2 Hz, 14.4 Hz, 1H, $CH_{\alpha\text{-Val}}$), 2.17-2.12 (m, 1H, $CH_{\beta\text{–Val}}$), 2.04 (s, 3H, $CH_{3\text{-Ac}}$), 1.48 [s, 9H, $(CH_3)_{3\text{-Boc}}$], 1.01 [d, J = 6.1 Hz, 3H, $(CH_3)_{\gamma\text{-aVal}}$], 0.96 [d, J = 6.1 Hz, 3H, $(CH_3)_{\gamma\text{-bVal}}$] ppm. **^{13}C-NMR** (150 MHz, $CDCl_3$) δ: 170.52(1C, $CO^a{}_{Fn}$), 169.98 (1C, CO_{Ac}), 153.80 (1C, $CO^b{}_{Fn}$), 80.58 (1C, C_{qBoc}), 74.45 (1C, $C_q\text{-}1_{Fn}$), 67.07, 66.59, 66.06, 64.59, 62.97, 62.90, 62.82, 62.76 (8C, CH_{Fn}), 60.54 (1C, $CH_{\alpha\text{-Val}}$), 31.26 (1C, $CH_{\beta\text{-Val}}$), 28.53 [3C, $(CH_3)_{3Boc}$], 23.48 (1C, $CH_{3\text{-Ac}}$), 19.47 [1C, $(CH_3)_{\gamma\text{-aVal}}$], 18.41 [1C, $(CH_3)_{\gamma\text{-bVal}}$] ppm.

Ac–D–Leu–NH–Fn–NH–Boc (31): IR (CH_2Cl_2) ν_{max}/cm^{-1}: 3426 m ($NH_{slobodni}$), 3305 w ($NH_{assoc.}$), 1701 s, 1688 s, 1670 s ($C{=}O_{CONH}$), 1530, 1505, 1436, 1420 (amide II). **^{1}H-NMR** (600 MHz, $CDCl_3$) δ: 8.16 (s, 1H, NH_{Fn}), 6.35 (s, 1H, NH_{Ac}), 6.07 (s, 1H, $NH^b{}_{Fn}$), 4.68-4.50 (m, 2H, CH_{Fn}), 4.30 (s, 2H, CH_{Fn}), 4.48-4.46 (m, 1H, $CH_{\alpha\text{-Leu}}$), 4.20-4.13 (m, 4H, CH_{Fn}), 2.01 (s, 3H, $CH_{3\text{-Ac}}$), 1.73-1.66 [m, 3H, $(CH_2)_{\beta\text{-Leu}}$, $CH_{\gamma\text{-Leu}}$], 1.48 [s, 9H, $(CH_3)_{3\text{-Boc}}$], 0.96-0.94 [m, 6H, $(CH_3)_{\delta\text{-a-Leu}}$, $(CH_3)_{\delta\text{-b-Leu}}$] ppm. **^{13}C-NMR** (150 MHz, $CDCl_3$) δ: 170.80 (1C, $CO^a{}_{Fn}$), 170.61 (1C, CO_{Ac}), 154.16 (1C, $CO^b{}_{Fn}$), 80.50 (1C, C_{qBoc}), 71.79 (1C, $C_q\text{-}1_{Fn}$), 68.17, 66.65, 66.16, 65.90, 64.80, 64.18, 63.13, 62.82 (8C, CH_{Fn}), 52.33 (1C, $CH_{\alpha\text{-Leu}}$), 41.38 [1C, $(CH_2)_{\beta\text{-Leu}}$], 28.48 [3C, $(CH_3)_{3Boc}$], 24.94 (1C, $CH_{\gamma\text{-Leu}}$), 23.36 (1C, $CH_{3\text{-Ac}}$), 23.06, 22.38 [2C, $(CH_3)_{2\text{-}\delta\text{-Leu}}$] ppm.

Ac–L–Phe–NH–Fn–NH–L–Phe–Boc (32)

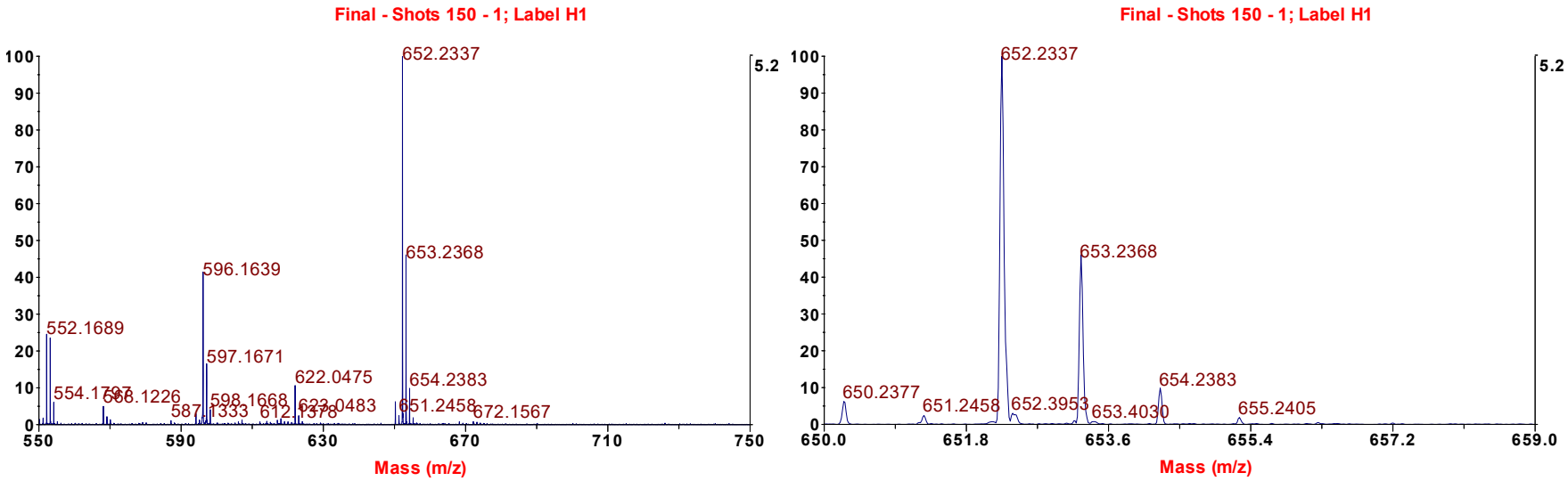

Figure S2. HRMS spectrum of compound **32.**

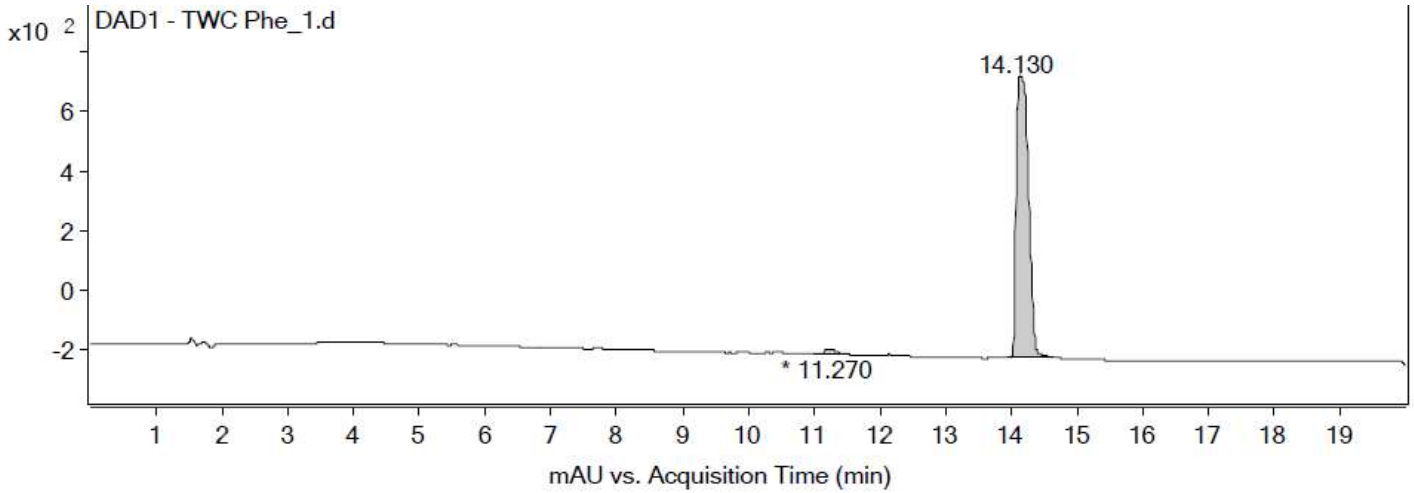

Integration Peak List

Peak	Start	RT	End	Height	Area	Area %
1	10.984	11.27	11.55	16.37	194.88	1.61
2	13.964	14.13	14.638	943.99	12117.92	100

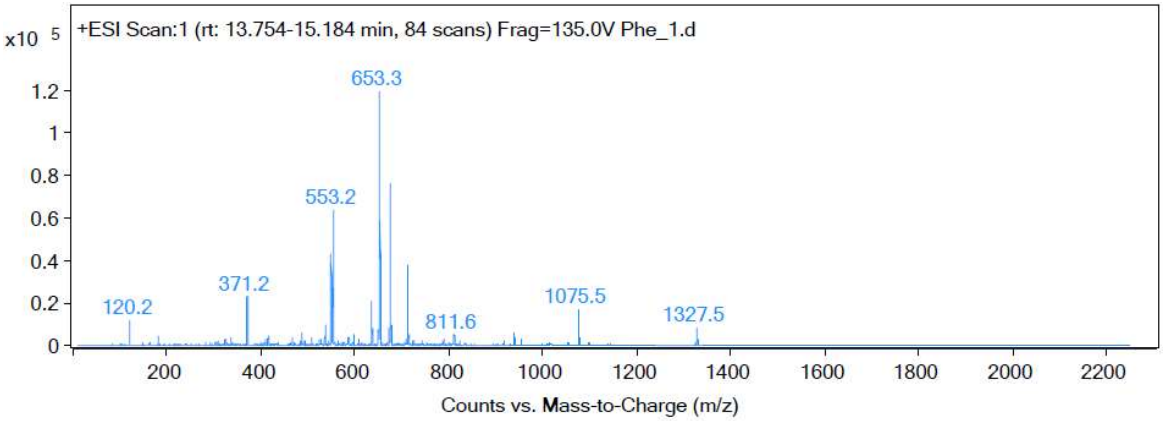

Peak List

m/z	z	Abund
371.2	1	23139.37
549.3	1	42951.14
553.2	1	63879.39
554.2	1	24076.97
652.3		97588.08
653.3	1	119554.73
654.2	1	42921.98
675.3	1	76776.57
676.2	1	34435.55
712.3	1	38095.04

Figure S3. HPLC-ESI spectra of compound **32.**

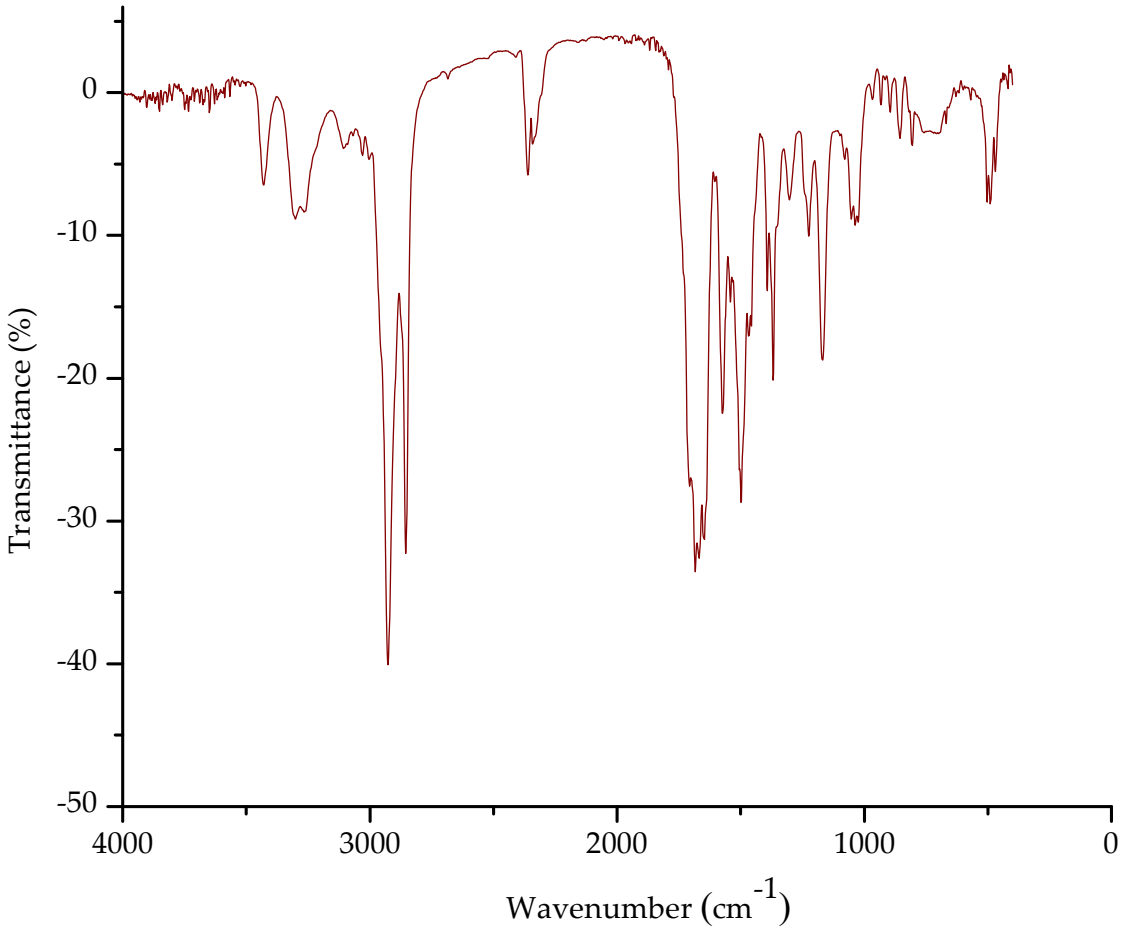

Figure S4. IR spectrum of compound **32** ($c = 5 \times 10^{-2}$ M) in DCM.

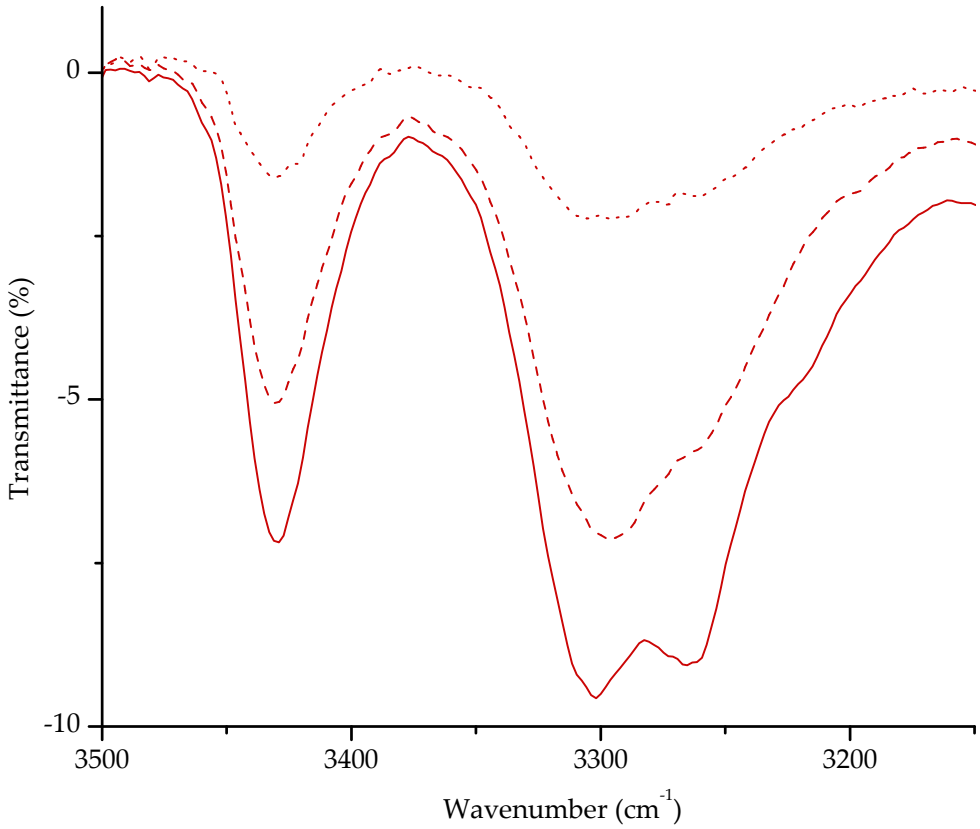

Figure S5. The NH stretching vibrations in concentration-dependent IR spectra of **32** in DCM [(—) $c = 5 \times 10^{-2}$ M, (——) $c = 2.5 \times 10^{-2}$ M, (· · ·) $c = 1.25 \times 10^{-2}$ M.

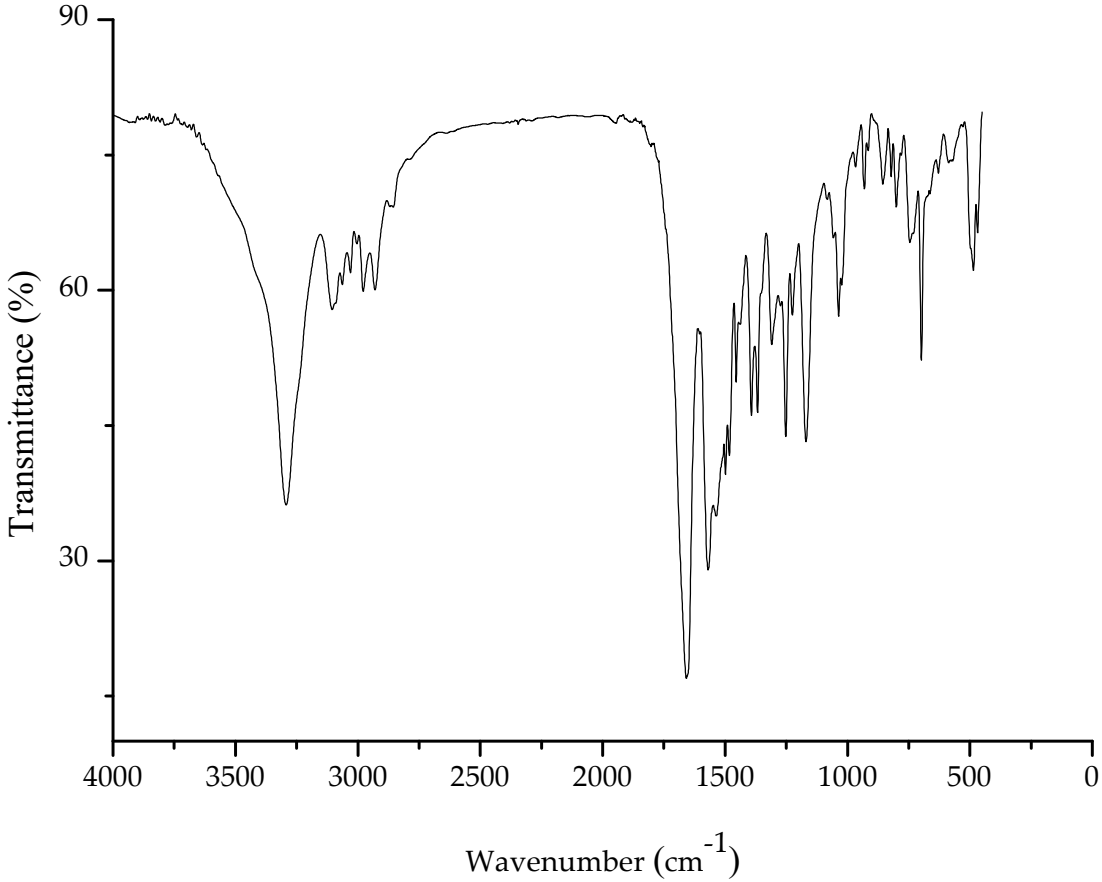

Figure S6. IR spectrum of compound **32** (2 mg) in KBr (200 mg).

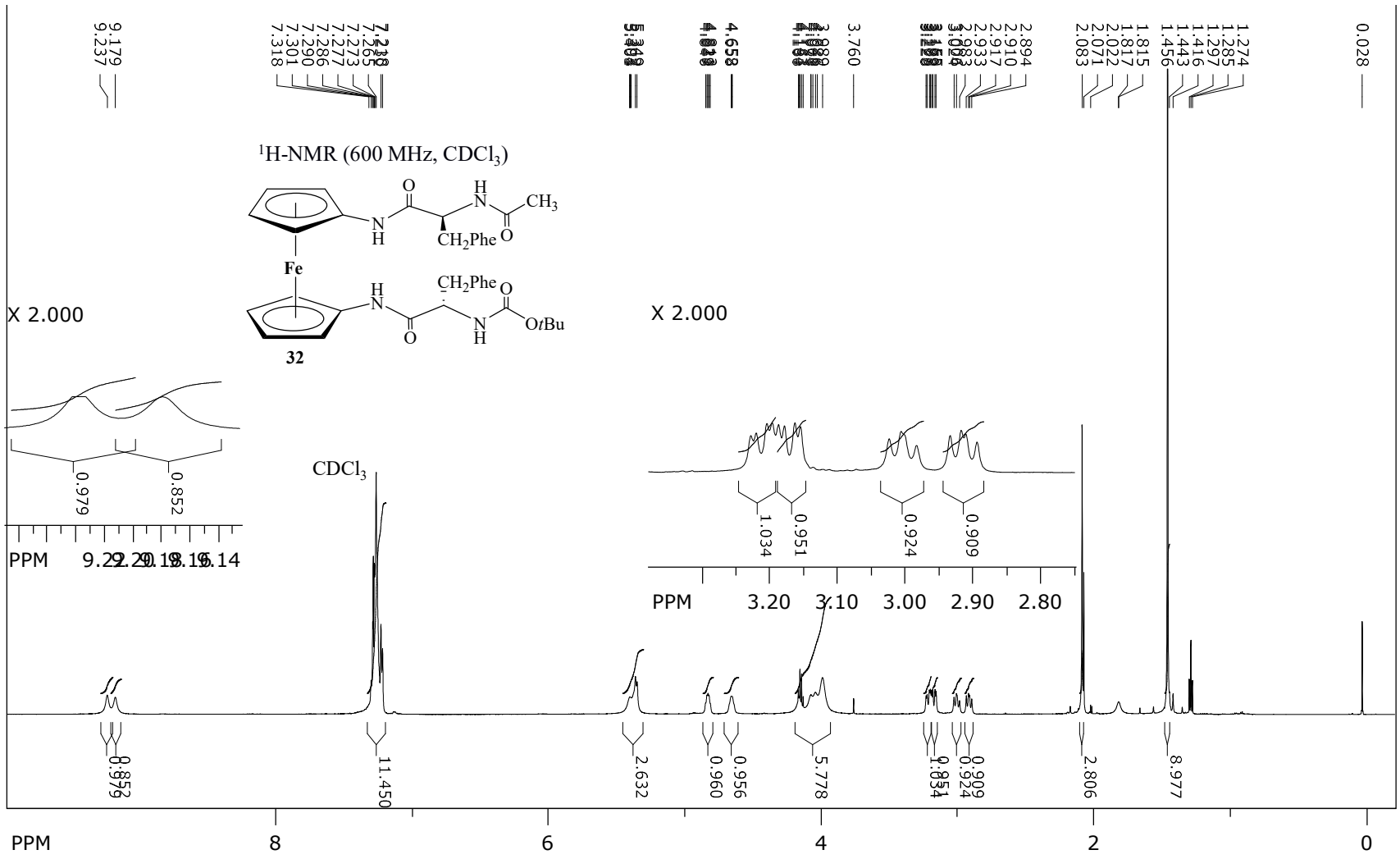

Figure S7. ^{1}H NMR spectrum of compound **32** ($c = 5 \times 10^{-2}$ M).

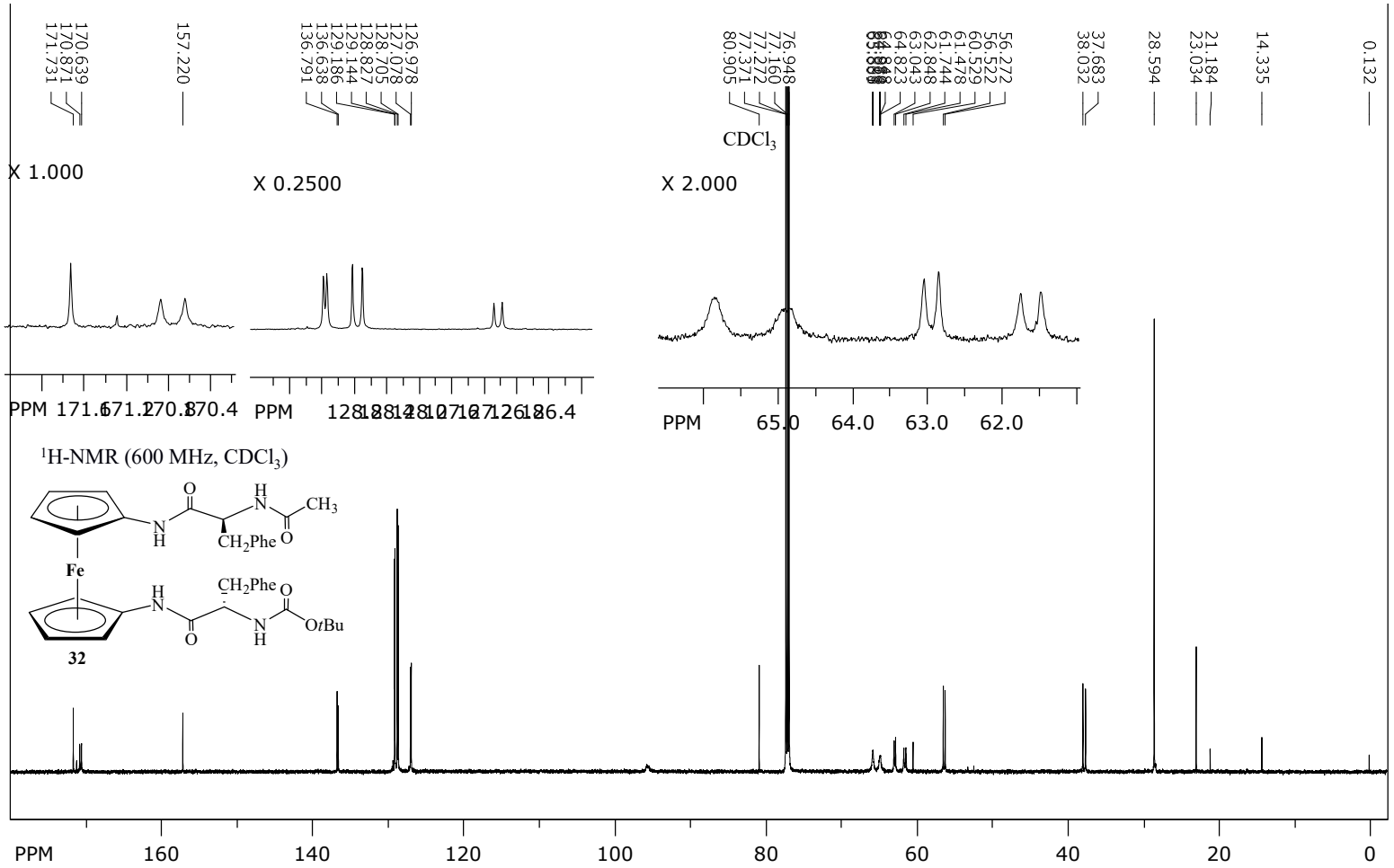

Figure S8. $^{13}C\{^{1}H\}$ NMR spectrum of compound **32** ($c = 5 \times 10^{-2}$ M).

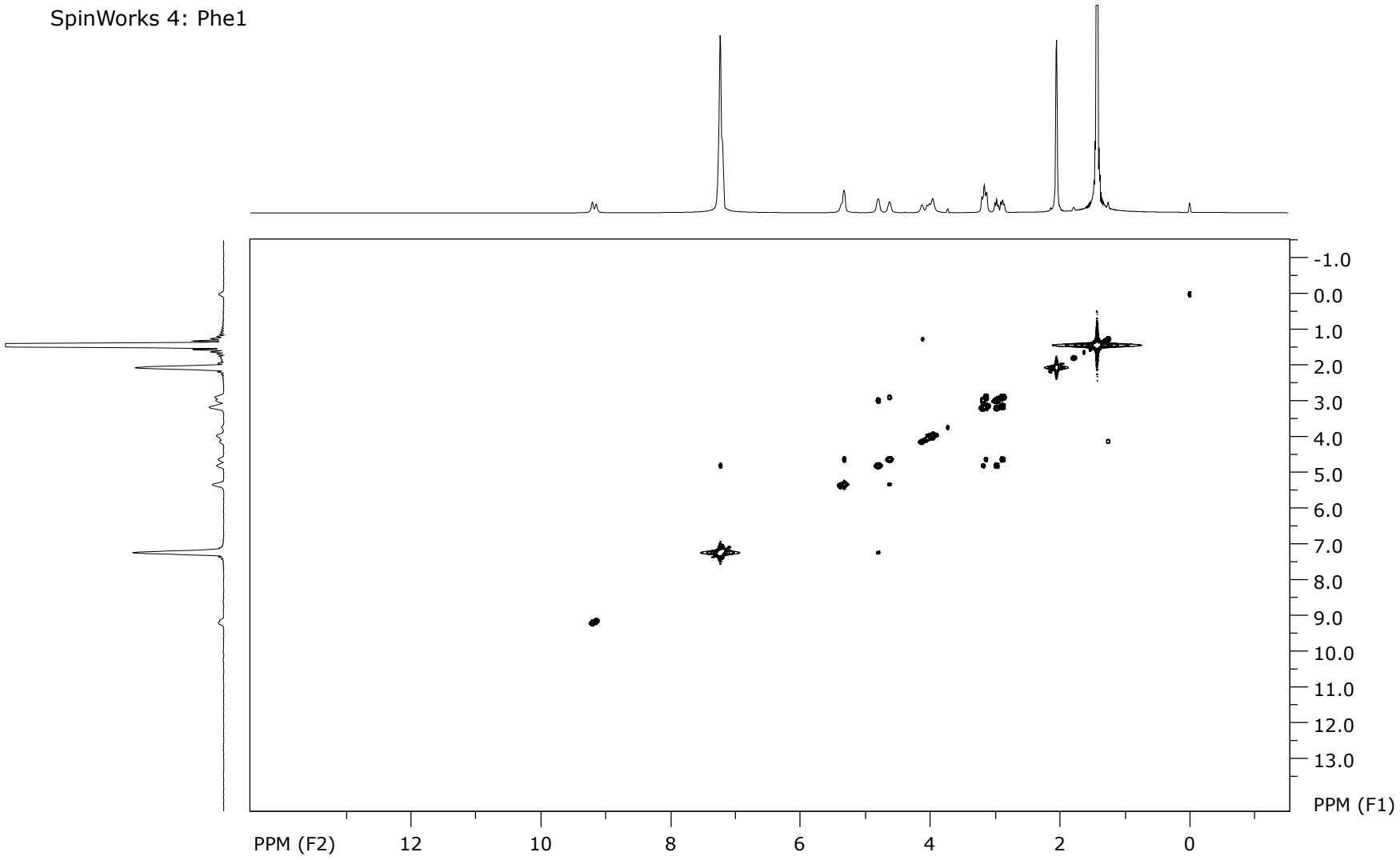

Figure S9. ^{1}H-^{1}H COSY NMR spectrum of compound **32** ($c = 5 \times 10^{-2}$ M).

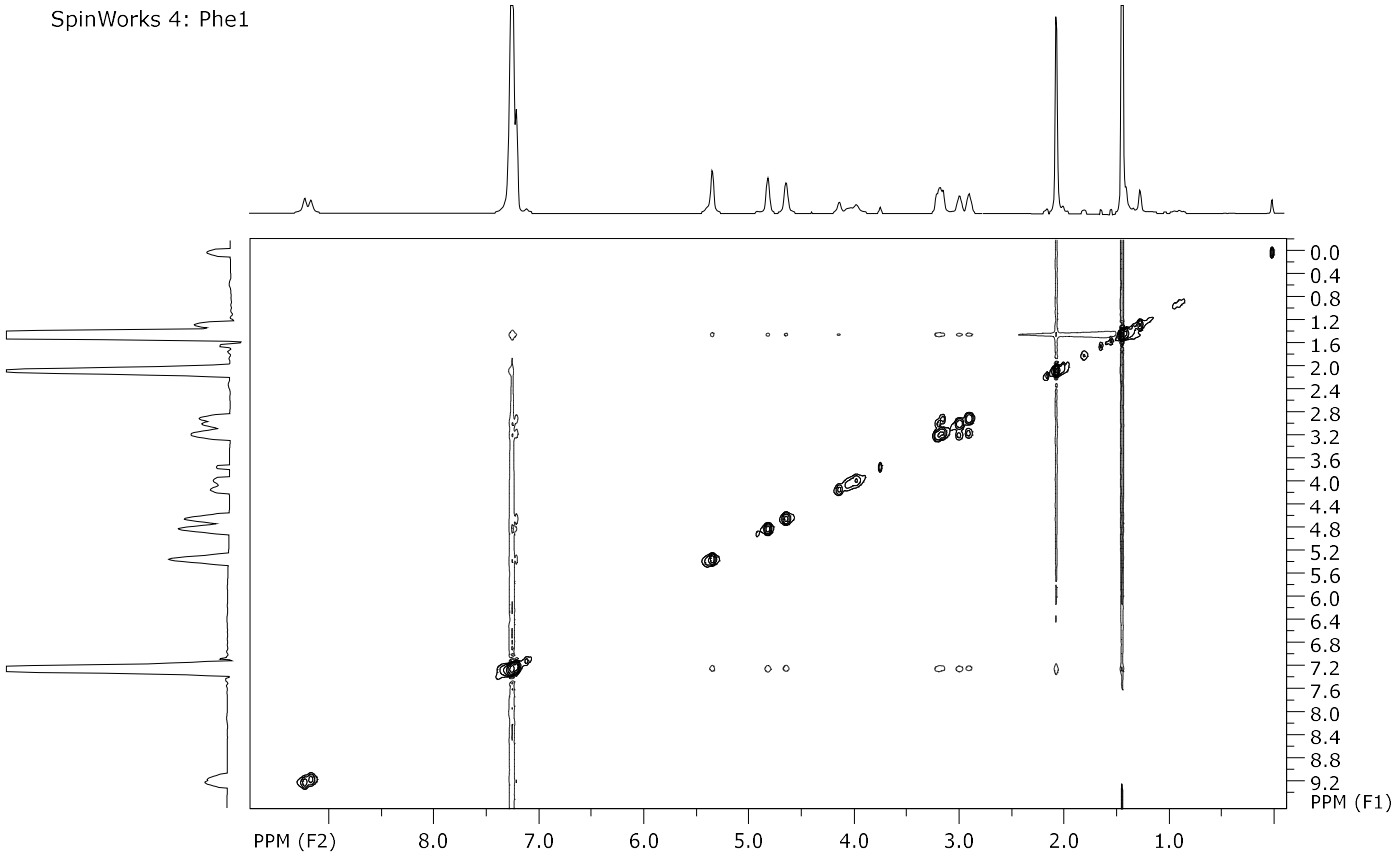

Figure S10. ^{1}H-^{1}H NOESY NMR spectrum of compound **32** ($c = 5 \times 10^{-2}$ M).

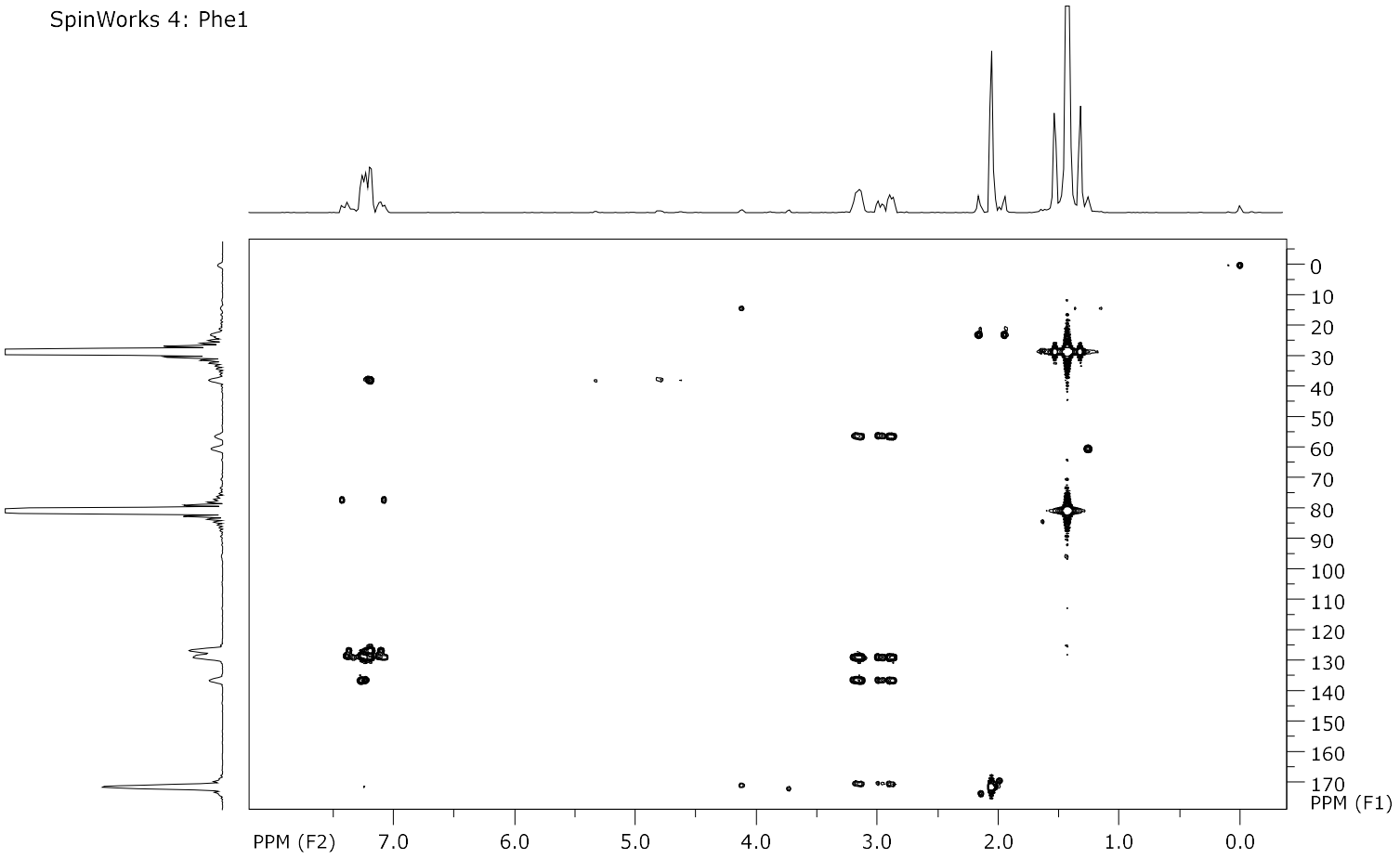

Figure S11. ^{1}H-^{13}C HMQC spectrum of compound **32** ($c = 5 \times 10^{-2}$ M).

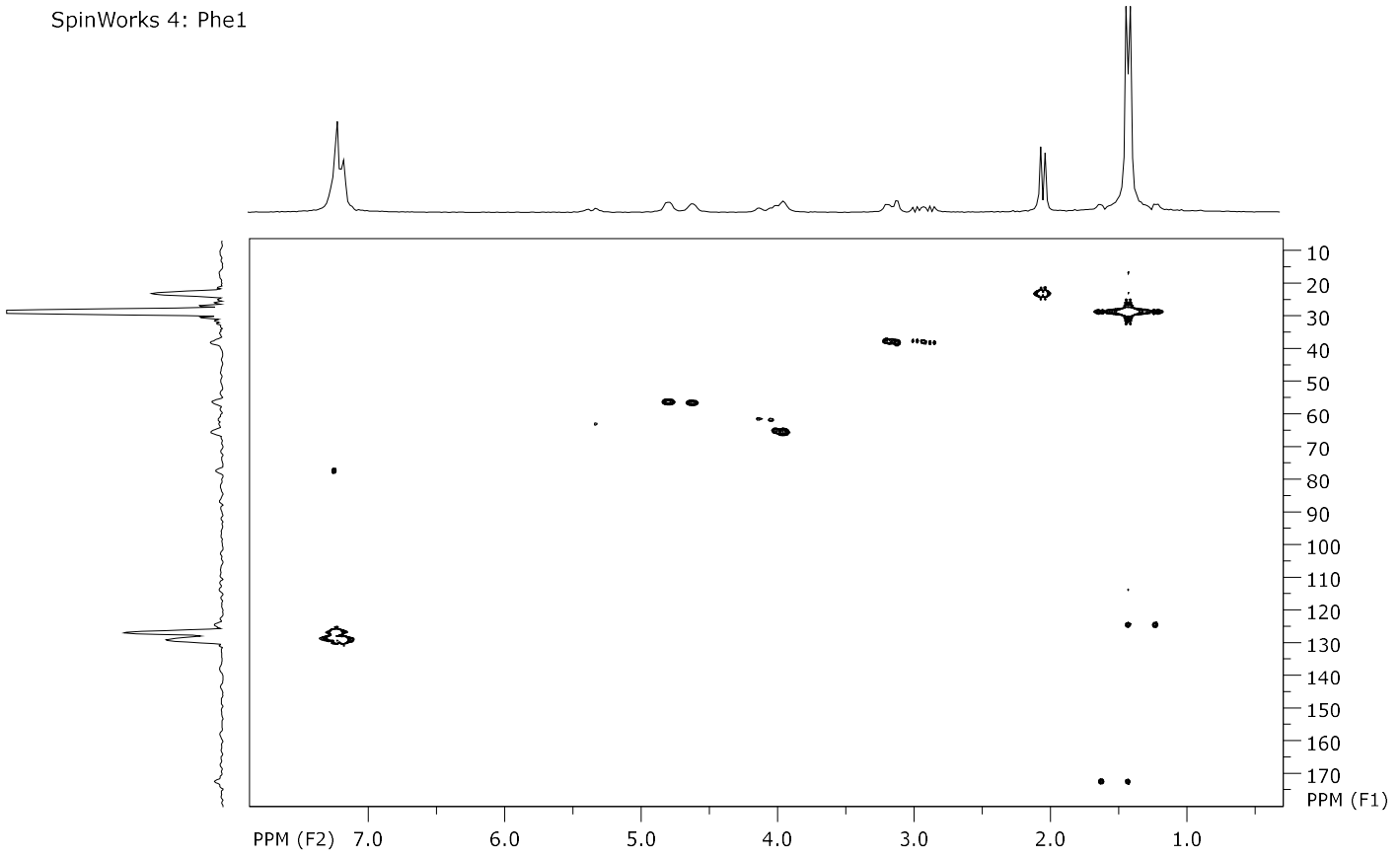

Figure S12. ^{1}H-^{13}C HMBC spectrum of compound **32** ($c = 5 \times 10^{-2}$ M).

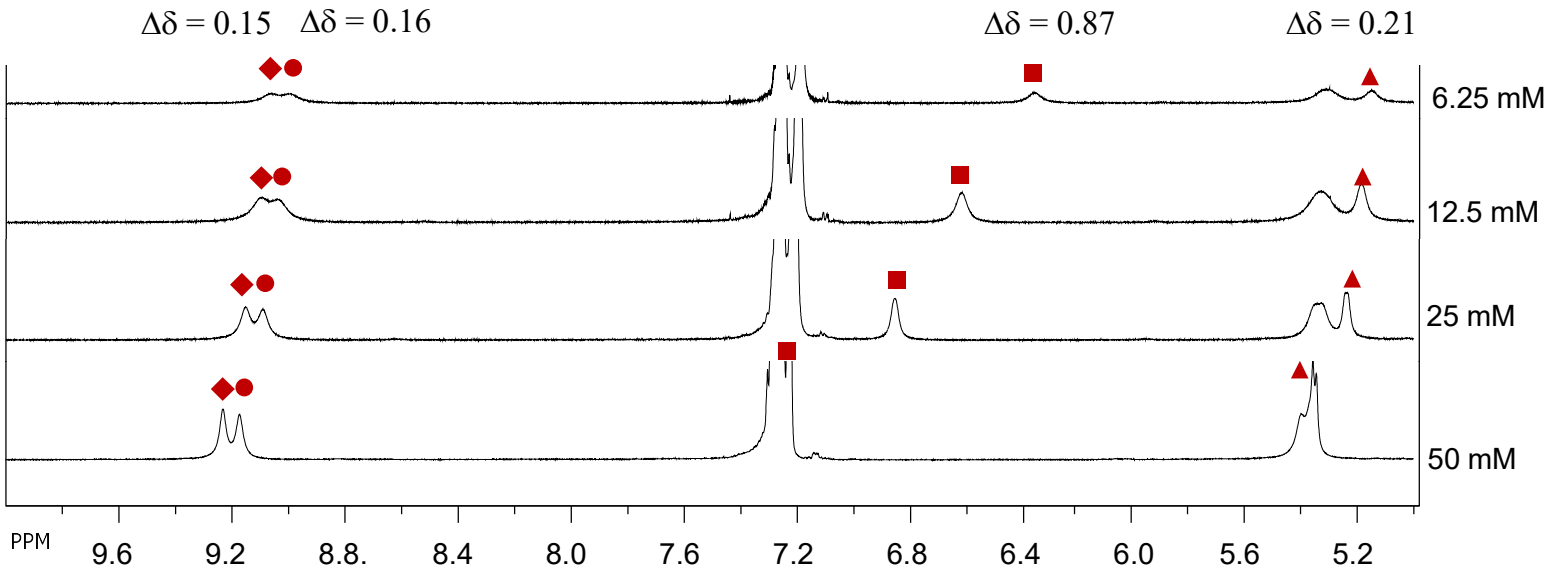

Figure S13. Concentration-dependent NH chemical shifts of compound **32** in $CDCl_3$.

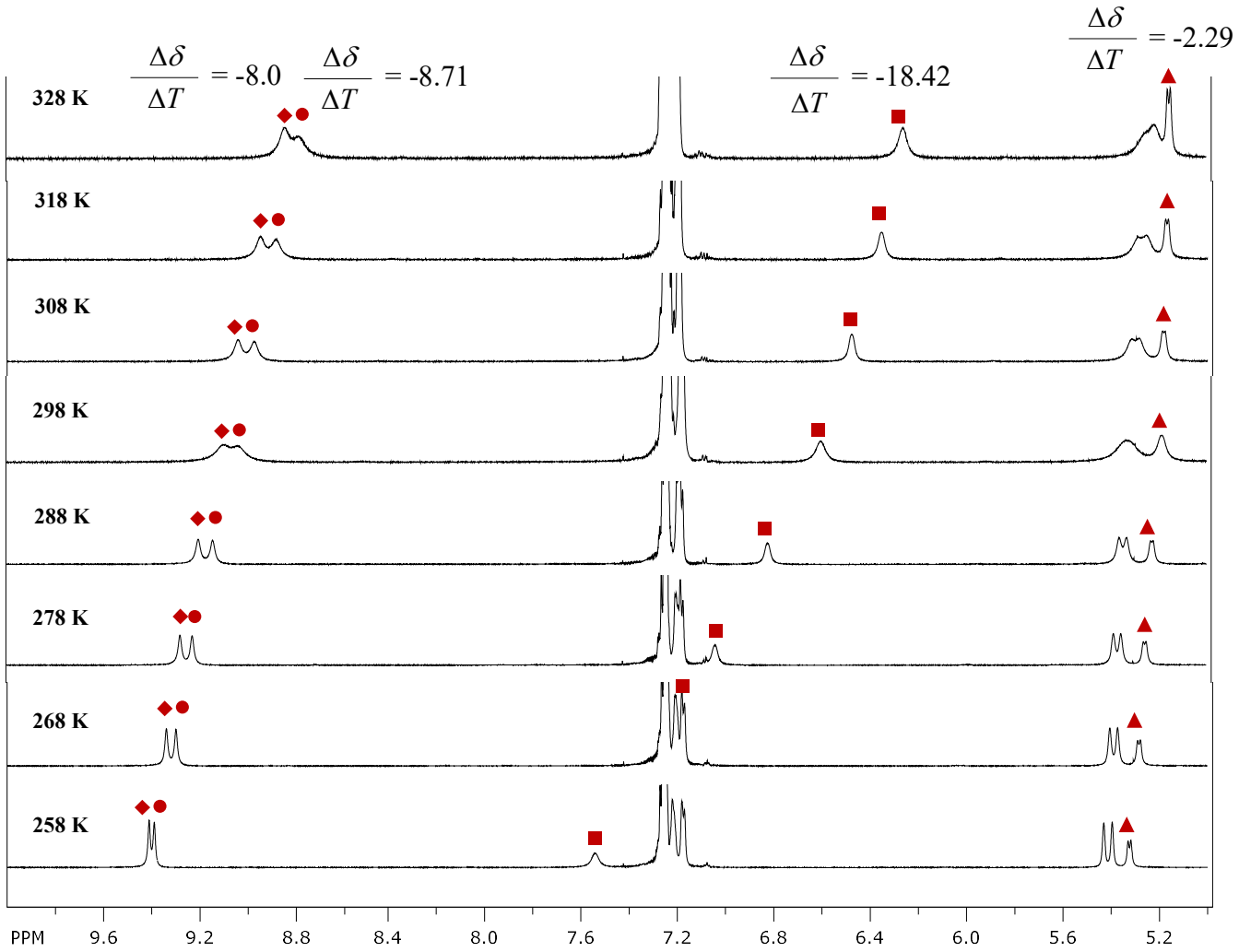

Figure S14. Temperature-dependent NH chemical shifts of compound **32** ($c = 1 \times 10^{-2}$ M).

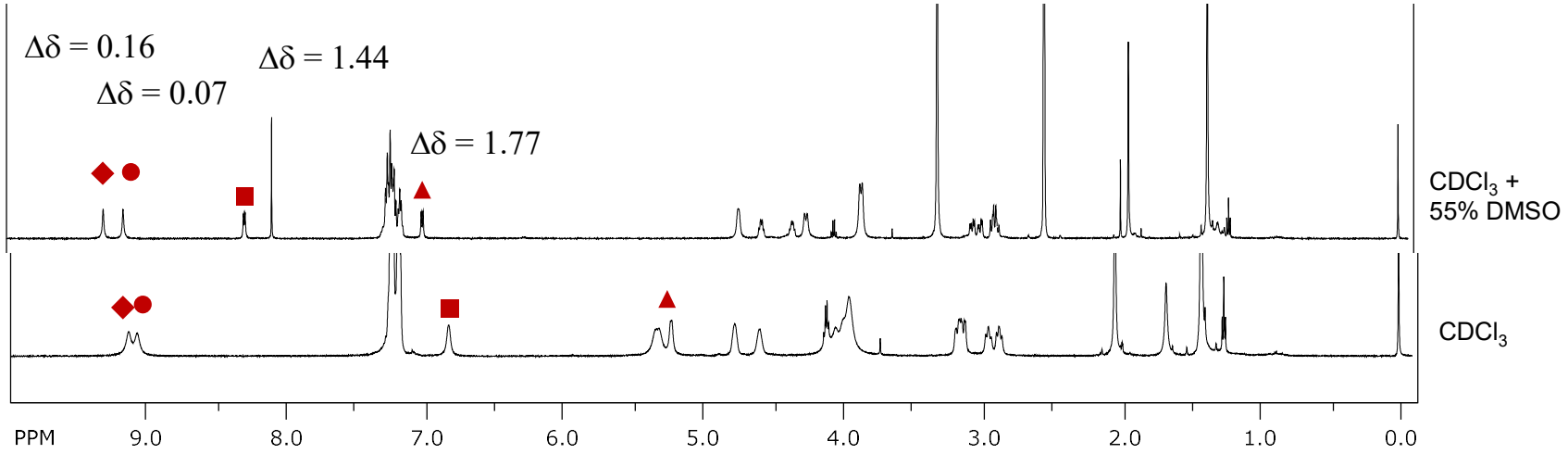

Figure S15. ^{1}H NMR spectra of compound **32** at varying concentrations of DMSO in $CDCl_3$ ($c = 2.5 \times 10^{-2}$ M).

Ac–D–Phe–NH–Fn–NH–D–Phe–Boc (35)

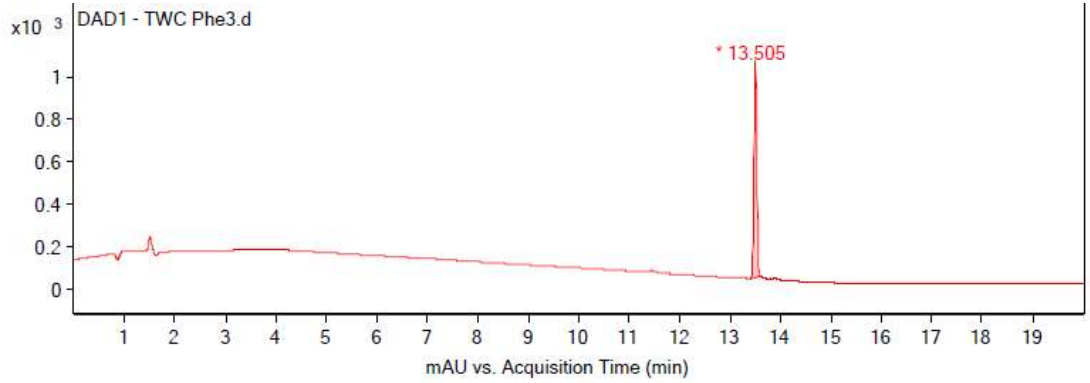

Integration Peak List

Peak	Start	RT	End	Height	Area	Area %
1	13.398	13.505	13.625	1015.37	3759.71	100

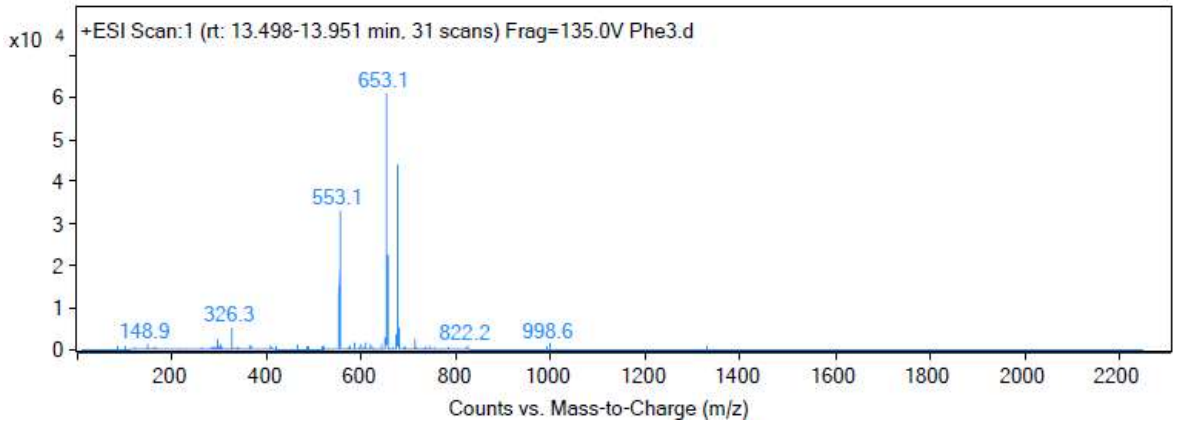

Peak List

m/z	z	Abund
326.3	1	5074.83
553.1	1	32871.92
554.1	1	12461.7
652.1		51132.72
653.1	1	60920.72
654.1	1	22339.01
655.1	1	4982.88
675.1	1	44003.48
676.1	1	18700.43
677.1	1	5240.64

Figure S16. HPLC-ESI spectra of compound **35.**

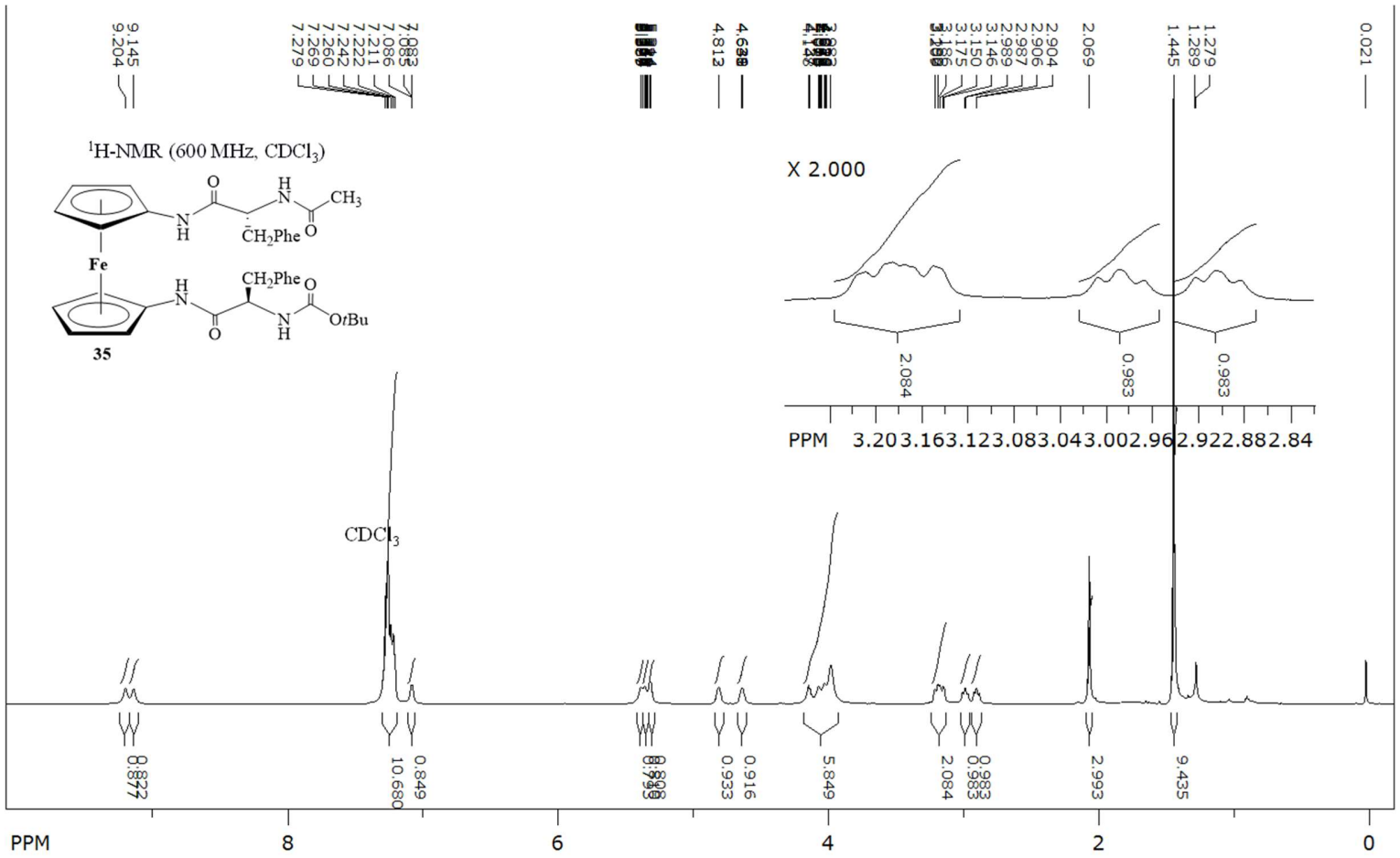

Figure S17. ^{1}H NMR spectrum of compound **35** ($c = 5 \times 10^{-2}$ M).

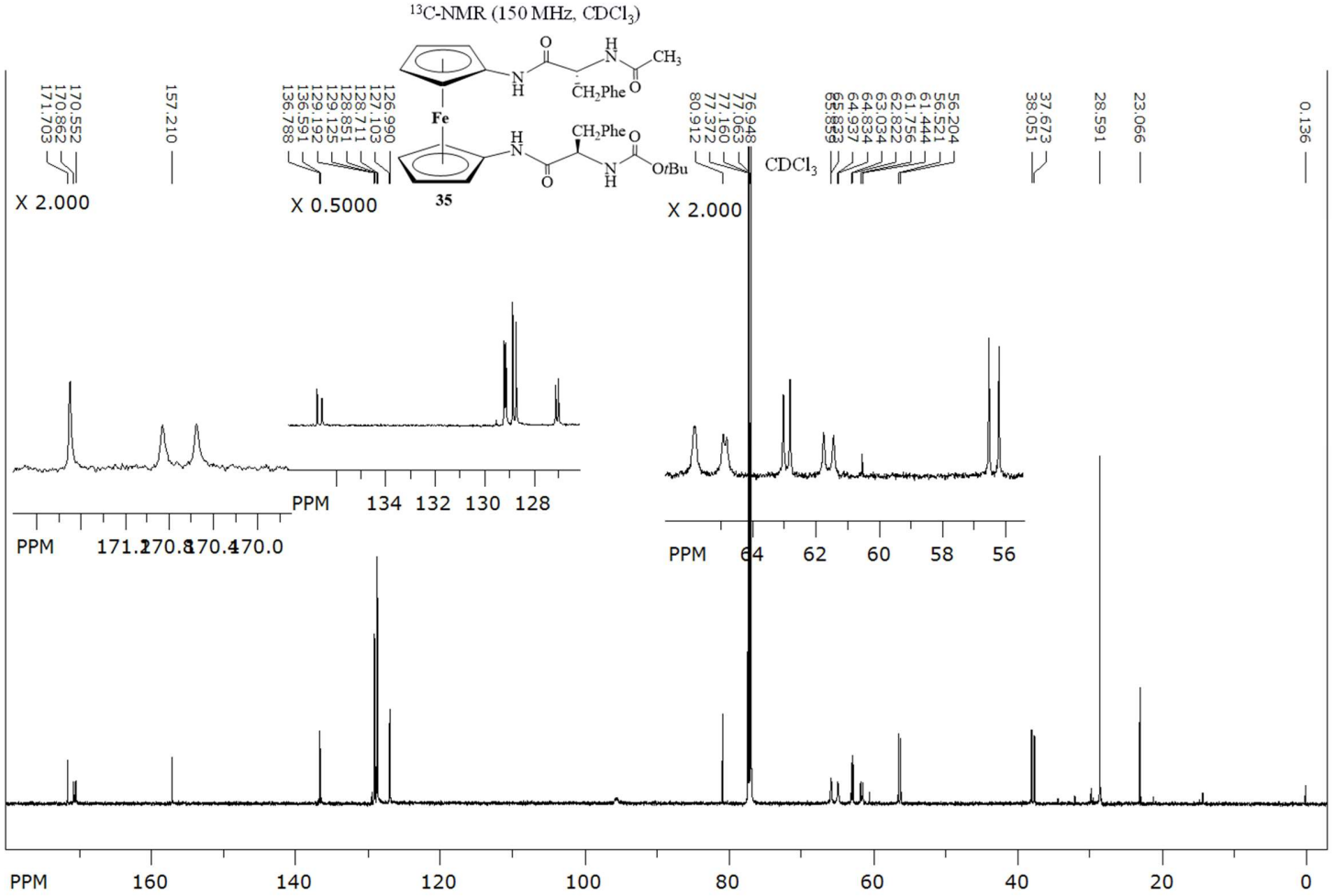

Figure S18. $^{13}C\{^{1}H\}$ NMR spectrum of compound **35** ($c = 5 \times 10^{-2}$ M).

Ac–L–Val–NH–Fn–NH–L–Val–Boc (33)

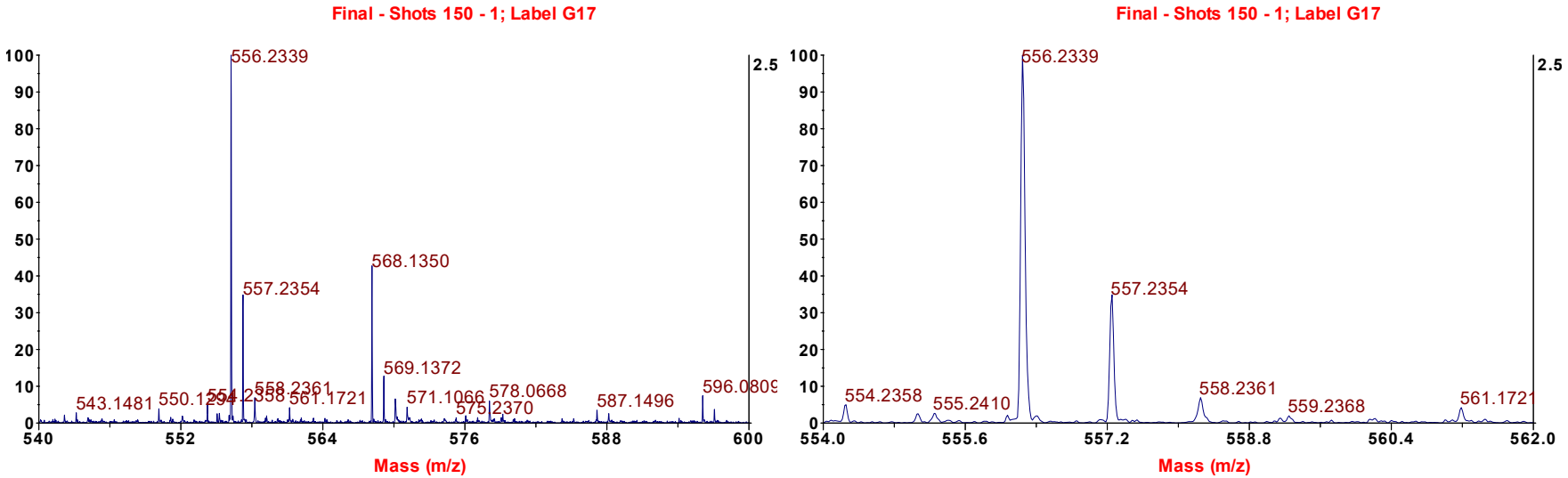

Figure S19. HRMS spectrum of compound **33.**

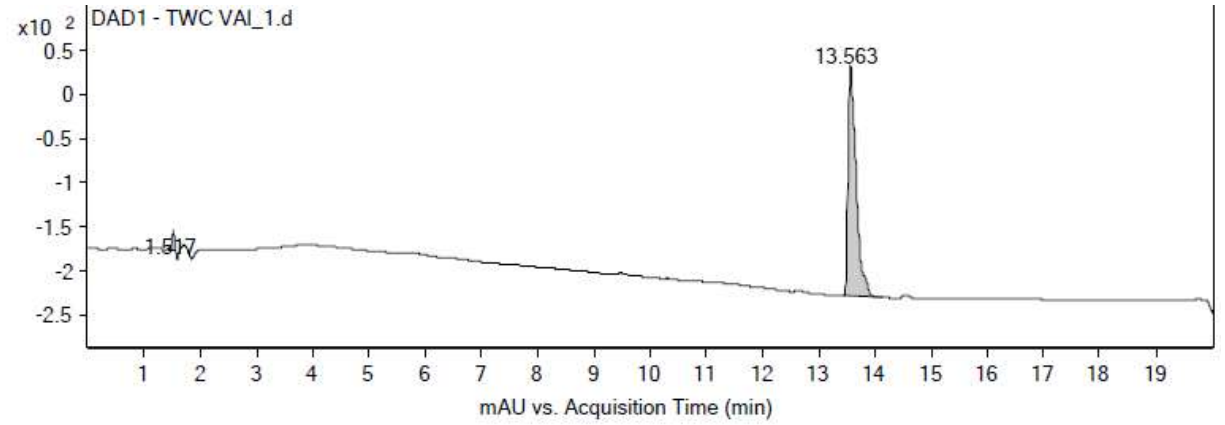

Integration Peak List

Peak	Start	RT	End	Height	Area	Area %
1	1.43	1.517	1.555	21.23	65.66	2.53
2	13.43	13.563	14.126	261.36	2593.39	100

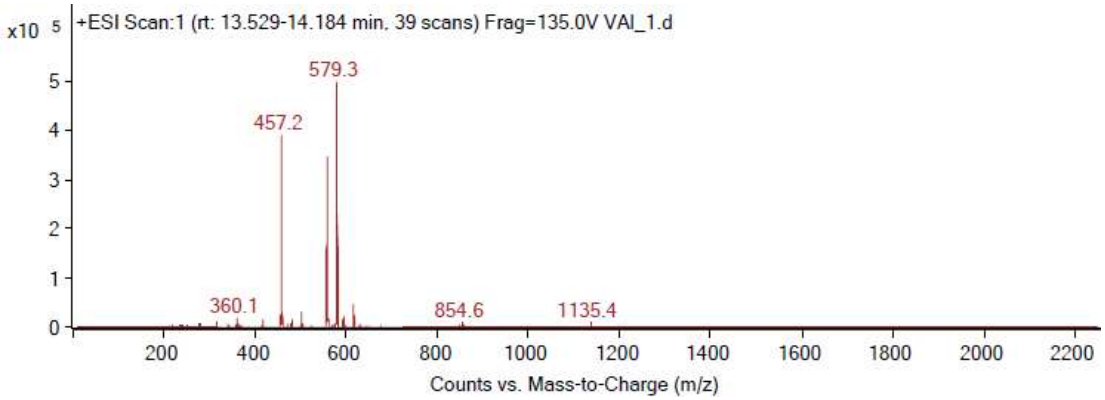

Peak List

m/z	z	Abund
457.2	1	387985.22
458.2	1	99976.73
556.3		176509.63
557.3	1	346304.03
558.2	1	107409.55
577.2		34858.21
579.3	1	497104.09
580.3	1	164582.95
581.3	1	32016.14
616.3	1	46668.61

Figure S20. HPLC-ESI spectra of compound **33.**

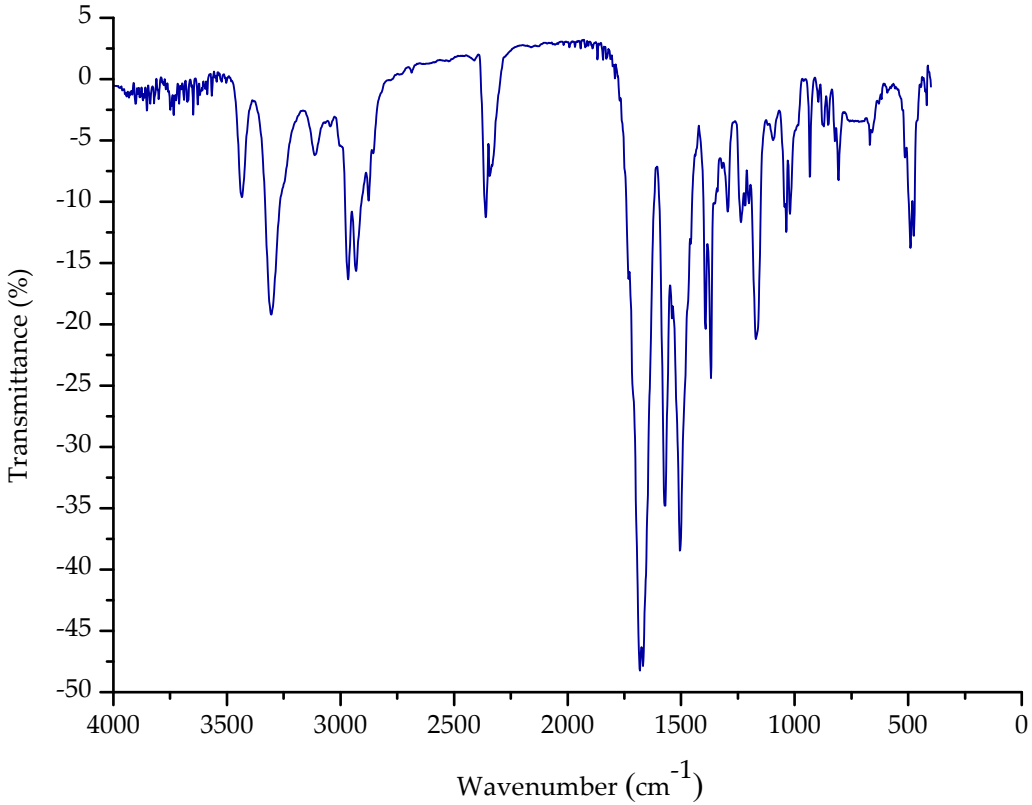

Figure S21. IR spectrum of compound **33** ($c = 5 \times 10^{-2}$ M) in DCM.

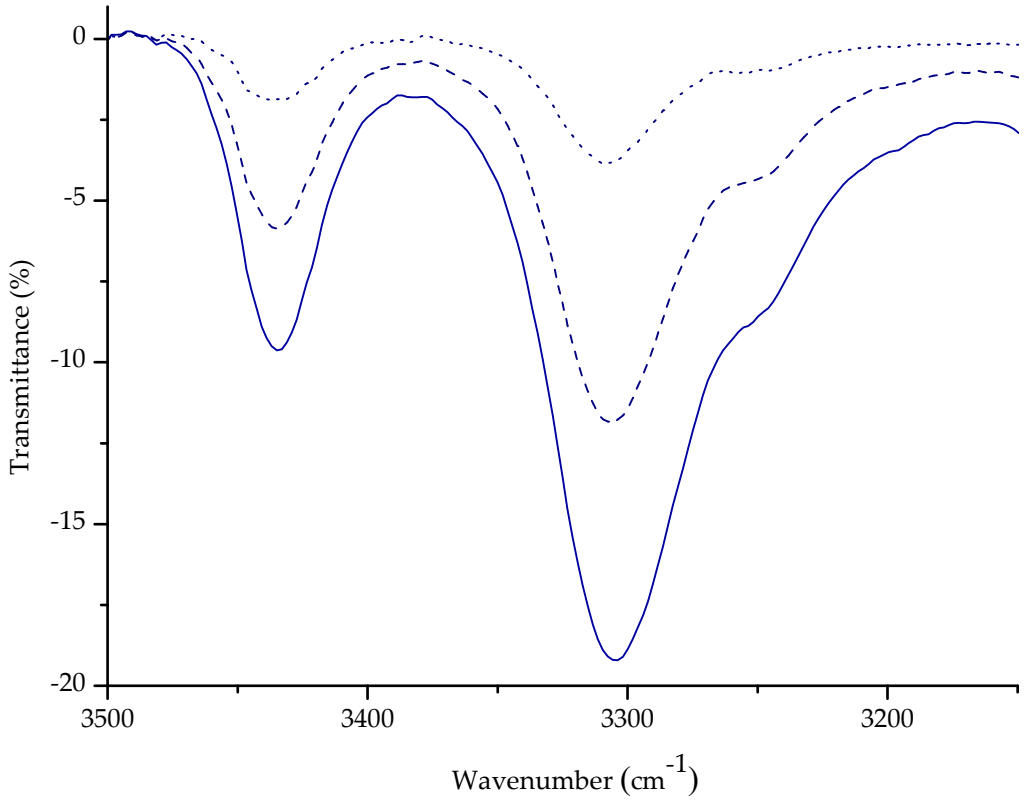

Figure S22. The NH stretching vibrations in concentration-dependent IR spectra of **33** in DCM [(—) $c = 5 \times 10^{-2}$ M, (——) $c = 2.5 \times 10^{-2}$ M, (· · ·) $c = 1.25 \times 10^{-2}$ M.

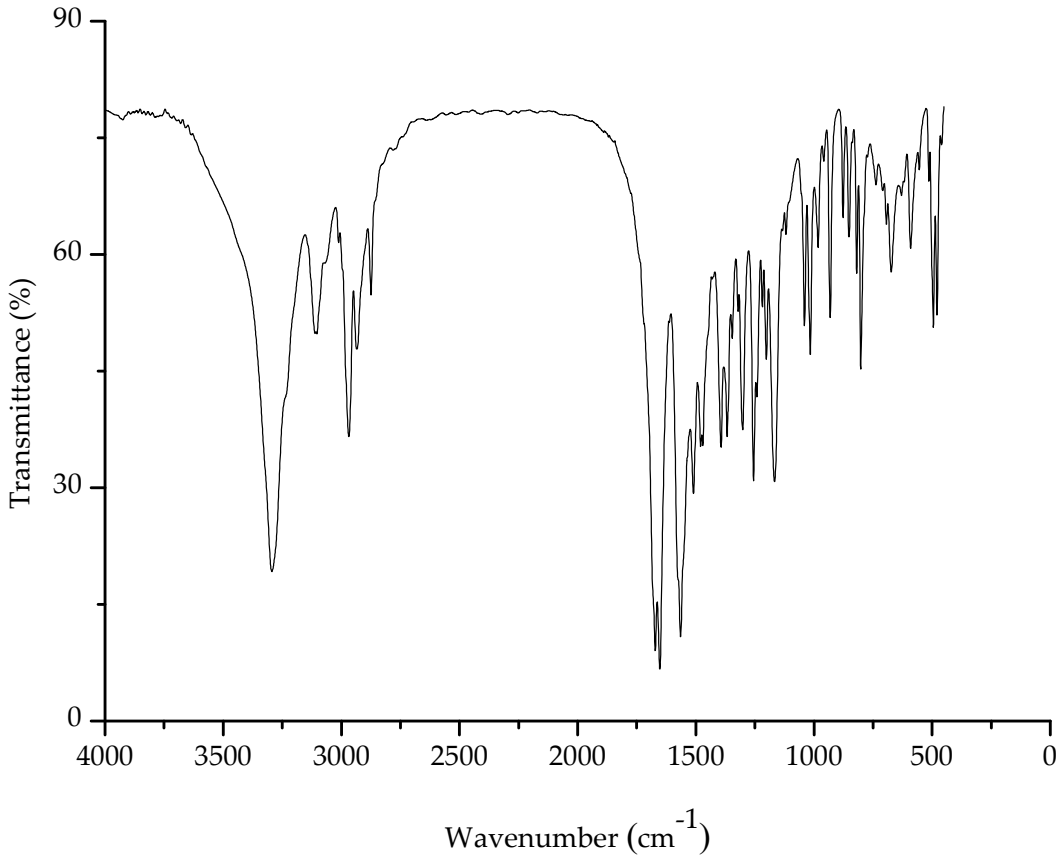

Figure S23. IR spectrum of compound **33** (2 mg) in KBr (200 mg).

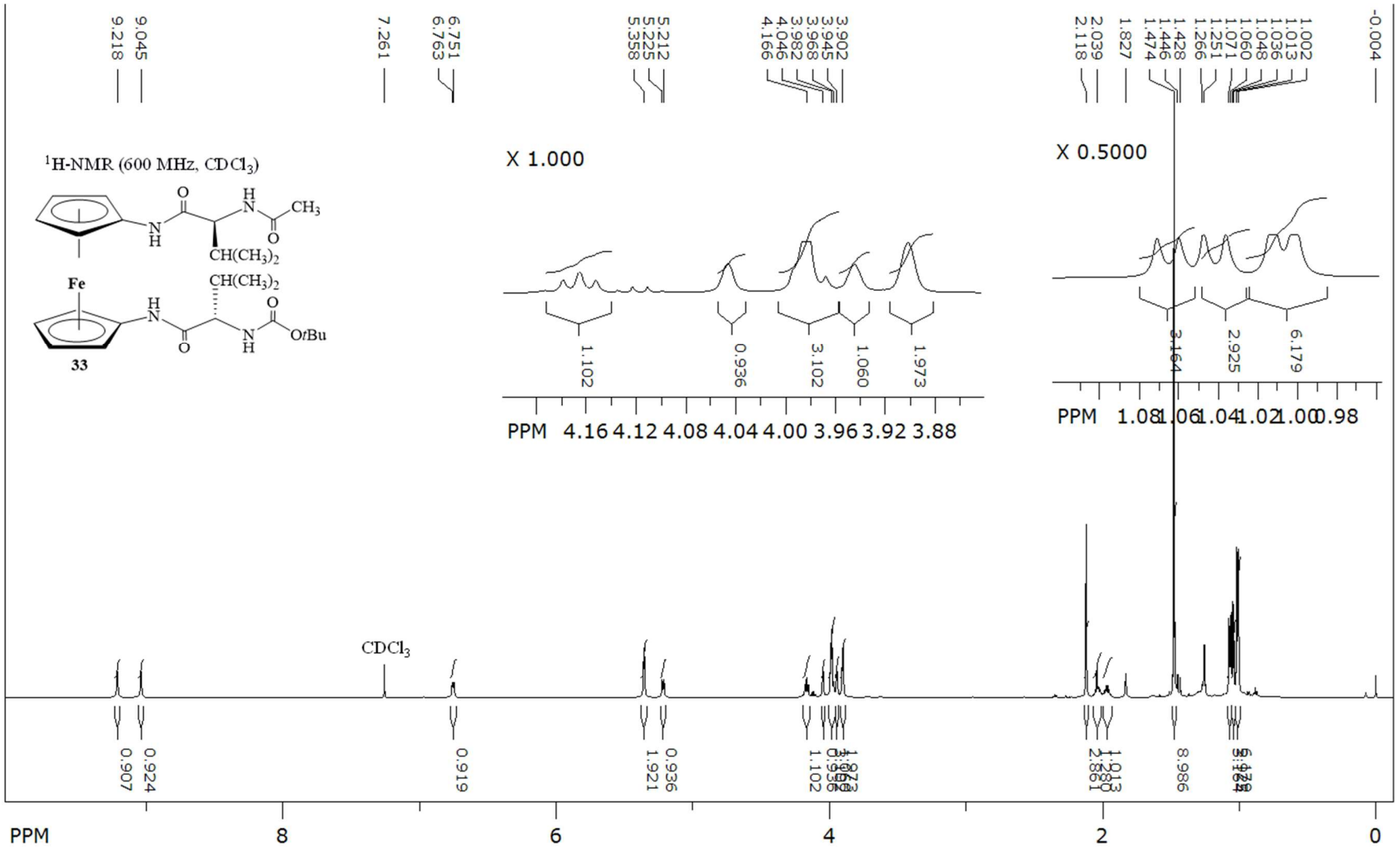

Figure S24. ^{1}H NMR spectrum of compound **33** ($c = 5 \times 10^{-2}$ M).

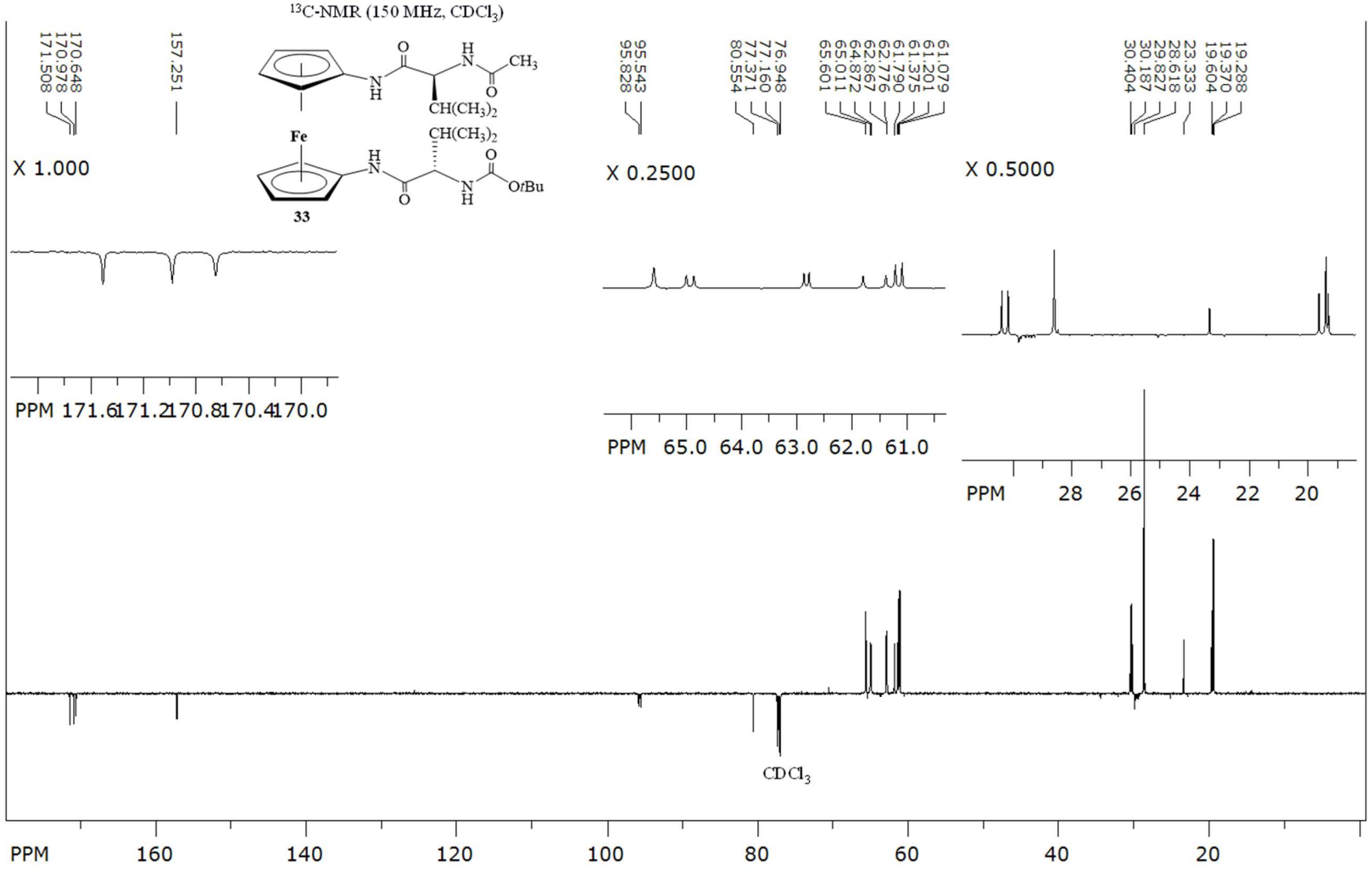

Figure S25. $^{13}C\{^{1}H\}$ NMR spectrum of compound **33** ($c = 5 \times 10^{-2}$ M).

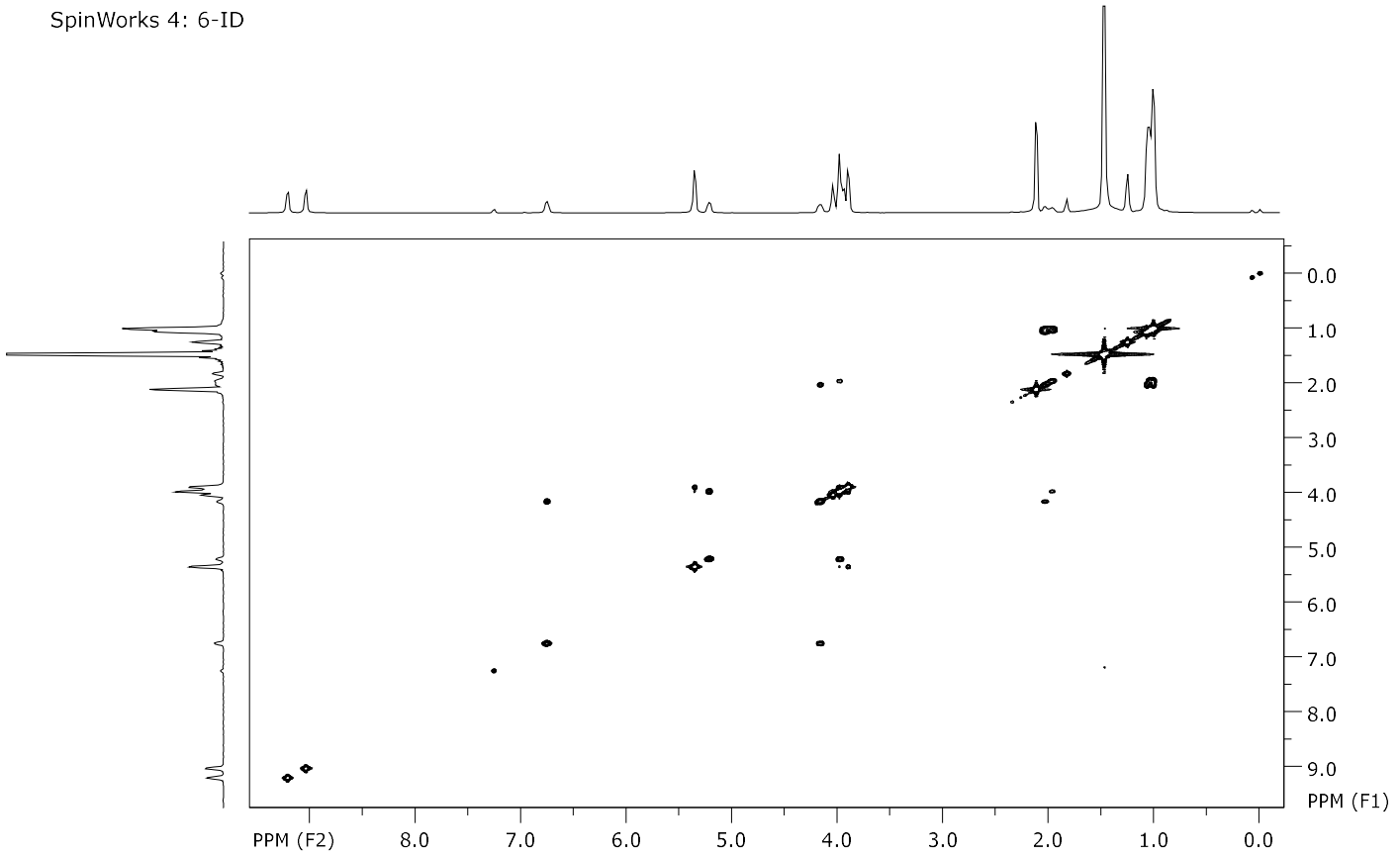

Figure S26. ^{1}H-^{1}H COSY NMR spectrum of compound **33** ($c = 5 \times 10^{-2}$ M).

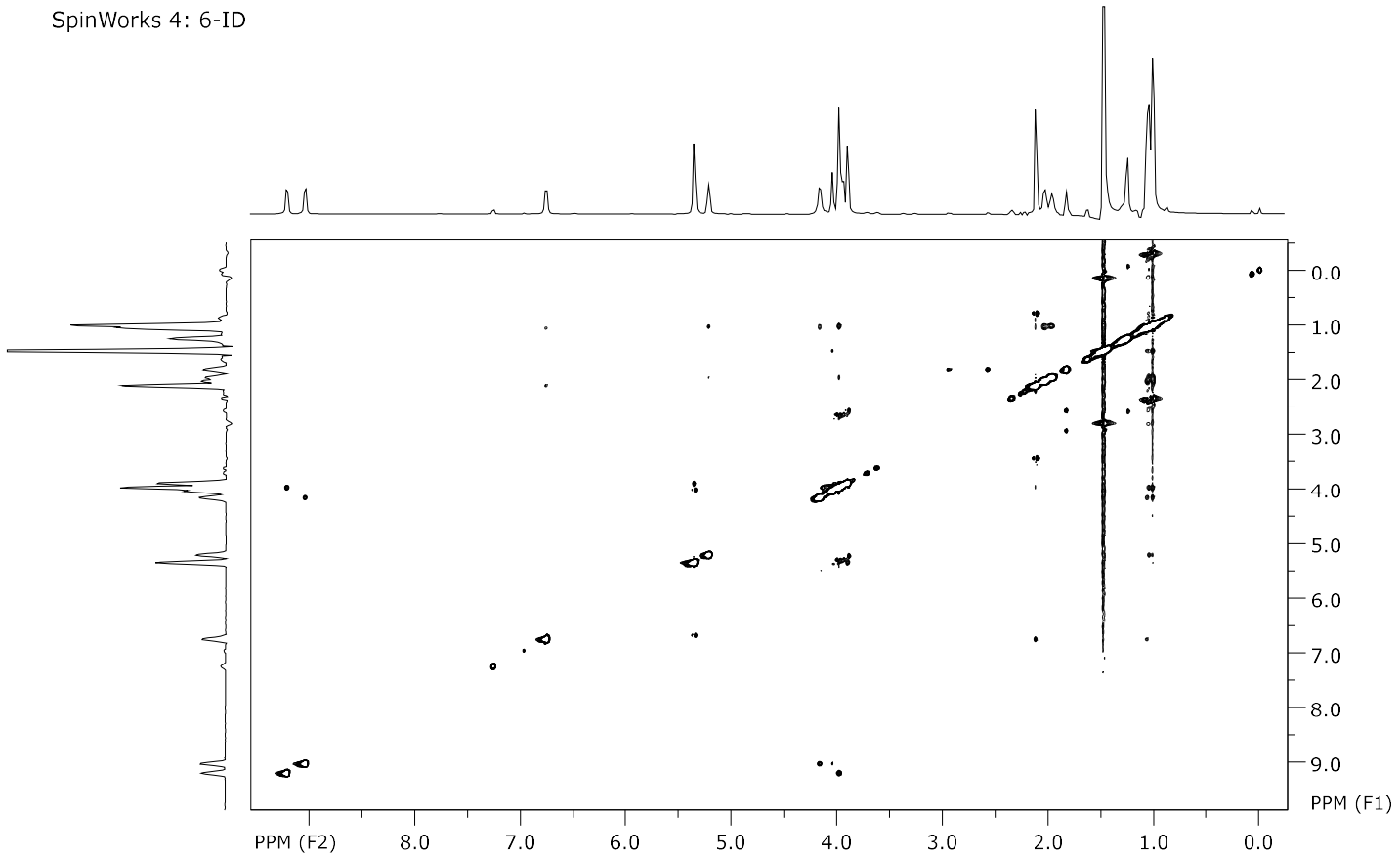

Figure S27. ^{1}H-^{1}H NOESY NMR spectrum of compound **33** ($c = 5 \times 10^{-2}$ M).

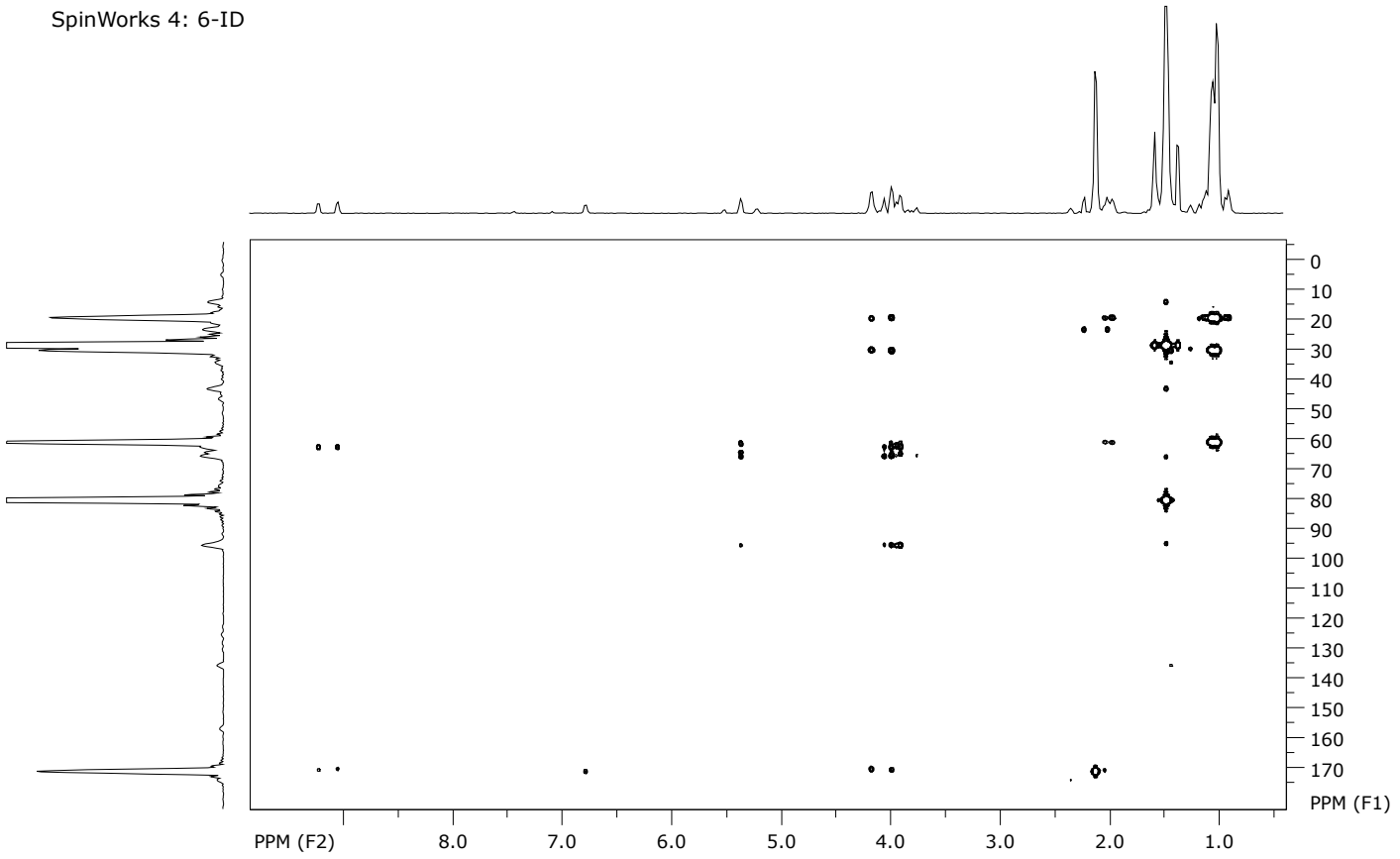

Figure S28. ^{1}H-^{13}C HMQC spectrum of compound **33** ($c = 5 \times 10^{-2}$ M).

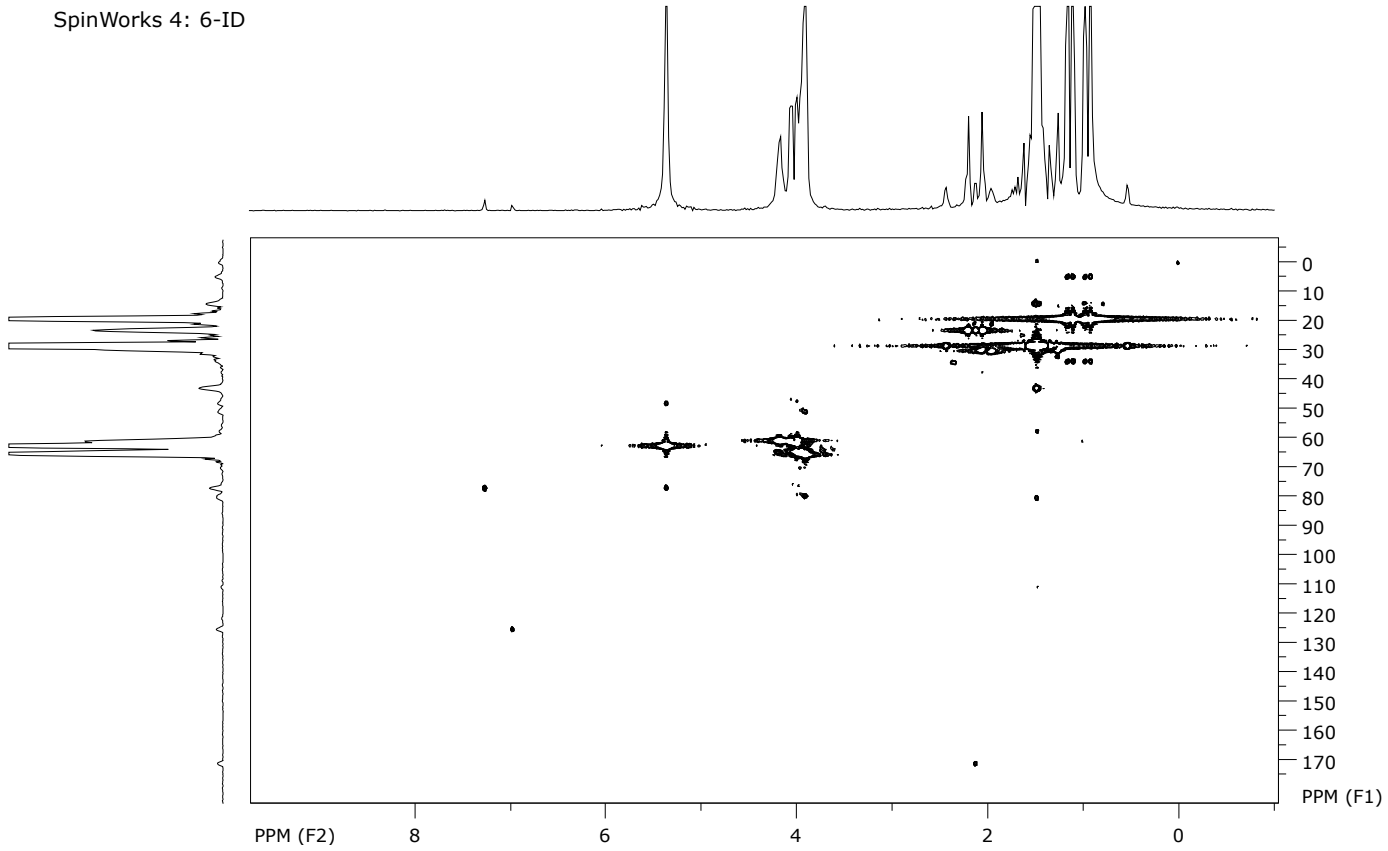

Figure S29. ^{1}H-^{13}C HMBC spectrum of compound **33** ($c = 5 \times 10^{-2}$ M).

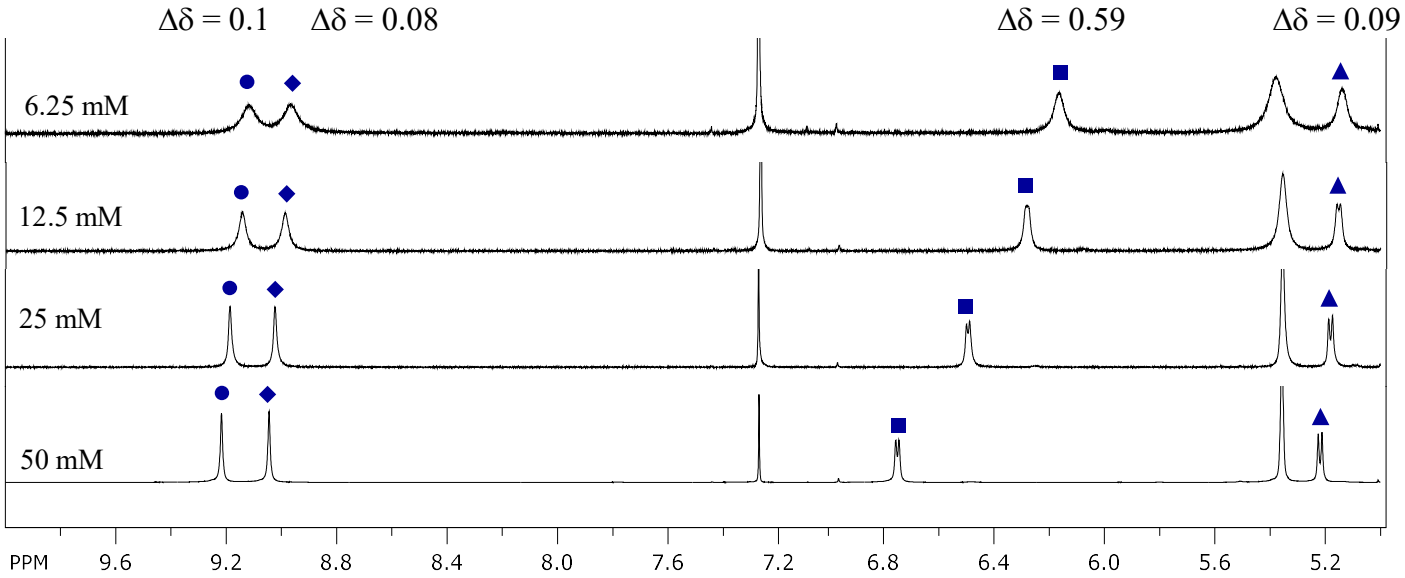

Figure S30. Concentration-dependent NH chemical shifts of compound **33** in $CDCl_3$.

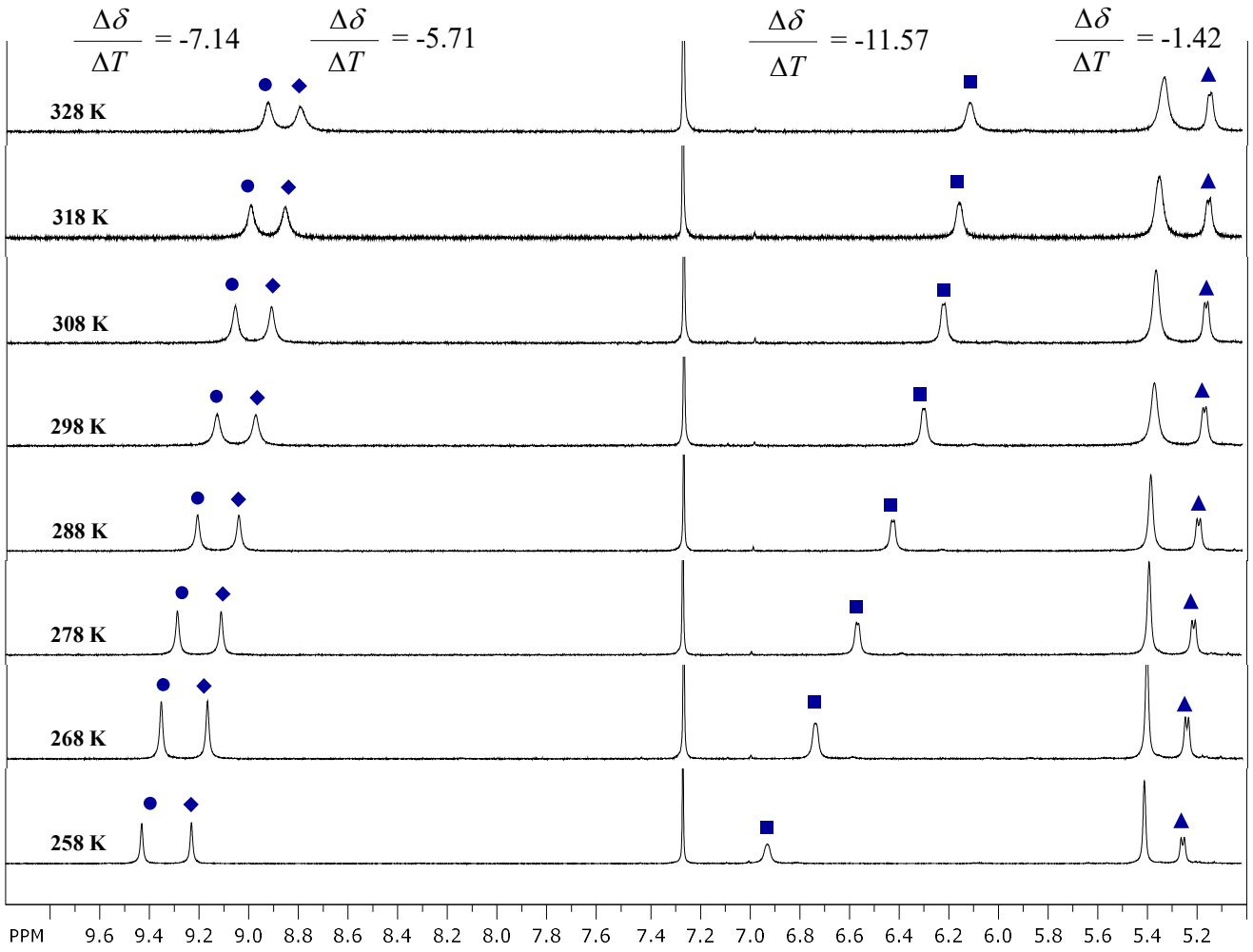

Figure S31. Temperature-dependent NH chemical shifts of compound **33** ($c = 1 \times 10^{-2}$ M).

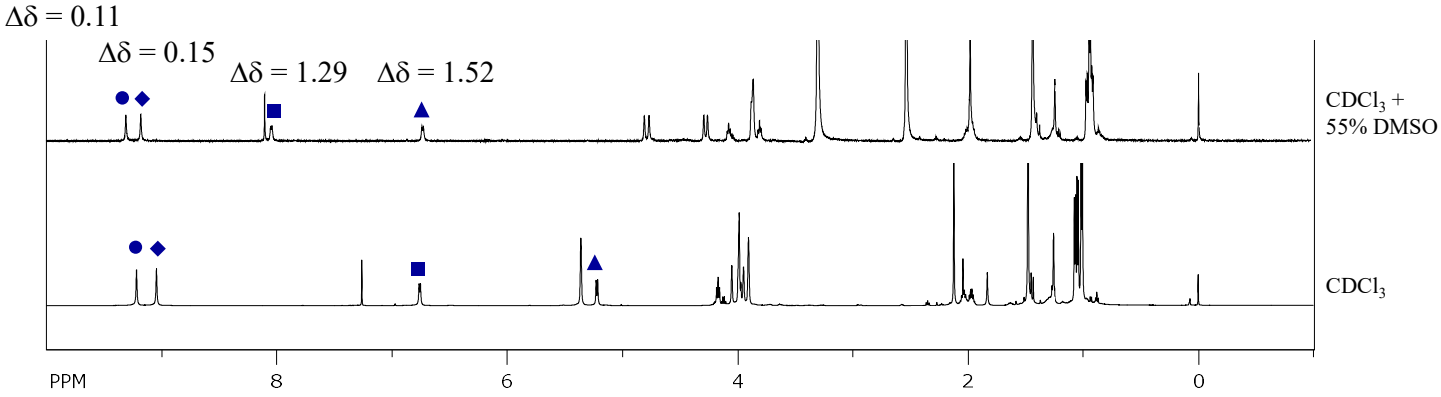

Figure S32. ^{1}H NMR spectra of compound **33** at varying concentrations of DMSO in $CDCl_3$ (c = 2.5 × 10-2 M).

Ac–D–Val–NH–Fn–NH–D–Val–Boc (36)

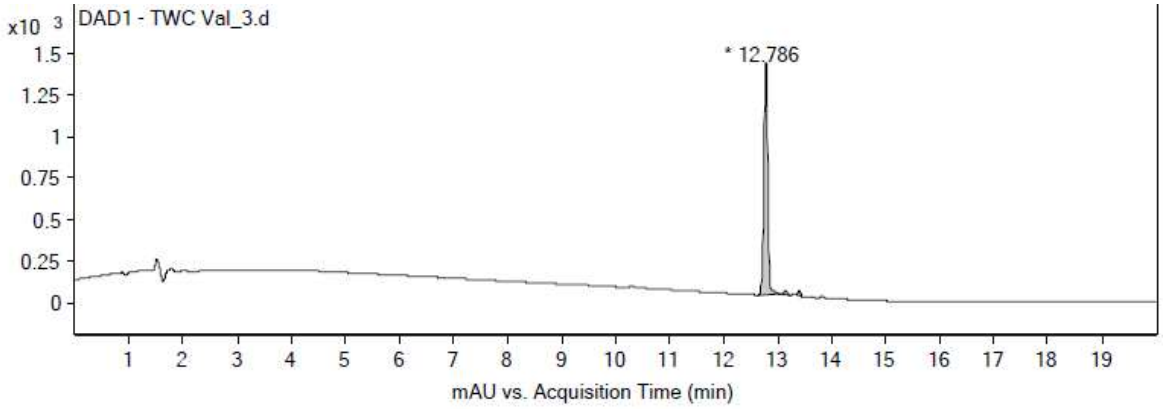

Integration Peak List

Peak	Start	RT	End	Height	Area	Area %
1	12.626	12.786	13.033	1388.83	7292.07	100
2	13.046	13.146	13.226	28.08	103.81	1.42
3	13.339	13.399	13.453	33.67	98.4	1.35

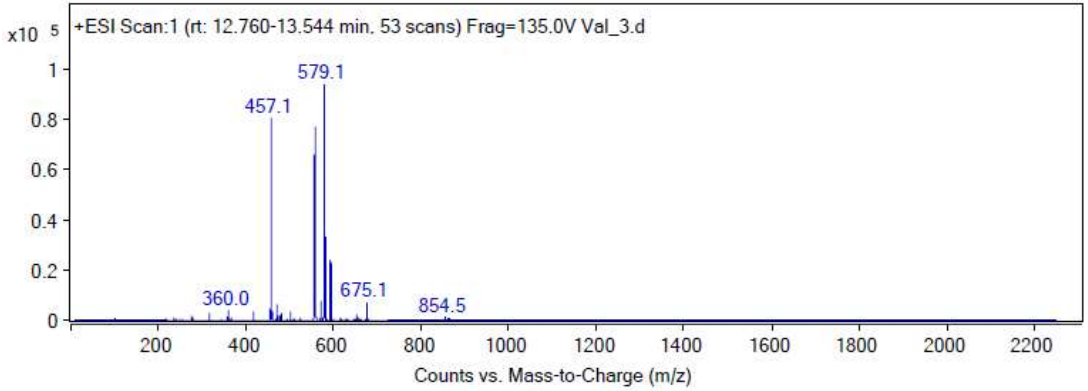

Peak List

m/z	z	Abund
457.1	1	80791.95
458.1	1	23177.79
556.1		66362.38
557.1	1	77432.63
558.1	1	24279.56
579.1	1	94219.45
580.1	1	33641.09
581.1	1	7447.52
593.1	1	23926.74
594.1	1	8303.44

Figure S33. HRMS spectrum of compound **36.**

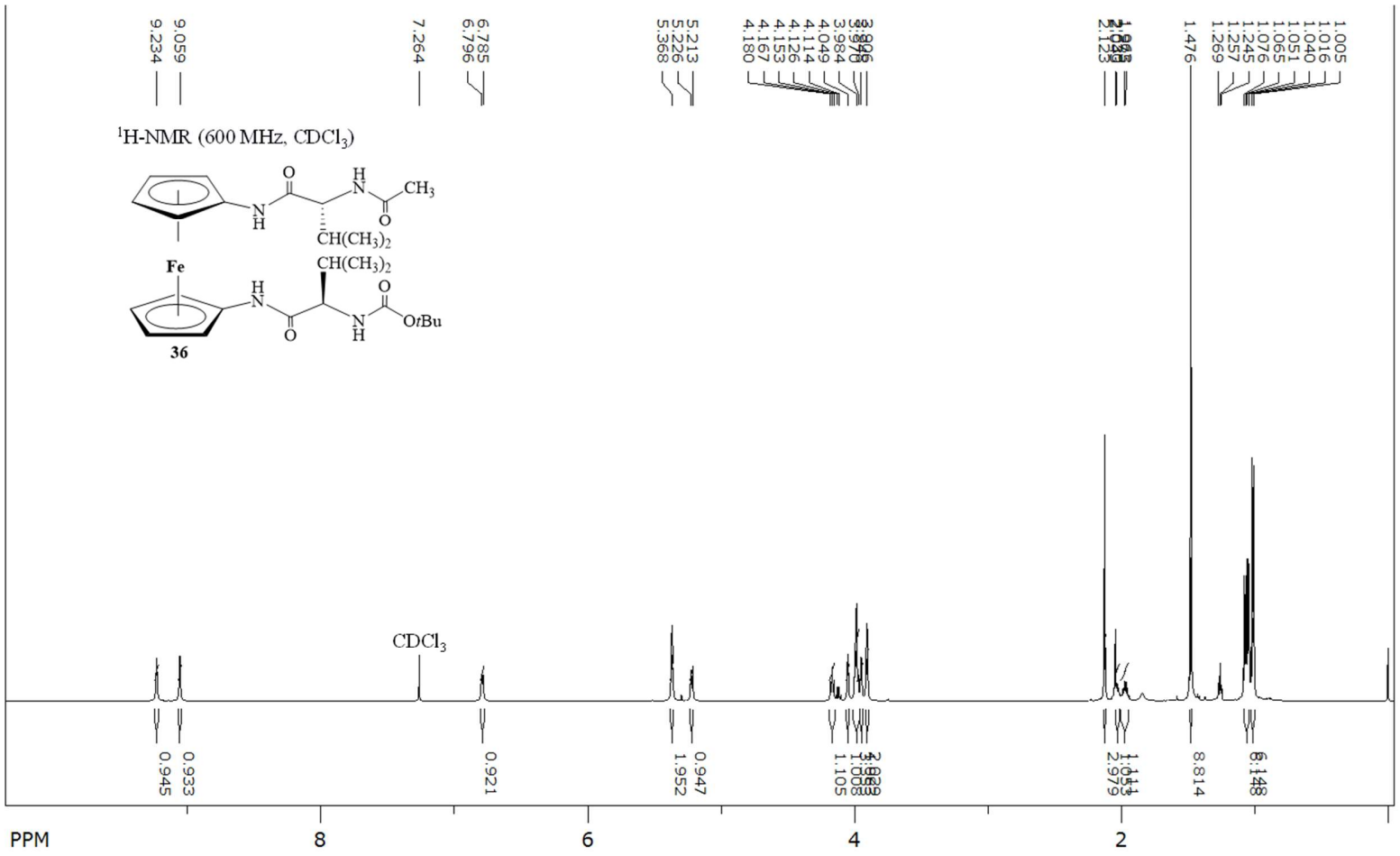

Figure S34. ^{1}H NMR spectrum of compound **36** ($c = 5 \times 10^{-2}$ M).

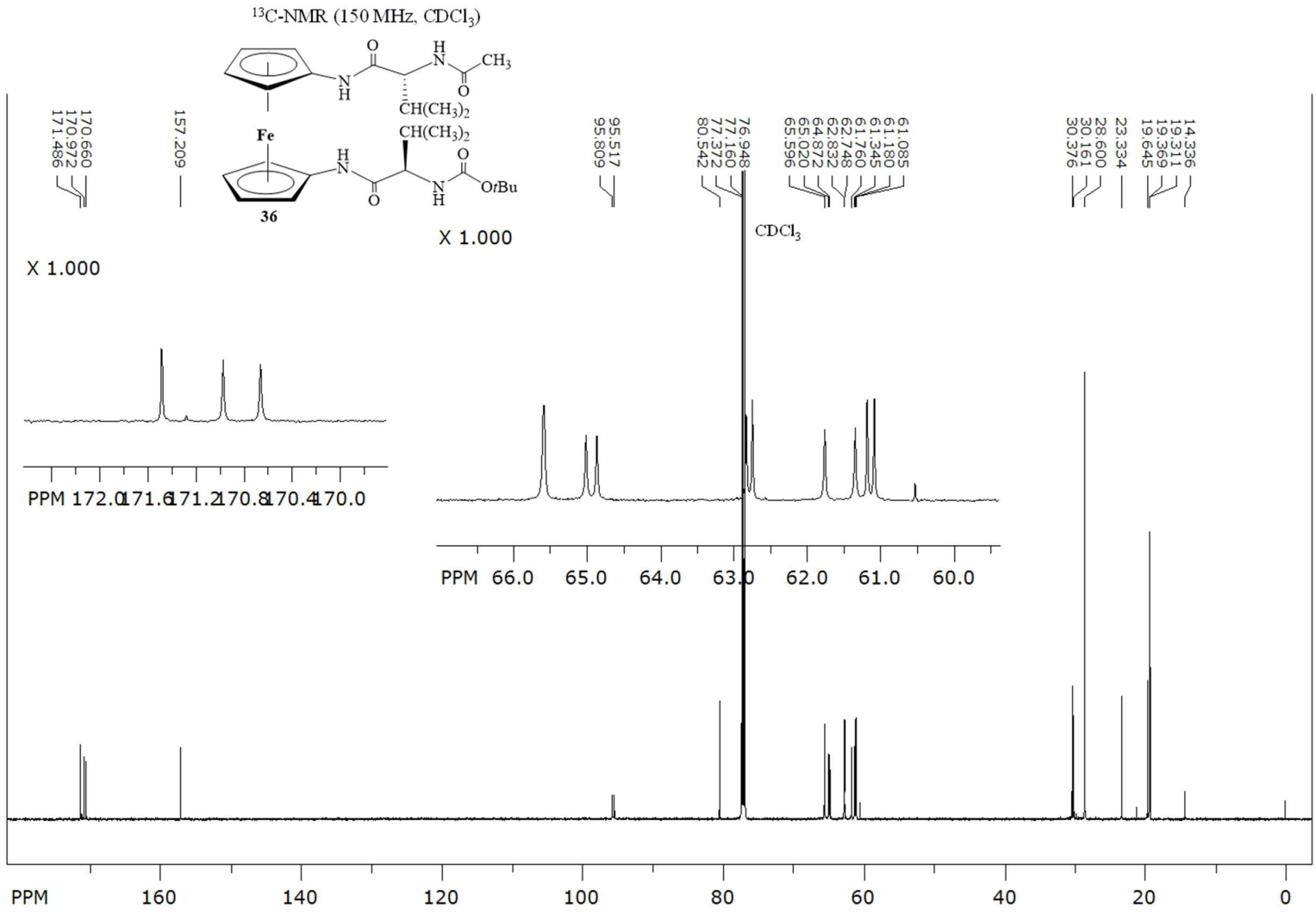

Figure S35. $^{13}C\{^{1}H\}$ NMR spectrum of compound **36** ($c = 5 \times 10^{-2}$ M).

Ac–L–Leu–NH–Fn–NH–L–Leu–Boc (34)

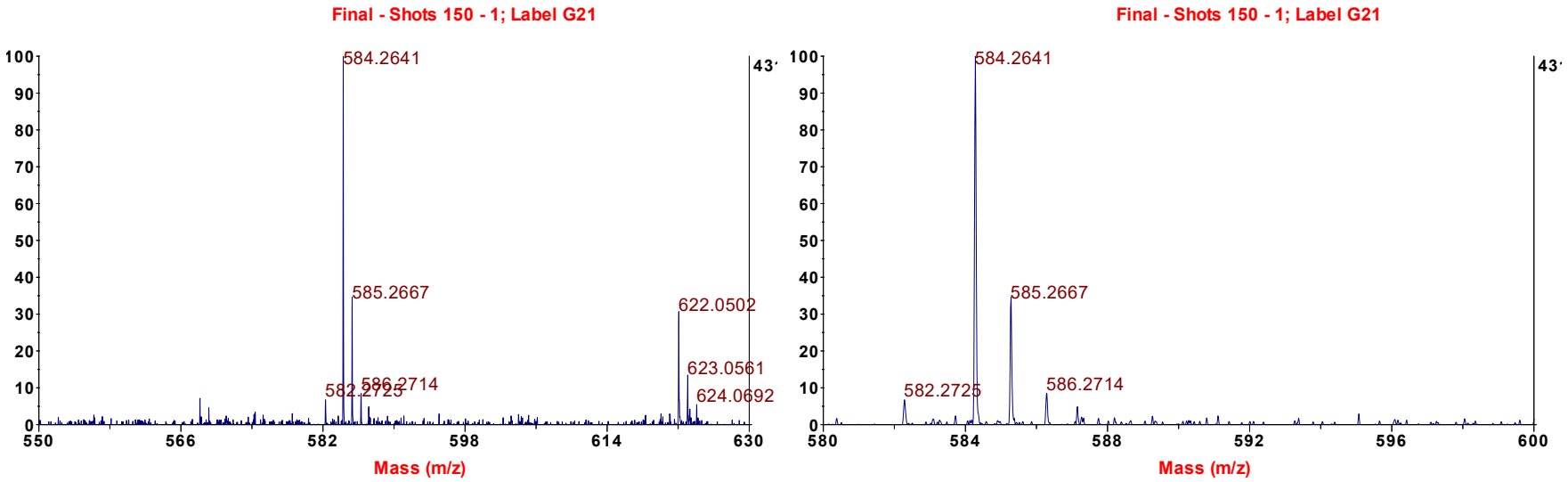

Figure S36. HRMS spectrum of compound **34.**

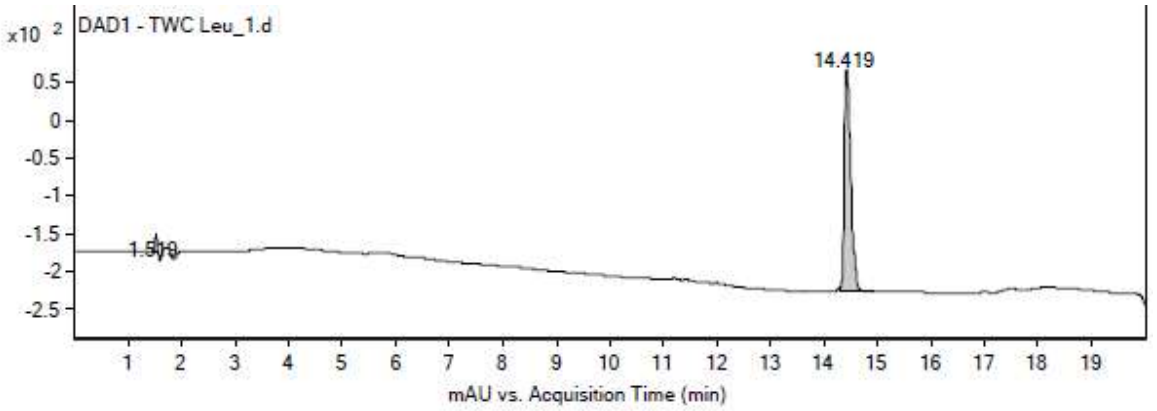

Integration Peak List

Peak	Start	RT	End	Height	Area	Area %
1	1.426	1.519	1.557	22.26	69.86	2.78
2	14.279	14.419	14.918	294.37	2510.88	100

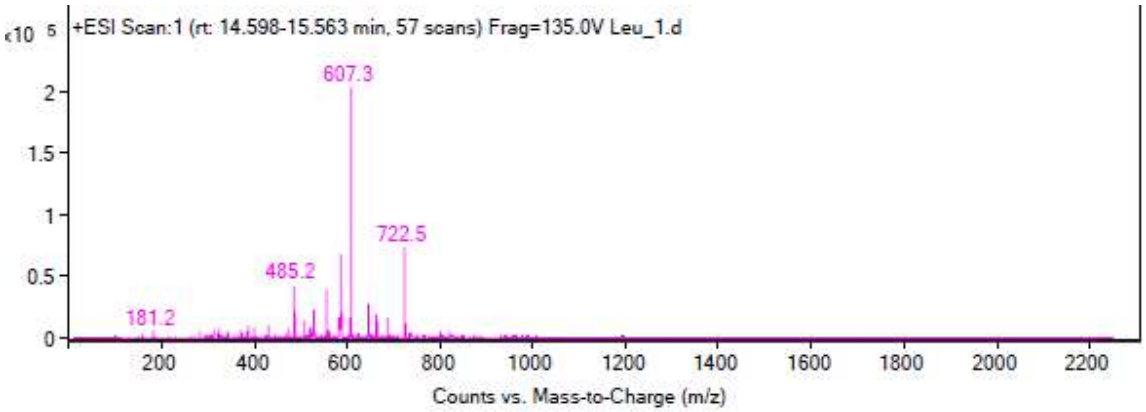

Peak List

m/z	z	Abund
485.2	1	42451.25
526.5	1	22780.45
554.5	1	38813.14
584.3		66515.44
585.3	1	68292.15
607.3	1	203895.69
608.3	1	68822.19
644.3	1	27674.21
722.5	1	73843.47
723.5	1	36041.13

Figure S37. HPLC-ESI spectra of compound **34.**

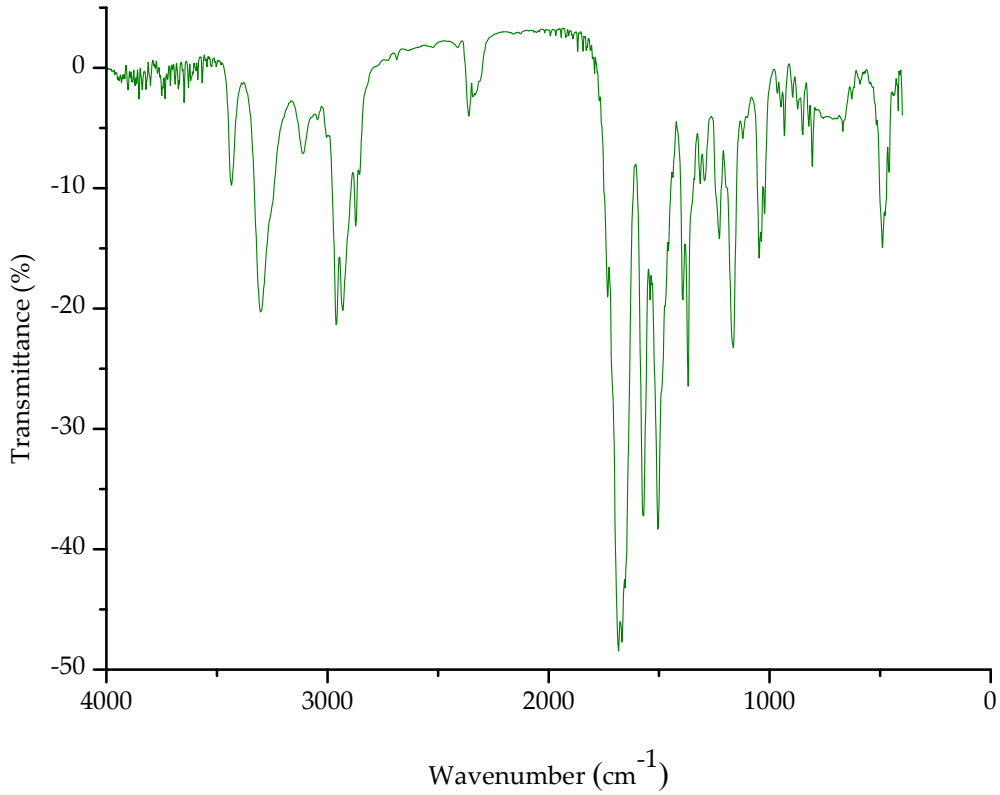

Figure S38. IR spectrum of compound **34** ($c = 5 \times 10^{-2}$ M) in DCM.

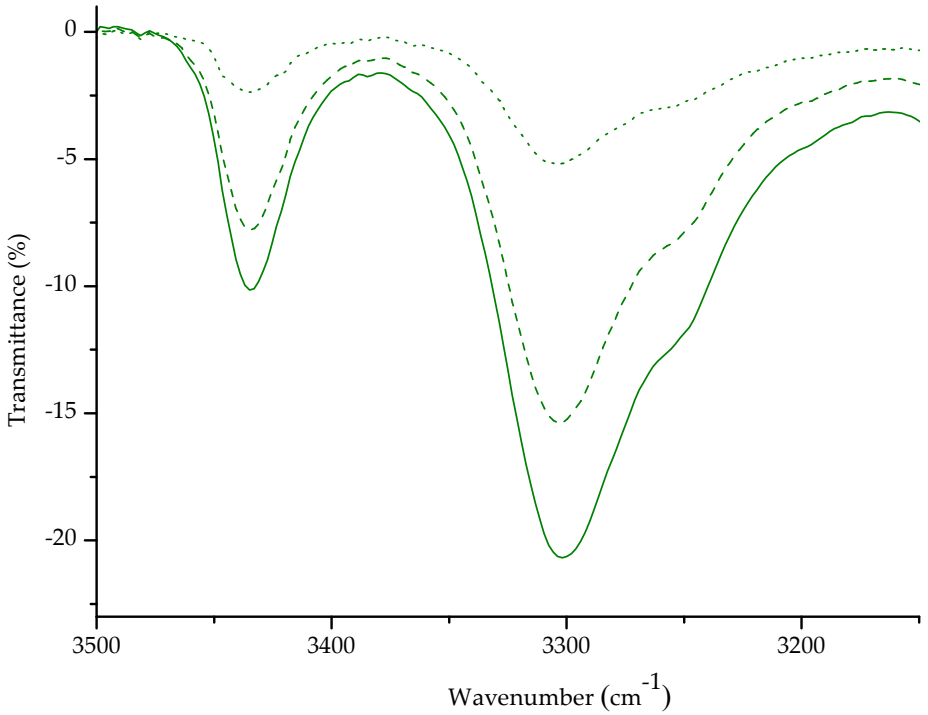

Figure S39. The NH stretching vibrations in concentration-dependent IR spectra of **34** in DCM [(—) $c = 5 \times 10^{-2}$ M, (——) $c = 2.5 \times 10^{-2}$ M, (· · ·) $c = 1.25 \times 10^{-2}$ M.

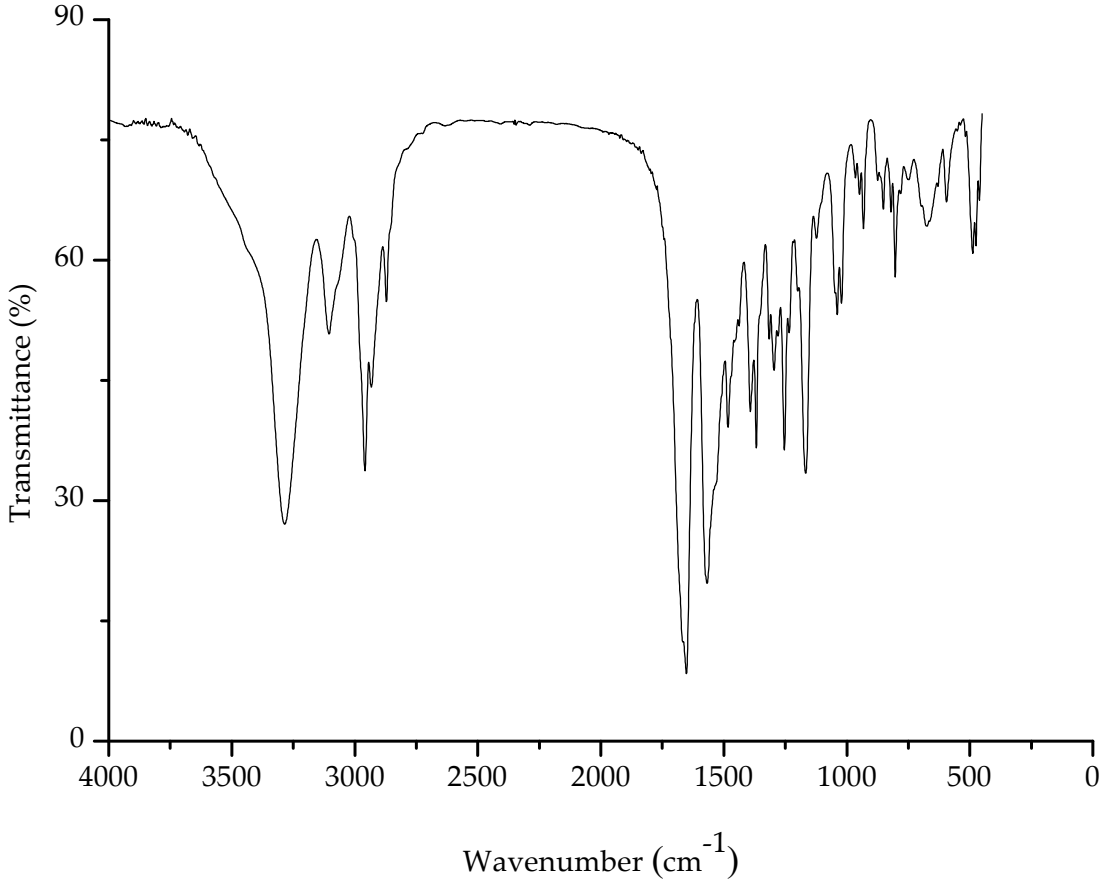

Figure S40. IR spectrum of compound **34** (2 mg) in KBr (200 mg).

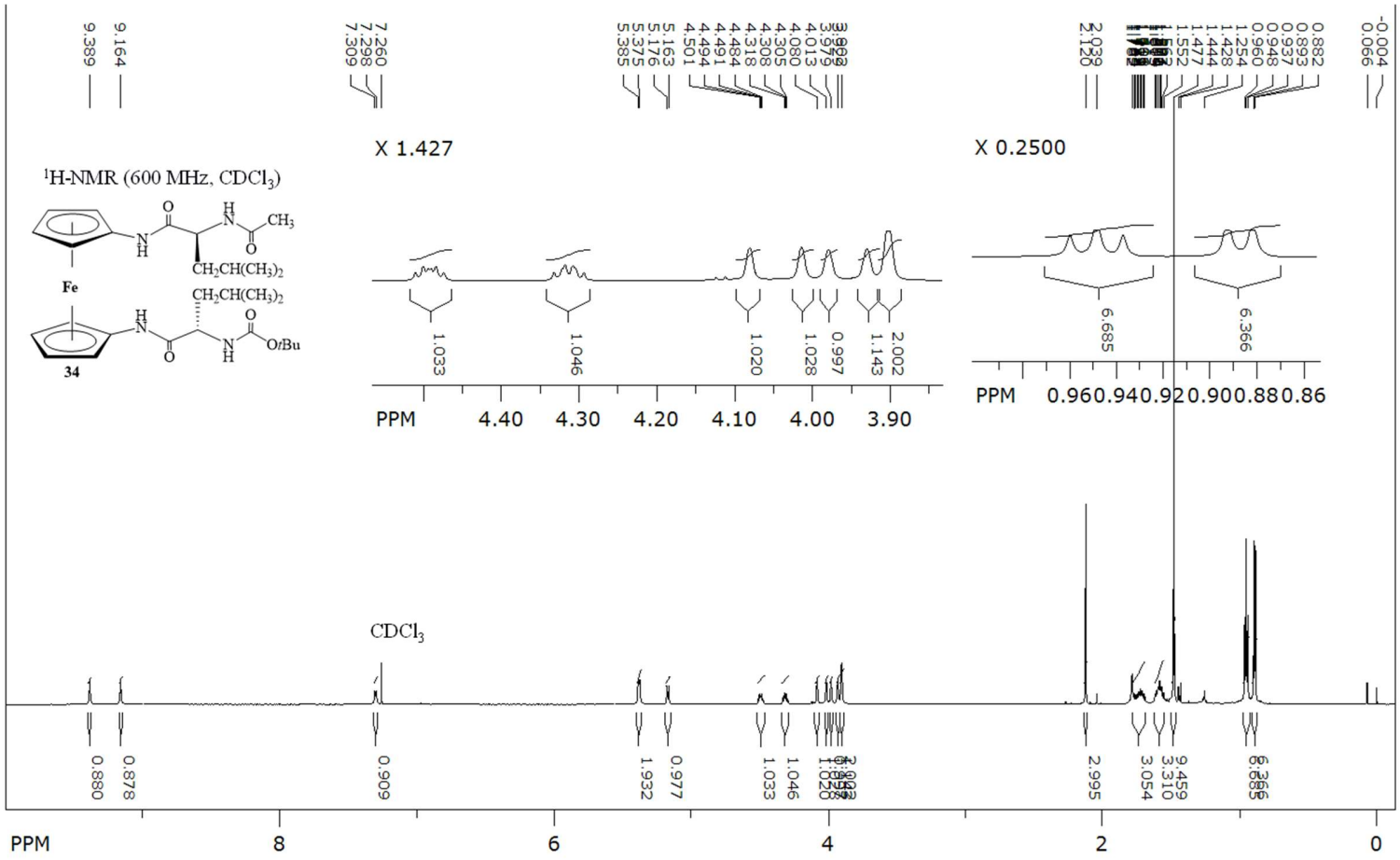

Figure S41. ^{1}H NMR spectrum of compound **34** ($c = 5 \times 10^{-2}$ M).

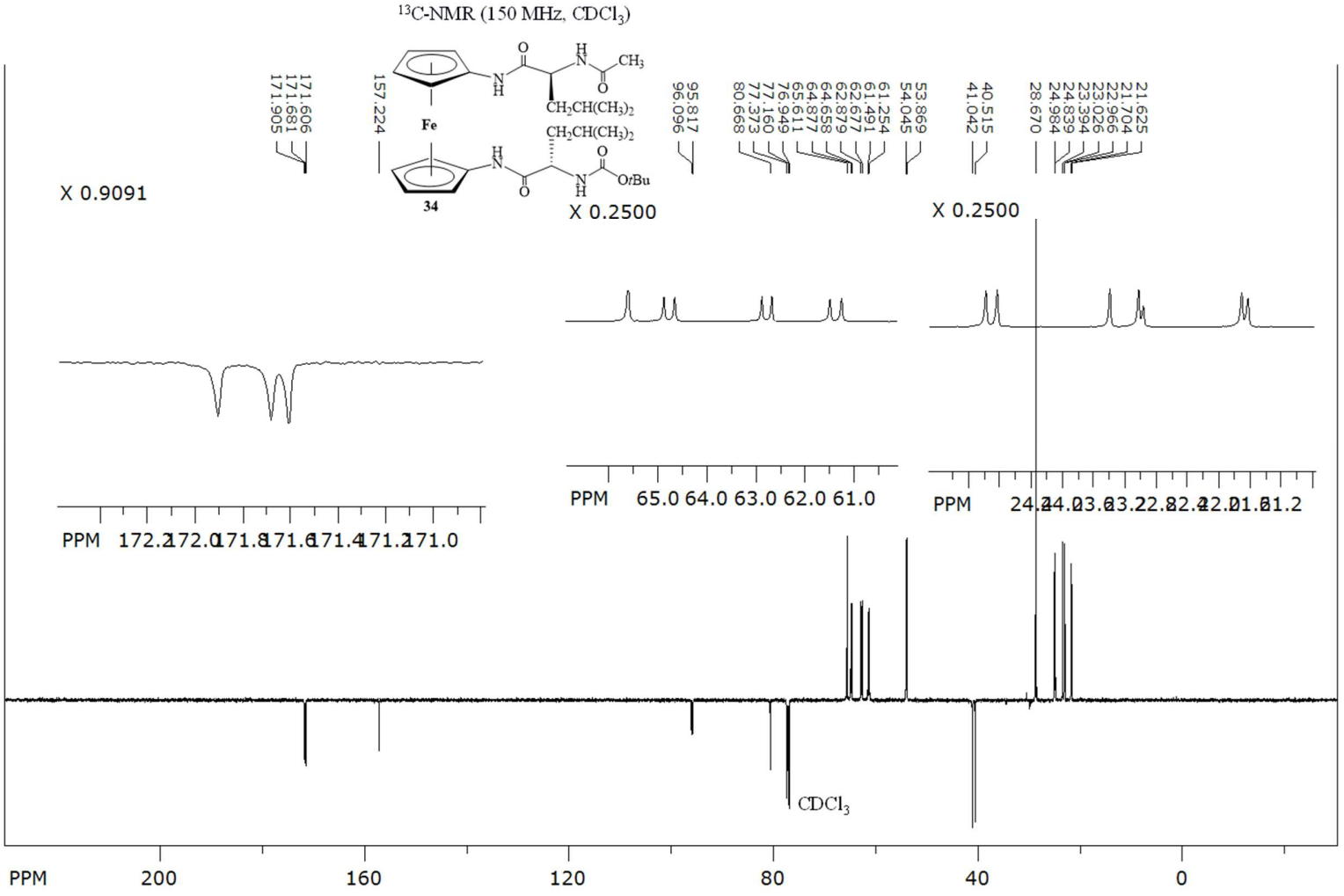

Figure S42. $^{13}C\{^{1}H\}$ NMR spectrum of compound **34** ($c = 5 \times 10^{-2}$ M).

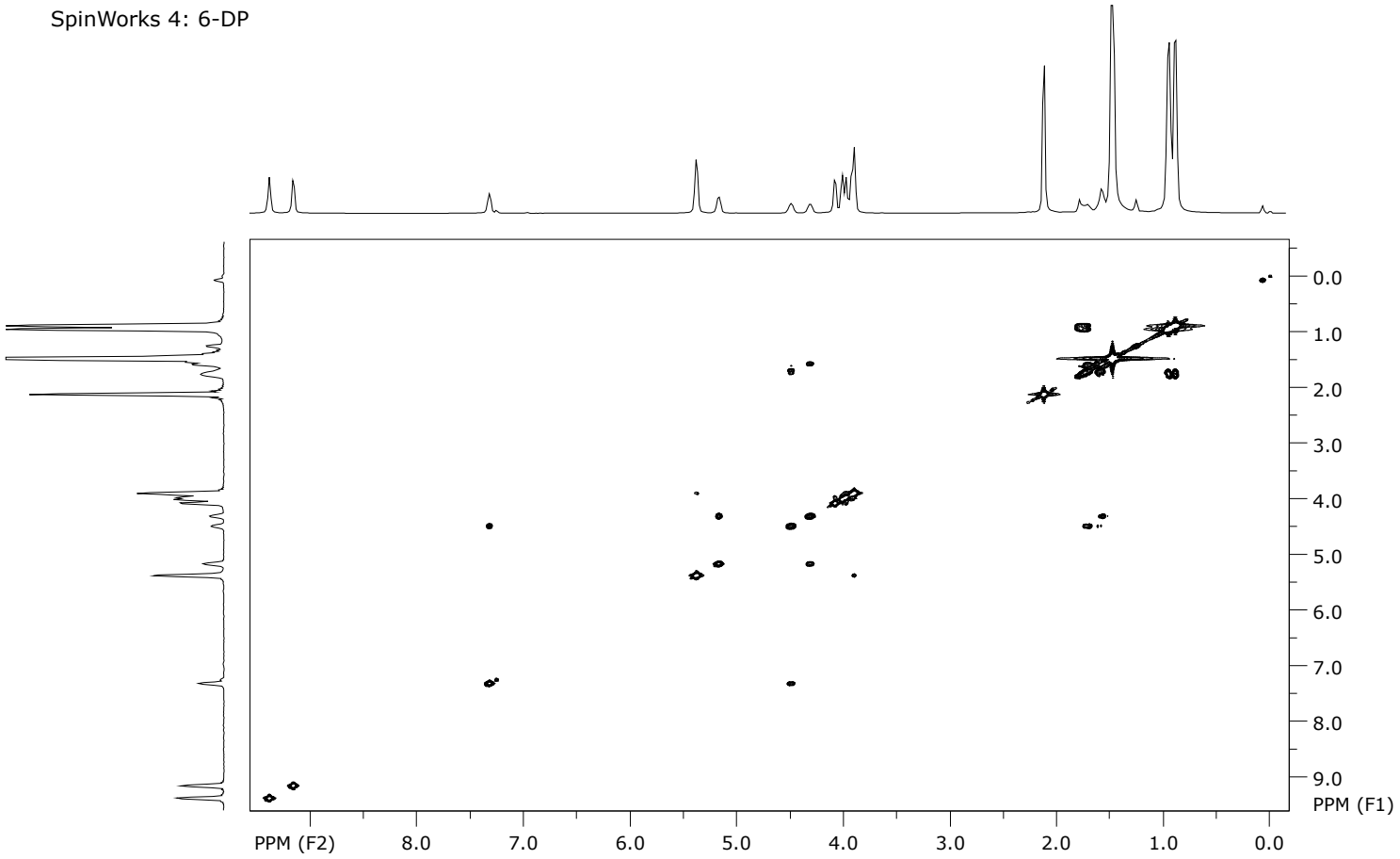

Figure S43. ^{1}H-^{1}H COSY NMR spectrum of compound **34** ($c = 5 \times 10^{-2}$ M).

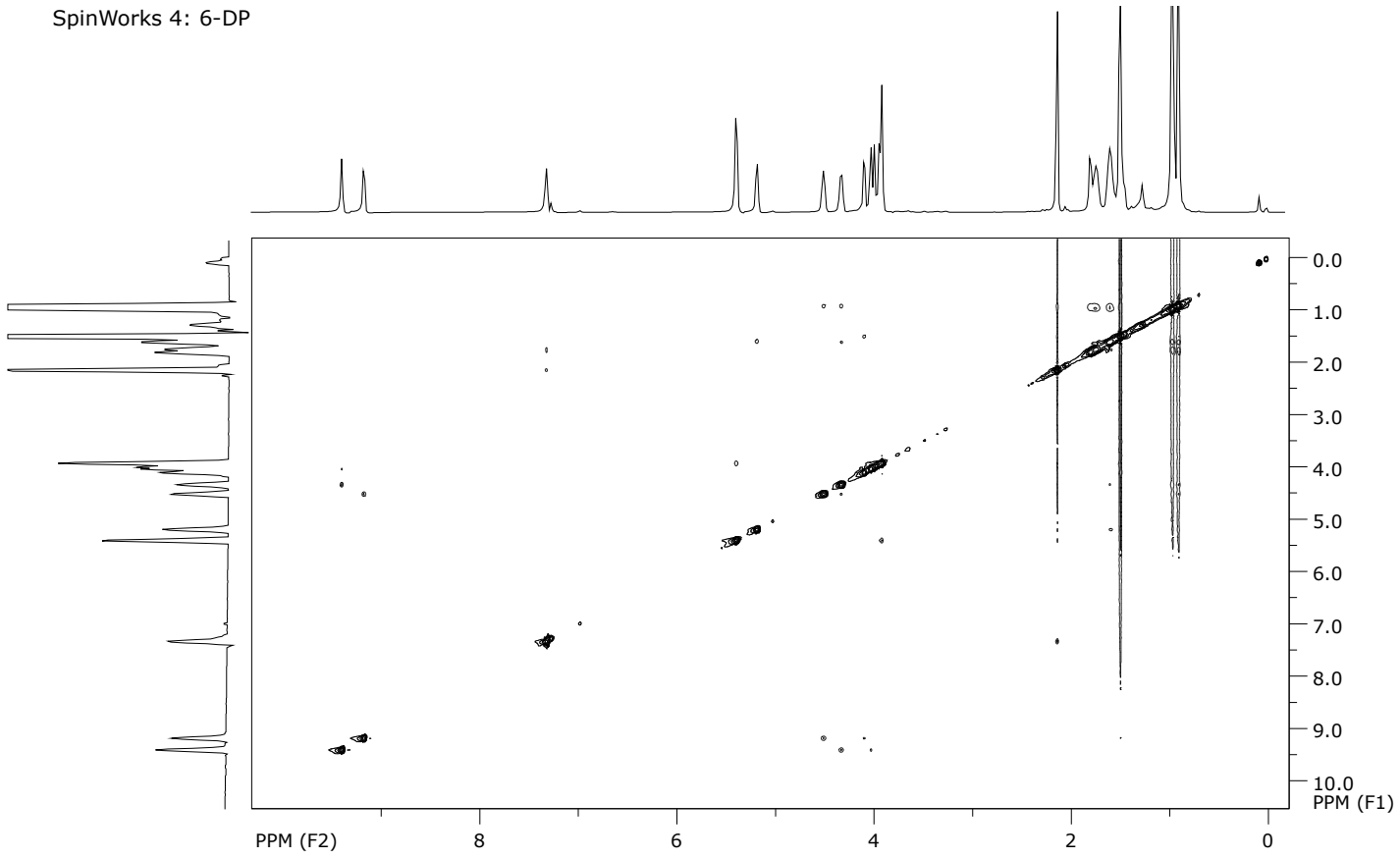

Figure S44. ^{1}H-^{1}H NOESY NMR spectrum of compound **34** ($c = 5 \times 10^{-2}$ M).

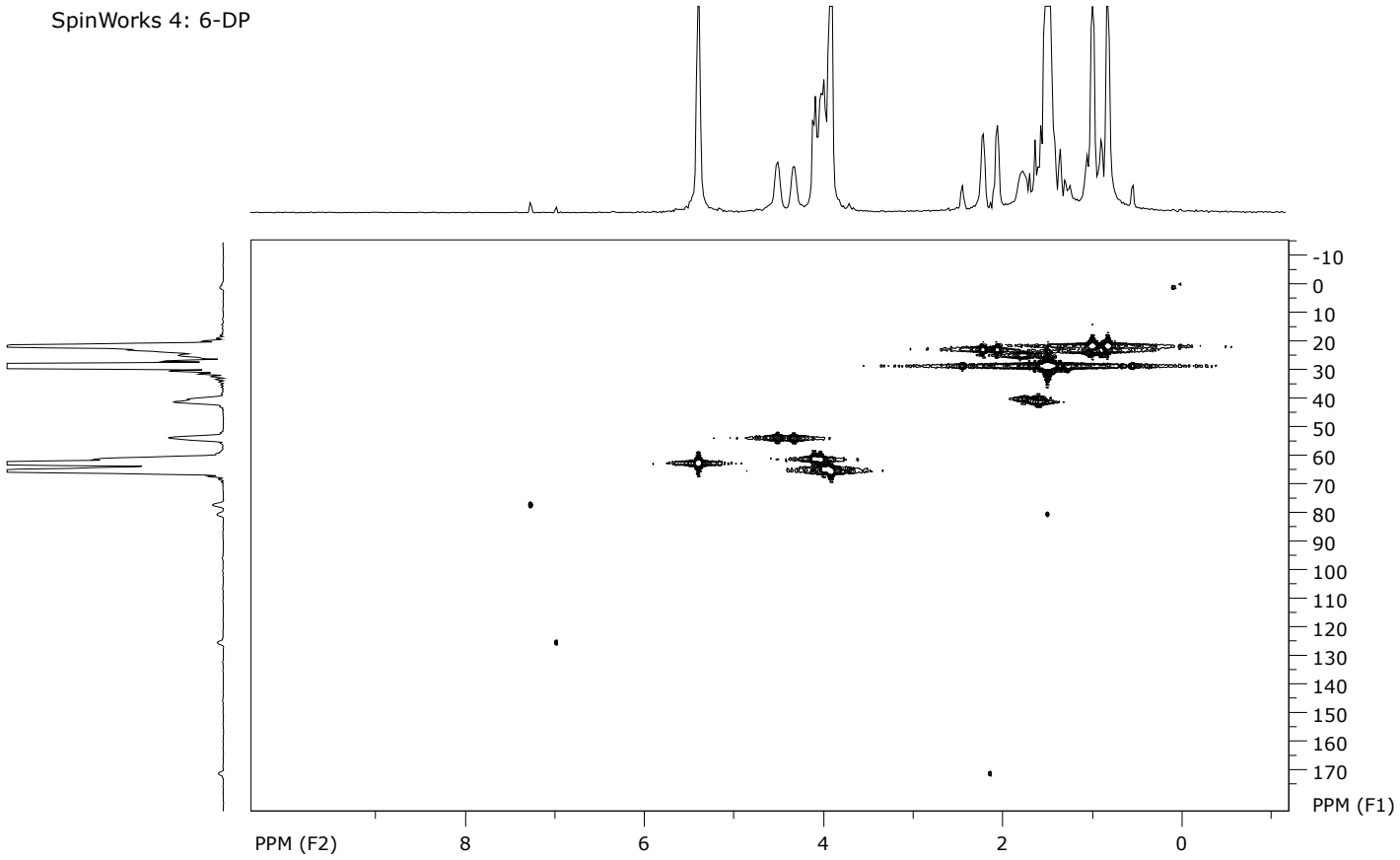

Figure S45. ^{1}H-^{13}C HMQC spectrum of compound **34** ($c = 5 \times 10^{-2}$ M).

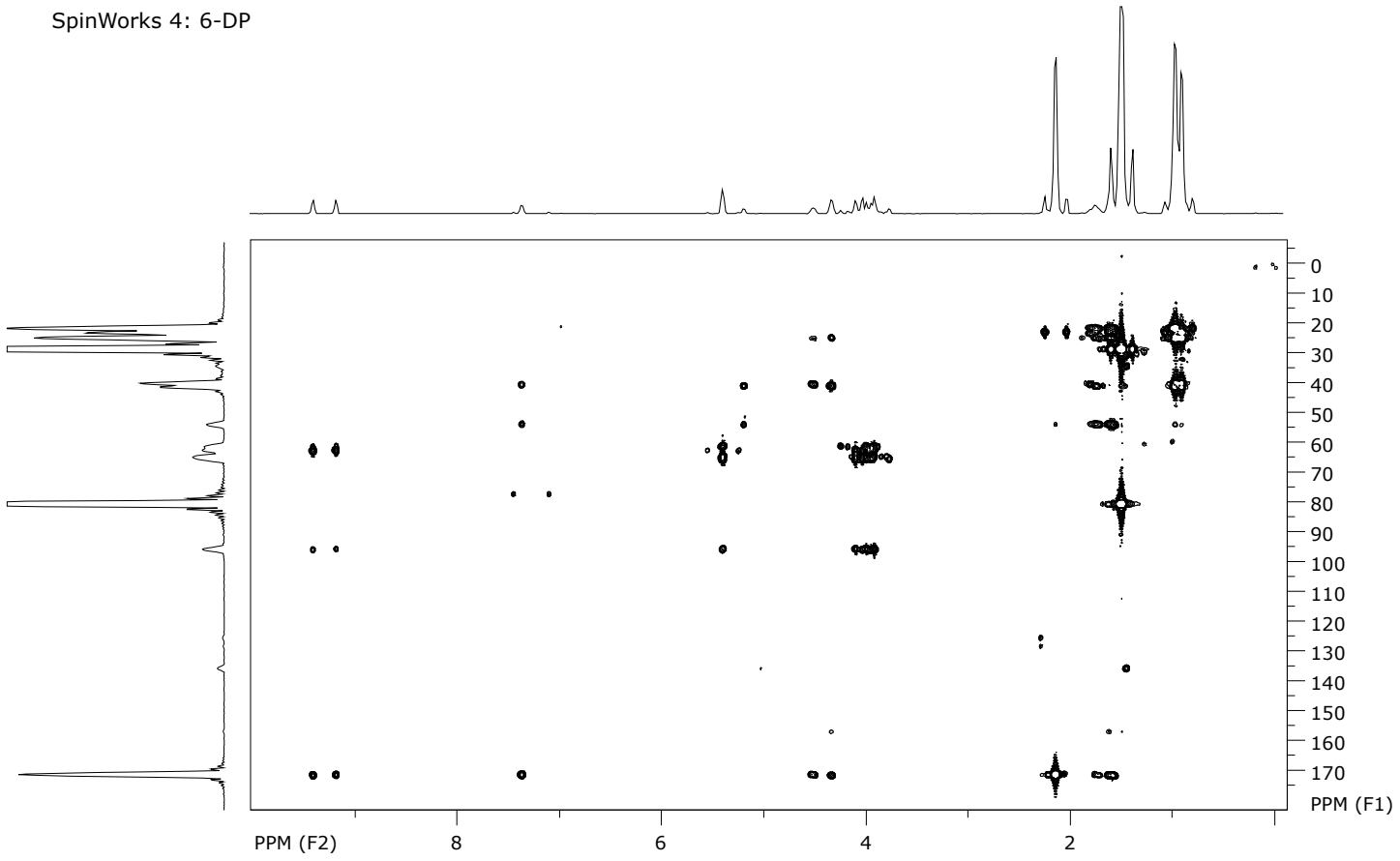

Figure S46. ^{1}H-^{13}C HMBC spectrum of compound **34** ($c = 5 \times 10^{-2}$ M).

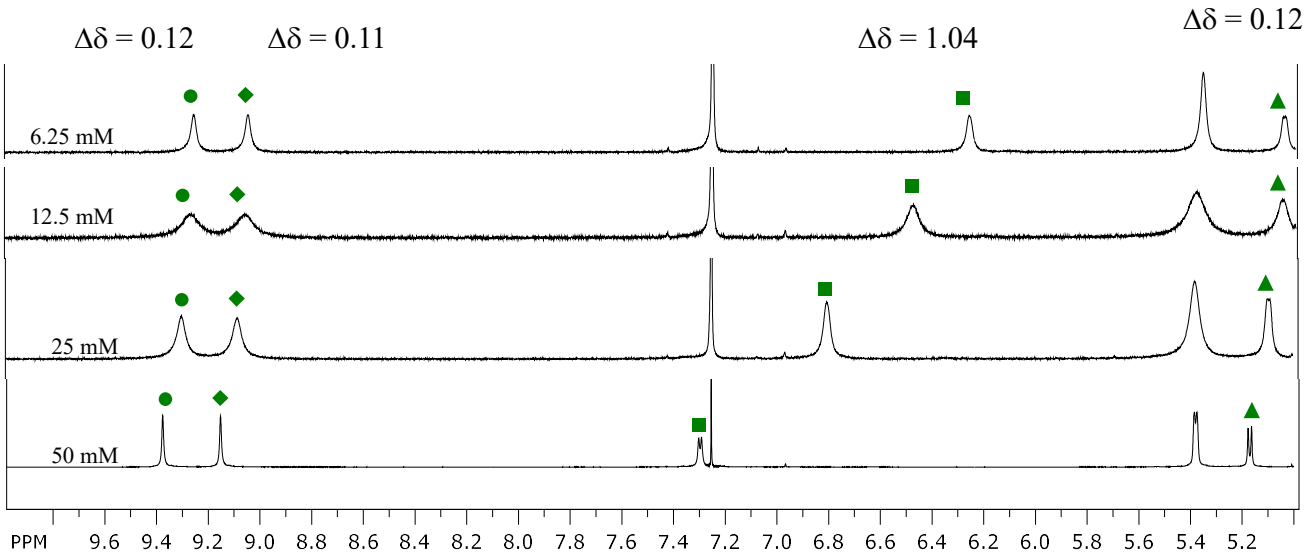

Figure S47. Concentration-dependent NH chemical shifts of compound **34** in $CDCl_3$.

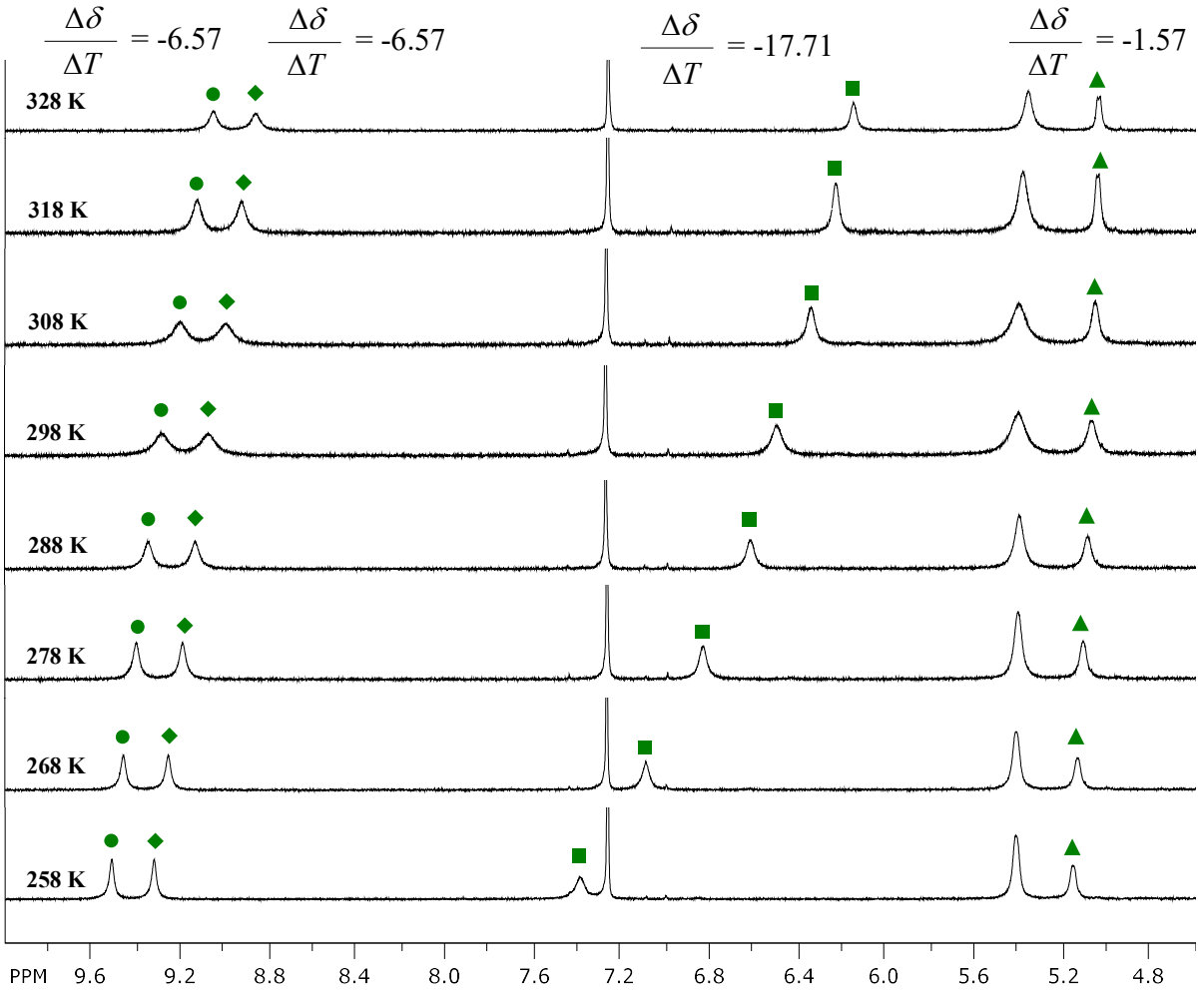

Figure S48. Temperature-dependent NH chemical shifts of compound **34** ($c = 1 \times 10^{-2}$ M).

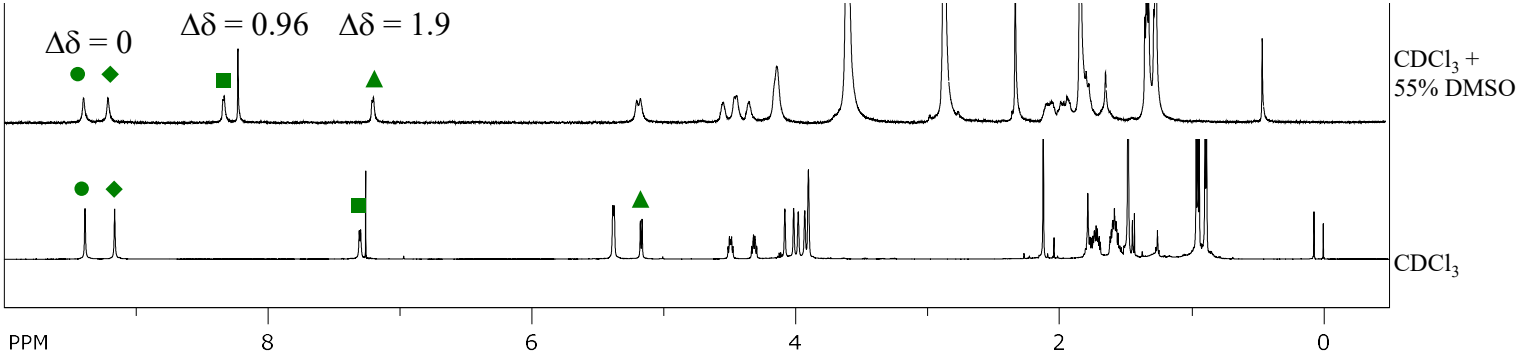

Figure S49. ^{1}H NMR spectra of compound **34** at varying concentrations of DMSO in $CDCl_3$ (c = 2.5 × 10-2 M).

Ac–D–Leu–NH–Fn–NH–D–Leu–Boc (37)

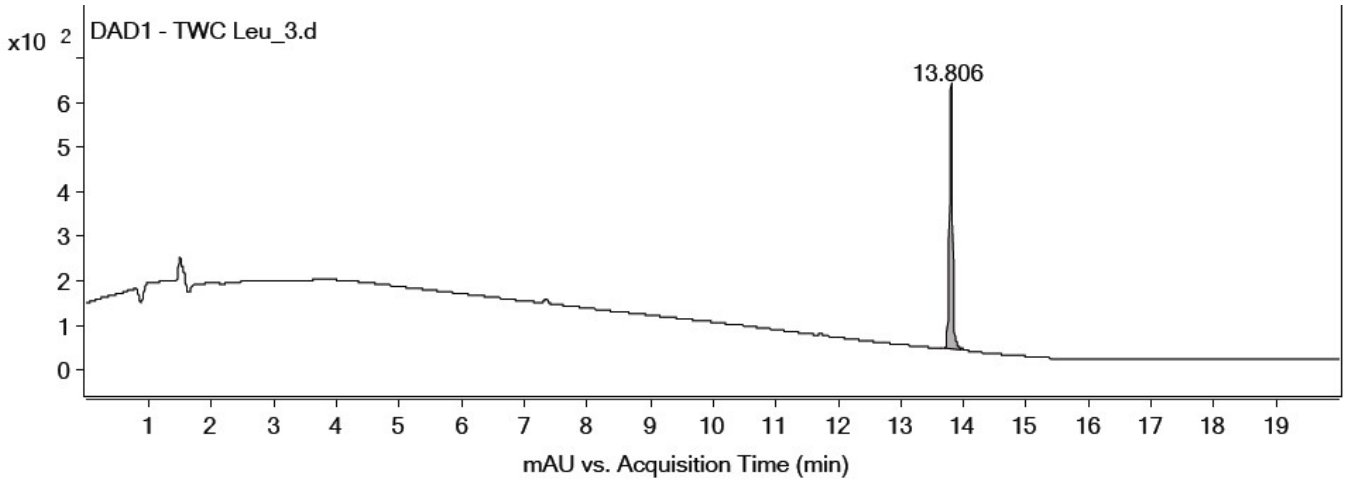

Integration Peak List

Peak	Start	RT	End	Height	Area	Area %
1	13.706	13.806	13.973	593.73	2177.34	100

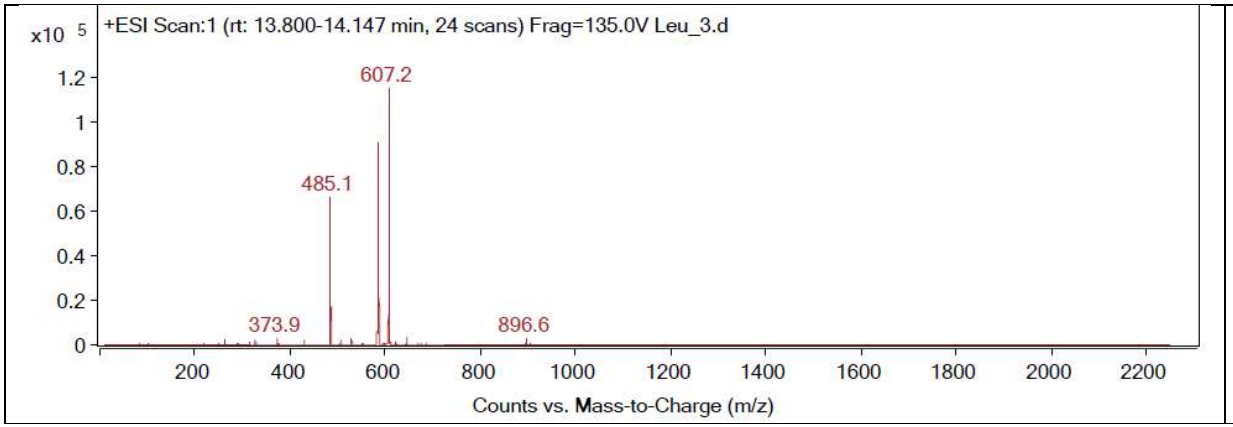

Peak List

m/z	z	Abund
485.1	1	66519.8
486.1	1	16861.59
583.1		6170.95
584.1		70845.26
585.1	1	90658.1
586.1	1	28849.23
605.1		8747.15
607.2	1	115051.34
608.1	1	40762.71
609.1	1	9568.72

Figure S50. HPLC-ESI spectra of compound **37.**

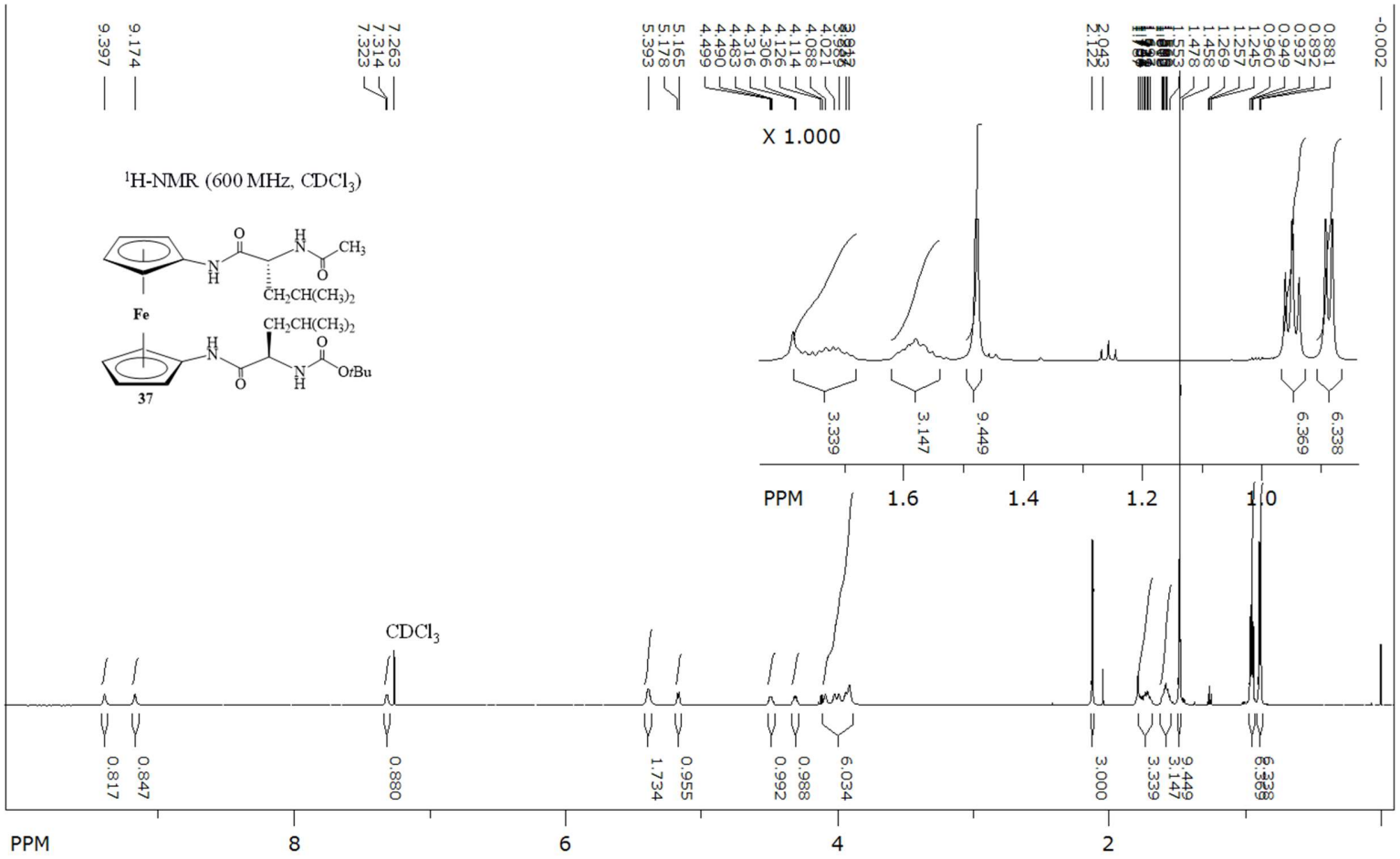

Figure S51. ^{1}H NMR spectrum of compound **37** ($c = 5 \times 10^{-2}$ M).

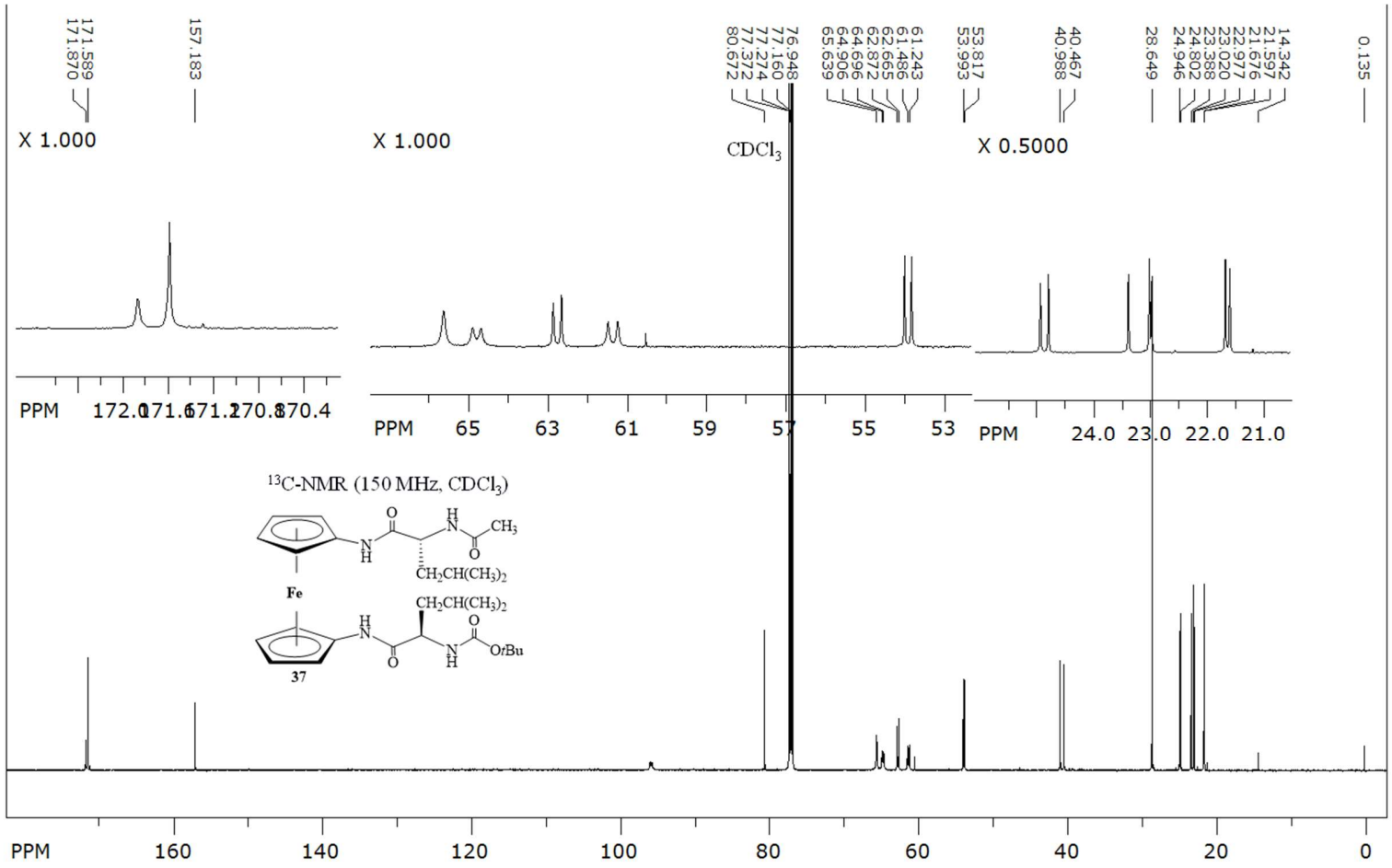

Figure S52. $^{13}C\{^{1}H\}$ NMR spectrum of compound **37** ($c = 5 \times 10^{-2}$ M).

Table S2. IR (ν in cm^{-1}) and NMR (δ in ppm) spectroscopic data of reference (Fn–NH–Ac and Fn–NH–Boc), model **(III)** and L-peptides **32–34.**

	ν (NH)		ν (CO)	δ			
	Free	Assoc.	Amide I	NH^{a}_{Fn} (●)	NH^{b}_{Fn} (◆)	NH_{Ac} (■)	NH_{Boc} (▲)
Fn–NH–Ac*	3436		1684			6.49	
Fn–NH–Boc*	3436		1723				5.55
Ac–L–Ala–NH^{a}–Fn–NH^{b}–L–Ala–Boc **(III)***	3439	3310 3253	1684 1665	9.02	9.06	6.85	5.21
Ac–L–Phe–NH^{a}–Fn–NH^{b}–L–Phe–Boc **(32)**	3430	3302 3266	1731 1706 1683 1668	9.15	9.21	7.21	5.43
Ac–L–Val–NH^{a}–Fn–NH^{b}–L–Val–Boc **(33)**	3434	3305 3249	1733 1716 1683 1666	9.21	9.04	6.75	5.21
Ac–L–Leu–NH^{a}–Fn–NH^{b}–L–Leu–Boc **(34)**	3434	3301 3253	1733 1684 1668	9.39	9.16	7.30	5.17

*Adapted from (19).

Table S3. Changes in chemical shifts (Δδ) observed for NH_{Fn} and NH_{Ac} in model **(III)** and L-peptides **32–34** at high (50 mM) vs. low concentrations (6.25 mM), from 258 – 328 K and at varying concentrations of DMSO in $CDCl_3$.

	NH^a_{Fn} (●)	NH^b_{Fn} (◆)	NH_{Ac} (■)	NH^a_{Fn} (●)	NH^b_{Fn} (◆)	NH_{Ac} (■)	NH^a_{Fn} (●)	NH^b_{Fn} (◆)	NH_{Ac} (■)	NH^a_{Fn} (●)	NH^b_{Fn} (◆)	NH_{Ac} (■)
	Concentration-dependent Δδ (ppm)			Temperature-dependent Δδ (ppm)			Temperature coefficients Δδ/ΔT (ppb K^{-1})			Solvent-dependent Δδ (ppm)		
Ac–L–Ala–NH^a–Fn–NH^b–L–Ala–Boc **(III)***	0.06	0.07	0.69	0.72	0.72	0.7	-10.33	-10.33	-10.0	0.13	0.11	1.71
Ac–L–Phe–NH^a–Fn–NH^b–L–Phe–Boc **(32)**	0.16	0.15	0.87	0.61	0.56	1.29	-8.0	-8.71	-18.42	0.07	0.16	1.44
Ac–L–Val–NH^a–Fn–NH^b–L–Val–Boc **(33)**	0.08	0.1	0.59	0.4	0.5	0.81	-7.14	-5.71	-11.57	0.15	0.11	1.29
Ac–L–Leu–NH^a–Fn–NH^b–L–Leu–Boc **(34)**	0.11	0.12	1.04	0.46	0.46	1.24	-6.57	-6.57	-17.71	0	0.08	0.96

*Adapted from (19).

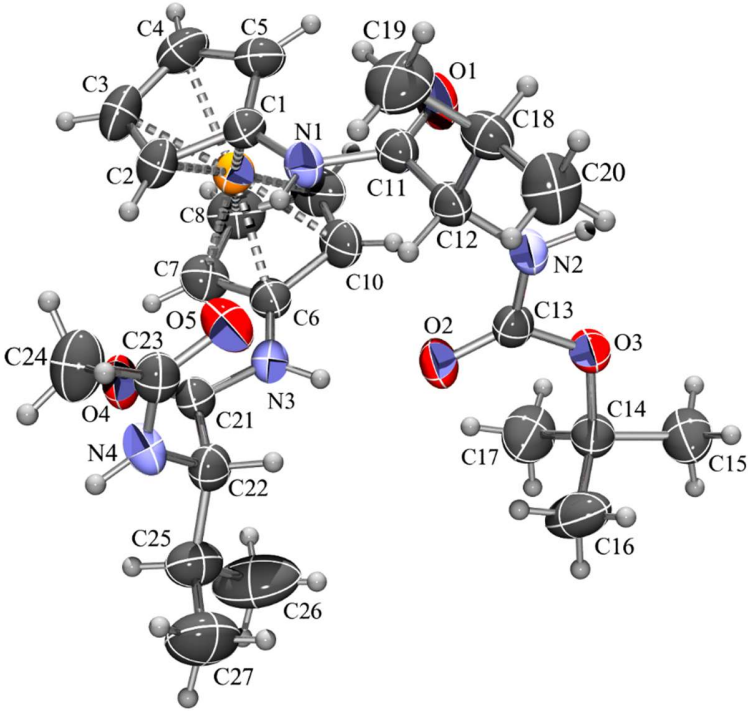

33

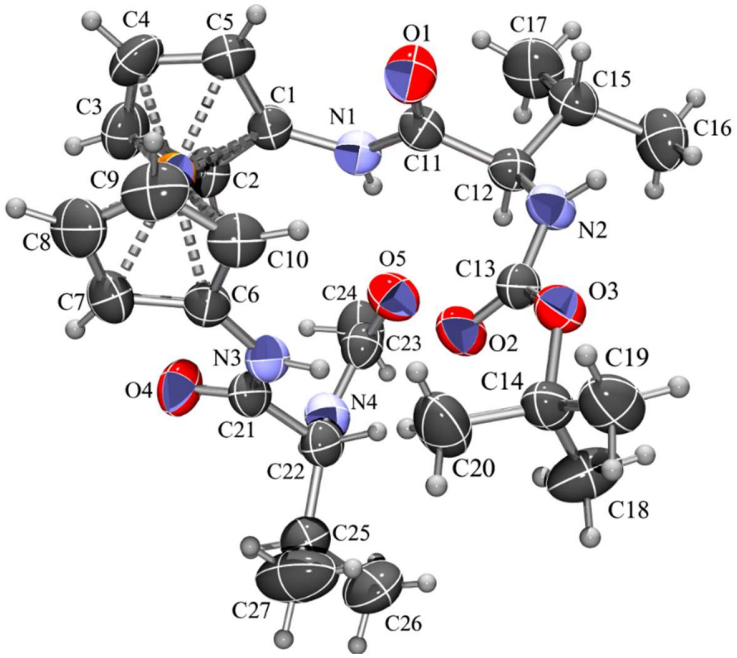

36

Figure S53. ORTEP-3 drawings of molecules of **33** and **36**. Displacement ellipsoids are drawn for the probability of 50 % and hydrogen atoms are shown as spheres of arbitrary radii.

1. NMR spectroscopy

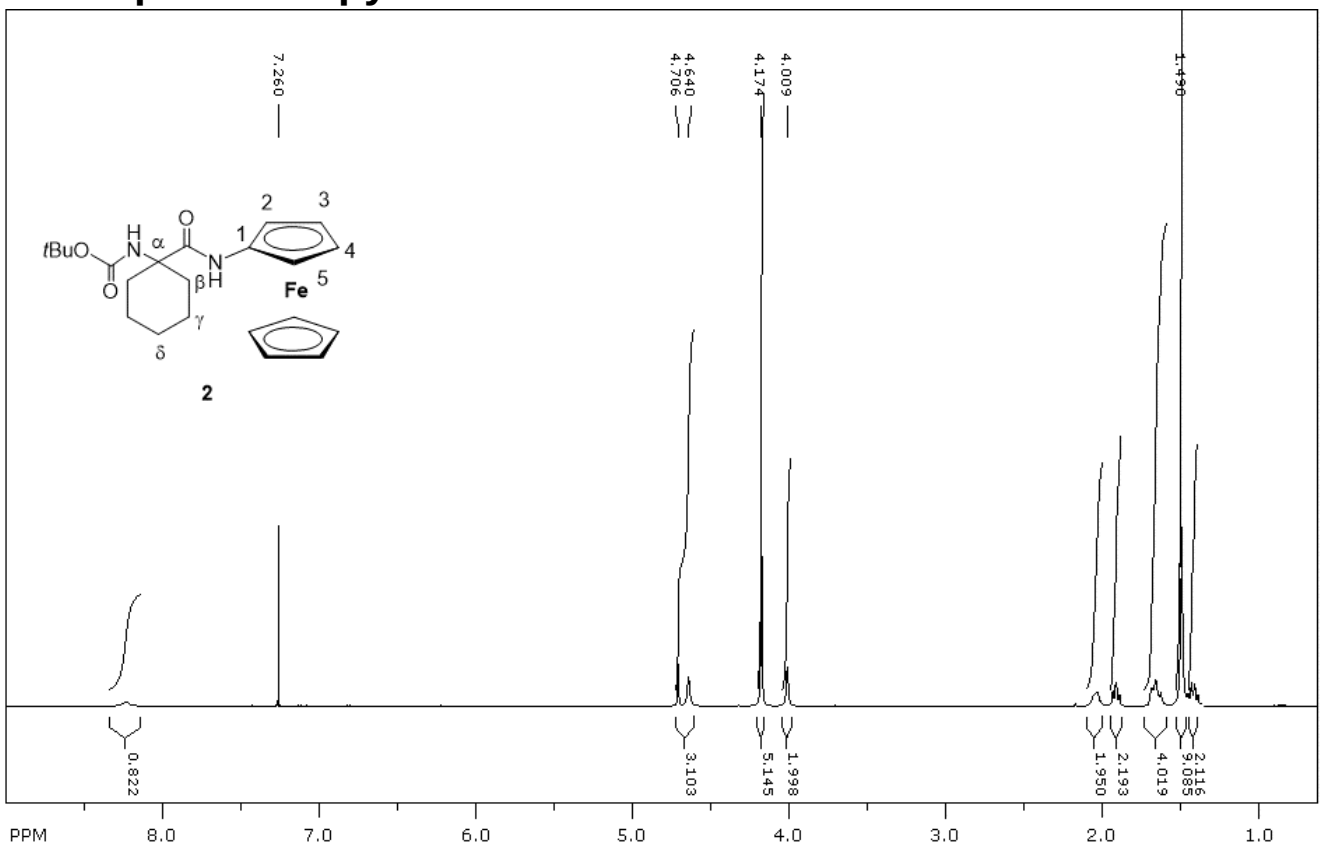

Figure S1. ^{1}H NMR spectrum of **2**, full range

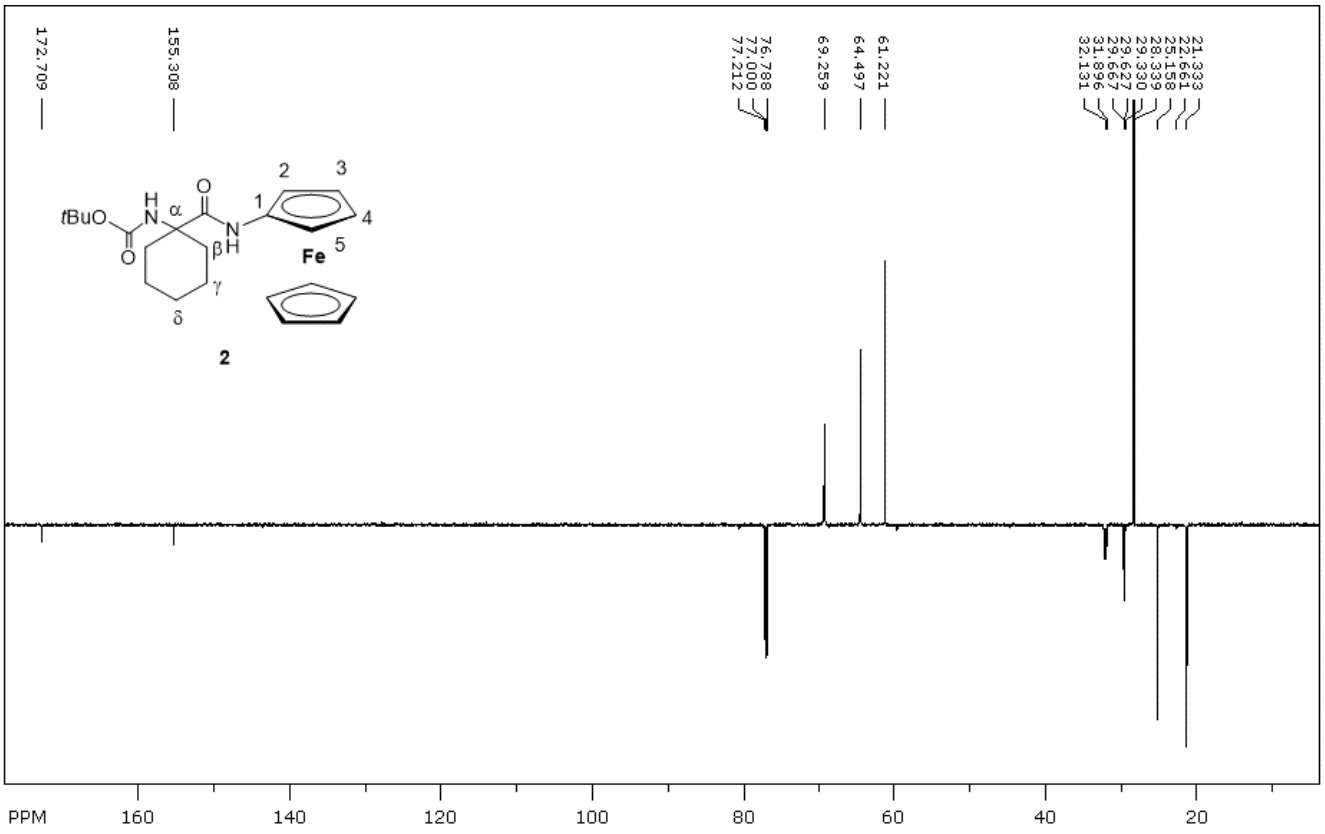

Figure S2. ^{13}C NMR spectrum of **2**, full range

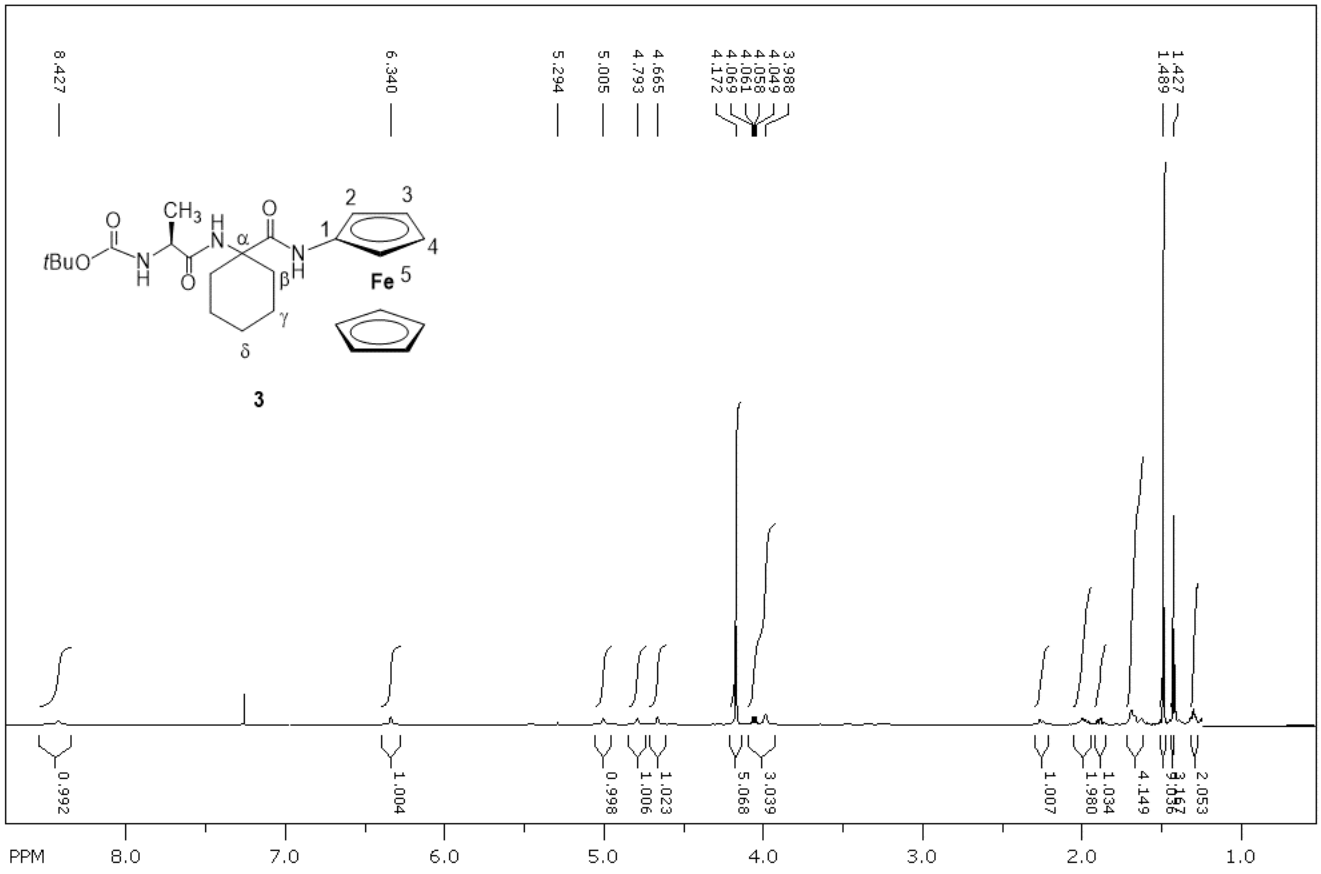

Figure S3. ^{1}H NMR spectrum of **3**, full range

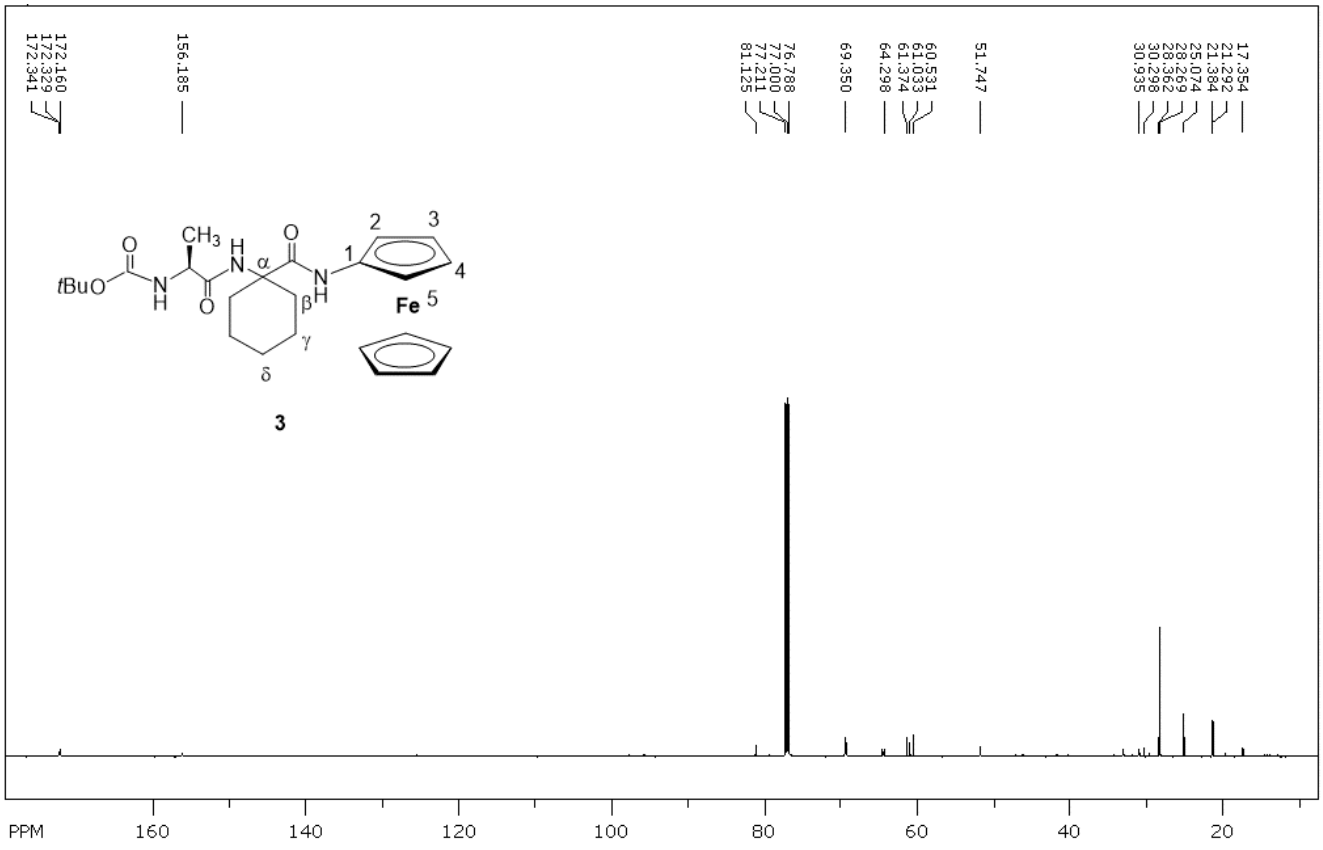

Figure S4. ^{13}C NMR spectrum of **3**, full range

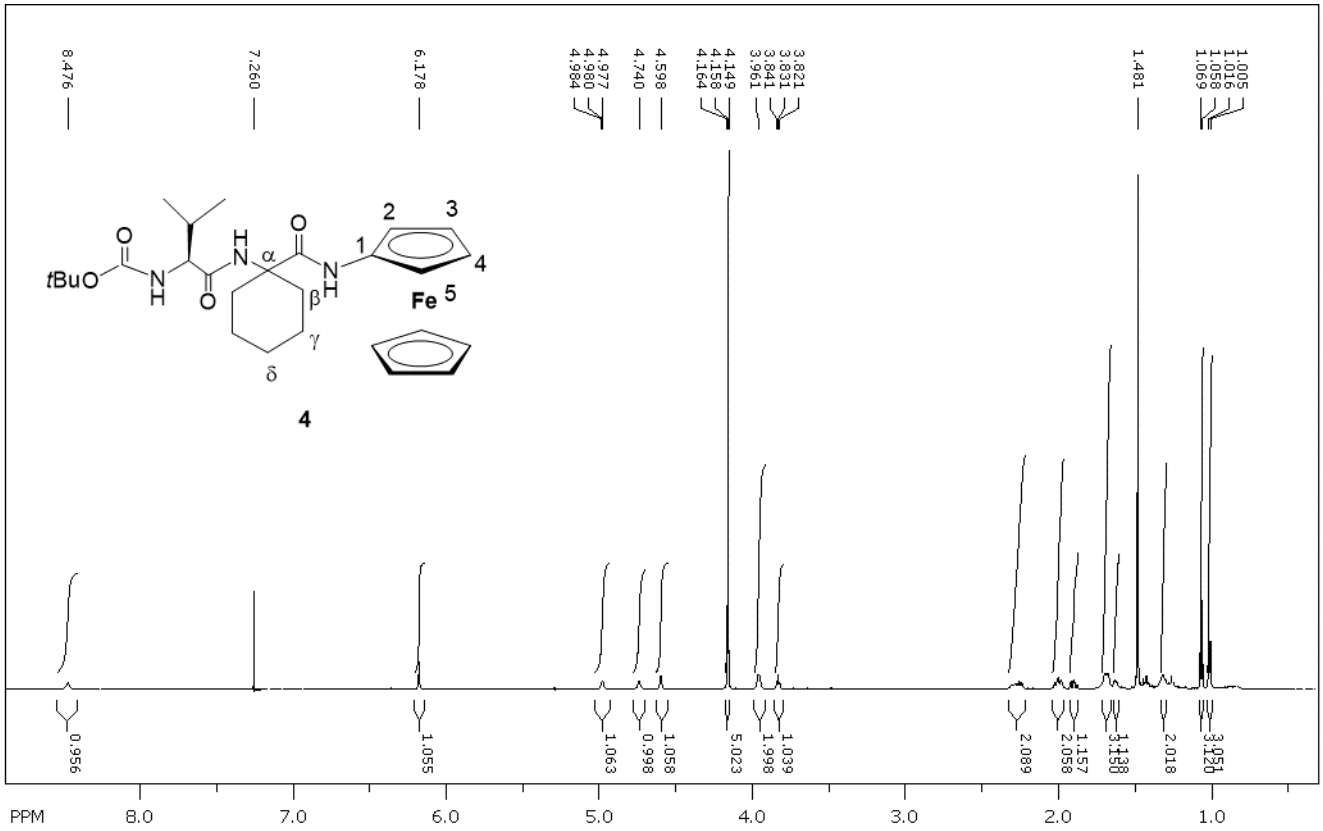

Figure S5. ^{1}H NMR spectrum of **4**, full range

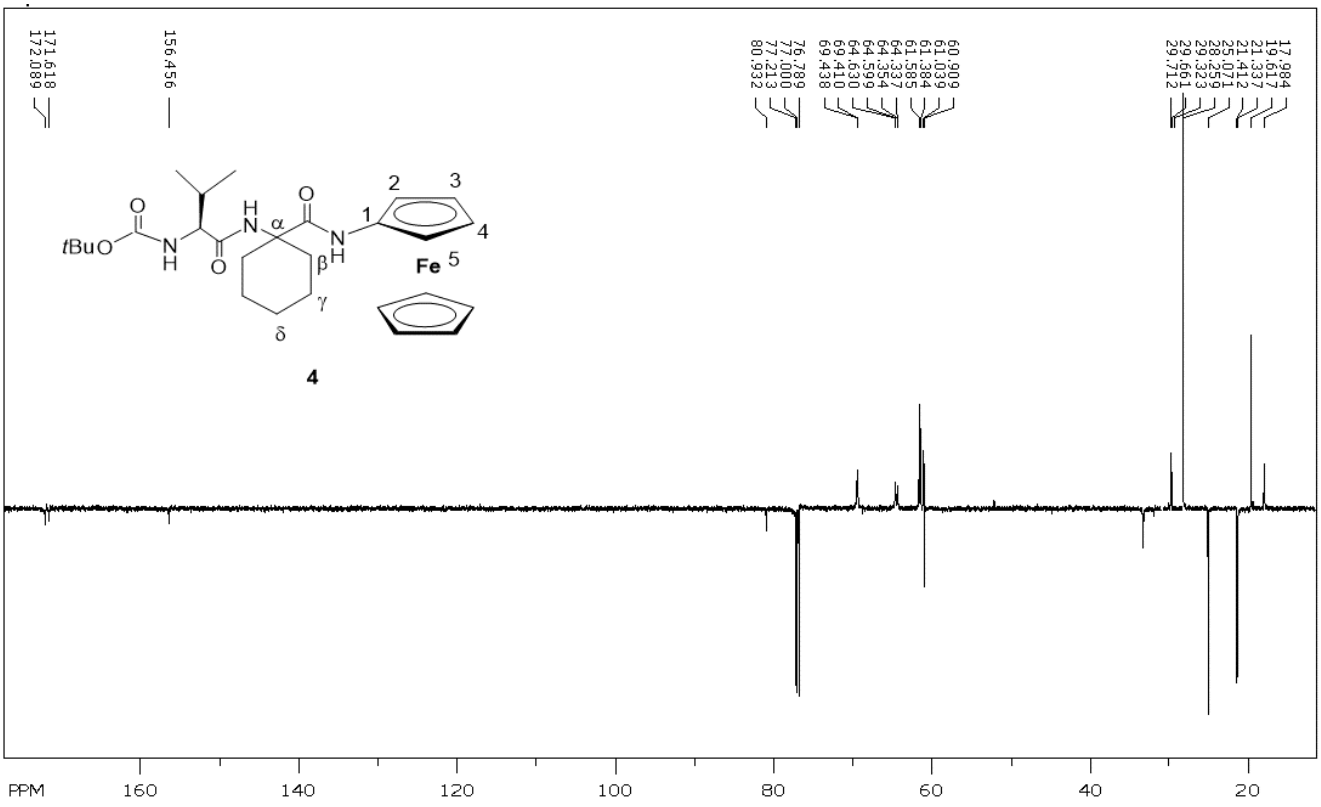

Figure S6. ^{13}C NMR spectrum of **4**, full range

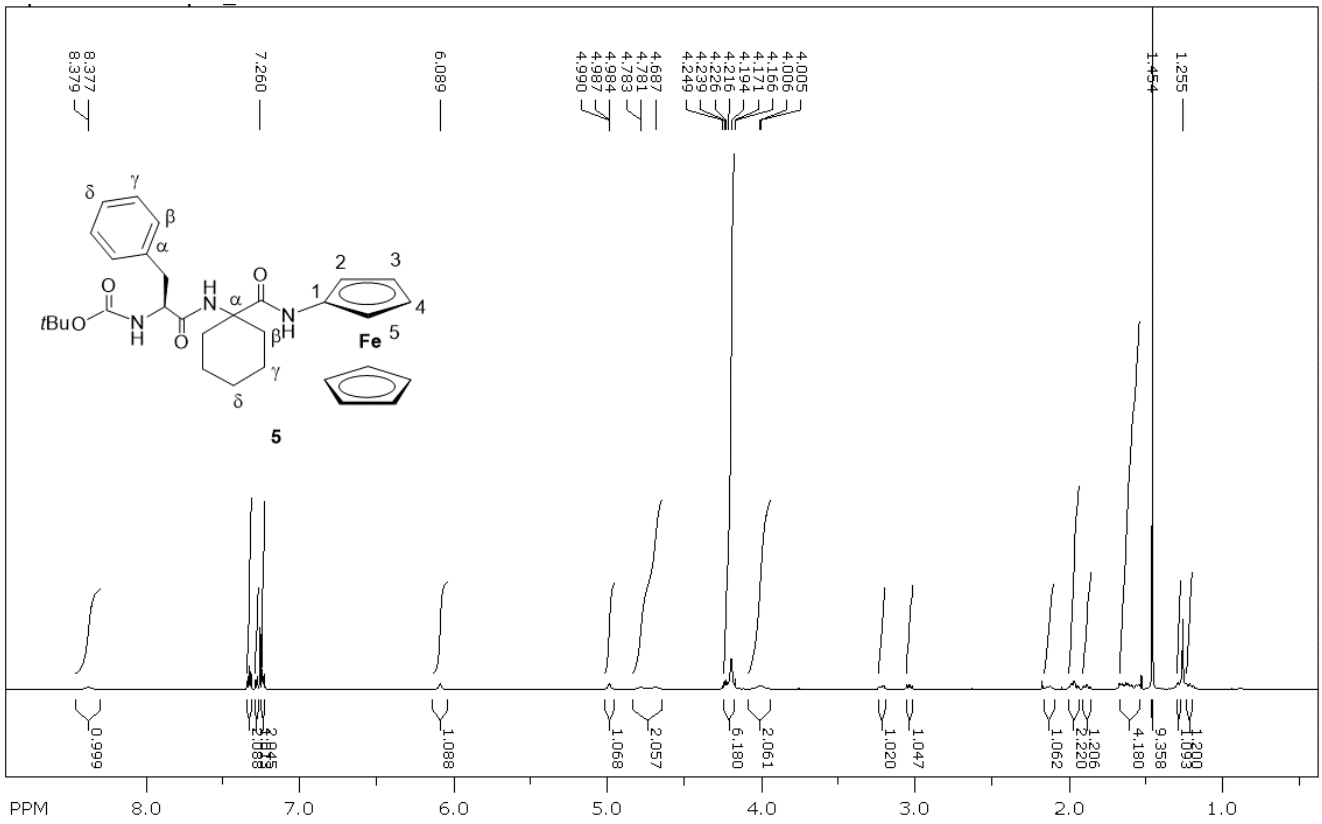

Figure S7. ^{1}H NMR spectrum of **5**, full range

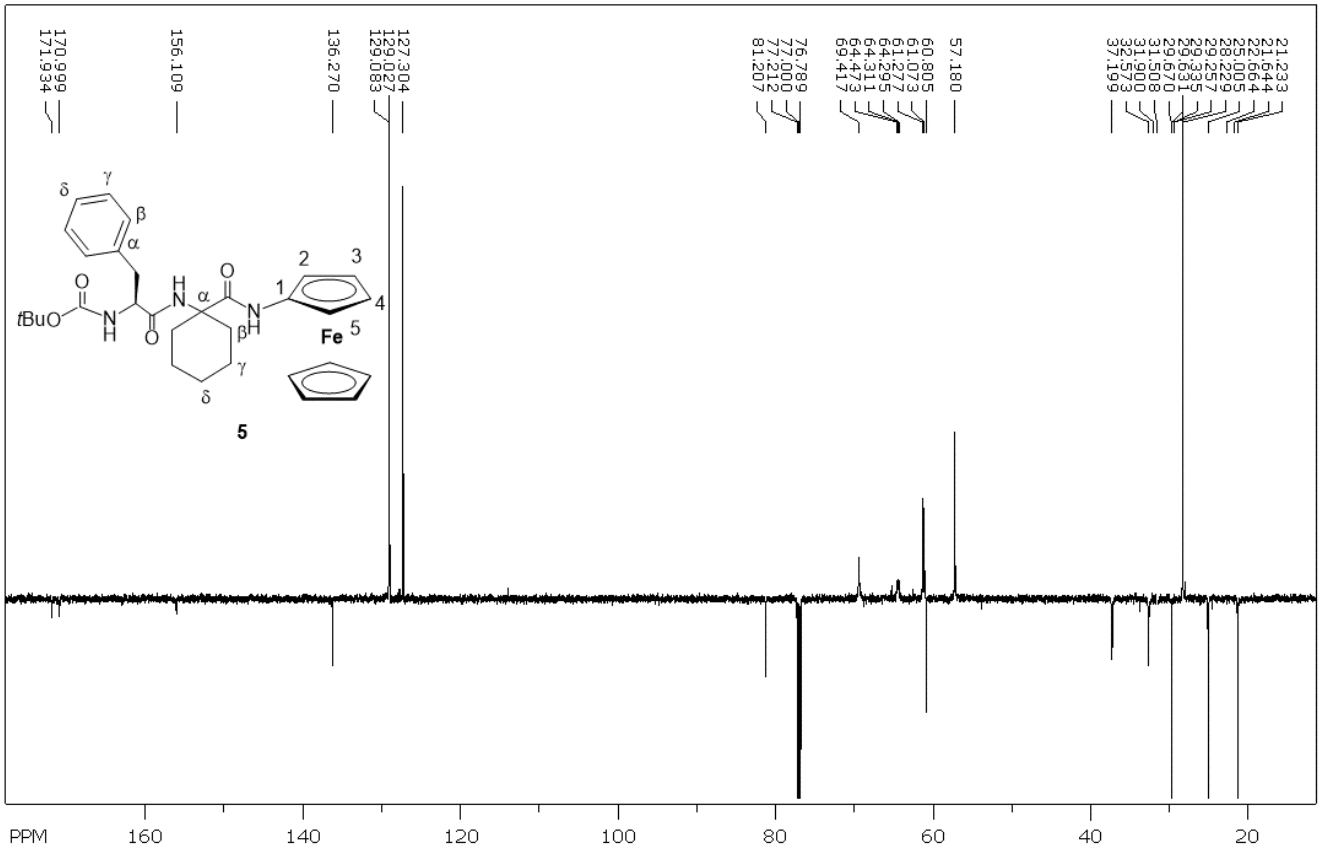

Figure S8. ^{13}C NMR spectrum of **5**, full range

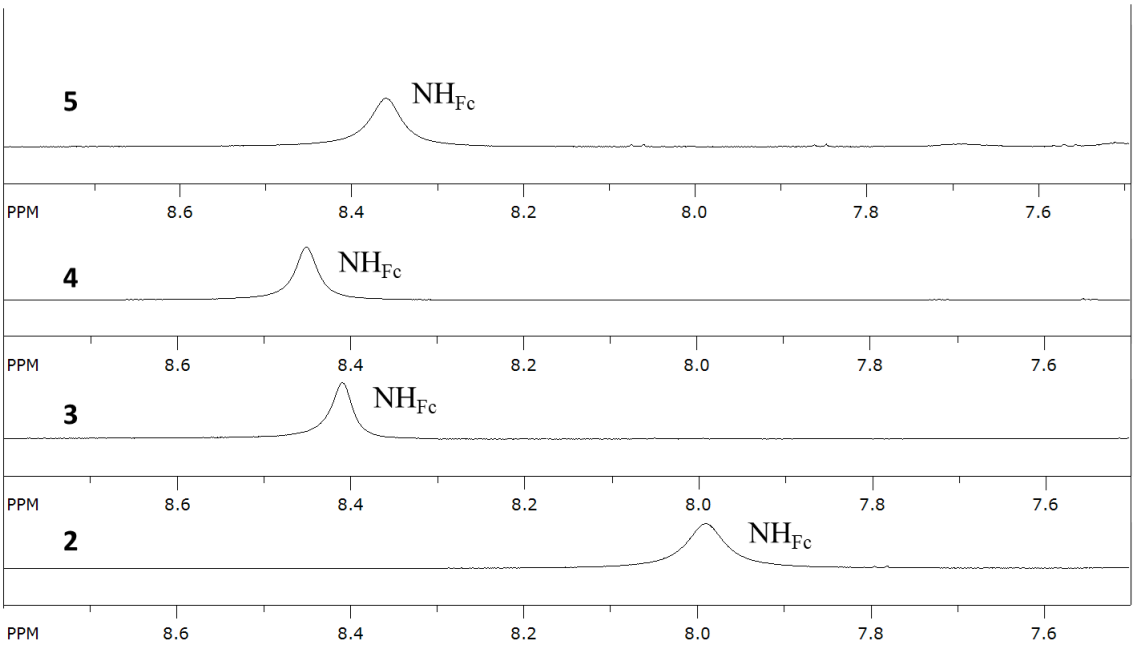

Figure S9. NH_{Fc} resonances in the NMR spectra of dilute solutions of **2**-**5** (*c* = 2 mmol dm^{-3})

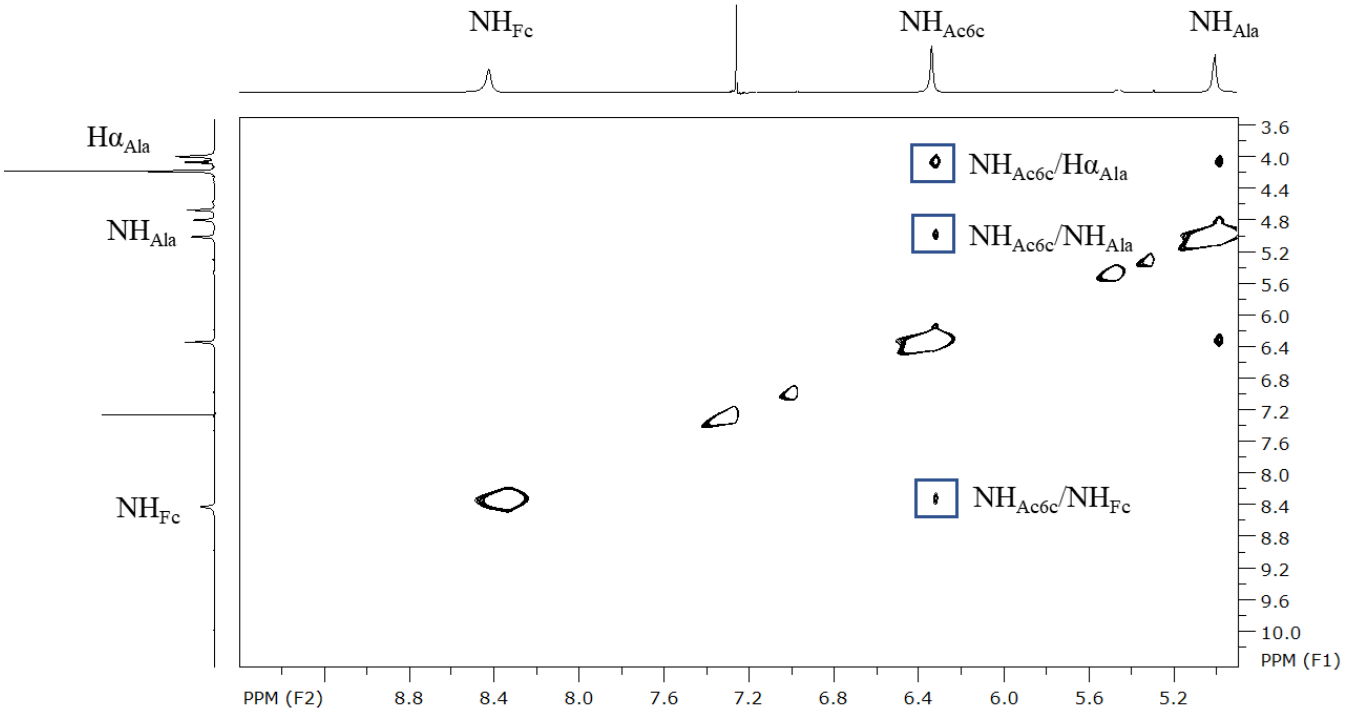

Figure S10. Sequential interactions in the NOESY spectrum of **3**

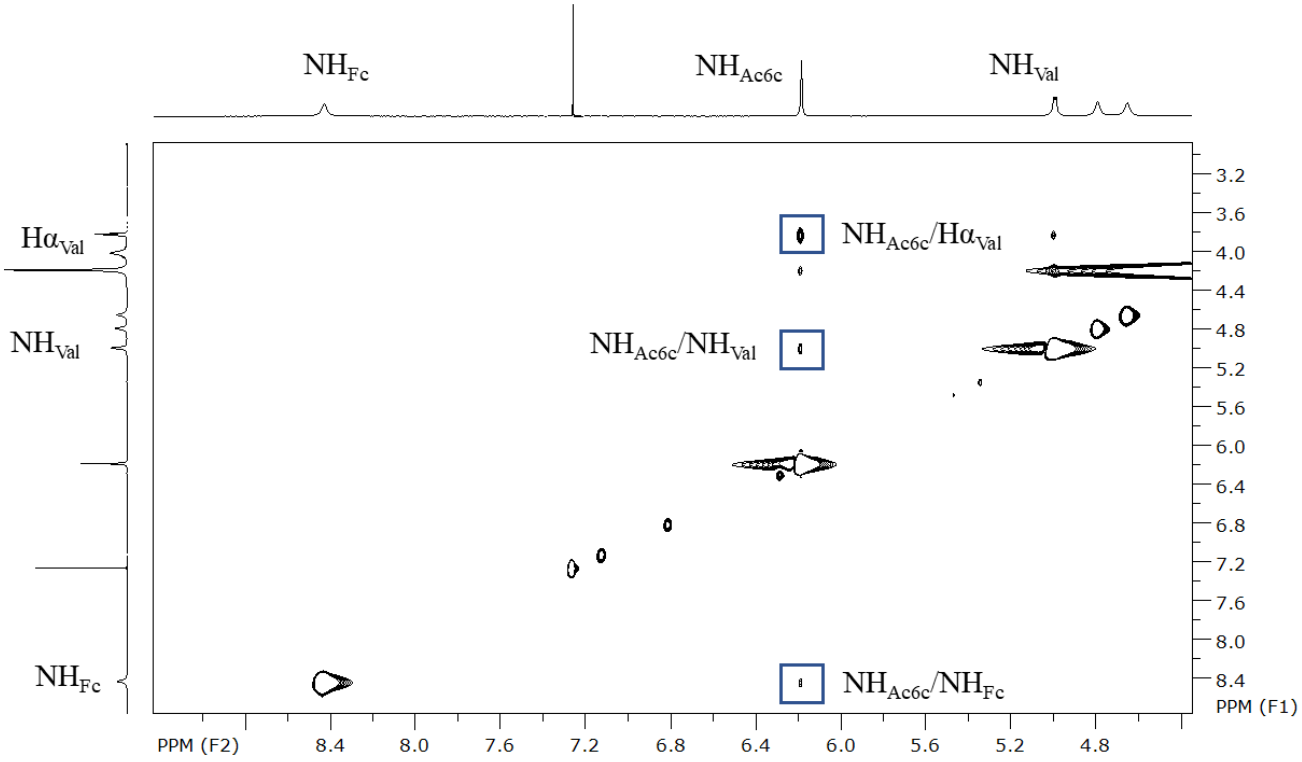

Figure S11. Sequential interactions in the NOESY spectrum of **4**

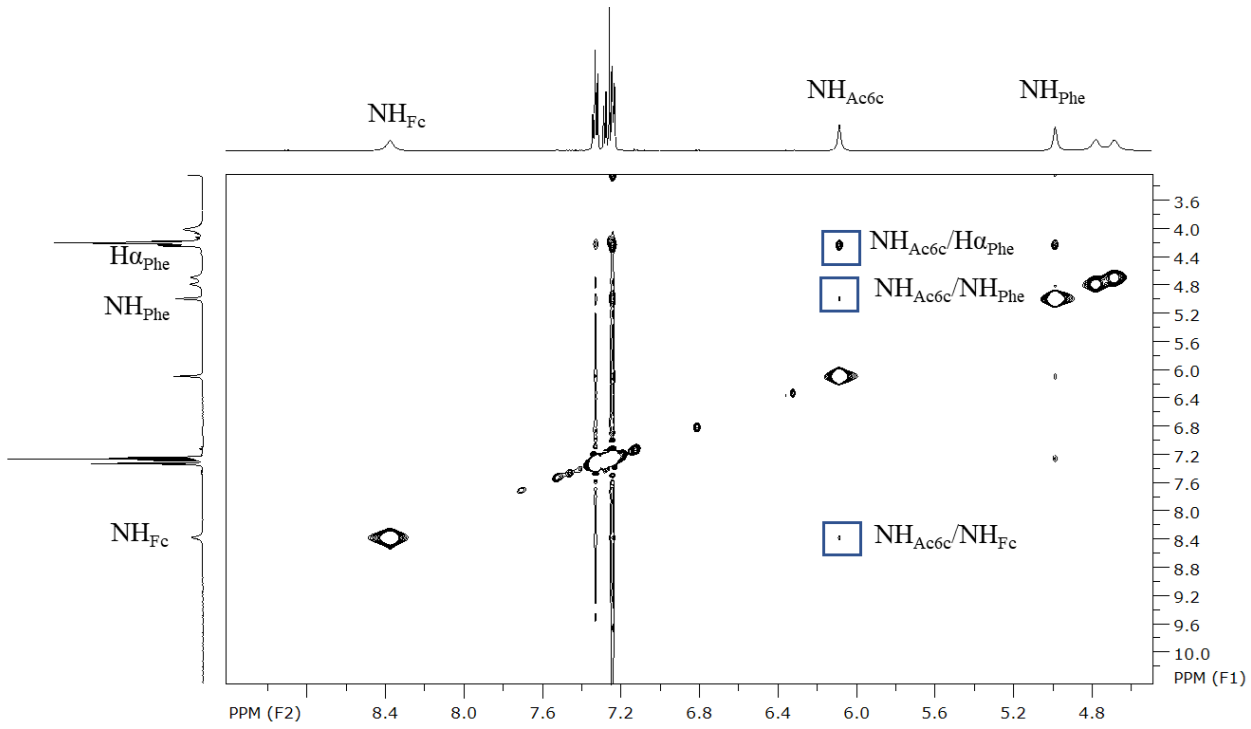

Figure S12. Sequential interactions in the NOESY spectrum of **5**

Table S1. Melting points of L-/D-**1a-3a** and L-/D-**1b-3b**

	Peptide	Melting point (°C)
L-**1b**	Boc-L-Val-NH-Fn-COOMe	112.3
L-**2b**	Boc-L-Leu-NH-Fn-COOMe	123
L-**3b**	Boc-L-Phe-NH-Fn-COOMe	130.6
D-**1b**	Boc-D-Val-NH-Fn-COOMe	112.5
D-**2b**	Boc-D-Leu-NH-Fn-COOMe	123.1
D-**3b**	Boc-D-Phe-NH-Fn-COOMe	130.7
L-**1a**	Ac-L-Val-NH-Fn-COOMe	156
L-**2a**	Ac-L-Leu-NH-Fn-COOMe	145.2
L-**3a**	Ac-L-Phe-NH-Fn-COOMe	198.6
D-**1a**	Ac-D-Val-NH-Fn-COOMe	156.1
D-**2a**	Ac-D-Leu-NH-Fn-COOMe	145.3
D-**3a**	Ac-D-Phe-NH-Fn-COOMe	198.7

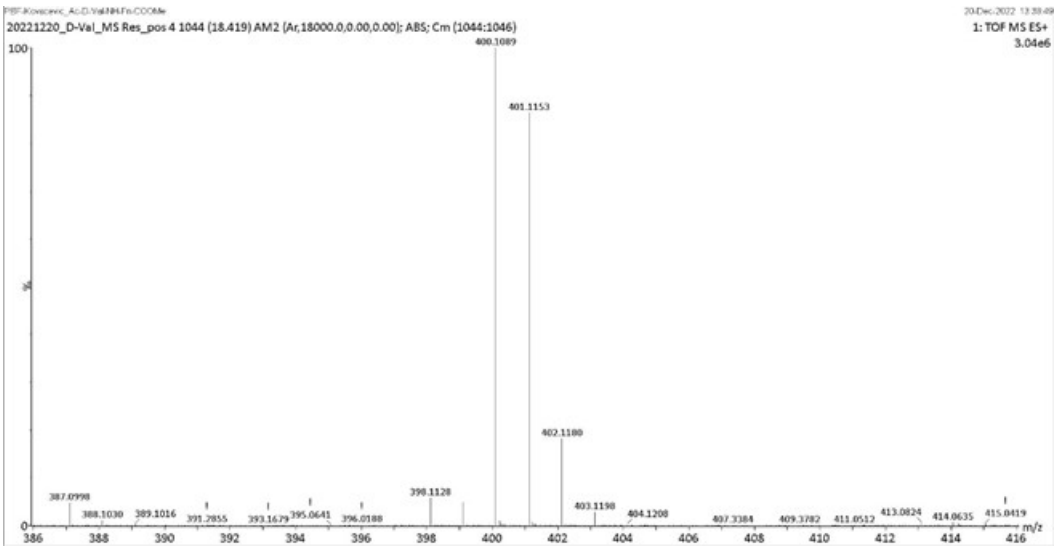

	Peptide	Molecular formula	Ion	Calculated mass	Measured mass
D-**1a**	Ac-D-Val-NH-Fn-COOMe	$C_{19}H_{24}FeN_2O_4$	$[M]^+$	400.1085	400.1089

Figure S1. HRMS spectrum of compound D-**1a**

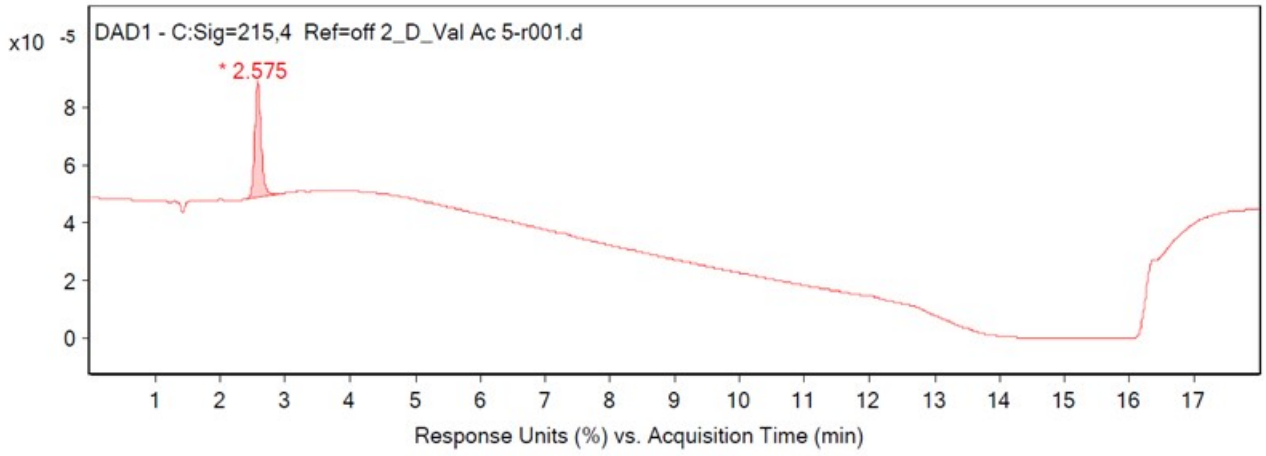

Integration Peak List

Peak	Start	RT	End	Height	Area	Area %
1	2.382	2.575	2.922	108.73	769.81	100

Figure S2. HPLC spectrum of compound D-**1a**

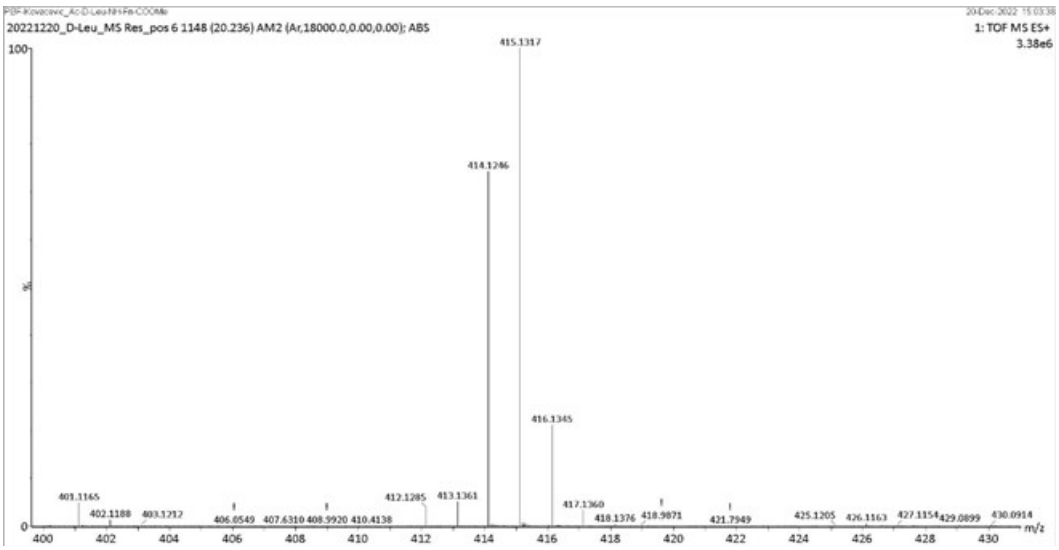

	Peptide	Molecular formula	Ion	Calculated mass	Measured mass
D-**2a**	Ac-D-Leu-NH-Fn-COOMe	$C_{20}H_{26}FeN_2O_4$	$[M+H]^+$	415.1320	415.1317

Figure S3. HRMS spectrum of compound D-**2a**

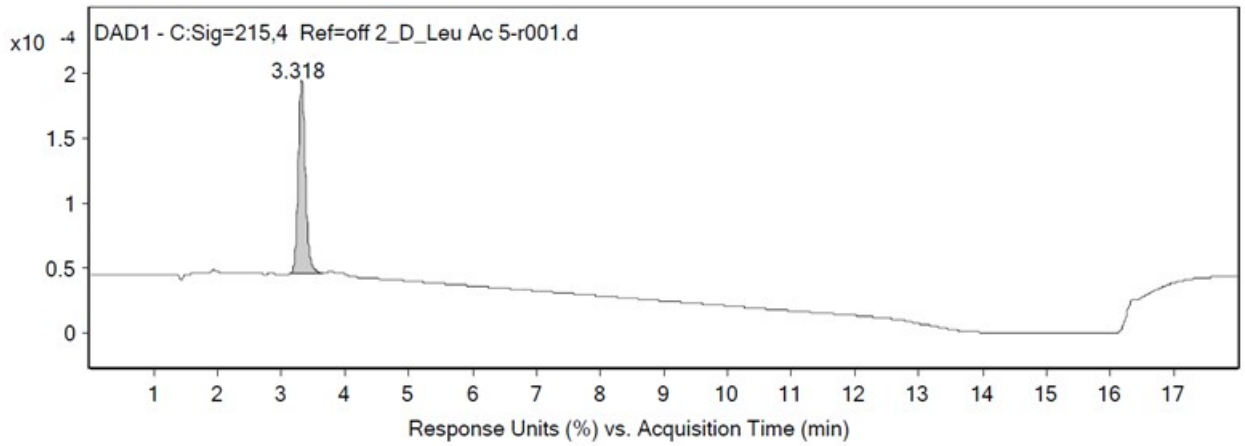

Integration Peak List

Peak	Start	RT	End	Height	Area	Area %
1	3.146	3.318	3.647	399.87	3184.69	100

Figure S4. HPLC spectrum of compound D-**2a**

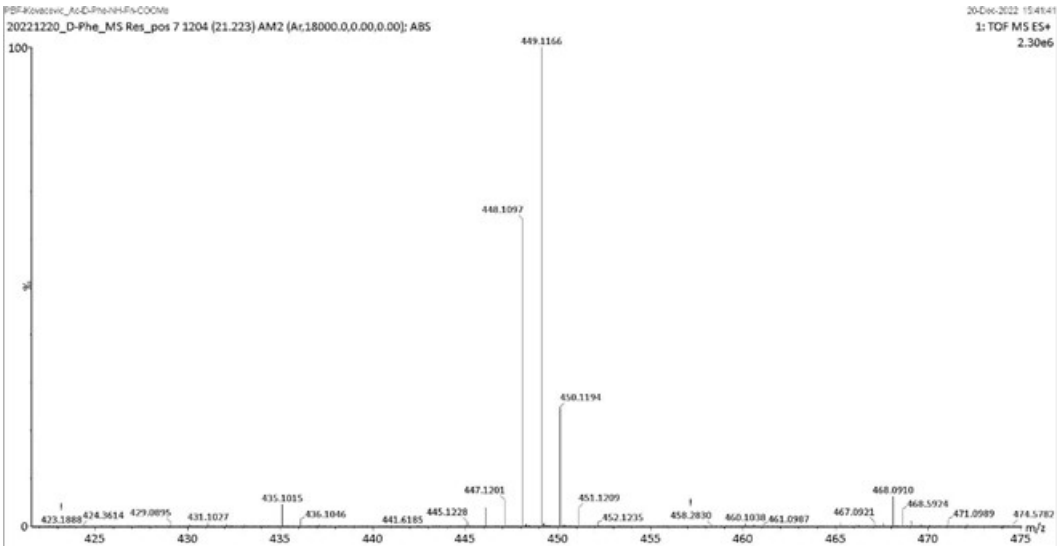

	Peptide	Molecular formula	Ion	Calculated mass	Measured mass
D-**3a**	Ac-D-Phe-NH-Fn-COOMe	$C_{23}H_{24}FeN_2O_4$	$[M+H]^+$	449.1164	449.1166

Figure S5. HRMS spectrum of compound D-**3a**

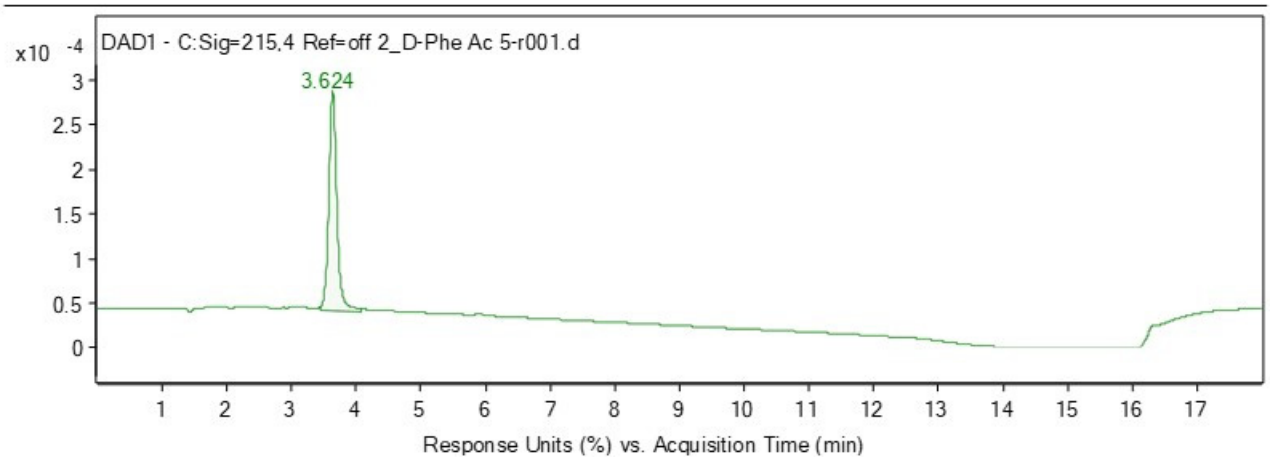

Integration Peak List

Peak	Start	RT	End	Height	Area	Area %
1	3.43	3.624	4.07	663.75	5882.13	100

Figure S6. HPLC spectrum of compound D-**3a**

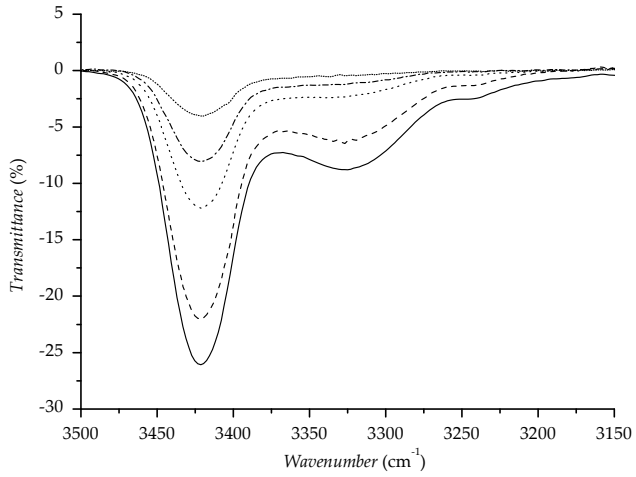

Figure S7. The NH stretching vibrations in concentration-dependent IR spectra of D-**1b** in DCM [(—) c = 5 × 10^{-2} M, (– – –) c = 2.5 × 10^{-2} M, (· · ·) c = 1.25 × 10^{-2} M, (-·-·-·) c = 0.6 × 10^{-2} M, (·····) c = 0.3 × 10^{-2} M.

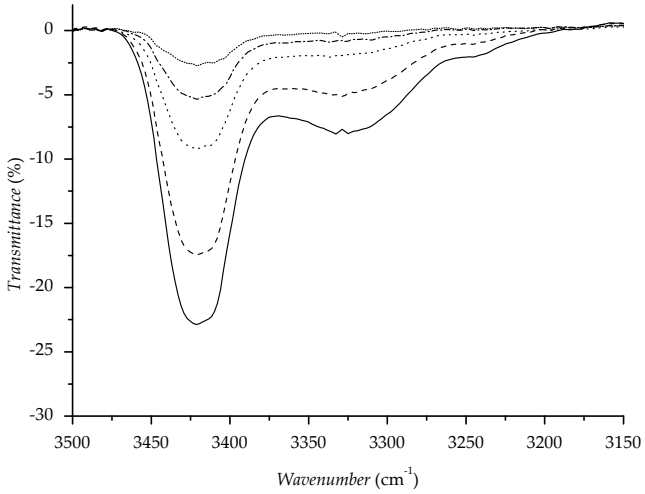

Figure S8. The NH stretching vibrations in concentration-dependent IR spectra of D-**2b** in DCM [(—) c = 5 × 10^{-2} M, (– – –) c = 2.5 × 10^{-2} M, (· · ·) c = 1.25 × 10^{-2} M, (-·-·-·) c = 0.6 × 10^{-2} M, (·····) c = 0.3 × 10^{-2} M.

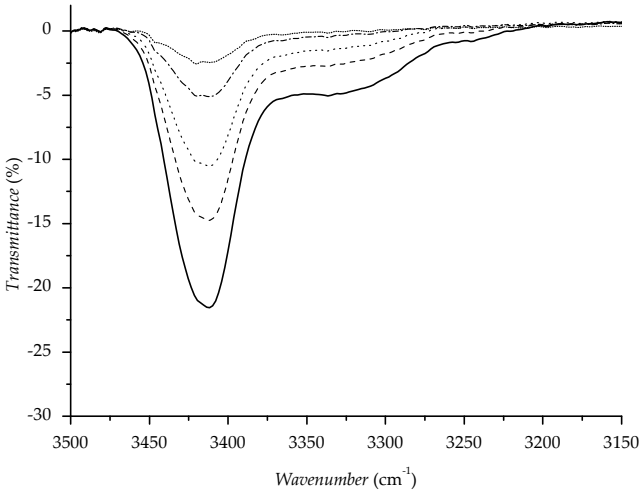

Figure S9. The NH stretching vibrations in concentration-dependent IR spectra of D-**3b** in DCM [(—) c = 5 × 10^{-2} M, (– – –) c = 2.5 × 10^{-2} M, (· · ·) c = 1.25 × 10^{-2} M, (-·-·-·) c = 0.6 × 10^{-2} M, (·····) c = 0.3 × 10^{-2} M.

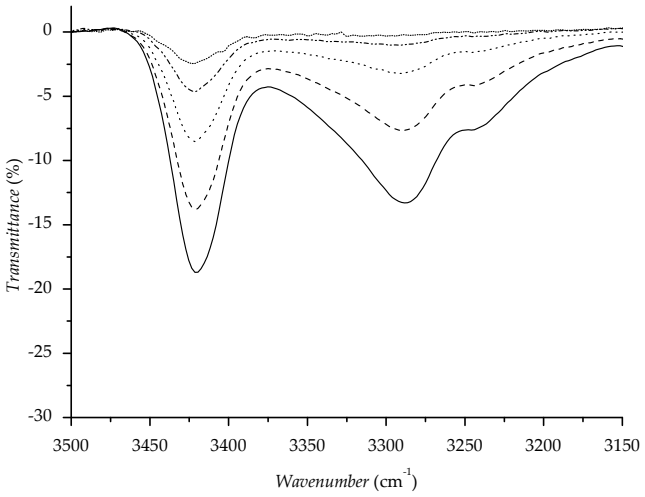

Figure S10. The NH stretching vibrations in concentration-dependent IR spectra of D-**1a** in DCM [(—) c = 5 × 10^{-2} M, (– – –) c = 2.5 × 10^{-2} M, (· · ·) c = 1.25 × 10^{-2} M, (-·-·-·) c = 0.6 × 10^{-2} M, (·····) c = 0.3 × 10^{-2} M.

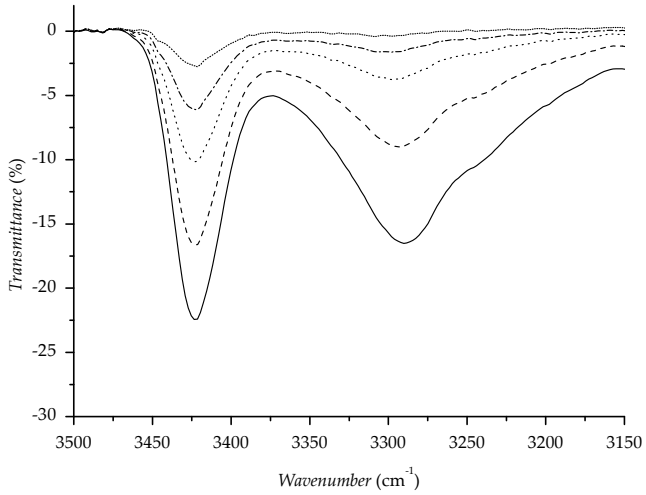

Figure S11. The NH stretching vibrations in concentration-dependent IR spectra of D-**2a** in DCM [(—) c = 5 × 10^{-2} M, (– – –) c = 2.5 × 10^{-2} M, (· · ·) c = 1.25 × 10^{-2} M, (-·-·-·) c = 0.6 × 10^{-2} M, (·····) c = 0.3 × 10^{-2} M.

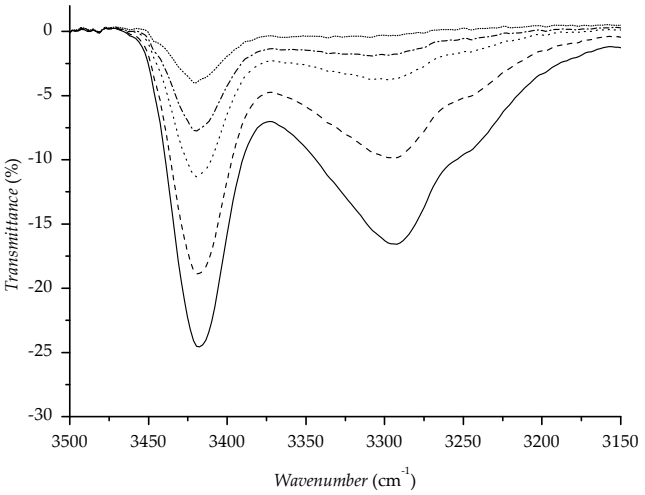

Figure S12. The NH stretching vibrations in concentration-dependent IR spectra of D-**3a** in DCM [(—) c = 5 × 10^{-2} M, (– – –) c = 2.5 × 10^{-2} M, (· · ·) c = 1.25 × 10^{-2} M, (-·-·-·) c = 0.6 × 10^{-2} M, (·····) c = 0.3 × 10^{-2} M.

Table S2. Concentration dependence of NH chemical shifts of derivatives D-**1a**, D-**2a** and D-**3a**

c (mM)	δ (ppm)					
	NH_{Fca}	NH_{Val}	NH_{Fca}	NH_{Leu}	NH_{Fca}	NH_{Phe}
50	8.19	6.46	8.15	6.38	7.73	6.44
25	7.93	6.33	7.89	6.17	7.56	6.35
12.5	7.69	6.23	7.73	6.05	7.37	6.24
6.25	7.56	6.19	7.63	5.98	7.3	6.18
$\Delta\delta$	**0.63**	**0.27**	**0.52**	**0.4**	**0.43**	**0.26**

Table S3. Temperature dependence of chemical shifts of ferrocene peptides D-**1a**, D-**2a** and D-**3a** [NMR-spectra are recorded in $CDCl_3$ (c = 2.5·10^{-2} M)]

	δ (ppm)					
T (K)	NH_{Fca}	NH_{Val}	NH_{Fca}	NH_{Leu}	NH_{Fca}	NH_{Phe}
258	8.8	6.74	8.68	6.76	8.3	6.81
268	8.59	6.63	8.39	6.53	8.04	6.65
278	8.43	6.55	8.16	6.36	7.84	6.53
288	8.24	6.46	8.00	6.24	7.69	6.42
298	8.06	6.38	7.86	6.15	7.55	6.35
308	7.9	6.31	7.75	6.08	7.46	6.3
318	7.75	6.25	7.68	6.03	7.37	6.23
328	7.62	6.19	7.6	5.97	7.31	6.17
$\Delta\delta$	**1.18**	**0.55**	**1.08**	**0.79**	**0.99**	**0.64**

Table S4. DMSO titration of ferrocene peptides D-**1a**, D-**2a** and D-**3a**

D-**1a**	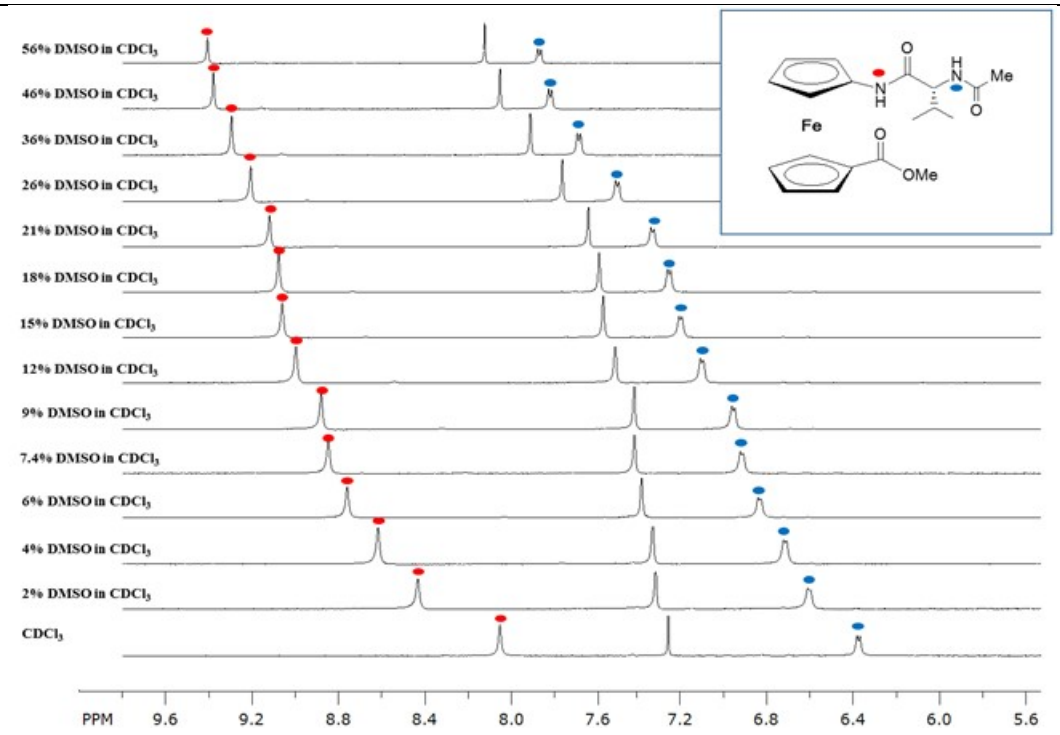
D-**2a**	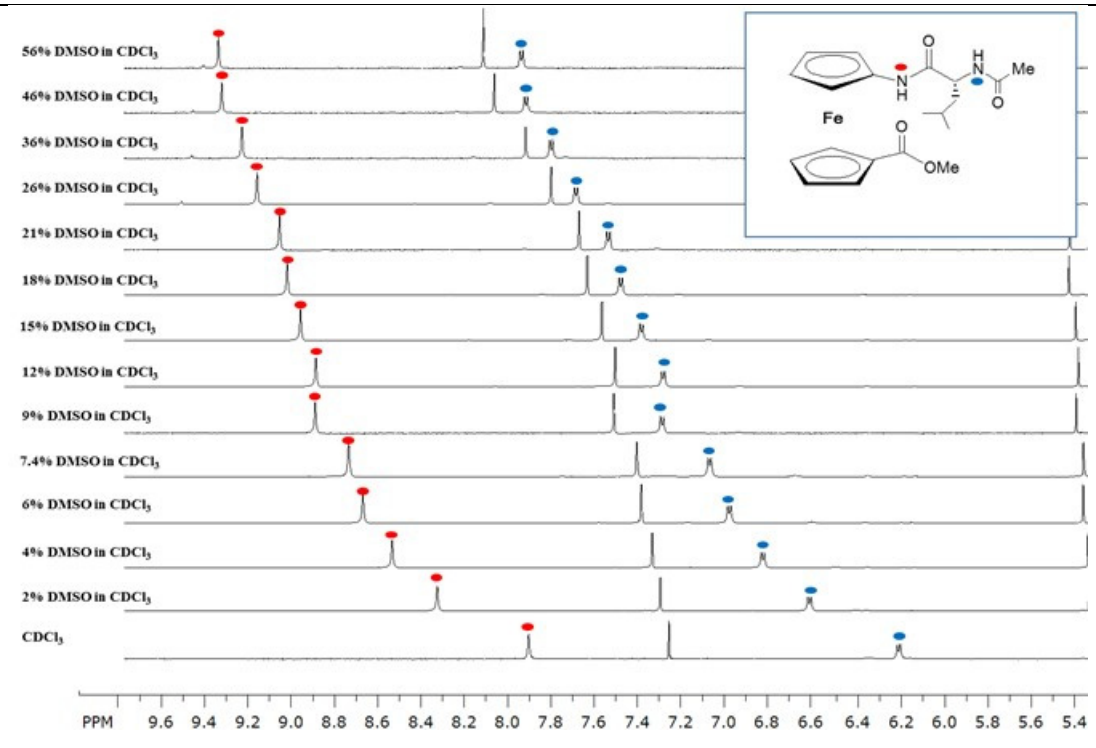

D-**3a**	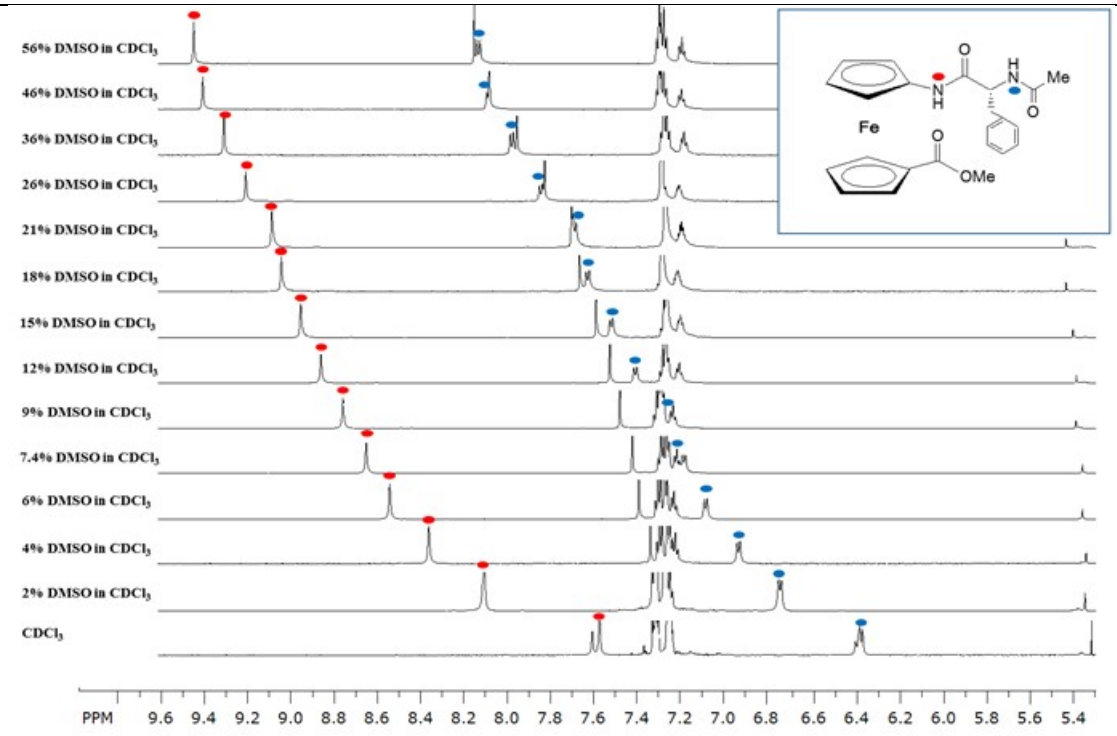

Table S5. UV/Vis-signals and Cottons efects in peptides L-/D-**1a**-**3a** and L-/D-**1b**-**3b**

	Peptide		λ_{max} / nm	[θ]/ deg cm² dmol⁻¹
L-**1b**	Boc-L-Val-NH-Fn-COOMe	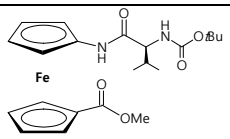	480	1227,62624
L-**2b**	Boc-L-Leu-NH-Fn-COOMe	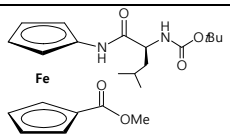	479,2	959,55305
L-**3b**	Boc-L-Phe-NH-Fn-COOMe	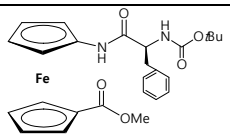	480	678,77391
D-**1b**	Boc-D-Val-NH-Fn-COOMe	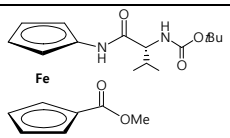	482,2	-1205,79523
D-**2b**	Boc-D-Leu-NH-Fn-COOMe	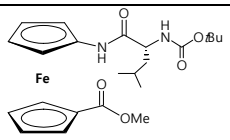	478,3	-957,2157

D-**3b**	Boc-D-Phe-NH-Fn-COOMe	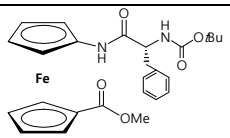	479,9	-676,39962
L-**1a**	Ac-L-Val-NH-Fn-COOMe	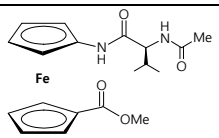	480,2	675,26792
L-**2a**	Ac-L-Leu-NH-Fn-COOMe	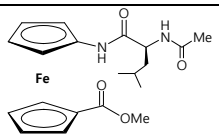	474,2	455,83704
L-**3a**	Ac-L-Phe-NH-Fn-COOMe	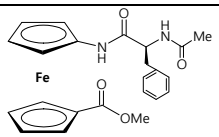	478,3	672,45099
D-**1a**	Ac-D-Val-NH-Fn-COOMe	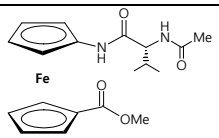	483,9	-687,37927
D-**2a**	Ac-D-Leu-NH-Fn-COOMe	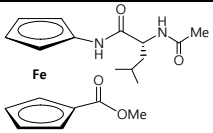	475,1	-479,18576
D-**3a**	Ac-D-Phe-NH-Fn-COOMe	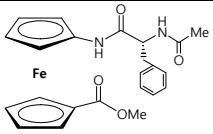	476,6	-643,06888

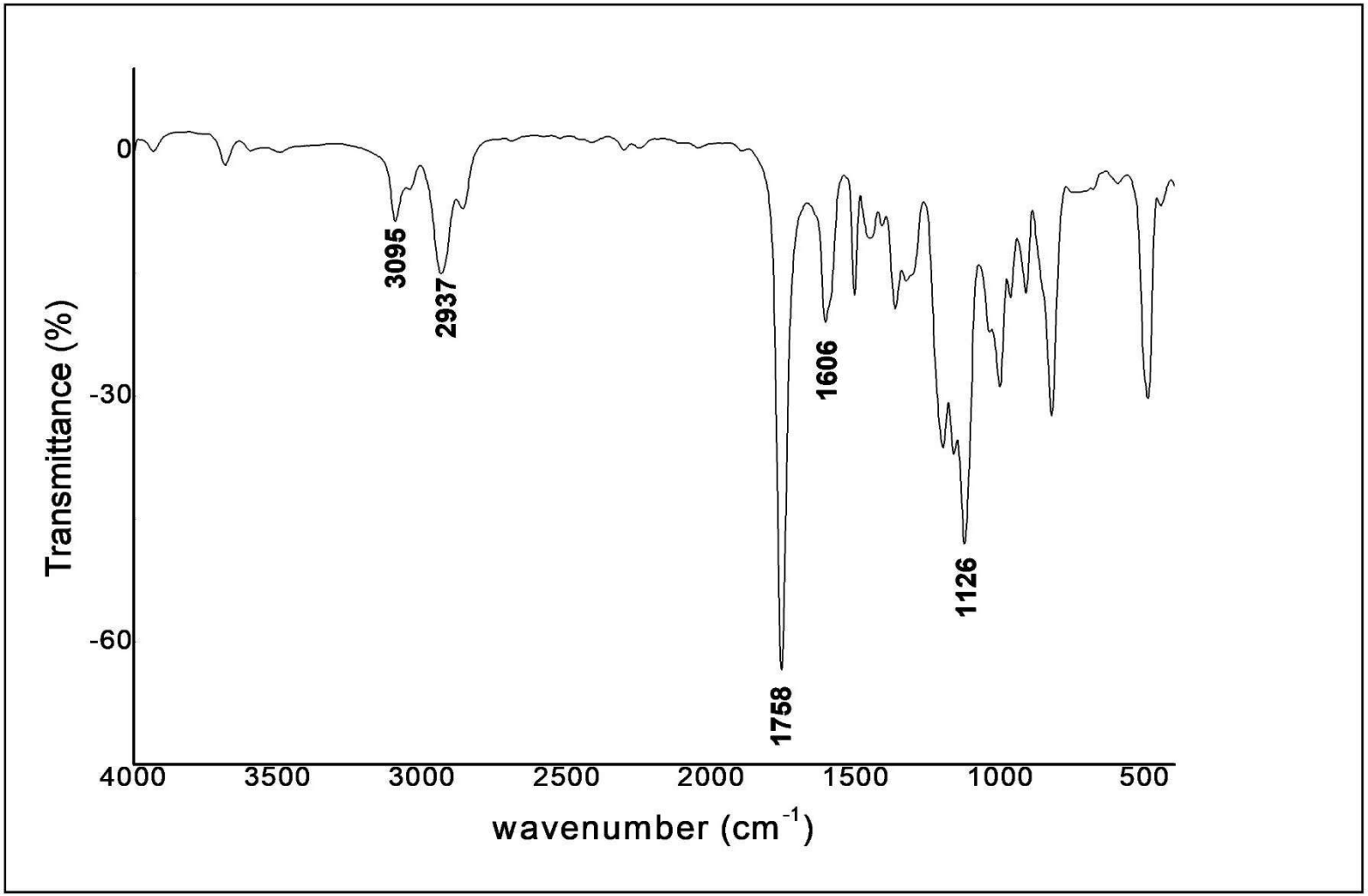

Figure S1: FTIR spectra (in CH_2Cl_2) of ferrocene-containing resveratrol derivative RF

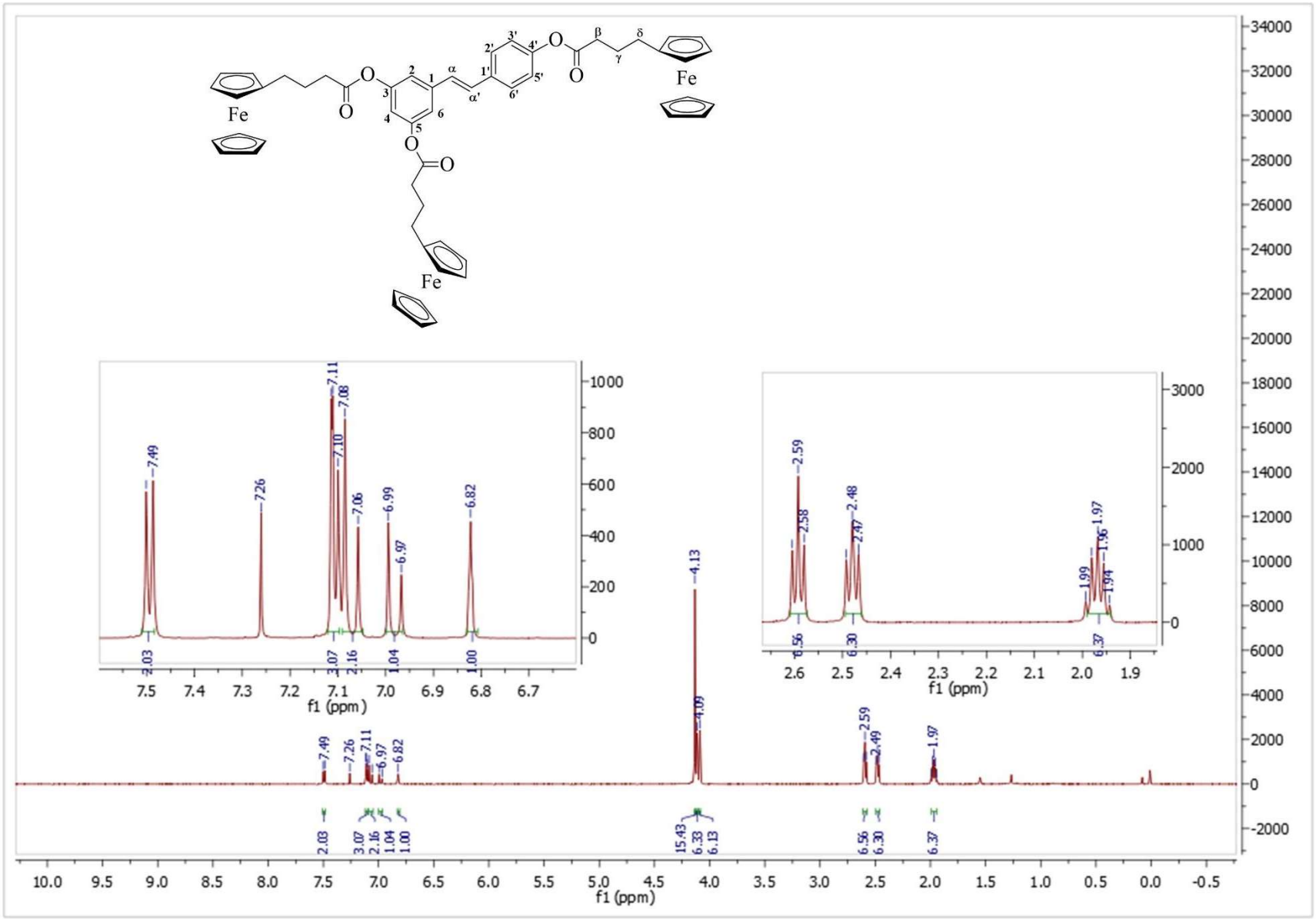

Figure S2: ^{1}H NMR spectra (in $CDCl_3$) of ferrocene-containing resveratrol derivative RF

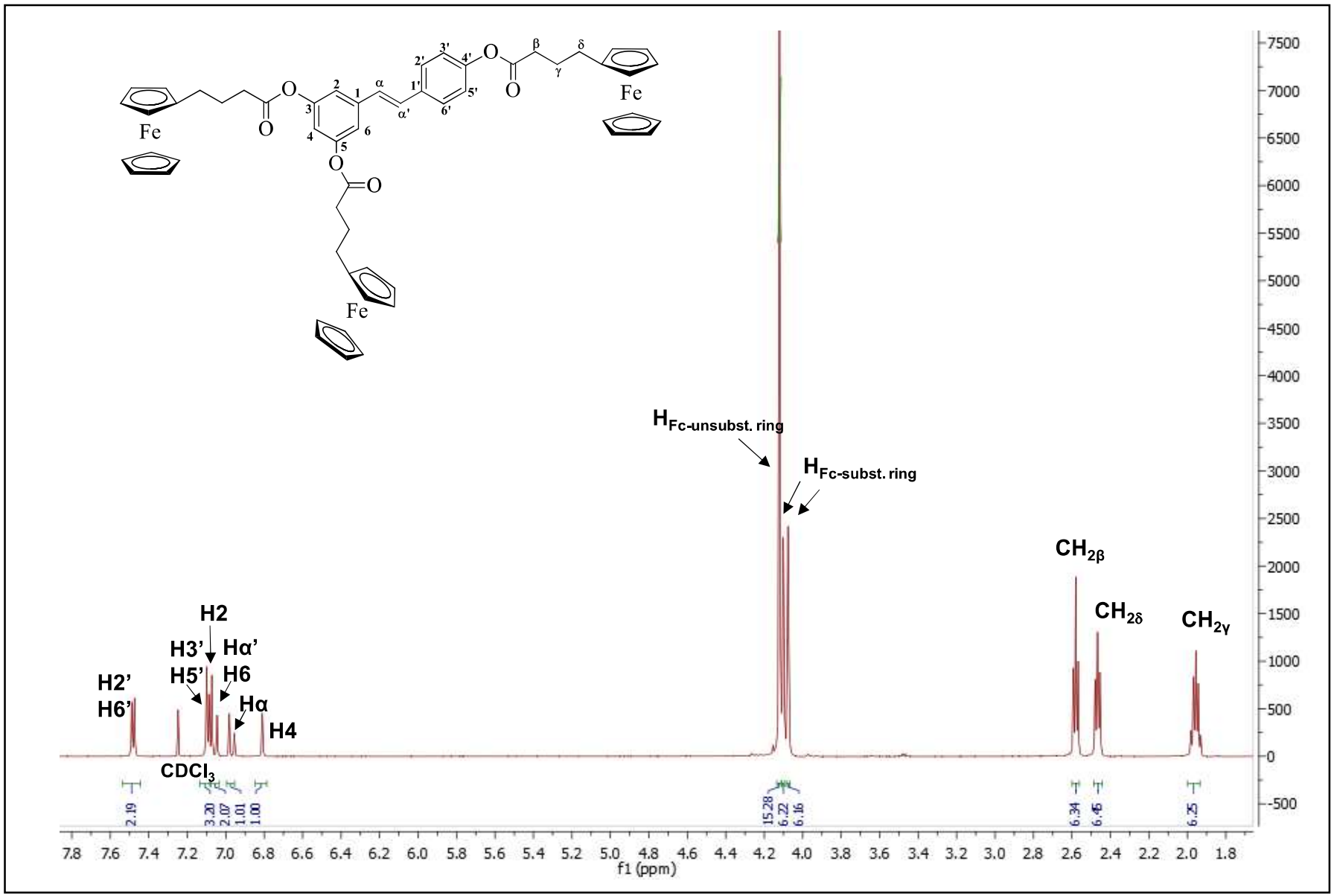

Figure S3: ^{1}H NMR spectra (in $CDCl_3$) of RF with signals assingment

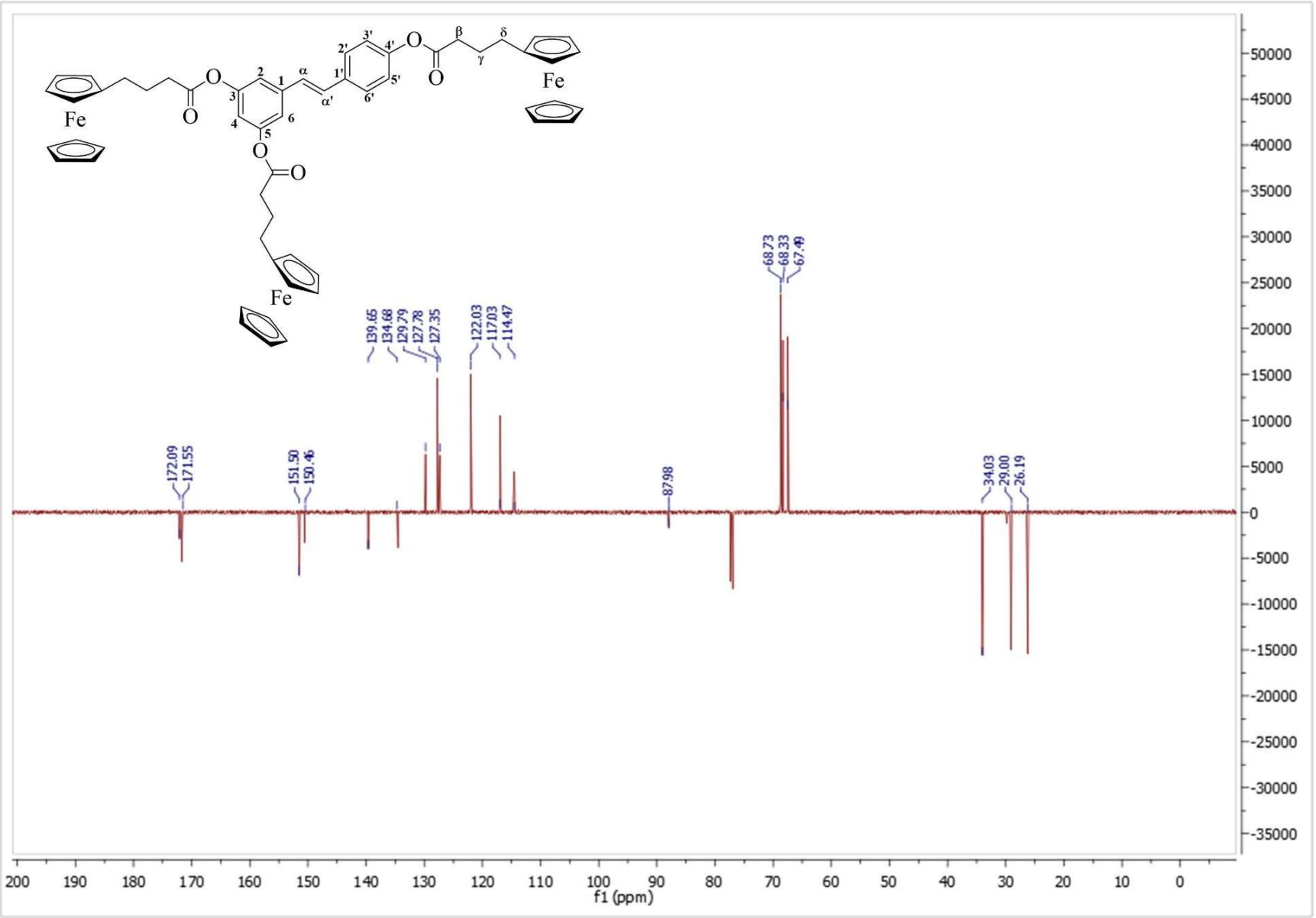

Figure S4: ^{13}C NMR APT spectra (in $CDCl_3$) of ferrocene-containing resveratrol derivative RF

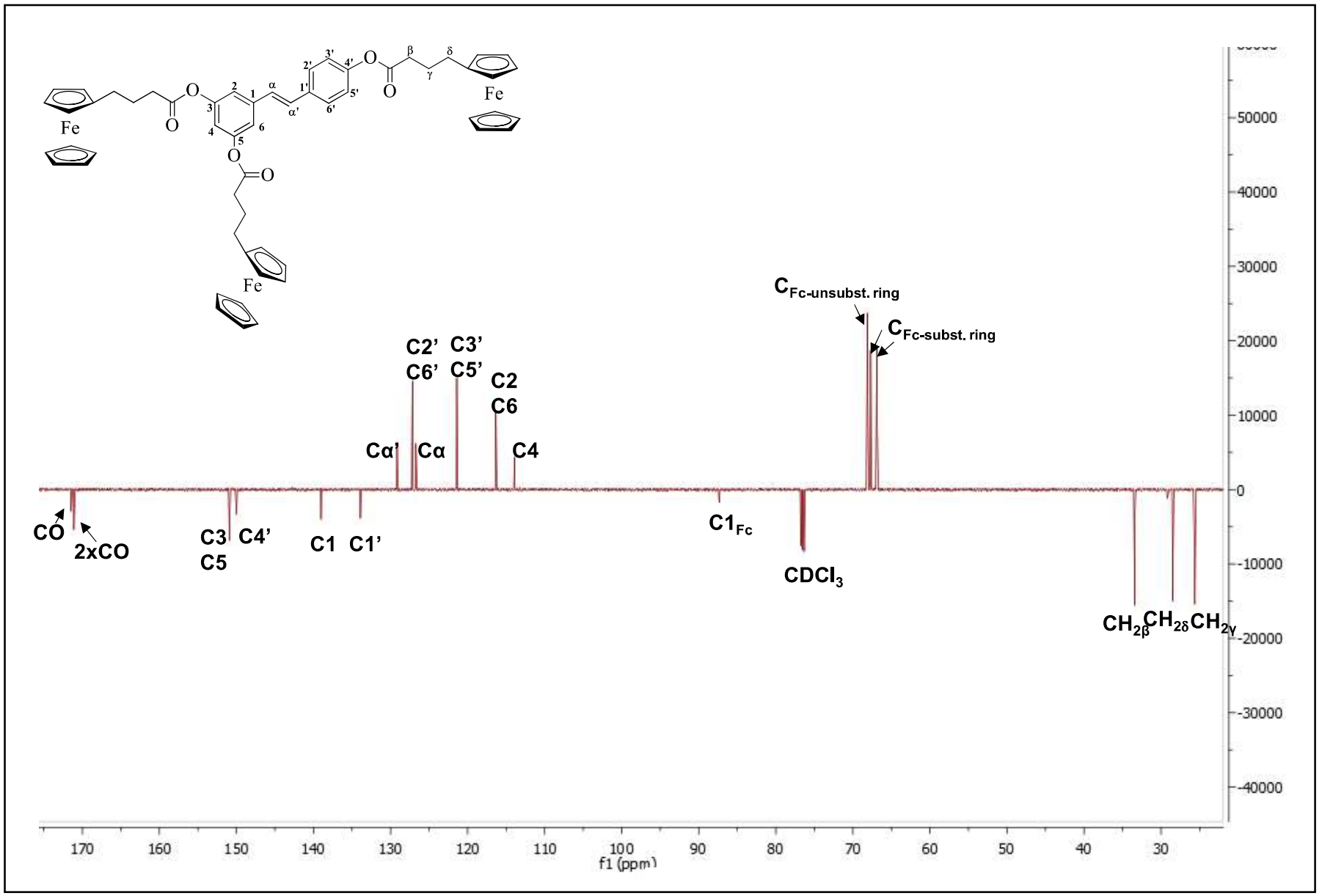

Figure S5: ^{13}C NMR APT spectra (in $CDCl_3$) of RF with signals assingment

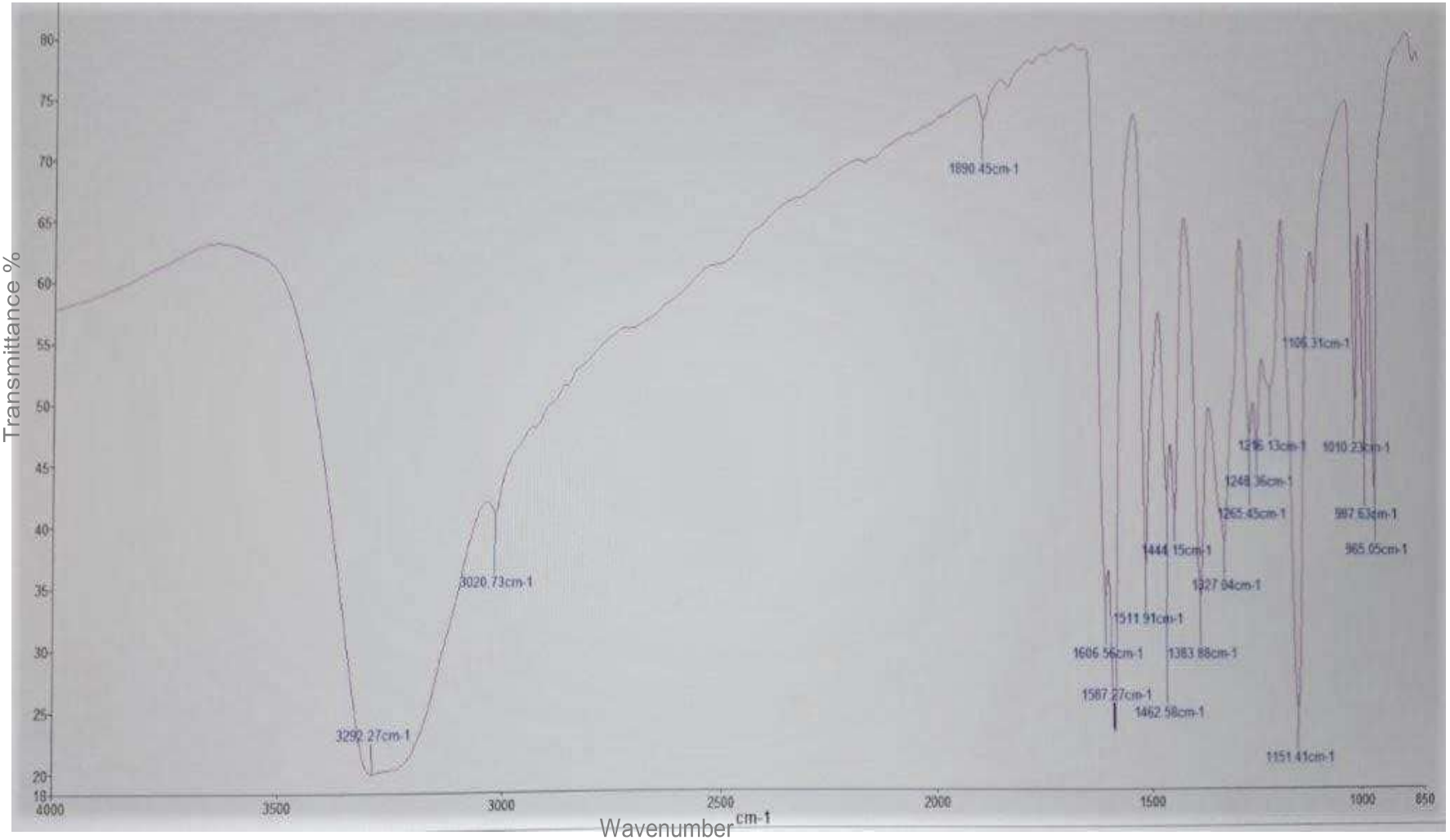

Figure S6: FTIR spectra (in KBr pastille) of resveratrol (RSV)

HRZZ_FER-AN-BIOMOL_biološka evaluacija

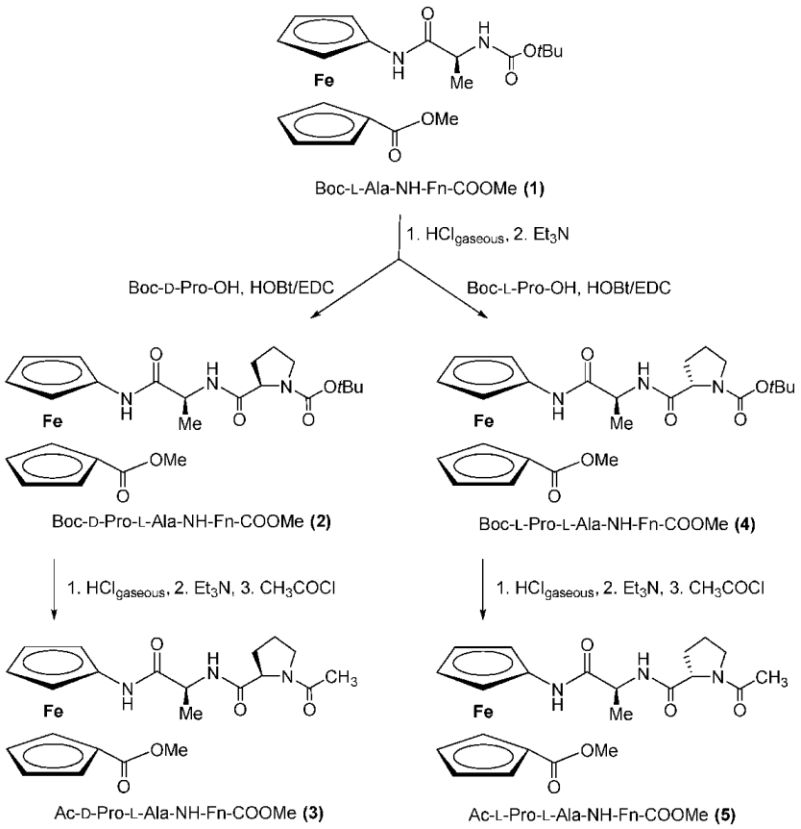

Boc-L-Ala-NH-Fn-COOMe **(1)**

Boc-D-Pro-L-Ala-NH-Fn-COOMe **(2)**

Boc-L-Pro-L-Ala-NH-Fn-COOMe **(4)**

Ac-D-Pro-L-Ala-NH-Fn-COOMe **(3)**

Ac-L-Pro-L-Ala-NH-Fn-COOMe **(5)**

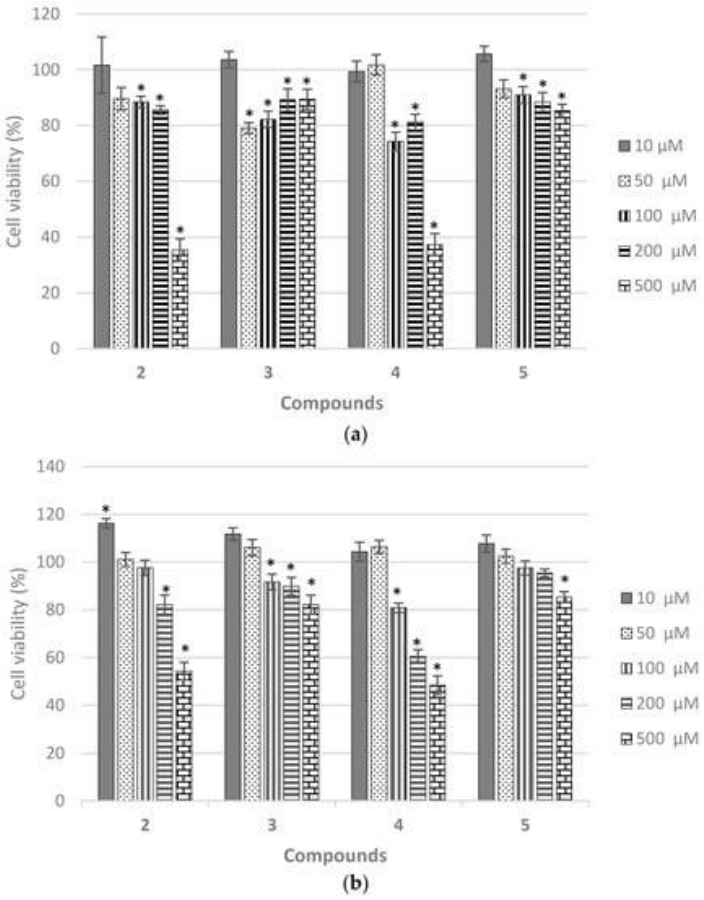

Figure 13. Cell viability of HeLa (**a**) and MCF-7 (**b**) cells treated with peptides **2**–**5** for 72 h in the range of concentration from 10 µM to 500 µM and assessed by the CellTiter 96® AQueous. One Solution Cell Proliferation Assay. Cell viability (%) was expressed as percentage of treated cells versus control cells. and the data from three individual experiments were expressed as the means (n = 5) ± S.D. * significant difference was considered at a *p* value < 0.05.

Table 1. IC_{50} values calculated from dose-response curves of cell viability on HeLa and MCF7 cells.

Table 1. IC_{50} values calculated from dose-response curves of cell viability on HeLa and MCF7 cells.

Compound	HeLa Cells	MCF-7 Cells
2	436.1959 µM	n.d. [1]
3	n.d. [1]	n.d. [1]
4	370.3969 µM	270.6925 µM
5	n.d. [1]	n.d. [1]

[1] n.d. = not detected.

Table 2. Plating efficiency (PE) and surviving fraction (SF) for peptides **2**–**5**.

Table 2. Plating efficiency (PE) and surviving fraction (SF) for peptides 2–5.

PE (%)	Concentration	SF (2)	SF (3)	SF (4)	SF (5)
31.75	100 µM	0.1575	1.0394	0	0.7874
	500 µM	0	0	0	0.0315

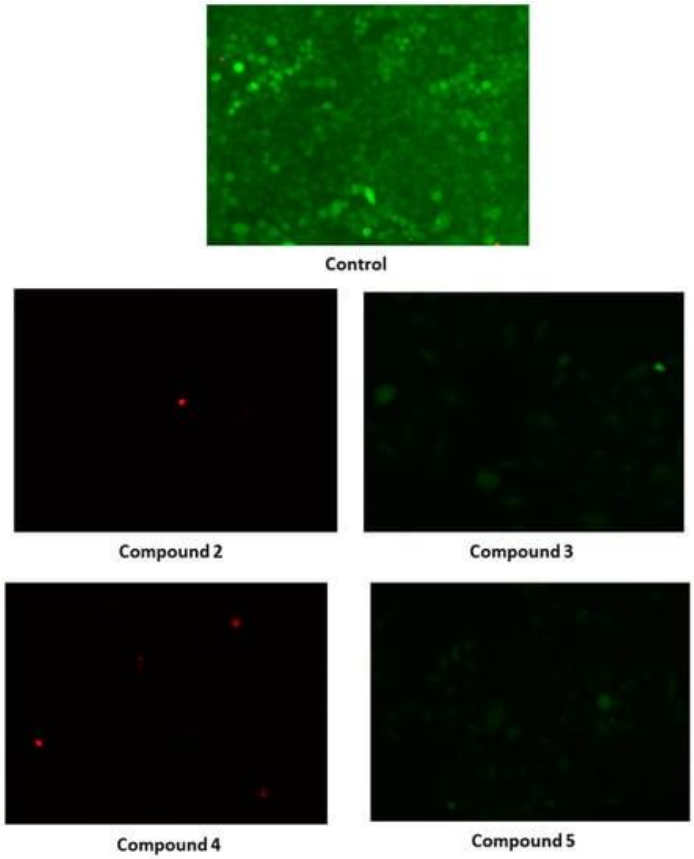

Figure 14. Morphological appearance of control, non-treated and HeLa cells treated with peptides **2**–**5** (500 µM) photographed after staining with FDA and PI under the fluorescence microscopy.

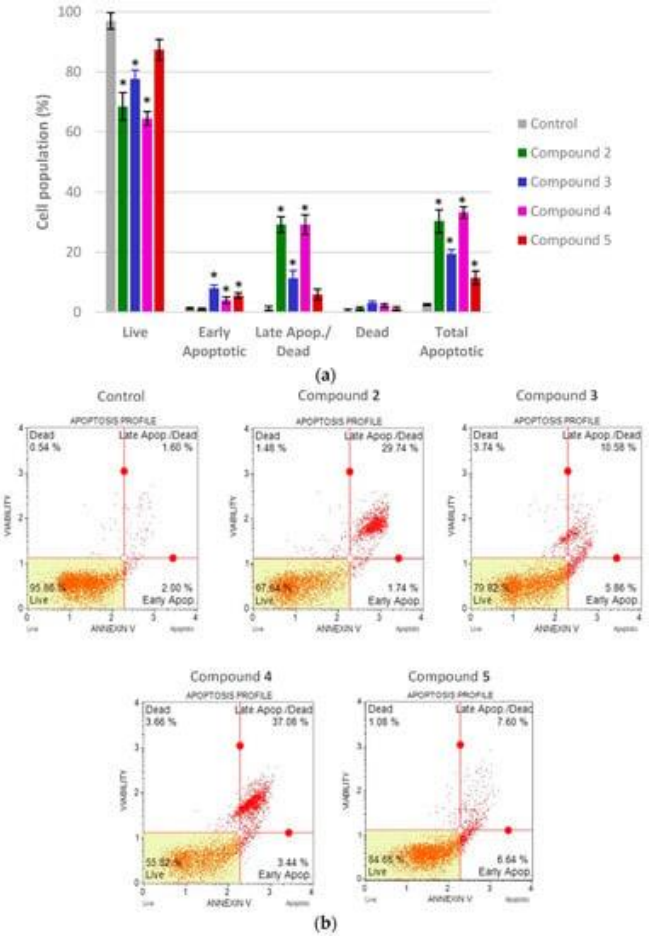

Figure 15. Cell death analysis of HeLa cells treated with the highest tested concentration of Boc-(**2**,**4**) and Ac-peptides (**3**,**5**) (500 µM) for 72 h. Distribution of four distinct cell populations (**a**). Values were represented as the mean (n = 2) ± SD from two independent experiments. * significant difference of treated cells versus control cells was considered at a *p* value < 0.05. Representative histograms for control and treated cells were given from the Muse Annexin V & Dead Cell assay (**b**).

3.1.5. Biological Activity

Materials: Trypsin-EDTA (0.25%), FBS (fetal bovine serum) and PBS (phosphate buffer saline) were purchased from Sigma-Aldrich while DMEM (Dulbecco's Modified Eagle Medium) was purchased from Capricorn Scientific GmbH (Ebsdorfergrund, Germany). The CellTiter 96® AQ_{ueous} One Solution Cell Proliferation Assay was purchased from Promega (Madison, WI, USA). Fluorescein diacetate (FDA) and propidium iodide (PI) were purchased from Sigma-Aldrich. The Muse Annexin V Dead Cell kit was purchased from EMD Milipore Corporation (Merck KGaA).

Cell culture and cultivation conditions: Two adherent human cell lines used in this work were obtained from the Ruđer Bošković Institute (Zagreb, Croatia). The HeLa cell line derived from the cervical adenocarcinoma (ATCC No. CCL-2) and the MCF-7 cell line derived from breast adenocarcinoma (ATCC No. HTB-22) were cultured in DMEM supplemented with 5% FBS and maintained in BioLite petri dishes for cell culture (Thermo Fisher Scientific, Waltham, MA, USA) in an incubator under a humidified atmosphere and 5% CO_2 at 37 °C. Cells in the exponential growth phase were trypsinized, counted by the trypan blue method using an improved Neubauer hemocytometer, and used to set up individual experiments. BioLite

6-well and 96-well plates were used for individual experiments to test compounds of interest (Thermo Fisher Scientific).

Evaluation of cytotoxicity: The effect of peptides **2**–**5** on cell viability was examined using the CellTiter 96® AQ_{ueous} One Solution Cell Proliferation Assay, which was performed according to the manufacturer's instructions with minor modifications and as described [69]. In brief, HeLa and MCF-7 cells were seeded in 96-well plates at a density of 3×10^4 cells per well in 100 µL of media. Stock solutions of peptides 2–5 were prepared as 10 mM solutions of compounds in ethanol, sterilized by filtration through a 0.22 µM filters and then, prior to each experiment, diluted in culture medium. After overnight incubation, HeLa and MCF-7 cells were treated with peptides 2–5 at nominal concentrations ranging from 10 µM to 500 µM. After the 72 h treatment, 10 µL of CellTiter 96® AQ_{ueous} One Solution Cell Proliferation reagent was added to each well, and the cells were incubated for an additional 3 h. Subsequently, absorbance was measured at 490 nm on the microplate reader (Tecan, Mannedorf,, Switzerland). Cell viability was expressed as the percentage of treated cells versus control cells. Experiments were performed three times with five parallels for each concentration of compound tested and data were expressed as mean ± SD. The corresponding IC_{50} values were calculated from the dose-response curves using equations of best-fitted trend lines.

Clonogenic assay: The clonogenic analysis began by seeding pre-cultured HeLa cells in 6-well plates at an initial concentration of 200 cells in 2 mL of culture medium per well. The cells were incubated under optimal conditions and treated with peptides **2**–**5** at a concentration of 100 µM and 500 µM after 24 h. There was also a control cells that were not treated with peptidomimetics. Three days after the cells were treated, the growth medium containing the test compounds was removed and replaced with fresh growth medium, after which the plate with the HeLa cells was returned to the incubator for further cultivation. After treatment with the test substances, the surviving cells need about 1–3 weeks to form colonies. In this work, the colonies formed were visible 17 days after initial seeding of the cells. Staining the grown colonies with crystal-violet begins by removing the growth medium and washing the cells with 1 mL of PBS buffer. Then 2.5 mL of methanol was added to fix the cells, which was removed after 10 min. The plates are then allowed to air dry completely. A 0.5% solution of crystal-violet is then added and incubated for 10 min. In the final step, the dye is removed and the colonies in the wells are rinsed with 1 mL of PBS buffer and deionized water. The number of colonies grown was then counted and the plating efficiency (PE) and survival fraction (SF) were calculated according to the equations in the protocol of Franken et al. [52]. PE is the ratio of the number of colonies to the number of seeded cells, while SF is the number of colonies formed after treatment of the cells, expressed as PE.

Analysis of cell death by fluorescence microscopy and flow cytometry: for fluorescein diacetate and propidium iodide staining, HeLa cells were seeded in 6-well plates at a concentration approximately about 1×10^5 cells mL^{-1} and treated with 500 µM of peptides **2**–**5** after 24 h. After the 72 h treatment, cells were washed with PBS, trypsinized, centrifuged, and resuspended in 0.2 mL of PBS. Cell were stained with FDA and PI according to the method described by us [70] and immediately examined with the fluorescent microscope EVOS FLoid Cell Imaging Station (Thermo Fisher Scientific).

Quantitative analysis of live, apoptotic, and dead cells treated with peptides **2**–**5** was performed with the Muse Cell Analyzer (EMD Millipore Corporation, Burlington, MA, USA) using the Muse Annexin V & Dead Cell Kit according to the manufacturer's specifications. In brief, HeLa cells were plated into a 6-well culture at a density of 5×10^4 cells mL^{-1} (2 mL per well) and treated with the 500 µM concentration of conjugates **2**–**5** for 72 h. After treatment with the test compounds, both floating and adherent cells were collected, centrifuged (600 g min^{-1}), and suspended in cell culture medium to adjust the cell concentration according to the manufacturer's protocol. Then, 100 µL aliquots of the cell suspension were added to 100 µL of Muse Annexin V & Dead Cell Reagent and incubated for 20 min in the dark at RT. Cells were then analyzed using the Muse Cell Analyzer. Each compound was tested in duplicate, and each experiment was performed twice.

The data in the graphs are expressed as mean ± standard deviation (±SD), and the error bars in the figures indicate the SD. Differences between means were analyzed using the ANOVA test, followed by post-hoc Tukey's test. A significant difference was considered at a p value < 0.05.

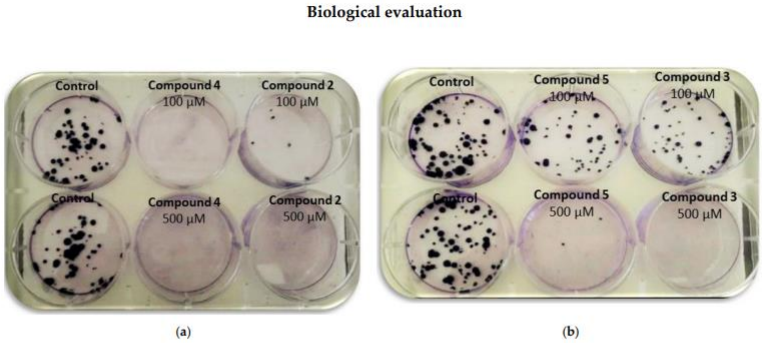

Figure S58. Results of clonogenic analysis after treatment with peptides **2-5** with two different concentrations [100 µM (**a**) and 500 µM (**b**)].

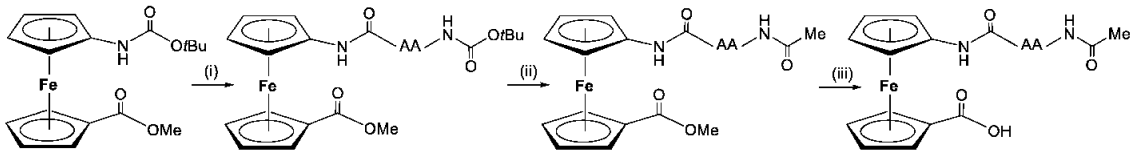

1 (Boc-NH-Fn-COOMe)

2 (Boc-L-Phe-NH-Fn-COOMe)
3 (Boc-L-Val-NH-Fn-COOMe)
4 (Boc-L-Leu-NH-Fn-COOMe)
5 (Boc-D-Phe-NH-Fn-COOMe)
6 (Boc-D-Val-NH-Fn-COOMe)
7 (Boc-D-Leu-NH-Fn-COOMe)

8 (Ac-L-Phe-NH-Fn-COOMe)
9 (Ac-L-Val-NH-Fn-COOMe)
10 (Ac-L-Leu-NH-Fn-COOMe)
11 (Ac-D-Phe-NH-Fn-COOMe)
12 (Ac-D-Val-NH-Fn-COOMe)
13 (Ac-D-Leu-NH-Fn-COOMe)

14 (Ac-L-Phe-NH-Fn-COOH)
15 (Ac-L-Val-NH-Fn-COOH)
16 (Ac-L-Leu-NH-Fn-COOH)
17 (Ac-D-Phe-NH-Fn-COOH)
18 (Ac-D-Val-NH-Fn-COOH)
19 (Ac-D-Leu-NH-Fn-COOH)

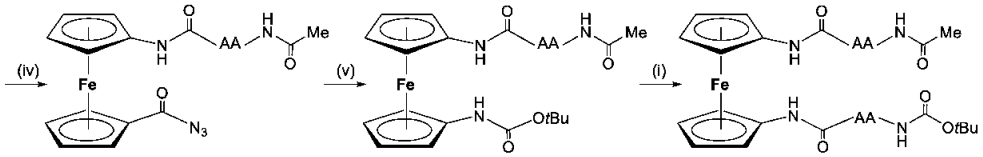

20 (Ac-L-Phe-NH-Fn-CON_3)
21 (Ac-L-Val-NH-Fn-CON_3)
22 (Ac-L-Leu-NH-Fn-CON_3)
23 (Ac-D-Phe-NH-Fn-CON_3)
24 (Ac-D-Val-NH-Fn-CON_3)
25 (Ac-D-Leu-NH-Fn-CON_3)

26 (Ac-L-Phe-NH-Fn-NH-Boc)
27 (Ac-L-Val-NH-Fn-NH-Boc)
28 (Ac-L-Leu-NH-Fn-NH-Boc)
29 (Ac-D-Phe-NH-Fn-NH-Boc)
30 (Ac-D-Val-NH-Fn-NH-Boc)
31 (Ac-D-Leu-NH-Fn-NH-Boc)

32 (Ac-L-Phe-NH-Fn-NH-L-Phe-Boc)
33 (Ac-L-Val-NH-Fn-NH-L-Val-Boc)
34 (Ac-L-Leu-NH-Fn-NH-L-Leu-Boc)
35 (Ac-D-Phe-NH-Fn-NH-D-Phe-Boc)
36 (Ac-D-Val-NH-Fn-NH-D-Val-Boc)
37 (Ac-D-Leu-NH-Fn-NH-D-Leu-Boc)

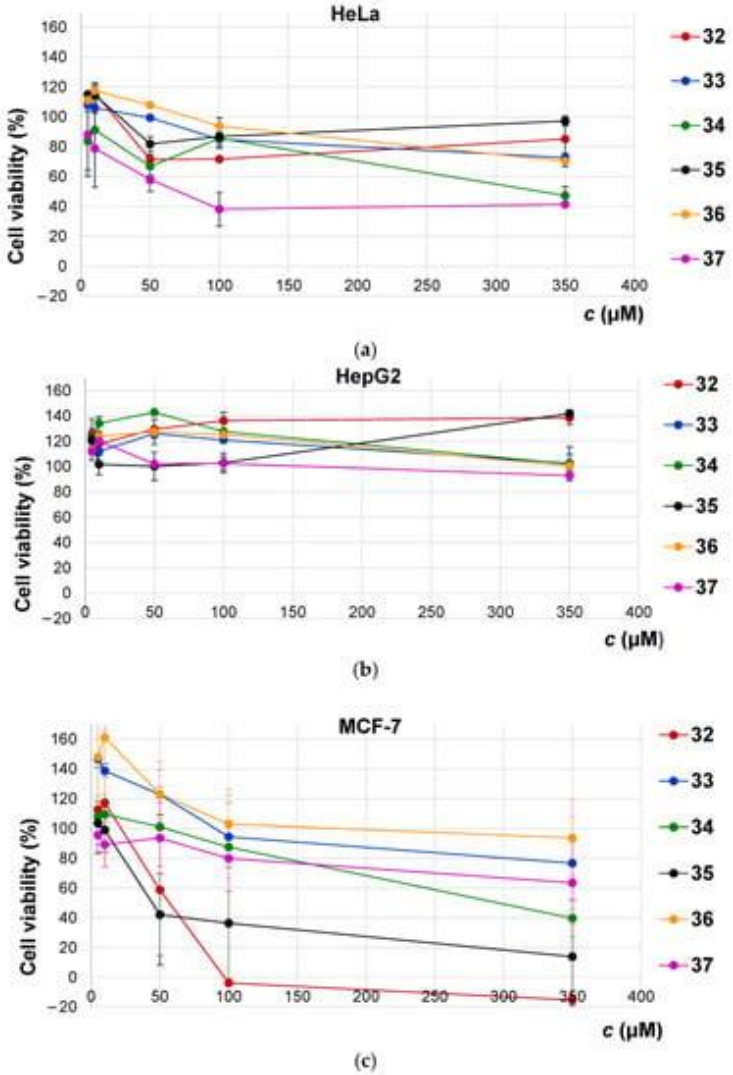

Figure 11. Dose response curves for tested compounds **32–37** in Hela (**a**), Hep G2 (**b**), and MCF-7 (**c**) cells. Cells were treated with 5 different concentrations of compounds (5, 10, 50, 100, and 350 uM) and their viability was assessed by MTT test after 72h of incubation. Average ± s.d. from 3 biological replicates is shown.

Table 2. IC_{50} values calculated from dose-response curves on HeLa, HepG2 and MCF-7 cells.

Table 2. IC_{50} values calculated from dose-response curves on HeLa, HepG2 and MCF-7 cells.

Ferrocene Peptidomimetics	HeLa	HepG2	MCF-7
Ac–L-Phe–NH–Fn–NH–L-Phe–Boc (**32**)	>350 μM	>350 μM	53.1 ± 23 μM
Ac–D-Phe–NH–Fn–NH–D-Phe–Boc (**35**)	>350 μM	>350 μM	32.7 ± 6.89 μM
Ac–L-Val–NH–Fn–NH–L-Val–Boc (**33**)	>350 μM	>350 μM	>350 μM
Ac–D-Val–NH–Fn–NH–D-Val–Boc (**36**)	>350 μM	>350 μM	>350 μM
Ac–L-Leu–NH–Fn–NH–L-Leu–Boc (**34**)	331 ± 39 μM	>350 μM	261 ± 97 μM
Ac–D-Leu–NH–Fn–NH–D-Leu–Boc (**37**)	80.8 ± 15 μM	>350 μM	>350 μM
III[a]	N.T.	259.33	N.T.
Cisplatin	46.14 [b]	15.9 [c]	97.86 [b]

[a] Adapted from ref [19]: N.T. not tested in ref [19]. [b] Adapted from ref [85]. [c] Adapted from ref [86].

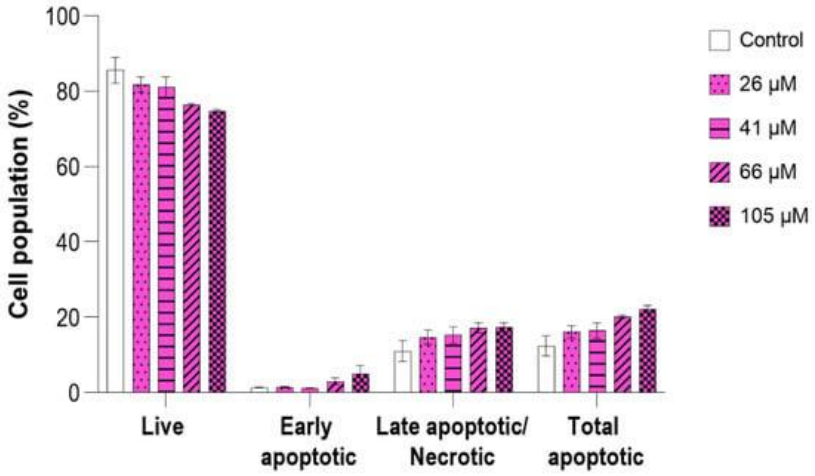

Figure 12. The effect of peptidomimetic **37** on apoptosis of HeLa cells. Cells were treated with four different concentrations of the tested compound (26 μM, 44 μM, 61 μM, and 105 μM) for 24 h. Bar graphs present the percentage of different cell subpopulations: live cells, early apoptotic cells, late apoptotic, and necrotic cells. Total apoptotic cells are the sum of the percentages of early apoptotic and late apoptotic/necrotic cells. Values are presented as mean ± SEM from two independent experiments.

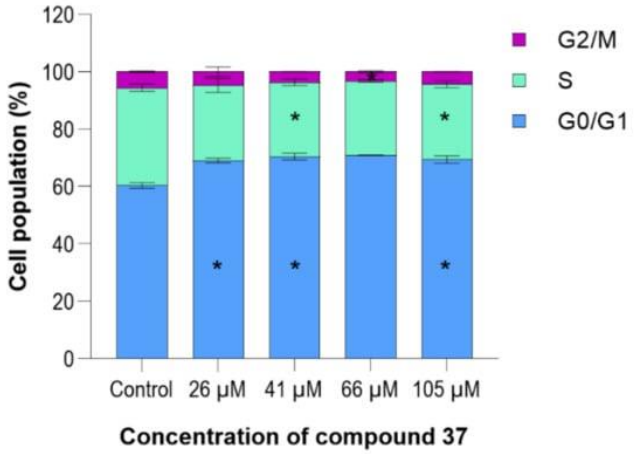

Figure 13. Cell cycle profiles for control HeLa cells and cells treated with four different concentrations of compound **37** (26 µM, 44 µM, 61 µM, and 105 µM) for 24 h. Cell cycle distribution was calculated as the percentage of cells in the G0/G1, S, and G2/M phase. Data are representative of two independent experiments and were calculated as mean ± SEM. Statistical significance was considered if * $p < 0.05$.

Table 3. Antioxidant activity of ferrocene peptides evaluated by 1,1-diphenyl-2-picryl-hydrazyl radical scavenging assay (DPPH) and ferric reducing antioxidant power methods (FRAP).

Table 3. Antioxidant activity of ferrocene peptides evaluated by 1,1-diphenyl-2-picryl-hydrazyl radical scavenging assay (DPPH) and ferric reducing antioxidant power methods (FRAP).

Ferrocene Peptidomimetics (c = 1 mM)	FRAP (mM Trolox)	DPPH (% Inhibition of 0.1 mM Trolox)
Ac–L-Phe–NH–Fn–NH–L-Phe–Boc **(32)**	0.63 ± 0.21	113.77 ± 4.02
Ac–D-Phe–NH–Fn–NH–D-Phe–Boc **(35)**	0.58 ± 0.20	116.80 ± 18.19
Ac–L-Val–NH–Fn–NH–L-Val–Boc **(33)**	0.52 ± 0.06	102.62 ± 20.66
Ac–D-Val–NH–Fn–NH–D-Val–Boc **(36)**	0.62 ± 0.15	88.68 ± 24.52
Ac–L-Leu–NH–Fn–NH–L-Leu–Boc **(34)**	0.56 ± 0.17	81.98 ± 7.04
Ac–D-Leu–NH–Fn–NH–D-Leu–Boc **(37)**	0.60 ± 0.10	122.75 ± 2.17
Trolox 0.1 mM	-	100.00 ± 0.0

3.1.4. Biological Activity

Antitumor activity

Materials: trypsin-EDTA (0.25%), FBS (fetal bovine serum), DMEM (Dulbecco's Modified Eagle Medium), RNAse A, insulin, glutamine, penicillin, and streptomycin were purchased from Sigma-Aldrich. PBS (phosphate buffer saline) was prepared from the following ingredients: sodium chloride was purchased from Honeywell Research Chemicals, calcium chloride was purchased from Gram-Mol, disodium phosphate and monopotassium phosphate were purchased from Merck. Accutase Cell Detachment Solution was purchased from Capricorn Scientific GmbH (Ebsdorfergrund, Germany). Annexin V-FITC and propidium iodide were purchased from BD Biosciences, while Annexin Binding Buffer was prepared from the following ingredients: HEPES was purchased from Carl Roth, and calcium chloride and sodium hydroxide were purchased from Gram-Mol. Absolute ethanol was purchased from Merck.

Cell culture: The HeLa (cervical adenocarcinoma), MCF-7 (breast adenocarcinoma), and HepG2 (hepatocellular carcinoma) cells were cultured as monolayers and maintained in DMEM supplemented with 10% (*v*/*v*) FBS, 2 mmol/L L-glutamine, 100 U/mL penicillin, and 100 mg/mL streptomycin in a humidified atmosphere with 5% CO_2 at 37 °C. Media for MCF-7 were additionally supplemented with 0.01 mg/mL human recombinant insulin. Cells were washed in PBS and detached with 0.25% (*v*/*v*) Trypsin-EDTA solution.

The growth inhibition activity was assessed according to the slightly modified procedure performed at the National Cancer Institute, Developmental Therapeutics Program [**85**]. The cells were inoculated onto standard 96-well microtiter plates on day 0. Cell concentrations were adjusted according to their respective growth rates: 3000 cells per well for HeLa and HepG2, and 5000 cells per well for MCF-7. Test agents were then added the next day in five dilutions (5, 10, 50, 100, and 350 umol/L) and incubated over a further 72 h. Working dilutions were freshly prepared on the day of testing. The solvent (EtOH) was also tested for possible inhibitory activity at the same concentration as in tested solutions. After 72 h of incubation, the cell growth rate was evaluated by the MTT assay, which detects dehydrogenase activity in viable cells [**23**,**105**] The absorbance (OD, optical density) was measured on a microplate reader at 595 nm. Percentage of growth (PG) of the cell lines was calculated using one of the following two expressions:

If (mean OD_{test} − mean OD_{tzero}) ≥ 0, then: PG = 100 × (mean OD_{test} − mean OD_{tzero})/(mean OD_{ctrl} − mean OD_{tzero})

If (mean OD_{test} − mean OD_{tzero}) < 0, then: PG = 100 × (mean OD_{test} − mean OD_{tzero})/OD_{tzero}

where mean OD_{tzero} = the average of optical density measurements before exposure of cells to the test compound; mean OD_{test} = the average of optical density measurements after the desired period of time; mean OD_{ctrl} = the average of optical density measurements after the desired period of time without exposure of cells to the test compound [**104**]. Each test point was performed in quadruplicate in three individual experiments. The results are expressed as IC_{50}, which is the concentration necessary for 50% inhibition. The IC_{50} values for each compound are calculated from dose response curves using linear regression analysis by fitting the test concentrations that give PG values above and below the reference value (i.e., 50%). If, however, for a given cell line all of the tested concentrations produce PGs exceeding the respective reference level of effect (e.g., PG value of 50), then the highest tested concentration is assigned as the default value, which is preceded by a sign >. Each result is the mean value from three separate experiments.

Based on the IC_{50} values determined by the MTT assay, compound **37** was selected for further analysis of apoptosis and cell cycle.

Treatment: for apoptosis, 10^5 cells per well were seeded in 12-well plates, while for the cell cycle, 2 × 10^5 cells per well were seeded in 6-well plates. Once the cell monolayers reached 80% of confluency, the cells were treated for 24 h with four different concentrations of the test compound (26 µM, 44 µM, 61 µM, and 105 µM) dissolved in DMEM completed medium. For both apoptosis and cell cycle, the medium containing ethanol without the tested compound was used as a negative control.

Apoptosis analysis by flow cytometry: after the 24-h treatment, the floating HeLa cells were collected while the attached cells were washed with PBS and detached with Accutase. Both attached and detached cells were pooled together, centrifuged, resuspended in 1× Annexin Binding Buffer, and stained with Annexin V-FITC and PI according to the manufacturer's instructions. Samples were analyzed using the Navios™ flow cytometer (Beckman Coulter Life Sciences, Miami, FL, USA) to detect viable (Annexin V-FITC-negative/PI-negative), total apoptotic (Annexin V-FITC-positive/ PI-negative and Annexin V-FITC-positive/PI-positive), and necrotic cells (Annexin V-FITC-negative/PI-positive). Ten thousand cells were analyzed per sample. Data were analyzed using the FlowLogic software (Inivai, Melbourne, Australia). Analysis was performed on two biological replicates, with each concentration of compound **37** tested in duplicate (**Figures S54 and S55**).

Cell cycle analysis by flow cytometry: after the 24-h treatment, the floating HeLa cells were collected, while the attached cells were washed with PBS and detached with Accutase. Both attached and detached cells were pooled together, centrifuged, and washed twice with PBS. After washing, cells were resuspended in 1.5 mL PBS and fixed by adding two volumes of the ice-cold absolute ethanol. After a minimum of 72 h of fixation, cells were centrifuged, washed twice in PBS, and then incubated with RNase A (0.1 mg/mL) and PI (50 µg/mL) at room temperature for 30 min in the dark. The cell cycle was analyzed using the DxFLEX flow cytometer (Beckman Coulter Life Sciences, Miami, FL, USA). Twenty thousand cells were analyzed per sample. FlowLogic software (Inivai, Melbourne, Australia) was used to determine the percentage of cells in each phase of the cell cycle (G0/G1, S, G2/M). Each concentration of compound **37** was tested in duplicate and each experiment was performed twice.

Statistical analysis: the obtained results were analyzed using GraphPad Prism 9 software. Data are presented as mean value ± SEM of two independent experiments performed in duplicate. For comparison between the control and treated groups, one-way ANOVA test, followed by post-hoc Tukey's test, was used. Statistical significance was considered at a p value < 0.05.

Antimicrobial activity

Microorganisms: To evaluate the antimicrobial properties of the tested peptides, thirteen microorganisms were used: Gramme-positive bacteria (*Staphylococcus aureus*, *Bacillus subtilis*, *Enterococcus faecium*, *Listeria monocytogenes*), Gramme-negative bacteria (*Pseudomonas aeruginosa*, *Escherichia coli*, *Salmonella enterica* s. Typhimurium), lactic acid bacteria (*Leuconostoc mesenteroides*, *Lactobacillus plantarum*) and yeasts (*Candida albicans*, *Candida utilis*, *Rhodotorula* sp. and *Saccharomyces cerevisiae*). The microorganisms were stored on slant agar in the microorganism collection of the Laboratory of General Microbiology and Food Microbiology and the Laboratory of Fermentation and Yeast Technology of the Faculty of Food Technology and Biotechnology, University of Zagreb (Croatia). Antimicrobial activity tests: In the first step, the antimicrobial activities of the tested peptides were determined using the disc diffusion method to verify the efficacy of the samples on all tested strains. After overnight growth of cultures under anaerobic conditions at 37 °C in Muler Hinton broth (Gramme-positive and Gramme-negative bacteria), MRS broth at 32 °C (lactic acid bacteria), and Muler Hinton broth with 2% glucose at 28 °C (yeast), cell density was adjusted to 0.5 McFarland using a spectrophotometer ($A_{550\,nm} \approx 0.125$). Agar plates were then inoculated directly from the suspension, and the inoculum was spread with a sterile swab according to the CLSI protocol. Ferrocene peptides were diluted in DMSO (0.1 g/mL). Philtre paper discs were then placed on the inoculated medium using flamed forceps and the ferrocene samples (10 µL) were applied to the discs (diameter = 6 mm; 1mg/disc). Kanamycin and nystatin were used as positive controls and DMSO as a negative control. Petri dishes were incubated anaerobically, and zones of inhibition were measured with a ruler after 24 h **Figure S56** in the **Supplementary Material**). For each peptide and microorganism, the experiments were performed in duplicate.

Antioxidant activity assays

The methods used to determine the antioxidant activity are based on the study of a reaction in which a free radical is generated and inhibited by the addition of the sample whose antioxidant activity is being measured. DPPH radical scavenging activity and ferric ion reducing antioxidant power (FRAP) are used to determine the antioxidant activity of the tested peptides (c = 1 mM).

DPPH assays: the DPPH radical scavenging assay (1,1-diphenyl-2-picrylhydrazyl) was performed according to the method of Brand-Williams et al. [**106**]. Ethanol (1 mL) and 0.1 mM DPPH working solution (2 mL) were added to the samples (150 µL). The absorbance at 525 nm was measured after 30 min of incubation in the dark. The DPPH reagent and ethanol were used as blank reference, and 0.1 mM and 0.5 mM Trolox were used to compare the percentage of DPPH radical inhibition. The percentage of DPPH

inhibition was calculated using the following formula: % of DPPH reduction = [Ao − As]/Ao × 100, where Ao is the absorbance of DPPH solution with ethanol and As is the absorbance of a DPPH solution with the sample. Results are expressed as percent inhibition of 0.1 mM Trolox. All experiments were performed in triplicate.

FRAP assay: the FRAP assay was performed as previously described [107], with some modifications. FRAP reagent solution was prepared from the mixture of acetate buffer (300 mM, pH = 3.6), TPTZ (10 mM solution of TPTZ in 40 mM HCl) and $FeCl_3 \times 6H_2O$ (20 mM) in a volume ratio of 10:1:1). The working reagent FRAP was freshly prepared. All samples, standards , and reagents were pre-incubated at 37 ˚C. The sample to be analyzed (80 µL) was mixed with FRAP reagent (2080 µL) and distilled water (240 µL) at 37 °C. After 5 min, the absorbance was measured at 593 nm. The standard curve was generated using a serial dilution (0.1–2.0 mM) of the stock Trolox solution. The results were expressed as mM Trolox equivalents. All experiments were also performed in triplicate.

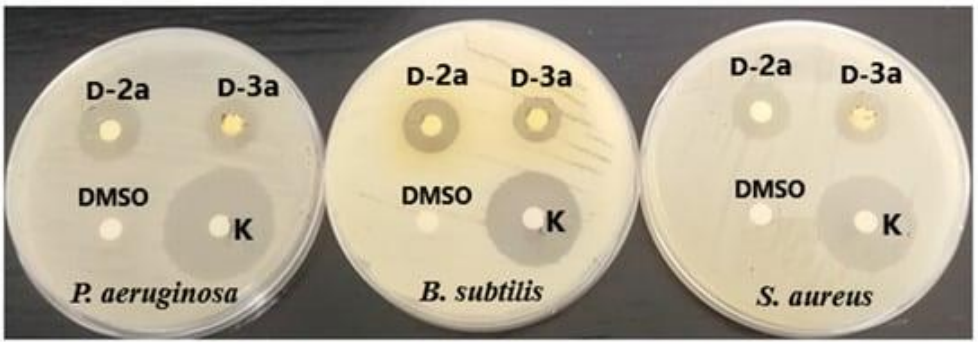

Figure 9. Inhibition zone of D-**2a** and D-**3a** against *P. aeruginosa*, *B. subtilis,* and *S. aureus* (D-**2a**, D-**3a**—1 mg/disk; K—Kanamycin 50 µg disk—positive control, DMSO—negative control).

Table 2. Growth inhibition zones of the tested microorganisms and minimum inhibitory concentrations (MIC) of the tested compounds D-**1a**, D-**2a,** and D-**3a**.

Table 2. Growth inhibition zones of the tested microorganisms and minimum inhibitory concentrations (MIC) of the tested compounds D-**1a**, D-**2a**, and D-**3a**.

Compound	Test Microorganisms	Molarity of Solutions for Disk Diffusion Method (mM)	Inhibition Zone (mm)	MIC (mM)
D-**1a**	*S. aureus*	251	nd	>2
	B. subtilis		7 ± 1	>2
	P. aeruginosa		nd	>2
D-**2a**	*S. aureus*	243	16 ± 1	>2
	B. subtilis		16 ± 1	>2
	P. aeruginosa		19 ± 2	>2
D-**3a**	*S. aureus*	224	14 ± 1	>2
	B. subtilis		14 ± 1	>2
	P. aeruginosa		14 ± 1	>2
Kanamycin	*S. aureus*	50 µg disk	25 ± 0	nd
	B. subtilis		25 ± 0	nd
	P. aeruginosa		28 ± 1	nd

nd—not detected.

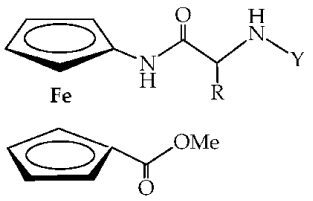

L- and D-**1a** (R = $CH(CH_3)_2$, Y = $COCH_3$)

L- and D-**2a** (R = $CH_2CH(CH_3)_2$, Y = $COCH_3$)

L- and D-**3a** (R = $CH_2C_6H_5$, Y = $COCH_3$)

L- and D-**1b** (R = $CH(CH_3)_2$, Y = $COOC(CH_3)_3$)

L- and D-**2b** (R = $CH_2CH(CH_3)_2$, Y = $COOC(CH_3)_3$)

L- and D-**3b** (R = $CH_2C_6H_5$, Y = $COOC(CH_3)_3$)

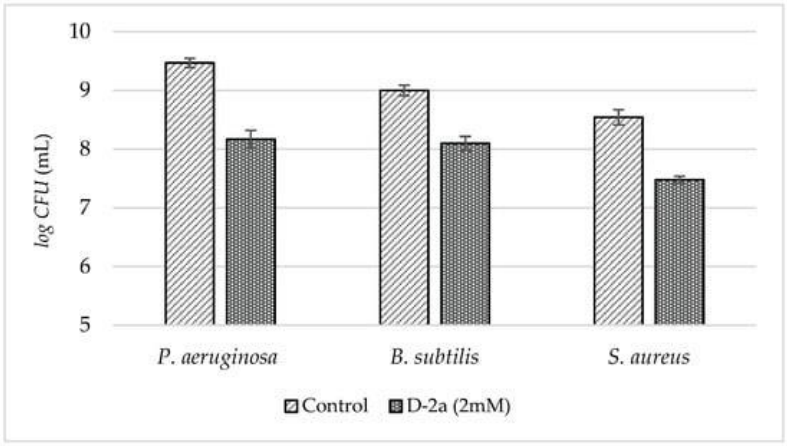

Figure 10. Bacterial density expressed as log CFU/mL of *S. aureus*, *B. subtilis,* and *P. aeruginosa* after 24 h of incubation without (control) and 2 mM of compound D-**2a**. Each column and bar represent the mean and the standard deviation, respectively (*n* = 2). CFU, colony-forming unit.

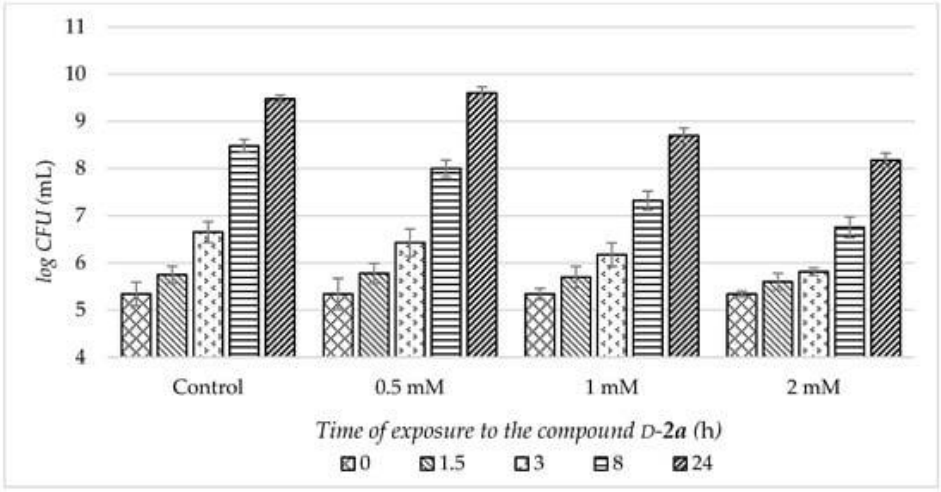

Figure 11. Bacterial density expressed as log CFU/mL of *P. aeruginosa* at baseline and after 1.5 h, 3 h, 8 h, and 24 h of incubation without (control) and in the presence of 0.5 mM, 1 mM, and 2 mM of compound D-**2a**. Each column and bar represent the mean and standard deviation, respectively (*n* = 2). CFU, colony-forming unit.

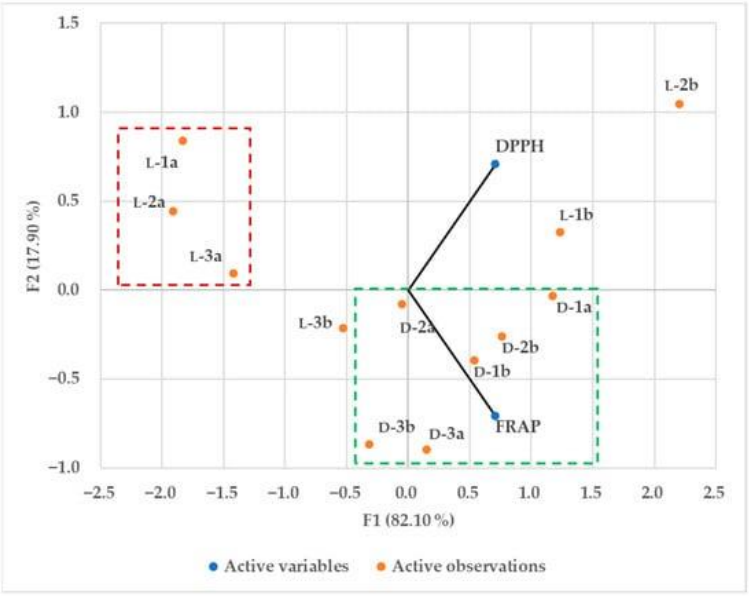

Figure 12. Principal component analysis (PCA) plot of different dipeptides based on their antioxidant activity; highlighted in green—dipeptides with D-amino acids and higher antioxidant activity; highlighted in red—dipeptides with L-amino acids and acetyl as the protecting group with the lowest antioxidant activity.

Table 3. Antioxidative activity of ferrocene compounds evaluated using free 1,1-diphenyl-2-picrylhydrazyl radical scavenging assay and ferric-reducing antioxidant power methods.

Table 3. Antioxidative activity of ferrocene compounds evaluated using free 1,1-diphenyl-2-picrylhydrazyl radical scavenging assay and ferric-reducing antioxidant power methods.

Compound (1 mM)	DPPH (% Inhibition)	DPPH (mM Trolox Equivalent)	FRAP (mM Trolox)
L-**1b**	11.75 ± 2.10	0.150	2.16 ± 0.013
L-**2b**	16.55 ± 1.77	0.211	2.27 ± 0.006
L-**3b**	5.50 ± 3.87	0.067	1.62 ± 0.001
D-**1b**	7.76 ± 0.65	0.099	2.17 ± 0.015
D-**2b**	8.79 ± 2.10	0.112	2.21 ± 0.003
D-**3b**	3.99 ± 0.48	0.051	2.00 ± 0.001
L-**1a**	4.57 ± 0.64	0.058	0.58 ± 0.009
L-**2a**	3.19 ± 1.29	0.041	0.72 ± 0.004
L-**3a**	3.65 ± 2.26	0.046	1.09 ± 0.030
D-**1a**	10.62 ± 1.13	0.135	2.29 ± 0.003
D-**2a**	6.96 ± 0.81	0.089	1.77 ± 0.001
D-**3a**	5.25 ± 2.26	0.067	2.22 ± 0.006
Standard (0.5 mM Trolox)	39.27 ± 8.40	0.500	

Table 4. List of the peptides used in the study. The abbreviation, retention time (t_R), and percentage of acetonitrile (% ACN) at elution are displayed.

Table 4. List of the peptides used in the study. The abbreviation, retention time (t_R), and percentage of acetonitrile (% ACN) at elution are displayed.

Compound	t_R/min	% ACN
L-**1b**	7.1	82.6
L-**2b**	8.3	87.5
L-**3b**	8.3	87.9
D-**1b**	7.1	82.6
D-**2b**	8.3	87.5
D-**3b**	8.3	87.9
L-**1a**	2.6	63.7
L-**2a**	3.3	66.6
L-**3a**	3.6	68.0
D-**1a**	2.6	63.7
D-**2a**	3.3	66.6
D-**3a**	3.6	68.0

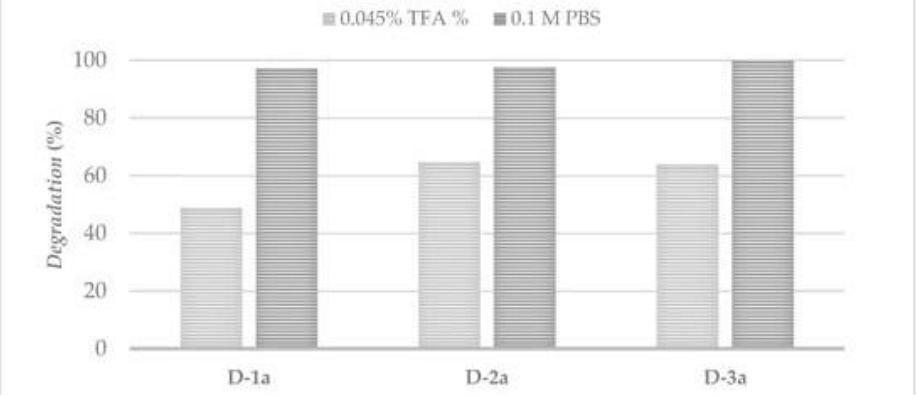

Figure 13. Percentage of degradation of ferrocene peptides in 0.045% TFA and 0.1 M buffer after 24 h.

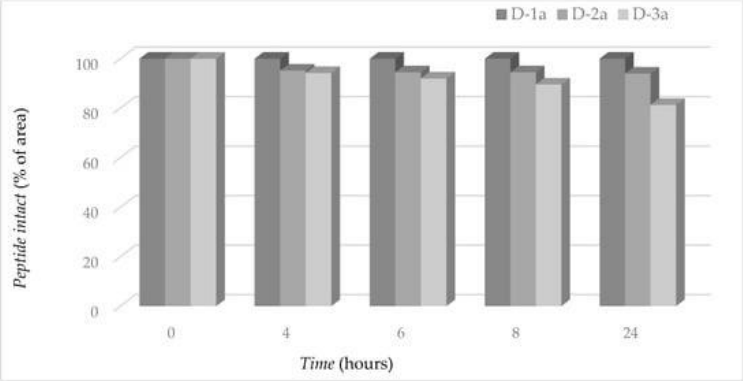

Figure 14. Proteolytic stability of ferrocene peptides during 24 h.

3.4. Antimicrobial Activity

Microorganisms: Gram-positive bacteria (*Staphylococcus aureus*, *Bacillus subtilis*, *Enterococcus faecium*, and *Listeria monocytogenes*), Gram-negative bacteria (*Pseudomonas aeruginosa*, *Escherichia coli*, and *Salmonella enterica* s. Typhimurium), lactic acid bacteria (*Leuconostoc mesenteroides* and *Lactobacillus plantarum*), and yeasts (*Candida albicans*, *Candida utilis*, *Rhodotorula sp.*, and *Saccharomyces cerevisiae*) were used to evaluate the antimicrobial properties of the tested peptides. The microorganisms were stored on slant agar in the microorganism collection of the Laboratory of General Microbiology and Food Microbiology and the Laboratory of Fermentation and Yeast Technology of the Faculty of Food Technology and Biotechnology, University of Zagreb (Croatia).

Antimicrobial disk diffusion testing: The disk diffusion method was used to preliminarily test the efficacy of the samples on all strains tested. The disk diffusion method is a common method for pretesting the antimicrobial activity of potential antimicrobial compounds. For this reason, and because the detailed description of the work was included in our previous manuscript [36] and is repeated identically here, we do not discuss it in detail in this manuscript.

Determination of MIC: The minimum inhibitory concentration (MIC) was determined spectrophotometrically using the broth microdilution method [82]. Briefly, Mueller–Hinton broth was used for bacterial growth. Fresh 24-h broth culture was used (*S. aureus*, *B. subtilis*, *P. aeruginosa*), and the final density was set at 1×10^5 CFU/mL. Twofold dilution series of the test compound (D-**1a**, D-**2a**, and D-**3a**) were prepared in 200 µL of the medium. The compound was tested in a concentration gradient of 2–0.125 mM. During the experiment, a growth control without the test compound, kanamycin as a positive control, and the compound (stained) in the medium without microorganisms as a negative control were maintained. The microtiter plate was incubated at 37 °C for 24 h, after which the optical density was measured. The minimum concentration of the test substance that completely inhibits bacterial growth is referred to as the MIC.

Time–kill curve determination: The broth macrodilution method was used to generate a time–kill curve against *P. aeruginosa*. Briefly, for the time–kill curve, compound D-**2a** was evaluated at different multiples of tentative MIC—2 mM (¼ × MIC, ½ × MIC, and MIC). Three milliliters of Mueller–Hinton broth containing the appropriate concentration of the test compound were inoculated for 24 h for freshly grown *P. aeruginosa* to obtain a final concentration of 105 colony-forming units per mL. All test tubes were incubated at 37 °C in a thermostat, and samples were taken from each test tube after 0, 1.5, 3, 8, and 24 h. To determine the number of live cells, serial tenfold dilutions were prepared in sterile saline and aseptically spread on Mueller–Hinton agar plates. All agar plates were incubated at 37 °C for 24 h, and colonies were counted to determine colony-forming units per ml. The time–kill curve was constructed by plotting log 10 of colony-forming units per mL against time.

3.5. Antioxidant Activity Assays

Methods for determining antioxidant activity are based on the study of a reaction in which a free radical is generated and inhibited by the addition of the sample whose antioxidant activity is measured. The antioxidant activity of the tested peptides (c = 1 mM) is determined using the radical scavenger DPPH and the antioxidant power of ferric ions (FRAP). A detailed description of the work was also included in our previous manuscript [36] and is repeated identically here.

3.6. Statistical Analysis

Statistical analysis was performed with the MS Excel tool XLStat (Addinsoft, Paris, France) program. The data shown are mean values (n = 2). Differences between control and dipeptide microbial groups were subjected to analysis of variance (ANOVA). Principal component analysis (PCA) was used to visualize differences between dipeptides based on their antioxidant activity.

3.7. Hydrophobicity

Hydrophobicity of the dipeptides was measured by RP-HPLC-UV at 215 nm (Agilent Technologies 1200 series HPLC-DAD-MS/MS; Agilent Technologies Inc., Palo Alto, CA, USA) on a Zorbax XDP C18 column (75 × 4.6 mm^2, 3.5 µm particle size) (Agilent Technologies Inc.). The solvents for the analysis were 95% 0.1% TFA in water + 5% ACN (solvent A) and 95% ACN + 5% 0.1% TFA in water (solvent B). The gradient was applied as follows: 0 min 50% B, 0–10 min 50% B–100% B, 10.1–13 min 100% B, 13.1–18 min 50% B. The flow rate was 0.5 mL/min. Samples were prepared as 100 µg/mL solution in acetonitrile. The injection volume was 10 µL. The percentage of B eluent was read on the instrument for the retention time of each ferrocene peptide and corrected for the percentage of water in the B eluent.

3.8. Chemical Stability

Analysis was performed on RP-HPLC-UV at 215 nm (Agilent Technologies 1200 series HPLC-DAD-MS/MS) on a Zorbax XDP C18 column (75 × 4.6 mm^2, 3.5 µm particle size) (Agilent Technologies Inc.) by observing the decrease in the peak area of samples prepared in buffer and in TFA immediately after preparation and 4 h, 6 h, 8 h, and 24 h after preparation. The solvents for the analysis were 95% 0.1% TFA in water + 5% ACN (solvent A) and 95% ACN + 5% 0.1% TFA in water (solvent B). The gradient was applied as follows: 0 min 30% B, 0–10 min 30% B–100% B, 10.1–13 min 100% B, 13.1–18 min 20% B. The flow rate was 0.5 mL/min [16,58,59]. The stock solution of peptides with the greatest potency against microbial activity (D-**1a**–**3a**) was prepared as a 10 mg/mL solution in ACN. The dilution was prepared in 0.1 M buffer or 0.045% TFA as a 200 µg/mL solution. Samples were analyzed immediately after preparation and 4, 6, 8, and 24 h after sample preparation.

3.9. Proteolytic Stability

To test the proteolytic stability of the compounds, the same RP-HPLC-UV analysis was performed as in the determination of stability in the buffer and in acid. Samples were prepared as a 200 µg/mL solution in 0.1 M PBS with the addition of 26.3 µg/mL chymotrypsin. Peak area was measured immediately after preparation and 4 h, 6 h, 8 h, and 24 h after sample preparation. The curves of degradation were plotted as the percentage of intact peptide measured by the analysis of peak area as a function of time.

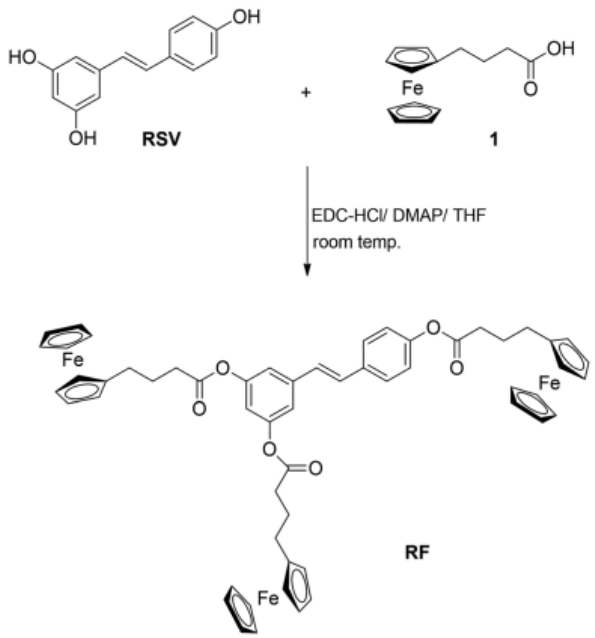

SCHEME 1 The synthesis of ferrocene-containing resveratrol derivative, RF

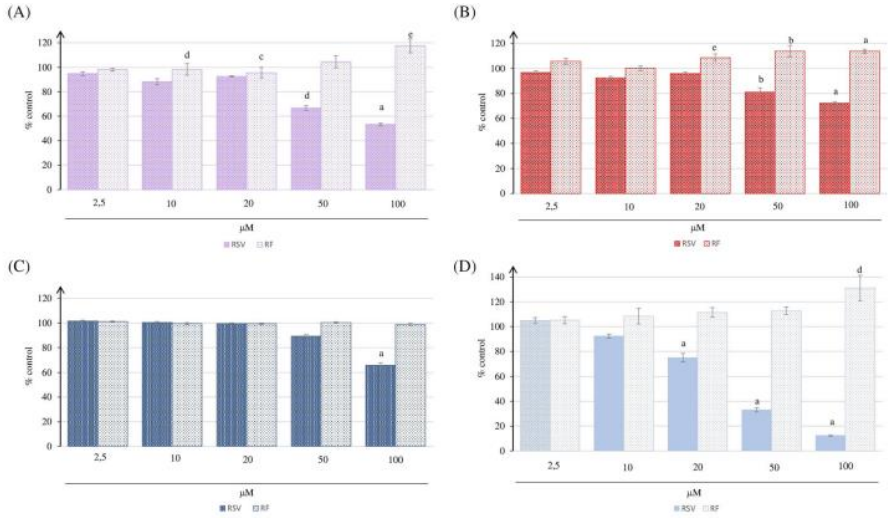

FIGURE 2 Effects of 2.5–100 μM resveratrol (RSV) and resveratrol-ferrocene derivative (RF) on CHO-K1 viability and rate of proliferation after 48 h of exposure obtained with MTT assay (A), Neutral Red (B), Kenacid Blue (C), and Trypan blue exclusion (D) assays. Data are presented as percentage of control (cells treated with 5 μl ml^{-1} DMSO) ± SEM. Statistically significant $^{a}p < 0.001$; $^{b}p < 0.005$; $^{c}p < 0.01$; $^{d}p < 0.025$; $^{e}p < 0.05$ *versus* control

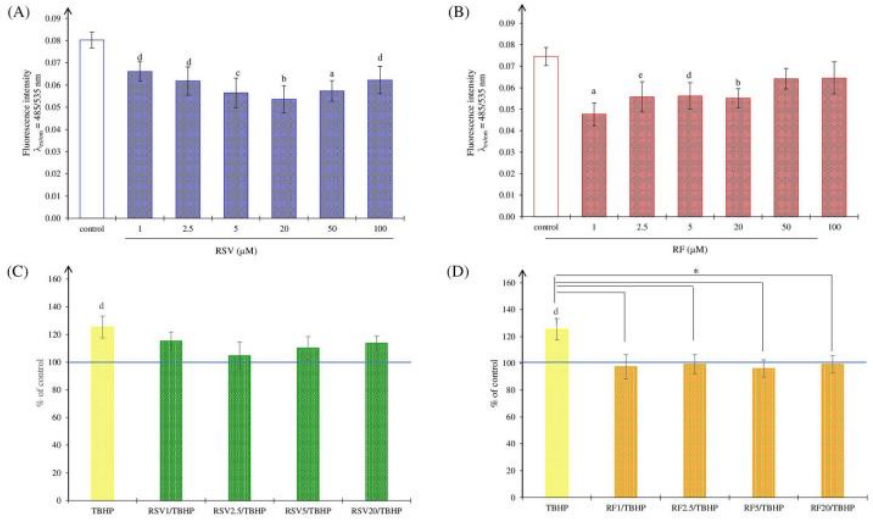

FIGURE 3 CHO-K1 cells treated with 1–100 μM resveratrol—RSV (A); 1–100 μM resveratrol-ferrocene derivative—RF (B); 1–20 μM resveratrol—RSV + 50 μM *t*BHP (*tert*-butyl hydroperoxide) (C); 1–20 μM resveratrol-ferrocene derivate—RF + 50 μM TBHP (*tert*-butyl hydroperoxide) (D). Data are presented as percentage of control ± SEM. Statistically significant [a]$p < 0.001$; [b]$p < 0.005$; [c]$p < 0.01$; [d]$p < 0.025$; [e]$p < 0.05$ versus control; *$p < 0.05$ *versus* TBHP

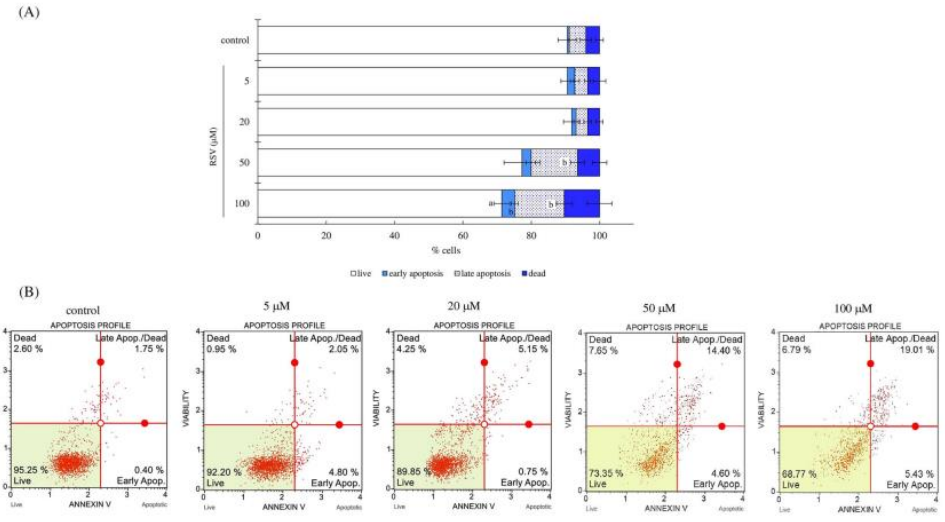

FIGURE 4 Flow cytometric analysis of apoptosis/necrosis in CHO-K1 cells after exposure to 5–100 μM resveratrol (RSV) for 48 h by Muse Cell Analyzer (Merck Millipore). (A) Percentage of live, early and late apoptotic, and dead cells in population; mean ± SEM. Statistically significant [a]$p < 0.01$; [b]$p < 0.05$ *versus* control. (B) Representative dot plots of control (treated with 5 μl ml^{-1} DMSO) and resveratrol treated cells

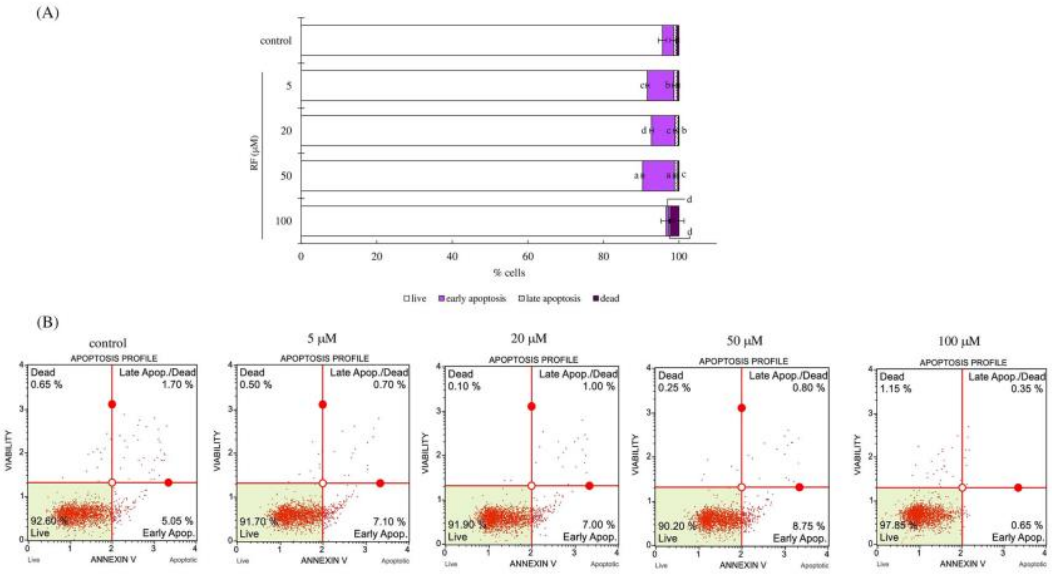

FIGURE 5 Flow cytometric analysis of apoptosis/necrosis in CHO-K1 cells after exposure to 5–100 μM resveratrol-ferrocene derivative (RF) for 48 h by Muse Cell Analyzer (Merck Millipore). (A) Percentage of live, early and late apoptotic, and dead cells in population; mean ± SEM. Statistically significant $^{a}p < 0.001$; $^{b}p < 0.005$; $^{c}p < 0.01$; $^{d}p < 0.05$ *versus* control. (B) Representative dot plots of control (treated with 5 μl ml^{-1} DMSO) and RF conjugate treated cells

2.2 | Pharmacology

2.2.1 | Reagents and tissue culture supplies

Dulbecco's Modified Eagle Medium/Nutrient Mixture F-12 (DMEM/F12), fetal bovine serum (FBS; heat inactivated), MTT (3-(4,5-dimethyl-2-thiazolyl)-2,5-diphenyl-2H-tetrazolium bromide; CAS 298–93-1), Trypan Blue dye (CAS 72-57-1), trypsin/EDTA solution (0.25% trypsin with EDTA 4Na), and RSV (CAS 501-36-0) were supplied by Sigma–Aldrich Co. The synthesis of the ferrocene-triacyl derivative of resveratrol ($C_{56}H_{54}Fe_3O_6$) is described in 2.1.2. Muse™ Annexin V & Dead Cell Kit (cat #MCH100105) and Neutral Red dye (CAS 553-24-2) were purchased from Merck (Billerica, MA, USA). Coomassie Brilliant Blue R-250 (CAS 6104-59-2) was supplied by LKB (Bromma, Sweden). DCFDA/H2DCFDA assay kit (cat #ab113851) was supplied from Abcam (Cambridge, UK). DMSO (CAS 67-68-5) was provided by Kemika (Zagreb, Croatia). Stock solutions of RSV and RF prepared in DMSO were diluted to the final concentration (2.5–100 μM) in cell culture medium. The final DMSO concentration was 1% (v/v). Tissue culture supplies (T-25 flasks, 6-well and black 96-well plates) were obtained from Beckton Dickinson (Franklin Lakes, New Jersey, USA) and Nunc (Roskilde, Denmark).

2.2.2 | Cell culturing and maintenance

CHO-K1: Chinese hamster ovary cell line (ATCC no. CCL-61) was routinely grown at 37°C in sterile 25 cm^2 polystyrene cell culture flasks (Falcon) in DMEM/F12 medium supplemented with 10% (v/v) FBS. No antibiotics were used during the experiments. CHO-K1 cell culture was maintained under a humidified atmosphere of 95% air and 5% CO_2. At >70% confluence, the cells were harvested with trypsin/EDTA solution, diluted to the required density, and transferred to multiwell plates for the experiment to be performed.

2.2.3 | Cytotoxicity and proliferation analysis

Cytotoxicity and proliferation endpoints were quantified using MTT, Neutral Red uptake (NR), Kenacid Blue (KB) assays, and Trypan Blue exclusion method (TB). The assays were performed as previously described (Kmetič et al., 2008) with minor modifications. Briefly, CHO-K1 cells were inoculated at a density of 2×10^4 cells ml^{-1} (2 m/well) in six-well culture plates. After 24 h, the cells were exposed to medium containing RSV or RF (2.5–100 μM) for 48 h at 37°C. To ensure that DMSO exposure had no effect on cell viability and proliferation, the cells (control) were treated with the same concentration of DMSO (1% of total medium v/v).

2.2.3 | Cytotoxicity and proliferation analysis

Cytotoxicity and proliferation endpoints were quantified using MTT, Neutral Red uptake (NR), Kenacid Blue (KB) assays, and Trypan Blue exclusion method (TB). The assays were performed as previously described (Kmetič et al., 2008) with minor modifications. Briefly, CHO-K1 cells were inoculated at a density of 2×10^4 cells ml^{-1} (2 m/well) in six-well culture plates. After 24 h, the cells were exposed to medium containing RSV or RF (2.5–100 μM) for 48 h at 37°C. To ensure that DMSO exposure had no effect on cell viability and proliferation, the cells (control) were treated with the same concentration of DMSO (1% of total medium v/v).

2.2.4 | Intracellular ROS determination

The formation of reactive oxygen species (ROS) in cells was investigated spectrofluorimetrically using the 2′,7′-dichlorofluorescein diacetate (DCFDA/H2DCFDA) assay. A detailed protocol of this method was described in Banella et al. (2020). Briefly, CHO-K1 cells from the exponential growth phase were plated in black 96-well plates at an initial density of 2.5×10^5 cells ml^{-1} (100 μl/well). After overnight incubation, cells were washed with buffer and incubated with 25 μM 2′,7′-dichlorofluorescin diacetate at 37°C for 45 min. Cells were then washed with buffer and exposed to RSV or RF (1–100 μM) at 37°C. After 3 h, fluorescence intensity was measured using the Cary Eclipse spectrofluorimeter (Varian, Palo Alto, California, USA) at $\lambda_{ex/em} = 485/535$ nm.

In addition, the production of ROS was induced in ovarian cells with 50 μM tBHP (*tert*-butyl hydroperoxide), and RSV or RF was added to reduce oxidative stress. For this purpose, the CHO-K1 cell suspension was seeded as previously described with the addition of RSV or RF (1–20 μM). After 24 h, the cells were washed with buffer and incubated for 45 min at 37°C with 100 μl DCFH-DA (at a concentration of 25 μM). After incubation, the cells were washed with buffer. The cells were then treated with 50 μM *t*BHP for 3 h at 37°C. Fluorescence intensity was measured as previously described. Cells treated with the same volume of DMSO in which the RSV/RF was dissolved were used as control samples. For each concentration tested, 6 to 15 replicates were analyzed.

2.2.5 | Cytofluorimetric analysis

The percentage of viable, necrotic, and apoptotic cells after treatment with RSV or RF was determined using the Muse™ Annexin V & Dead Cell Kit according to the manufacturer's protocol. A detailed protocol of this method has been described in Murati et al. (2019). In brief, CHO-K1 cells from the exponential growth phase were seeded in six-well plates at an initial concentration of 2×10^4 cells ml^{-1} (4 ml per well). After overnight incubation, cells were treated with various concentrations of RSV or RF (5–100 μM) and incubated at 37°C for the next 48 h. Muse™ Annexin V & Dead Cell Reagent (100 μl) was added to aliquots of the trypsinized cell suspensions (100 μl), incubated in the dark at RT/20 min, and then analyzed using the Muse™ Cell Analyzer (Merck). Each RSV and RF concentration was tested (at least) in triplicate.

2.3 | Statistical analysis

Shown data present means ± SEM. A two-tailed Student's *t* test was used, and $p < 0.05$ was defined as the significance level.